NOAA Technical Memorandum NMFS-AFSC-468

Advancing Model-Based Essential Fish Habitat Descriptions for North Pacific Species in the Gulf of Alaska

J. L. Pirtle, E. A. Laman, J. Harris, M. C. Siple,
C. N. Rooper, T. P. Hurst, C. L. Conrath, and G. A. Gibson

April 2023

U.S. DEPARTMENT OF COMMERCE

National Oceanic and Atmospheric Administration
National Marine Fisheries Service
Alaska Fisheries Science Center

The National Marine Fisheries Service's Alaska Fisheries Science Center uses the NOAA Technical Memorandum series to issue informal scientific and technical publications when complete formal review and editorial processing are not appropriate or feasible. Documents within this series reflect sound professional work and may be referenced in the formal scientific and technical literature.

The NMFS-AFSC Technical Memorandum series of the Alaska Fisheries Science Center continues the NMFS-F/NWC series established in 1970 by the Northwest Fisheries Center. The NMFS-NWFSC series is currently used by the Northwest Fisheries Science Center.

This document should be cited as follows:

Pirtle, J. L., Laman, E. A., Harris, J., Siple, M. C., Rooper, C. N., Hurst, T. P., Conrath, C. L., and Gibson, G. A. 2023. Advancing model-based essential fish habitat descriptions for North Pacific species in the Gulf of Alaska. U.S. Dep. Commer., NOAA Tech. Memo. NMFS-AFSC-468, 541 p.

This document is available online at:

Document available: https://repository.library.noaa.gov

NOAA FISHERIES

Advancing Model-Based Essential Fish Habitat Descriptions for North Pacific Species in the Gulf of Alaska

J. L. Pirtle[1], E. A. Laman[2], J. Harris[3], M. C. Siple[2], C. N. Rooper[4], T. P. Hurst[2], C. L. Conrath[2], and G. A. Gibson[5]

[1]Habitat Conservation Division
Alaska Regional Office
National Marine Fisheries Service
National Oceanic and Atmospheric Administration
709 West 9th Street
Juneau, AK 99801

[2]Alaska Fisheries Science Center
National Marine Fisheries Service
National Oceanic and Atmospheric Administration
7600 Sand Point Way NE
Seattle, WA 98115

[3]Washington Department of Fish and Wildlife
1111 Washington St. SE
Olympia, WA 98501

[4]Pacific Biological Station
Fisheries and Oceans Canada
3190 Hammond Bay Road
Nanaimo, BC V9T 6N7
Canada

[5]International Arctic Research Center
University of Alaska
Fairbanks, AK 99775–7340

U.S. DEPARTMENT OF COMMERCE

National Oceanic and Atmospheric Administration
National Marine Fisheries Service
Alaska Fisheries Science Center

NOAA Technical Memorandum NOAA-TM-AFSC-468

April 2023

ABSTRACT

Councils and NMFS are required to review the essential fish habitat (EFH) components of Fishery Management Plans (FMPs) and revise or amend these components based on available information at least every five years (50 CFR 600.815(a)(10)) in an EFH 5-year Review. This study demonstrates advances in EFH component 1 descriptions and identification (maps) based on refinements to the habitat-based species distribution modeling (SDM) approach to mapping EFH established in the 2017 EFH 5-year Review[1]. All of the SDM ensembles constructed for FMP species in the Gulf of Alaska (GOA) in this present work describe and map EFH Level 2 (habitat-related abundance), meeting a key objective of the EFH Research Plan for Alaska[2]. For early juvenile life stages in the GOA, SDMs describe and map EFH Level 1 (distribution) for the first time. Another objective of the Research Plan was met by introducing maps for a subset of species with EFH Level 3 information (habitat-related vital rates) for the first time. In this study, EFH was described and mapped for 41 North Pacific groundfish species and one octopus in the GOA across up to three life stages. Companion studies have also described and mapped EFH for species' life stages in the Bering Sea and Aleutian Islands. A total of 96 new or revised EFH Level 1, 2, and 3 descriptions and maps for 86 individual species' life stages and four stock complexes were made available for the GOA for the 2023 EFH 5-year Review, out of 224 new or revised EFH descriptions and maps for 211 species' life stages and 10 stock complexes available across all regions modeled. The SDMs provided insight into the environmental conditions affecting patterns of species distribution and abundance, where geographic location, bottom depth, and bottom temperature were the most common top contributors to the deviance explained by the SDMs and rockiness, sponge presence, and BPI were relatively more influential for GOA species' life stages than for those in other regions modeled. The type of SDM used in the 2017 EFH 5-year Review had a large effect on the model

[1] https://repository.library.noaa.gov/view/noaa/17257
[2] https://www.fisheries.noaa.gov/resource/document/alaska-essential-fish-habitat-research-plan-processed-report-2017-05

performance and EFH areas in comparison to the 2022 ensembles; in the majority of cases, 2022 ensemble performance demonstrated clear improvements over the 2017 SDMs. The maps and descriptions here present the best available science to form a basis for assessing anthropogenic impacts to habitats in Alaska and are extensible to other fishery and ecosystem management information needs. Future research is recommended, including developing methods for combining disparate data sources to expand spatial and seasonal coverage of Alaska species distribution and abundance as well as increasing the scope of EFH research to address rapidly changing environmental conditions in the region.

CONTENTS

INTRODUCTION

The purpose of this project is to advance levels of essential fish habitat (EFH) information for federally managed groundfish species in the Gulf of Alaska (GOA) using species distribution models (SDMs). We are guided by the Alaska EFH Research Plan (Sigler et al. 2017) Research Priority #1 near-term objectives and by the Magnuson-Stevens Act (MSA) EFH requirements.

Alaska EFH Research Plan, Research Priority #1 of 5 – Characterize habitat utilization and productivity by using the best available science to accomplish—

Objective #1 – Develop EFH Level 1 information (distribution) for life stages and areas where missing, and

Objective #2 – Raise EFH level from 1 or 2 (habitat-related densities or abundance) to Level 3 (habitat-related growth, reproduction, or survival rates).

The Final Environmental Impact Statement for EFH Identification and Conservation in Alaska defines EFH as the area inhabited by 95% of a species' population (NMFS 2005)[3]. Our habitat-based modeling approach characterizes EFH for species' life stages as the spatial domain containing 95% of occupied habitat (where occupied habitat is defined as locations where predicted species encounter probability is greater than 5%). To meet the research priority and objectives described above, we applied 1) SDMs to predict the distribution and abundance of species life stages by incorporating new and updated data sources to develop SDM EFH Level 1 and 2 maps, and 2) used habitat-related vital rates to map EFH Level 3 information as an adjunct to the SDM EFH Level 1 and 2 maps.

[3] https://repository.library.noaa.gov/view/noaa/17391

Essential fish habitat is defined as those waters and substrate necessary to fish for spawning, breeding, feeding, or growth to maturity (50 CFR 600.10). EFH regulations require that the National Marine Fisheries Service (NMFS) and Fishery Management Councils (Councils) describe and identify EFH for managed species and minimize to the extent practicable the adverse effects of anthropogenic activities (e.g., fishing, mineral and oil extraction, coastal development). As part of this requirement, EFH text descriptions and maps (EFH component 1, descriptions and identification) are necessary for each life stage of species in an FMP (50 CFR 600.815(a)(1)) with an overarching consideration that the science related to this effort meets the standards of best available science (NMFS National Standard 2 – Scientific Information 50 CFR 600.315).

Councils and NMFS must also periodically review the EFH components of FMPs and revise or amend these components with new information at least every 5 years (50 CFR 600.815(a)(10)). In the 2017 EFH 5-year Review, habitat-based SDMs incorporating Level 1 and 2 EFH information were developed for 36 FMP species and their life stages in the GOA (Rooney et al. 2018). That project, along with related projects in the Aleutian Islands (AI) (Turner et al. 2017) and eastern Bering Sea (EBS) (Laman et al. 2017), replaced qualitative EFH Level 1 maps based on adult distributions (Fisheries Leadership and Sustainability Forum 2016; Simpson et al. 2017) with SDM-based estimates for individual life stages, substantially refining Alaska groundfish and crab EFH designation and, in many cases, producing EFH Level 2 information for the first time. The EFH descriptions and maps produced for the 2017 EFH 5-year Review were approved by the U.S. Secretary of Commerce as part of the EFH Omnibus Amendment package (83 FR 31340, July 5, 2018) to revise the FMPs[4].

In this EFH 5-year Review, we assessed the forecasting accuracy of the 2017 SDM approach for describing EFH[5] (e.g., Rooney et al. 2018, Laman et al. 2018), refined our modeling approach, and

[4] https://alaskafisheries.noaa.gov/portal/apps/webappviewer
[5] EFH component 1 descriptions and maps discussion paper and presentation prepared for the June 2020 SSC meeting are available at https://www.npfmc.org/efh-distribution/

updated the data sources. EFH in this present work is now represented as life stage-specific and spatially-explicit population percentiles predicted from an ensemble of best-performing constituent SDMs for 41 groundfish species across up to three life stages per species in the GOA and one octopus species. To achieve this, we expanded the SDM approach from the 2017 5-year EFH Review to include up to five constituent SDMs (three SDMs were assessed in 2017) in an ensemble and refined our methodology by using the lowest cross-validated root mean square error (RMSE) to identify the best-fitting models. We incorporated new sources of response data (e.g., nearshore survey data, Grüss et al. 2021 - AFSC Nearshore Fish Atlas updated in 2019), updated several independent predictor variables (e.g., survey-dependent bottom temperature observations), and enhanced existing data sets (both response and predictor variables) with recent survey results (summer bottom trawl surveys 1993–2019; e.g., von Szalay and Raring 2018). In addition, we extended EFH to include a critical ontogenetic habitat transition by separately accounting for and, when possible, modeling, settled early juvenile groundfish life stages. In general, SDMs were revised for species where maturity schedules or life stage definitions were recently updated (e.g., yellowfin sole and flathead sole; Tenbrink and Wilderbuer 2015).

METHODS

Study Area

The GOA study area for these modeling studies extends from Dixon Entrance (131°W longitude) in southeastern Alaska to Unimak Pass (165°W° longitude) at the western edge of the Alaska Peninsula (Fig. 1). The GOA coastline in this region forms an intricate complex of many bays and islands with diverse terrestrial and marine habitats (Johnson et al. 2012, Zimmermann 2019). The GOA continental shelf and upper continental slope encompass a mosaic of benthic habitats with extensive rocky substrate that has been uplifted due to tectonic activity and deposited by glacial retreat (Carlson et al. 1982, Zimmermann et al. 2019). Much of the continental shelf is dominated by soft unconsolidated sediments (Golden et al. 2016) and is narrow in southeastern Alaska and the western GOA, but is relatively broad in the central GOA with numerous glacial troughs (Carlson et al. 1982, Goldstein et al. 2020) and islands

throughout. The shelf break occurs at about 200 m throughout the GOA, and the shelf itself is deeply incised by numerous gullies and troughs. Oceanic currents in the GOA ecosystem are the Alaska Coastal Stream and Alaska Coastal Current which flow westward (counter-clockwise) around the GOA from Dixon Entrance to the Aleutian Island chain (Stabeno et al. 2004). These currents result in downwelling of surface water at the coast, while seasonal freshwater discharge results in a highly stratified system in the summer (Stabeno et al. 2004, 2016).

Dependent Variables: Fish and Invertebrate Data

Large-mesh summer bottom-trawl survey

The Alaska Fisheries Science Center's (AFSC) Resource Assessment and Conservation Engineering-Groundfish Assessment Program (RACE-GAP) conducts bottom trawl surveys of the GOA study area to describe the distribution and abundance of federally managed fish and invertebrate species in the region (Table 1). These regular, fishery-independent AFSC RACE-GAP summer bottom trawl surveys (1993–2001 triennial, 2003–2019 biennial) provide the primary source of groundfish data in the GOA. These surveys follow a stratified random design applied to a fixed survey grid (von Szalay and Raring 2018) constrained by the 1,000 m isobath between Dixon Entrance in the southeast and Unimak Pass to the west. Strata are based on six depth intervals (10–100 m, 101–200 m, 201–300 m, 301–500 m, 501–700 m, and 701–1,000 m) and established survey districts. Four recent surveys (2011, 2013, 2017, and 2019) out of the 13 survey years represented in this data set did not sample in the deepest stratum. Assignment of sampling effort within strata was determined using a Neyman optimal allocation sampling strategy (Cochran 1977), which considers the relative abundance and variance of commercially important groundfish species from previous surveys of the area as well as each species' ex-vessel price in the previous year.

The fishing gear used on the RACE-GAP GOA bottom trawl survey consists of the RACE-GAP Poly Nor'Eastern high-opening bottom trawl with a 27.2 m headrope, a 36.3 m footrope, and 24.2 m roller gear constructed with 36 cm rubber bobbins separated by 10 cm rubber disks (Stauffer 2004).

Under fishing conditions, the average net width is 16.0 m, and average height is 6.7 m based on acoustic net mensuration equipment mounted on the wing-tips and headrope of the trawl. Each trawl was certified as conforming to measurements and dimension standards prior to its use in the survey as stipulated in the National Trawling Standards (Stauffer 2004). All fishes and invertebrates captured by the trawl net were sorted either by species or into higher-level taxonomic groups and weighed. Non-colonial taxa were also counted, or estimates of total count were made.

During the period of these data collections, changes in taxonomic classifications have resulted in different effective time series for different species and these are reflected in the analyses presented here (see Table 1). For example, dusky and dark rockfishes were considered a single species prior to the 1996 survey, so only data since 1996 were used to model these two species separately. For species where length-based definitions of life stages were available, length ranges for settled early juveniles, subadults, and adults were used to partition the catch based on proportionality estimated from the random length subsample taken from each catch. These length-based definitions of ontogenetic life stages came from scientific literature, web resources (e.g., the Ichthyoplankton Information System; AFSC RACE[6]), or length data recorded in the updated Nearshore Fish Atlas and collected in beach seines, purse seines, and small-mesh bottom-trawls (as described in Grüss et al. 2021).

Small-mesh Bottom-trawl Survey

The Alaska Department of Fish and Game (ADFG) has conducted a series of fishery-independent small-mesh bottom trawl surveys (Jackson and Ruccio 2003, Spalinger 2020), which provided a new source of groundfish distribution and abundance data for the GOA. This summer survey targets shrimp, forage fishes, and commercially important groundfish species on the central and western GOA continental shelf, including areas inshore of the GOA RACE-GAP survey grid. The small-mesh survey uses a fixed-grid station design where stations are pre-selected randomly and deploys a high-opening box trawl

[6] https://access.afsc.noaa.gov/ichthyo/speciesdict.php

constructed with 3.2 cm mesh throughout and designed to sweep a 9.8 m path at a height of 4 m which is the ADFG, NMFS, and Department of Fisheries and Oceans of Canada standard for shrimp trawl research. Since 1973, either ADFG or NMFS have conducted this small-mesh bottom trawl survey annually in the GOA (Jackson and Ruccio 2003, Spalinger 2020). In 2015, funding was reduced, and a fishery-independent small-mesh survey was no longer possible. However, the survey was continued in bays around Kodiak Island to provide a baseline to monitor the shrimp population from 2016 to 2019. Additional funding was made available to continue the survey more broadly in 2020 and 2021.

In the present study, we used ADFG small-mesh bottom trawl survey data to parameterize SDMs of settled early juvenile life stages of groundfishes from survey years in the GOA spanning 1989–2019. Groundfishes collected on the survey were identified to species or genus level, and fish lengths were measured to the nearest millimeter. This small-mesh survey catches all demersal life stages of our target groundfish species, providing the opportunity to use length data from the small-mesh survey to contribute to defining limits for length-based life stage definitions. In addition, these data hold the potential for future SDM EFH mapping that accounts for habitat use of other groundfish life history stages in areas inshore of the GOA RACE-GAP survey grid.

Nearshore Mixed Gear Surveys

The AFSC's Auke Bay Laboratories (ABL) has historically curated their nearshore fish surveys in a centralized, relational database called the Nearshore Fish Atlas of Alaska[7] (NFAA). The NFAA database was developed in 2003 to consolidate the ABL's southeastern Alaska beach seine data dating back to 1998 when NOAA's EFH funds first became available. By 2012, the NFAA database was made available online and contained 19 years of fish catch data from more than 1,300 beach seine hauls made in shallow, nearshore waters (within 20 m of shore and shallower than 5 m) of southeastern Alaska, the

[7] NOAA Fisheries Nearshore Fish Atlas of Alaska database https://alaskafisheries.noaa.gov/mapping/sz/index.html?tab=fa

Aleutian Islands, Prince William Sound (PWS), Cook Inlet, Bristol Bay, and the Arctic region, making it the largest online repository of Alaska nearshore fish data (Johnson et al. 2012).

In 2020, the offline NFAA database was updated for the primary purpose of modeling and mapping EFH (e.g., Grüss et al. 2021). Although the NFAA started as a beach seine database, catch data from other gear types have been archived in the offline version for years. The 2020 expansion of the NFAA with contemporary survey data from multiple gear types, including beach seines, purse seines, bottom and midwater trawls, gillnets, jigs, fyke nets, and minnow traps, quintupled the number of data entries (to 85,827), with the majority of these entries in the GOA. The online NFAA database was updated in 2022[8].

In the present studies, we used survey data from the updated NFAA (1995-2019) to parameterize SDMs of settled early juvenile life stages of groundfishes in the GOA. We restricted data extracts to survey gear types of beach seine (3.2 cm mesh), purse seine (3.2 cm mesh), bottom trawl (various mesh sizes), and jigs. This wide variety of gear types represents several sampling designs in a variety of habitats inshore of the GOA RACE-GAP survey grid. The NFAA provides the opportunity to use length data collected by the inshore surveys to define lower limits for length-based life stage definitions of the settled early juvenile stage. The lower length limits of settled early juvenile stages from inshore surveys were compared to the maximum transformation lengths of the pelagic early juvenile stages sampled in the field prior to settlement (e.g., Doyle et al. 2019). Additional details about the NFAA are available with the online database and in Johnson et al. (2012) and Grüss et al. (2021).

Juvenile Sablefish Tagging Program

Beginning in 1985, juvenile sablefish have been sampled by jig, tagged, and released in a number of bays and inlets in southeast Alaska by ABL's Marine Ecology and Stock Assessment Program

[8] NOAA Fisheries Nearshore Fish Atlas of Alaska database https://alaskafisheries.noaa.gov/mapping/sz/index.html?tab=fa

(MESA) (Echave et al. 2013). Annual sampling in St. John Baptist Bay near Sitka on Baranof Island is used as an indicator of the potential strength of an upcoming cohort. Tagging efforts have expanded to several areas of the central GOA following reports of high catch rates in recent years (Goethel et al. 2020). The juvenile sablefish tagging program is included in the present study as an additional data source to parameterize SDMs for the sablefish settled early juvenile life stage, using capture locations throughout the GOA for years 1985–2020.

Independent Covariates: Habitat Data

The independent covariates used to parameterize SDMs (Table 2) were chosen based on their potential to influence the distribution and abundance of North Pacific groundfish and crab life stages in the ecosystems where these species have been sampled. To eliminate strongly collinear terms, variance inflation factors (VIF) were calculated (Table 3) using the methods of Zuur et al. (2009), and covariates with VIFs greater than or equal to 5.0 were eliminated (Sigler et al. 2015). These independent covariates (or predictor variables) represent dynamic or static habitat attributes observed on the bottom trawl surveys (Fig. 2) as well as modeled variables describing the marine environment in the study area (e.g., bottom current from Northeast Pacific 5 km resolution Regional Ocean Modeling System (NEP5 ROMS; Danielson et al. 2011). To apply these covariates to modeling species distribution and abundance, we balanced the consideration of spatial scale when describing influential habitat processes for several groundfish life stages with the need to map EFH on the differing scales appropriate for each of those ontogenetic phases. Habitat covariates mapped on a finer spatial scale (e.g., 100 m^2) may be more informative of the nursery habitat processes influencing the settled early juvenile life stages of many groundfish species, whereas a broader covariate scale (e.g., 1 km^2) is more appropriate for modeling more widely distributed subadult and adult life stages. For these reasons, we developed two sets of covariate rasters using different grid cell sizes (100 m^2 and 1 km^2) for SDMs of the settled early juvenile life stage and the subadult and adult life stages, respectively.

Independent habitat covariates from the time series (1993–2019) were interpolated on regular spatial grids of 100 m^2 for settled early juvenile life stages and 1 km^2 for subadult and adult life stages using natural neighbor interpolation (Sibson 1981), inverse distance weighting (Watson and Philip 1985), ordinary kriging (Venables and Ripley 2002) with an exponential semi-variogram, or empirical Bayesian kriging with a semi-variogram estimated using restricted maximum likelihood (REML; Diggle and Ribeiro 2002). Interpolation by inverse distance weighting and ordinary kriging was accomplished on the R computing platform[9] (R Core Development Team 2019), and Bayesian kriging was generated in ESRI ArcGIS mapping software[10]. All rasters were projected in the Alaska Albers Equal Area Conic (EAC) projection (standard parallels = 55° and 65°N and center longitude = 154°W).

To represent local conditions in the SDMs and to incorporate inter-annual variability in our EFH maps and descriptions, we utilized a mixture of observed, modeled, and derived predictors. For the RACE-GAP survey data, covariate raster values were extracted as averaged values along the towpaths at the bottom trawl stations. For other species data sources supporting the settled early juvenile stage models only, covariate raster values were extracted at point locations representing the geographic location of each sampling site. These extracted predictors were used in both cases to train and identify the best-fitting SDMs. When predicting species distribution and abundance, the complete raster of each retained covariate was used as input into the final models for a species and life stage. In the case of observed, dynamic predictor variables such as bottom temperature from the 13 RACE-GAP surveys conducted between 1993 and 2019, the rasterized multi-year averages of each grid cell were used to represent average conditions in the study area over time.

[9] R version 3.6.3 "Holding the Windsock"
[10] ESRI 2018, version 10.7

Bottom Depth and Temperature

Bottom depth and temperature were routinely collected during each haul, but different instruments were used to measure these values over the survey years (Buckley et al. 2009). From 1982 to 1992, depth and temperature were recorded using expendable bathythermographs (XBTs). In 1993, the XBTs were replaced by the Brancker XL200 digital bathythermographic data logger (Richard Brancker Research, Ltd., Kanata, Ontario, Canada) mounted on the headrope of the trawl net. With the advent of continuous recording devices, the survey began reporting on-bottom depth and temperature averaged over the tow duration. Starting in 2004, the Brancker data logger was replaced by the SeaBird SBE-39 microbathythermograph (Sea-Bird Electronics, Inc., Bellevue, WA). In 1993–1995, mean gear depth measured at the headrope was equated with bottom depth. Since 1996, mean gear depth has been added to mean net height measured during the on-bottom period of the trawl to estimate mean bottom depth.

We used two kinds of bathymetry data when formulating the SDMs modeling groundfish distribution and abundance in the GOA. When identifying the best-fitting constituent SDMs for the subadult and adult life stages, the bottom depth measured at each trawl station was used as a covariate predictor variable to train and test the SDMs. When predicting groundfish distribution and abundance for all life stages modeled, we used a bathymetry raster built from several compiled data sources (Zimmermann and Prescott 2014, 2015; Zimmermann et al. 2019). The primary sources for the bathymetry raster were depth soundings from digitized NOAA's National Ocean Service (NOS) smooth sheets from early hydrographic (Hawley 1931) and other surveys (hydrographic and non-hydrographic) that used manual soundings (e.g., lead lines), single-beam, or multi-beam acoustic echosounders. Details on the preparation and processing of the bathymetry datasets were documented in Zimmermann and Benson (2013) and Zimmermann et al. (2019). Occasional gaps in these bathymetric compilations were filled using bathymetry data modeled and attributed to the CGOA ROMS 3 km grid (e.g., Coyle et al. 2019). Point data from these combined datasets were interpolated to a 100 m^2 grid and to coarser

resolution by averaging 100 m^2 point data over 1 km^2 grid cells, using natural neighbor interpolation (Sibson 1981) in ArcMap.

Similar to how we used depth data, we used temperatures measured at each trawl station in the GOA (1993–2019) to train and identify the best-fitting SDMs and used a complete raster surface of those temperatures to predict groundfish distributions and abundances for subadult and adult life stages from the final ensembles. A bottom temperature raster was created by interpolating the observed temperatures at each trawl station over the study area and over the time series using empirical Bayesian kriging in ArcGIS (Diggle and Ribeiro 2002) with a semi-variogram estimated using restricted maximum likelihood (REML). The bottom temperature raster was interpolated over a 1 km^2 grid of the GOA study area.

The GOA ROMS with integrated nutrient-phytoplankton-zooplankton (NPZ) is a high-resolution hydrodynamic model that is run using two domains, including a 3 km^2 resolution grid of the CGOA (coastal Gulf of Alaska) and an 11 km^2 grid of the Northeast Pacific with 42 vertical layers, as described in Coyle et al. (2019). The CGOA ROMS 3 km grid extends from Haida Gwaii in British Columbia to the Shumagin Islands and from the coastline to 1,200 km offshore. Bottom temperature values (°C) from May-September 1999–2019, were extracted from the deepest (closest to the seafloor) vertical layer at each point of the CGOA ROMS 3 km grid and averaged to produce a gridded 100 m^2 (natural neighbor interpolation) climatology surface of mean modeled bottom temperature (Fig. 3). This surface was used in the analysis of the settled early juvenile life stage SDMs and provided bottom temperature estimates for areas inshore of the GOA RACE-GAP survey grid.

Water Movement

Three attributes of water movement were used as habitat covariates in modeling and prediction: maximum tidal speed, combined bottom current speed and direction, and combined bottom current speed and direction variability. We estimated maximum tidal speed at each survey station over a lunar year (369 consecutive days between 1 January 2009 and 4 January 2010) using a tidal inversion program parameterized for the GOA on a 1 km^2 grid (Egbert and Erofeeva 2002). This tidal prediction model was

used to produce a series of tidal currents for spring and neap cycles at every bottom trawl survey station. The maximum of the lunar annual series of predicted tidal current was then extracted at each bottom trawl survey haul location. A 1 km^2 raster surface of maximum tidal current speed was kriged over the GOA using an exponential semi-variogram and used as input to the SDMs and final ensembles. An interpolated maximum tidal current speed 100 m^2 raster was used as the covariate input when making spatial predictions in SDMs of the settled early juvenile stage.

A second water movement variable was the predicted bottom water layer current speed and direction from NEP5 ROMS model runs from 1969 to 2005 (Danielson et al. 2011). These long-term current projections are available as points on a 10 km^2 grid. The ROMS model was based on a three-dimensional grid with 60 depth tiers for each grid cell. For example, a point at 60 m water depth would have 60 depth bins at 1 m intervals, while a point at 120 m depth would have 60 depth bins at 2 m depth intervals, etc.). The bottom current speed and direction for the deepest depth bin at each point (closest to the seafloor) were used in our analyses. These regularly spaced projections were interpolated to a 100 m^2 raster grid covering the GOA using inverse distance weighting and then averaged over a 1 km^2 for our analyses.

Bottom current variability across summer months (May to September) was included as a third bottom current-related predictor in the SDMs. It was computed separately as the pooled standard deviation (*Pooled* SD_j) of the northing and easting components of bottom current at each NEP5 ROMS prediction locus through time such that:

$$Pooled\ SD_j = \sqrt{\frac{\sum_{i=1}^{k}\left[(n_i-1)*s_{ij}^2\right]}{\sum_{i=1}^{k}[n_i-1]}}\ ,$$

where j is the location of a prediction on the ROMS grid, n_i is the number of months in year i, s_{ij}^2 is the variance at location j in year i, and k is the total number of survey years (13 in the GOA). Bottom current variability can be considered a proxy for current stability near the bottom.

Geographic Location

Spatial modeling, such as the SDMs presented here, commonly includes a location variable to represent geographic location and account for spatial autocorrelation (Ciannelli et al. 2008, Politou et al. 2008, Boldt et al. 2012). To reduce the effects of spatial autocorrelation on the results, we chose to combine latitude and longitude into a smoothed bivariate geographic location term included as an independent predictor in SDM formulations. Rooper et al. (2020) demonstrated that this approach can reduce spatial autocorrelation in the modeled results. Geographic location was collected during each haul using a variety of positioning systems through time (e.g., manual charting, long-range navigation (LORAN-C), digital global positioning system [dGPS]). Since 2005, start and end locations for the vessel during the on-bottom portion of the trawl haul were collected from a dGPS receiver mounted on the vessel. We corrected vessel location to represent the location of the bottom trawl by triangulating how far the trawl net was behind the vessel (based on the seafloor depth and the length of wire out) and subtracting this distance from the vessel location. We assumed that the bottom trawl was directly behind the vessel during the tow and that all bottom trawl hauls were conducted in a straight line without a catenary from the beginning to the end point. The mid-point of the net's trawl path between the start and end locations was used as the location variable in the SDMs. EAC projected longitude and latitude data for each haul's latitude and longitude were projected and transformed into eastings and northings for modeling.

Seafloor Terrain

Several seafloor terrain metrics were derived from the bathymetry surface and describe attributes of seafloor morphology. The attributes included in the present study were slope, aspect, curvature, and bathymetric position index (BPI). Seafloor terrain metrics were derived at the original scale of the compiled bathymetry surface (100 m^2) using neighborhood-based analytical methods in ArcGIS 10.7 (ESRI) with the Benthic Terrain Modeler (Wright et al. 2012, Walbridge et al. 2018). All seafloor terrain

metrics were derived using a 3 × 3 neighborhood of grid cells, with the exception of BPI. Computation algorithms are provided by Walbridge et al. (2018).

Seafloor slope is the rate of change in bathymetry over a defined area. Slope is the first derivative of the bathymetry surface and was reported in degrees of incline (Horn 1981, Dolan and Lucieer 2014). Terrain slope may be a determinant of colonization since flatter areas support different substrata and communities than those found on steeper slopes (Pirtle et al. 2019).

Aspect measures the direction of the maximum gradient of slope and was expressed as angular compass direction, which is a circular variable (Horn 1981). Aspect was decomposed into sine (west-east or "eastness") and cosine (south-north or "northness") components to be used in the SDMs as continuous surfaces ranging from -1.0 to 1.0, where negative values indicate westness or southness and positive values indicate eastness or northness. Aspect eastness and northness were derived from the aspect surface. Terrain aspect is considered an indirect indicator of current velocity over and around seafloor terrain features (Mienis et al. 2007, Dolan et al. 2008).

Terrain curvature is the second derivative of the bathymetry surface and the first derivative of the slope (Zevenbergen and Thorne 1987, Schmidt et al. 2003). Curvature defines convex, concave, and linear slopes and can be used to identify seafloor features such as mounds and depressions that may be ecologically meaningful (Wilson et al. 2007). Curvature is also an indicator of how currents interact with the seafloor, either accelerating or decelerating parallel to the direction of slope and converging or diverging perpendicular to the direction of slope. We derived standard curvature as a single terrain surface, incorporating curvature in directions parallel and perpendicular to the slope (Zevenbergen and Thorne 1987, Schmidt et al. 2003). With this surface, positive values are convex slopes where currents may decelerate or diverge, negative values are concave slopes where currents may accelerate or converge, and values near zero are linear slopes where the rate and direction of flow are not expected to change.

Bathymetric position index (BPI) describes the elevation of one location relative to the mean of neighboring locations in an annulus-shaped neighborhood around a central cell or cells (Guisan et al. 1999, Weiss 2000). BPI emphasizes features shallower or deeper than the surrounding landscape area, such as ridges and valleys and places with abrupt changes in slope, such as the continental shelf break and the base of the continental slope. Broad-scale measures of BPI (> 1 km) have been useful in distinguishing between areas of trawlable and untrawlable seafloor encountered by the RACE-GAP bottom-trawl survey (Pirtle et al. 2015). BPI has been used as an SDM covariate describing groundfish habitat in the GOA (Pirtle et al. 2019) and other habitat analyses (Wilson et al. 2007, Howell et al. 2011). We derived BPI from GOA bathymetry using a 65-cell radius neighborhood with an inner radius of 3 cells. This is equivalent to a horizontal scale of 6.5 km, representing relatively broad-scale terrain features in our study area, such as banks, and glacial moraines and troughs (Pirtle et al. 2019, Goldstein et al. 2020). In the resulting surface, positive values are shallower than the surrounding area (e.g., ridges and crests), and negative values are deeper (e.g., channels and valleys).

Seafloor Substrate

A seafloor rockiness surface was developed for the GOA based on a compilation of rock features and sediment attributes to represent a continuous gradient from areas with high occurrence of rocky substrate to areas with low occurrence, using methods similar to Pirtle et al. (2019). The following datasets were included for the GOA region: 1) dbSEABED format sediment and substrate features (Golden et al. 2016); 2) sediment and substrate features from digitized smooth sheets (Zimmermann and Prescott 2014, 2015); 3) EBSSED-2 regional selection of samples collected from bottom grabs and cores (Richwine et al. 2018); 4) modeled untrawlable and trawlable seafloor locations based on a generalized linear model of multibeam acoustic backscatter and terrain metrics available as a 6 m^2 raster dataset (Pirtle et al 2015) that was re-gridded to 1 km^2 and exported as point locations (model predictions of untrawlable and trawlable locations are proxies for high and low occurrence of rocky substrate); 5) RACE-GAP bottom-trawl survey historic haul locations, including hauls that incurred gear damage from

seafloor contact to represent locations where untrawlable rocky features were likely encountered using the corrected start positions of the on-bottom portion of tows; and 6) RACE-GAP bottom-trawl survey grid, using centroid locations for grid cells with codes indicating presence of rocky substrate features (rocky, pinnacles, snags, ledges, bottom too hard) and non-rocky substrate features (sand waves). Compiled point location data from the six datasets were gridded using natural neighbor interpolation to produce raster surfaces of 100 m^2 and 1 km^2 resolution (ArcGIS 10.7, ESRI).

Biogenic Structure

Previous studies have indicated that structure-forming invertebrates (SFI) such as sponges, corals, and pennatulaceans (sea pens and sea whips) can form important structural habitat for North Pacific groundfishes (e.g., Rooper et al. 2010, Stone et al. 2011, Laman et al. 2015). SFIs can also indicate substratum type (Du Preez and Tunnicliffe 2011) because these sponges and corals attach to rocks and hard substrata, whereas sea pens and sea whips anchor into soft substrata. Therefore, we included the presence and absence of SFIs as binomial factors in the suite of habitat covariates. Presence-absence of SFIs in trawl catches was used to train and identify the best-fitting SDMs. Rasters of modeled SFI presence-absence (Rooper et al. 2014, 2016, 2017; Sigler et al. 2015) were used as covariate inputs into the final ensembles for predicting groundfish distribution and abundance.

Statistical Modeling

Our modeling strategy for this 5-year EFH Review has been to fit multiple habitat-based SDMs to groundfish abundances, skill test among SDMs using the root-mean-square-error to indicate model performance (RMSE; Hastie et al. 2009), and incorporate the best-performing models into an ensemble in R (R Core Team 2020). Ensemble models essentially average predictions across constituent models, making them more robust to overfitting and less sensitive to differences in predictive performance among constituents. Rooper et al. (2017) found that ensembles performed better than the generalized linear or generalized additive models alone when predicting distributions of structure-forming invertebrates.

Overall, the ensemble modeling approach provides a universal SDM application across multiple FMPs and can be easily expanded to consider additional constituent models in the future.

Previous EFH descriptions in Alaska (e.g., Laman et al. 2017) were based on habitat-based SDMs modeling species abundances from 4^{th}-root transformed catch-per-unit-effort (CPUE; $kg \cdot ha^{-1}$) using the area swept method (Wakabayashi et al. 1985) and assuming a Gaussian distribution. Modeling 4th-root transformed CPUE has several shortcomings with respect to our study objectives, including: 1) residuals were not informative due to the zero-inflation and over-dispersion that a Gaussian distribution cannot properly address 2) the *a priori* and *ad hoc* nature of deciding to use a 4^{th}-root transformation relative to other equally defensible transformations; 3) the inability to interpret the scale of the output, which is in units of 4^{th}-root CPUE and hence must be back-transformed to calculate a total predicted CPUE in any subarea; and 4) the scale-dependence of results, where the 4^{th}-root transformation implies that estimated density would change if the area swept in the survey changed (i.e., if sampling had occurred at a different scale). To improve on the challenges associated with using the 4^{th}-root transformed CPUE, we directly modeled numerical abundance with an area-swept offset to generate EFH descriptions that were less derived than those using a transformed CPUE approach; this more precisely represents survey effort.

For this EFH review cycle, we modeled numerical abundance using five different SDMs (Table 4; Fig. 4): a maximum entropy model (MaxEnt), a presence-absence gam (paGAM), a hurdle GAM (hGAM), and two forms of standard gam using the Poisson distribution (GAMP) and the negative binomial distribution (GAMnb). The MaxEnt and paGAM use presence or presence-absence data to estimate probabilities of occurrence (Phillips et al. 2006, Wood 2017). Using these models in conjunction with the complementary log-log (cloglog) link function allowed us to approximate abundance from the estimated probabilities (Fithian et al. 2015). Transforming these native model outputs (probability) into approximate numerical abundance yields predictions in the same units as the response variables from the other three SDMs, which facilitated skill testing and model comparison while meeting the requirements to qualify predictions as EFH Level 2, habitat-related density or abundance. Because some models (notably

MaxEnt) produce results on different scales, a scaling factor was calculated for each model by dividing the mean of the observed abundance by the mean of the model predictions. This ensures that predictions from all models are directly comparable and can be used to construct a weighted ensemble.

Maximum Entropy Models (MaxEnt)

Settled Early Juvenile Life Stage

Modeling the settled early juvenile life stage presented different challenges than those encountered when modeling later life stages. These smaller animals are not as readily retained in the standard RACE-GAP large mesh bottom trawl survey as larger animals, and they typically reside in inshore areas not sampled by the GOA RACE-GAP survey. To address these data gaps and so that we could model the distribution of this critical life stage, we incorporated fishery-independent surveys with a variety of sampling designs and gear types into our analyses, including the GOA RACE-GAP survey and surveys from areas inshore of the GOA RACE-GAP survey grid (e.g., Pirtle et al. 2019). These additional sources consisted of the ADFG small-mesh bottom trawl survey (Jackson and Ruccio 2003, Spalinger 2020), data from multiple surveys stored in the NFAA database (e.g., Grüss et al. 2021), and the AFSC MESA juvenile sablefish tagging program (Echave et al. 2013). However, integrating data from disparate surveys makes it difficult to separate catchability and fishing gear effects from actual differences in population abundance. To address these concerns, we modeled settled early juvenile life stages from presence-only data rather than use the ensemble approach used for subadults and adults modeled solely from the GOA RACE-GAP summer bottom trawl surveys.

As a method for combining multiple surveys with different designs and gear types (i.e., various bottom trawls, beach and purse seines, and jigs), we reduced all settled early juvenile stage observations to presence-absence only for inclusion in the MaxEnt model. MaxEnt treats data within a presence-only framework (Phillips et al. 2006), which has been useful to combine data obtained from multiple sampling designs and for data-limited species (Guisan et al. 2007, Elith et al. 2011). MaxEnt models have been previously applied to the settled early juvenile life stages of groundfish species in the GOA (Pirtle et al.

2019, Shotwell et al. 2022) and to juvenile and adult groundfish life stages in the GOA, EBS, and AI for the 2017 EFH 5-year Review (GOA-Rooney et al. 2018, EBS-Laman et al. 2017, AI-Turner et al. 2017). Here, we modeled the probability of suitable habitat with the *maxnet* package, which incorporates a newer MaxEnt algorithm and the cloglog link (Phillips et al. 2017). The GOA settled early juvenile MaxEnt models utilized the suite of covariates developed as 100 m^2 raster grids (Table 2) and omitted geographic location (lat/long) since MaxEnt cannot distinguish spatial variation in sampling probability from spatial variation in resource density (Elith et al. 2011). For GOA settled early juvenile EFH, we produce Level 1 (habitat-related distribution) maps as a first approximation of the distribution of these groundfish early life stages based on the predicted probability of suitable habitat. This approach advanced the level of settled early juvenile life stage EFH information from none to EFH Level 1 for 11 groundfish species in this EFH 5-year Review (Objective 1; Sigler et al. 2017).

MaxEnt automatically constructs and selects terms based on several feature classes that determine relationships between the species response data and covariates. The default feature set was used in this study, which includes linear, quadratic, and product interaction terms. By default, hinge features are included in models with more than 80 presence records and threshold features are not used. As part of the fitting process, a variety of these different features were tested in different combinations. MaxEnt uses a regularization multiplier to determine the penalty applied to larger models and to help regulate overall model complexity. For settled early juvenile stage MaxEnt models, we evaluated regularization multiplier values between 0.5 and 3.0 in intervals of 0.5. All evaluations were carried out using the 10-fold cross-validation methods described below (see subsection *Cross-Validation and Skill Testing*), with the exception that instead of using RMSE, we used AIC_c (Akaike 1974) to identify the best fit model:

$$AICc = \sum_{k=1}^{10} 2q_k - 2\, ln\, \widehat{L_k} + \frac{q_k^2+2q_k}{n_k-q_k-1} ,$$

where q_k is the number of non-zero coefficients in the model for cross-validation fold k, n_k is the number of data points where the species is present for cross-validation fold k, and $\widehat{L_k}$ is the likelihood for the

model in fold *k*. Since MaxEnt does not utilize a standard error distribution and thus does not provide a likelihood, the *aic.maxent* function from the *ENMeval* package (Muscarella et al. 2014) was used to provide an approximation of AIC_c.

To assess model fit for settled early juvenile MaxEnt models, we calculated the area under the receiver operator curve (AUC) as a measure of overall prediction skill. The AUC measures the ability of model predictions to accurately discriminate between two options, such as a species being present or absent. An AUC of near 0.50 indicates poor performance, whereas a score of 1.0 indicates perfect discrimination (Hosmer and Lemeshow 2005). We also presented the spatial variation in model predictions as the standard deviation among the 10 replicates. Because the MaxEnt predictions were in units of probability bounded between zero and one, the standard deviation is easily interpretable without further modification (Pirtle et al. 2019).

Subadult and Adult Life Stages

MaxEnt models of the subadult and adult life stages only use distribution and abundance data from the GOA RACE-GAP summer bottom trawl survey. The MaxEnt model implemented with *maxnet* (Phillips et al. 2017, R Core Team 2020) reformulates the model as an inhomogeneous Poisson process, which constructs the predicted probabilities as a proportion of the product of underlying relative abundance and sampling probabilities. Because of this, it was possible to estimate species abundance by treating the cloglog link output of the MaxEnt model as if it were the linear predictor in a Poisson model. The relative abundance estimate was then calculated by adding an additional parameter, the entropy, to the cloglog linear predictor and exponentiating the sum. In this case, for GOA subadult and adult EFH, we comprehensively produced Level 2 (habitat-related abundance) maps and advanced the level of EFH information available for several species in this EFH 5-year Review.

As with the settled early juvenile stage MaxEnt models above, the subadult and adult MaxEnt models utilized the same suite of covariates as the GAMs described below, but omitted geographic location (lat/long) from the suite of predictor variables since MaxEnt cannot distinguish spatial variation

in sampling probability from spatial variation in resource density (Elith et al. 2011). The MaxEnt algorithm automatically selected various feature classes, and we tested a range (0.5-3.0) of regularization multipliers with the best value determined by the lowest RMSE after 10-fold cross-validation as described below in the subsection *Cross-Validation and Skill Testing*.

Generalized Additive Models (GAM)

We used three classes of GAMs in this study: the paGAM (Wood 2017), the hGAM (Cragg 1971, Barry and Welsh 2002, Potts and Elith 2006), and the standard GAM with a Poisson distribution (GAM_P; Hastie and Tibshirani 1990) and with the negative-binomial distribution (GAM_{nb}; Zuur et al. 2009). All GAMs were fit using the *mgcv* package (Wood 2011) in R. The paGAM uses the binomial distribution and the cloglog link function, allowing numerical abundance to be approximated from model-predicted encounter probabilities (Fithian et al. 2015). The hGAM models presence-absence and abundance in two stages and accounts for zero-inflation commonly seen in field-collected data (McCullagh and Nelder 1989). In the first stage of the hGAM, the probability of occurrence was predicted from presence-absence data using a paGAM and binomial distribution. In the second stage of the hGAM, a standard GAM was constructed for the positive catches using a "zero-adjusted" (Zuur et al. 2009) Poisson distribution. Finally, an abundance estimate was obtained by multiplying the predicted probability of presence from step one with the abundance estimate from step two (Manel et al. 2001, Barry and Welsh 2002, Wilson et al. 2005). The GAM_P estimates abundance directly using the Poisson distribution and a log link. The GAMnb was structurally similar to the GAMP but used a negative binomial distribution with a log link, allowing the GAMnb to account for overdispersion in the data (McCullagh and Nelder 1989).

For all GAMs, we used iterative backward stepwise term elimination to remove covariate predictors based on minimizing the model-dependent generalized cross-validation (GCV) or unbiased risk estimator (UBRE) scores, thereby identifying the best-fitting model formulations (Weinberg and Kotwicki 2008; Zuur et al. 2009). Since the Poisson and negative binomial GAMs were structurally very

similar models, we used RMSE-base skill testing to identify the best-performing model (lowest RMSE) of this pair and keep it in the ensemble.

All GAMs in this study used a variety of two-dimensional smoothing terms, one-dimensional smoothing terms, and categorical variables to fit the data. To avoid overfitting in the GAMs, the basis degrees of freedom used in the smoothing function for each habitat covariate were constrained following the methods of Weinberg and Kotwicki (2008). However, attempting to extrapolate model predictions into areas with few data points required additional consideration. In particular, the default smoother when fitting GAMs, a "thin-plate spline," sometimes produced exaggerated predictions in areas of sparse data (Wood 2003). To counter this behavior in one-dimensional smooth terms, we used a smoothing penalty based on the first derivative (as opposed to the default second derivative), which tended to push the effect curve towards zero where data were unavailable. For two-dimensional smooth terms, the same method was applied, but "Duchon" splines were used instead of thin-plate or cubic splines (Duchon 1977), which did a better job of penalizing the smooth function in areas with sparse data. Finally, if a GAM based on thin-plate splines failed, a second version using cubic splines in the one-dimensional smooth terms was attempted. If both versions failed to converge or produced unreasonable results, that particular GAM was excluded from the final ensemble.

Cross-Validation and Skill Testing

Species distribution models were subjected to *k*-fold cross-validation to estimate RMSE and assess accuracy and uncertainty. We computed the error at each cross-validation fold (k) by fitting an SDM to a randomly selected "in-bag" partition containing 90% of the observed abundance at trawl stations (i), predicting abundance at the remaining "out-of-bag" partition containing the other 10% of trawl stations, and comparing the predicted (y) and observed (x) values for the testing subset. The *k*-fold cross-validation was repeated 10 times until every point in the data set had been tested and the RMSE from the accumulated out-of-bag sample was calculated as:

$$RMSE = \sqrt{\frac{\sum_{k=1}^{10}\sum_{i=1}^{n_k}(y_{ki}-x_{ki})^2}{\sum_{k=1}^{10} n_k}} \ ,$$

where y_{ki} is the predicted numerical abundance in cross-validation fold k, x_{ki} is the observed numerical abundance at trawl station i in cross-validation fold k, and n_k is the number of stations sampled in the kth fold. This process provides a test of prediction skill at unsampled locations within the cross-validation, and provides a performance measure used to compare models. We used the RMSE to assess the ability of a model to accurately predict the abundance at a series of locations (Hastie et al. 2009). The cross-validation also allows for a consistent method of calculating the variance in model predictions by computing it at each location across folds.

Skill testing was used to eliminate constituent SDMs from the ensemble by identifying and dropping low-performing models with high RMSEs. Constituent SDMs retained in the ensemble were weighted by the inverse squared RMSE following the formula,

$$w_i = \frac{RMSE_i^{-2}}{\sum_{i=1}^{m} RMSE_i^{-2}} \ ,$$

where w_i is the weight for model i, $RMSE_i$ is the cross-validated RMSE for model i, and m is the number of constituent models. The inclusion of poor performing models may degrade ensemble performance if any constituent SDM received less than a 10% relative weight, it was eliminated from the ensemble, and the weights of the remaining SDMs were recalculated.

The ensemble can extrapolate abundance predictions into areas of sparse data and into areas that have rarely or never been sampled. Under these conditions, SDMs that fit the majority of the data quite well can still produce unacceptable predictions in these areas. The unacceptable predictions usually take the form of unrealistically high abundance. To address this challenge, a criterion was implemented so that any SDM generating abundance predictions > 10 times the highest observed survey abundance was excluded from the ensemble. The resulting cumulative ensemble-predicted numerical abundance, based

on the combined effects of all retained constituent SDMs, was translated into a map of the complete EFH area for each species.

Ensemble Models and Uncertainty

Ensemble modeling is a robust method to predict species distributions and abundances (Aruajo and New 2007). Potential advantages include better estimates of uncertainty, reduced bias, and results that are less sensitive to minor changes in the underlying data (e.g., accumulating data through annual surveys; Stewart and Hicks 2018). In the present study, we combined the best-fit constituent SDMs into single species life stage-specific ensemble predictions of habitat-related abundance to inform descriptions of EFH. In practice, this means we first identified the best-performing MaxEnt, paGAM, hGAM, and GAM SDMs. In the MaxEnt models, this entailed testing a range of regularization multipliers, while in the GAMs this involved backward stepwise term elimination. For the standard GAM, the Poisson and negative binomial error distributions were modeled separately, and skill testing using the RMSE was employed to select the distribution that best characterized the data. The set of best SDMs from each category was then weighted by the inverse of its cross-validated RMSE and constituent SDM weights were normalized to sum to one. Predictions from the ensemble were made by multiplying each constituent prediction by its weight and summing the weighted predictions across SDMs. The result of this exercise was a final ensemble for each species' life stage that predicts habitat-related abundance.

The variance of the ensemble prediction can be obtained based on a weighted combination of the variance in the predictions of each constituent model. For each constituent, 10 abundance prediction rasters were made using the 10 models fit during cross-validation. The variance across these 10 folds at each location was then calculated to provide a variance estimate for that constituent model. After repeating this process for all constituent models in the ensemble, we adapted the following equation from Burnham and Anderson (2002), substituting our RMSE-derived weights for their AIC weights:

$$SD_j(ensemble) = \sum_{i=1}^{m} w_i \times \sqrt{var_{ij} + \left(y_j^* - y_{ij}\right)^2} \ ,$$

where SD_j is the standard deviation of the ensemble at location j, w_i is the weight for model i, m is the number of constituent models, var_{ij} is the variance for model i at location j, y_j^* is the ensemble abundance prediction at location j, and y_{ij} is the abundance prediction for model i at location j. Then we computed the coefficient of variation (CV) from the *SD (ensemble)* as:

$$CV_j = \frac{SD_j}{y_j^* + c} \ ,$$

where CV_j is the coefficient of variation at location j, SD_j is the ensemble standard deviation at location j, and y^*_j is the ensemble prediction at location j. Because the term y^*_j in the denominator can sometimes be zero, a small constant c, which was set at 1% of the max predicted abundance for that species and life stage, must be added to all abundance estimates when calculating the CV.

Species Distribution Model Performance Metrics

In addition to the RMSE described above for skill testing among SDMs and constituent model weighting in the ensemble, we computed three commonly used metrics of SDM performance for constituent models and the ensembles. The three fit metrics we reported were the Spearman's rank correlation coefficient (ρ), the area under the receiver-operator-characteristics curve (AUC; Hosmer and Lemeshow 2005), and the percent deviance explained based on the Poisson distribution (PDE). Each fit metric measures a different aspect of model performance and has distinct strengths and weaknesses. A model that scores poorly on one metric may still be useful once the others are considered, and all models should be assessed with reference to the underlying biology of the species being studied.

The ρ compares predicted densities with observations for each sample, computing their rank correlation and measuring how well a model accurately distinguished between high and low-density areas (Best and Roberts 1975, Zar 1984). We employ ρ instead of the more familiar Pearson correlation because the ρ is more appropriate to count data that do not follow a normal distribution (Legendre and Legendre 2012). Additionally, the EFH maps produced in this project are based on ranked percentiles of abundance, and ρ may provide some insight into the EFH maps' accuracy. While there is no objective standard for

what constitutes a "good enough" correlation, for this project, we will adopt the framework that less than 0.2 represents "poor" predictive performance, between 0.2 and 0.4 is "fair," between 0.4 and 0.6 is "good," and greater than 0.6 is "excellent." Our framework is based on our knowledge of the ecology of the species being modeled and the available data. Because ρ is the rank correlation, a high value is easiest to obtain when there is a large difference between the lowest and highest abundances, so small prediction errors do not affect the rankings. Conversely, a low value can result if the observed densities occupy a narrow range and a small prediction error will change the rankings.

The AUC is a measure of the ability of a model to discriminate between binary outcomes, such as presence and absence. The value of the curve at any point represents the ratio of true positives to false positives at that point, and the total area under the curve represents the overall performance across the entire range of values. The AUC has a minimum value of 0.5 (i.e., random 50/50 chance) and a maximum of 1, and values under 0.7 are generally considered poor, values between 0.7 and 0.9 are average to good, and values greater than 0.9 suggest excellent discrimination ability (Hosmer and Lemeshow 2005). The AUC provides a measure of discrimination ability standardized across the range of probability predictions, which makes it useful as a summary of discrimination ability. In this case, discriminating where the RACE-GAP bottom trawl survey catches individuals and where it does not. However, it can sometimes be misleading when an overwhelming majority of observations are either present or absent, and only a small portion of the probability space has been adequately sampled.

The PDE provides a generalization of "variance explained" for the constituent SDMs as well as the ensemble. We assume the Poisson distribution when computing the deviance explained for these models because count data are not normally distributed and traditional estimates of the variance explained tend to be misleading. Additionally, with the Poisson distribution, as with other distributions the size of errors is expected to change with the mean of the predictions. Therefore, it is common to compute the deviance explained by a model. This value is a measure of the percent reduction in the residual deviance of a model compared to a naïve null model, which contains only an intercept and no predictor terms.

Because we employ a variety of models that utilize different distributions (binomial, Poisson, negative binomial), and different underlying data types (presence-absence, count), we estimate the deviance explained in comparison to a fixed null Poisson model. Therefore, the PDE represents the percent deviance explained in relation to a null Poisson model, which allows for a fairer comparison of the different models. In this case, we adopt a similar metric to the correlation, where less than 0.2 indicates "poor" performance, between 0.2 and 0.4 "fair" performance, between 0.4 and 0.6 "good" performance, and greater than 0.6 is "excellent" performance. A high PDE can result when model predictions are accurate or when the observed data are highly variable, and the model represents a significant improvement over a simple null model. Similarly, a low value can sometimes occur even when predictions are accurate if there is no improvement over the null model, indicating that a simpler method would probably be acceptable. Deviance is calculated as,

$$D = 2\sum_{i=1}^{n}\left[x_i ln\left(\frac{x_i}{exp(y_i)}\right) - \left(x_i - exp(y_i)\right)\right],$$

$$D_0 = 2\sum_{i=1}^{n}\left[x_i ln\left(\frac{x_i}{exp(\bar{x})}\right) - \left(x_i - exp(\bar{x})\right)\right], \text{ and}$$

$$PDE = \frac{D}{D_0},$$

where D represents the deviance of a given model, D_0 is the deviance of the null model, x_i represents the observed abundance for data point i, $\bar{x}$ represents the mean of observed abundance, and y_i represents the predicted abundance for data point i (Pardoe 2012).

Species Distribution Model Performance Metric Rubric:

ρ: < 0.20 (poor), 0.21–0.40 (fair), 0.41–0.60 (good), 0.61–0.99 (excellent)

AUC: < 0.70 (poor), 0.71–0.90 (good), 0.90–0.99 (excellent)

PDE: < 0.20 (poor), 0.21–0.40 (fair), 0.41–0.60 (good), 0.61–0.99 (excellent)

Essential Fish Habitat (EFH) Maps

Encounter Probability

Encounter rates were derived from model predictions and used to eliminate locations with low encounter probabilities from inclusion in the EFH area. For settled early juvenile MaxEnt SDMs, the cloglog probability of suitable habitat was used in place of encounter probability. In ensembles for subadult and adult life stages, we assumed that the abundance predictions approximately followed a Poisson distribution. Under this assumption, the probability of encounter was equal to one minus the likelihood of zero abundance, given the predicted abundance at that location.

Mapping EFH from SDMs

New Level 1 EFH maps, based on habitat-related species distribution for the settled early juvenile life stage in the GOA, met an Alaska EFH Research Plan objective for this EFH 5-year Review (i.e., Objective 1: Develop EFH Level 1 information (distribution) for life stages and areas where missing; Sigler et al. 2017). For subadults and adults, maps of species' habitat-related abundance predicted from the ensembles were used to describe and map new EFH Level 2 information for this EFH 5-year Review.

Occupied habitat was defined as all locations where a species' life stage had a probability of suitable habitat (settled early juveniles) or encounter probability (subadults and adults) greater than 5%. Four areas containing 95%, 75%, 50%, and 25% of the occupied habitat were identified, where habitat is defined as areas exceeding a threshold of 5% predicted species encounter probability. The definition of EFH area in Alaska is the area containing 95% of the occupied habitat (NMFS 2005). Each of the lower quantiles (hereafter referred to as subareas) describes a more focused partition of the total EFH area. The area containing 75% of the occupied habitat based on SDM predictions is referred to as the "principal EFH area." For the fishing effects analysis of the 2017 EFH 5-year Review (EFH component 2; Simpson et al. 2017), the area containing 50% of the occupied habitat is termed the "core EFH area," and we have applied this terminology to our results. The areas containing the top 25% of the occupied area are referred to as "EFH hot spots." Mapping habitat percentiles for EFH subareas like these helps demonstrate the

heterogeneity of species distributions over available habitat within the larger area identified as EFH and aligns our results with those of other EFH-related projects.

Species Complexes

Some groundfishes in Alaska are managed as members of stock complexes (e.g., the Other Rockfish Stock Complex in the Gulf of Alaska). While EFH must be designated for each managed species, EFH may be designated for assemblages of species with justification or scientific rationale provided (50 CFR 600.815(a)(1)(iv)(E)). In the present study, and for the first time in an EFH 5-year Review, we presented EFH descriptions of multi-species stock complexes using aggregated single species SDMs to produce descriptions of EFH to serve as proxies for individual species in the stock complex where an SDM EFH map was not possible due to data limitations (i.e., < 50 catches over the study period). To achieve this, we first generated multi-species abundance maps by summing the predicted abundances at each raster cell for each species in the complex that supported an ensemble. Then, using the same method described above for single species maps, we constructed an EFH map for the stock complex. In complexes where there was a mixture of available life history information (e.g., some species with known length-based life stage definitions and some without), life stages were combined for the species mapped together from the complex. See the introductory section of each species complex chapter (see section *Results*) for details about the species and life stages that were included.

EFH Level 3 Habitat-related Vital Rates

We advanced EFH information to Level 3 (habitat-related vital rates) in the GOA for a set of groundfish species' settled early juvenile life stages to achieve a key Alaska EFH Research Plan objective for this EFH 5-year Review (Objective 2; Raise EFH level from 1 (distribution) or 2 (habitat-related densities or abundance) to Level 3 (habitat-related growth, reproduction, or survival rates); Sigler et al. 2017). This was done by integrating temperature-dependent vital rates developed from field and laboratory studies with SDM predictions of the probability of suitable habitat. Temperature-dependent vital rates have been published or are in development for groundfish species in Alaska (Table 5). A

representative example that can be applied in this context is from Laurel et al. (2016), who described the temperature-dependent growth rate of early juvenile walleye pollock as:

$$GR = y_0 + a * T + b * T^2 - c * T^3,$$

$$GR = 0.2023 + 0.0092 * T + 0.0335 * T^2 - 0.0019 * T^3 \ ,$$

where *GR* is the growth rate expressed as the % change in body weight per day (% body weight per day), *T* is temperature in degrees Celsius, and y_0, a, b, and c are estimated parameters. Species-specific vital rate formulations are detailed in each Results chapter where EFH Level 3 information was generated.

We constructed the EFH Level 3 maps by first mapping the temperature-dependent vital rates across the survey study area, using the CGOA ROMS 3 km bottom temperature covariate raster as the temperature value in the rate equations. Next, we computed the product of the rate map and the SDM-predicted probability of habitat map by multiplying the two rasters. The product map was then transformed onto a relative scale ranging from zero to one, where zero indicates areas of low probability of suitable habitat and low habitat-related temperature-dependent growth potential, and one indicates areas of high probability of suitable habitat and high habitat-related temperature-dependent growth potential. The Level 3 maps provide additional context when interpreting EFH Level 1 or Level 2 maps developed from the same SDMs.

Table 1. -- North Pacific groundfish and crab species from AFSC RACE GAP summer bottom trawl surveys (and summer surveys of mixed gear types for the settled early juvenile stage) modeled to describe essential fish habitat in the Gulf of Alaska. The years modeled were determined by taxonomic validity, life stage length ranges are in fork lengths (FL) in mm with sources indicated ("--" indicates no length known from literature); "All" RACE GAP years modeled = 1993–2019, and for example, "1996–" indicates RACE GAP 1996 to present (2019). "All EJ" years modeled = 1989–2019 (except sablefish, 1985–2020).

Common Names	**Years Modeled**	**Life Stage**	**Length Ranges (FL)**		**Source**
flatfishes		early juvenile	subadult	adult	
Alaska plaice	All	35–140	141–319	> 319	NFAA[1], Doyle et al. 2019, Tenbrink and Wilderbuer 2015
arrowtooth flounder	All EJ; 1993–	35–160	161–480	> 480	NFAA, Debenham et al. 2019, Doyle et al. 2018, 2019, Stark 2012b
butter sole	All	--	--	--	
Dover sole	All	30–140	141–439	> 380	NFAA, Doyle et al. 2019, Abookire and Macewicz 2003
English sole	All EJ; All	20–140	141–250	> 250	NFAA, Sampson and Al-Jufaily 1998
flathead sole	All EJ; All	20–140	141–333	> 333	NFAA, Doyle et al. 2019, Stark 2004
northern rock sole	All EJ; 1996–	20–140	141–328	> 328	NFAA, Doyle et al. 2019, Stark 2012a
Pacific sanddab	All	--	--	--	
Petrale sole	All	--	10–331	> 331	Parker and Fruth 2002
rex sole	All EJ; All	60–140	141–352	> 352	Doyle et al. 2019, Abookire 2006
slender sole	All	--	--	--	
southern rock sole	All EJ; 1996–	--	20–347	> 347	Doyle et al. 2019, Stark and Somerton 2002
starry flounder	All EJ; All	20–150	151–369	> 369	NFAA, Orcutt 1950
yellowfin sole	All EJ; All	30–140	141–296	> 296	NFAA, Doyle et al. 2019, Yeung and Cooper 2020, Tenbrink and Wilderbuer 2015
roundfishes					
Atka mackerel	All	--	49–344	> 344	McDermott and Lowe 1997
Pacific cod	All EJ; All	40–150	151–503	> 503	NFAA, Doyle et al. 2019, Laurel et al. 2009, Stark 2007
sablefish	1985–; All	150–399	400–585	> 585	Sasaki 1985, Hanselman pers. comm.
walleye pollock	All EJ; All	40–140	141–381	> 381	NFAA, Doyle et al. 2019, Pirtle et al. 2019, Stahl and Kruse 2008 (L_{50})
rockfishes					

Common Names	Years Modeled	Life Stage	Length Ranges (FL)		Source
flatfishes		early juvenile	subadult	adult	
blackspotted rockfish	2006–	--	25–453	> 453	IIS[2], Moser 1996, Conrath 2017
dusky rockfish	1996–	--	25–365	> 365	Chilton 2010
greenstriped rockfish	All	--	25–220	> 220	Love et al. 2002
harlequin rockfish	All	--	25–188	> 230	Tenbrink and Helser 2021
northern rockfish	All	--	25–310	> 310	IIS, Moser 1996, Chilton 2007
Pacific ocean perch	All EJ; All	25–200	201–250	> 250	IIS, Moser 1996, Pirtle et al. 2019, Rooper 2008, Rooper pers. comm.
pygmy rockfish	All	--	--	--	
quillback rockfish	All	--	25–290	> 290	IIS, Moser 1996, Rooper 2008
redbanded rockfish	All	--	25–420	> 420	IIS, Moser 1996, Love et al. 2002
redstripe rockfish	All	--	25–290	> 290	IIS, Moser 1996, Rooper 2008
rosethorn rockfish	All	--	25–215	> 215	IIS, Moser 1996, Rooper 2008
rougheye rockfish	2006–	--	25–450	> 450	IIS, Moser 1996, Conrath 2017
sharpchin rockfish	All	--	25–265	> 265	IIS, Moser 1996, Malecha et al. 2007, Tribuzio and Echave 2019
shortraker rockfish	All	--	25–499	> 499	IIS, Moser 1996, Conrath 2017
shortspine thornyhead	All	--	20–215	> 215	IIS, Pearson and Gunderson 2003
silvergray rockfish	All	--	25–405	> 405	IIS, Moser 1996, Rooper 2008
yelloweye rockfish	All	--	25–450	> 450	IIS, Moser 1996, O'Connell and Funk 1987
sharks and skates					
spiny dogfish	All	--	200–973	> 973	Stehlik 2007, Tribuzio et al. 2010
Alaska skate	1999–	--	<= 930	> 930	Matta and Gunderson 2007
Aleutian skate	1999–	--	<= 1320	> 1320	Ebert et al. 2007
Bering skate	1999–	--	<= 690	> 690	Ainsley et al. 2011
big skate	All	--	<= 1486	> 1486	Ebert et al. 2008
longnose skate	All	--	<= 1131	> 1131	Ebert et al. 2008
invertebrates					
giant octopus	All	--	--	--	--

[1] NFAA = Updated Nearshore Fish Atlas of Alaska, NMFS Auke Bay Laboratories, Juneau, AK: https://alaskafisheries.noaa.gov/mapping/sz/index.html?tab=fa
[2] IIS = Ichthyoplankton Information System, Alaska Fisheries Science Center, Resource Assessment and Conservation Engineering: https://access.afsc.noaa.gov/ichthyo/speciesdict.php

Table 2. -- Covariates used in habitat-based species distribution models (SDM) to fit (identify best-fitting formulation) and then predict distributions and abundances from the final ensembles or final model (settled early juvenile stage) of North Pacific groundfish species in the GOA to describe essential fish habitat (EFH). Covariates applied to SDMs of distribution or abundance in the GOA are indicated by life stage (settled early juvenile = EJ; subadult = SA; and adult = A).

Covariate	Unit	Description of Prediction Raster	Interpolation Method	SDM Life Stages
Bottom temperature (observed)	°C	Mean bottom temperatures measured on bottom trawls during AFSC RACE-GAP summer trawl surveys (1982–2019).	Empirical Bayesian kriging	SA, A
Bottom temperature (modeled)	°C	Bottom temperature (deepest depth bin) predicted from the CGOA ROMS 3 km grid (Coyle et al. 2019) from May-September and averaged (1999–2019).	Natural neighbor	EJ
Bottom current Northing and Easting	--	Seafloor ocean current speed and direction components predicted from the NEP5 ROMS (Danielson et al. 2011) averaged for the bottom layer across summer years (1969–2005).	Inverse distance weighting	SA, A
Bottom current Northing and Easting variability	--	Pooled standard deviation of seafloor ocean current speed and direction components predicted from the NEP5 ROMS (Danielson et al. 2011) averaged for the bottom layer across summer years (1969–2005).	Inverse distance weighting	SA, A
Maximum tidal current	$cm \cdot sec^{-1}$	Predicted tidal current maximum at each bottom trawl location over a lunar year cycle (Egbert and Erofeeva 2002).	Ordinary kriging	EJ, SA, A
Geographic Location	Latitude, Longitude	Midpoint of bottom trawl hauls corrected for location of the trawl net relative to the vessel in Alaska Albers Equal Area conic projection.	--	SA, A
Bottom Depth	meters (m)	Bathymetry of the seafloor based on acoustic seafloor mapping data and digitized, location corrected NOS charts.	Natural neighbor	EJ, SA, A
Slope	degrees	Maximum gradient in depth between adjacent cells, derived from bathymetry (Horn 1981) applied with Benthic Terrain Modeler in ArcGIS (Walbridge et al. 2018).	--	EJ, SA, A

Covariate	Unit	Description of Prediction Raster	Interpolation Method	SDM Life Stages
Aspect Eastness and Northness	--	Describes concavity/convexity as well as sloping nature, derived from bathymetry (Horn 1981) applied in ArcGIS (Walbridge et al. 2018)	--	EJ, SA, A
Curvature	--	Combined plan and profile curvature to return "standard" curvature; derived from bathymetry (Schmidt et al. 2003) applied in ArcGIS (Walbridge et al. 2018).	--	EJ, SA, A
Bathymetric Position Index	--	Relative difference of elevation between neighboring locations, illustrates bathymetric highs and lows across the landscape, derived from bathymetry (Guisan et al. 1999) applied in ArcGIS (Walbridge et al. 2018).	--	EJ, SA, A
Rockiness	--	Continuous surface of compiled datasets representing locations of rocky and not rocky substrate (updated for this study from Pirtle et al. 2019).	Natural neighbor	EJ, SA, A
Coral presence or absence	probability	Coral presence-absence in bottom trawl catches / model-predicted coral presence-absence (Rooper et al. 2014, Sigler et al. 2015).	--	EJ, SA, A
Sponge presence or absence	probability	Sponge presence-absence in bottom trawl catches / model-predicted sponge presence-absence (Rooper et al. 2014, Sigler et al. 2015).	--	EJ, SA, A
Pennatulacean presence-absence	probability	Pennatulacean presence-absence in bottom trawl catches / model-predicted penn. presence-absence (Rooper et al. 2014, Sigler et al. 2015).	--	EJ, SA, A

Table 3. -- Variance inflation factors (VIF) of covariates used as predictors in species distribution models (SDM) for federally managed groundfishes and invertebrates in the Gulf of Alaska; SD = pooled standard deviation.

Covariate	**VIF**
*Longitude	2.25
*Latitude	2.25
Bottom depth	1.80
Slope	1.31
Aspect Eastness	1.04
Aspect Northness	1.09
Curvature	1.14
Bottom temperature	1.74
*Bottom Current Eastings	1.22
*Bottom Current Northings	1.22
*SD bottom current Eastings	1.65
*SD bottom current Northings	1.68
Tidal maximum current	1.31
Rockiness	1.21
Bathymetric position index	1.21
Sponge presence-absence	1.00
Coral presence-absence	1.02
Pennatulacean presence-absence	1.01

*represent components of covariates that form bivariate smoothed interaction terms in the generalized additive models (Longitude & Latitude = “geographic location”, Eastings & Northings = “bottom current”, SD Eastings & SD Northings = “bottom current SD”).

Table 4. -- Species distribution models (SDMs) trained and skill tested for inclusion in an ensemble; the Maximum Entropy model (MaxEnt) uses the *maxnet*[a] package and the generalized additive models (GAMs) use the *mgcv*[b] package.

Species Distribution Model (SDM)	**Family**	**Link**	**Documentation**
Maximum Entropy (MaxEnt)	*	cloglog approx.	Phillips et al. (2017)
Generalized Additive Models (GAM)			
presence-absence GAM (paGAM)	binomial	log	Woods (2011)
hurdle GAM (hGAM)	zero-adjusted Poisson	cloglog & log	Zuur et al. (2009), Woods (2011)
standard GAM (GAM_P)	Poisson	log	Woods (2011)
negative-binomial GAM (GAM_{nb})	negative-binomial	log	Woods (2011)

* - the distribution applied to the MaxEnt model is a heavily modified Poisson distribution representing an inhomogeneous Poisson process

a - R v3.6.1; Fitting 'MaxEnt' species distribution models with 'glmnet'; *maxnet*: R package version 0.1.2.

b - R v3.6.1; Fast stable restricted maximum likelihood and marginal likelihood estimation of semiparametric generalized linear models; *mgcv*: R package version 1.8-29

Table 5. -- Groundfish species in the Gulf of Alaska and life stages for which vital rates are available from the literature or ongoing studies; combining these vital rates with EFH will advance EFH information to Level 3. Settled early juvenile = EJ.

Species	**Life Stage**	**Region**	**Vital Rate**
walleye pollock	age-0, EJ	AI [a, b], GOA [a, b]	growth [a], lipid accumulation (condition) [b]
Pacific cod	age-0, EJ	EBS [a, b], GOA [a, b]	growth [a], lipid accumulation (condition) [b]
sablefish	EJ	GOA	growth [c]
yellowfin sole	EJ	GOA	growth [d]
northern rock sole	EJ	GOA	growth [d]
Pacific ocean perch	EJ	GOA	growth [e]

[a] Laurel et al. 2016, [b] Copeman et al. 2017, [c] Krieger et al. 2019, [d] Hurst *in preparation*, and [e] Rooper et al. 2012.

FIGURES

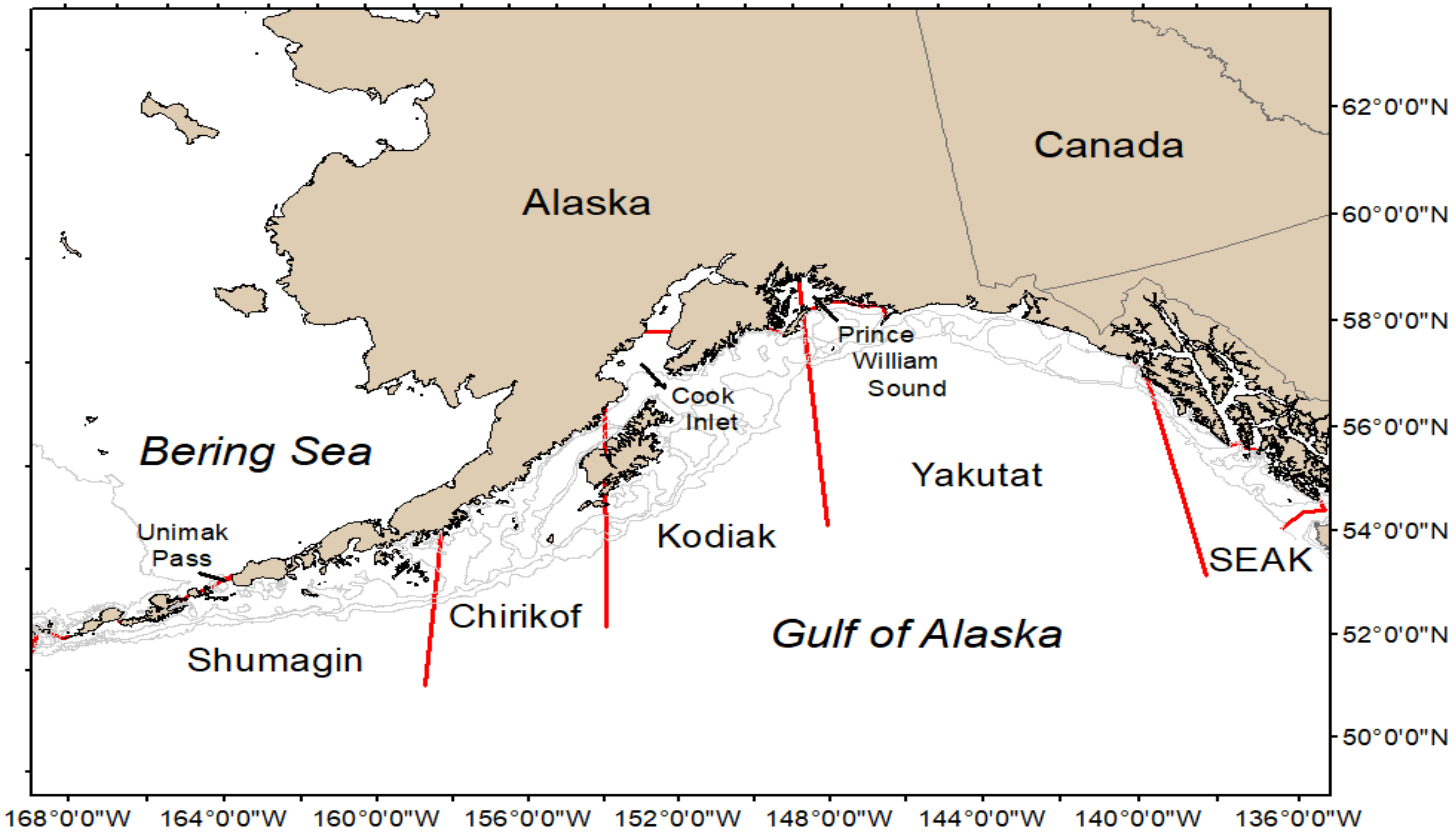

Figure 1. -- Gulf of Alaska (GOA) from Unimak Pass to Dixon Entrance where data for this modeling study were collected on Alaska Fisheries Science Center (AFSC), Resource Assessment and Conservation Engineering-Groundfish Assessment Program (RACE-GAP) summer bottom trawl surveys (1993-2019).

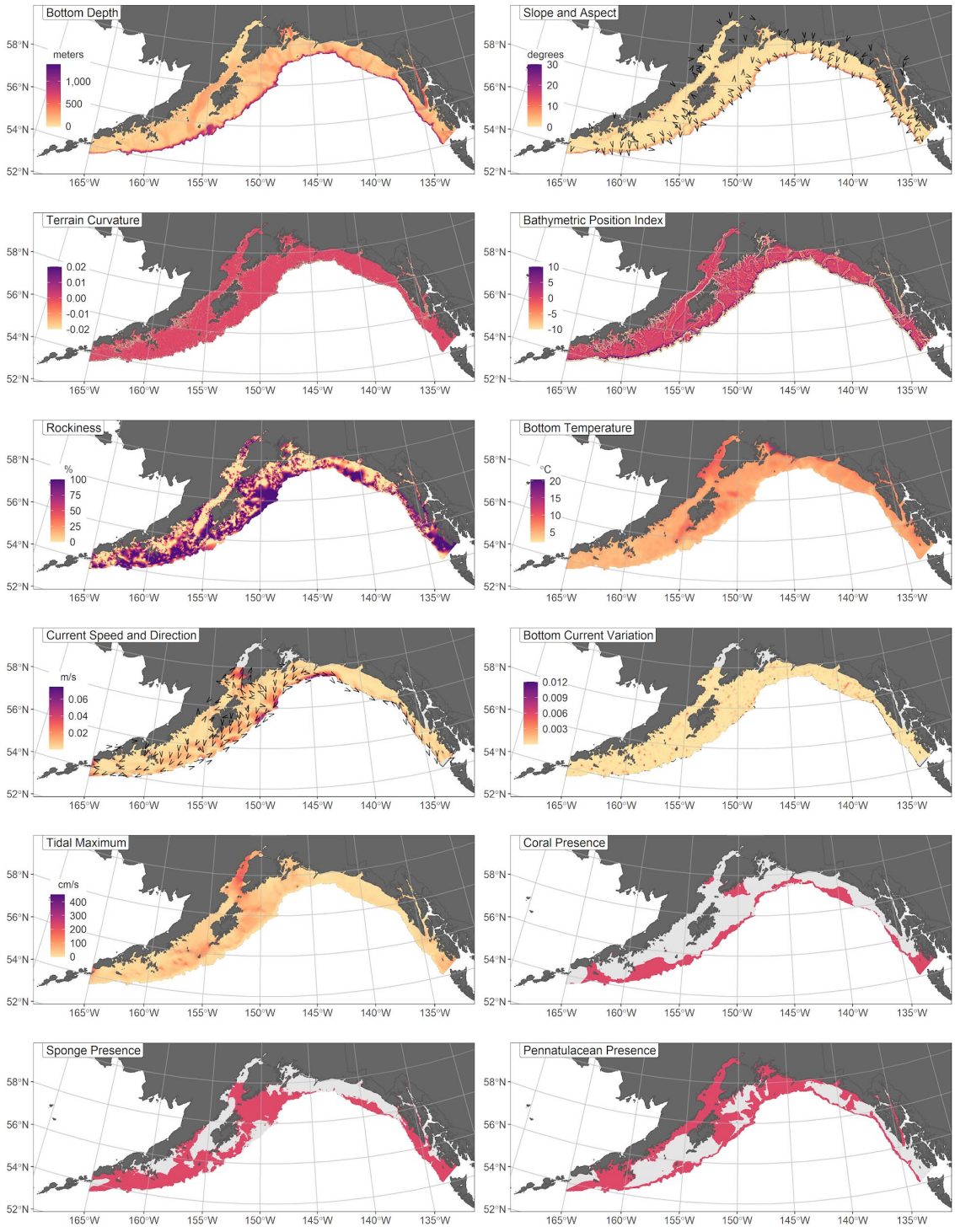

Figure 2. -- Predictor variables used to represent environmental and habitat covariates in the Gulf of Alaska; scale of structure-forming invertebrates (SFI: corals, sponges, and pennatulaceans) is light shading = absent and darker shading = present.

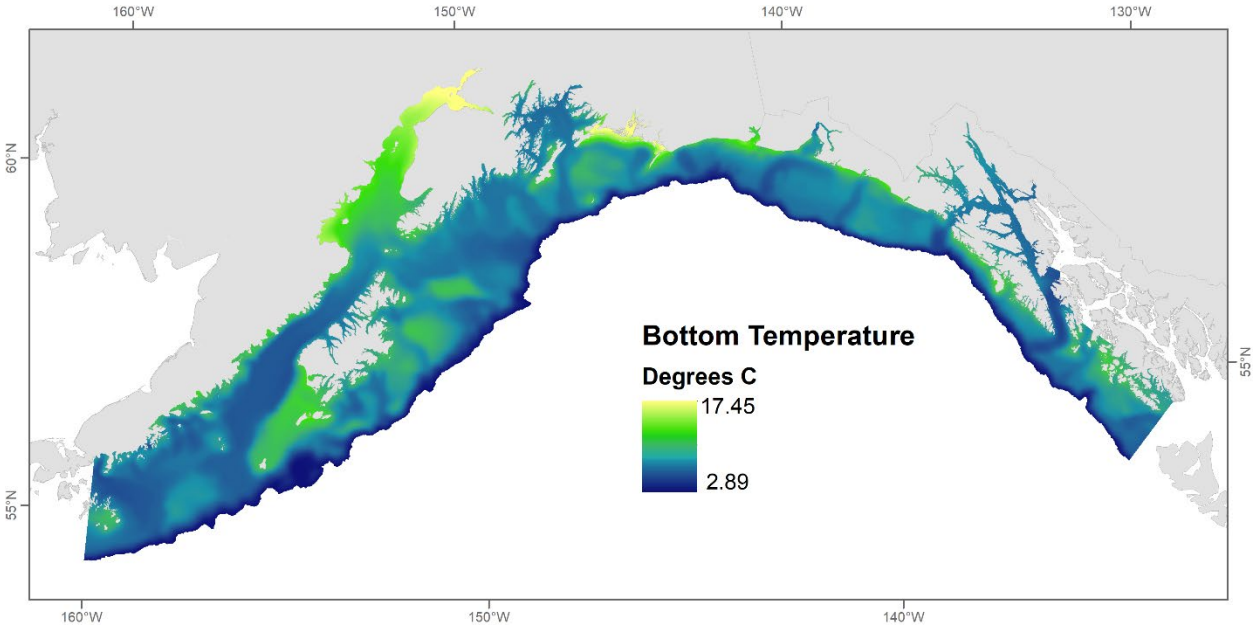

Figure 3. -- Bottom temperature (deepest depth bin) predicted from the CGOA ROMS 3 km grid (Coyle et al. 2019) from May-September and averaged (1999-2019). Applied to settled early juvenile stage (EJS) SDMs. The spatial extent of the EJS SDMs is limited by the spatial extent of the CGOA ROMS data.

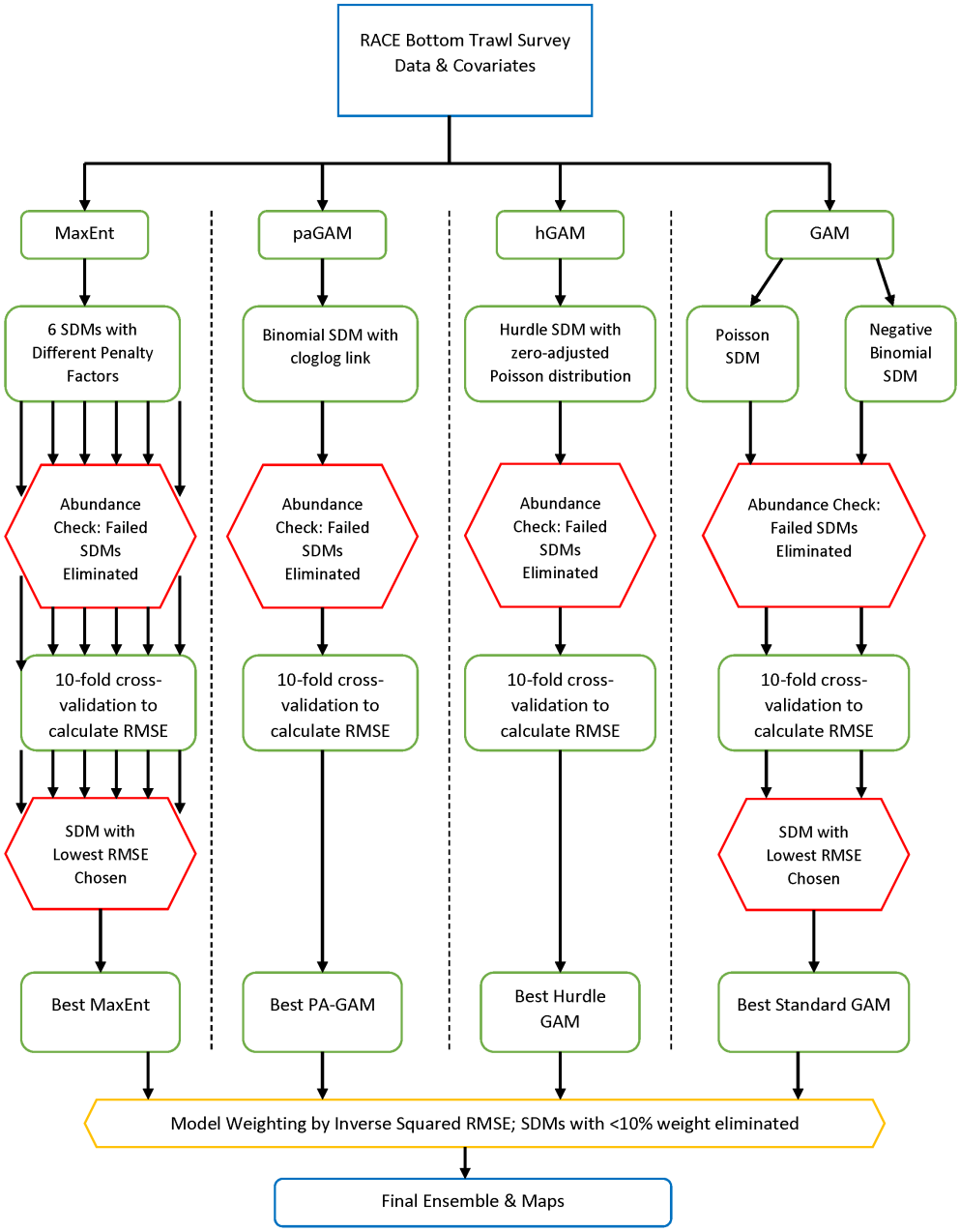

Figure 4. -- Pathways to formulation and assessment of five species distribution models (MaxEnt = maximum entropy, paGAM = presence-absence generalized additive model, hGAM = hurdle GAM, GAM = standard Poisson GAM, GAMnb = standard negative-binomial GAM) for inclusion in or elimination from a final ensemble predicting habitat-related distribution and abundance used to describe and map essential fish habitat (EFH) in Alaska: RMSE = root mean square error.

RESULTS

Flatfishes

Arrowtooth flounder (*Atheresthes stomias*)

Arrowtooth flounder (*Atheresthes stomias*, ATF) is a large-bodied flatfish that can be found from Russia in the west, through the Aleutian Islands, Bering Sea, and Gulf of Alaska (GOA) into central California (Mecklenberg et al. 2002). Arrowtooth flounder are the most abundant flatfish in the GOA (Spies et al. 2019). They are morphologically similar to the Kamchatka flounder (*A. evermanni*), which is rare in this region. Doyle et al. (2018) reports an estimated maximum length for the ATF settled early juvenile stage of 160 mm, and a minimum length for this life stage of 35 mm was found in the NFAA and corresponds to the maximum size range of transformed pelagic early juveniles (Doyle et al. 2019). The mesh size of the RACE-GAP bottom trawl is large enough that these smaller life stages may not be wholly retained in the catch[11]. The majority of ATF become sexually mature at an approximate size of 460 mm (L_{50}; Stark 2012a) in the GOA, and although the length at maturity appears consistent across regions, the age of maturity can vary considerably (Spies et al. 2019). This species is highly predatory and is considered an important component of the trophic system in the GOA (Yang 1993; Hollowed et al. 1995, 2000).

Settled early juvenile arrowtooth flounder distribution predicted from mixed gear-type summer surveys in the Gulf of Alaska -- Settled early juvenile ATF (N = 1,825) caught in mixed gear-type summer surveys (1989–2019), using large and small mesh bottom trawls and purse and beach seines, were distributed from Cook Inlet across the continental shelf and onto the upper continental slope (Fig. 1). Settled early juvenile ATF presence records from multiple surveys were combined in a habitat-related MaxEnt SDM predicting suitable habitat probabilities for this life stage in the GOA. The best model had a β-multiplier of 3.0 and an AUC of 0.79 (Table 6). The covariates contributing the majority of influence to the MaxEnt model (88%) were tidal maximum current, terrain aspect, bottom depth, and BPI (Table 7). The highest predicted probabilities of suitable habitat were broadly distributed across the continental shelf in the Yakutat and southeastern Alaska management areas in 150 m depths with tidal current speeds around 25 cm/s over relatively flat seafloor terrain (Fig. 6). The standard deviation among k-folds as a result of cross-validation for the final SDM was higher in coastal areas along the Alaska Peninsula, Kodiak Island, and mainland Alaska.

[11] A recommenation from the stock author review to incorporate longline survey data in future SDM ensemble EFH mapping for this species will be included as a research recommendation from the 2023 EFH 5-year Review.

Subadult arrowtooth flounder abundance and distribution predicted from RACE-GAP summer bottom trawl surveys in the Gulf of Alaska -- Subadult ATF (N = 7,390) caught in GOA RACE-GAP summer bottom trawl surveys (1993–2019) were widely distributed across the GOA continental shelf and onto the upper continental slope (Fig. 7). Five SDMs considered for inclusion in the ensemble to predict numerical abundance of subadult ATF in the GOA converged (Table 8); the GAM_{nb} was eliminated by skill testing based on RMSE. The GAM_P carried the highest weight in the final ensemble, and the hGAM carried the lowest. The overall ensemble fit to the observed subadult ATF distribution and abundance data was fair. The ensemble was excellent at predicting high and low abundance catches ($\rho = 0.64$), and fair at discriminating presence-absence (AUC = 0.70) and explaining deviance (PDE = 0.28). Bottom depth, geographic location, and bottom temperature explained 77.1% of the deviance in the ensemble-predicted subadult ATF numerical abundance (Table 7). Their highest abundances were predicted in the Shelikof Strait and over the continental shelf to the west at depths around 200 m and in cooler bottom temperatures (Fig. 8). Higher CVs from cross-validating these predictions were associated with deeper waters along the upper continental slope. The probability of encountering subadult ATF was high throughout the survey area (Fig. 9).

Adult arrowtooth flounder abundance and distribution predicted from RACE-GAP summer bottom trawl surveys in the Gulf of Alaska -- Adult ATF (N = 7,043) were widely distributed across the continental shelf and onto the upper continental slope in GOA RACE-GAP summer bottom trawl survey catches (1993–2019; Fig. 6). Five SDMs converged to predict numerical abundance of adult ATF in the GOA (Table 8); the GAM_{nb} was eliminated by skill testing. The four remaining best-performing SDMs were weighted relatively evenly in the final ensemble. The overall ensemble fit to observed adult ATF distribution and abundance data was good. The ensemble was good at predicting high and low abundance catches ($\rho = 0.55$) and discriminating presence-absence (AUC = 0.76), and fair at explaining deviance (PDE = 0.29). Bottom depth, geographic location, bottom temperature, slope, and rockiness accounted for 78.1% of the deviance in the ensemble-predicted adult ATF numerical abundance (Table 7), which was highest in Shelikof Strait into the southern end of Cook Inlet at in glacial troughs in the central GOA. Adult ATF distribution and abundance were related to depths around 200 m with cooler bottom temperatures in sloping and non-rocky terrain (Fig. 11). The CVs from cross-validation of ensemble predictions were relatively low (< 0.30) throughout the region. The probability of encountering adult ATF was high throughout the survey area, similar to subadults (Fig. 12).

Essential Fish Habitat of three life stages of arrowtooth flounder in the Gulf of Alaska -- Habitat-related predictions of arrowtooth flounder demersal life stage distribution and abundance from summer surveys of the GOA (mixed gear-type summer surveys (1989–2019) and RACE-GAP bottom

trawl surveys (1993–2019)) were mapped as EFH areas and subareas (Fig. 13). Settled early juvenile ATF EFH extended from the 200 m isobaths at the edge of the continental shelf well into inshore areas throughout the region. The EFH areas for subadult and adult ATF extended to the margins of the GOA survey. Settled early juvenile core EFH areas and EFH hot spots were present across the western GOA shelf, around Kodiak Island, and into Cook Inlet, and hot spots were particularly prominent for this life stage in the central and eastern GOA. Subadult and adult ATF core EFH dominated much of the GOA survey area from southeastern Alaska to the western GOA. EFH hot spots for both life stages were prominent in Shelikof Strait and in glacial troughs throughout the GOA. The EFH maps for these life stages collectively demonstrated a shift in habitat-related distribution and abundance to deeper depths with increasing size and age.

Table 6. -- Maximum entropy model (MaxEnt) used to construct Essential Fish Habitat (EFH) for settled early juvenile arrowtooth flounder: regularization multiplier (β); *k*-fold cross-validation root-mean-square-error (RMSE), area under the receiver operating characteristic curve (AUC), and areal extent of EFH (km^2).

Model	**β**	**RMSE**	**AUC**	**EFH area (km^2)**
MaxEnt	3.0	4.06	0.79	242,500

Table 7. -- Covariates retained in the a) settled early juvenile habitat-related maximum entropy (MaxEnt) species distribution model (SDM), and b) subadult and c) adult SDM final ensembles for arrowtooth flounder with the percent contribution of each covariate to the deviance explained by the SDMs and the cumulative deviance explained: SD = standard deviation and BPI = bathymetric position index.

arrowtooth flounder	**Covariate**	**% Contribution**	**Cumulative %**
a) settled early juvenile	tidal maximum	26.3	26.3
	aspect east	18.8	45.1
	aspect north	15.6	60.7
	bottom depth	14.1	74.8
	BPI	13.3	88.1
	bottom temperature	4.4	92.5
	slope	3.1	95.7
	rockiness	2.4	98.1
	curvature	1.9	100.0
b) subadult	bottom depth	55.8	55.8
	location	12.6	68.4
	bottom temperature	8.7	77.1
	rockiness	4.3	81.4
	tidal maximum	4.1	85.5
	slope	2.9	88.4
	current	2.8	91.2
	current SD	2.3	93.5
	BPI	2.1	95.6
	aspect north	1.2	96.8
	sponge presence	1.1	97.9
	aspect east	1.0	98.9
	curvature	0.8	99.7
	pennatulacean presence	0.3	100.0
c) adult	bottom depth	31.0	31.0
	location	18.4	49.4
	bottom temperature	12.9	62.2
	slope	11.5	73.7
	rockiness	4.4	78.1
	current SD	3.7	81.8
	tidal maximum	3.7	85.5
	sponge presence	3.3	88.8
	current	3.2	92.0
	aspect north	2.4	94.4
	BPI	2.2	96.6
	curvature	1.7	98.3

arrowtooth flounder

Covariate	% Contribution	Cumulative %
aspect east	1.3	99.6
coral presence	0.2	99.8
pennatulacean presence	0.2	100.0

Table 8. -- Constituent species distribution models (SDMs) used to construct Essential Fish Habitat (EFH) for a) subadult and b) adult arrowtooth flounder: MaxEnt = Maximum entropy; paGAM = presence-absence generalized additive model; hGAM = zero-adjusted Poisson hurdle GAM; GAM_P = standard Poisson GAM; GAM_{nb} = standard negative-binomial GAM; RMSE = root mean square error; ρ (*rho*) = Spearman's rank correlation coefficient; AUC = area under the receiver operating characteristic curve; and PDE = Poisson deviance explained *. The "--" indicates that this model was not included in the final ensemble.

a) subadult arrowtooth flounder

Models	**RMSE**	**Relative Weight**	**ρ**	**AUC**	**PDE**	**EFH area (km^2)**
MaxEnt	333.2	0.22	0.63	0.90	0.00	280,400
paGAM	294.4	0.28	0.48	0.86	0.08	281,800
hGAM	371.6	0.17	0.59	0.87	0.24	281,800
GAM_P	271.0	0.33	0.60	0.66	0.29	272,300
GAM_{nb}	279.8	0	--	--	--	--
ensemble	276.1	1	0.64	0.70	0.28	281,800

b) adult arrowtooth flounder

Models	**RMSE**	**Relative Weight**	**ρ**	**AUC**	**PDE**	**EFH area (km^2)**
MaxEnt	209.0	0.22	0.52	0.84	0.12	280,900
paGAM	200.2	0.24	0.51	0.84	0.02	281,800
hGAM	188.6	0.27	0.43	0.84	0.28	281,800
GAM_P	189.1	0.27	0.41	0.66	0.27	281,800
GAM_{nb}	191.9	0	--	--	--	--
ensemble	189.5	1	0.55	0.76	0.29	281,800

* Refer to the Species Distribution Model Performance Metrics subsection within the Statistical Modeling section of the Methods for detailed descriptions of individual model performance metrics.

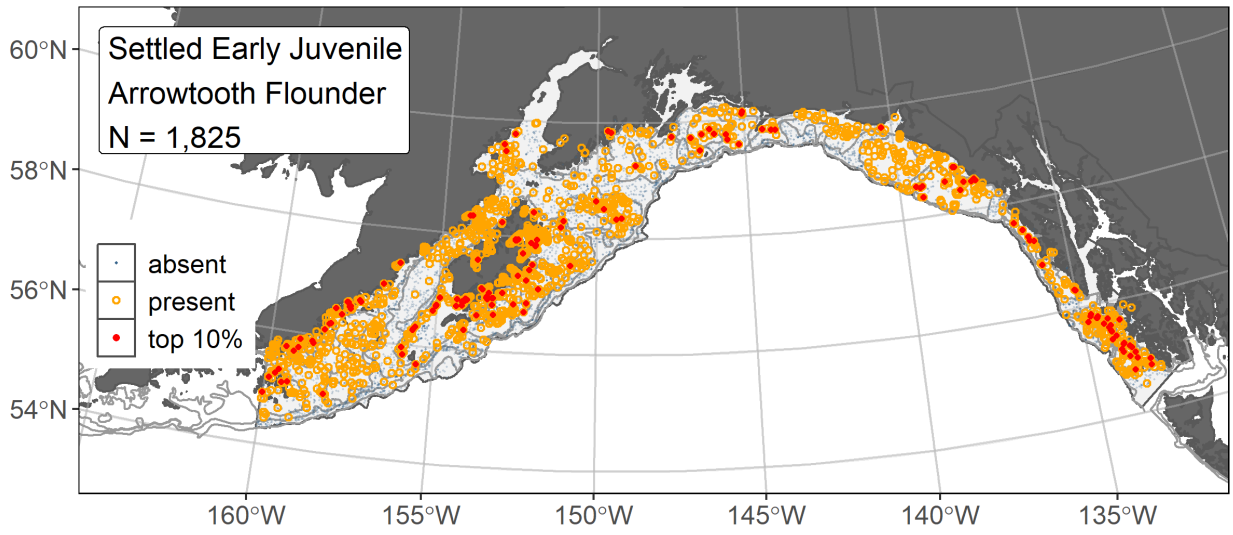

Figure 5. -- Distribution of settled early juvenile arrowtooth flounder catches (N = 1,825) in mixed gear-type summer surveys of the Gulf of Alaska (1989–2019) with the 100 m, 200 m, and 700 m isobaths indicated; filled red circles indicate locations in top 10% of overall abundance, open orange circles indicate presence in remaining catches, and blue dots indicate stations sampled where the animals were not present.

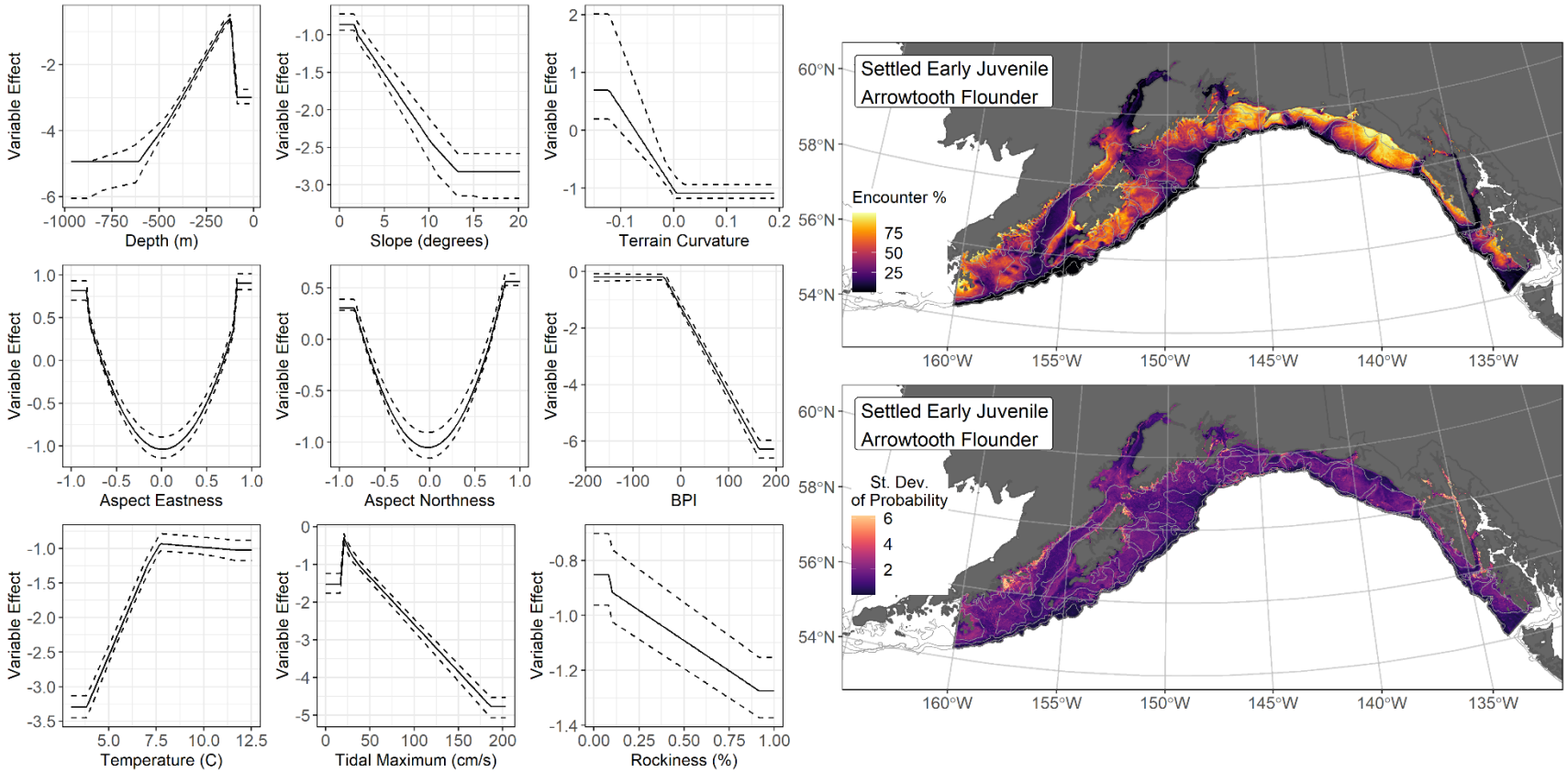

Figure 6. -- The top nine covariate effects (left panel) from a habitat-related species distribution model (MaxEnt) of settled juvenile arrowtooth flounder probability of suitable habitat in the Gulf of Alaska (upper right panel) with the standard deviation of the probability predictions (lower right panel).

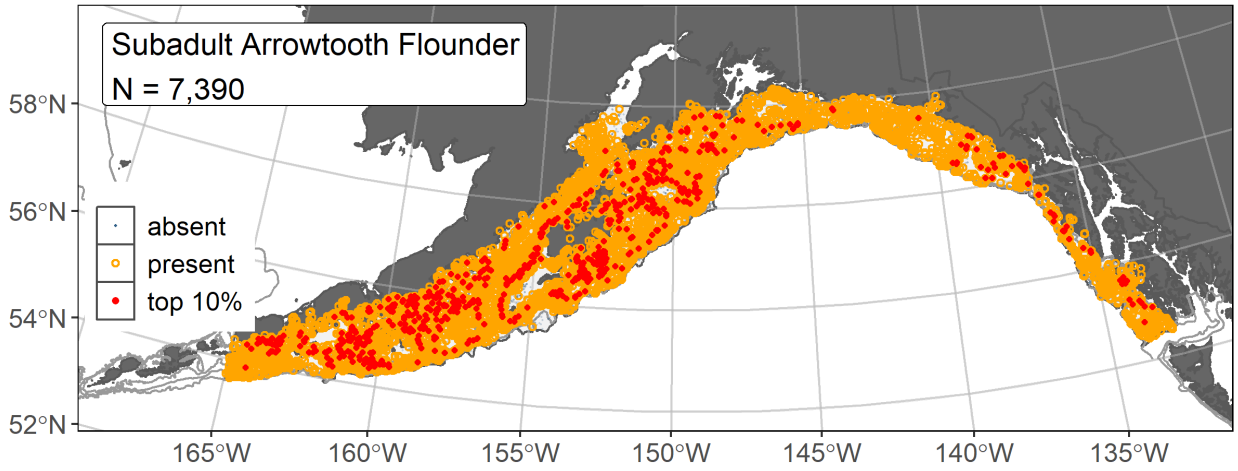

Figure 7. -- Distribution of subadult arrowtooth flounder catches (N = 7,390) in 1993–2019 AFSC RACE-GAP summer bottom trawl surveys of the Gulf of Alaska with the 100 m, 200 m, and 700 m isobaths indicated; filled red circles indicate locations in top 10% of overall abundance, open orange circles indicate presence in remaining catches, and blue dots indicate stations sampled where the animals were not present.

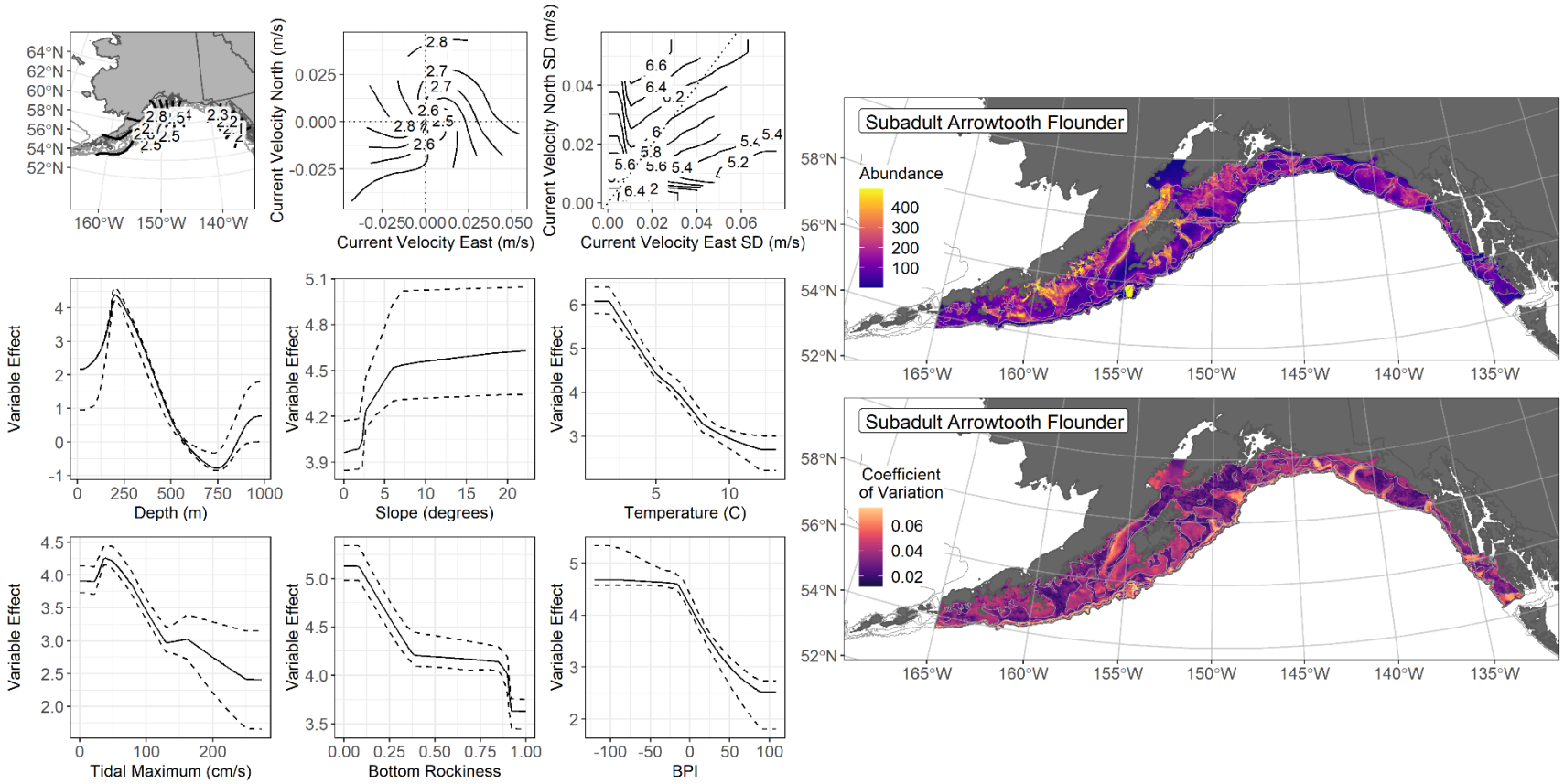

Figure 8. -- The top nine covariate effects (left panel) on ensemble-predicted subadult arrowtooth flounder numerical abundance across the Gulf of Alaska (upper right panel) along with the coefficient of variation (CV) of the ensemble predictions (lower right panel).

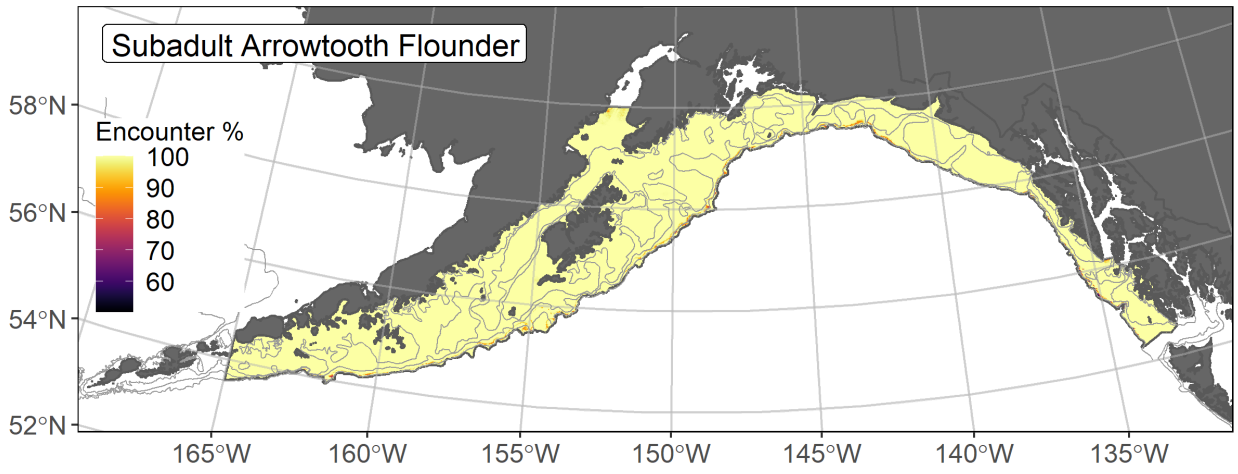

Figure 9. -- Encounter probability of subadult arrowtooth flounder from AFSC RACE-GAP summer bottom trawl surveys (1993–2019) of the Gulf of Alaska with the 100 m, 200 m, and 700 m isobaths indicated.

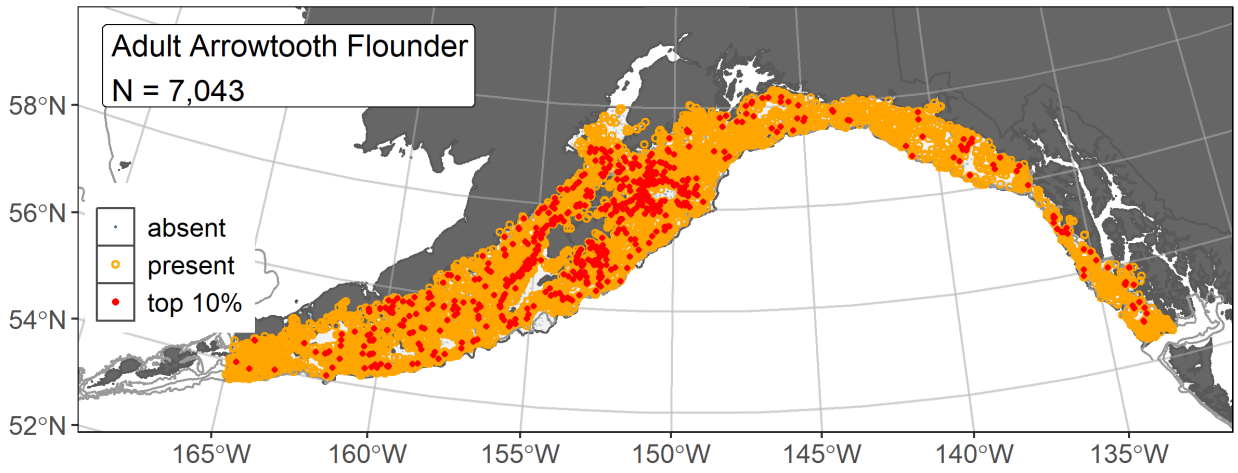

Figure 10. -- Distribution of adult arrowtooth flounder catches (N = 7,043) in 1993–2019 AFSC RACE-GAP summer bottom trawl surveys of the Gulf of Alaska with the 100 m, 200 m, and 700 m isobaths indicated; filled red circles indicate locations in top 10% of overall abundance, open orange circles indicate presence in remaining catches, and blue dots indicate stations sampled where the animals were not present.

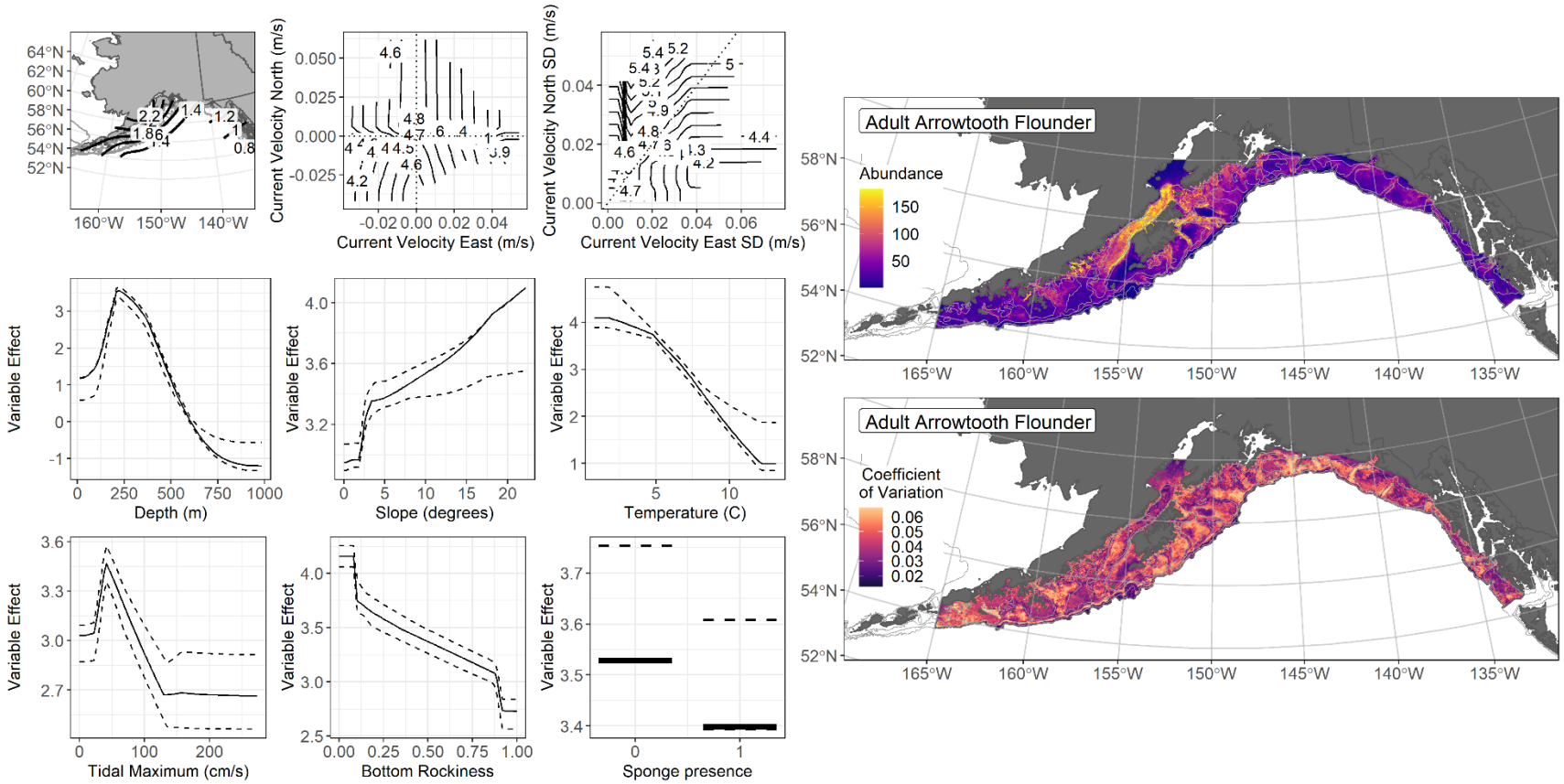

Figure 11. -- The top nine covariate effects (left panel) on ensemble-predicted adult arrowtooth flounder numerical abundance across the Gulf of Alaska (upper right panel) along with the coefficient of variation (CV) of the ensemble predictions (lower right panel).

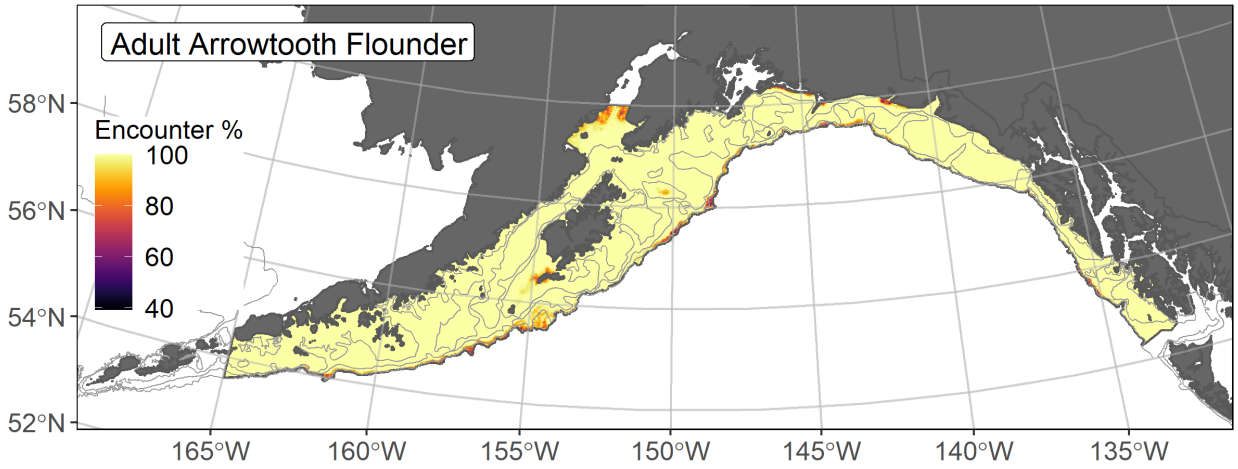

Figure 12. -- Encounter probability of adult arrowtooth flounder from AFSC RACE-GAP summer bottom trawl surveys (1993–2019) of the Gulf of Alaska with the 100 m, 200 m, and 700 m isobaths indicated.

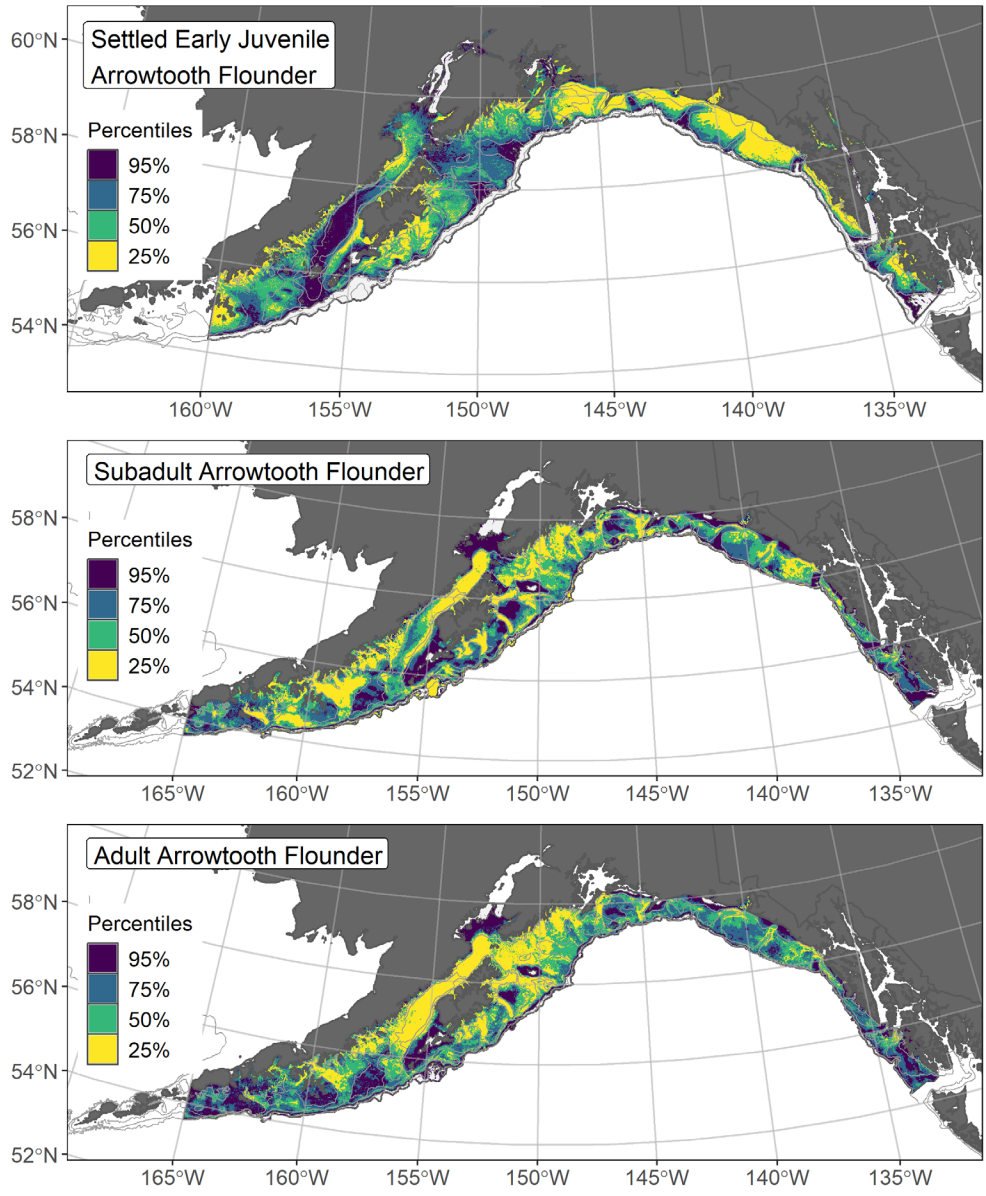

Figure 13. -- Essential fish habitat (EFH) is the area containing the top 95% of occupied habitat (defined as greater than 5% predicted probability of suitable habitat) for settled early juvenile (top panel) arrowtooth flounder from an SDM fitted to their distribution in Gulf of Alaska (GOA) mixed gear-type summer surveys (1989–2019), and for subadults (middle panel) and adults (bottom panel) is the area containing the top 95% of occupied habitat (defined as model estimated encounter probabilities greater than 5%) from an SDM ensemble fitted to arrowtooth flounder distribution and abundance in AFSC RACE-GAP GOA summer bottom trawl surveys (1993–2019) with 100 m, 200 m, and 700 m isobaths indicated; within the EFH area map are the subareas of the top 25% (EFH hot spots), top 50% (core EFH area), and top 75% (principal EFH area).

Flathead sole (*Hippoglossoides elassodon*)

Flathead sole (*Hippoglossoides elassodon*) is distributed across the North Pacific from northern California across the Aleutian Islands and Bering Sea at least as far as the Kuril archipelago (Hart 1973). This study uses a length range of 20–140 mm for settled early juvenile flathead sole (Doyle et al. 2019, NFAA), and the majority become mature at L_{50} = 333 mm TL (Stark 2004). Adults may grow to 520 mm TL and live more than 30 years, maturing around nine years of age. Spawning occurs between March and June on the continental shelf, frequently in bays or other shallow habitats close to nursery areas (Porter 2005). In the GOA region, flathead sole are managed as a single species (Turnock et al. 2017a). The mesh size of the RACE-GAP bottom trawl is large enough that the smaller juvenile life stages may not be wholly retained in the catch[12].

Settled early juvenile flathead sole distribution predicted from mixed gear-type summer surveys in the Gulf of Alaska -- Settled early juvenile flathead sole (N = 2,017) caught in mixed gear-type summer surveys (1989–2019) were fairly common and widely distributed across the continental shelf throughout the GOA and into Cook Inlet with higher abundance catches centered in the Shumagin management area and around Kodiak Island (Fig. 14). For these early juvenile flathead sole, presence records from multiple surveys were combined in an habitat-related MaxEnt model predicting suitable habitat probabilities for this life stage. The best model had a β-multiplier of 2.5 and an AUC of 0.90 (Table 9). The covariates contributing the majority of influence to the MaxEnt model (80%) were BPI, bottom depth, tidal current, and seafloor aspect (Table 10). The highest probabilities of suitable habitat for early juvenile flathead sole in the GOA were predicted in nearshore areas along the Alaska Peninsula, around Kodiak Island, and along the mainland in the southeastern Alaska management area over relatively flat, non-rocky bottom at shallower depths (Fig. 15). The areas with the highest error around the MaxEnt predictions for settled early juvenile suitable habitat loosely corresponded to the locations where high probabilities of suitable habitat were predicted.

Subadult flathead sole abundance and distribution predicted from RACE-GAP summer bottom trawl surveys in the Gulf of Alaska -- Subadult flathead sole (N = 4,064) caught in GOA RACE-GAP summer bottom trawl surveys (1993–2019) were widely distributed across the GOA continental shelf throughout the survey area with concentrations of high abundance catches around Kodiak Island and the Alaska Peninsula in the western GOA (Fig. 16). Five SDMs were considered for inclusion in the ensemble to predict numerical abundance of subadult flathead sole in the GOA

[12] Adding other high quality sources of data if available to future SDM ensemble EFH mapping for this species will be included as a research recommendation from the 2023 EFH 5-year Review.

(Table 11); the MaxEnt and GAM_{nb} was eliminated by skill testing. The three remaining SDMs were weighted by RMSE in the final ensemble, which attained an excellent fit to the observed subadult flathead sole distribution and abundance data. The ensemble was excellent at predicting high and low abundance catches (ρ = 0.71), good at discriminating presence-absence (AUC = 0.86), and excellent at explaining deviance (PDE = 0.65). Geographic location, bottom depth, tidal current, and BPI accounted for the majority of covariate contribution (74.3%) to the deviance explained by the ensemble (Table 10). The highest subadult flathead sole abundances were predicted in upper Shelikof Strait, in nearshore waters around Kodiak Island, and along the coast of the western Alaska Peninsula in shallower waters with slower maximum tidal currents over submarine channels or valleys (Fig. 17). The higher CVs from cross-validating these predictions appeared to be associated with Shelikof Strait and over the shallower continental shelf in the Kodiak, Yakutat, and southeastern Alaska management areas. The probability of encountering subadult flathead sole was high across the GOA continental shelf at depths < 250 m and low over the continental slope and in submarine canyons of southeast Alaska (Fig. 18).

Adult flathead sole abundance and distribution predicted from RACE-GAP summer bottom trawl surveys in the Gulf of Alaska -- Adult flathead sole (N = 4,201) caught in GOA RACE-GAP summer bottom trawl surveys (1993–2019) were common and widely distributed across the continental shelf in western and central GOA with concentrations of higher abundance catches around Kodiak Island and along the Alaska Peninsula (Fig. 19). Five SDMs were considered for inclusion in the ensemble to predict numerical abundance of adult flathead sole in the GOA (Table 11); the MaxEnt and GAM_{nb} were eliminated by skill testing. The three remaining SDMs were weighted by RMSE in the final ensemble, which attained a good fit to the observed subadult flathead sole distribution and abundance data. The ensemble was excellent at predicting high and low abundance catches (ρ = 0.72), and good at discriminating presence-absence (AUC = 0.88) and at explaining deviance (PDE = 0.54). Geographic location, BPI, and bottom depth accounted for 68.9% of covariate contribution to the deviance explained by the ensemble (Table 10). Adult flathead sole predicted abundance was highest in Shelikof Strait, in coastal waters around Kodiak Island, and the shallower, nearshore waters of the Alaska Peninsula over submarine channels or valleys with relatively non-rocky seafloor (Fig. 20). The CV from cross-validating ensemble predictions was high across the continental shelf but near zero at depths along the continental slope. The probability of encountering adult flathead sole was high across the continental shelf at depths < 300 m (Fig. 21).

Essential Fish Habitat of three life stages of flathead sole in the Gulf of Alaska -- Habitat-related predictions of flathead sole life stage distribution and abundance from summer surveys of the GOA (mixed gear-type summer surveys (1989–2019) and RACE-GAP bottom trawl surveys (1993–

2019)) were mapped as EFH areas and subareas (Fig. 22). Settled early juvenile flathead sole EFH was scattered across the continental shelf and into inshore areas throughout the region. Core EFH areas and EFH hot spots for settled early juveniles were also scattered throughout the region but generally associated with shallower continental shelf habitats and nearshore areas. The EFH areas for subadult and adult flathead sole extended from southeast Alaska to the western GOA. The core EFH areas of subadults extended slightly further into the southeast Alaska management area than did that of adults but generally overlapped elsewhere in the GOA. For both the subadult and adult life stages of flathead sole, EFH hot spots were prominent in Shelikof Strait and over the continental shelf as well as along the coast of the Alaska Peninsula west of there. EFH hot spots for these two life stages were also located in the nearshore and south of Kodiak Island. The SDM and EFH area maps demonstrated an ontogenetic shift to deeper depths among the three life stages.

Table 9. -- Maximum entropy model (MaxEnt) used to construct Essential Fish Habitat (EFH) for settled early juvenile flathead sole: regularization multiplier (β); *k*-fold cross-validation root-mean-square-error (RMSE), area under the receiver operating characteristic curve (AUC), and areal extent of EFH (km^2).

Model	**β**	**RMSE**	**AUC**	**EFH area (km^2)**
MaxEnt	2.5	10.85	0.90	150,100

Table 10. -- Covariates retained in the a) settled early juvenile habitat-related maximum entropy (MaxEnt) species distribution model (SDM), and b) subadult and c) adult SDM final ensembles for flathead sole with the percent contribution of each covariate to the deviance explained by the SDMs and the cumulative deviance explained: SD = standard deviation and BPI = bathymetric position index.

flathead sole	**Covariate**	**% Contribution**	**Cumulative %**
a) settled early juvenile	BPI	27.4	27.4
	bottom depth	19.0	46.4
	tidal maximum	11.6	58.0
	aspect north	11.2	69.2
	aspect east	11.1	80.3
	bottom temperature	8.6	88.9
	slope	3.6	92.5
	rockiness	2.8	95.3
	pennatulacean presence	1.9	97.2
	curvature	1.3	98.5
	sponge presence	1.1	99.6
	coral presence	0.4	100.0
b) subadult	location	24.6	24.6
	bottom depth	21.0	45.6
	tidal maximum	16.6	62.3
	BPI	12.0	74.3
	current	8.6	82.9
	rockiness	5.5	88.4
	sponge presence	4.0	92.4
	current SD	3.0	95.4
	slope	1.8	97.2
	aspect north	0.9	98.1
	bottom temperature	0.7	98.8
	curvature	0.5	99.3
	aspect east	0.4	99.7
	pennatulacean presence	0.2	99.9
	coral presence	0.1	100.0
c) adult	location	34.7	34.7
	BPI	18.7	53.4
	bottom depth	15.5	68.9
	current	8.8	77.7
	rockiness	4.5	82.2
	tidal maximum	4.3	86.5
	slope	3.7	90.2
	sponge presence	3.4	93.6

flathead sole

Covariate	% Contribution	Cumulative %
current SD	1.9	95.5
bottom temperature	1.7	97.2
aspect east	0.8	98.0
curvature	0.8	98.8
aspect north	0.7	99.5
coral presence	0.4	99.9
pennatulacean presence	0.1	100.0

Table 11. -- Constituent species distribution models (SDMs) used to construct Essential Fish Habitat (EFH) for a) subadult and b) adult flathead sole: MaxEnt = Maximum entropy; paGAM = presence-absence generalized additive model; hGAM = zero-adjusted Poisson hurdle GAM; GAM_P = standard Poisson GAM; GAM_{nb} = standard negative-binomial GAM; RMSE = root mean square error; ρ (*rho*) = Spearman's rank correlation coefficient; AUC = area under the receiver-operating characteristic curve; and PDE = Poisson deviance explained *. The "--" indicates that this model was not included in the final ensemble.

a) subadult flathead sole

Models	**RMSE**	**Relative Weight**	**ρ**	**AUC**	**PDE**	**EFH area (km^2)**
MaxEnt	375.8	0	--	--	--	--
paGAM	132.9	0.27	0.72	0.89	0.48	258,800
hGAM	113.8	0.37	0.68	0.88	0.64	252,900
GAM_P	113.8	0.37	0.68	0.88	0.64	252,900
GAM_{nb}	--	--	--	--	--	--
ensemble	109.4	1	0.71	0.86	0.65	257,900

b) adult flathead sole

Models	**RMSE**	**Relative Weight**	**ρ**	**AUC**	**PDE**	**EFH area (km^2)**
MaxEnt	171.9	0	--	--	--	--
paGAM	70.7	0.30	0.73	0.90	0.45	258,900
hGAM	64.6	0.35	0.70	0.89	0.52	253,200
GAM_P	65.0	0.35	0.69	0.87	0.51	255,900
GAM_{nb}	78.6	0	--	--	--	--
ensemble	63.3	1	0.72	0.88	0.54	257,900

* Refer to the Species Distribution Model Performance Metrics subsection within the Statistical Modeling section of the Methods for detailed descriptions of individual model performance metrics.

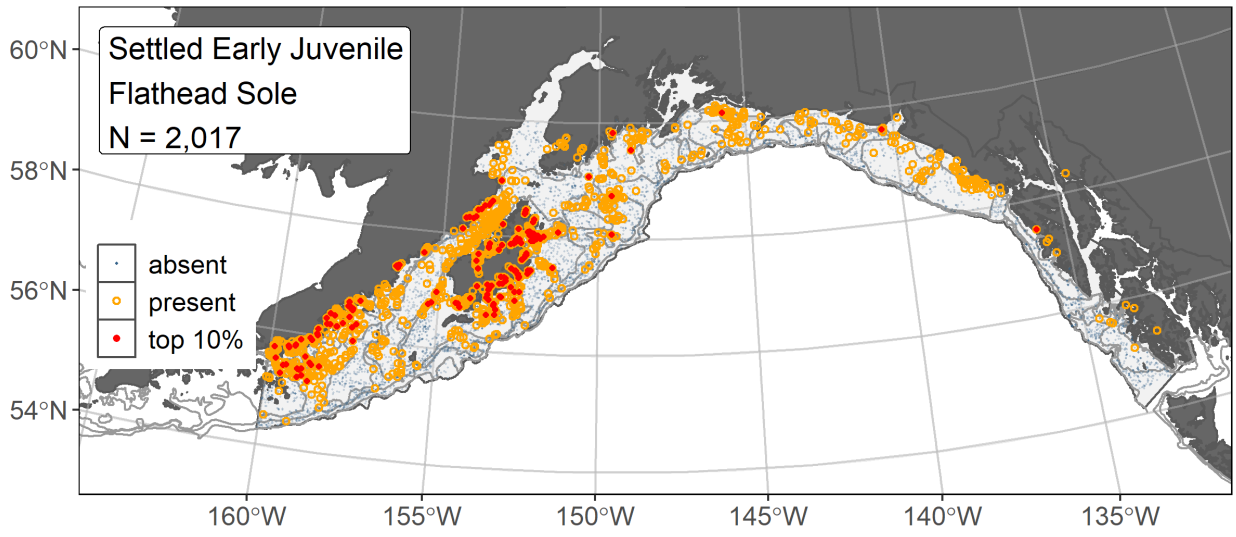

Figure 14. -- Distribution of settled early juvenile flathead sole catches (N = 2,017) in mixed gear-type summer surveys of the Gulf of Alaska (1989–2019) with the 100 m, 200 m, and 700 m isobaths indicated; filled red circles indicate locations in top 10% of overall abundance, open orange circles indicate presence in remaining catches, and blue dots indicate stations sampled where the animals were not present.

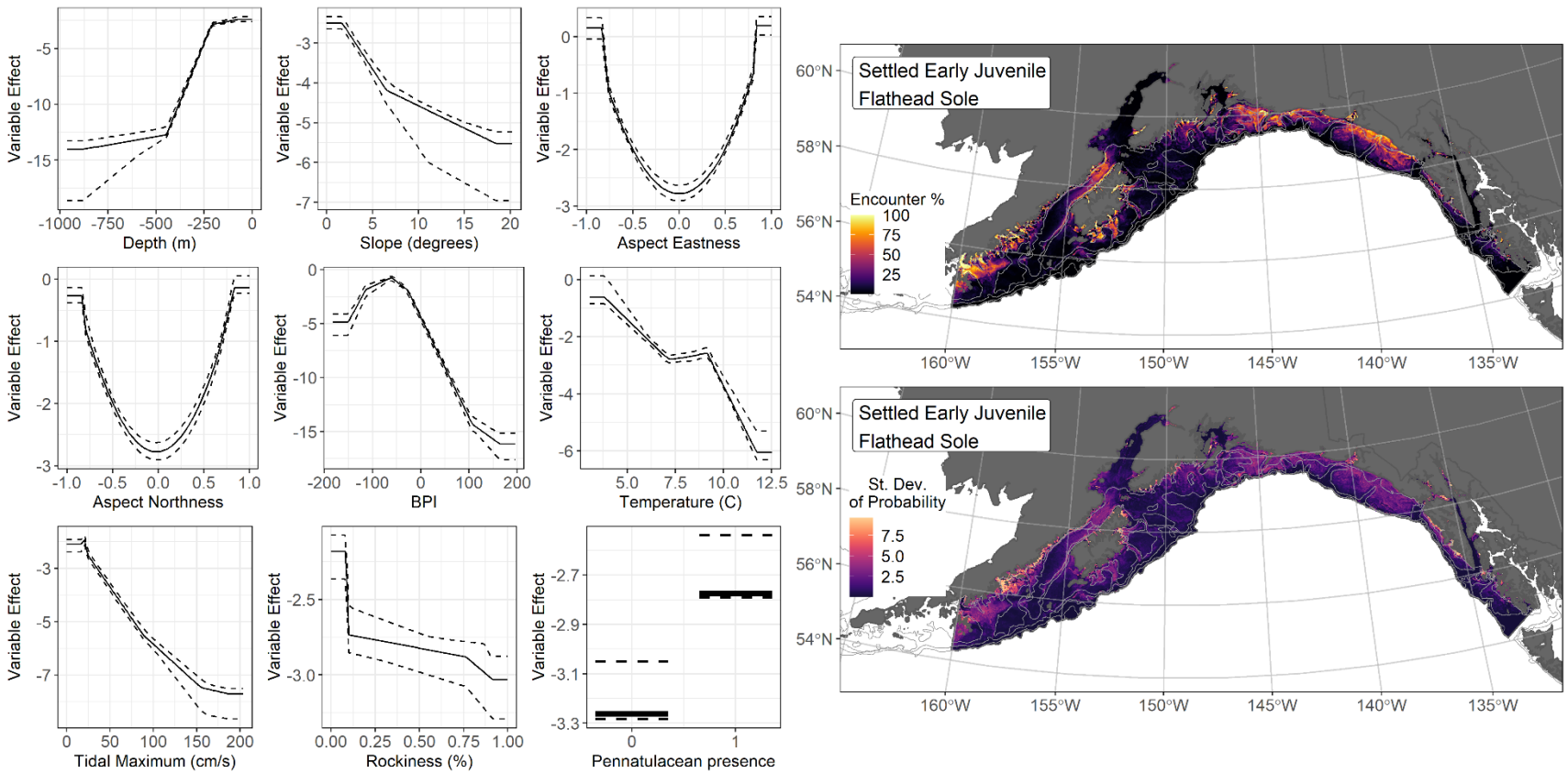

Figure 15. -- The top nine covariate effects (left panel) from a habitat-related species distribution model (MaxEnt) of settled early juvenile flathead sole probability of suitable habitat in the Gulf of Alaska (upper right panel) with the standard deviation of the probability predictions (lower right panel).

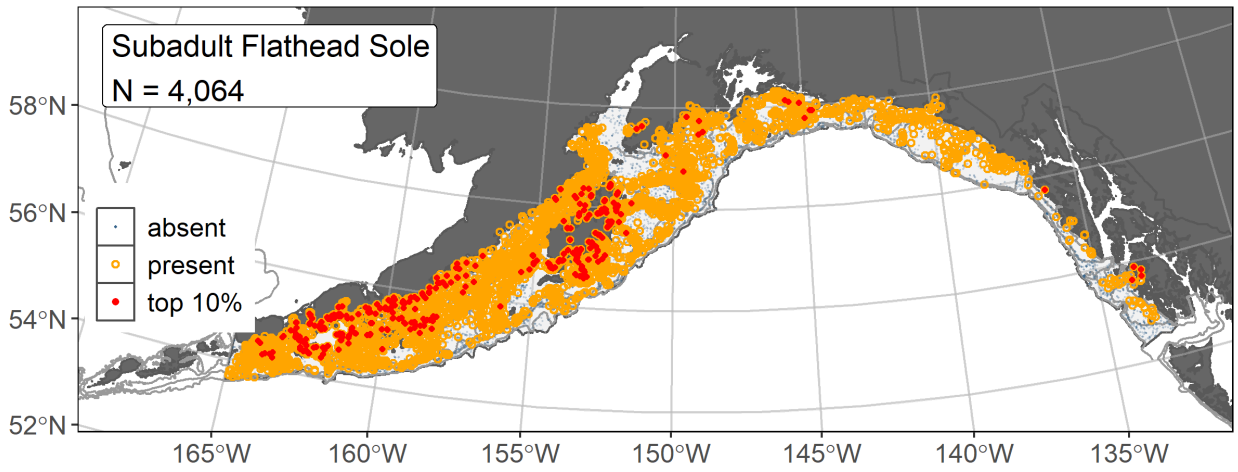

Figure 16. -- Distribution of subadult flathead sole catches (N = 4,064) in 1993–2019 AFSC RACE-GAP summer bottom trawl surveys of the Gulf of Alaska with the 100 m, 200 m, and 700 m isobaths indicated; filled red circles indicate locations in top 10% of overall abundance, open orange circles indicate presence in remaining catches, and blue dots indicate stations sampled where the animals were not present.

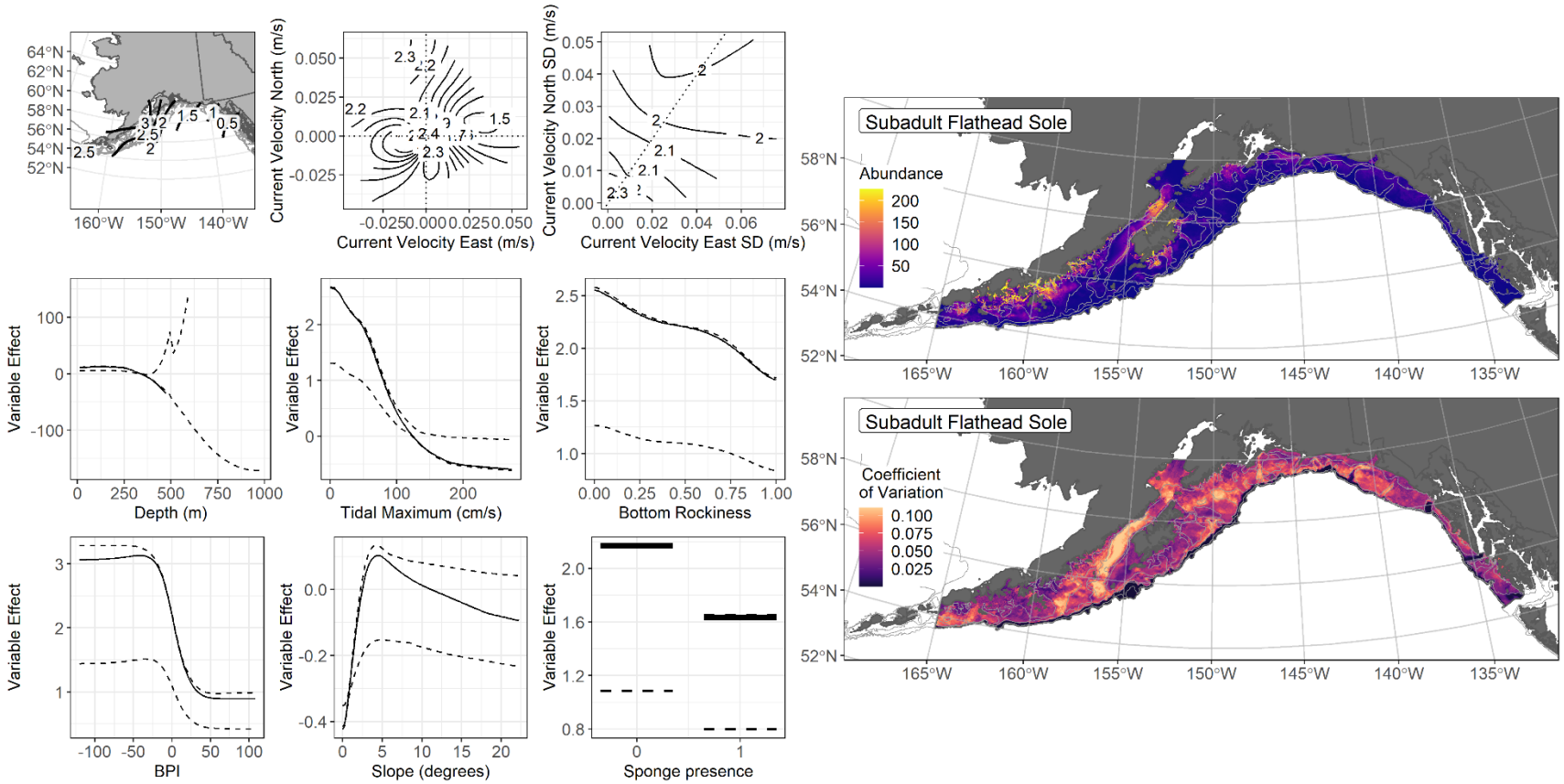

Figure 17. -- The top nine covariate effects (left panel) on ensemble-predicted subadult flathead sole numerical abundance across the Gulf of Alaska (upper right panel) along with the coefficient of variation (CV) of the ensemble predictions (lower right panel).

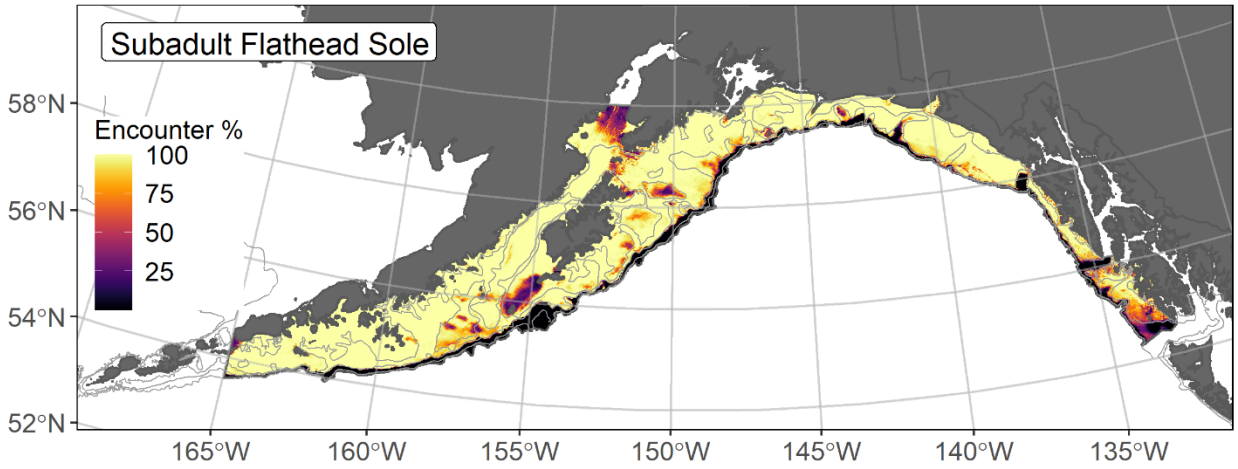

Figure 18. -- Encounter probability of subadult flathead sole from AFSC RACE-GAP summer bottom trawl surveys (1993–2019) of the Gulf of Alaska with the 100 m, 200 m, and 700 m isobaths indicated.

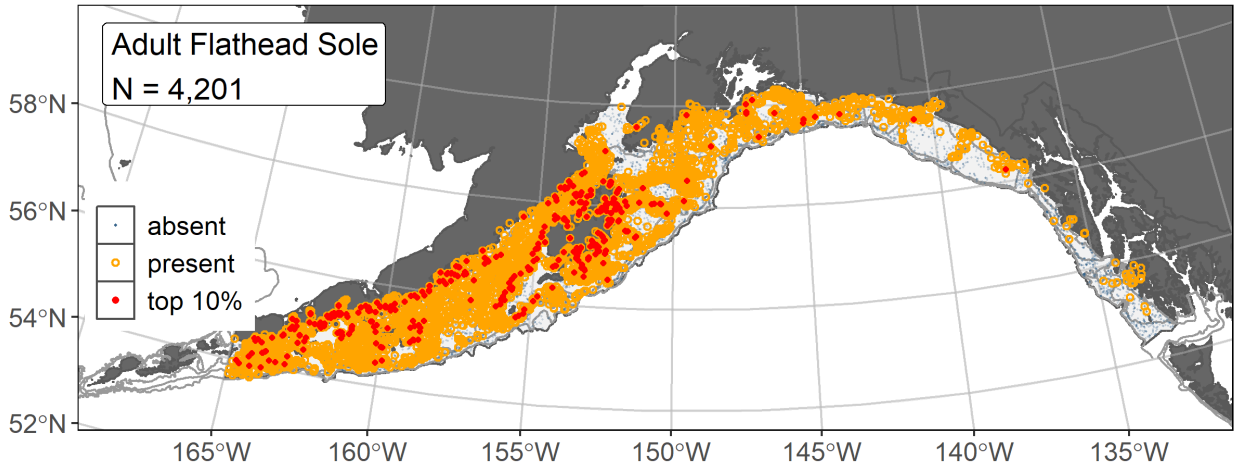

Figure 19. -- Distribution of adult flathead sole catches (N = 4,201) in 1993–2019 AFSC RACE-GAP summer bottom trawl surveys of the Gulf of Alaska with the 100 m, 200 m, and 700 m isobaths indicated; filled red circles indicate locations in top 10% of overall abundance, open orange circles indicate presence in remaining catches, and blue dots indicate stations sampled where the animals were not present.

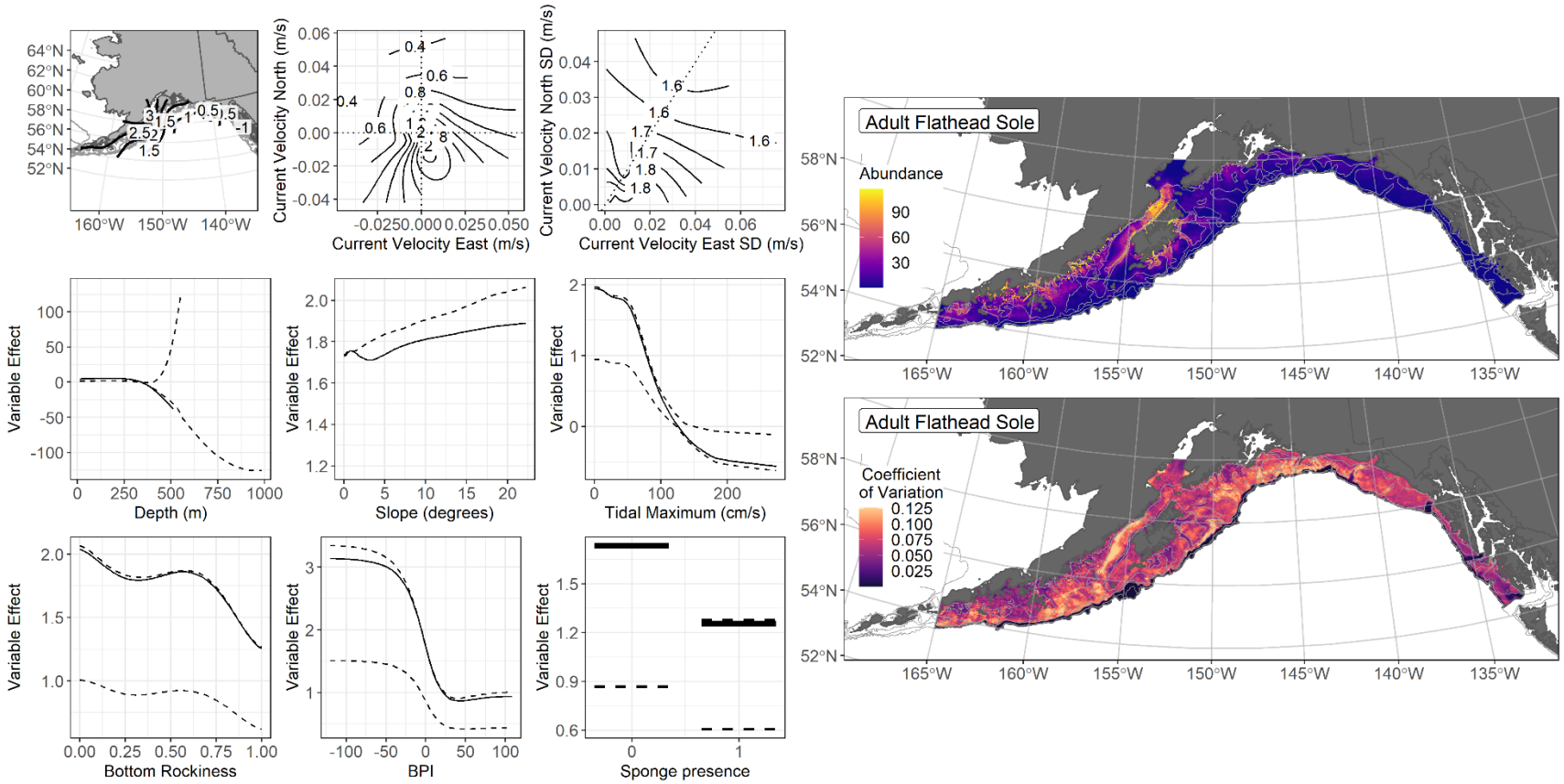

Figure 20. -- The top nine covariate effects (left panel) on ensemble-predicted adult flathead sole numerical abundance across the Gulf of Alaska (upper right panel) along with the coefficient of variation (CV) of the ensemble predictions (lower right panel).

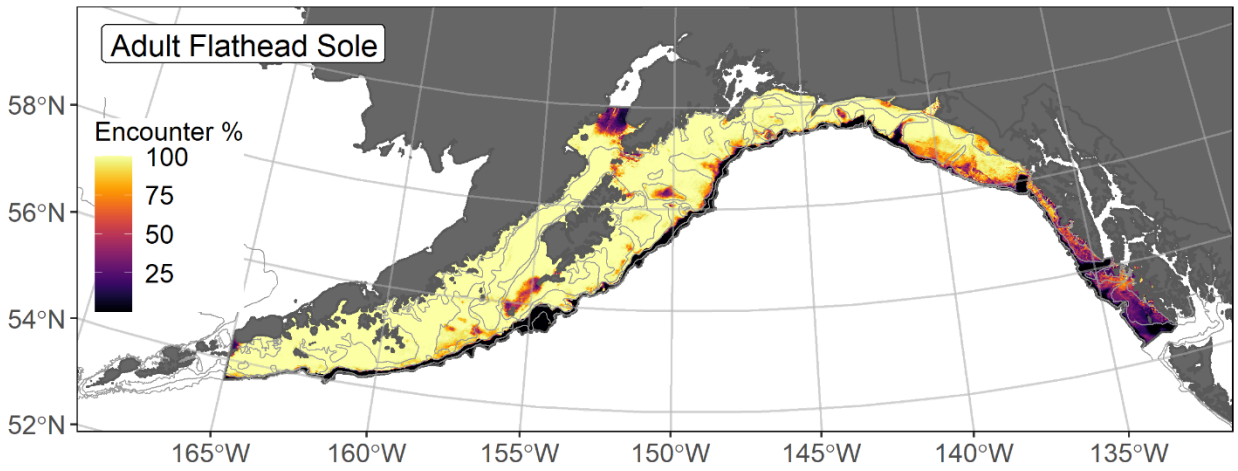

Figure 21. -- Encounter probability of adult flathead sole from AFSC RACE-GAP summer bottom trawl surveys (1993–2019) of the Gulf of Alaska with the 100 m, 200 m, and 700 m isobaths indicated.

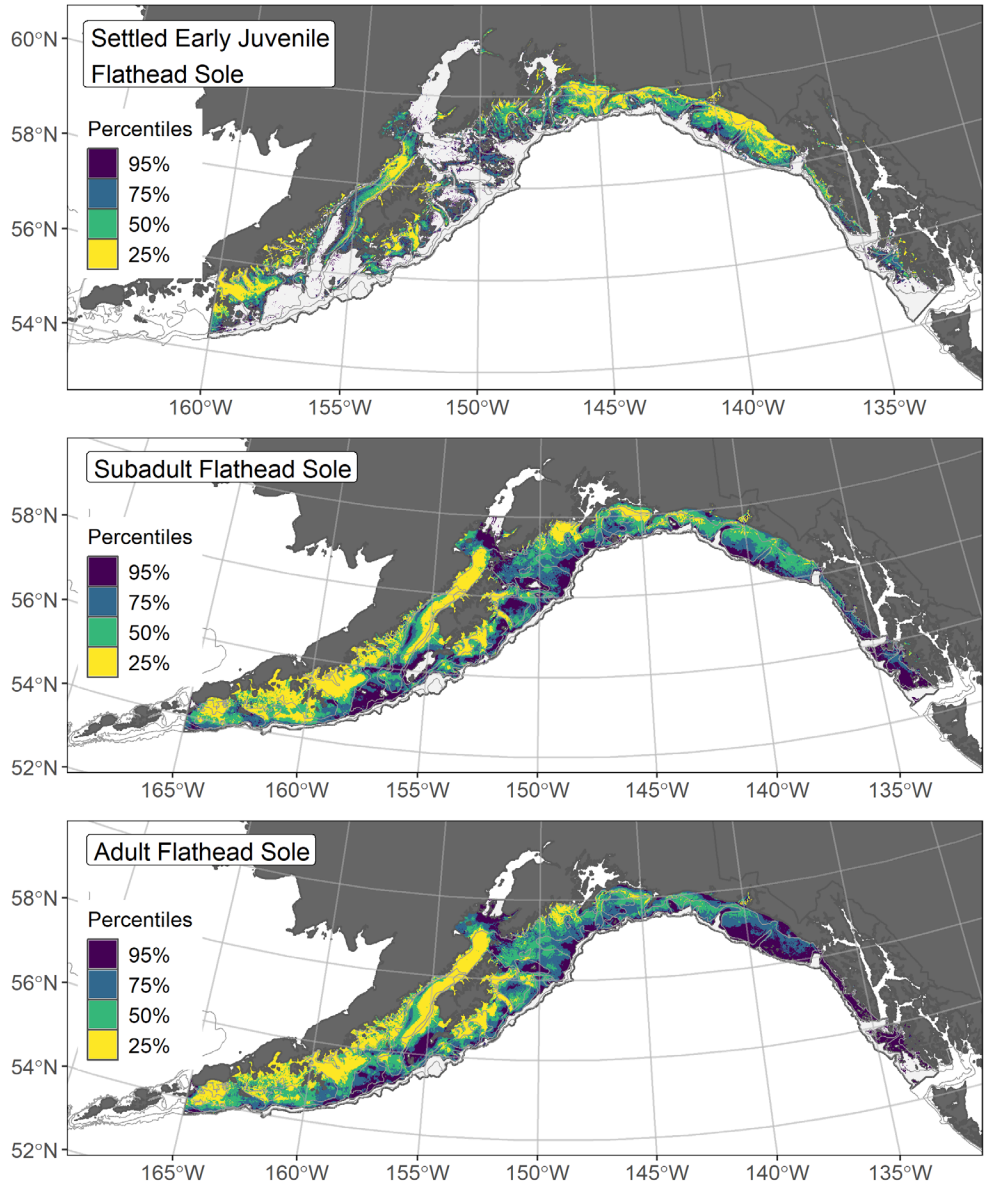

Figure 22. -- Essential fish habitat (EFH) is the area containing the top 95% of occupied habitat (defined as greater than 5% predicted probability of suitable habitat) for settled early juvenile (top panel) flathead sole from an SDM fitted to their distribution in Gulf of Alaska (GOA) mixed gear-type summer surveys (1989–2019), and for subadults (middle panel) and adults (bottom panel) is the area containing the top 95% of occupied habitat (defined as model estimated encounter probabilities greater than 5%) from an SDM ensemble fitted to flathead sole distribution and abundance in AFSC RACE-GAP GOA summer bottom trawl surveys (1993–2019) with 100 m, 200 m, and 700 m isobaths indicated; within the EFH area map are the subareas of the top 25% (EFH hot spots), top 50% (core EFH area), and top 75% (principal EFH area).

Rex sole (*Glyptocephalus zachirus*)

Rex sole (*Glyptocephalus zachirus*) is a widely distributed flatfish with a native range that extends from Baja California to the western Gulf of Alaska (Mecklenburg et al. 2002). This study uses a length range for settled early juvenile rex sole of 60–140 mm (Abookire 2006, Abookire and Bailey 2007, Doyle et al. 2019), consistent with catches from the NFAA and ADFG small mesh bottom trawl survey. The majority of rex sole reach maturity (L_{50}) at 352 mm (Abookire 2006). Adults may grow to 800 mm (RACE unpubl. data) and can be found from the surface to depths of 850 m (Abookire and Bailey 2007). Spawning occurs offshore and in deeper water along the edge of the continental slope, with most juveniles occurring inshore and in shallower water. This species has an extended spawning period estimated to last from October to May in the GOA (Abookire 2006) and an extended larval stage that can last from nine months to two years (Abookire 2006, Pearcy et al. 1977). Significant regional differences in rex sole growth rates have been observed in the GOA and along the Oregon coast, with Alaska populations having higher growth rates (Abookire 2006). Any redefinition of the length-based life stage breaks for rex sole (and Dover sole) based on temporal and spatial differences will require additional research[13]. Rex sole are managed independently as an individual stock in the Gulf of Alaska (McGilliard and Palsson 2017).

Settled early juvenile rex sole distribution predicted from mixed gear-type summer surveys in the Gulf of Alaska -- Settled early juvenile rex sole (N = 480) caught in multiple mixed gear-type summer surveys (1989–2019), using large and small mesh bottom trawls and purse and beach seines, were widely distributed across the GOA (Fig. 23). Settled early juvenile rex sole presence records from multiple surveys were combined in a habitat-related MaxEnt SDM predicting suitable habitat probabilities for this life stage. The best model had a β-multiplier of 3.0 and an AUC of 0.85 (Table 12). The covariates contributing the majority of influence to the MaxEnt model (85%) were tidal current speed, terrain aspect, BPI, and rockiness (Table 13). The highest predicted probabilities of suitable habitat for early juvenile rex sole in the GOA occurred along the Alaska Peninsula from the western GOA through the Shelikof Strait and into southeast Alaska, including areas of low-lying terrain such as channels and glacial troughs with low occurrence of rocky substrate (Fig. 24). The standard deviation among k-folds as a result of cross-validation for the final SDM was higher in western GOA and in Prince William Sound.

[13] A request from the stock author review to redefine how life stages are incorporated in the SDM ensemble for this species with spatially varying sub-regional growth in future EFH mapping will be included as a research recommendation from the 2023 EFH 5-year Review.

Subadult rex sole abundance and distribution predicted from RACE-GAP summer bottom trawl surveys in the Gulf of Alaska -- Subadult rex sole (N = 4,744) caught in GOA RACE-GAP summer bottom trawl surveys (1993–2019) were common and broadly distributed across the continental shelf and upper continental slope (Fig. 25). Concentrations of higher abundance catches were often associated with glacial troughs. Five SDMs considered for inclusion in the ensemble to predict numerical abundance of subadult rex sole in the GOA converged (Table 14); the GAM_{nb} was eliminated by skill testing based on RMSE. The four remaining, best-performing SDMs were nearly equally weighted in the final ensemble. The final ensemble was a good fit to the observed subadult rex sole distribution and abundance data. The ensemble was good at predicting high and low abundance catches (ρ = 0.56) and discriminating presence-absence (AUC = 0.80), and fair at explaining deviance (PDE = 0.32). Bottom depth, geographic location, tidal current speed, and BPI accounted for 86.1% of the contribution among covariates to the deviance explained by the ensemble (Table 13). Subadult rex sole abundance was highest in the Yakutat and southeastern Alaska management areas at depths around 350 m with reduced tidal current speeds (Fig. 26). The CV of abundance predictions was higher in Cook Inlet, around Kodiak Island, and into the western GOA. The probability of encountering subadult rex sole was high throughout the GOA, with notable exceptions in Cook Inlet and off southwestern Kodiak Island (Fig. 27).

Adult rex sole abundance and distribution predicted from RACE-GAP summer bottom trawl surveys in the Gulf of Alaska -- Adult rex sole (N = 4,455) caught in GOA RACE-GAP summer bottom trawl surveys (1993–2019) were distributed similarly to the subadults, across the continental shelf and upper slope with higher abundance catches associated with the glacial troughs (Fig. 28). Five SDMs considered for inclusion in the ensemble to predict numerical abundance of adult rex sole in the GOA converged (Table 14); the GAM_{nb} was eliminated by skill testing. The final ensemble was a good fit to the observed adult rex sole distribution and abundance data. The ensemble was good at predicting high and low abundance catches (ρ = 0.59) and discriminating presence-absence (AUC = 0.80), and fair at explaining deviance (PDE = 0.37). Bottom depth, geographic location, and tidal current speed accounted for 72.6% of the contribution among covariates to the deviance explained by the final ensemble (Table 13). Adult rex sole abundance was predicted to be highest in glacial troughs south and west of the outlet to Shelikof Strait and south and east of Kodiak Island (Fig. 29). The CV of abundance predictions was highest between lower Cook Inlet and northern Kodiak Island in upper Shelikof Strait. The probability of encountering adult rex sole was high throughout most of the GOA study area, with notable exceptions off southwestern Kodiak Island, in Cook Inlet, and the nearshore areas of the Yakutat and southeast Alaska management areas (Fig. 30).

Essential Fish Habitat of three life stages of rex sole in the Gulf of Alaska -- Habitat-related predictions of rex sole life stage distribution and abundance from summer surveys of the GOA (mixed gear-type summer surveys (1989–2019) and RACE-GAP bottom trawl surveys (1993–2019)) were mapped as EFH areas and subareas (Fig. 31). Settled early juvenile rex sole EFH occurred across the continental shelf with exceptions in shallow water (< 100 m) from Cook Inlet around Kodiak Island and into the western GOA. Core EFH areas and EFH hot spots for the settled early juveniles were present from the southeastern to the western extent of the survey area, with large hot spots over the shelf from southeast Alaska into the Kodiak management area as well as in the Shelikof Strait. The EFH areas for subadult and adult rex sole extended from southeast Alaska to the western GOA with a few similar gaps to those observed for settled early juveniles over shallow banks on the continental shelf. The core EFH areas and EFH hot spots of subadults generally overlapped those of adult rex sole, though the subadult hot spots extended from the Kodiak management area into southeast Alaska while the adult hot spots extended from the Yakutat into the Chirikof and Shumagin management areas.

Table 12. -- Maximum entropy model (MaxEnt) used to construct Essential Fish Habitat (EFH) for settled early juvenile rex sole: regularization multiplier (β); k-fold cross-validation root-mean-square-error (RMSE), area under the receiver operating characteristic curve (AUC), and EFH area (km^2).

Model	**β**	**RMSE**	**AUC**	**EFH area (km^2)**
MaxEnt	3.0	1.07	0.85	209,900

Table 13. -- Covariates retained in the a) settled early juvenile habitat-related maximum entropy (MaxEnt) species distribution model (SDM), and b) subadult and c) adult SDM final ensembles for rex sole with the percent contribution of each covariate to the deviance explained by the SDMs and the cumulative deviance explained: SD = standard deviation and BPI = bathymetric position index.

rex sole

	Covariate	**% Contribution**	**Cumulative %**
a) settled early juvenile	tidal maximum	26.2	26.2
	aspect north	18.8	45.0
	BPI	15.1	60.1
	aspect east	13.4	73.5
	rockiness	11.1	84.6
	bottom depth	6.9	91.5
	pennatulacean presence	3.9	95.5
	slope	2.1	97.6
	curvature	1.0	98.6
	bottom temperature	0.8	99.4
	sponge presence	0.6	100.0
b) subadult	bottom depth	37.6	37.6
	location	33.5	71.1
	tidal maximum	8.6	79.7
	BPI	6.4	86.1
	current SD	2.8	88.9
	rockiness	2.8	91.7
	current	2.0	93.7
	bottom temperature	1.7	95.4
	aspect north	1.5	96.9
	sponge presence	1.1	98.0
	aspect east	0.6	98.6
	slope	0.5	99.1
	pennatulacean presence	0.4	99.5
	curvature	0.4	99.9
	coral presence	0.1	100.0
c) adult	bottom depth	33.9	33.9
	location	27.1	60.9
	tidal maximum	11.7	72.6
	bottom temperature	5.5	78.1
	current	5.3	83.4
	BPI	3.6	87.0
	rockiness	3.2	90.2
	aspect north	2.9	93.1
	current SD	2.6	95.7

rex sole

Covariate	% Contribution	Cumulative %
sponge presence	2.2	97.9
slope	1.2	99.1
aspect east	0.5	99.6
pennatulacean presence	0.2	99.8
curvature	0.2	100.0

Table 14. -- Constituent species distribution models (SDMs) used to construct Essential Fish Habitat (EFH) for a) subadult and b) adult rex sole: MaxEnt = Maximum entropy; paGAM = presence-absence generalized additive model; hGAM = zero-adjusted Poisson hurdle GAM; GAM_P = standard Poisson GAM; GAM_{nb} = standard negative-binomial GAM; RMSE = root mean square error; ρ (*rho*) = Spearman's rank correlation coefficient; AUC = area under the receiver-operating characteristic curve; and PDE = Poisson deviance explained *. The "--" indicates that this model was not included in the final ensemble.

a) subadult rex sole

Models	**RMSE**	**Relative Weight**	**ρ**	**AUC**	**PDE**	**EFH area (km^2)**
MaxEnt	35.3	0.24	0.53	0.80	0.20	279,100
paGAM	35.0	0.24	0.52	0.79	0.22	281,800
hGAM	34.1	0.26	0.51	0.79	0.29	281,800
GAM_P	34.0	0.26	0.51	0.77	0.30	281,800
GAM_{nb}	35.5	0	--	--	--	--
ensemble	33.6	1	0.56	0.80	0.32	281,800

b) adult rex sole

Models	**RMSE**	**Relative Weight**	**ρ**	**AUC**	**PDE**	**EFH area (km^2)**
MaxEnt	38.5	0.24	0.60	0.83	0.26	272,700
paGAM	38.4	0.24	0.56	0.80	0.24	281,700
hGAM	36.5	0.26	0.49	0.80	0.35	277,500
GAM_P	36.6	0.26	0.49	0.74	0.34	277,800
GAM_{nb}	38.0	0	--	--	--	--
ensemble	36.3	1	0.59	0.80	0.37	280,100

* Refer to the Species Distribution Model Performance Metrics subsection within the Statistical Modeling section of the Methods for detailed descriptions of individual model performance metrics.

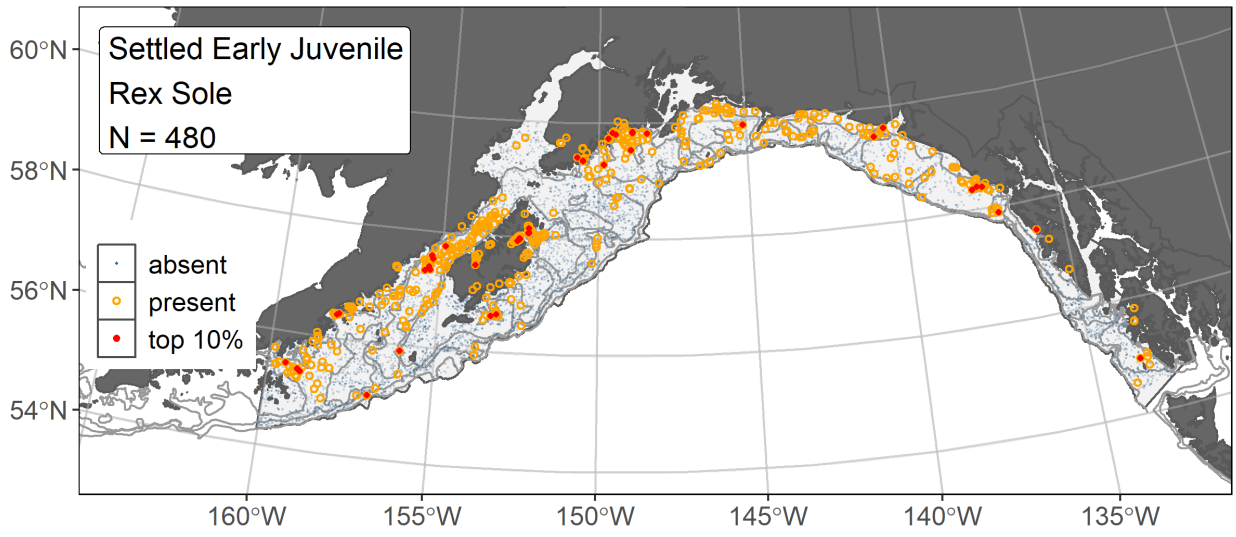

Figure 23. -- Distribution of settled early juvenile rex sole catches (N = 480) in mixed gear-type summer surveys of the Gulf of Alaska (1989–2019) with the 100 m, 200 m, and 700 m isobaths indicated; filled red circles indicate locations in top 10% of overall abundance, open orange circles indicate presence in remaining catches, and blue dots indicate stations sampled where the animals were not present.

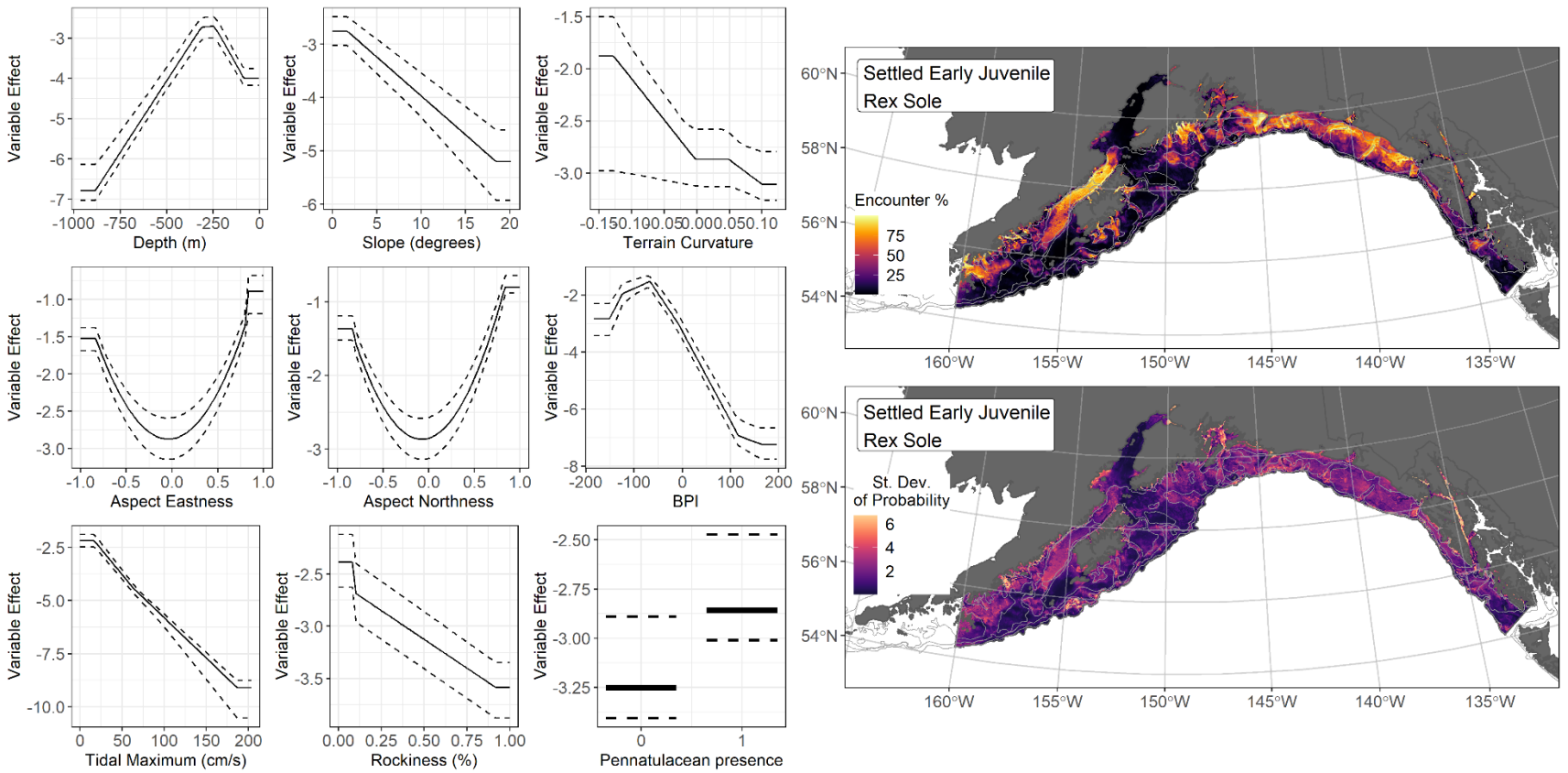

Figure 24. -- The top nine covariate effects (left panel) from a habitat-related species distribution model (MaxEnt) of settled early juvenile rex sole probability of suitable habitat in the Gulf of Alaska (upper right panel) with the standard deviation of the probability predictions (lower right panel).

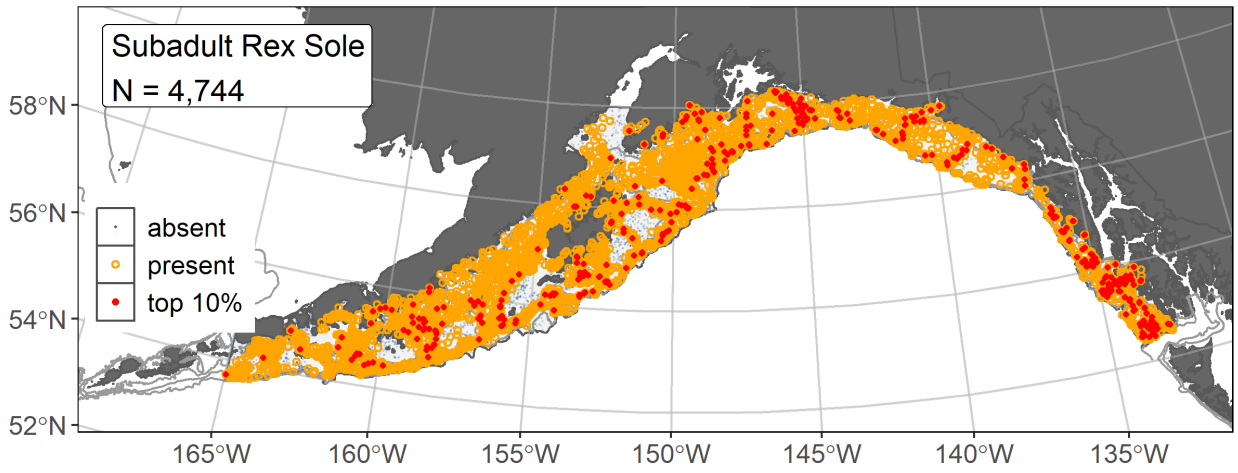

Figure 25. -- Distribution of subadult rex sole catches (N = 4,744) in 1993–2019 AFSC RACE-GAP summer bottom trawl surveys of the Gulf of Alaska with the 100 m, 200 m, and 700 m isobaths indicated; filled red circles indicate locations in top 10% of overall abundance, open orange circles indicate presence in remaining catches, and blue dots indicate stations sampled where the animals were not present.

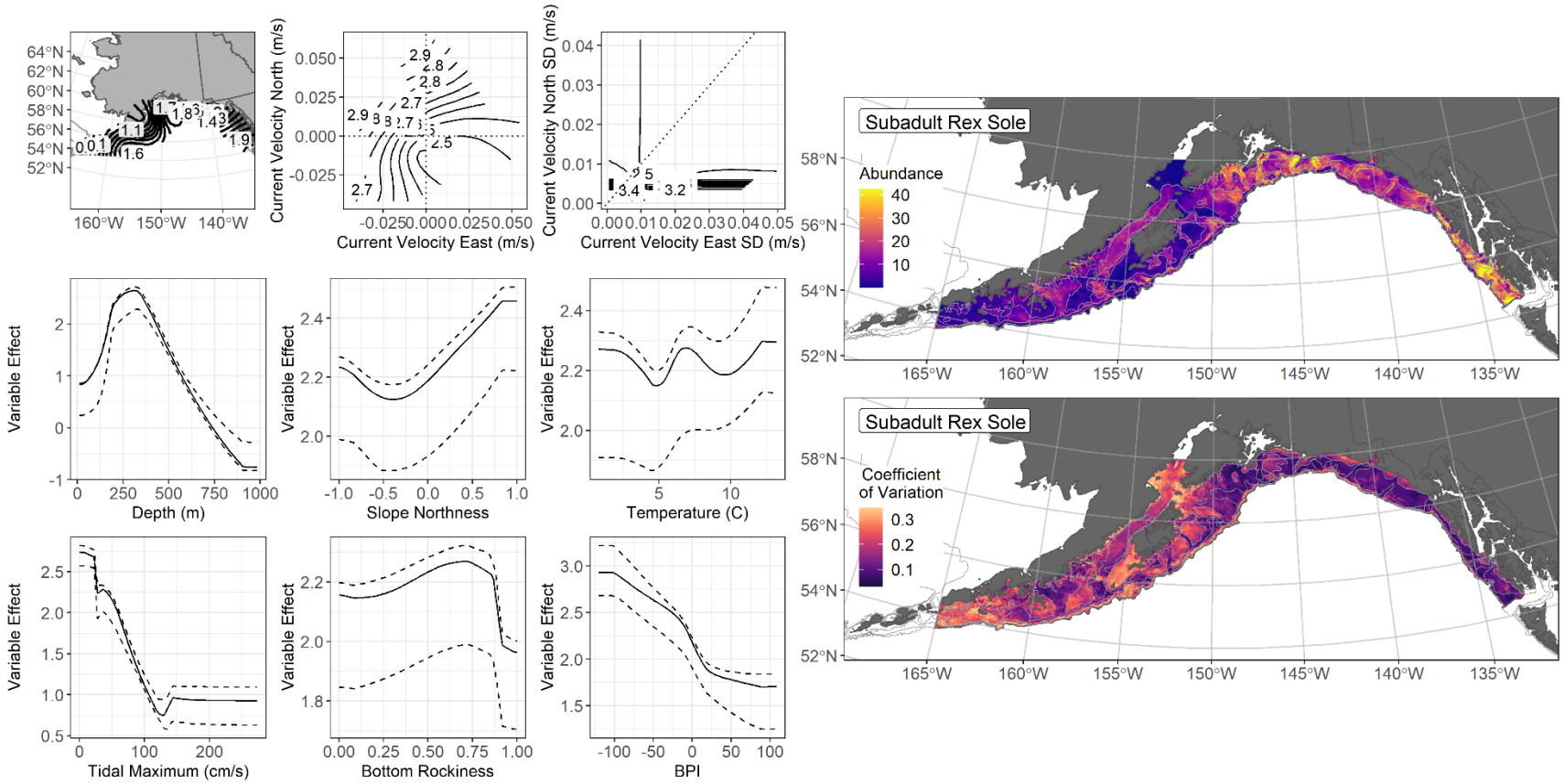

Figure 26. The top nine covariate effects (left panel) on ensemble-predicted subadult rex sole numerical abundance across the Gulf of Alaska (upper right panel) along with the coefficient of variation (CV) of the ensemble predictions (lower right panel).

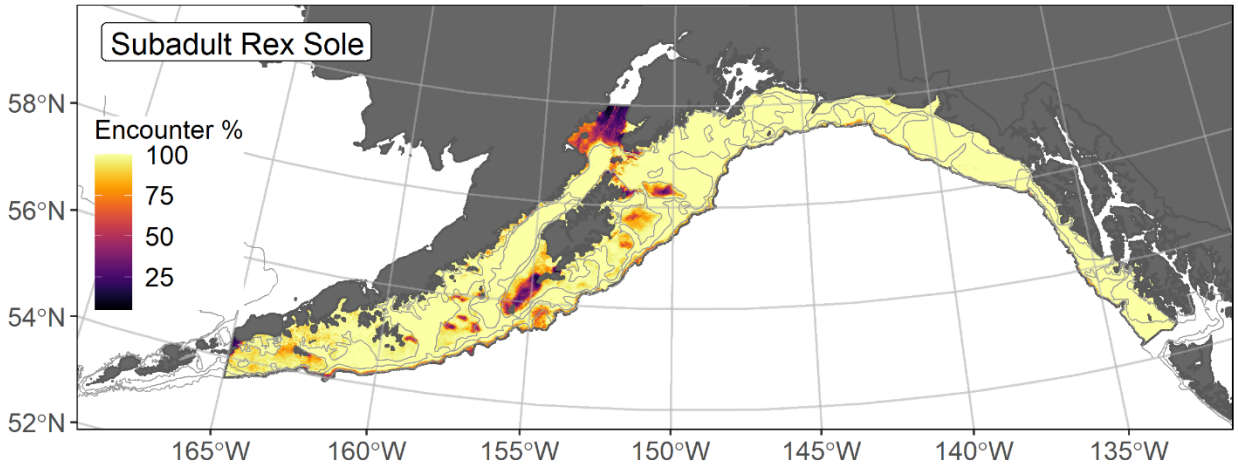

Figure 27. -- Encounter probability of subadult rex sole from AFSC RACE-GAP summer bottom trawl surveys (1993–2019) of the Gulf of Alaska with the 100 m, 200 m, and 700 m isobaths indicated.

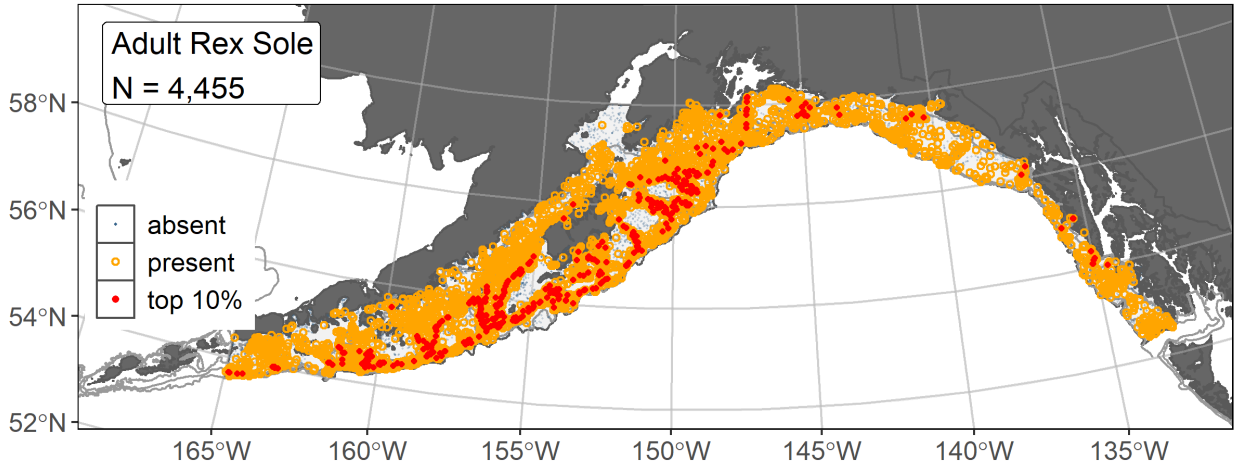

Figure 28. -- Distribution of adult rex sole catches (N = 4,455) in 1993–2019 AFSC RACE-GAP summer bottom trawl surveys of the Gulf of Alaska with the 100 m, 200 m, and 700 m isobaths indicated; filled red circles indicate locations in top 10% of overall abundance, open orange circles indicate presence in remaining catches, and blue dots indicate stations sampled where the animals were not present.

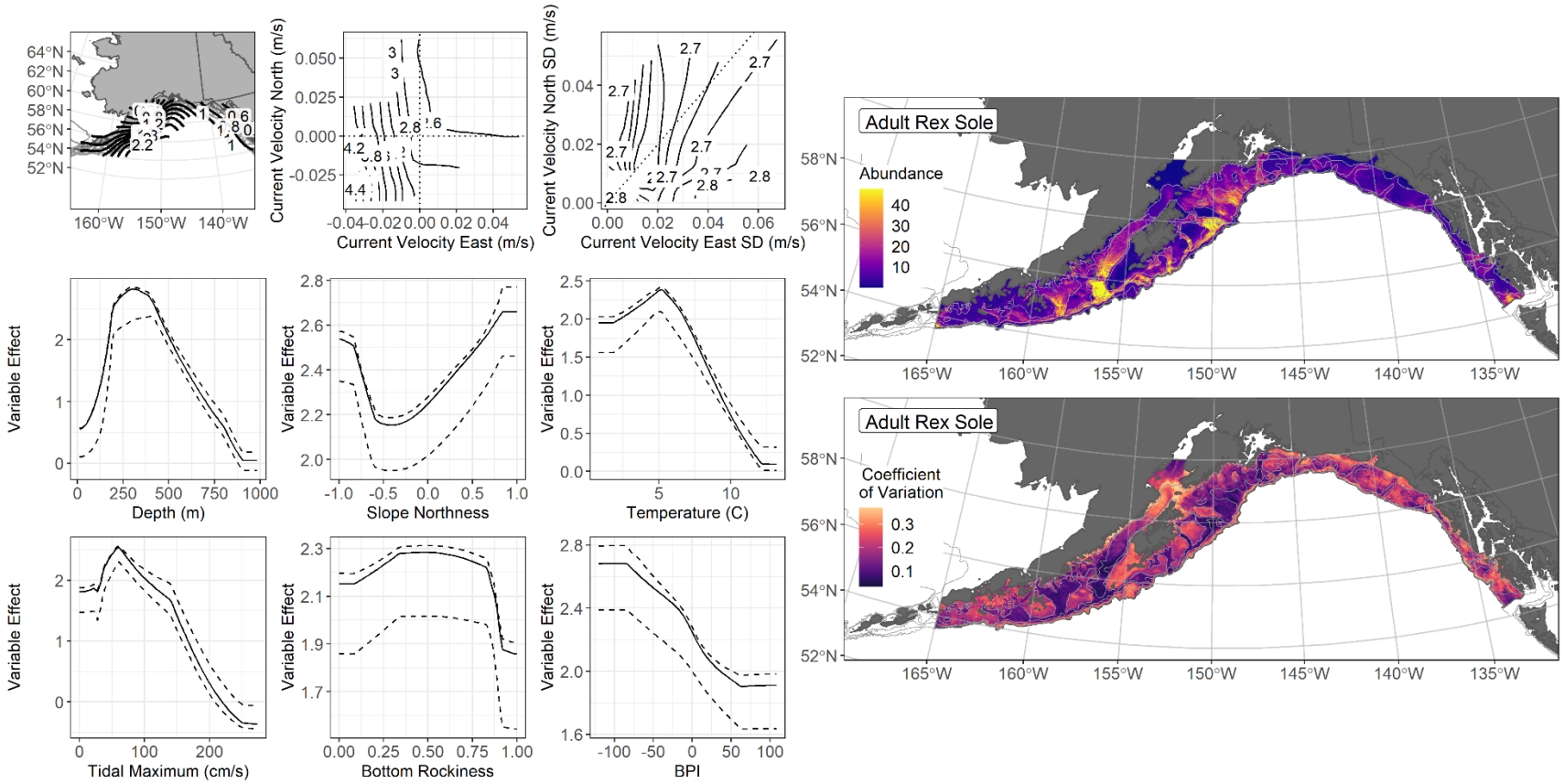

Figure 29. -- The top nine covariate effects (left panel) on ensemble-predicted adult rex sole numerical abundance across the Gulf of Alaska (upper right panel) along with the coefficient of variation (CV) of the ensemble predictions (lower right panel).

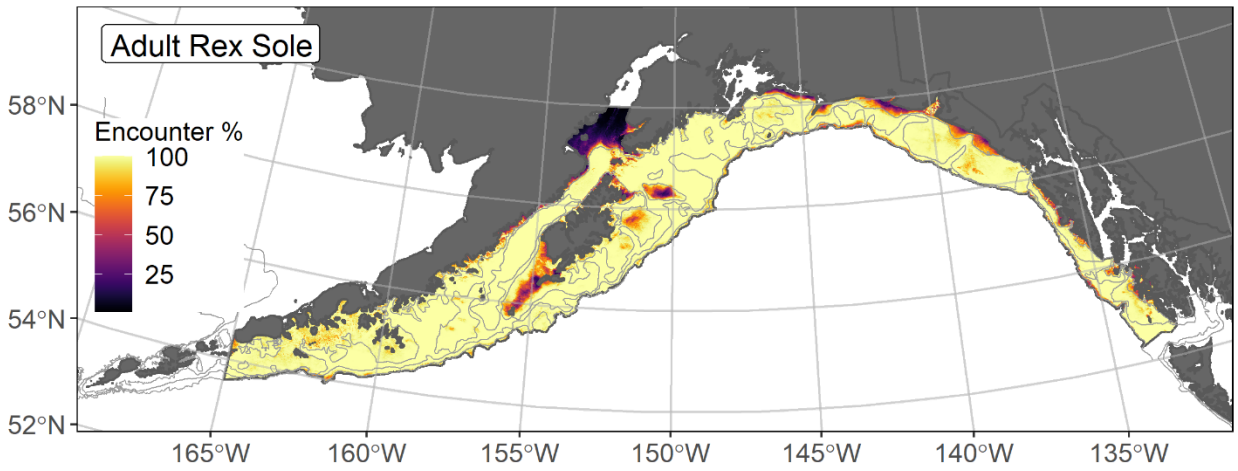

Figure 30. -- Encounter probability of adult rex sole from AFSC RACE-GAP summer bottom trawl surveys (1993–2019) of the Gulf of Alaska with the 100 m, 200 m, and 700 m isobaths indicated.

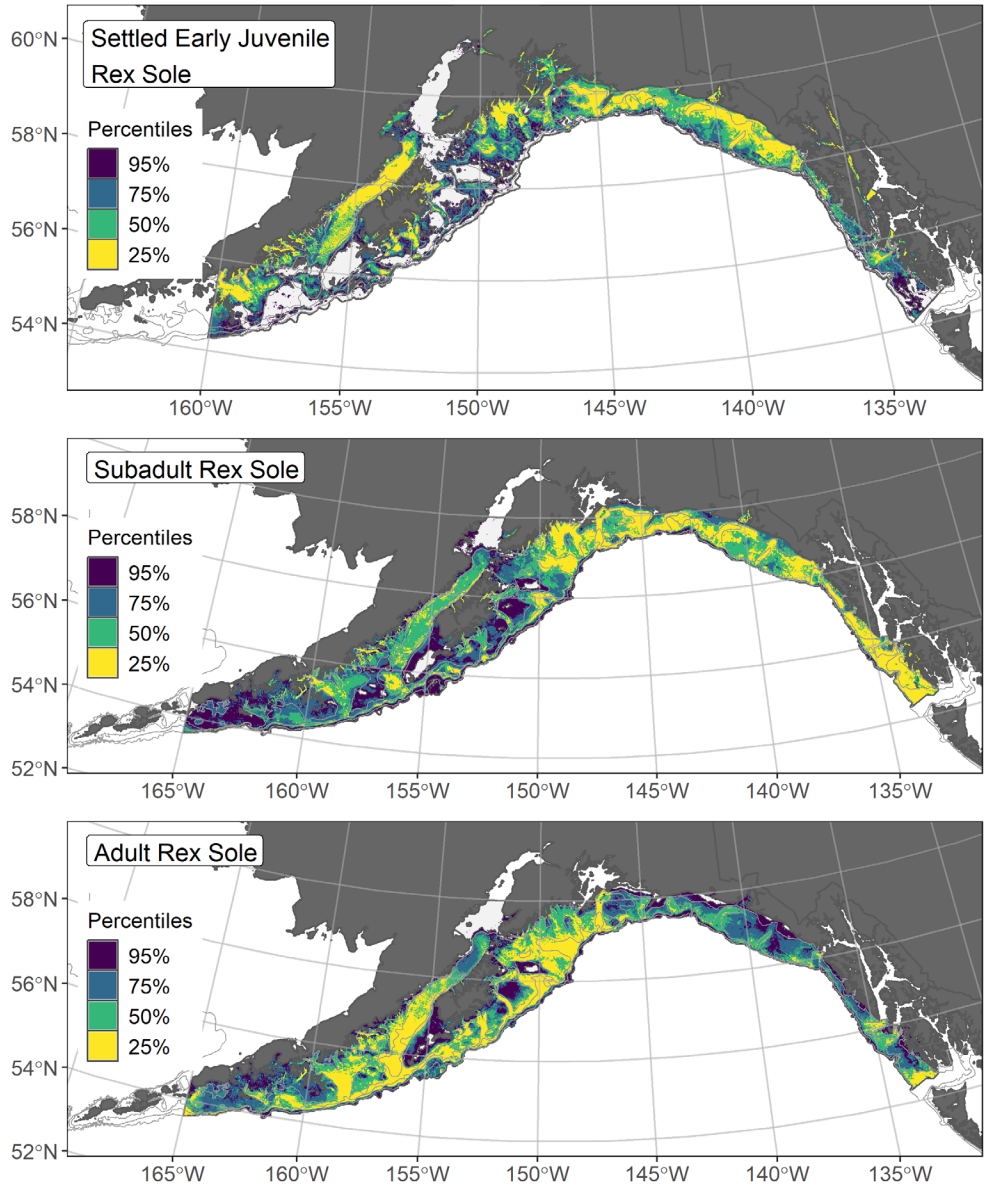

Figure 31. -- Essential fish habitat (EFH) is the area containing the top 95% of occupied habitat (defined as greater than 5% predicted probability of suitable habitat) for settled early juvenile (top panel) rex sole from an SDM fitted to their distribution in Gulf of Alaska (GOA) mixed gear-type summer surveys (1989–2019), and for subadults (middle panel) and adults (bottom panel) is the area containing the top 95% of occupied habitat (defined as model estimated encounter probabilities greater than 5%) from an SDM ensemble fitted to rex sole distribution and abundance in AFSC RACE-GAP GOA summer bottom trawl surveys (1993–2019) with 100 m, 200 m, and 700 m isobaths indicated; within the EFH area map are the subareas of the top 25% (EFH hot spots), top 50% (core EFH area), and top 75% (principal EFH area).

Dover sole (*Microstomus pacificus*)

Dover sole (*Microstomus pacificus*) is distributed from Baja California to the Aleutian Islands and into the southeastern Bering Sea (Mecklenburg et al. 2002). Length at 50% maturity (L_{50}) in the GOA (439 mm FL; Abookire and Macewicz 2003) was used to separate subadult and adult life stages of Dover sole for these analyses. Adults attain a size of up to 660 mm FL, and this species' depth range extends below 1200 m. Spawning occurs offshore and in deeper water along the edge of the continental slope, with most juveniles occurring inshore and in shallower water. Dover sole have a moderately extended spawning period from late January to early June in the GOA (Abookire 2006). Development in Dover sole appears to be complex and may exhibit significant regional and individual variation in the timing of metamorphosis and juvenile settlement (Pearcy 1977, Bailey et al. 2008). Juveniles and adults move to deeper water as they age, with the oldest individuals favoring deeper depths. Dover sole growth exhibits temporal and spatial patterns in the GOA, which are influenced by cohort and ontogenetic movement to deeper depth with age (McGilliard et al. 2019). Any redefinition of length-based life stage breaks for Dover sole (and rex sole) based on these differences will require additional research[14]. Dover sole are managed as a part of a three species "deepwater flatfish" stock complex that includes deepsea sole and Greenland turbot (McGilliard et al. 2019). There were too few deepsea sole or Greenland turbot catches in GOA RACE-GAP summer bottom trawl surveys (1993–2019) to support SDMs for these species. Dover sole are the one representative of this stock complex modeled in this study to map EFH.

Subadult Dover sole abundance and distribution predicted from RACE-GAP summer bottom trawl surveys in the Gulf of Alaska -- Subadult Dover sole (N = 3,710) caught in GOA RACE-GAP summer bottom trawl surveys (1993–2019) were distributed throughout the survey area with higher abundance catches typically associated with deeper stations (Fig. 32). Five SDMs considered for inclusion in the subadult Dover sole ensemble (Table 15); the GAM_{nb} was eliminated by skill testing. The four remaining best-performing SDMs were weighted by RMSE in the final ensemble, attaining a good overall fit to the observed distribution and abundance data for subadult Dover sole. The ensemble was excellent at predicting high and low abundance catches (ρ = 0.62), and good at discriminating presence-absence (AUC = 0.83) and explaining deviance (PDE = 0.46). Geographic location and bottom depth accounted for the majority of the covariate contribution (73.6%) to the deviance explained by the final ensemble (Table 16). The highest abundances of subadult Dover sole occurred in the glacial troughs of the Yakutat and southeastern Alaska management areas of the GOA (Fig. 32). The CV of ensemble

[14] A request from the stock author review to redefine how life stages are incorporated in the SDM ensemble for this species with spatially varying sub-regional growth in future EFH mapping will be included as a research recommendation from the 2023 EFH 5-year Review.

predictions was higher in the central and western GOA than off of Yakutat and southeastern Alaska. The probability of encountering subadult Dover sole was near zero in the western GOA, off southwestern Kodiak Island, and in southern Cook Inlet (Fig. 34).

Adult Dover sole abundance and distribution predicted from m RACE-GAP summer bottom trawl surveys in the Gulf of Alaska -- Adult Dover sole (N = 2,973) caught in GOA RACE-GAP summer bottom trawl surveys (1993–2019) were distributed across the continental shelf and onto the continental slope with many higher abundance catches associated with deeper depths (Fig. 35). Five SDMs were considered for inclusion in the adult Dover sole ensemble (Table 15); the GAM_{nb} was eliminated by skill testing. The remaining four best-performing SDMs were weighted similarly by RMSE in the final ensemble, which was a good fit overall to the observed adult Dover sole distribution and abundance data. The ensemble was excellent at predicting high and low abundance catches ($\rho = 0.62$), and good at discriminating presence-absence (AUC = 0.87) and explaining deviance (PDE = 0.42). Bottom depth and geographic location accounted for the majority of the contribution among covariates (65.7%) to the deviance explained by the final ensemble (Table 16). Adult Dover sole abundance was highest from the Kodiak management area into southeastern Alaska in the glacial troughs extending down the slope at depths around 400 m (Fig. 36). The CV of ensemble predictions was generally higher at shallower depths over the continental shelf. The probability of encountering adult Dover sole was near zero in the western GOA and at shallower depths throughout the study area (Fig. 37).

Essential Fish Habitat of subadult and adult Dover sole in the Gulf of Alaska -- Ensemble-predicted habitat-related numerical abundance of Dover sole life stages collected in RACE-GAP summer bottom trawl surveys of the GOA (1993–2019) was mapped as EFH areas and subareas (Fig. 38). EFH areas of subadults and adults covered similar spatial extents that included most of the GOA study area. Core EFH and EFH hot spots for both life stages were prominent in the central GOA and southeast Alaska. For subadult Dover sole, EFH hot spots were primarily located in the Kodiak, Yakutat, and southeastern Alaska management areas of the GOA while hot spots for adults were found in these areas and extended into the Chirikof area as well.

Table 15. -- Constituent species distribution models (SDMs) used to construct Essential Fish Habitat (EFH) for a) subadult and b) adult Dover sole: MaxEnt = Maximum entropy; paGAM = presence-absence generalized additive model; hGAM = zero-adjusted Poisson hurdle GAM; GAM_P = standard Poisson GAM; GAM_{nb} = standard negative-binomial GAM; RMSE = root mean square error; ρ (*rho*) = Spearman's rank correlation coefficient; AUC = area under the receiver-operating characteristic curve; and PDE = Poisson deviance explained *. The "--" indicates that this model was not included in the final ensemble.

a) subadult Dover sole

Models	RMSE	Relative Weight	ρ	AUC	PDE	EFH area (km^2)
MaxEnt	24.8	0.15	0.57	0.82	0.17	278,200
paGAM	18.4	0.26	0.60	0.83	0.38	281,400
hGAM	17.5	0.30	0.58	0.83	0.45	271,000
GAM_P	17.5	0.29	0.58	0.81	0.44	269,100
GAM_{nb}	18.9	0	--	--	--	--
ensemble	17.4	1	0.62	0.83	0.46	281,300

b) adult Dover sole

Models	RMSE	Relative Weight	ρ	AUC	PDE	EFH area (km^2)
MaxEnt	12.0	0.23	0.59	0.85	0.21	244,300
paGAM	11.6	0.24	0.61	0.86	0.33	277,700
hGAM	11.0	0.27	0.59	0.86	0.41	268,000
GAM_P	11.1	0.26	0.58	0.83	0.39	270,000
GAM_{nb}	11.8	0	--	--	--	--
ensemble	11.0	1	0.62	0.87	0.42	272,900

* Refer to the Species Distribution Model Performance Metrics subsection within the Statistical Modeling section of the Methods for detailed descriptions of individual model performance metrics.

Table 16. -- Covariates retained in the a) subadult and b) adult Dover sole species distribution model (SDM) final ensembles, the percent contribution to the ensemble deviance explained by each covariate, and the cumulative deviance explained: SD = standard deviation and BPI = bathymetric position index.

Dover sole	**Covariate**	**% Contribution**	**Cumulative %**
a) subadult	location	41.5	41.5
	bottom depth	32.2	73.6
	current	6.0	79.7
	slope	4.7	84.4
	bottom temperature	4.1	88.5
	tidal maximum	3.1	91.6
	current SD	1.7	93.3
	BPI	1.7	95.0
	rockiness	1.6	96.6
	aspect east	1.1	97.7
	aspect north	1.1	98.8
	sponge presence	0.7	99.5
	pennatulacean presence	0.3	99.8
	coral presence	0.1	99.9
b) adult	bottom depth	35.3	35.3
	location	30.3	65.7
	current	6.6	72.3
	tidal maximum	6.0	78.3
	rockiness	5.3	83.6
	bottom temperature	4.4	88.0
	slope	3.3	91.3
	current SD	2.6	93.9
	BPI	2.3	96.2
	aspect north	1.8	98.0
	aspect east	1.6	99.6
	curvature	0.4	100.0

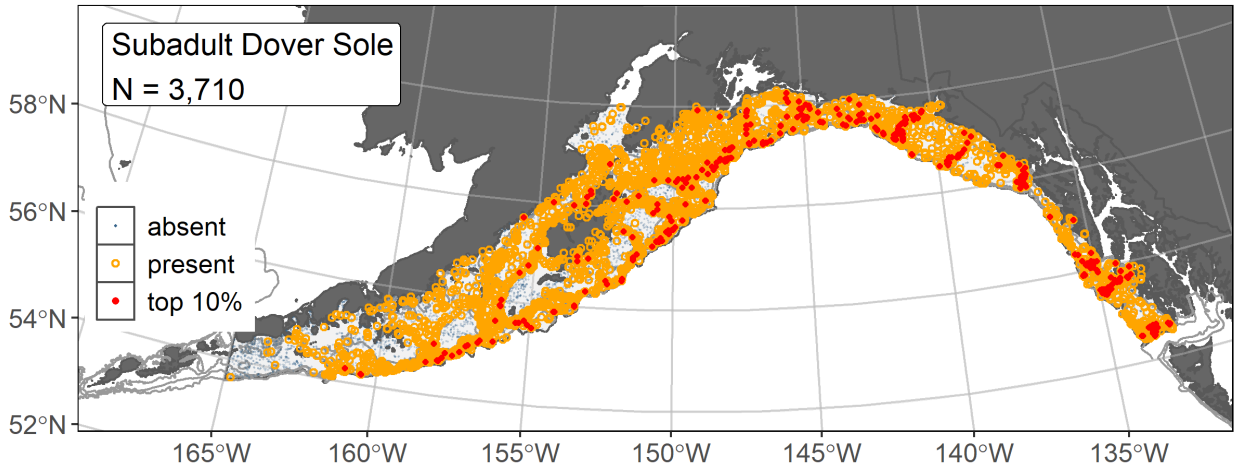

Figure 32. -- Distribution of subadult Dover sole catches (N = 3,710) in 1993–2019 AFSC RACE-GAP summer bottom trawl surveys of the Gulf of Alaska with the 100 m, 200 m, and 700 m isobaths indicated; filled red circles indicate locations in top 10% of overall abundance, open orange circles indicate presence in remaining catches, and blue dots indicate stations sampled where the animals were not present.

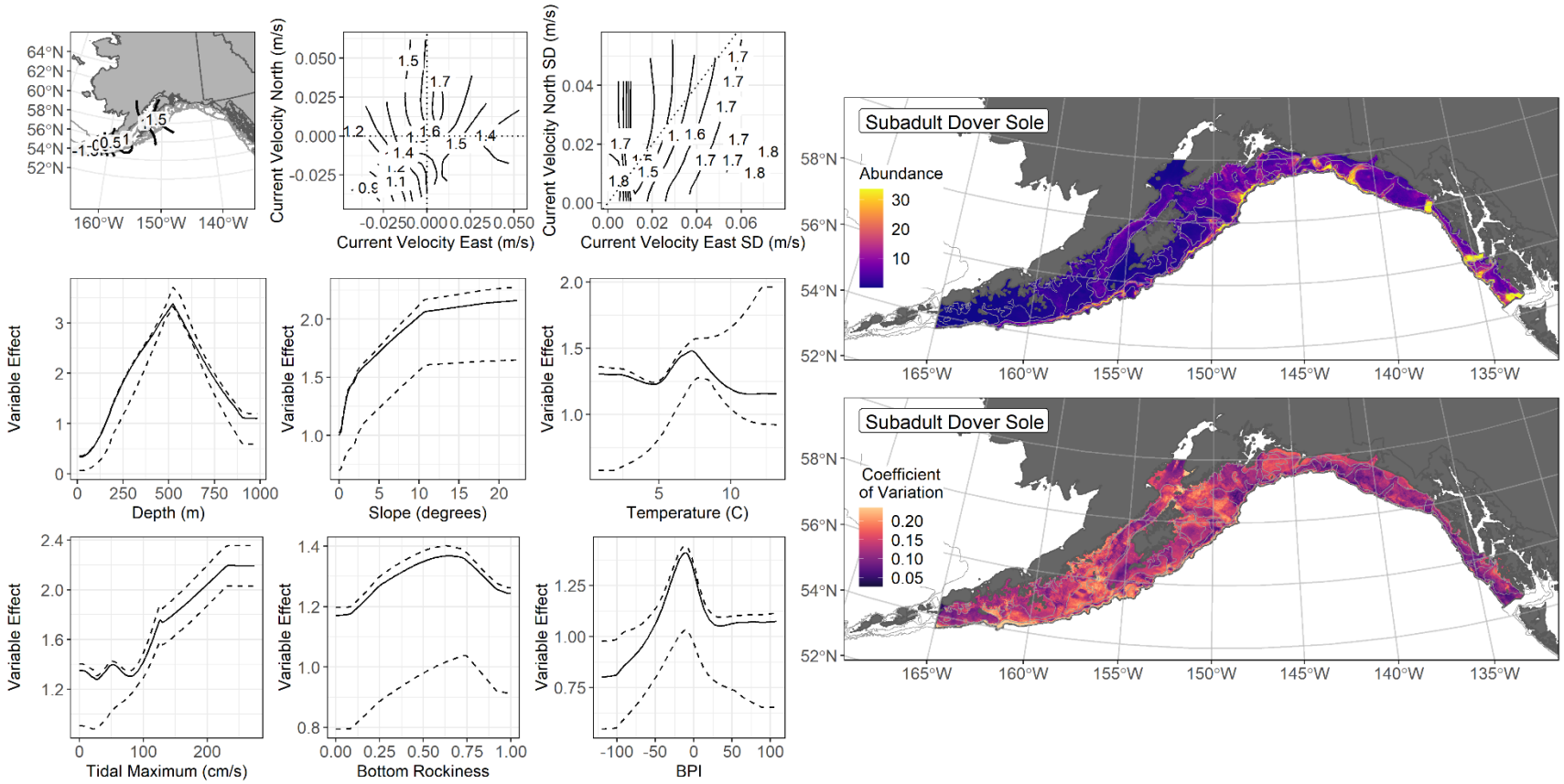

Figure 33. -- The top nine covariate effects (left panel) on ensemble-predicted subadult Dover sole numerical abundance across the Gulf of Alaska (upper right panel) along with the coefficient of variation (CV) of the ensemble predictions (lower right panel).

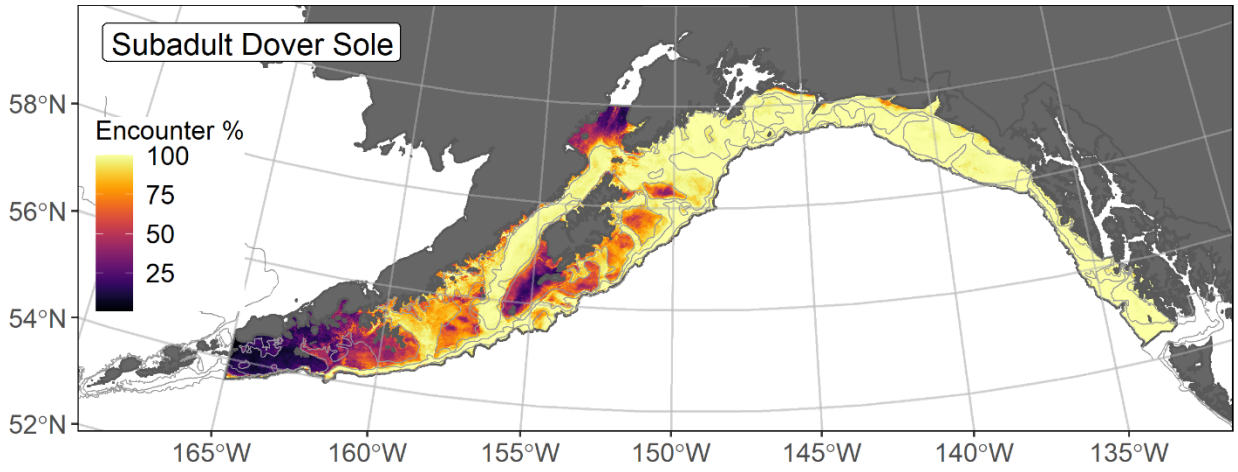

Figure 34. -- Encounter probability of subadult Dover sole from AFSC RACE-GAP summer bottom trawl surveys (1993–2019) of the Gulf of Alaska with the 100 m, 200 m, and 700 m isobaths indicated.

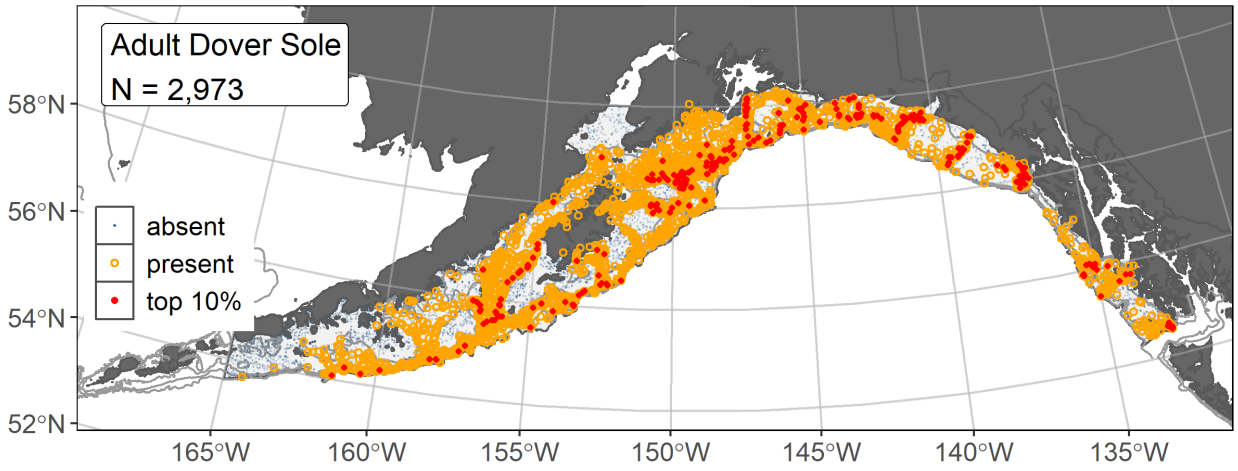

Figure 35. -- Distribution of adult Dover sole catches (N = 2,973) in 1993–2019 AFSC RACE-GAP summer bottom trawl surveys of the Gulf of Alaska with the 100 m, 200 m, and 700 m isobaths indicated; filled red circles indicate locations in top 10% of overall abundance, open orange circles indicate presence in remaining catches, and blue dots indicate stations sampled where the animals were not present.

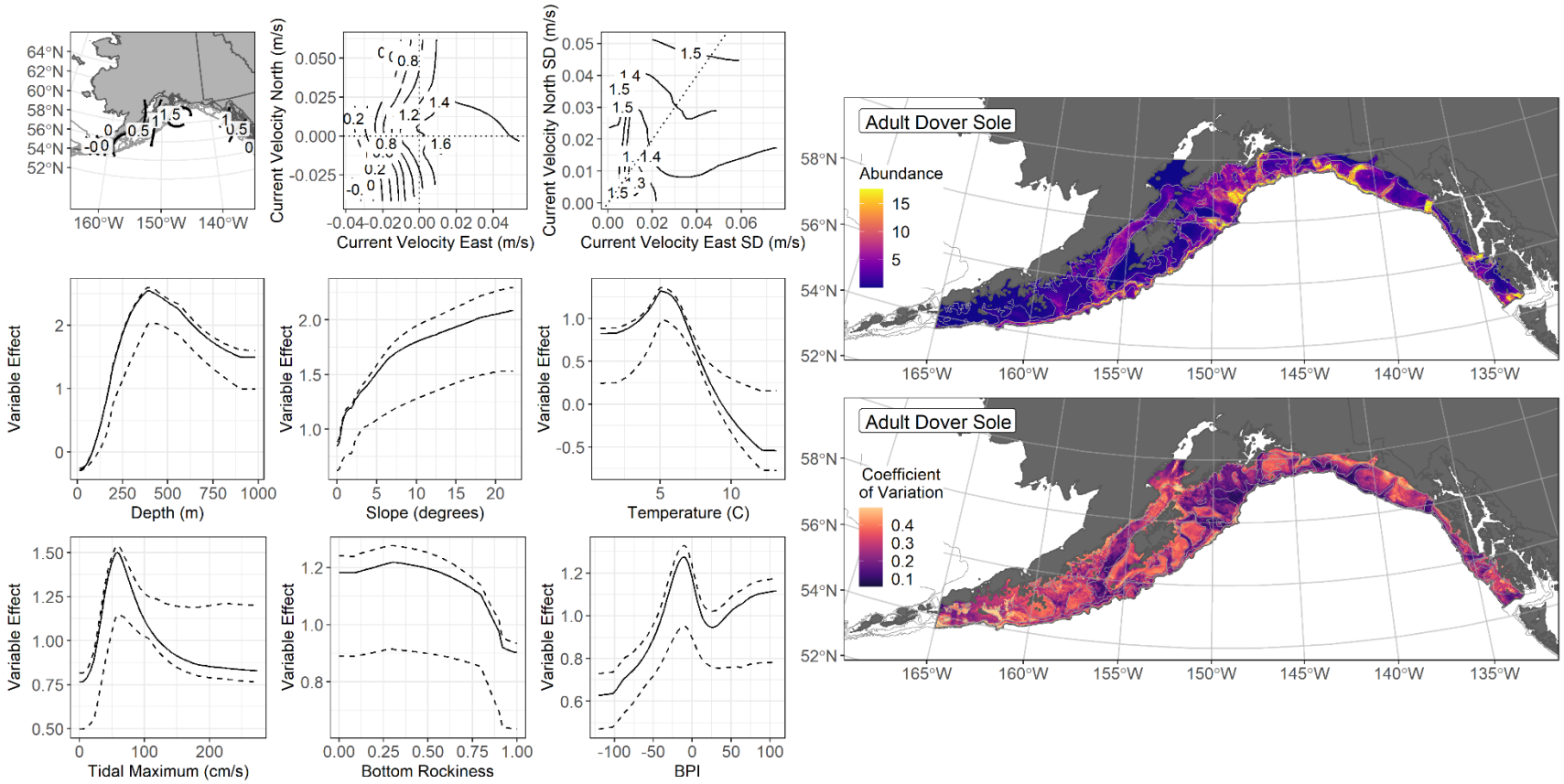

Figure 36. -- The top nine covariate effects (left panel) on ensemble-predicted adult Dover sole numerical abundance across the Gulf of Alaska (upper right panel) with the coefficient of variation (CV) of the ensemble predictions (lower right panel).

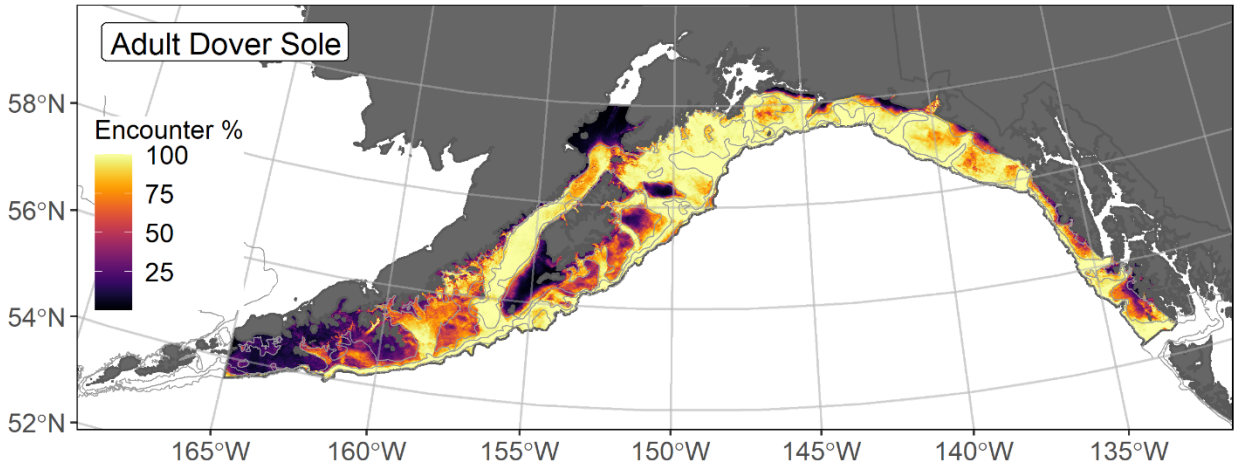

Figure 37. -- Encounter probability of adult Dover sole from AFSC RACE-GAP summer bottom trawl surveys (1993–2019) of the Gulf of Alaska with the 100 m, 200 m, and 700 m isobaths indicated.

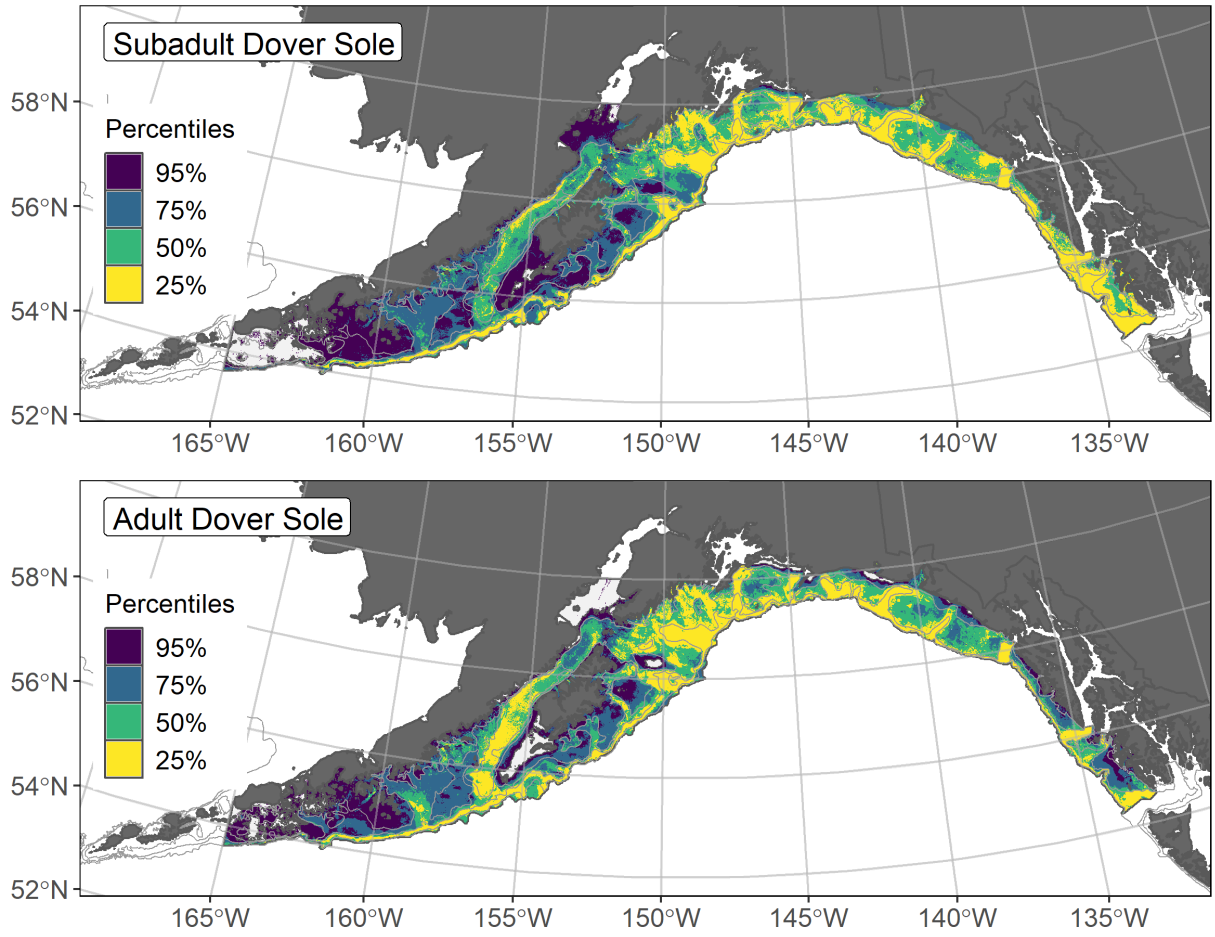

Figure 38. -- Essential fish habitat (EFH) is the area containing the top 95% of occupied habitat (defined as model estimated encounter probabilities greater than 5%) from an SDM ensemble fitted to subadult (top panel) and adult (bottom panel) Dover sole distribution and abundance in AFSC RACE-GAP summer bottom trawl surveys (1993–2019) with 100 m, 200 m, and 700 m isobaths indicated; within the EFH area map are the subareas of the top 25% (EFH hot spots), top 50% (core EFH area), and top 75% (principal EFH area) of habitat-related, ensemble-predicted numerical abundance.

Shallow water flatfish complex

In the GOA, the shallow water flatfish stock complex is comprised of Alaska plaice, butter sole, English sole, northern and southern rock soles, sand sole, starry flounder, and yellowfin sole (Turncock et al. 2017b). Additional "other flatfish" species with relatively low biomass are also included in this group; Pacific sanddab, petrale sole, and slender sole (NPFMC 2020). In GOA RACE-GAP summer bottom trawl survey catches (1993–2019) and mixed gear-type summer surveys (1989–2019), all member species except sand sole were common enough (N > 50) to support SDMs of probability of suitable habitat or habitat-related abundance to map EFH. To map the EFH of the shallow water flatfish complex, the subadult and adult SDMs of these species were combined additively to generate a composite habitat-related abundance and EFH map, which represents the EFH of shallow water flatfish complex species where an individual EFH map was not possible due to insufficient data[15].

Shallow water flatfish abundance and distribution predicted from RACE-GAP summer bottom trawl surveys in the Gulf of Alaska -- Habitat-related, ensemble-predicted numerical abundance was combined for the subadult and adult life stages of shallow water flatfish species to represent this stock complex in the GOA and mapped along with the combined encounter probability and EFH area (Fig. 1). The composite, ensemble-predicted abundance of the shallow water flatfish reflects the higher abundance catches of certain species on the continental shelf of the GOA, notably the rock soles. Encounter probabilities for shallow water flatfish were higher throughout the GOA continental shelf except for Shelikof Strait and other deeper glacial troughs. Encounter probability was also low along the continental slope.

Essential Fish Habitat of the shallow water flatfish stock complex in the Gulf of Alaska -- EFH of the shallow water flatfish stock complex extended from southeast Alaska in the eastern GOA through the western GOA boundary of the study area at 165°W (Fig. 1). Core EFH area was limited to the bathymetric rises and inshore areas of the GOA continental shelf. EFH hot spots occurred in nearshore areas throughout the GOA, on the banks south of Kodiak Island, and bathymetric rises to the west.

[15] 50 CFR 600.815(a)(1)(iv)(E).

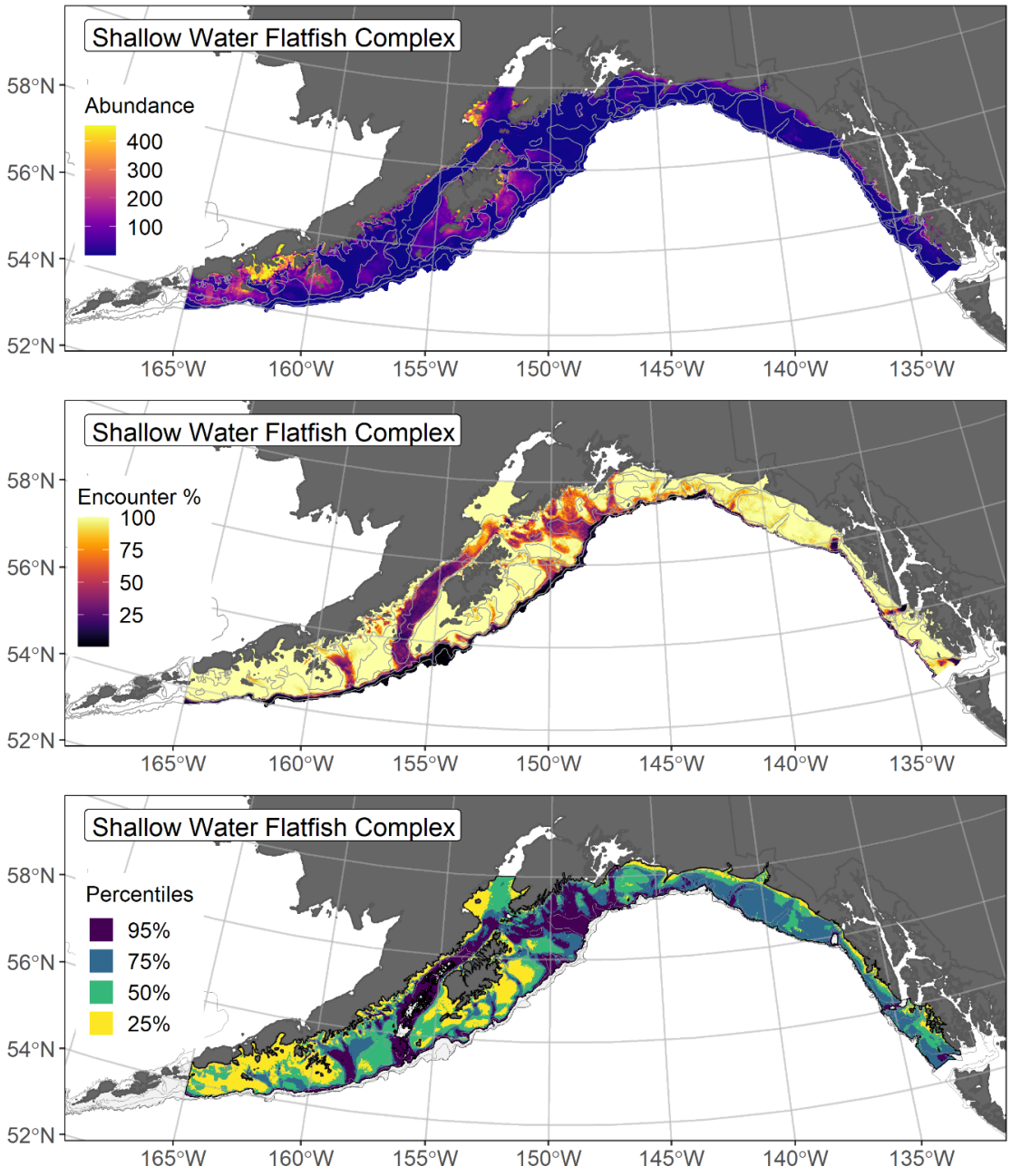

Figure 39. -- Composite habitat-related, ensemble-predicted numerical abundance (top panel), encounter probability (middle panel), and essential fish habitat (EFH) (the area containing the top 95% of occupied habitat defined as model estimated encounter probabilities greater than 5%) (bottom panel) of the shallow water flatfish complex from the Gulf of Alaska in AFSC RACE-GAP summer bottom trawl surveys (1993–2019) with 100 m, 200 m, and 700 m isobaths indicated; within the EFH area map are the subareas of the top 25% (EFH hot spots), top 50% (core EFH area), and top 75% (principal EFH area) of habitat-related, ensemble-predicted numerical abundance.

Alaska plaice (*Pleuronectes quadrituberculatus*)

Alaska plaice (*Pleuronectes quadrituberculatus*) is a flatfish species distributed in RACE-GAP summer bottom trawl surveys from the northern GOA, across the eastern Bering Sea shelf, and into the Chukchi and Northern Bering seas. This species is adapted to low water temperatures with an antifreeze glycoprotein in their blood to prevent ice crystal formation (Knight et al. 1991). Alaska plaice are not commercially targeted in Alaska waters but are caught incidentally and managed in the GOA Shallow Water Flatfish stock complex (Turncock et al. 2017b). Length-based life stage breaks distinguish between demersal life stages; settled early juvenile (35–140 mm FL) (Doyle et al. 2019, NFAA), subadults (141–319 mm FL), and adults (> 319 mm FL) (Tenbrink and Wilderbuer 2015). The mesh size of the RACE-GAP bottom trawl is large enough that the smaller juvenile life stages may not be wholly retained in the catch[16]. SDMs of subadults and adults were possible in this study (N > 50).

Subadult Alaska plaice abundance and distribution predicted from RACE-GAP summer bottom trawl surveys in the Gulf of Alaska -- Subadult Alaska plaice (N = 85) caught in GOA RACE-GAP summer bottom trawl surveys (1993–2019) were caught infrequently and west of the Kenai Peninsula (Fig. 40). Five SDMs were considered for inclusion in the ensemble to predict numerical abundance of subadult Alaska plaice in the GOA (Table 17); the hGAM and GAM_P did not converge. These remaining SDMs were weighted by RMSE in the final ensemble, which attained a good fit overall to the observed subadult Alaska plaice distribution and abundance data. The ensemble was fair at predicting high and low abundance catches (ρ = 0.23), and excellent at discriminating presence-absence (AUC = 0.98) and explaining deviance (PDE = 0.62). Geographic location, bottom depth, tidal maximum, and BPI accounted for 73.8% of the deviance explained by the ensemble (Table 18). Higher subadult Alaska plaice abundance occurred in nearshore areas in Kachemak Bay and along the Alaska Peninsula and western Kodiak Island (Fig. 41). The CV of ensemble predictions was higher in the western GOA (Fig. 2), where the probability of encountering subadult Alaska plaice was higher at shallower depths on the continental shelf and in nearshore areas (Fig. 42).

Adult Alaska plaice abundance and distribution predicted from RACE-GAP summer bottom trawl surveys in the Gulf of Alaska -- Adult Alaska plaice (N = 442) caught in GOA RACE-GAP summer bottom trawl surveys (1993–2019) west of the Kenai Peninsula (Fig. 43). All five SDMs considered for inclusion in the ensemble to predict numerical abundance of adult Alaska plaice in the GOA converged (Table 17); the GAM_{nb} was eliminated by skill testing. The four remaining SDMs were

[16] Adding other high quality sources of data if available to future SDM ensemble EFH mapping for this species will be included as a research recommendation from the 2023 EFH 5-year Review.

weighted by RMSE in the final ensemble, which attained a good fit to the observed adult Alaska plaice distribution and abundance data. The ensemble was fair at predicting high and low abundance catches (ρ = 0.38), and excellent at discriminating presence-absence (AUC = 0.97) and explaining deviance (PDE = 0.71). Geographic location, bottom depth, and current metrics accounted for 75.9% of the deviance explained by the ensemble (Table 18). Similar to subadults, higher adult Alaska plaice abundance was predicted to occur in nearshore areas in Kachemak Bay and along the Alaska Peninsula and western Kodiak Island (Fig. 44). The CV of ensemble predictions was higher on bathymetric rises and at shallower depths throughout the GOA continental shelf (Fig. 44). The probability of encountering adult Alaska plaice was higher at shallower depths, particularly for the western GOA (Fig. 45).

Essential Fish Habitat of subadult and adult Alaska plaice in the Gulf of Alaska -- Ensemble-predicted, habitat-related numerical abundance of Alaska plaice life stages collected in RACE-GAP summer bottom trawl surveys of the GOA (1993–2019) was mapped as EFH areas and subareas (Fig. 46). Alaska plaice subadult EFH occurred from the Kenai Peninsula and west in nearshore areas in Kachemak Bay and lower Cook Inlet, and along the Alaska Peninsula and west Kodiak Island. Adult EFH was more extensive than that predicted for subadults, extending to deeper depths along bathymetric rises on the GOA continental shelf. EFH of adults was predicted to occur in the eastern GOA, where the RACE-GAP summer bottom trawl survey did not catch this species. Adult EFH hotspots and core area were concentrated in the western GOA.

Table 17. -- Constituent species distribution models (SDMs) used to construct Essential Fish Habitat (EFH) for a) subadult and b) adult Alaska plaice: MaxEnt = Maximum entropy; paGAM = presence-absence generalized additive model; hGAM = zero-adjusted Poisson hurdle GAM; GAM_P = standard Poisson GAM; GAM_{nb} = standard negative-binomial GAM; RMSE = root mean square error; ρ (rho) = Spearman's rank correlation coefficient; AUC = area under the receiver-operating characteristic curve; and PDE = Poisson deviance explained *. The "--" indicates that this model was not included in the final ensemble.

a) subadult Alaska plaice

Models	RMSE	Relative Weight	ρ	AUC	PDE	EFH area (km^2)
MaxEnt	0.89	0.33	0.22	0.97	0.60	29,900
paGAM	0.86	0.35	0.23	0.97	0.51	23,700
hGAM	--	--	--	--	--	--
GAM_P	--	--	--	--	--	--
GAM_{nb}	0.90	0.32	0.26	0.98	0.58	16,900
ensemble	0.83	1	0.23	0.98	0.62	28,500

b) adult Alaska plaice

Models	RMSE	Relative Weight	ρ	AUC	PDE	EFH area (km^2)
MaxEnt	4.28	0.22	0.36	0.95	0.53	117,600
paGAM	4.02	0.25	0.41	0.97	0.64	66,200
hGAM	3.89	0.27	0.43	0.97	0.99	47,300
GAM_P	3.92	0.26	0.42	0.97	0.64	53,300
GAM_{nb}	4.84	0	--	--	--	--
ensemble	3.60	1	0.38	0.97	0.71	87,500

* Refer to the Species Distribution Model Performance Metrics subsection within the Statistical Modeling section of the Methods for detailed descriptions of individual model performance metrics.

Table 18. -- Covariates retained in the a) subadult and b) adult Alaska plaice species distribution model (SDM) final ensembles, the percent contribution to the total deviance explained by each, and the cumulative percent deviance: SD = standard deviation, and BPI = bathymetric position index.

Alaska plaice			
	Covariate	**% Contribution**	**Cumulative %**
a) subadult	bottom depth	35.8	35.8
	location	20.6	56.3
	tidal maximum	10.7	67.0
	BPI	6.8	73.8
	current	6.3	80.1
	bottom temperature	4.1	84.2
	aspect north	3.9	88.1
	aspect east	3.7	91.8
	rockiness	2.7	94.5
	current SD	1.7	96.2
	curvature	1.1	97.3
	sponge presence	1.0	98.3
	slope	0.9	99.2
	coral presence	0.8	100.0
b) adult	location	32.4	32.4
	bottom depth	25.7	58.1
	tidal maximum	11.8	69.9
	current SD	6.0	75.9
	BPI	5.9	81.8
	current	4.8	86.6
	rockiness	4.3	90.9
	slope	2.7	93.6
	bottom temperature	2.3	95.9
	aspect east	1.5	97.4
	pennatulacean presence	1.4	98.8
	aspect north	0.8	99.6
	coral presence	0.3	99.9
	sponge presence	0.1	100.0

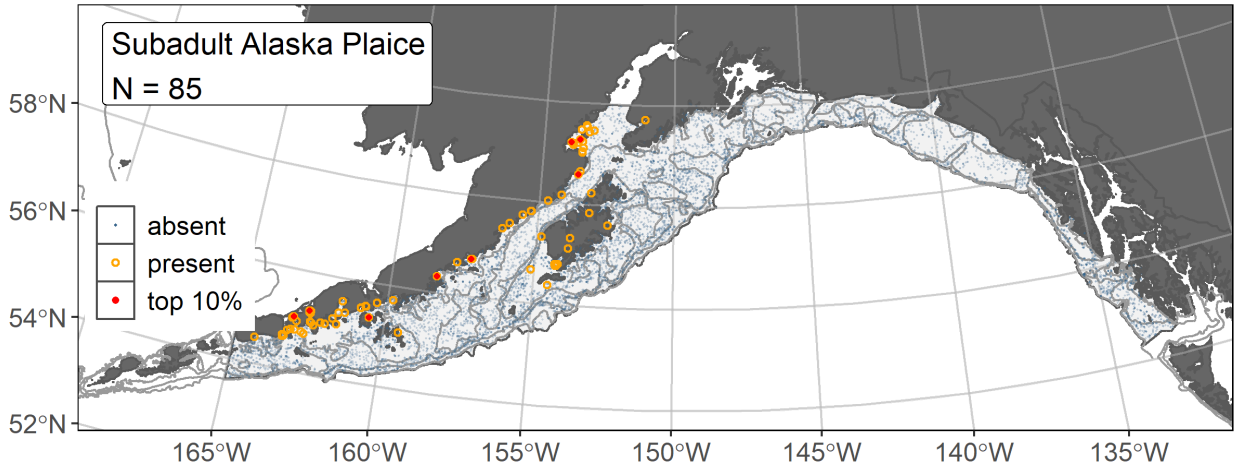

Figure 40. -- Distribution of subadult Alaska plaice catches (N = 85) in 1993–2019 AFSC RACE-GAP summer bottom trawl surveys of the Gulf of Alaska with the 100 m, 200 m, and 700 m isobaths indicated; filled red circles indicate locations in top 10% of overall abundance, open orange circles indicate presence in remaining catches, and blue dots indicate stations sampled where the animals were not present.

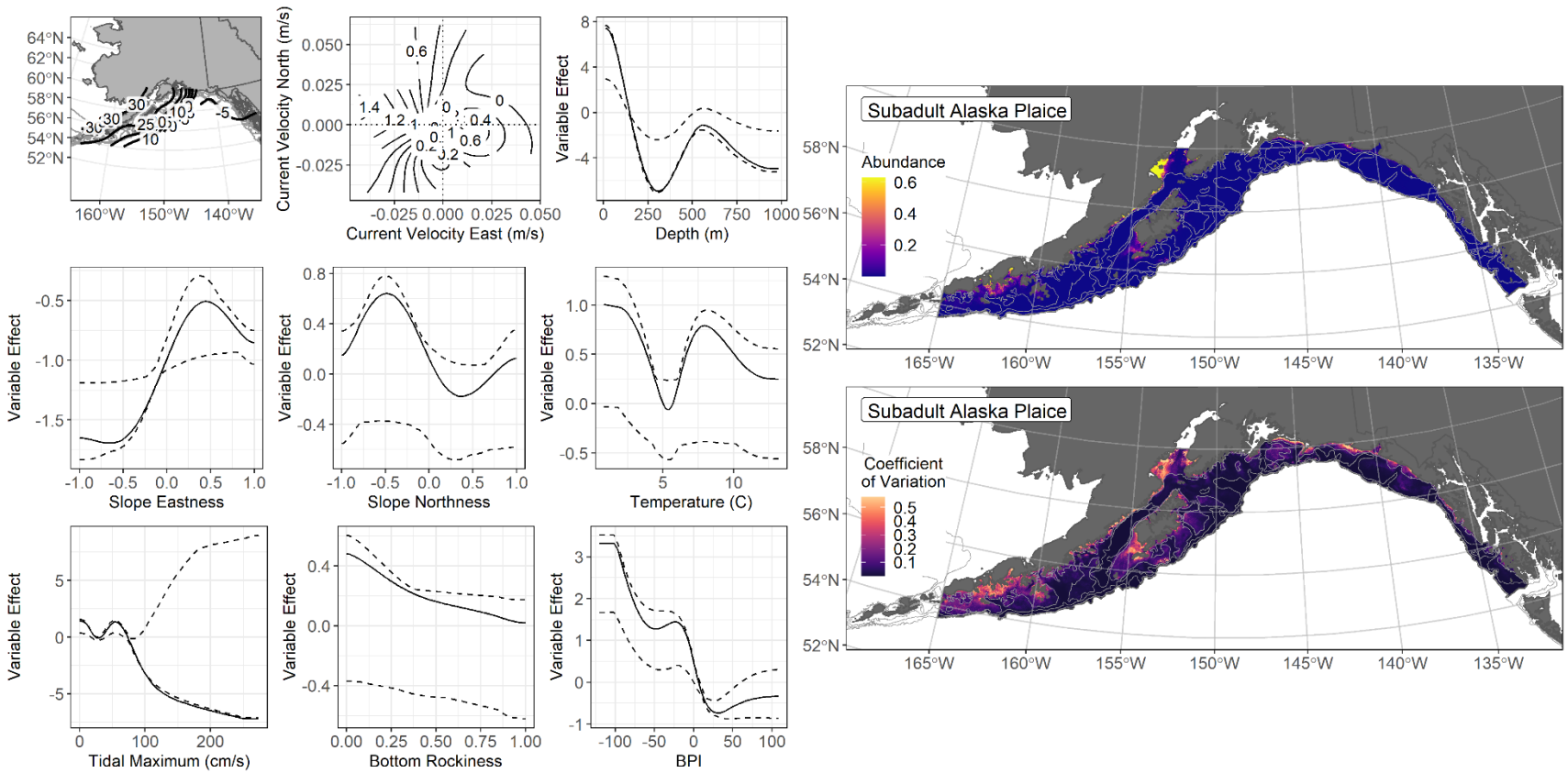

Figure 41. -- The top nine covariate effects (left panel) on ensemble-predicted subadult Alaska plaice numerical abundance across the Gulf of Alaska (upper right panel) along with the coefficient of variation (CV) of the ensemble predictions (lower right panel).

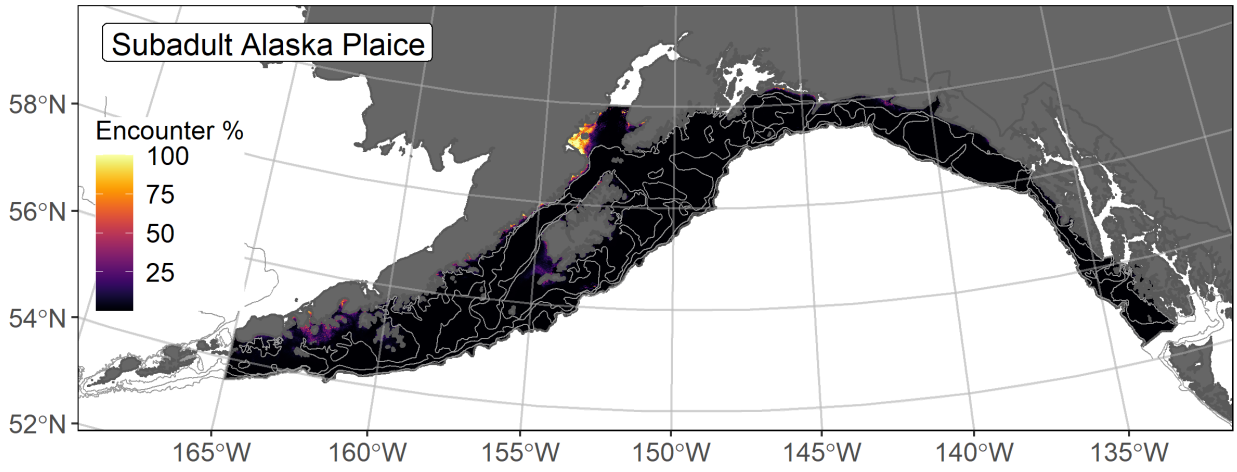

Figure 42. -- Encounter probability of subadult Alaska plaice from AFSC RACE-GAP summer bottom trawl surveys (1993–2019) of the Gulf of Alaska with the 100 m, 300 m, and 700 m isobaths indicated.

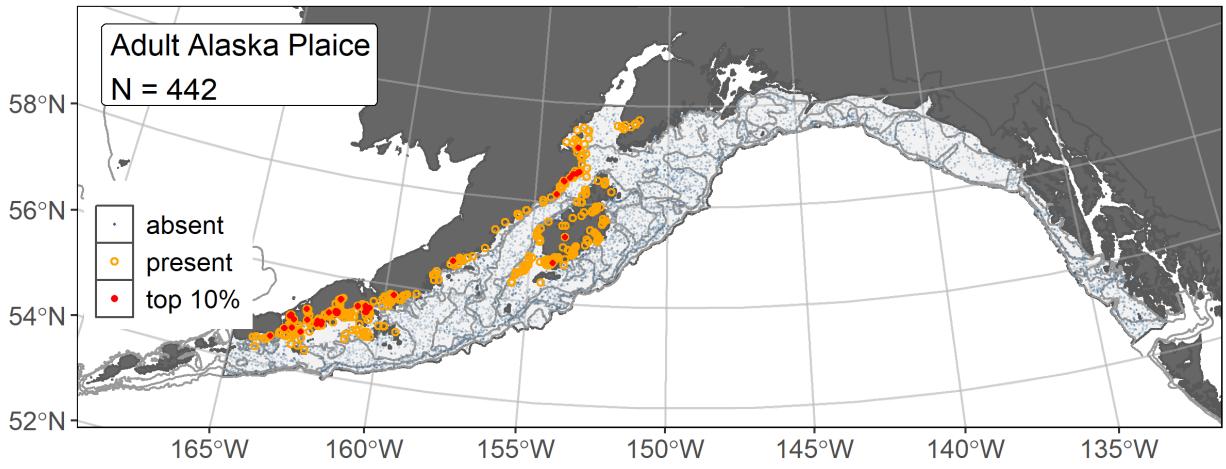

Figure 43. -- Distribution of adult Alaska plaice catches (N = 442) in 1993–2019 AFSC RACE-GAP summer bottom trawl surveys of the Gulf of Alaska with the 100 m, 200 m, and 700 m isobaths indicated; filled red circles indicate locations in top 10% of overall abundance, open orange circles indicate presence in remaining catches, and blue dots indicate stations sampled where the animals were not present.

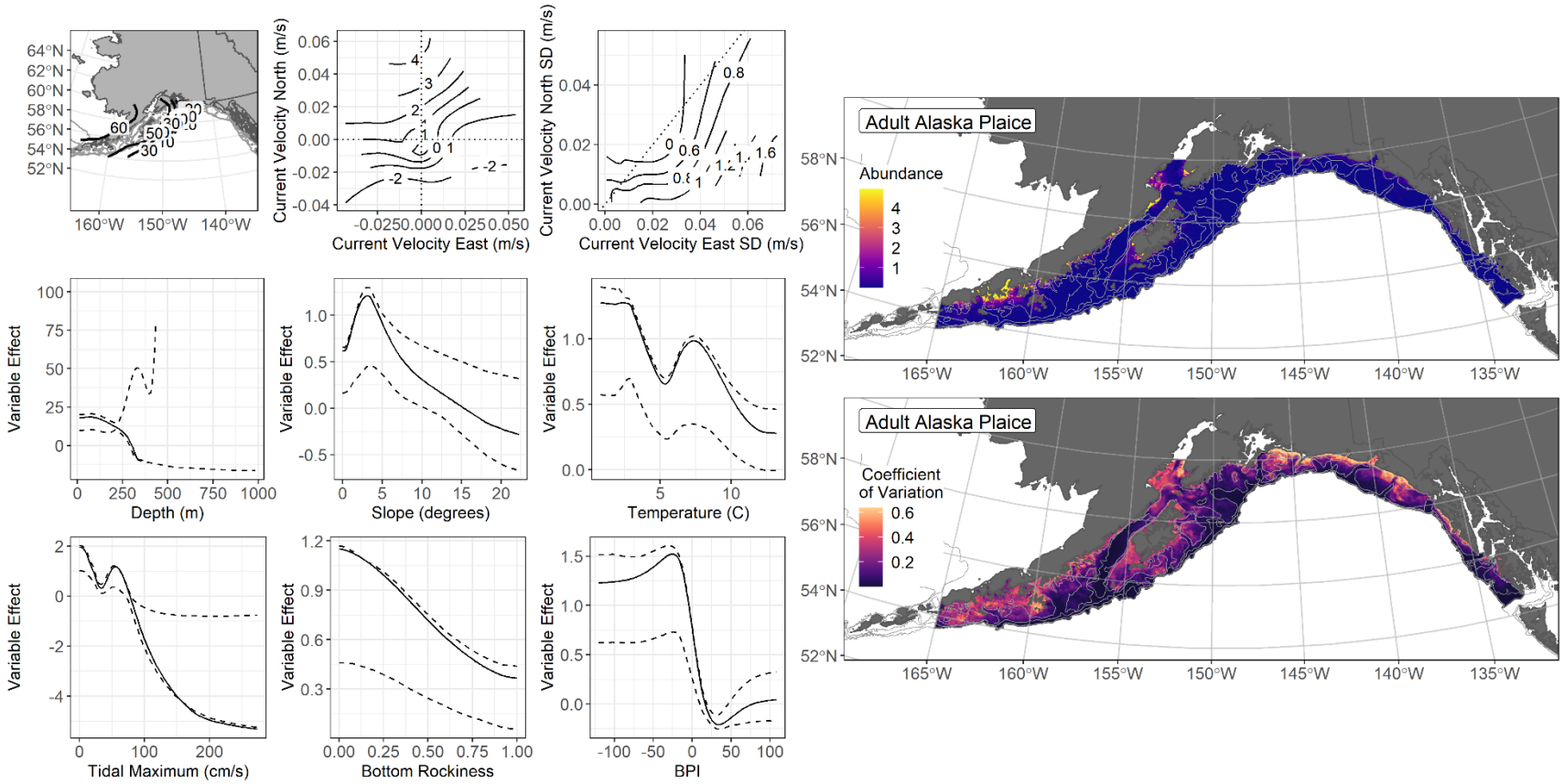

Figure 44. -- The top nine covariate effects (left panel) on ensemble-predicted adult Alaska plaice numerical abundance across the Gulf of Alaska (upper right panel) along with the coefficient of variation (CV) of the ensemble predictions (lower right panel).

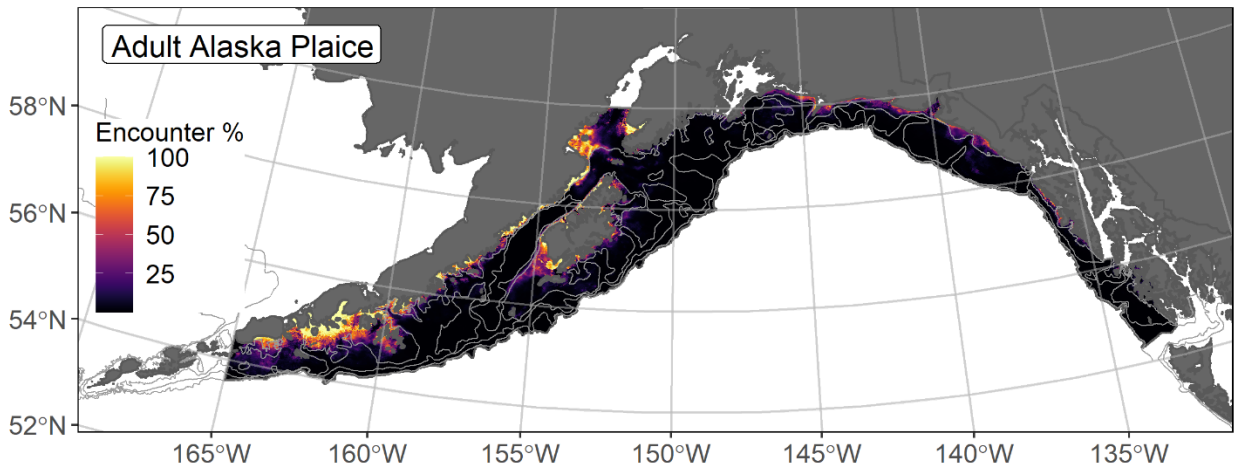

Figure 45. -- Encounter probability of adult Alaska plaice from AFSC RACE-GAP summer bottom trawl surveys (1993–2019) of the Gulf of Alaska with the 100 m, 200 m, and 700 m isobaths indicated.

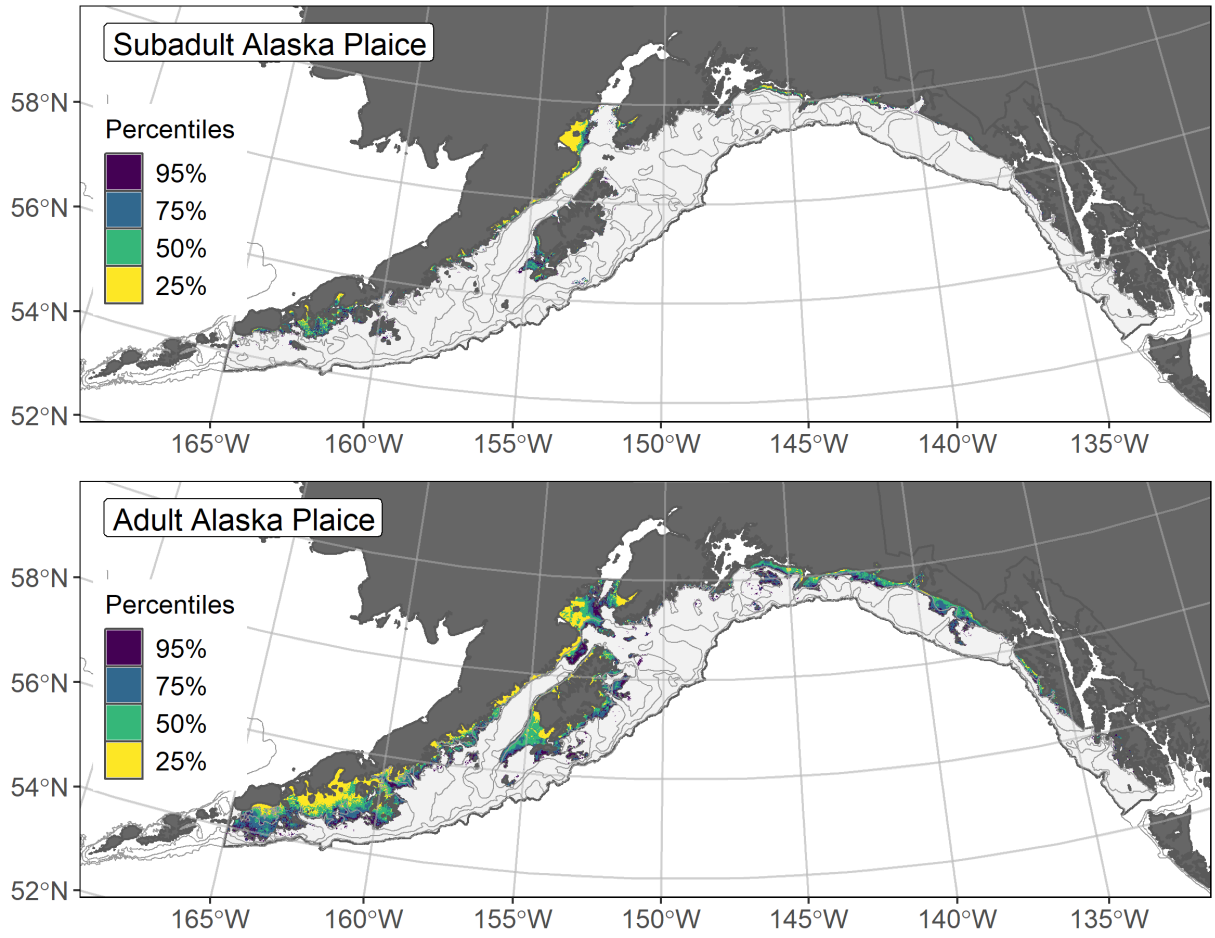

Figure 46. -- Essential fish habitat (EFH) is the area containing the top 95% of occupied habitat (defined as model estimated encounter probabilities greater than 5%) from an SDM ensemble fitted to subadult (top panel) and adult (bottom panel) Alaska plaice distribution and abundance in AFSC RACE-GAP summer bottom trawl surveys (1993–2019) with 100 m, 200 m, and 700 m isobaths indicated; within the EFH area map are the subareas of the top 25% (EFH hot spots), top 50% (core EFH area), and top 75% (principal EFH area) of habitat-related, ensemble-predicted numerical abundance.

Butter sole (*Isopsetta isolepis*)

Butter sole (*Isopsetta isolepis*) range from the southeastern Bering Sea and Aleutian Islands at Amchitka Island to southern California over soft bottom habitats in relatively shallow (< 150 m) water (Mecklenburg et al. 2002). In the GOA, butter sole are managed in the GOA Shallow Water Flatfish stock complex (Turncock et al. 2017b). Although butter sole are one of five species that account for most of the current biomass of this stock complex, little is known about their life history. Doyle et al. (2019) reported a maximum observed transformation length from pelagic larvae to early juveniles of 15–20 mm TL in the GOA, and settled individuals as small as 11 mm FL were captured in summer beach seine surveys (NFAA), yet not in sufficient numbers to model (N < 50)[17]. Without length-based information to distinguish between the older subadult and adult life stages, all individuals caught by RACE-GAP summer bottom trawl surveys in the GOA were modeled in composite to map EFH for this species.

Butter sole demersal life stage abundance and distribution predicted from RACE-GAP summer bottom trawl surveys in the Gulf of Alaska -- Butter sole demersal life stages (N = 881) caught in GOA RACE-GAP summer bottom trawl surveys (1993–2019) were caught primarily from Yakutat Trough through the western GOA (Fig. 47). Five SDMs were considered for inclusion in the ensemble to predict numerical abundance of butter sole in the GOA (Table 19); the hGAM did not converge, and the GAM_{nb} was eliminated by skill testing. The remaining three SDMs were weighted by RMSE in the final ensemble, which attained a good fit to the observed butter sole distribution and abundance data. The ensemble was good at predicting high and low abundance catches (ρ = 0.46), excellent at discriminating presence-absence (AUC = 0.93), and good at explaining deviance (PDE = 0.54). Bottom depth and rockiness alone accounted for 56.8% of the deviance explained by the ensemble, although other covariates contributed (Table 20). Higher butter sole abundance was predicted at less than 200 m depth in areas with low presence of rocky substrate (Fig. 48). Predicted abundance was highest in nearshore areas and at bathymetric rises on the GOA continental shelf. The CV of ensemble predictions was higher at shallower depths on the GOA continental shelf. The probability of encountering butter sole was generally higher in nearshore areas and at bathymetric rises on the continental shelf (Fig. 49).

Essential Fish Habitat of butter sole demersal life stages in the Gulf of Alaska -- Ensemble-predicted, habitat-related numerical abundance of butter sole demersal life stages collected in RACE-GAP summer bottom trawl surveys of the GOA (1993–2019) was mapped as EFH areas and subareas

[17] Adding other high quality sources of data if available to future SDM ensemble EFH mapping for this species will be included as a research recommendation from the 2023 EFH 5-year Review.

(Fig. 50). Butter sole EFH occurred on the continental shelf of the GOA from southeast Alaska to the extent of the study area at 165°W. Core EFH areas and EFH hot spots are more extensive at shallower depths for this species. This SDM-based EFH map is the first developed for butter sole in the GOA, which is the case for many constituent species of the GOA Shallow Water Flatfish stock complex.

Table 19. -- Constituent species distribution models (SDMs) used to construct Essential Fish Habitat (EFH) for butter sole: MaxEnt = Maximum entropy; paGAM = presence-absence generalized additive model; hGAM = zero-adjusted Poisson hurdle GAM; GAM_P = standard Poisson GAM; GAM_{nb} = standard negative-binomial GAM; RMSE = root mean square error; ρ (rho) = Spearman's rank correlation coefficient; AUC = area under the receiver-operating characteristic curve; and PDE = Poisson deviance explained *. The "--" indicates that this model was not included in the final ensemble.

butter sole

Models	RMSE	Relative Weight	ρ	AUC	PDE	EFH area (km^2)
MaxEnt	33.1	0.32	0.45	0.92	0.43	210,100
paGAM	32.4	0.33	0.45	0.92	0.46	207,500
hGAM	--	--	--	--	--	--
GAM_P	31.5	0.35	0.43	0.91	0.48	168,200
GAM_{nb}	57.5	0	--	--	--	--
ensemble	30.4	1	0.46	0.93	0.54	206,500

* Refer to the Species Distribution Model Performance Metrics subsection within the Statistical Modeling section of the Methods for detailed descriptions of individual model performance metrics.

Table 20. -- Covariates retained in the butter sole species distribution model (SDM) final ensembles, the percent contribution to the total deviance explained by each, and the cumulative percent deviance: SD = standard deviation, and BPI = bathymetric position index.

butter sole

Covariate	% Contribution	Cumulative %
bottom depth	45.7	45.7
rockiness	11.2	56.8
location	7.8	64.6
BPI	7.2	71.8
tidal maximum	7.1	78.9
current	5.2	84.1
sponge presence	5.0	89.1
bottom temperature	3.3	92.4
current SD	2.1	94.5
aspect east	1.5	96.0
aspect north	1.4	97.4
slope	1.2	98.6
curvature	1.0	99.6
coral presence	0.2	99.8
pennatulacean presence	0.2	100.0

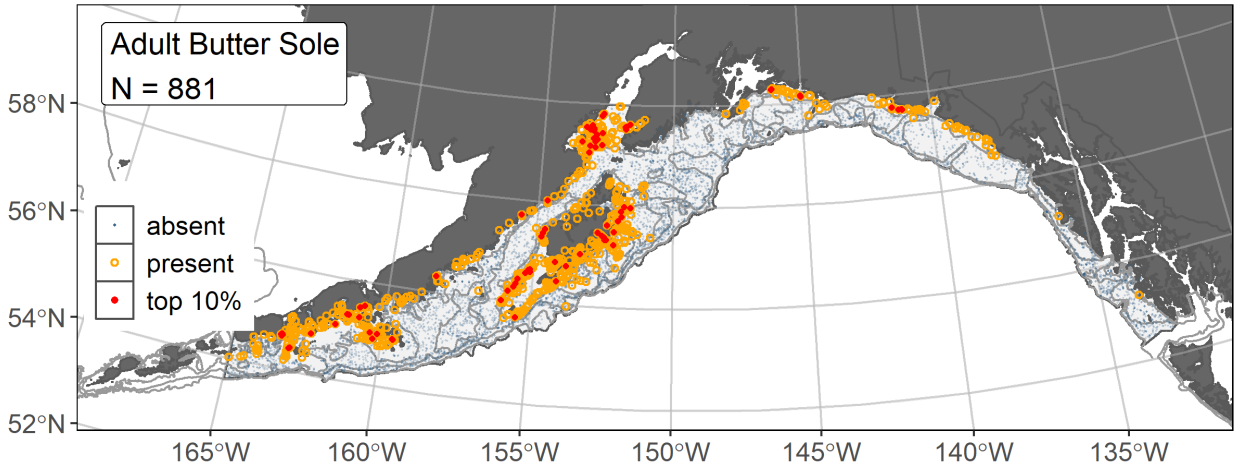

Figure 47. -- Distribution of butter sole catches (N = 881) in 1993–2019 AFSC RACE-GAP summer bottom trawl surveys of the Gulf of Alaska with the 100 m, 200 m, and 700 m isobaths indicated; filled red circles indicate locations in top 10% of overall abundance, open orange circles indicate presence in remaining catches, and blue dots indicate stations sampled where the animals were not present.

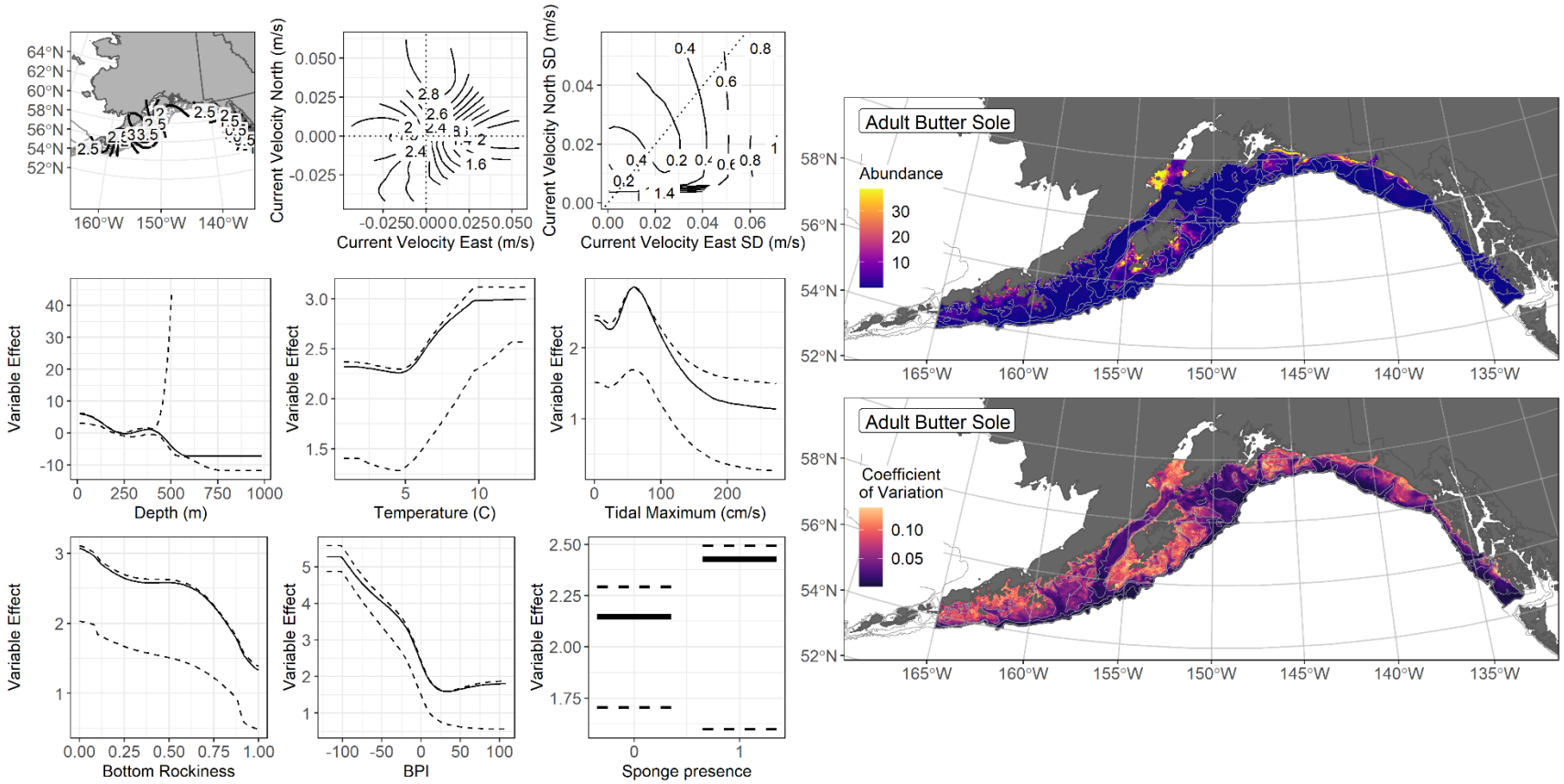

Figure 48. -- The top nine covariate effects (left panel) on ensemble-predicted butter sole numerical abundance across the Gulf of Alaska (upper right panel) along with the coefficient of variation of the ensemble predictions (lower right panel).

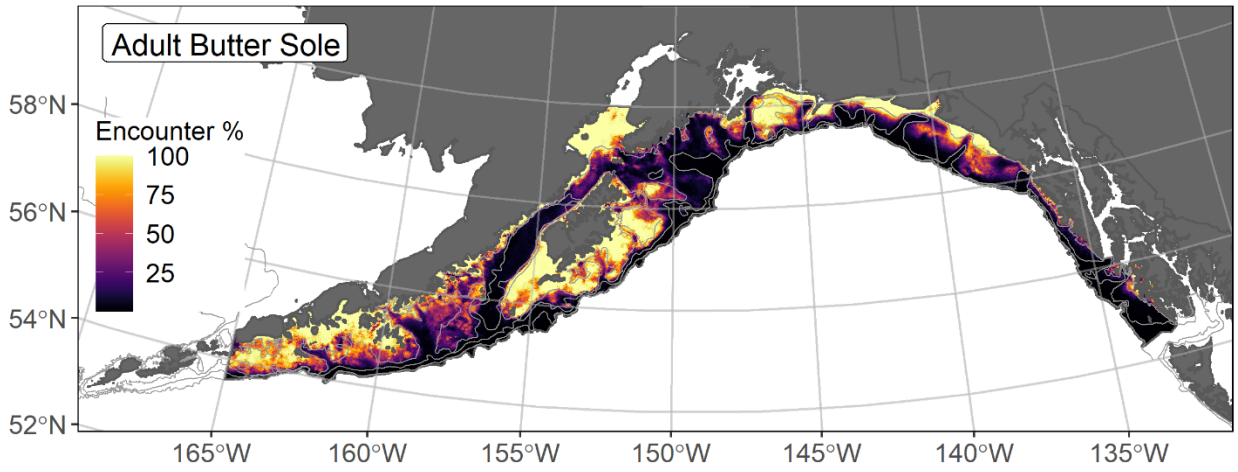

Figure 49. -- Encounter probability of butter sole from AFSC RACE-GAP summer bottom trawl surveys (1993–2019) of the Gulf of Alaska with the 100 m, 300 m, and 700 m isobaths indicated.

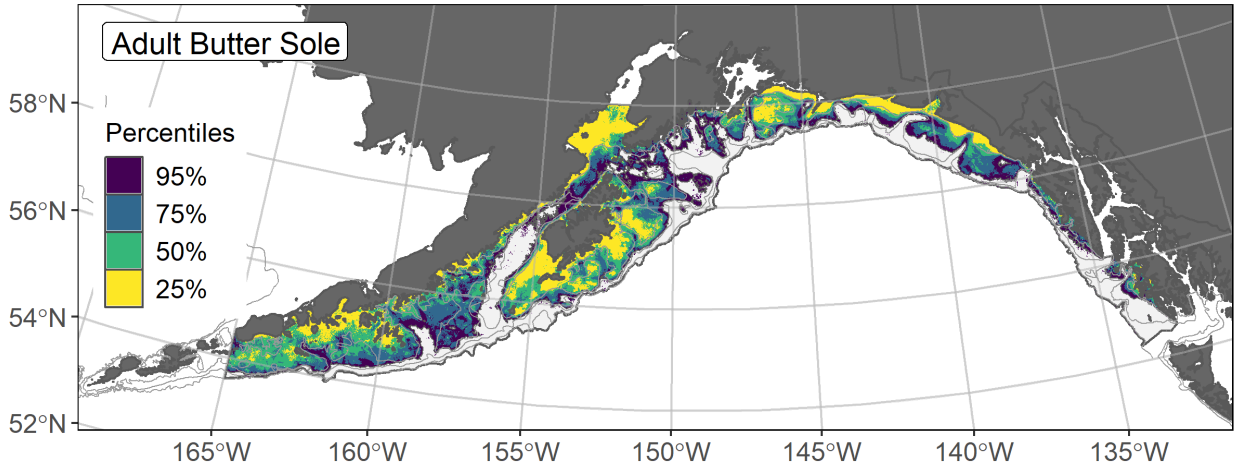

Figure 50. -- Essential fish habitat (EFH) is the area containing the top 95% of occupied habitat (defined as model estimated encounter probabilities greater than 5%) from an SDM ensemble fitted to butter sole distribution and abundance from AFSC RACE-GAP Gulf of Alaska (GOA) summer bottom trawl surveys (1993–2019) with 100 m, 200 m, and 700 m isobaths indicated; within the EFH area map are the subareas of the top 25% (EFH hot spots), top 50% (core EFH area), and top 75% (principal EFH area) of habitat-related, ensemble-predicted numerical abundance.

English sole (*Parophrys vetulus*)

English sole (*Parophrys vetulus*) in the GOA are managed in the Shallow Water Flatfish stock complex as a member of the "other flatfish" species in this group (Turncock et al. 2017b). Little is known about English sole life history in the GOA. The smallest settled early juvenile English sole caught by beach seine gear in summer surveys in the GOA was 17 mm FL (mean 31 mm FL; NFAA). This study used the maximum length reported for settled early juvenile YFS as a proxy (140 mm FL; Yeung and Cooper 2020). The mesh size of the RACE-GAP bottom trawl is large enough that the smaller juvenile life stages may not be wholly retained in the catch[18]. Subadults and adults were distinguished in all regions using L50 = 230 mm FL (Sampson and Al-Jufaily 1999). We used these length breaks to separate English sole demersal life stages in our analysis, including settled early juveniles (20–140 mm), subadults (141–230 mm), and adults (> 230 mm).

Settled early juvenile English sole distribution predicted from mixed gear-type summer surveys in the Gulf of Alaska -- Settled early juvenile English sole (N = 56) were caught in mixed gear-type summer surveys (1989–2019) using bottom trawls and seines in nearshore areas of the GOA (Fig. 51). Settled early juvenile presence records from multiple surveys were combined in a habitat-related MaxEnt SDM predicting suitable habitat probabilities for this life stage in the GOA. The best model had a β-multiplier of 3.0 and an AUC of 0.99 (Table 21). Bottom depth alone accounted for 89.9% of the total deviance explained by the SDM (Table 22). The highest predicted probabilities of suitable habitat for settled early juvenile English sole occurred at locations less than 100 m depth (Fig. 52). The model may be overpredicting in certain areas where these surveys did not observe this life stage. The standard deviation among k-folds for the final SDM was relatively low across the GOA.

Subadult English sole abundance and distribution predicted from RACE-GAP summer bottom trawl surveys in the Gulf of Alaska -- Subadult English sole (N = 116) caught in GOA RACE-GAP summer bottom trawl surveys (1993–2019) were caught inshore on the continental shelf of the GOA from southeast Alaska to the western extent of the study area (Fig. 53). Three of the five SDMs considered for inclusion in the ensemble to predict numerical abundance of subadult English sole in the GOA converged (Table 23); the GAM_P was eliminated through skill testing. The remaining two best-performing SDMs were weighted by RMSE in the final ensemble, which attained a fair fit to the observed subadult English sole data. The ensemble was fair at predicting high and low abundance catches (ρ = 0.20), excellent at discriminating presence-absence (AUC = 0.95), and good at explaining deviance

[18] Adding other high quality sources of data if available to future SDM ensemble EFH mapping for this species will be included as a research recommendation from the 2023 EFH 5-year Review.

(PDE = 0.57). Bottom depth, tidal maximum speed, and geographic location accounted for 70.4% of the contribution among covariates to the deviance explained by the ensemble predicting subadult English sole numerical abundance (Table 22). The highest abundances were predicted in inshore areas east of 148°W and in western Cook Inlet (Fig. 54). The CV of ensemble predictions was higher at shallower depths on the GOA continental shelf. The probability of encountering subadult English sole was higher in areas of predicted high abundance (Fig. 55).

Adult English sole abundance and distribution predicted from RACE-GAP summer bottom trawl surveys in the Gulf of Alaska -- Adult English sole (N = 746) caught in GOA RACE-GAP summer bottom trawl surveys (1993–2019) were distributed on the GOA continental shelf from southeast Alaska to the western extent of the study area (Fig. 56). Four of the five SDMs considered for inclusion in the ensemble to predict numerical abundance of adult English sole in the GOA converged (Table 23); the GAM_{nb} was eliminated through skill testing. The remaining three best-performing SDMs were weighted by RMSE in the final ensemble, which attained a good fit to the observed adult English sole data. The ensemble was fair at predicting high and low abundance catches (ρ = 0.34), and good at discriminating presence-absence (AUC = 0.84) and explaining deviance (PDE = 0.52). Bottom depth and geographic location accounted for 57% of the contribution among covariates to the deviance explained by the ensemble predicting adult English sole numerical abundance (Table 22). The highest adult English sole abundances were predicted in inshore areas east of 148°W, similar to subadults, and off southeast Alaska Fig. 57). The CV of ensemble predictions was relatively even across the GOA. The probability of encountering adult English sole was higher at shallower depths throughout the GOA continental shelf (Fig. 58).

Essential Fish Habitat of three life stages of English sole in the Gulf of Alaska -- Habitat-related predictions of English sole demersal life stage distribution and abundance from summer surveys of the GOA (mixed gear-type summer surveys (1989–2019) and RACE-GAP bottom trawl surveys (1993–2019)) were mapped as EFH areas and subareas (Fig. 59). Settled early juvenile EFH occurred in nearshore areas and at shallow depths in the GOA. Subadult EFH occurred inshore in the GOA with core EFH areas and EFH hot spots concentrated east of 148°W. In contrast, adult English sole EFH was extensive across the GOA continental shelf, with EFH hot spots more prevalent east of 148°W. English sole may demonstrate ontogenetic migrations to deeper depths with increasing size or age.

Table 21. -- Maximum entropy model (MaxEnt) used to construct Essential Fish Habitat (EFH) for settled early juvenile English sole: regularization multiplier (β); *k*-fold cross-validation root-mean-square-error (RMSE), area under the receiver operating characteristic curve (AUC), and areal extent of EFH (km^2).

Model	**β**	**RMSE**	**AUC**	**EFH area (km^2)**
MaxEnt	3.0	1.8	0.99	39,300

Table 22. -- Covariates retained in the a) settled early juvenile habitat-related maximum entropy (MaxEnt) species distribution model (SDM), and b) subadult and c) adult SDM final ensembles for English sole with the percent contribution of each covariate to the deviance explained by the SDMs and the cumulative deviance explained: SD = standard deviation and BPI = bathymetric position index.

English sole	**Covariate**	**% Contribution**	**Cumulative %**
a) settled early juvenile	bottom depth	89.9	89.9
	slope	4.1	93.9
	aspect east	2.4	96.3
	aspect north	1.6	98.0
	rockiness	1.0	99.0
	curvature	0.7	99.6
	coral presence	0.4	100.0
b) subadult	bottom depth	42.5	42.5
	tidal maximum	16.0	58.6
	position	11.8	70.4
	bottom temperature	8.5	78.9
	BPI	7.3	86.2
	sponge presence	5.2	91.4
	current	3.7	95.1
	current SD	3.0	98.1
	slope	1.1	99.2
	coral presence	0.5	99.7
	pennatulacean presence	0.3	100.0
c) adult	bottom depth	31.8	31.8
	location	25.2	57.0
	tidal maximum	6.2	63.2
	current SD	5.7	68.9
	aspect east	5.5	74.4
	slope	5.1	79.5
	BPI	4.7	84.2
	current	4.3	88.5
	aspect north	3.2	91.7
	sponge presence	3.0	94.7
	bottom temperature	2.8	97.5
	rockiness	1.3	98.8
	curvature	0.8	99.6
	coral presence	0.3	99.9
	pennatulacean presence	0.1	100.0

Table 23. -- Constituent species distribution models (SDMs) used to construct Essential Fish Habitat (EFH) for a) subadult and b) adult English sole: MaxEnt = Maximum entropy; paGAM = presence-absence generalized additive model; hGAM = zero-adjusted Poisson hurdle GAM; GAM_P = standard Poisson GAM; GAM_{nb} = standard negative-binomial GAM; RMSE = root mean square error; ρ (*rho*) = Spearman's rank correlation coefficient; AUC = area under the receiver operating characteristic curve; and PDE = Poisson deviance explained *. The "--" indicates that this model was not included in the final ensemble.

a) subadult English sole

Models	RMSE	Relative Weight	ρ	AUC	PDE	EFH area (km^2)
MaxEnt	--	--	--	--	--	--
paGAM	2.29	0.51	0.19	0.94	0.49	66,900
hGAM	--	--	--	--	--	--
GAM_P	2.54	0	--	--	--	--
GAM_{nb}	2.34	0.49	0.21	0.93	0.46	35,400
ensemble	2.25	1	0.20	0.95	0.57	55,700

b) adult English sole

Models	RMSE	Relative Weight	ρ	AUC	PDE	EFH area (km^2)
MaxEnt	--	--	--	--	--	--
paGAM	14.6	0.42	0.33	0.83	0.38	254,800
hGAM	21.7	0.19	0.25	0.83	-0.98	187,700
GAM_P	15.0	0.40	0.30	0.81	0.41	177,100
GAM_{nb}	22.3	0	--	--	--	--
ensemble	13.3	1	0.34	0.84	0.52	241,600

* Refer to the Species Distribution Model Performance Metrics subsection within the Statistical Modeling section of the Methods for detailed descriptions of individual model performance metrics.

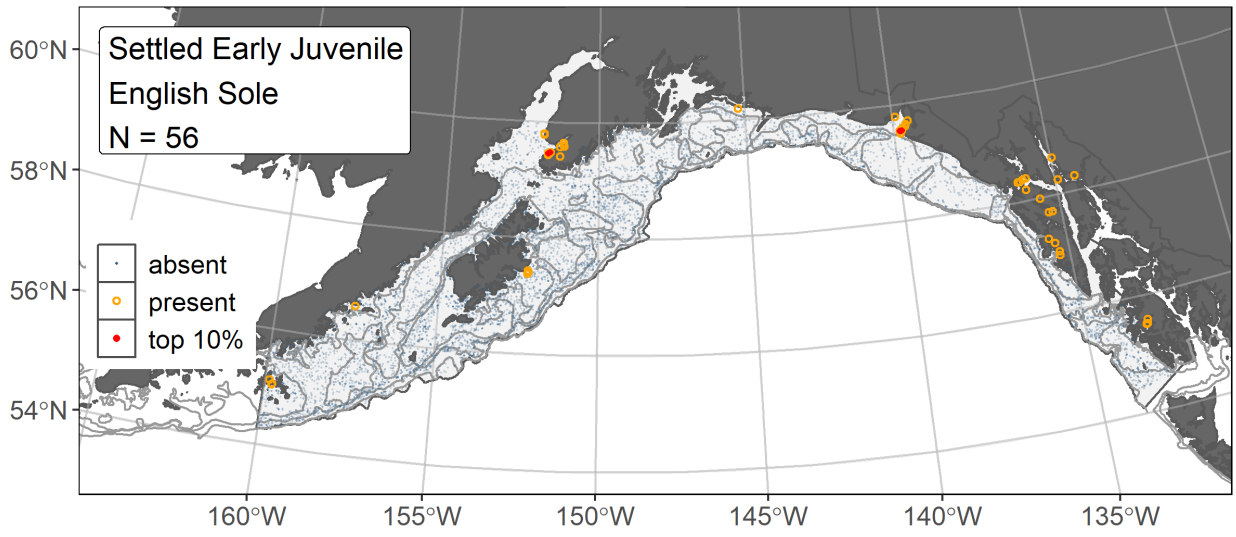

Figure 51. -- Distribution of settled early juvenile English sole catches (N = 56) in mixed gear-type summer surveys of the Gulf of Alaska (1989–2019) with the 100 m, 200 m, and 700 m isobaths indicated; filled red circles indicate locations in top 10% of overall abundance, open orange circles indicate presence in remaining catches, and blue dots indicate stations sampled where the animals were not present.

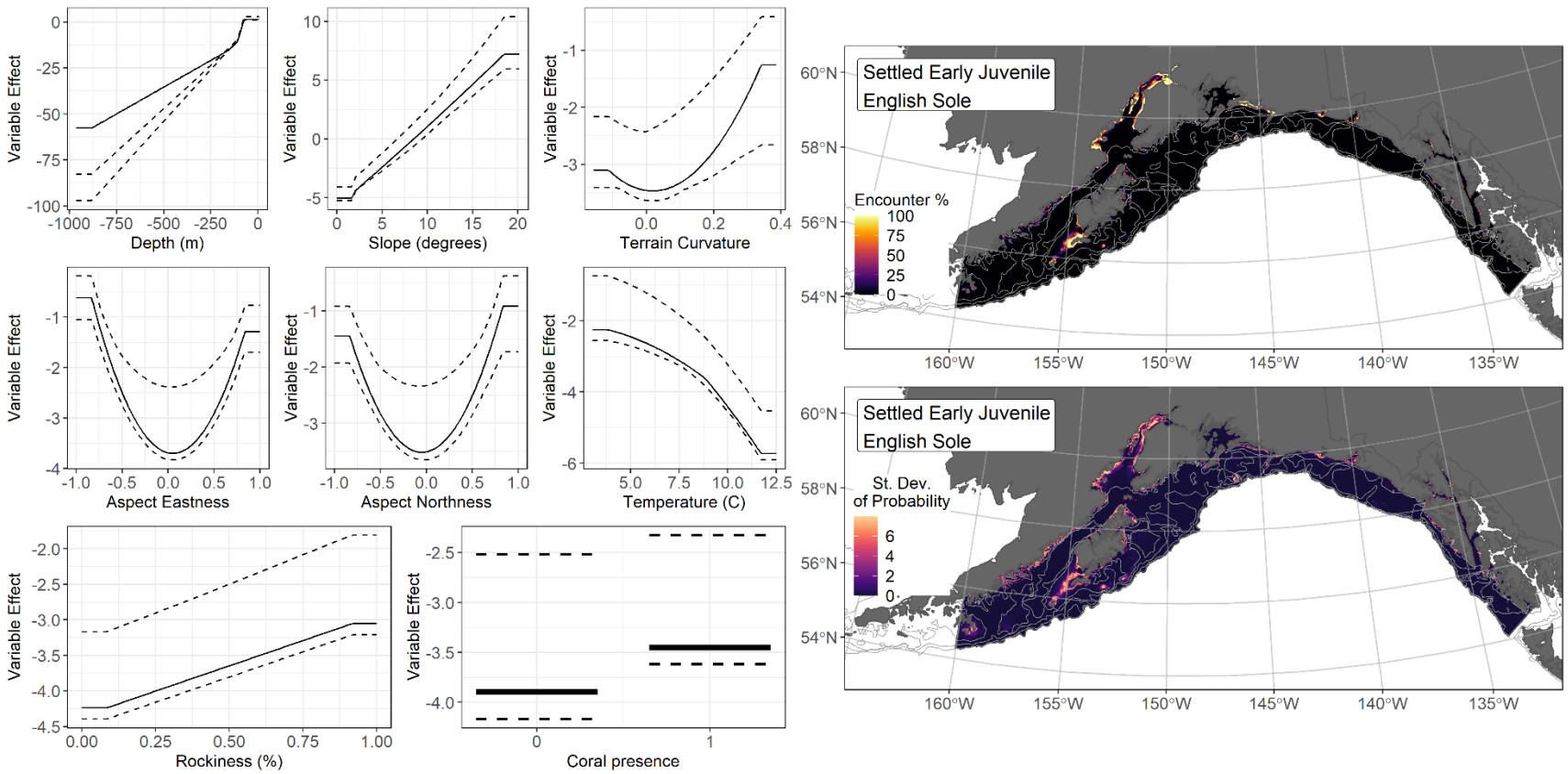

Figure 52. -- The top nine covariate effects (left panel) from a habitat-related species distribution model (MaxEnt) of settled early juvenile English sole probability of suitable habitat in the Gulf of Alaska (upper right panel) with the standard deviation of the probability predictions (lower right panel).

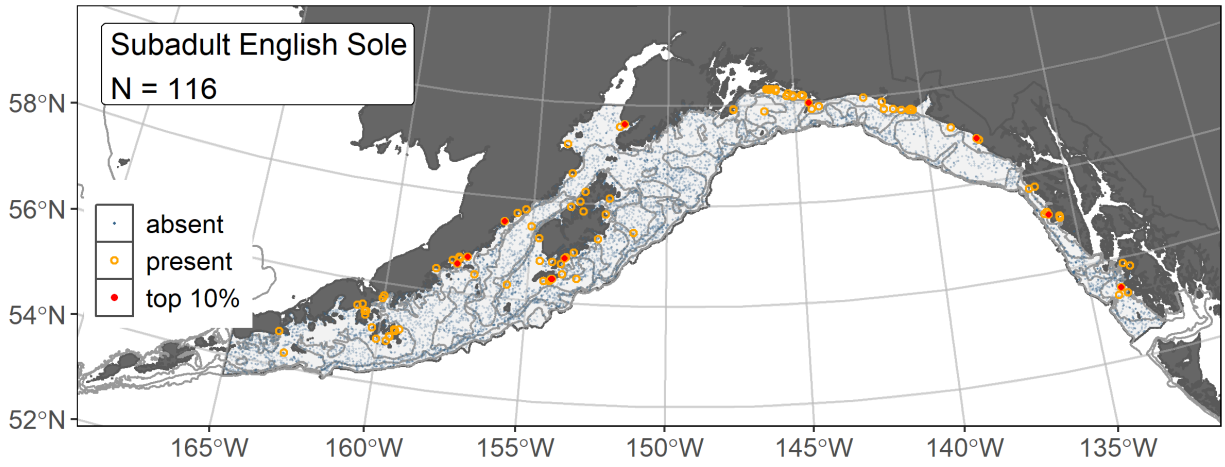

Figure 53. -- Distribution of subadult English sole catches (N = 116) in 1993–2019 AFSC RACE-GAP summer bottom trawl surveys of the Gulf of Alaska with the 100 m, 200 m, and 700 m isobaths indicated; filled red circles indicate locations in top 10% of overall abundance, open orange circles indicate presence in remaining catches, and blue dots indicate stations sampled where the animals were not present.

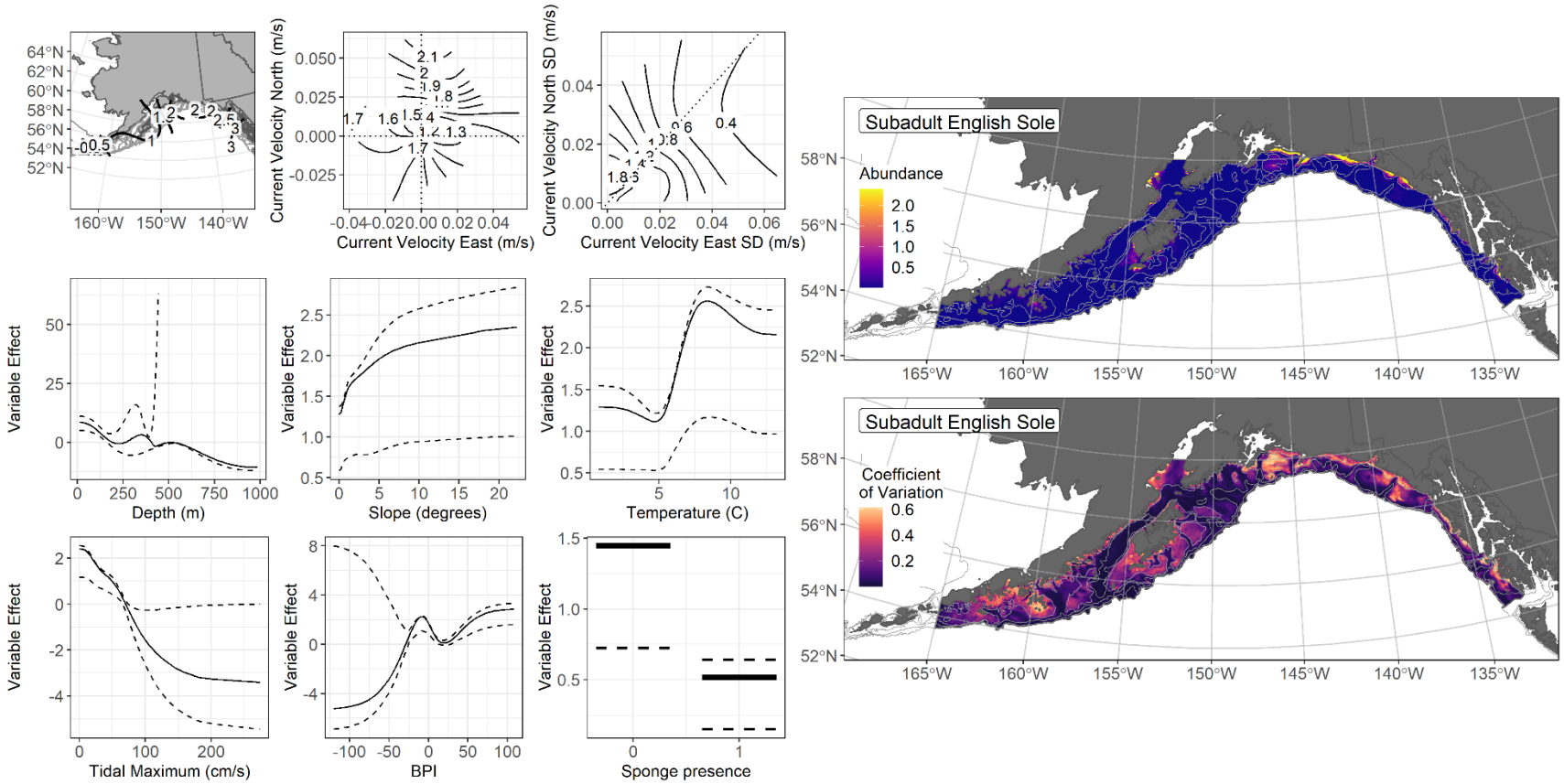

Figure 54. -- The top nine covariate effects (left panel) on ensemble-predicted subadult English sole numerical abundance across the Gulf of Alaska (upper right panel) along with the coefficient of variation (CV) of the ensemble predictions (lower right panel).

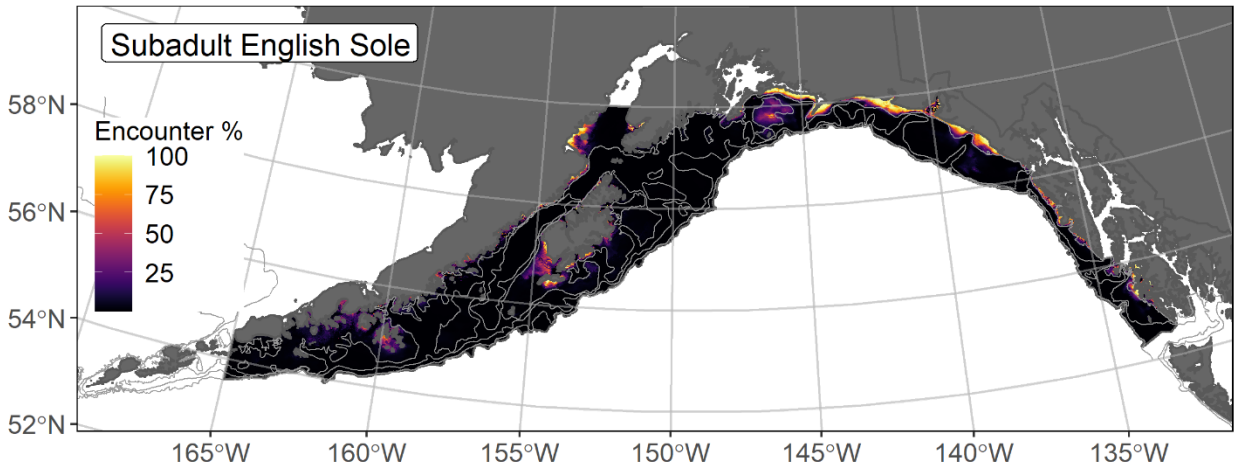

Figure 55. -- Encounter probability of subadult English sole from AFSC RACE-GAP summer bottom trawl surveys (1993–2019) of the Gulf of Alaska with the 100 m, 200 m, and 700 m isobaths indicated.

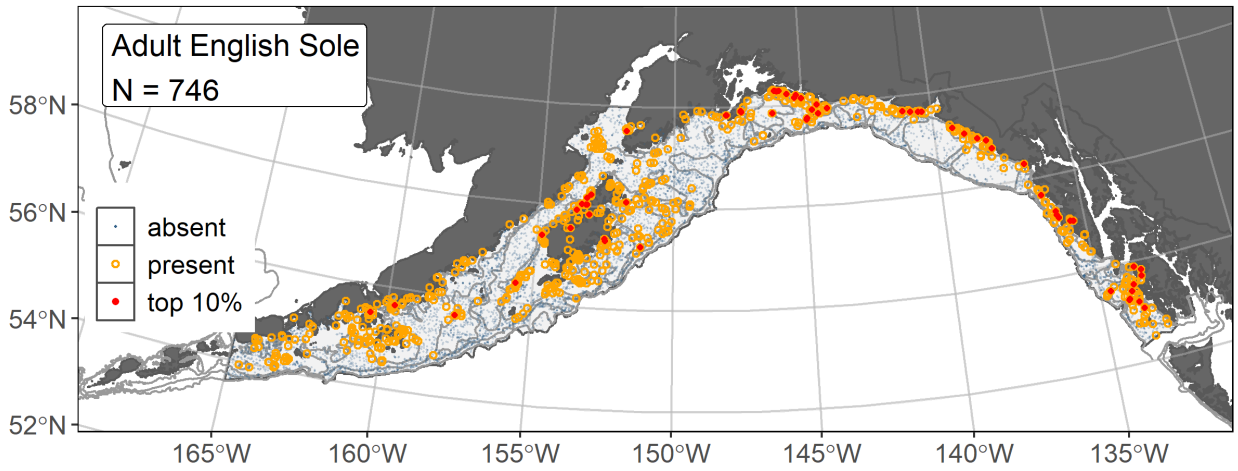

Figure 56. -- Distribution of adult English sole catches (N = 746) in 1993–2019 AFSC RACE-GAP summer bottom trawl surveys of the Gulf of Alaska with the 100 m, 200 m, and 700 m isobaths indicated; filled red circles indicate locations in top 10% of overall abundance, open orange circles indicate presence in remaining catches, and blue dots indicate stations sampled where the animals were not present.

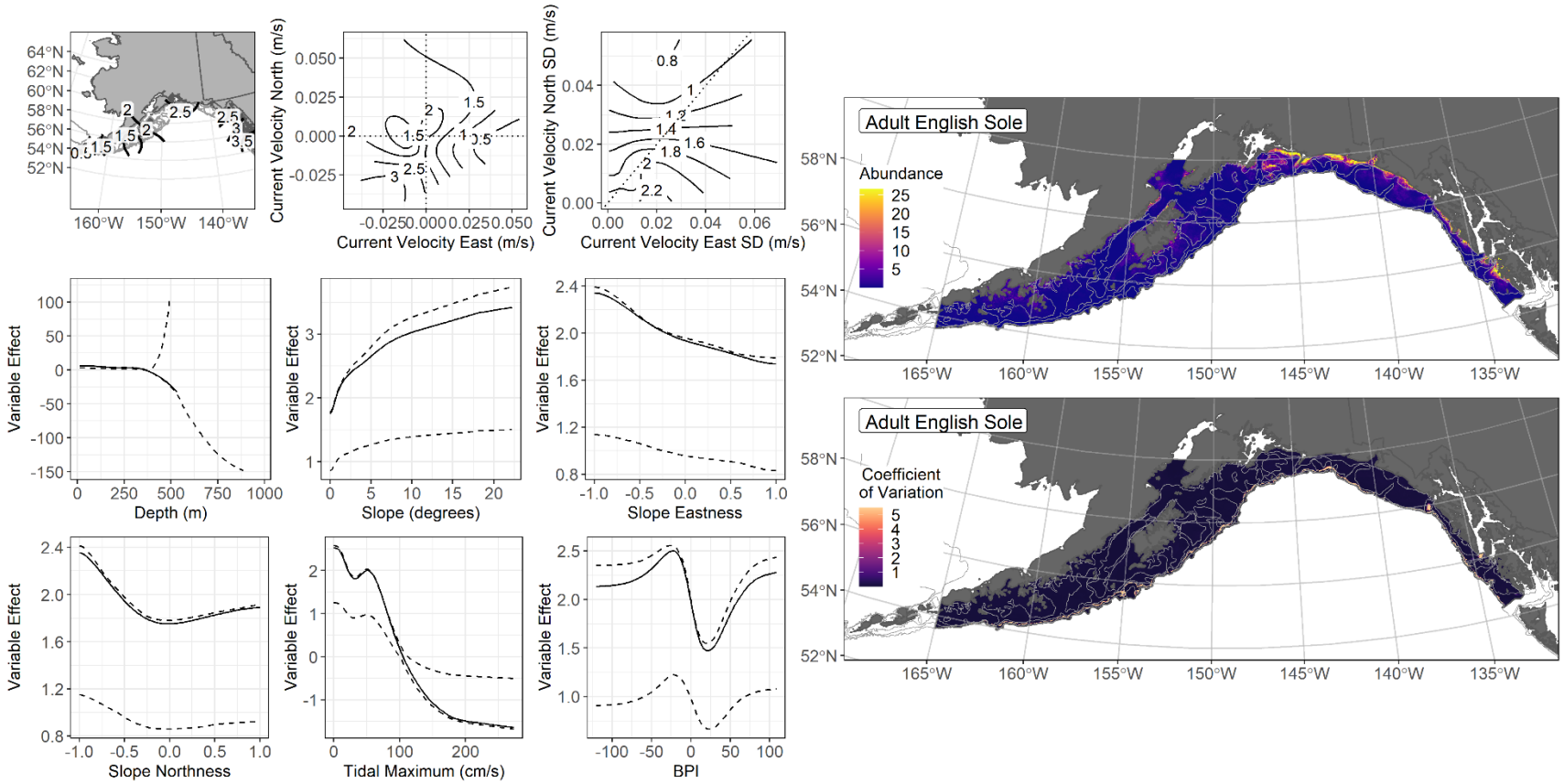

Figure 57. -- The top nine covariate effects (left panel) on ensemble-predicted adult English sole numerical abundance across the Gulf of Alaska (upper right panel) along with the coefficient of variation (CV) of the ensemble predictions (lower right panel).

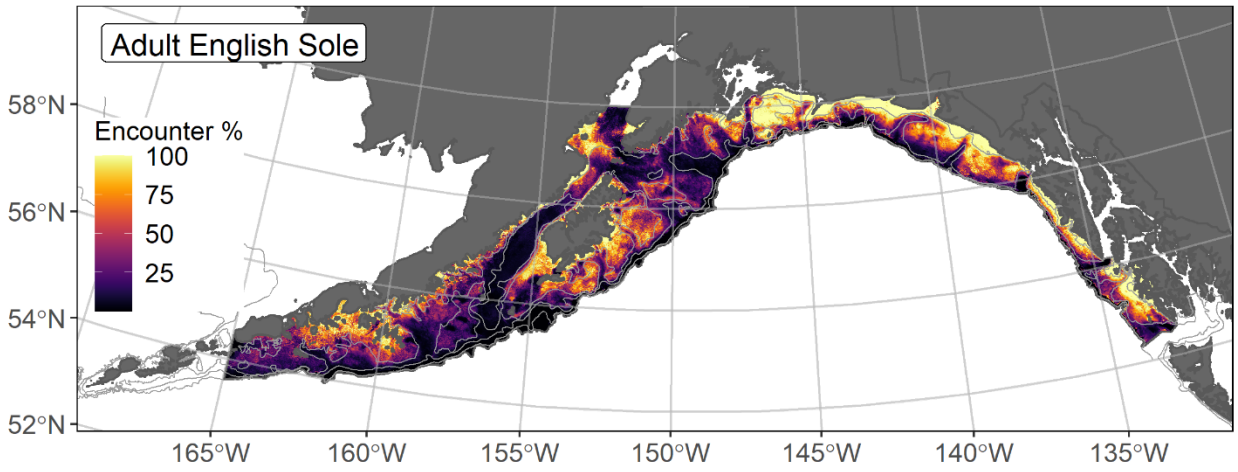

Figure 58. -- Encounter probability of adult English sole from AFSC RACE-GAP summer bottom trawl surveys (1993–2019) of the Gulf of Alaska with the 100 m, 200 m, and 700 m isobaths indicated.

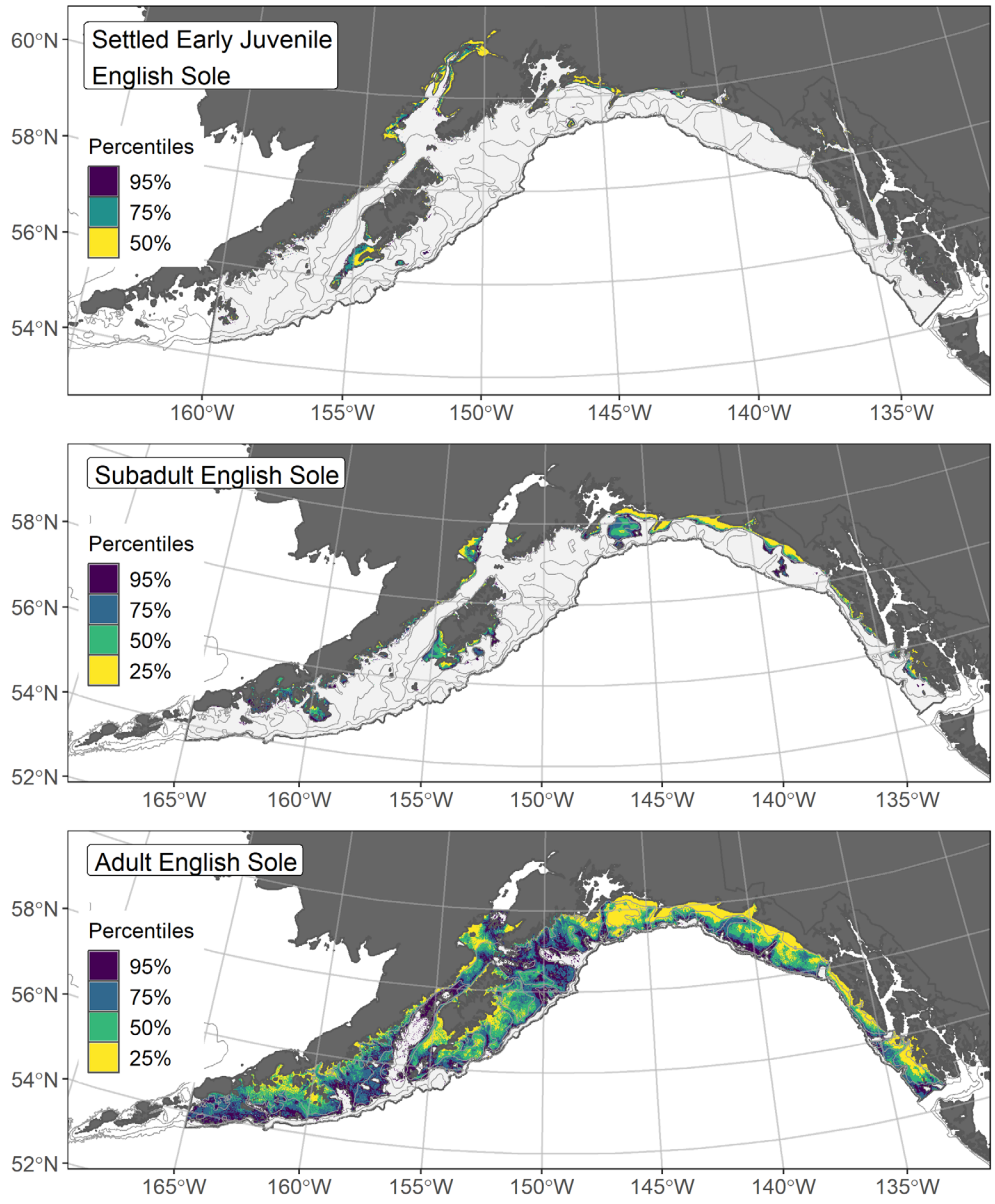

Figure 59. -- Essential fish habitat (EFH) is the area containing the top 95% of occupied habitat (defined as greater than 5% predicted probability of suitable habitat) for settled early juvenile (top panel) English sole from an SDM fitted to their distribution in Gulf of Alaska (GOA) mixed gear-type summer surveys (1989–2019), and for subadults (middle panel) and adults (bottom panel) is the area containing the top 95% of occupied habitat (defined as model estimated encounter probabilities greater than 5%) from an SDM ensemble fitted to English sole distribution and abundance in AFSC RACE-GAP GOA summer bottom trawl surveys (1993–2019) with 100 m, 200 m, and 700 m isobaths indicated; within the EFH area map are the subareas of the top 25% (EFH hot spots), top 50% (core EFH area), and top 75% (principal EFH area).

Northern rock sole (*Lepidopsetta polyxystra*)

Northern rock sole (*Lepidopsetta polyxystra*, NRS) is present across the north Pacific, from Puget Sound through the Aleutian Islands and Bering Sea to the Kuril Islands (Orr and Matarese 2000). The species is a close congener of southern rock sole (*L. bilineata*, SRS). NRS and SRS in the GOA region are managed in the Shallow Water Flatfish stock complex, where they are two of the five species that account for a majority of the biomass of this group (Turncock et al. 2017b). Length-based life stage breaks distinguish between the three demersal life stages modeled in this study; settled early juveniles (20–140 mm; Doyle et al. 2019, NFAA), subadults (141–328 mm FL), and adults (> 328 mm FL) (Stark 2012b). The mesh size of the RACE-GAP bottom trawl is large enough that the smaller juvenile life stages may not be wholly retained in the catch[19]. This study combines the settled early juvenile life stages of NRS and SRS, which have not been consistently distinguished in the field by surveys. Otherwise, NRS and SRS subadults and adults are modeled separately, using RACE-GAP summer bottom trawl survey data from 1996–2019 when the survey reliably distinguished the two species.

Settled early juvenile rock sole distribution predicted from mixed gear-type summer surveys in the Gulf of Alaska -- Settled early juvenile rock soles (N = 252) caught in mixed gear-type summer surveys (1989–2019), using large and small mesh bottom trawls and purse and beach seines, were distributed in shallow and nearshore areas of the GOA continental shelf (Fig. 60). Settled early juvenile rock sole presence records from multiple surveys were combined in a habitat-related MaxEnt SDM predicting suitable habitat probabilities for this life stage in the GOA. The best model had a β-multiplier of 3.0 and an AUC of 0.95 (Table 24). Bottom depth alone accounted for 74.6.3% of the contribution among covariates to the deviance explained by the final SDM (Table 25). The highest predicted probabilities of suitable habitat for settled early juvenile rock sole were nearshore or less than 125 m depth on the GOA continental shelf, including Cook Inlet and the bathymetric rises south and west of Kodiak Island (Fig. 61). The standard deviation among k-folds as a result of cross-validation for the final SDM was relatively low.

Subadult northern rock sole abundance and distribution predicted from RACE-GAP summer bottom trawl surveys in the Gulf of Alaska -- Subadult NRS (N = 1,854) caught in GOA RACE-GAP summer bottom trawl surveys (1996–2019) occurred primarily on the GOA continental shelf west of the Kenai Peninsula (Fig. 62). Four of the five SDMs considered for inclusion in the ensemble to predict numerical abundance of subadult NRS in the GOA converged (Table 26); the GAM_{nb} was

[19] Adding other high quality sources of data if available to future SDM ensemble EFH mapping for this species will be included as a research recommendation from the 2023 EFH 5-year Review.

eliminated by skill testing. The three remaining best-performing SDMs were weighted by RMSE in the final ensemble, which attained an excellent overall fit to the observed subadult NRS distribution and abundance data. The ensemble was excellent at predicting high and low abundance catches (ρ = 0.68), at discriminating presence-absence (AUC = 0.96), and at explaining deviance (PDE = 0.68). Bottom depth and geographic location accounted for 83.4% of the contribution among covariates to the deviance explained by the final ensemble, where bottom depth alone accounted for 59.7% (Table 25). The highest abundances of subadult NRS were predicted at less than 125 m depth on bathymetric rises, such as the banks south of Kodiak Island, with abundance increasing further west in the GOA (Fig. 63). The CV of ensemble predictions was higher in nearshore areas and bathymetric rises on the continental shelf throughout the GOA. The probability of encountering subadult NRS was highest at bathymetric rises and shallow nearshore locations on the GOA continental shelf, particularly west of the Kenai Peninsula (Fig. 64).

Adult northern rock sole abundance and distribution predicted from RACE-GAP summer bottom trawl surveys in the Gulf of Alaska -- Adult NRS (N = 1,980) caught in GOA RACE-GAP summer bottom trawl surveys (1996–2019) occurred primarily on the GOA continental shelf west of the Kenai Peninsula, similar to subadults (Fig. 65). The five SDMs considered for inclusion in the ensemble to predict numerical abundance of adult NRS in the GOA converged (Table 26); the hGAM and GAM_{nb} were eliminated by skill testing. The three remaining best-performing SDMs were weighted by RMSE in the final ensemble, which attained an excellent overall fit to the observed adult NRS distribution and abundance data. The ensemble was excellent at predicting high and low abundance catches (ρ = 0.68) and at discriminating presence-absence (AUC = 0.95), and good at explaining deviance (PDE = 0.58). Similar to subadults, bottom depth alone accounted for 63.4% of the contribution among covariates to the deviance explained by the final ensemble (Table 25). The highest abundances of adult NRS were predicted at less than 125 m depth on bathymetric rises, such as the banks south of Kodiak Island, with abundance increasing west in the GOA around the Shumagin Islands and the Alaska Peninsula (Fig. 66). The CV of ensemble predictions was higher in nearshore areas and bathymetric rises on the continental shelf throughout the GOA. Similar to subadults, the probability of encountering adult NRS was highest at bathymetric rises and at shallow nearshore locations on the GOA continental shelf (Fig. 67).

Essential Fish Habitat of three life stages of northern rock sole in the Gulf of Alaska -- Habitat-related predictions of rock sole demersal life stage distribution and abundance from summer surveys of the GOA (mixed gear-type summer surveys (1989–2019) and RACE-GAP bottom trawl surveys (1996–2019)) were mapped as EFH areas and subareas (Fig. 68). EFH of settled early juvenile rock soles (NRS and SRS combined) occurred in inshore areas of the GOA continental shelf, with EFH

hot spots nearshore. The EFH areas for subadult and adult NRS were similar, occurring at bathymetric rises throughout the GOA continental shelf, with core EFH area and EFH hot spots most concentrated west of the Kenai Peninsula.

Essential Fish Habitat Level 3 habitat-related vital rates of settled early juvenile rock soles in the Gulf of Alaska -- Temperature-dependent growth rate of laboratory-reared early juvenile NRS is described by the following equation (Hurst *in prep*aration):

$$GR = 0.000454 - 0.000687 * T + 0.000328 * T^2 - 0.000015 * T^3 \ ,$$

where *GR* is the growth rate (% body weight (g) per day (d)), and *T* is the temperature. The raster product of early juvenile rock soles (NRS and SRS combined in the present study) predicted probability of suitable habitat from a MaxEnt SDM, and their temperature-dependent growth is an EFH Level 3 map of habitat-related growth potential (Fig. 69). The temperature of maximum growth for early juvenile NRS is 13.5°C (Hurst *in prep*aration), which was within the range (2.9–17.5°C) of the CGOA ROMS 3 km summer bottom temperature covariate raster (2000–2019) in the SDM and to the EFH Level 3 map of habitat-related growth potential (Fig. 69). The bottom temperature range at settled early juvenile rock sole catch locations in the SDM was 5.9–12.5°C (Fig. 60). In the map of temperature-dependent growth, the highest growth areas occurred inshore and along the coast, as well as on the banks and bathymetric rises on the GOA continental shelf (Fig. 69). The SDM of settled early juvenile rock soles suitable habitat limited areas of high predicted habitat-related growth potential (Fig. 69), notably to shallower depths, suggesting that temperature was not the only driver of distribution for this life stage in the GOA. EFH subareas of core EFH and EFH hot spots corresponded with locations of high habitat-related growth potential for settled early juvenile stage rock soles, which added value in interpreting the EFH Level 1 map (Fig. 68).

Table 24. -- Maximum entropy model (MaxEnt) used to construct Essential Fish Habitat (EFH) for settled early juvenile rock sole: regularization multiplier (β); *k*-fold cross-validation root-mean-square-error (RMSE), area under the receiver operating characteristic curve (AUC), and areal extent of EFH (km^2).

Model	**β**	**RMSE**	**AUC**	**EFH area (km^2)**
MaxEnt	3.0	18.55	0.95	128,100

Table 25. -- Covariates retained in the a) settled early juvenile habitat-related maximum entropy (MaxEnt) species distribution model (SDM) for rock soles, and b) subadult and c) adult SDM final ensembles for northern rock sole with the percent contribution of each covariate to the deviance explained by the SDMs and the cumulative deviance explained: SD = standard deviation and BPI = bathymetric position index.

rock sole	**Covariate**	**% Contribution**	**Cumulative %**
a) settled early juvenile	bottom depth	74.6	74.6
	tidal maximum	6.0	80.6
	slope	4.0	84.7
	rockiness	3.9	88.6
	aspect north	3.3	91.9
	aspect east	3.1	95.0
	curvature	2.3	97.3
	BPI	1.7	98.9
	pennatulacean presence	1.1	100.0
northern rock sole	bottom depth	59.7	59.7
b) subadult	location	24.0	83.7
	bottom temperature	4.0	87.7
	current	3.5	91.2
	BPI	1.8	93.0
	current SD	1.3	94.3
	tidal maximum	1.2	95.5
	rockiness	1.1	96.6
	aspect east	0.8	97.4
	aspect north	0.7	98.1
	sponge presence	0.7	98.8
	slope	0.6	99.4
	pennatulacean presence	0.3	99.7
	coral presence	0.2	99.9
	curvature	0.1	100.0
	bottom depth	59.7	59.7
c) adult	bottom depth	63.4	63.4
	location	22.6	86.0
	bottom temperature	3.8	89.8
	current	2.5	92.3
	current SD	1.9	94.2
	rockiness	1.7	95.9
	BPI	1.2	97.1
	tidal maximum	0.7	97.8
	slope	0.4	98.2
	aspect north	0.4	98.6

rock sole

Covariate	% Contribution	Cumulative %
sponge presence	0.3	98.9
coral presence	0.3	99.2
pennatulacean presence	0.3	99.5
curvature	0.3	99.8
aspect east	0.2	100.0

Table 26. -- Constituent species distribution models (SDMs) used to construct Essential Fish Habitat (EFH) for a) subadult and b) adult northern rock sole: MaxEnt = Maximum entropy; paGAM = presence-absence generalized additive model; hGAM = zero-adjusted Poisson hurdle GAM; GAM_P = standard Poisson GAM; GAM_{nb} = standard negative-binomial GAM; RMSE = root mean square error; ρ (*rho*) = Spearman's rank correlation coefficient; AUC = area under the receiver operating characteristic curve; and PDE = Poisson deviance explained *. The "--" indicates that this model was not included in the final ensemble.

a) subadult northern rock sole

Models	RMSE	Relative Weight	*P*	AUC	PDE	EFH area (km^2)
MaxEnt	64.5	0.32	0.65	0.93	0.50	192,700
paGAM	63.4	0.33	0.69	0.96	0.59	171,000
hGAM	--	--	--	--	--	--
GAM_P	60.9	0.36	0.70	0.95	0.65	122,800
GAM_{nb}	63.1	0	--	--	--	--
ensemble	57.3	1	0.68	0.96	0.68	182,200

b) adult northern rock sole

Models	RMSE	Relative Weight	ρ	AUC	PDE	EFH area (km^2)
MaxEnt	26.8	0.32	0.65	0.92	0.46	202,900
paGAM	25.8	0.34	0.69	0.95	0.54	189,200
hGAM	120.5	0	--	--	--	--
GAM_P	25.8	0.34	0.71	0.94	0.55	124,200
GAM_{nb}	27.4	0	--	--	--	--
ensemble	25.0	1	0.68	0.95	0.58	190,700

* Refer to the Species Distribution Model Performance Metrics subsection within the Statistical Modeling section of the Methods for detailed descriptions of individual model performance metrics.

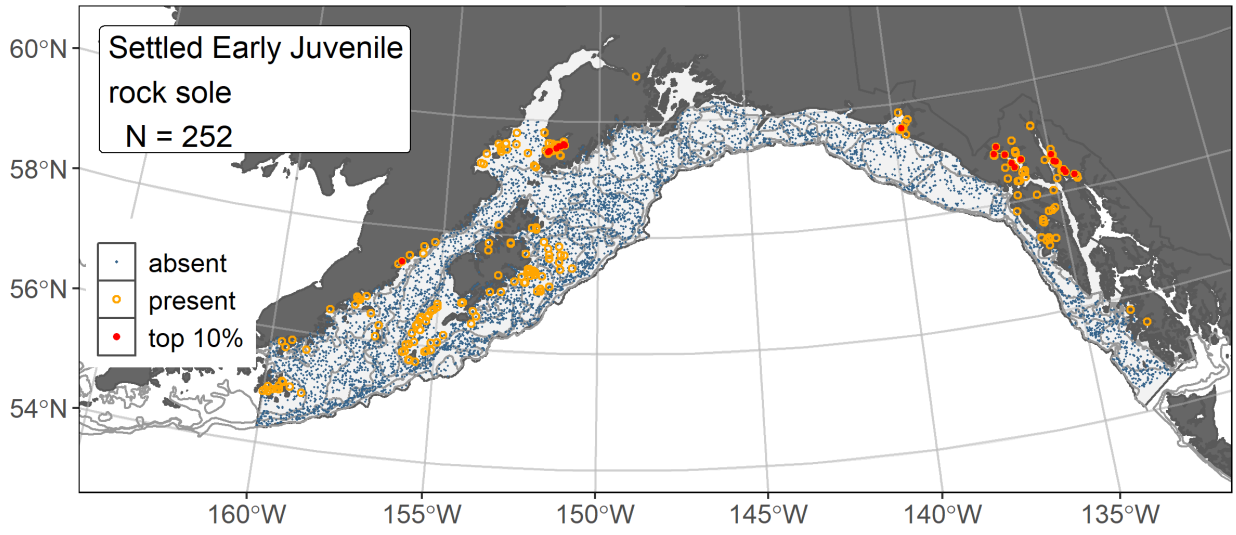

Figure 60. -- Distribution of settled early juvenile rock sole catches (N = 252) in mixed gear-type summer surveys of the Gulf of Alaska (1989–2019) with the 100 m, 200 m, and 700 m isobaths indicated; filled red circles indicate locations in top 10% of overall abundance, open orange circles indicate presence in remaining catches, and blue dots indicate stations sampled where the animals were not present.

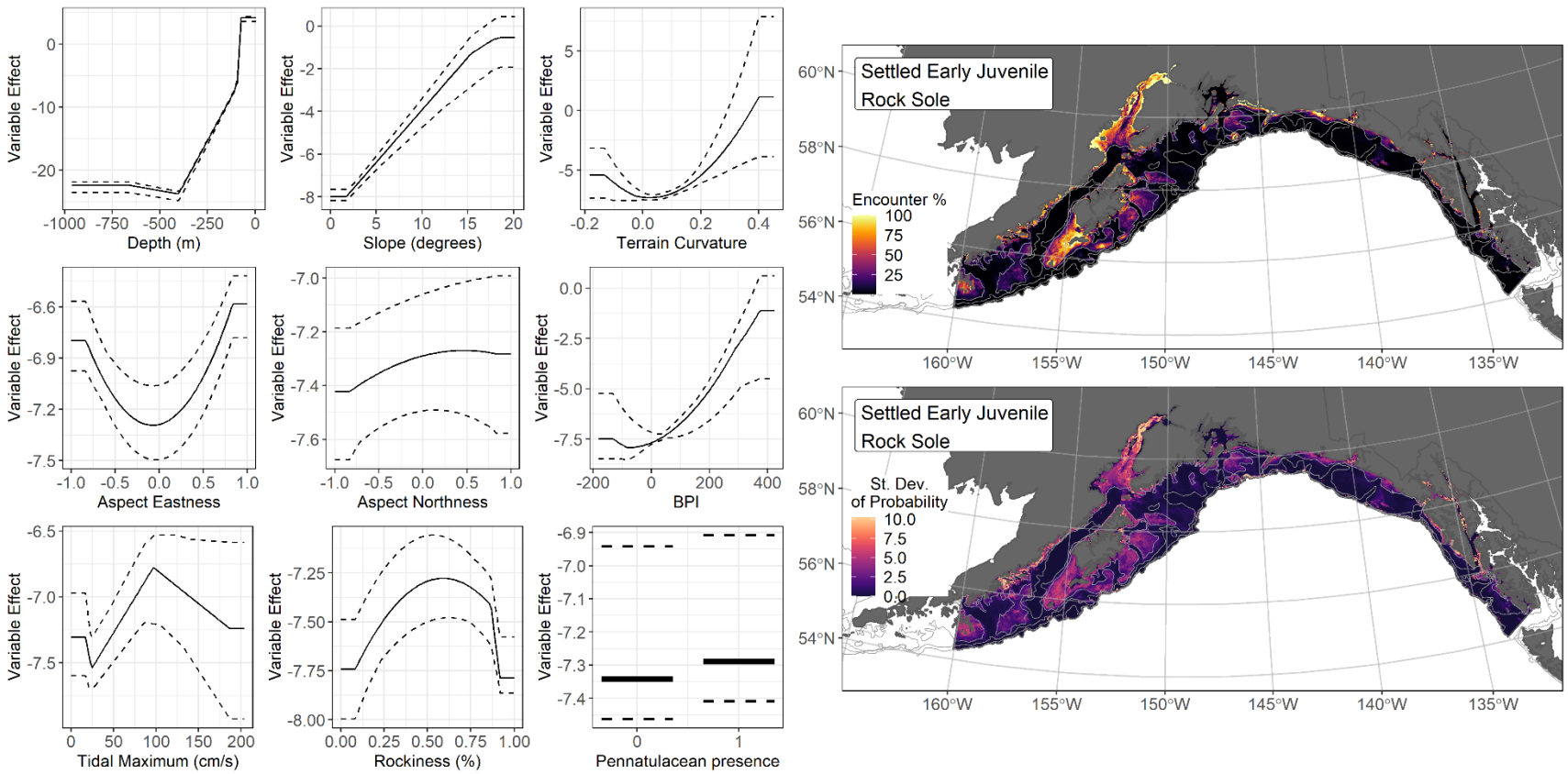

Figure 61. -- The top nine covariate effects (left panel) from a habitat-related species distribution model (MaxEnt) of settled early juvenile rock sole probability of suitable habitat in the Gulf of Alaska (upper right panel) with the standard deviation of the probability predictions (lower right panel).

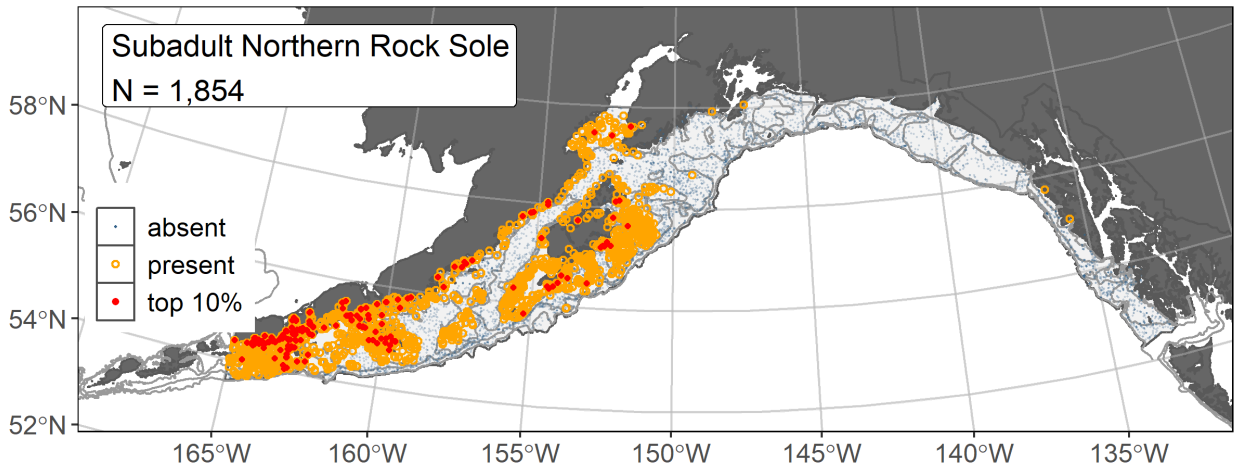

Figure 62. -- Distribution of subadult northern rock sole catches (N = 1,854) in 1996–2019 AFSC RACE-GAP summer bottom trawl surveys of the Gulf of Alaska with the 100 m, 200 m, and 700 m isobaths indicated; filled red circles indicate locations in top 10% of overall abundance, open orange circles indicate presence in remaining catches, and blue dots indicate stations sampled where the animals were not present.

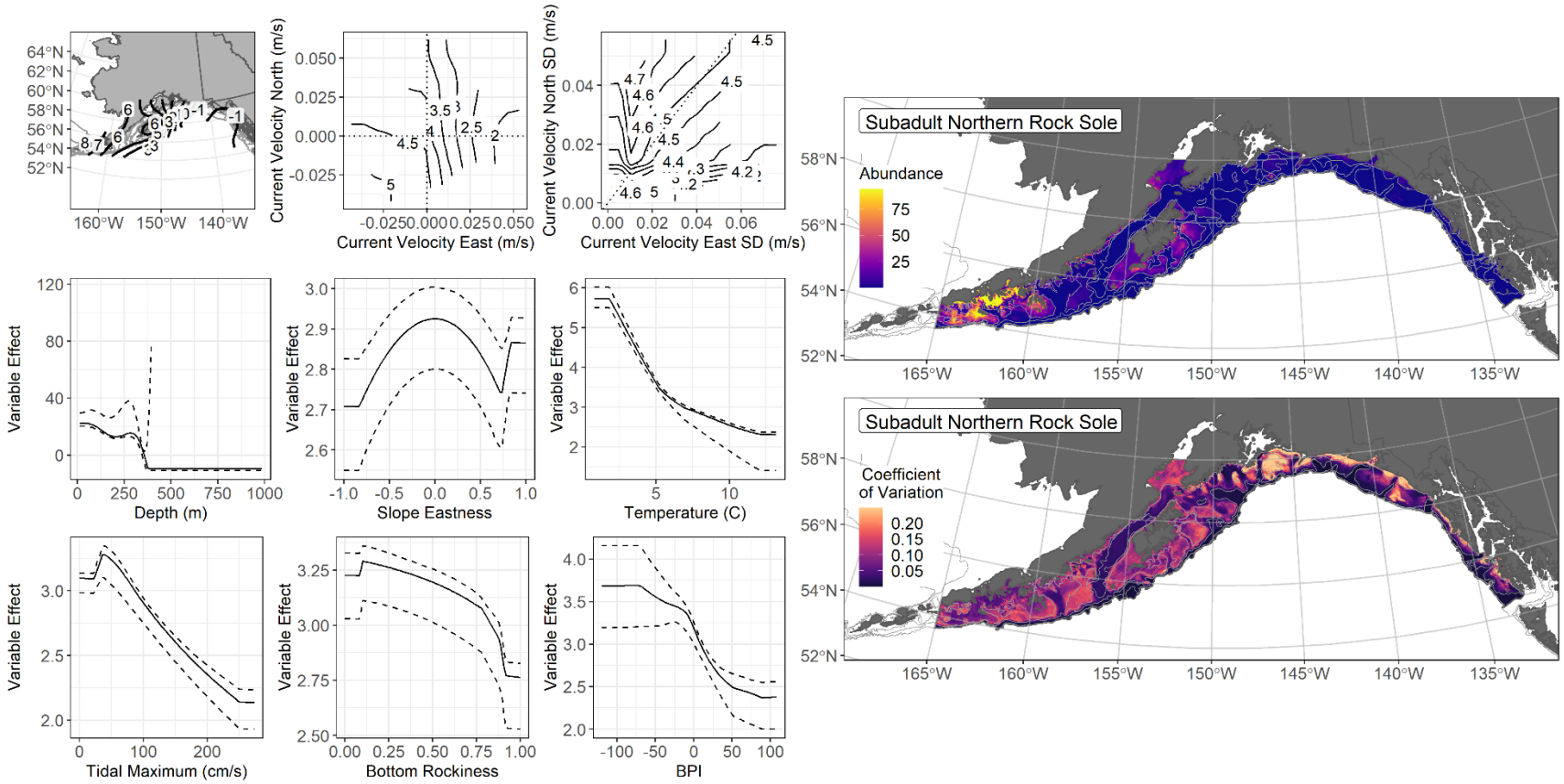

Figure 63. -- The top nine covariate effects (left panel) on ensemble-predicted subadult northern rock sole numerical abundance across the Gulf of Alaska (upper right panel) along with the coefficient of variation (CV) of the ensemble predictions (lower right panel).

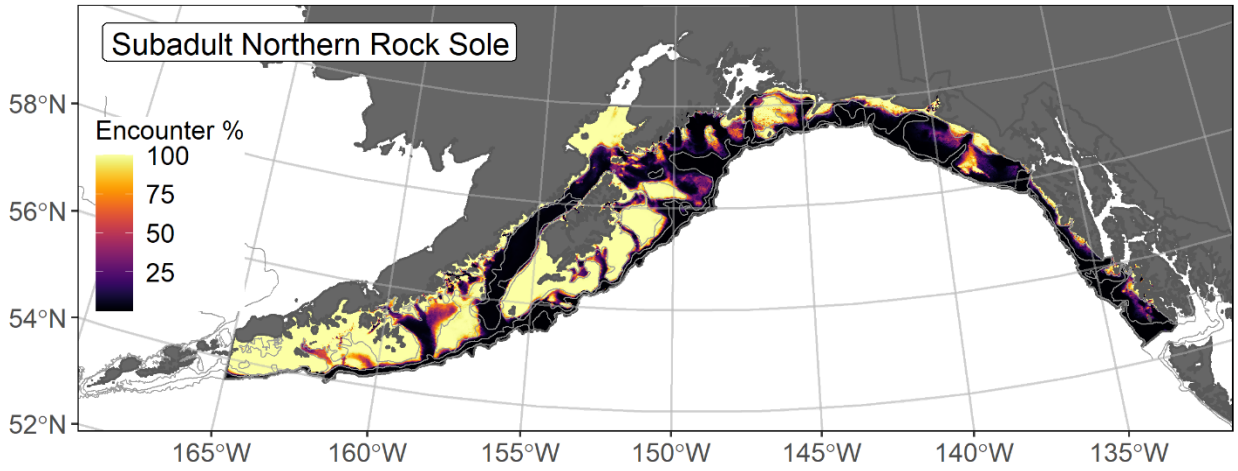

Figure 64. -- Encounter probability of subadult northern rock sole from AFSC RACE-GAP summer bottom trawl surveys (1996–2019) of the Gulf of Alaska with the 100 m, 200 m, and 700 m isobaths indicated.

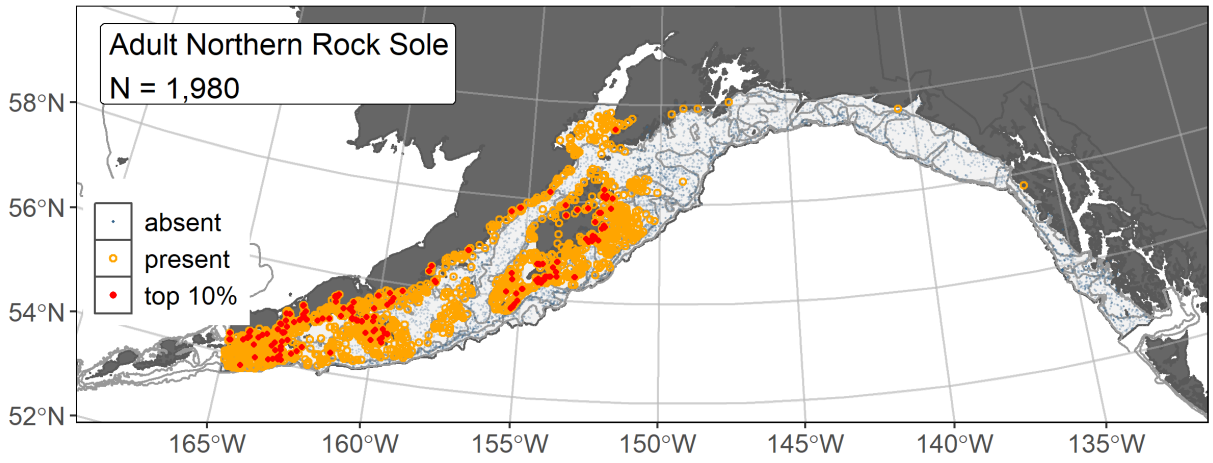

Figure 65. -- Distribution of adult northern rock sole catches (N = 1,980) in 1996–2019 AFSC RACE-GAP summer bottom trawl surveys of the Gulf of Alaska with the 100 m, 200 m, and 700 m isobaths indicated; filled red circles indicate locations in top 10% of overall abundance, open orange circles indicate presence in remaining catches, and blue dots indicate stations sampled where the animals were not present.

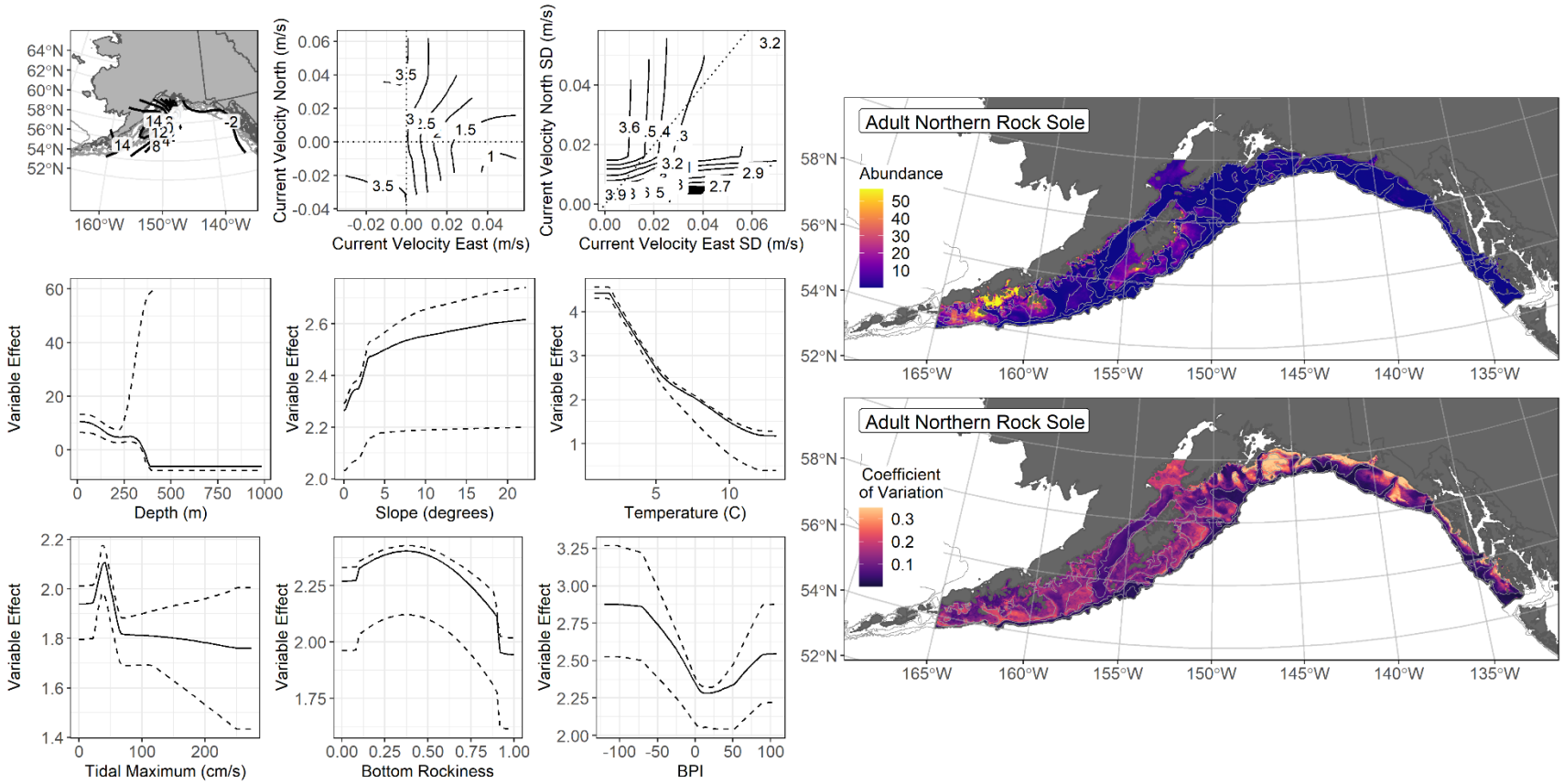

Figure 66. -- The top nine covariate effects (left panel) on ensemble-predicted adult northern rock sole numerical abundance across the Gulf of Alaska (upper right panel) along with the coefficient of variation (CV) of the ensemble predictions (lower right panel).

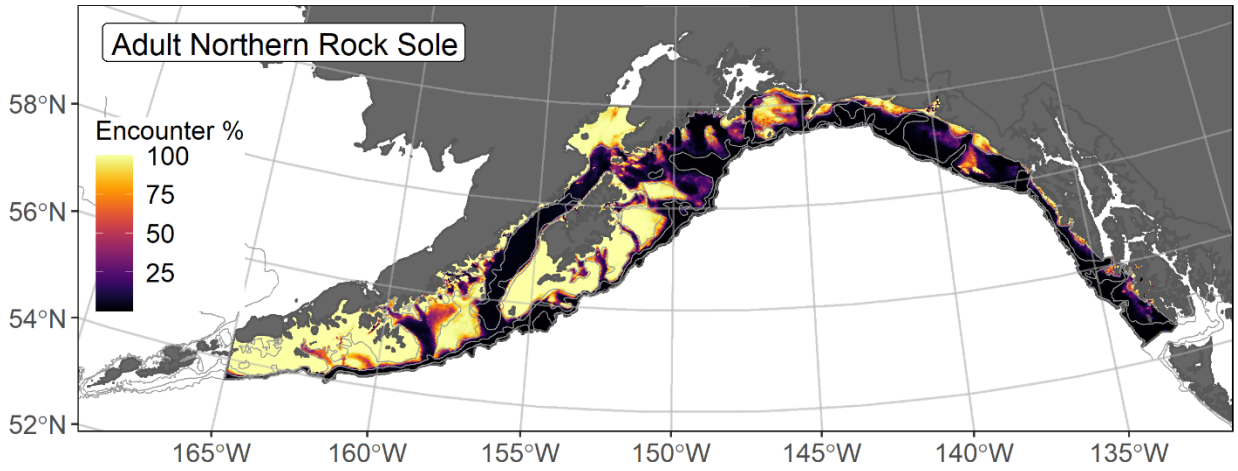

Figure 67. -- Encounter probability of adult northern rock sole from AFSC RACE-GAP summer bottom trawl surveys (1996–2019) of the Gulf of Alaska with the 100 m, 200 m, and 700 m isobaths indicated.

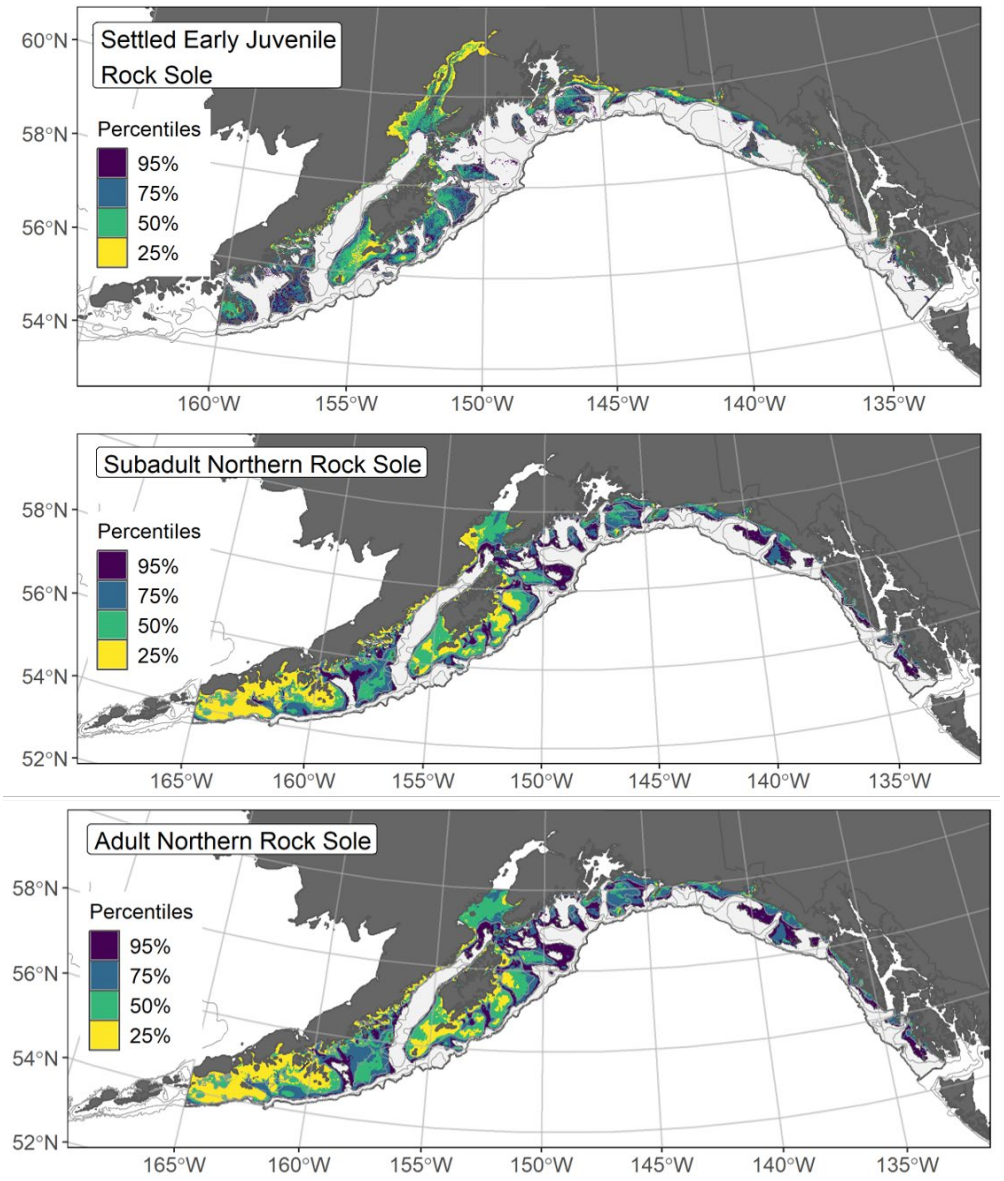

Figure 68. -- Essential fish habitat (EFH) is the area containing the top 95% of occupied habitat (defined as greater than 5% predicted probability of suitable habitat) for settled early juvenile (top panel) rock sole from an SDM fitted to their distribution in Gulf of Alaska (GOA) mixed gear-type summer surveys (1989–2019), and for subadults (middle panel) and adults (bottom panel) is the area containing the top 95% of occupied habitat (defined as model estimated encounter probabilities greater than 5%) from an SDM ensemble fitted to northern rock sole distribution and abundance in AFSC RACE-GAP GOA summer bottom trawl surveys (1993–2019) with 100 m, 200 m, and 700 m isobaths indicated; within the EFH area map are the subareas of the top 25% (EFH hot spots), top 50% (core EFH area), and top 75% (principal EFH area).

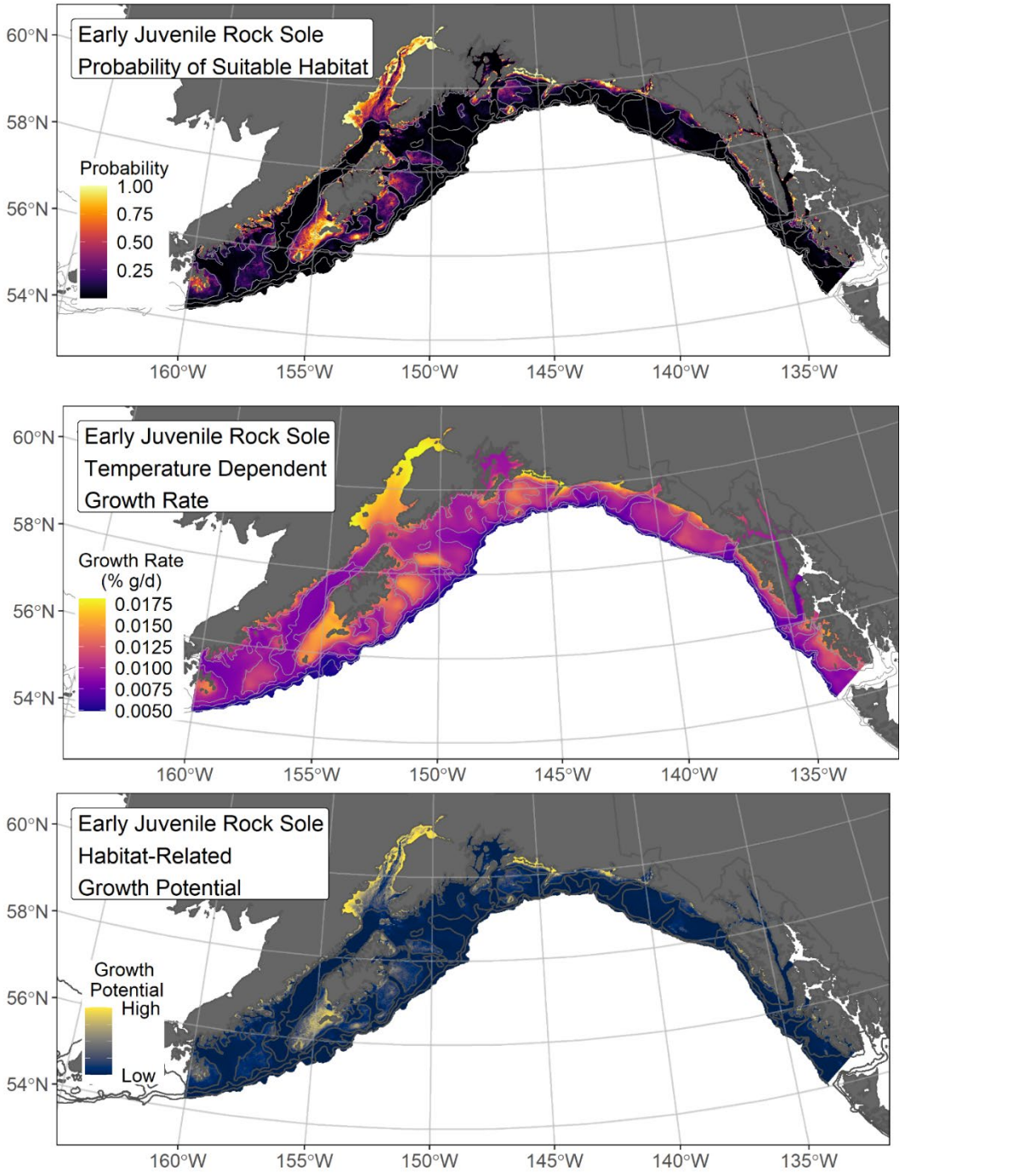

Figure 69. -- Settled early juvenile rock sole predicted probability of suitable habitat from a habitat-related species distribution model fitted to their distribution in Gulf of Alaska mixed gear-type summer surveys (1989–2019; top panel), temperature-dependent growth rate ($GR = \%\ body\ weight\ (g) \cdot day^{-1}$; center panel), and EFH Level 3 map of habitat-related growth potential (bottom panel), which is the raster product of probability of suitable habitat and temperature-dependent growth rate.

Pacific sanddab (*Citharichthys sordidus*)

Pacific sanddab (*Citharichthys sordidus*) is a shallow-water flatfish species ranging from Baja California to southeast Alaska (Lamb and Edgell 2010). In the GOA, Pacific sanddab are managed in the Shallow Water Flatfish stock complex as a member of the "other flatfish" species in this group (Turncock et al. 2017b). Little is known about Pacific sanddab life history in the GOA, encompassing the northern part of their range. The mesh size of the RACE-GAP bottom trawl is large enough that the smaller juvenile life stages may not be wholly retained in the catch[20]. Without length-based information to distinguish between the demersal life stages, all individuals caught by RACE-GAP summer bottom trawl surveys in the GOA were modeled in composite to map EFH for this species.

Pacific sanddab demersal life stage abundance and distribution predicted from RACE-GAP summer bottom trawl surveys in the Gulf of Alaska -- Pacific sanddab demersal life stages (N = 77) caught in GOA RACE-GAP summer bottom trawl surveys (1993–2019) were primarily caught on the continental shelf off of southeast Alaska and were present in the central and western GOA (Fig. 70). Three of the five SDMs considered for inclusion in the ensemble to predict numerical abundance of Pacific sanddab in the GOA converged (Table 27). The three best-performing SDMs were weighted by RMSE in the final ensemble, which attained a fair fit to the observed Pacific sanddab data. The ensemble was poor at predicting high and low abundance catches (ρ = 0.19) and excellent at discriminating presence-absence (AUC = 0.98) and explaining deviance (PDE = 0.74). Geographic location and bottom temperature accounted for 61.1% of the contribution among covariates to the deviance explained by the ensemble predicting Pacific sanddab numerical abundance (Table 28). Higher Pacific sanddab abundance was predicted to occur at shallower depths on the continental shelf of the eastern GOA (Fig. 71). The CV of ensemble predictions was higher in the eastern GOA. The probability of encountering Pacific sanddab was higher in areas of predicted high abundance, including off southeast Alaska (Fig. 72).

Essential Fish Habitat of Pacific sanddab demersal life stages in the Gulf of Alaska -- Habitat-related predictions of Pacific sanddab demersal life stage distribution and abundance from RACE-GAP summer bottom-trawl surveys of the GOA (1993–2019) were mapped as EFH areas and subareas (Fig. 73). Pacific sanddab EFH area included shallower depths of the continental shelf in the eastern GOA off southeast Alaska. This SDM-based EFH map is the first developed for Pacific sanddab in the GOA, which is the case for many of the constituent species of the GOA Shallow Water Flatfish stock complex.

[20] Adding other high quality sources of data if available to future SDM ensemble EFH mapping for this species will be included as a research recommendation from the 2023 EFH 5-year Review.

Table 27. -- Constituent species distribution models (SDMs) used to construct Essential Fish Habitat (EFH) for demersal life stages of Pacific sanddab: MaxEnt = Maximum entropy; paGAM = presence-absence generalized additive model; hGAM = zero-adjusted Poisson hurdle GAM; GAM_P = standard Poisson GAM; GAM_{nb} = standard negative-binomial GAM; RMSE = root mean square error; ρ (*rho*) = Spearman's rank correlation coefficient; AUC = area under the receiver-operating characteristic curve; and PDE = Poisson deviance explained *. The "--" indicates that this model was not included in the final ensemble.

Pacific sanddab

Models	**RMSE**	**Relative Weight**	**ρ**	**AUC**	**PDE**	**EFH area (km^2)**
MaxEnt	2.40	0.35	0.17	0.95	0.58	26,800
paGAM	2.22	0.40	0.20	0.96	0.70	31,200
hGAM	--	0	--	--	--	--
GAM_P	--	0	--	--	--	--
GAM_{nb}	2.82	0.25	0.29	0.98	0.70	22,900
ensemble	2.15	1	0.19	0.98	0.74	32,000

* Refer to the Species Distribution Model Performance Metrics subsection within the Statistical Modeling section of the Methods for detailed descriptions of individual model performance metrics.

Table 28. -- Covariates retained in the species distribution model (SDM) final ensemble for Pacific sanddab demersal life stages with the percent contribution of each covariate to the deviance explained by the SDMs and the cumulative deviance explained: SD = standard deviation and BPI = bathymetric position index.

Pacific sanddab

Covariate	% Contribution	Cumulative %
location	43.9	43.9
bottom temperature	17.1	61.1
tidal maximum	11.3	72.4
bottom depth	11.2	83.6
current	5.1	88.7
rockiness	3.1	91.8
slope	2.5	94.3
BPI	1.9	96.2
current SD	1.4	97.6
sponge presence	0.8	98.4
aspect north	0.6	99.0
coral presence	0.5	99.5
aspect east	0.3	99.8
pennatulacean presence	0.2	100.0

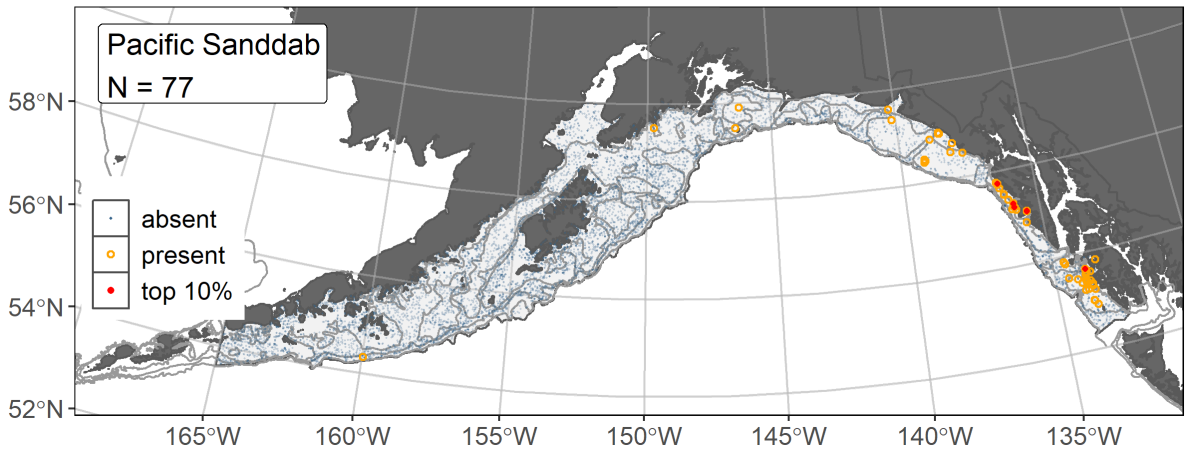

Figure 70. -- Distribution of Pacific sanddab catches (N = 77) in 1993–2019 AFSC RACE-GAP summer bottom trawl surveys of the Gulf of Alaska with the 100 m, 200 m, and 700 m isobaths indicated; filled red circles indicate locations in top 10% of overall abundance, open orange circles indicate presence in remaining catches, and blue dots indicate stations sampled where the animals were not present.

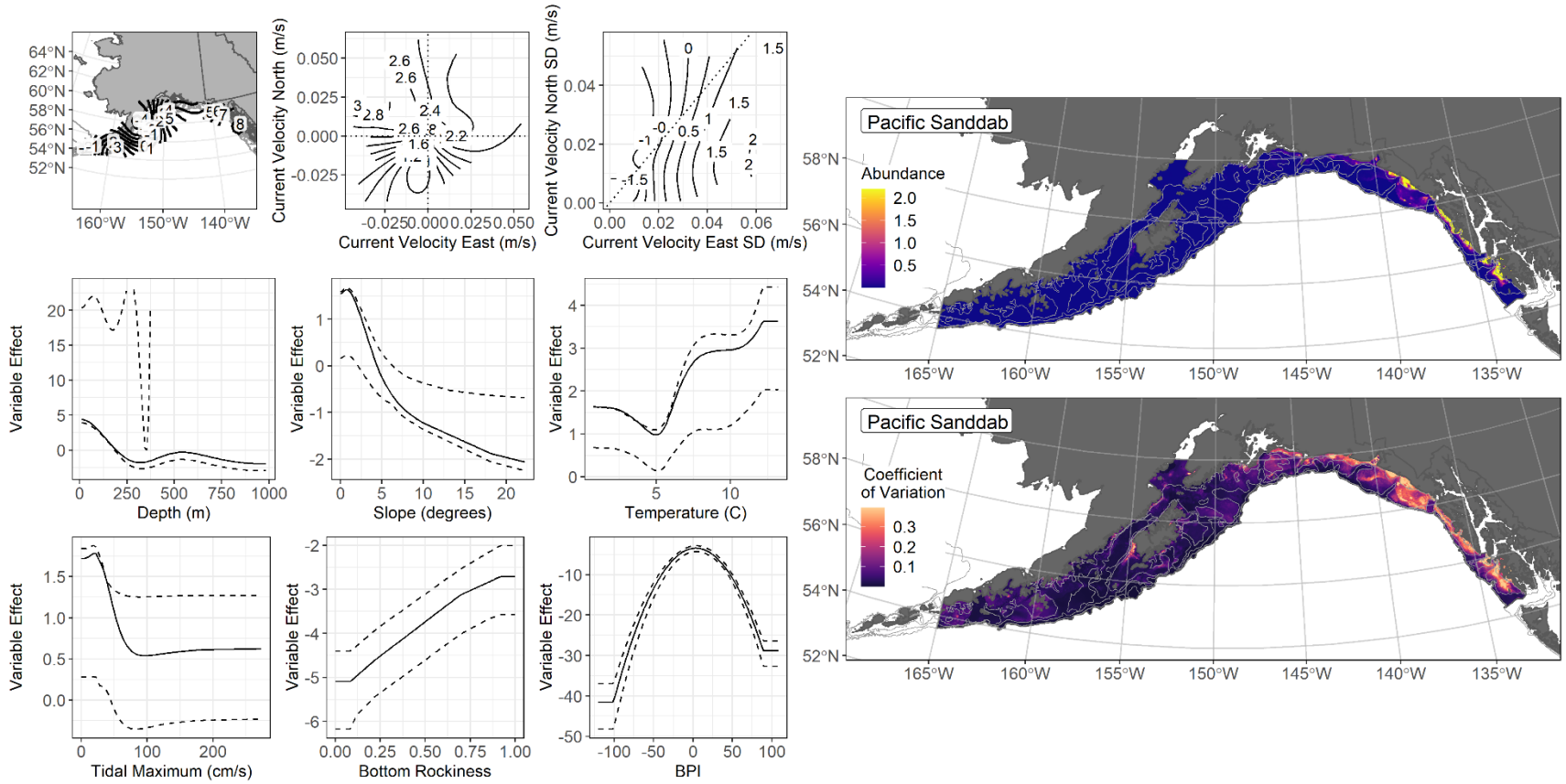

Figure 71. -- The top nine covariate effects (left panel) on ensemble-predicted Pacific sanddab numerical abundance across the Gulf of Alaska (upper right panel) along with the coefficient of variation (CV) of the ensemble predictions (lower right panel).

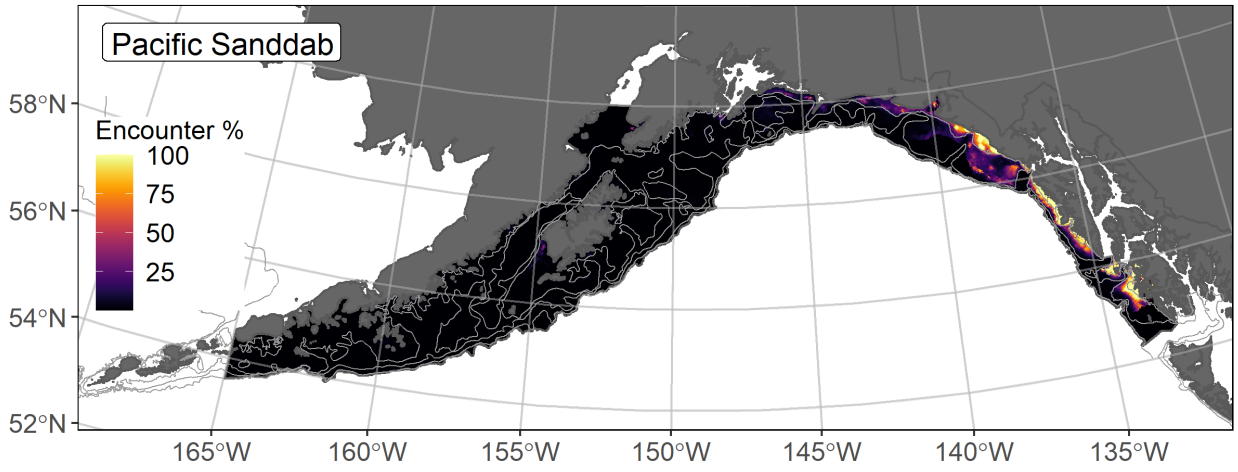

Figure 72. -- Encounter probability of Pacific sanddab from AFSC RACE-GAP summer bottom trawl surveys (1993–2019) of the Gulf of Alaska with the 100 m, 200 m, and 700 m isobaths indicated.

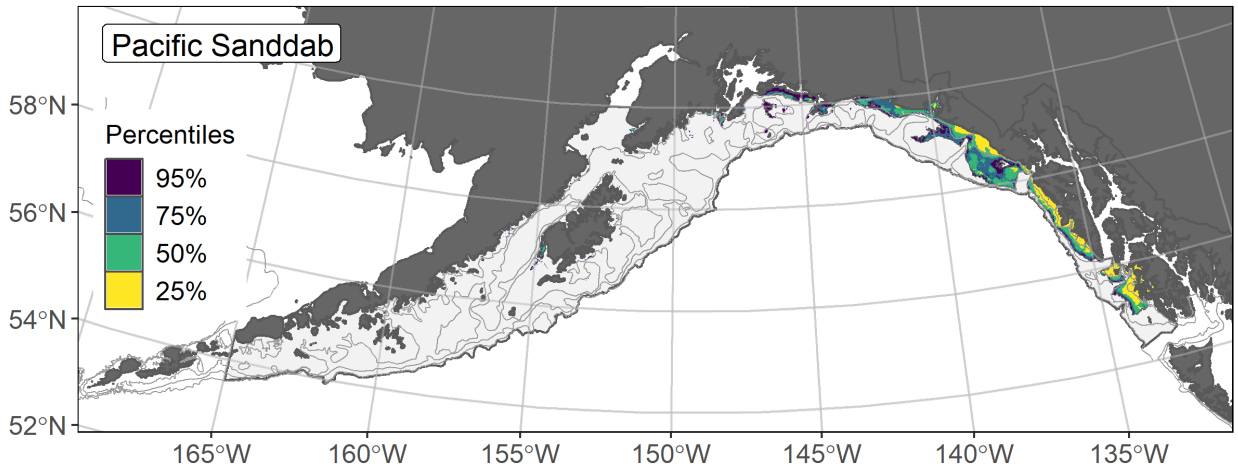

Figure 73. -- Essential fish habitat (EFH) is the area containing the top 95% of occupied habitat (defined as model estimated encounter probabilities greater than 5%) from an SDM ensemble fitted to Pacific sanddab distribution and abundance from AFSC RACE-GAP Gulf of Alaska (GOA) summer bottom trawl surveys (1993–2019) with 100 m, 200 m, and 700 m isobaths indicated; within the EFH area map are the subareas of the top 25% (EFH hot spots), top 50% (core EFH area), and top 75% (principal EFH area) of habitat-related, ensemble-predicted numerical abundance.

Petrale sole (*Eopsetta jordani*)

Petrale sole (*Eopsetta jordani*) is a right-eyed flounder ranging from Baja California to the western GOA (Wetzel 2019). In the GOA, petrale sole are managed in the Shallow Water Flatfish stock complex as a member of the "other flatfish" species in this group (Turncock et al. 2017b). Little is known about petrale sole life history in the GOA at the northern extent of their range. The mesh size of the RACE-GAP bottom trawl is large enough that the smaller juvenile life stages may not be wholly retained in the catch[21]. However, maturity studies of individuals from the US West Coast estimated L50 = 331 mm FL (Hannah et al. 2002), which is used in this study to distinguish the subadult ($\leq$ 331 mm FL) and adult (> 331 mm FL) life stages.

Subadult petrale sole abundance and distribution predicted from RACE-GAP summer bottom trawl surveys in the Gulf of Alaska -- Subadult petrale sole (N = 59) caught in GOA RACE-GAP summer bottom trawl surveys (1993–2019) occurred primarily in the eastern GOA off southeast Alaska and were incidentally present through the western extent of the GOA study area (Fig. 74). Four of the five SDMs considered for inclusion in the ensemble to predict numerical abundance of subadult petrale sole in the GOA converged (Table 29); the GAM_P was eliminated by skill testing. The three SDMs were weighted by RMSE in the final ensemble, which attained a fair fit to the observed subadult petrale sole distribution and abundance data. The ensemble was poor at predicting high and low abundance catches (ρ = 0.18), excellent at discriminating presence-absence (AUC = 0.98), and good at explaining deviance (PDE = 0.56). Geographic location, bottom temperature, and tidal current accounted for 52.4% of the contribution among covariates to the deviance explained by the final ensemble (Table 30). The highest abundances were predicted less than 100 m depth in the eastern GOA off southeast Alaska (Fig. 75). The CV of ensemble predictions was highest in the eastern GOA. The probability of encountering subadult petrale sole was highest off southeast Alaska (Fig. 76).

Adult petrale sole abundance and distribution predicted from RACE-GAP summer bottom trawl surveys in the Gulf of Alaska -- Adult petrale sole (N = 271) caught in GOA RACE-GAP summer bottom trawl surveys (1993–2019) also occurred primarily in the eastern GOA off southeast Alaska, where the highest density catches were observed and were present through the western extent of the GOA study area (Fig. 77). All five SDMs considered for inclusion in the ensemble to predict numerical abundance of adult petrale sole in the GOA converged (Table 29); the hGAM and GAM_P were eliminated by skill testing. The three remaining best-performing SDMs were weighted by RMSE in the final

[21] Adding other high quality sources of data if available to future SDM ensemble EFH mapping for this species will be included as a research recommendation from the 2023 EFH 5-year Review.

ensemble, which attained a good fit to the observed adult petrale sole distribution and abundance data. The ensemble was fair at predicting high and low abundance catches (ρ = 0.29), and excellent at discriminating presence-absence (AUC = 0.96) and at explaining deviance (PDE = 0.65). Geographic location, bottom depth, and bottom temperature accounted for 72.4% of the contribution among covariates to the deviance explained by the final ensemble (Table 30). The highest abundances were predicted less than 125 m depth in the eastern GOA off southeast Alaska, similar to subadults (Fig. 78). The CV of ensemble predictions was highest in the eastern GOA (Fig. 78). The probability of encountering adult petrale sole was highest off southeast Alaska (Fig. 79).

Essential Fish Habitat of subadult and adult petrale sole in the Gulf of Alaska -- Ensemble-predicted, habitat-related numerical abundance of petrale sole life stages collected in RACE-GAP summer bottom trawl surveys of the GOA (1993–2019) was mapped as EFH areas and subareas (Fig. 80). Petrale sole EFH areas for subadults and adults occurred in the eastern GOA, with EFH hot spots most prevalent off southeast Alaska. Adult petrale sole EFH area was larger than the subadult EFH area, extending into the central GOA with core EFH area over most of the eastern GOA continental shelf. These SDM-based EFH maps are the first developed for petrale sole in the GOA, which is the case for many of the constituent species of the GOA Shallow Water Flatfish stock complex.

Table 29. -- Constituent species distribution models (SDMs) used to construct Essential Fish Habitat (EFH) for a) subadult and b) adult petrale sole: MaxEnt = Maximum entropy; paGAM = presence-absence generalized additive model; hGAM = zero-adjusted Poisson hurdle GAM; GAM_P = standard Poisson GAM; GAM_{nb} = standard negative-binomial GAM; RMSE = root mean square error; ρ (rho) = Spearman's rank correlation coefficient; AUC = area under the receiver-operating characteristic curve; and PDE = Poisson deviance explained *. The "--" indicates that this model was not included in the final ensemble.

a) subadult petrale sole

Models	RMSE	Relative Weight	ρ	AUC	PDE	EFH area (km^2)
MaxEnt	0.32	0.34	0.13	0.91	0.38	14,800
paGAM	0.32	0.34	0.22	0.96	0.51	16,800
hGAM	--	--	--	--	--	--
GAM_P	0.34	--	--	--	--	--
GAM_{nb}	0.33	0.32	0.25	0.98	0.59	11,600
ensemble	0.31	1	0.18	0.98	0.56	15,400

b) adult petrale sole

Models	RMSE	Relative Weight	ρ	AUC	PDE	EFH area (km^2)
MaxEnt	1.47	0.33	0.25	0.91	0.45	77,000
paGAM	1.42	0.35	0.33	0.96	0.60	60,300
hGAM	4.23	0	--	--	--	--
GAM_P	1.46	0.33	0.39	0.95	0.58	48,200
GAM_{nb}	1.46	--	--	--	--	--
ensemble	1.32	1	0.29	0.96	0.65	64,600

* Refer to the Species Distribution Model Performance Metrics subsection within the Statistical Modeling section of the Methods for detailed descriptions of individual model performance metrics.

Table 30. -- Covariates retained in the a) subadult and b) adult petrale sole species distribution model (SDM) final ensembles, the percent contribution to the total deviance explained by each, and the cumulative percent deviance: SD = standard deviation, and BPI = bathymetric position index.

petrale sole	**Covariate**	**% Contribution**	**Cumulative %**
a) subadult	location	23.1	23.1
	bottom temperature	15.1	38.2
	tidal maximum	14.3	52.4
	bottom depth	9.7	62.1
	aspect east	8.7	70.8
	pennatulacean presence	8.4	79.2
	BPI	4.5	83.7
	coral presence	3.8	87.5
	curvature	3.6	91.1
	slope	3.2	94.3
	rockiness	1.9	96.2
	sponge presence	1.9	98.1
	current SD	1.0	99.1
	current	0.5	99.6
	aspect north	0.4	100.0
b) adult	location	51.8	51.8
	bottom depth	11.8	63.6
	bottom temperature	8.8	72.4
	rockiness	5.6	78.0
	current	4.9	82.9
	tidal maximum	4.7	87.6
	current SD	4.0	91.6
	BPI	3.2	94.8
	curvature	1.7	96.5
	aspect east	1.6	98.1
	slope	0.8	98.9
	aspect north	0.7	99.6
	pennatulacean presence	0.3	99.9
	coral presence	0.1	100.0

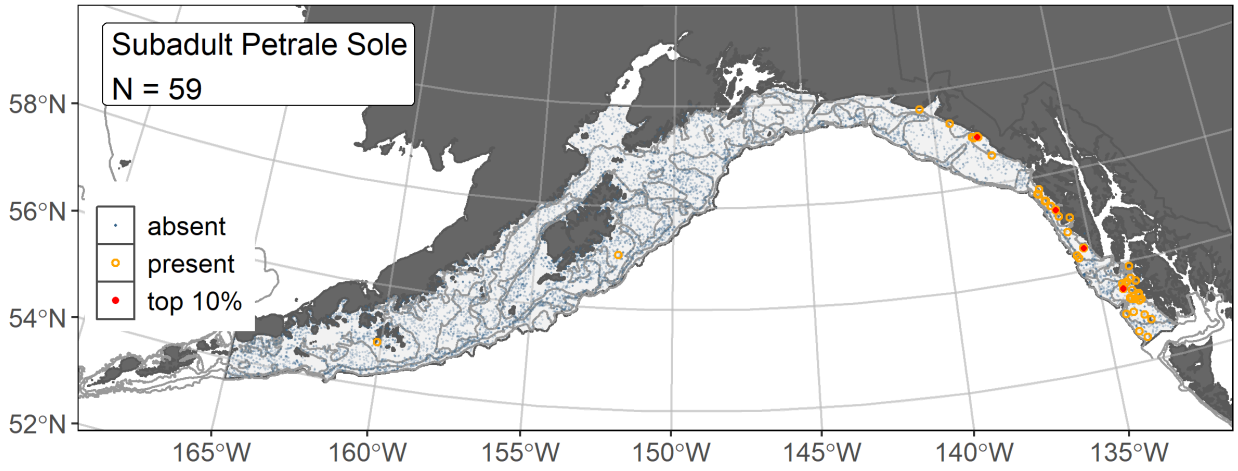

Figure 74. -- Distribution of subadult petrale sole catches (N = 59) in 1993–2019 AFSC RACE-GAP summer bottom trawl surveys of the Gulf of Alaska with the 100 m, 200 m, and 700 m isobaths indicated; filled red circles indicate locations in top 10% of overall abundance, open orange circles indicate presence in remaining catches, and blue dots indicate stations sampled where the animals were not present.

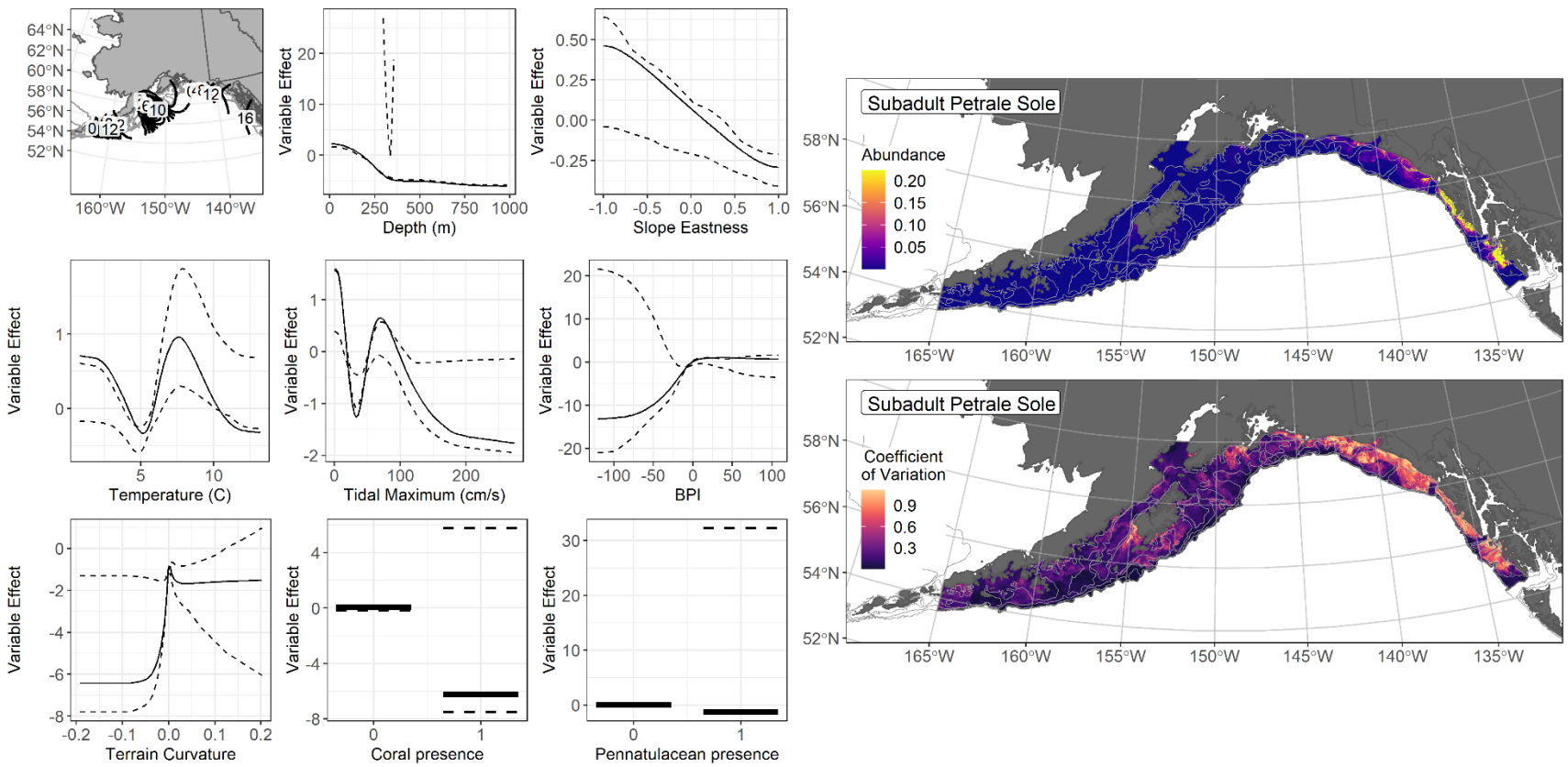

Figure 75. -- The top nine covariate effects (left panel) on ensemble-predicted subadult petrale sole numerical abundance across the Gulf of Alaska (upper right panel) along with the coefficient of variation (CV) of the ensemble predictions (lower right panel).

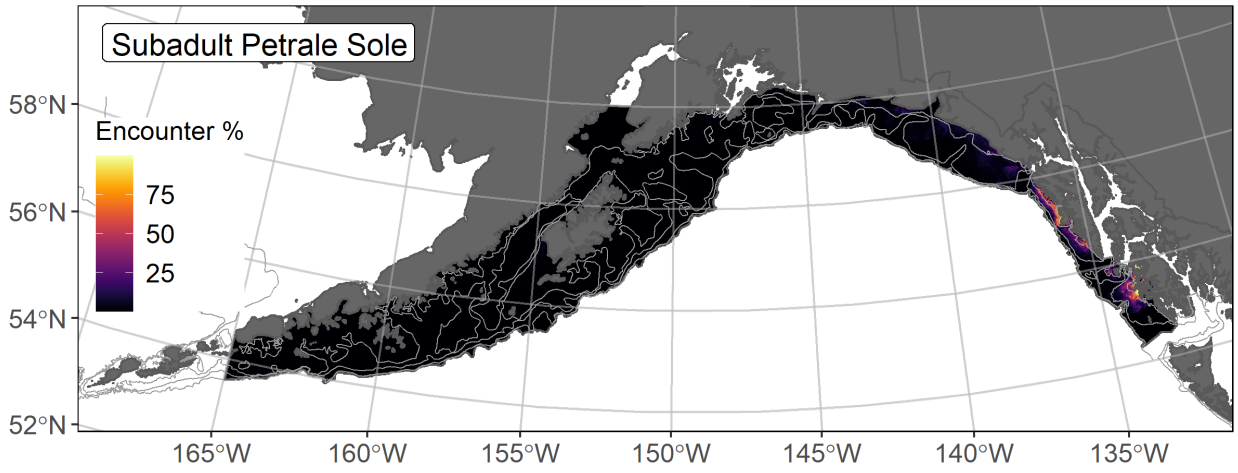

Figure 76. -- Encounter probability of subadult petrale sole from AFSC RACE-GAP summer bottom trawl surveys (1993–2019) of the Gulf of Alaska with the 100 m, 300 m, and 700 m isobaths indicated.

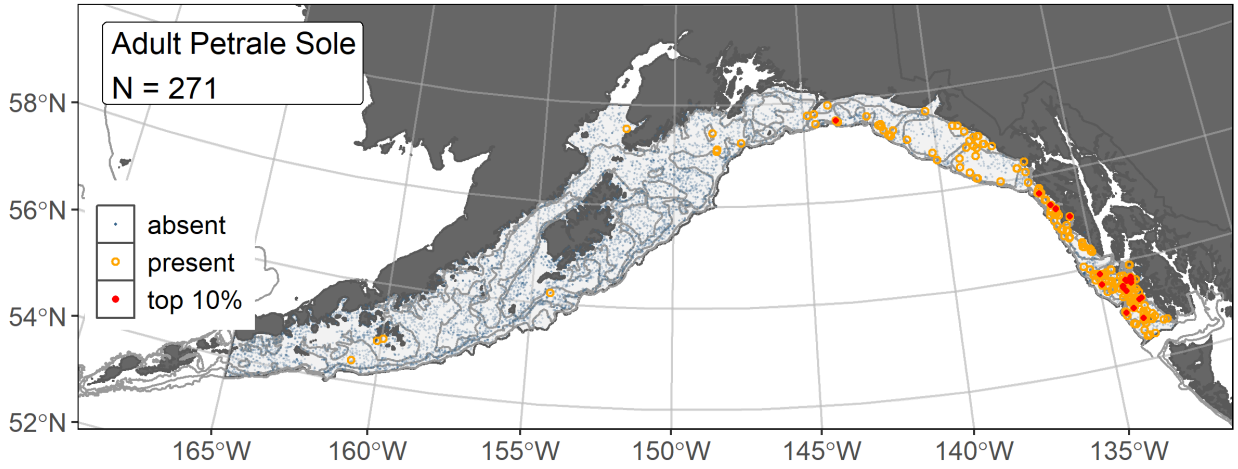

Figure 77. -- Distribution of adult petrale sole catches (N = 271) in 1993–2019 AFSC RACE-GAP summer bottom trawl surveys of the Gulf of Alaska with the 100 m, 200 m, and 700 m isobaths indicated; filled red circles indicate locations in top 10% of overall abundance, open orange circles indicate presence in remaining catches, and blue dots indicate stations sampled where the animals were not present.

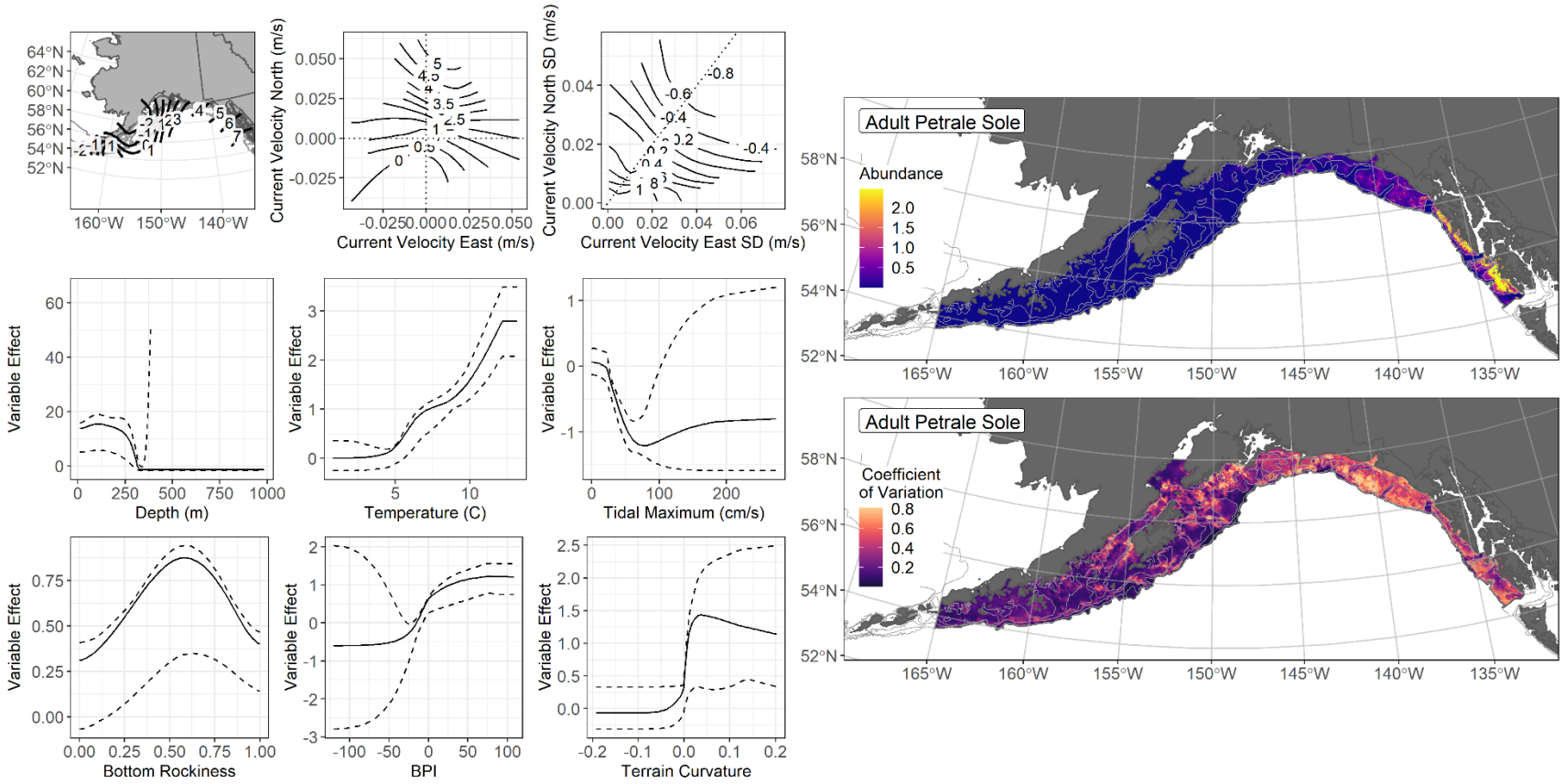

Figure 78. -- The top nine covariate effects (left panel) on ensemble-predicted adult petrale sole numerical abundance across the Gulf of Alaska (upper right panel) along with the coefficient of variation (CV) of the ensemble predictions (lower right panel).

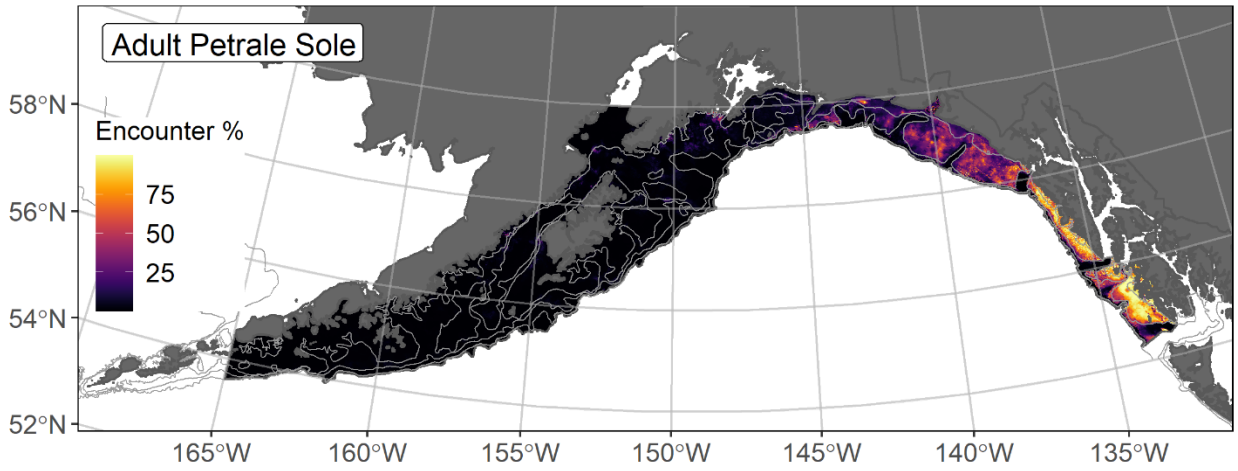

Figure 79. -- Encounter probability of adult petrale sole from AFSC RACE-GAP summer bottom trawl surveys (1993–2019) of the Gulf of Alaska with the 100 m, 200 m, and 700 m isobaths indicated.

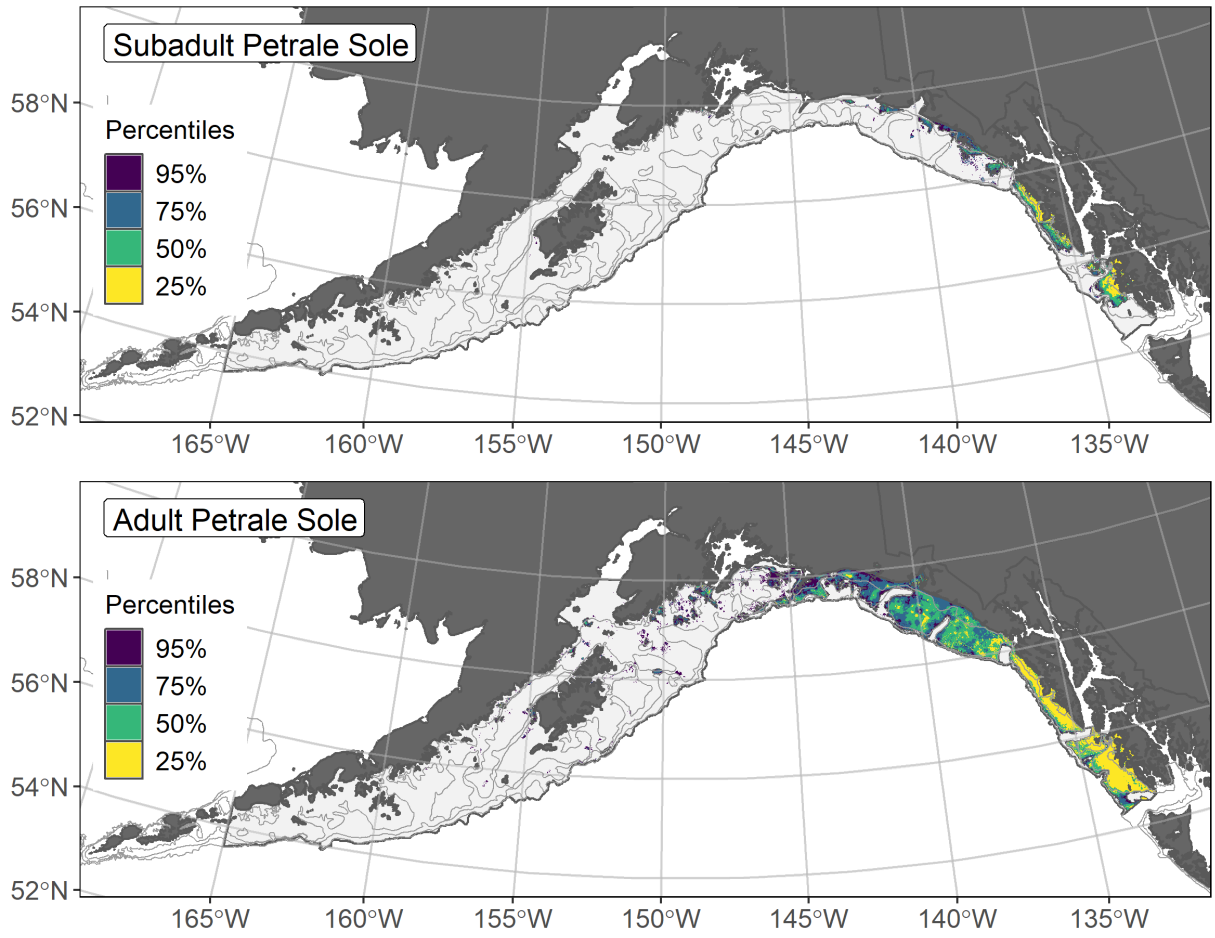

Figure 80. -- Essential fish habitat (EFH) is the area containing the top 95% of occupied habitat (defined as model estimated encounter probabilities greater than 5%) from an SDM ensemble fitted to subadult (top panel) and adult (bottom panel) petrale sole distribution and abundance in AFSC RACE-GAP summer bottom trawl surveys (1993–2019) with 100 m, 200 m, and 700 m isobaths indicated; within the EFH area map are the subareas of the top 25% (EFH hot spots), top 50% (core EFH area), and top 75% (principal EFH area) of habitat-related, ensemble-predicted numerical abundance.

Slender sole (*Lyopsetta exilis*)

Slender sole (*Lyopsetta exilis*) range from Baja California to the eastern Bering Sea (Mecklenburg et al. 2002). In the GOA, slender sole are managed in the Shallow Water Flatfish stock complex as a member of the "other flatfish" species (Turncock et al. 2017b). Little is known about slender sole life history in the GOA. The mesh size of the RACE-GAP bottom trawl is large enough that the smaller juvenile life stages may not be wholly retained in the catch[22]. Without length-based information to distinguish between the demersal life stages, all individuals caught by RACE-GAP summer bottom trawl surveys in the GOA were modeled in composite to map EFH for this species.

Slender sole demersal life stage abundance and distribution predicted from RACE-GAP summer bottom trawl surveys in the Gulf of Alaska -- Slender sole demersal life stages (N = 751) caught in GOA RACE-GAP summer bottom trawl surveys (1993–2019) were primarily caught on the continental shelf off of southeast Alaska and were present throughout the GOA (Fig. 81); the highest density catches (top 10%) were concentrated in the eastern GOA. All five SDMs considered for inclusion in the ensemble to predict numerical abundance of slender sole in the GOA converged (Table 31); the GAM_{nb} was eliminated by skill testing. The four best-performing SDMs were weighted by RMSE in the final ensemble, which attained a good fit to the observed slender sole data. The ensemble was good at predicting high and low abundance catches ($\rho = 0.44$) and excellent at discriminating presence-absence (AUC = 0.94) and explaining deviance (PDE = 0.68). Geographic location and bottom depth accounted for 61.4% of the deviance explained by the ensemble predicting slender sole numerical abundance, although other covariates contributed (Table 32). Higher slender sole demersal life stage abundance was predicted to peak around 250 m depth on the outer continental shelf and glacial troughs of the eastern GOA (Fig. 82). The CV of ensemble predictions was higher in the eastern GOA and at deeper depths on the continental shelf, such as in the glacial troughs, including Shelikof Strait. The probability of encountering slender sole was higher in the eastern GOA and in glacial troughs of the central GOA (Fig. 83).

Essential Fish Habitat of slender sole demersal life stages in the Gulf of Alaska -- Habitat-related predictions of slender sole demersal life stage distribution and abundance from RACE-GAP summer bottom-trawl surveys of the GOA (1993–2019) were mapped as EFH areas and subareas (Fig. 84). Slender sole EFH area occurred primarily in the eastern GOA, where EFH hot spots were also concentrated. EFH area was also mapped through the central and western GOA, with core EFH area

[22] Adding other high quality sources of data if available to future SDM ensemble EFH mapping for this species will be included as a research recommendation from the 2023 EFH 5-year Review.

extensive in the glacial troughs and along the outer continental shelf and upper slope. This SDM-based EFH map is the first developed for slender sole in the GOA, which is the case for many of the constituent species of the GOA Shallow Water Flatfish stock complex.

Table 31. -- Constituent species distribution models (SDMs) used to construct Essential Fish Habitat (EFH) for demersal life stages of slender sole: MaxEnt = Maximum entropy; paGAM = presence-absence generalized additive model; hGAM = zero-adjusted Poisson hurdle GAM; GAM_P = standard Poisson GAM; GAM_{nb} = standard negative-binomial GAM; RMSE = root mean square error; ρ (*rho*) = Spearman's rank correlation coefficient; AUC = area under the receiver-operating characteristic curve; and PDE = Poisson deviance explained *. The "--" indicates that this model was not included in the final ensemble.

slender sole

Models	**RMSE**	**Relative Weight**	$\boldsymbol{\rho}$	**AUC**	**PDE**	**EFH area (km^2)**
MaxEnt	6.40	0.25	0.40	0.91	0.41	133,600
paGAM	6.40	0.24	0.44	0.95	0.50	107,700
hGAM	6.26	0.26	0.44	0.95	0.56	90,000
GAM_P	6.29	0.25	0.45	0.93	0.57	87,500
GAM_{nb}	6.35	--	--	--	--	--
ensemble	4.99	1	0.44	0.94	0.68	127,100

* Refer to the Species Distribution Model Performance Metrics subsection within the Statistical Modeling section of the Methods for detailed descriptions of individual model performance metrics.

Table 32. -- Covariates retained in the species distribution model (SDM) final ensemble for slender sole demersal life stages with the percent contribution of each covariate to the deviance explained by the SDMs and the cumulative deviance explained: SD = standard deviation and BPI = bathymetric position index.

slender sole

Covariate	% Contribution	Cumulative %
location	32.4	32.4
bottom depth	29.0	61.4
bottom temperature	8.8	70.2
tidal maximum	6.5	76.7
current	6.2	82.9
current SD	5.9	88.8
aspect east	2.5	91.3
rockiness	2.2	93.5
BPI	2.2	95.7
aspect north	1.4	97.1
slope	1.1	98.2
curvature	1.1	99.3
coral presence	0.3	99.6
sponge presence	0.2	99.8
pennatulacean presence	0.2	100.0

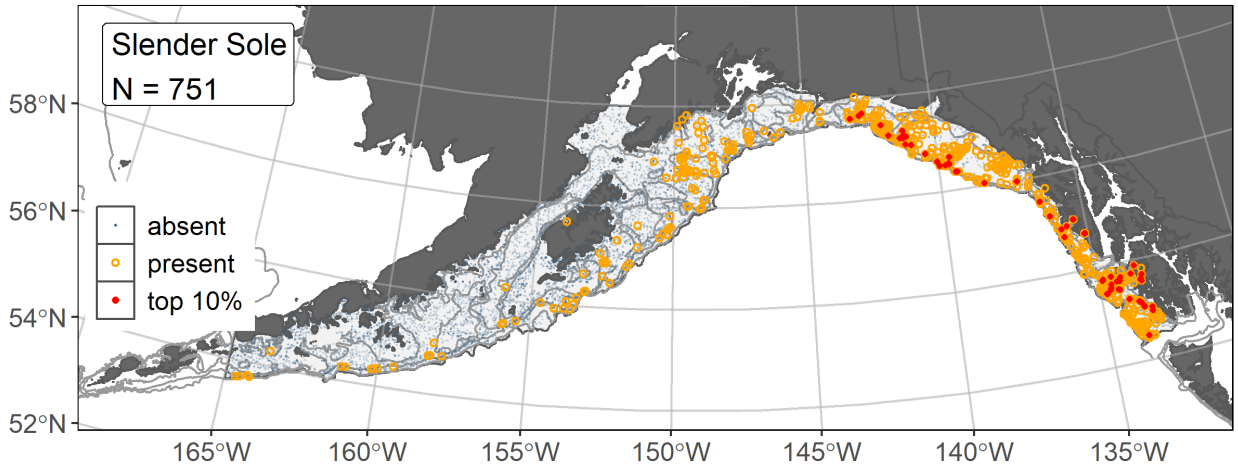

Figure 81. -- Distribution of slender sole catches (N = 751) in 1993–2019 AFSC RACE-GAP summer bottom trawl surveys of the Gulf of Alaska with the 100 m, 200 m, and 700 m isobaths indicated; filled red circles indicate locations in top 10% of overall abundance, open orange circles indicate presence in remaining catches, and blue dots indicate stations sampled where the animals were not present.

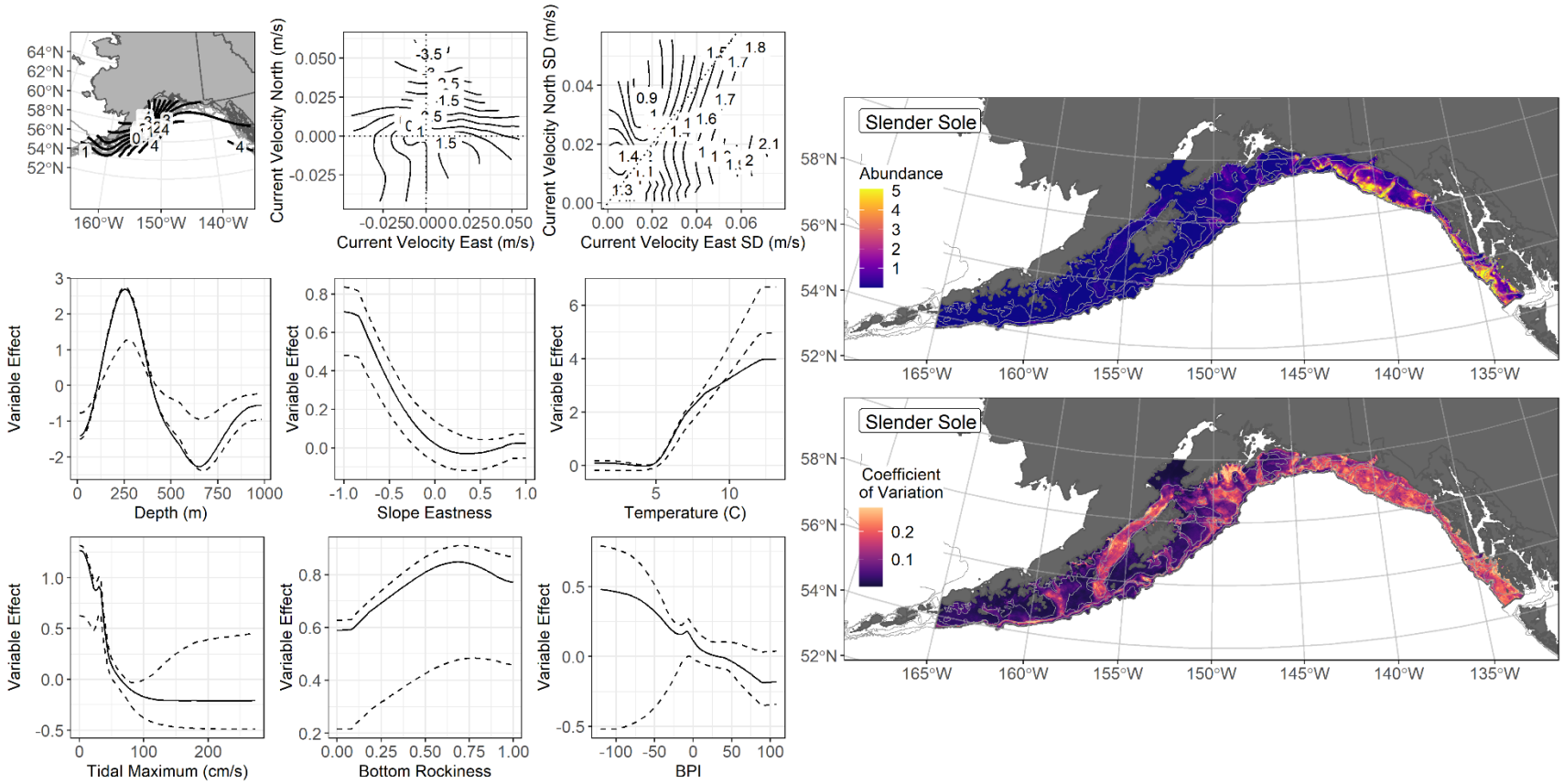

Figure 82. -- The top nine covariate effects (left panel) on ensemble-predicted slender sole numerical abundance across the Gulf of Alaska (upper right panel) along with the coefficient of variation (CV) of the ensemble predictions (lower right panel).

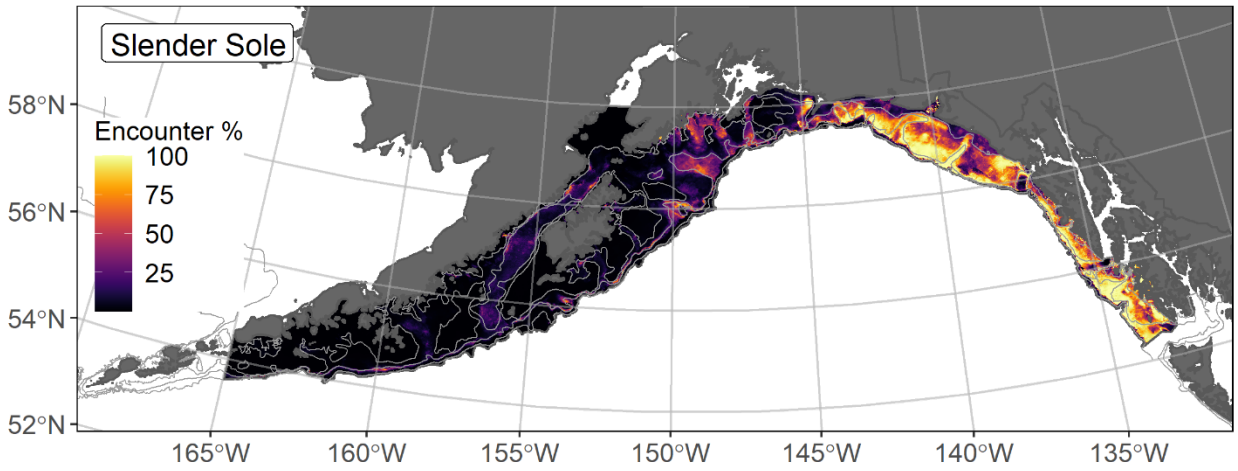

Figure 83. -- Encounter probability of slender sole from AFSC RACE-GAP summer bottom trawl surveys (1993–2019) of the Gulf of Alaska with the 100 m, 200 m, and 700 m isobaths indicated.

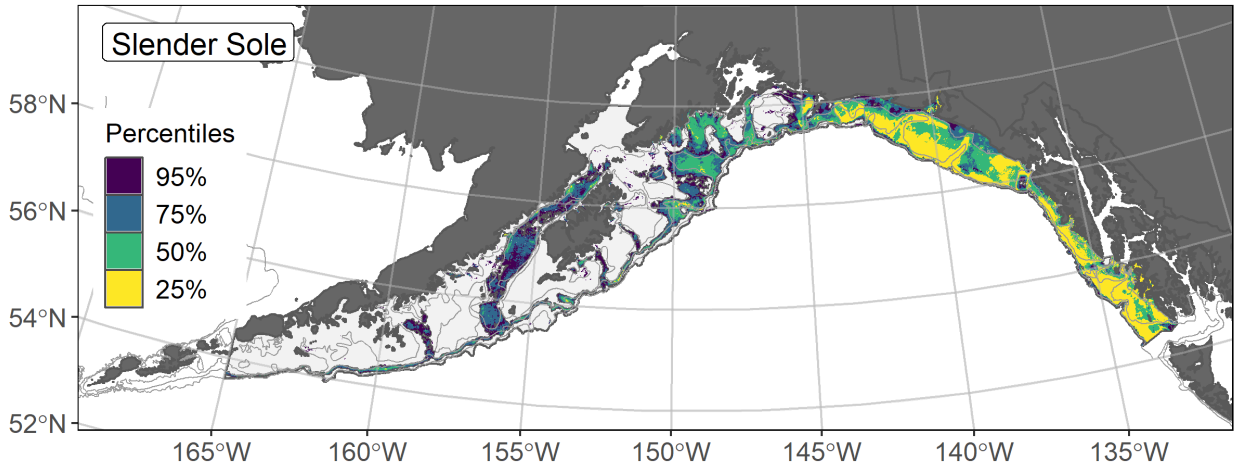

Figure 84. -- Essential fish habitat (EFH) is the area containing the top 95% of occupied habitat (defined as model estimated encounter probabilities greater than 5%) from an SDM ensemble fitted to slender sole distribution and abundance from AFSC RACE-GAP Gulf of Alaska (GOA) summer bottom trawl surveys (1993–2019) with 100 m, 200 m, and 700 m isobaths indicated; within the EFH area map are the subareas of the top 25% (EFH hot spots), top 50% (core EFH area), and top 75% (principal EFH area) of habitat-related, ensemble-predicted numerical abundance.

Southern rock sole (*Lepidopsetta bilineata*)

Southern rock sole (*Lepidopsetta bilineata*, SRS) is found in coastal waters from the eastern Aleutian Islands to Baja California (Orr and Matarese 2000). The species is morphologically similar to northern rock sole (*L. polyxstra*, NRS). There is broad overlap between the two species in the GOA and the eastern Aleutian Islands. Compared to NRS, there has been comparatively little research specific to SRS, and the species are often confounded in older literature. In the GOA region, SRS is managed in the Shallow Water Flatfish stock complex, where they are one of the five species that account for a majority of the biomass of this group (Turncock et al. 2017b). Length-based life stage breaks distinguish between the three demersal life stages modeled in this study; settled early juveniles (20–140 mm; Doyle et al. 2019, NFAA), subadults (141–347 mm FL), and adults (> 347 mm FL) (Stark and Somerton 2002). The mesh size of the RACE-GAP bottom trawl is large enough that the smaller juvenile life stages may not be wholly retained in the catch[23]. This study combines the settled early juvenile life stages of SRS and NRS, which have not been consistently distinguished in the field by surveys (reported in NRS chapter). Otherwise, SRS and NRS subadults and adults are modeled separately in the GOA, using RACE-GAP summer bottom trawl survey data from 1996–2019 when the two species were reliably distinguished by the survey.

Subadult southern rock sole abundance and distribution predicted from RACE-GAP summer bottom trawl surveys in the Gulf of Alaska -- Subadult SRS (N = 2,213) caught in GOA RACE-GAP summer bottom trawl surveys (1996–2019) occurred primarily on the GOA continental shelf west of the Kenai Peninsula (Fig. 1). SRS catch locations in the top 10% of overall abundance also occurred off of southeast Alaska. All five SDMs considered for inclusion in the ensemble to predict numerical abundance of subadult SRS in the GOA converged (Table 33); the GAM_{nb} was eliminated by skill testing. The four remaining best-performing SDMs were weighted by RMSE in the final ensemble, which attained an excellent overall fit to the observed subadult SRS distribution and abundance data. The ensemble was excellent at predicting high and low abundance catches ($\rho = 0.71$), at discriminating presence-absence (AUC = 0.94), and at explaining deviance (PDE = 0.65). Bottom depth alone accounted for 61.8% of the contribution among covariates to the deviance explained by the final ensemble (Table 34). The highest abundances were predicted at less than 125 m depth on bathymetric rises, such as the banks south of Kodiak Island and west in the GOA (Fig. 2). Nearshore areas along the outer coast of southeast Alaska were also areas of predicted high abundance for subadult SRS. The CV of ensemble

[23] Adding other high quality sources of data if available to future SDM ensemble EFH mapping for this species will be included as a research recommendation from the 2023 EFH 5-year Review.

predictions was greater at shallower depths on the GOA continental shelf, although not high overall. The probability of encountering subadult SRS was highest at bathymetric rises and shallow nearshore locations on the GOA continental shelf (Fig. 3).

Adult southern rock sole abundance and distribution predicted from RACE-GAP summer bottom trawl surveys in the Gulf of Alaska -- Adult SRS (N = 2,772) caught in GOA RACE-GAP summer bottom trawl surveys (1996–2019) occurred primarily on the GOA continental shelf west of the Kenai Peninsula and also off of southeast Alaska, similar to subadults (Fig. 4). The five SDMs considered for inclusion in the ensemble to predict numerical abundance of adult SRS in the GOA converged (Table 33); the GAM_{nb} was eliminated by skill testing. The four remaining best-performing SDMs were weighted by RMSE in the final ensemble, which attained an excellent overall fit to the observed adult SRS distribution and abundance data. The ensemble was excellent at predicting high and low abundance catches (ρ = 0.76), discriminating presence-absence (AUC = 0.94), and explaining deviance (PDE = 0.64). Bottom depth accounted for 68.3% of the contribution among covariates to the deviance explained by the final ensemble, where bottom depth alone accounted for 70.2% (Table 34). The highest abundances were predicted at less than 125 m depth on bathymetric rises, such as the banks south of Kodiak Island, around the Shumagin Islands, and the Alaska Peninsula (Fig. 5). Inshore areas along the outer coast of southeast Alaska were also areas of predicted high abundance for adult SRS. The CV of ensemble predictions was higher in nearshore areas and bathymetric rises on the continental shelf throughout the GOA. Similar to subadults, the probability of encountering adult SRS was highest at bathymetric rises and at shallow nearshore locations on the GOA continental shelf (Fig. 6).

Essential Fish Habitat of subadult and adult southern rock sole in the Gulf of Alaska -- Ensemble-predicted, habitat-related numerical abundance of SRS life stages collected in RACE-GAP summer bottom trawl surveys of the GOA (1996–2019) was mapped as EFH areas and subareas (Fig. 7). The EFH areas of subadult and adult SRS were similar, occurring on bathymetric rises on the GOA continental shelf, with EFH hot spots and core EFH area concentrated west of the Kenai Peninsula on the banks south of Kodiak Island, the Shumagin Islands, and along inshore areas of the Alaska Peninsula. EFH hot spots for these life stages were also notably present off southeast Alaska.

Table 33. -- Constituent species distribution models (SDMs) used to construct Essential Fish Habitat (EFH) for a) subadult and b) adult southern rock sole: MaxEnt = Maximum entropy; paGAM = presence-absence generalized additive model; hGAM = zero-adjusted Poisson hurdle GAM; GAM_P = standard Poisson GAM; GAM_{nb} = standard negative-binomial GAM; RMSE = root mean square error; ρ (rho) = Spearman's rank correlation coefficient; AUC = area under the receiver-operating characteristic curve; and PDE = Poisson deviance explained *. The "--" indicates that this model was not included in the final ensemble.

a) subadult southern rock sole

Models	RMSE	Relative Weight	ρ	AUC	PDE	EFH area (km^2)
MaxEnt	33.9	0.24	0.68	0.93	0.49	205,200
paGAM	33.4	0.24	0.70	0.94	0.54	218,000
hGAM	32.2	0.26	0.69	0.94	0.60	161,600
GAM_P	32.4	0.26	0.70	0.93	0.59	151,000
GAM_{nb}	32.9	0	--	--	--	--
ensemble	30.2	1	0.71	0.94	0.65	198,100

b) adult southern rock sole

Models	RMSE	Relative Weight	ρ	AUC	PDE	EFH area (km^2)
MaxEnt	26.8	0.20	0.74	0.93	0.47	198,100
paGAM	23.5	0.25	0.75	0.94	0.57	229,300
hGAM	22.7	0.27	0.74	0.94	0.99	190,200
GAM_P	22.6	0.28	0.74	0.93	0.63	188,600
GAM_{nb}	23.9	0	--	--	--	--
ensemble	22.1	1	0.76	0.94	0.64	212,100

* Refer to the Species Distribution Model Performance Metrics subsection within the Statistical Modeling section of the Methods for detailed descriptions of individual model performance metrics.

Table 34. -- Covariates retained in the a) subadult and b) adult southern rock sole species distribution model (SDM) final ensembles, the percent contribution to the total deviance explained by each, and the cumulative percent deviance: SD = standard deviation, and BPI = bathymetric position index.

southern rock sole

	Covariate	**% Contribution**	**Cumulative %**
a) subadult	bottom depth	61.8	61.8
	location	16.9	78.7
	tidal maximum	3.9	82.6
	current	3.6	86.2
	rockiness	2.5	88.7
	current SD	2.2	90.9
	BPI	2.2	93.1
	slope	1.6	94.7
	bottom temperature	1.4	96.1
	aspect east	1.1	97.2
	curvature	1.1	98.3
	aspect north	1.0	99.3
	coral presence	0.5	99.8
	sponge presence	0.2	100.0
b) adult	bottom depth	68.3	68.3
	location	14.9	83.2
	tidal maximum	3.4	86.6
	BPI	3.0	89.6
	current	2.7	92.3
	rockiness	2.2	94.5
	bottom temperature	1.3	95.8
	aspect north	1.2	97.0
	current SD	0.9	97.9
	aspect east	0.8	98.7
	sponge presence	0.4	99.1
	slope	0.3	99.4
	curvature	0.3	99.7
	pennatulacean presence	0.2	99.9
	coral presence	0.1	100.0

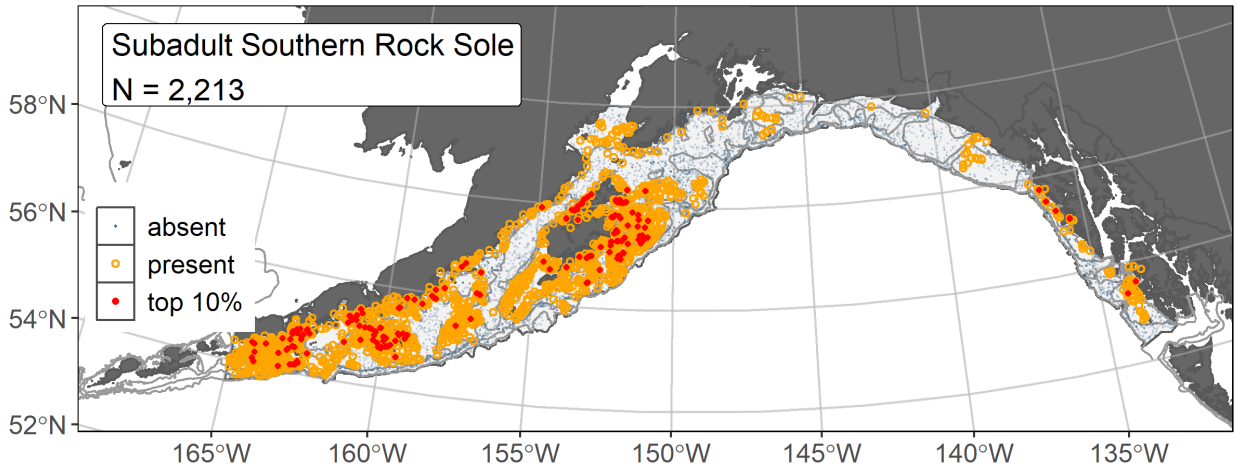

Figure 85. -- Distribution of subadult southern rock sole catches (N = 2,213) in 1996–2019 AFSC RACE-GAP summer bottom trawl surveys of the Gulf of Alaska with the 100 m, 200 m, and 700 m isobaths indicated; filled red circles indicate locations in top 10% of overall abundance, open orange circles indicate presence in remaining catches, and blue dots indicate stations sampled where the animals were not present.

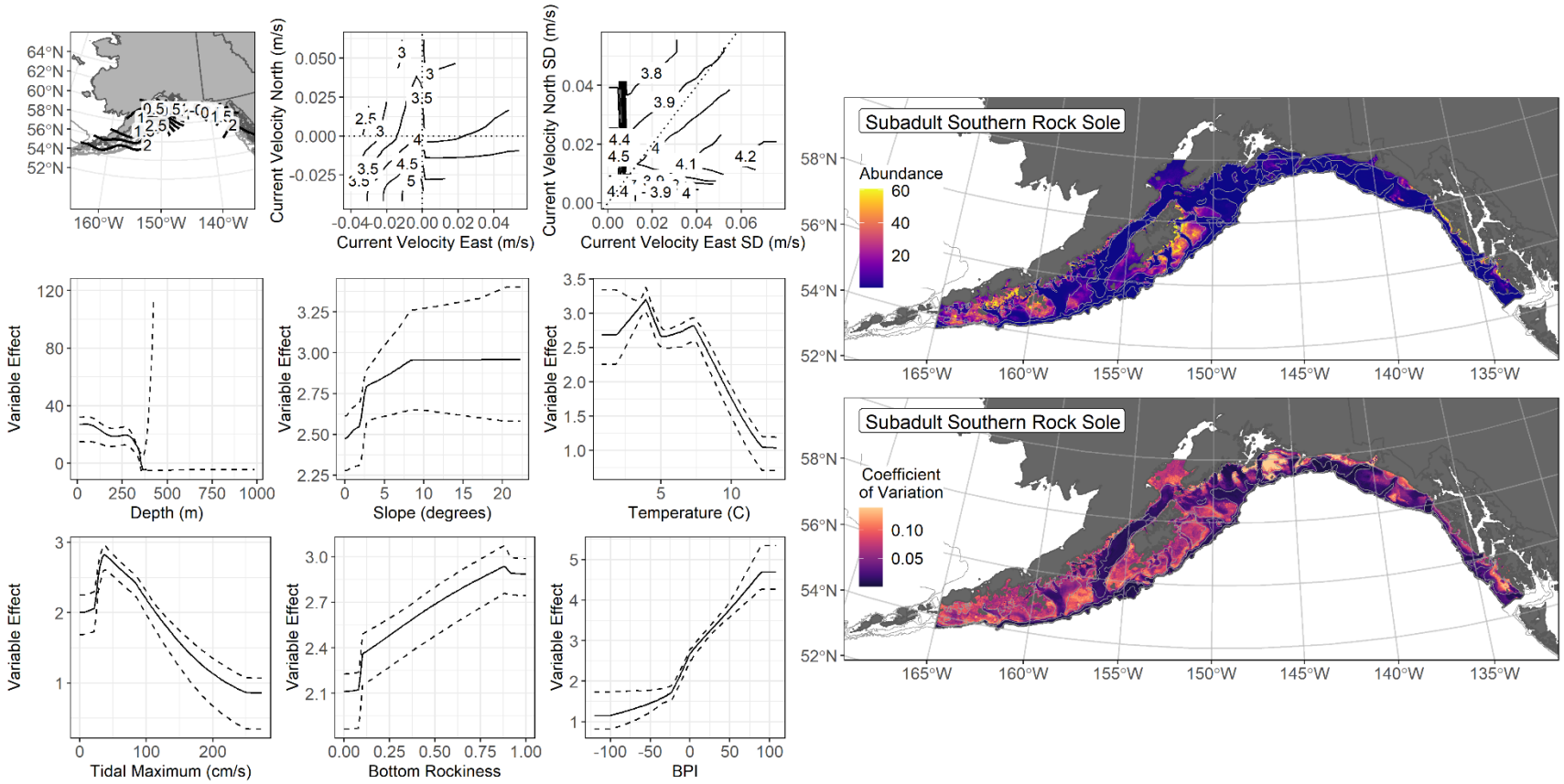

Figure 86. -- The top nine covariate effects (left panel) on ensemble-predicted subadult southern rock sole numerical abundance across the Gulf of Alaska (upper right panel) along with the coefficient of variation (CV) of the ensemble predictions (lower right panel).

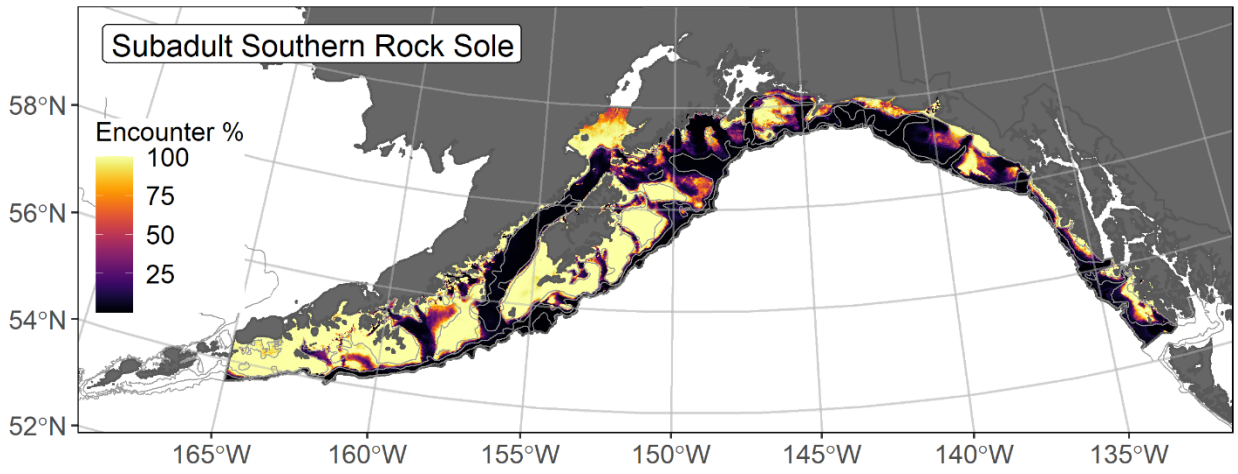

Figure 87. -- Encounter probability of subadult southern rock sole from AFSC RACE-GAP summer bottom trawl surveys (1996–2019) of the Gulf of Alaska with the 100 m, 300 m, and 700 m isobaths indicated.

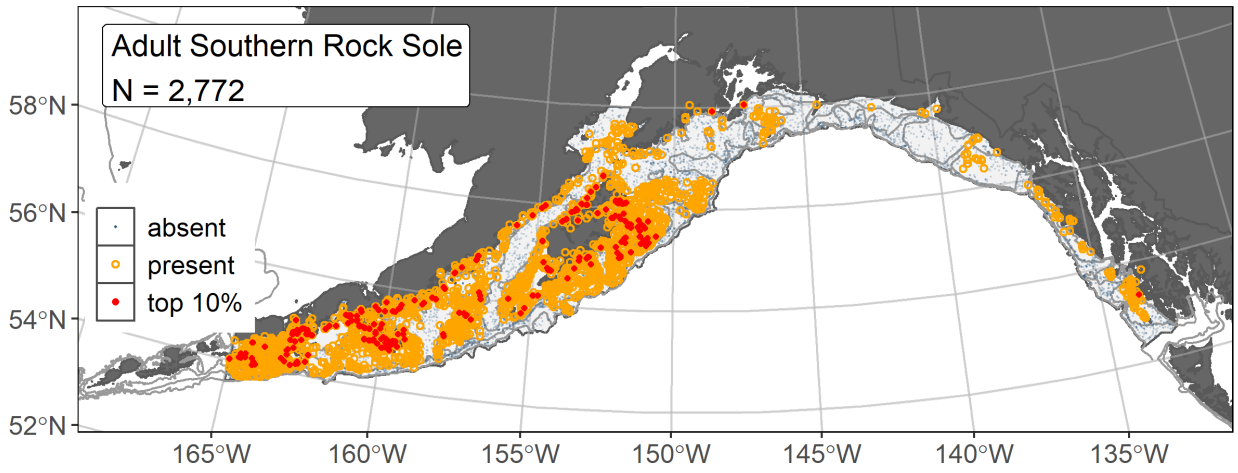

Figure 88. -- Distribution of adult southern rock sole catches (N = 2,772) in 1996–2019 AFSC RACE-GAP summer bottom trawl surveys of the Gulf of Alaska with the 100 m, 200 m, and 700 m isobaths indicated; filled red circles indicate locations in top 10% of overall abundance, open orange circles indicate presence in remaining catches, and blue dots indicate stations sampled where the animals were not present.

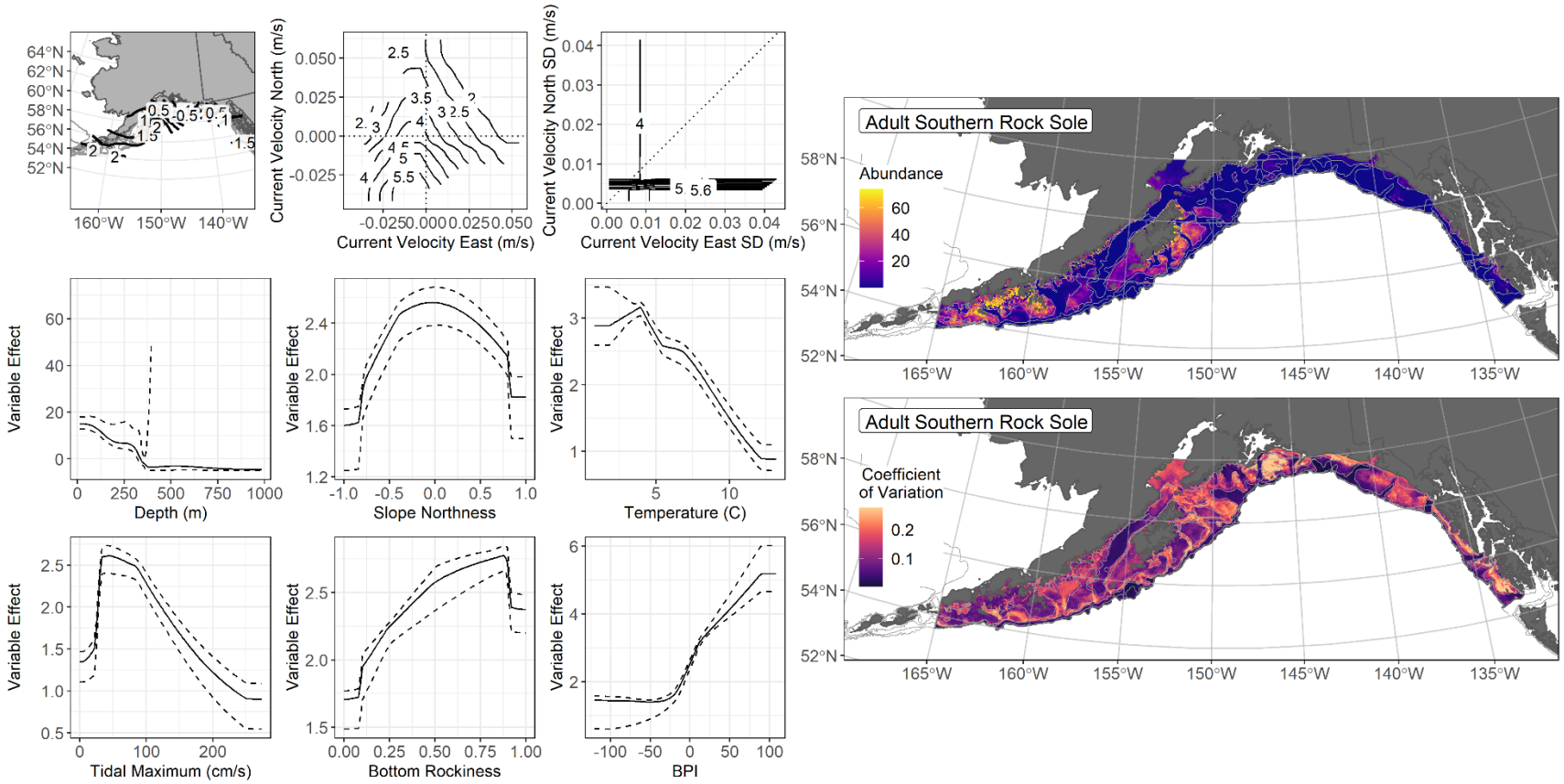

Figure 89. -- The top nine covariate effects (left panel) on ensemble-predicted adult southern rock sole numerical abundance across the Gulf of Alaska (upper right panel) along with the coefficient of variation (CV) of the ensemble predictions (lower right panel).

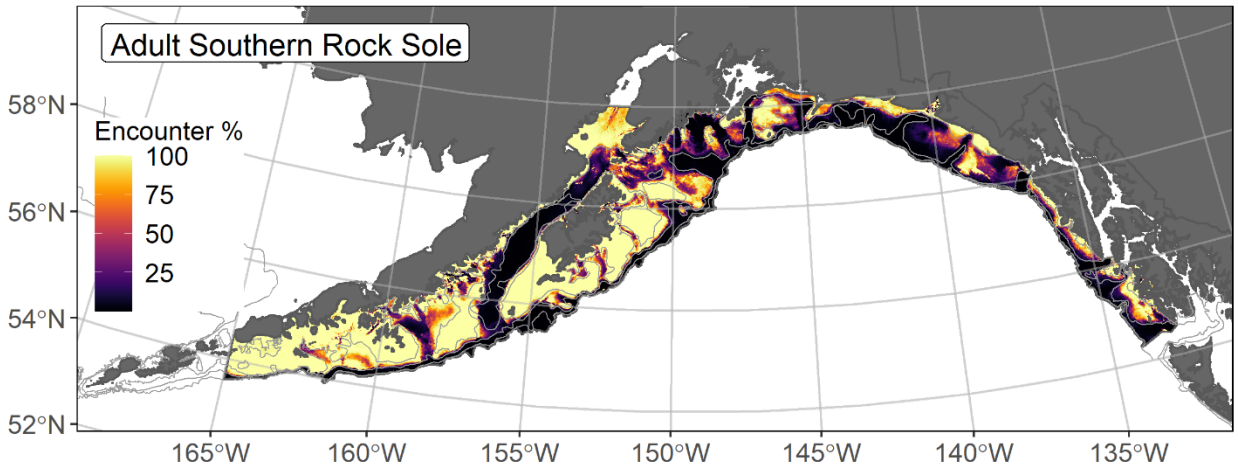

Figure 90. -- Encounter probability of adult southern rock sole from AFSC RACE-GAP summer bottom trawl surveys (1996–2019) of the Gulf of Alaska with the 100 m, 200 m, and 700 m isobaths indicated.

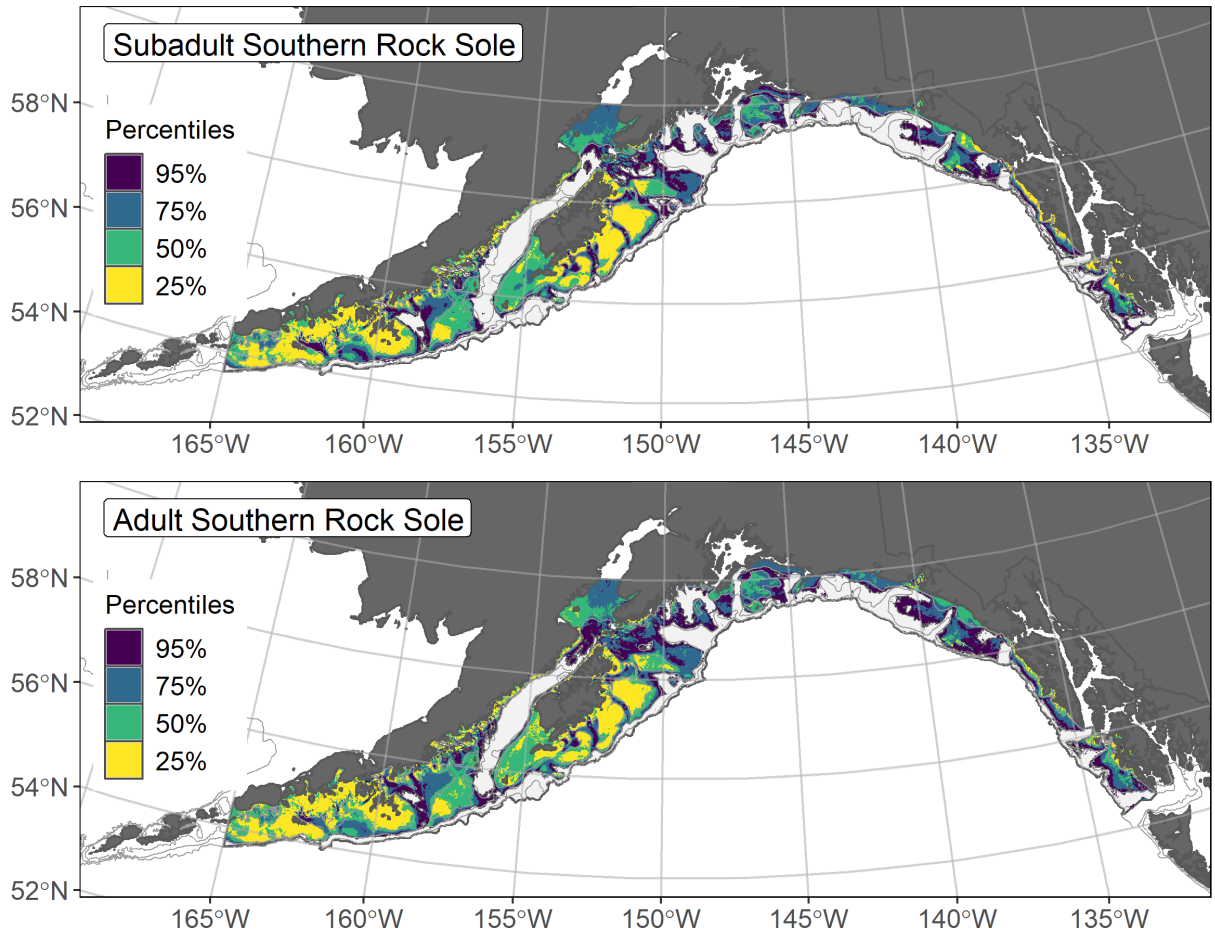

Figure 91. -- Essential fish habitat (EFH) is the area containing the top 95% of occupied habitat (defined as model estimated encounter probabilities greater than 5%) from an SDM ensemble fitted to subadult (top panel) and adult (bottom panel) southern rock sole distribution and abundance in AFSC RACE-GAP summer bottom trawl surveys (1993–2019) with 100 m, 200 m, and 700 m isobaths indicated; within the EFH area map are the subareas of the top 25% (EFH hot spots), top 50% (core EFH area), and top 75% (principal EFH area) of habitat-related, ensemble-predicted numerical abundance.

Starry flounder (*Platichthys stellatus*)

Starry flounder (*Platichthys stellatus*) range from the Beaufort Sea to Southern California, typically over soft bottom habitats in relatively shallow (< 100 m) water (Mecklenburg et al. 2002). This euryhaline species can tolerate a wide range of salinities and has been collected from marine to essentially freshwater environments (Orcutt 1950, Ralston 2005). Doyle et al. (2019) reported a maximum observed transformation length from pelagic larvae to early juveniles of 10–15 mm TL in the GOA, and the smallest settled early juvenile starry flounder caught in summer beach seine surveys in the GOA were 12 mm FL (mean 26 mm FL; NFAA). Orcutt (1950) reported a settled early juvenile length range of 20–150 mm along with a reproductive maturity for female starry flounder in California at 3 years and 369 mm FL. We used these length breaks to separate starry flounder demersal life stages in our analysis, including settled early juveniles (20–150 mm), subadults (151–369 mm), and adults (> 369 mm). The mesh size of the RACE-GAP bottom trawl is large enough that the smaller juvenile life stages may not be wholly retained in the catch[24]. Starry flounder are managed in the Shallow Water Flatfish stock complex, where they are one of the five species that account for a majority of the biomass of this group (Turncock et al. 2017b).

Settled early juvenile starry flounder distribution predicted from mixed gear-type summer surveys in the Gulf of Alaska -- Settled early juvenile starry flounder (N = 61) were caught in mixed gear-type summer surveys (1989–2019) using bottom trawls and seines in nearshore areas of the GOA (Fig. 92). Settled early juvenile starry flounder presence records from multiple surveys were combined in a habitat-related MaxEnt SDM predicting suitable habitat probabilities for this life stage in the GOA. The best model had a β-multiplier of 1.5 and an AUC of 0.98 (Table 35). Bottom depth alone accounted for 85.2% of covariate contribution to the deviance explained by the SDM (Table 36). The highest predicted probabilities of suitable habitat for settled early juvenile starry flounder occurred at locations less than 100 m depth in nearshore areas throughout the GOA (Fig. 93). The standard deviation among k-folds in the final SDM was relatively low.

Subadult starry flounder abundance and distribution predicted from RACE-GAP summer bottom trawl surveys in the Gulf of Alaska -- Subadult starry flounder (N = 68) caught in GOA RACE-GAP summer bottom trawl surveys (1993–2019) were caught inshore on the continental shelf of the GOA from southeast Alaska to the western extent of the study area (Fig. 94). Three of the five SDMs considered for inclusion in the ensemble to predict numerical abundance of subadult starry flounder in the

[24] Adding other high quality sources of data if available to future SDM ensemble EFH mapping for this species will be included as a research recommendation from the 2023 EFH 5-year Review.

GOA converged (Table 37); the GAM_P were eliminated through skill testing. The remaining three best-performing SDMs were weighted by RMSE in the final ensemble, which attained a fair fit to the observed subadult starry flounder data. The ensemble was poor at predicting high and low abundance catches (ρ = 0.19), and excellent at discriminating presence-absence (AUC = 0.98) and explaining deviance (PDE = 0.65). Bottom depth and geographic location accounted for 55.7% of the contribution among covariates to the deviance explained by the ensemble predicting subadult starry flounder numerical abundance (Table 36). Their highest abundances were predicted in nearshore areas and at shallow depths on the GOA continental shelf (Fig. 95). The CV of ensemble predictions was higher at shallower depths on the GOA continental shelf. The probability of encountering subadult starry flounder was higher in areas of predicted high abundance (Fig. 96).

Adult starry flounder abundance and distribution predicted from RACE-GAP summer bottom trawl surveys in the Gulf of Alaska -- Adult starry flounder (N = 604) caught in GOA RACE-GAP summer bottom trawl surveys (1993–2019) were distributed on the GOA continental shelf from southeast Alaska to the western extent of the study area (Fig. 97). Four of the five SDMs considered for inclusion in the ensemble to predict numerical abundance of adult starry flounder in the GOA converged (Table 37); the GAM_{nb} was eliminated through skill testing. The remaining three best-performing SDMs were weighted by RMSE in the final ensemble, which attained a good fit to the observed adult starry flounder data. The ensemble was good at predicting high and low abundance catches (ρ = 0.43), excellent at discriminating presence-absence (AUC = 0.96), and good at explaining deviance (PDE = 0.59). Bottom depth alone accounted for 63.6% of the contribution to the deviance explained by the ensemble predicting adult starry flounder numerical abundance (Table 36). The highest abundances were predicted in nearshore areas and at shallow depths on the GOA continental shelf (Fig. 98). The CV of ensemble predictions was higher at shallower depths on the GOA continental shelf. The probability of encountering adult starry flounder was higher in areas of predicted high abundance (Fig. 99).

Essential Fish Habitat of three life stages of starry flounder in the Gulf of Alaska -- Habitat-related predictions of starry flounder demersal life stage distribution and abundance from summer surveys of the GOA (mixed gear-type summer surveys (1989–2019) and RACE-GAP bottom trawl surveys (1993–2019)) were mapped as EFH areas and subareas (Fig. 100). The EFH areas of settled early juvenile and subadult starry flounder occurred in nearshore areas and at shallower depths over bathymetric rises in the GOA, with EFH hot spots inside Cook Inlet and offshore of the Copper and Bering rivers. The EFH area of adult starry flounder included nearshore areas and was more extensive than the EFH area of the juvenile life stages on the bathymetric rises of the continental shelf. EFH hot spots for adults occurred at shallower depths within the total EFH area for this life stage. The SDM-based EFH maps are the first

developed for starry flounder in the GOA, which is the case for many of the constituent species of the GOA Shallow Water Flatfish stock complex.

Table 35. -- Maximum entropy model (MaxEnt) used to construct Essential Fish Habitat (EFH) for settled early juvenile starry flounder: regularization multiplier (β); *k*-fold cross-validation root-mean-square-error (RMSE), area under the receiver operating characteristic curve (AUC), and areal extent of EFH (km^2).

Model	**β**	**RMSE**	**AUC**	**EFH area (km^2)**
MaxEnt	1.5	20.24	0.98	63,800

Table 36. -- Covariates retained in the a) settled early juvenile habitat-related maximum entropy (MaxEnt) species distribution model (SDM), and b) subadult and c) adult SDM final ensembles for starry flounder with the percent contribution of each covariate to the deviance explained by the SDMs and the cumulative deviance explained: SD = standard deviation and BPI = bathymetric position index.

starry flounder	**Covariate**	**% Contribution**	**Cumulative %**
a) settled early juvenile	bottom depth	85.2	85.2
	curvature	3.5	88.8
	slope	3.2	92.0
	bottom temperature	2.3	94.3
	aspect east	2.3	96.6
	aspect north	1.1	97.7
	rockiness	0.9	98.6
	sponge presence	0.9	99.5
	tidal maximum	0.5	99.9
	pennatulacean presence	0.1	100.0
b) subadult	bottom depth	45.4	45.4
	location	10.4	55.7
	bottom temperature	7.7	63.4
	current	7.3	70.7
	rockiness	6.7	77.4
	BPI	5.0	82.4
	tidal maximum	4.1	86.5
	slope	3.5	90.0
	aspect east	2.5	92.5
	sponge presence	1.8	94.3
	current SD	1.5	95.8
	coral presence	1.5	97.3
	curvature	1.2	98.5
	pennatulacean presence	1.2	99.7
	aspect north	0.3	100.0
c) adult	bottom depth	63.6	63.6
	location	7.4	71.0
	BPI	5.6	76.7
	sponge presence	4.3	81.0
	tidal maximum	3.8	84.8
	current SD	3.6	88.4
	rockiness	2.8	91.2
	current	2.6	93.8
	slope	1.8	95.6
	bottom temperature	1.8	97.4

starry flounder

Covariate	% Contribution	Cumulative %
aspect north	0.8	98.2
aspect east	0.5	98.7
coral presence	0.5	99.2
curvature	0.4	99.6
pennatulacean presence	0.4	100.0

Table 37. -- Constituent species distribution models (SDMs) used to construct Essential Fish Habitat (EFH) for a) subadult and b) adult starry flounder: MaxEnt = Maximum entropy; paGAM = presence-absence generalized additive model; hGAM = zero-adjusted Poisson hurdle GAM; GAM_P = standard Poisson GAM; GAM_{nb} = standard negative-binomial GAM; RMSE = root mean square error; ρ (*rho*) = Spearman's rank correlation coefficient; AUC = area under the receiver operating characteristic curve; and PDE = Poisson deviance explained *. The "--" indicates that this model was not included in the final ensemble.

a) subadult starry flounder

Models	**RMSE**	**Relative Weight**	**ρ**	**AUC**	**PDE**	**EFH area (km^2)**
MaxEnt	0.81	0.68	0.20	0.97	0.54	25,600
paGAM	--	--	--	--	--	--
hGAM	--	--	--	--	--	--
GAM_P	1.41	0	--	--	--	--
GAM_{nb}	1.19	0.32	0.20	0.97	0.61	8,000
ensemble	0.80	1	0.19	0.98	0.65	23,100

b) adult starry flounder

Models	**RMSE**	**Relative Weight**	**ρ**	**AUC**	**PDE**	**EFH area (km^2)**
MaxEnt	22.4	0.16	0.42	0.96	0.38	110,100
paGAM	13.5	0.44	0.43	0.96	0.53	122,900
hGAM	--	--	--	--	--	--
GAM_P	14.0	0.41	0.44	0.95	0.49	93,500
GAM_{nb}	61.3	0	--	--	--	--
ensemble	13.3	1	0.43	0.96	0.59	115,300

* Refer to the Species Distribution Model Performance Metrics subsection within the Statistical Modeling section of the Methods for detailed descriptions of individual model performance metrics.

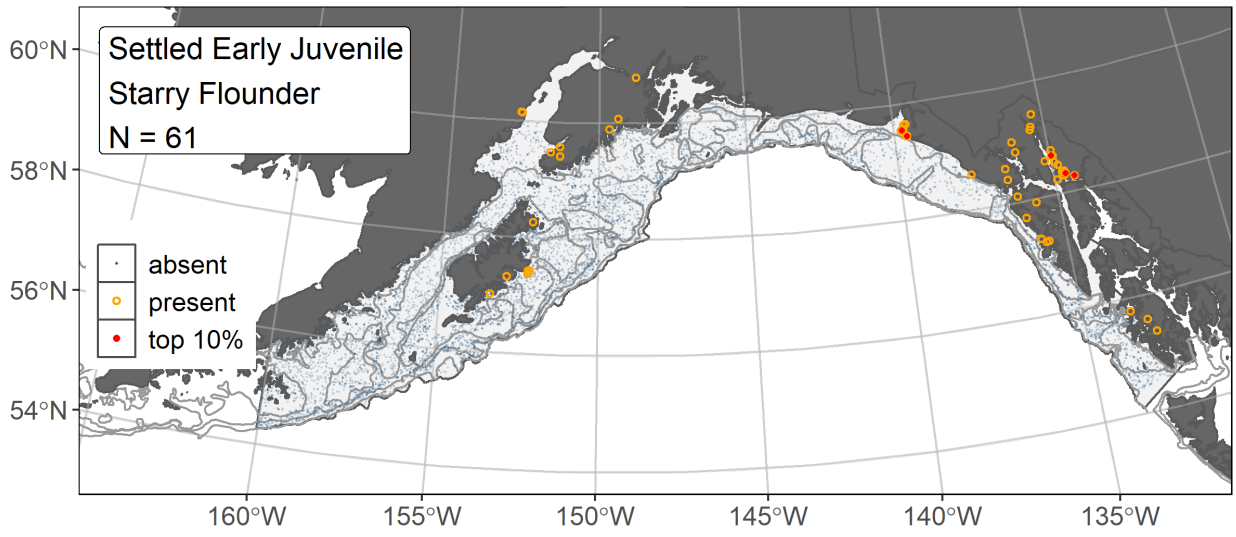

Figure 92. -- Distribution of settled early juvenile starry flounder catches (N = 61) in mixed gear-type summer surveys of the Gulf of Alaska (1989–2019) with the 100 m, 200 m, and 700 m isobaths indicated; filled red circles indicate locations in top 10% of overall abundance, open orange circles indicate presence in remaining catches, and blue dots indicate stations sampled where the animals were not present.

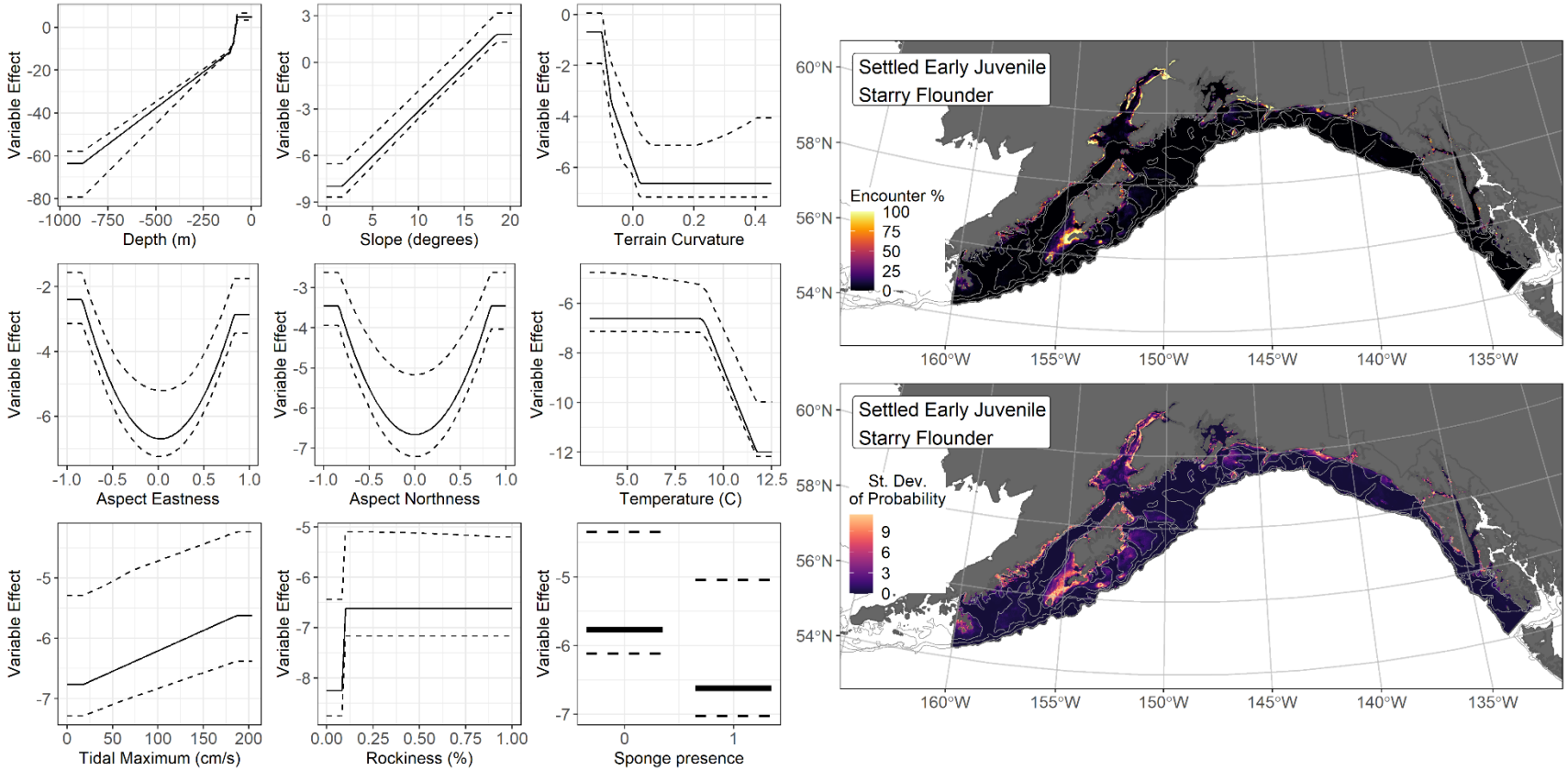

Figure 93. -- The top nine covariate effects (left panel) from a habitat-related species distribution model (MaxEnt) of settled early juvenile starry flounder probability of suitable habitat in the Gulf of Alaska (upper right panel) with the standard deviation of the probability predictions (lower right panel).

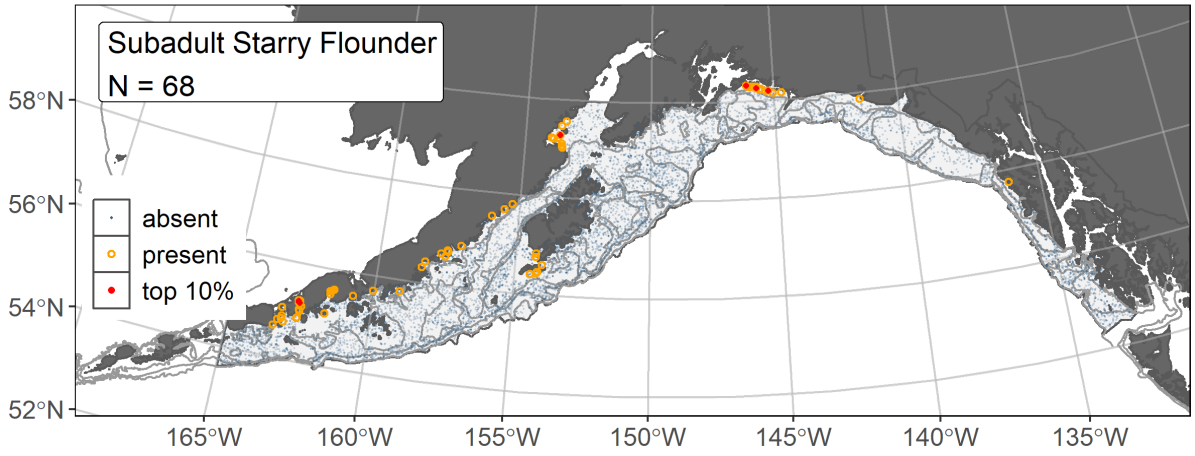

Figure 94. -- Distribution of subadult starry flounder catches (N = 68) in 1993–2019 AFSC RACE-GAP summer bottom trawl surveys of the Gulf of Alaska with the 100 m, 200 m, and 700 m isobaths indicated; filled red circles indicate locations in top 10% of overall abundance, open orange circles indicate presence in remaining catches, and blue dots indicate stations sampled where the animals were not present.

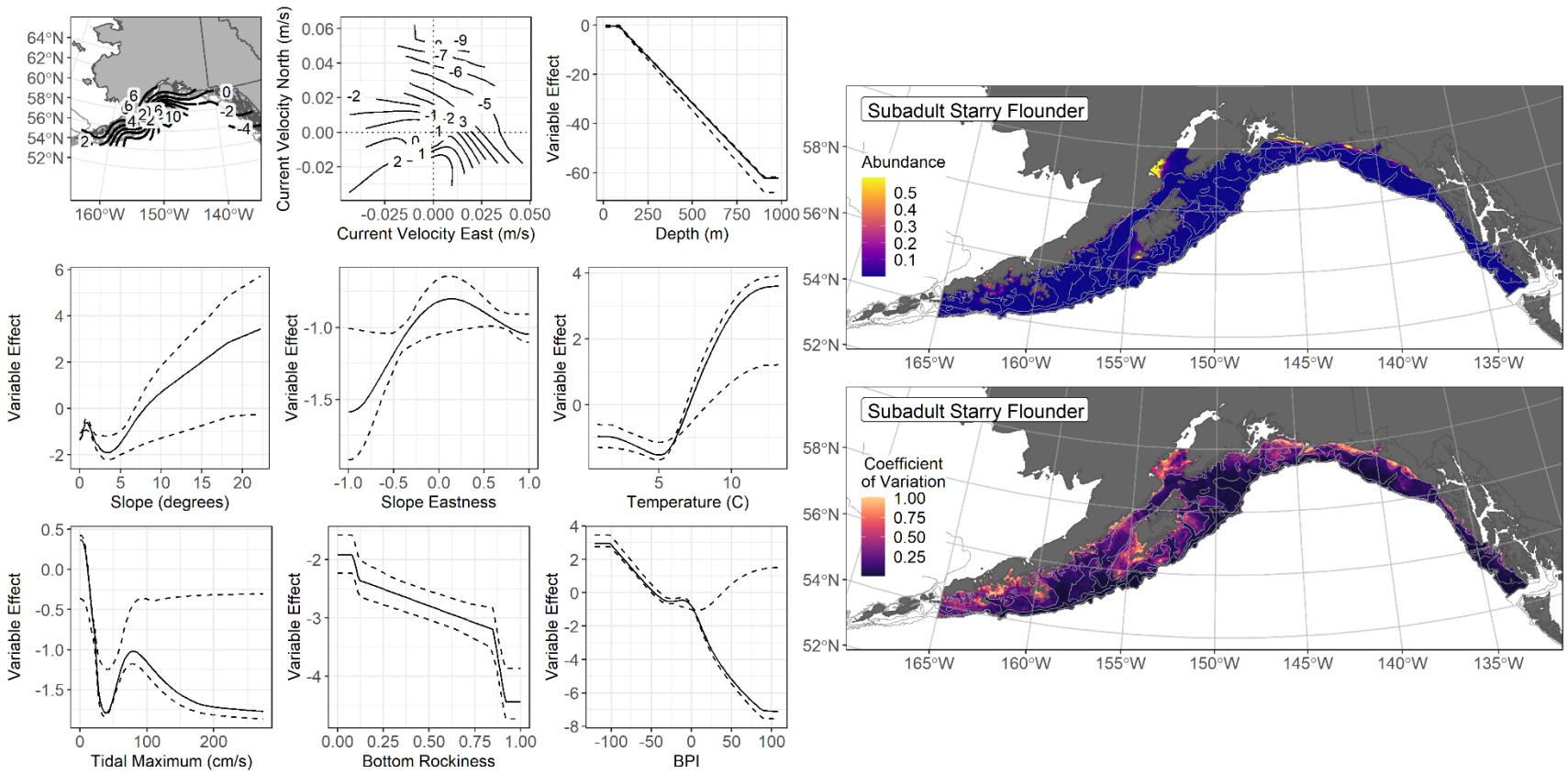

Figure 95. -- The top nine covariate effects (left panel) on ensemble-predicted subadult starry flounder numerical abundance across the Gulf of Alaska (upper right panel) along with the coefficient of variation (CV) of the ensemble predictions (lower right panel).

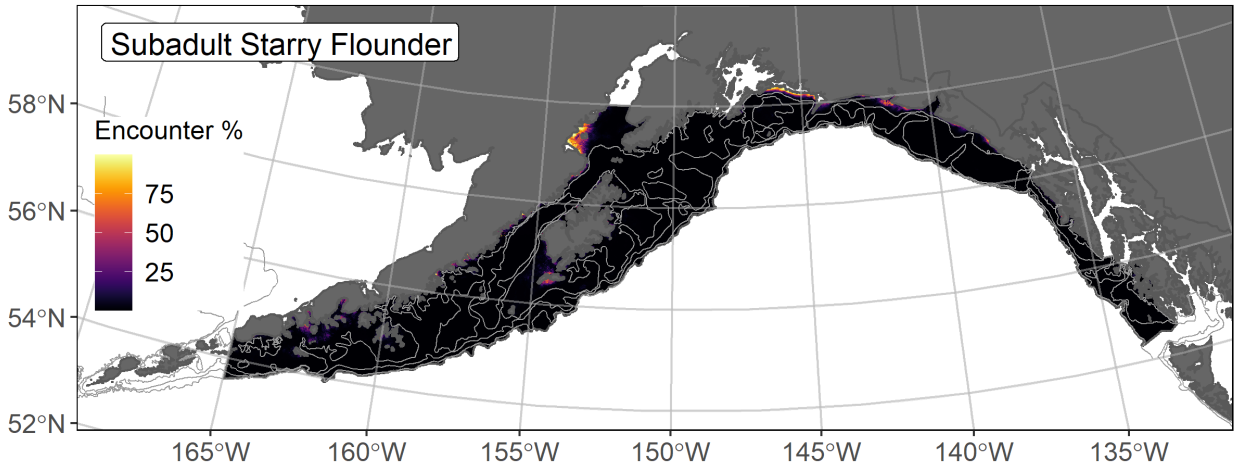

Figure 96. -- Encounter probability of subadult starry flounder from AFSC RACE-GAP summer bottom trawl surveys (1993–2019) of the Gulf of Alaska with the 100 m, 200 m, and 700 m isobaths indicated.

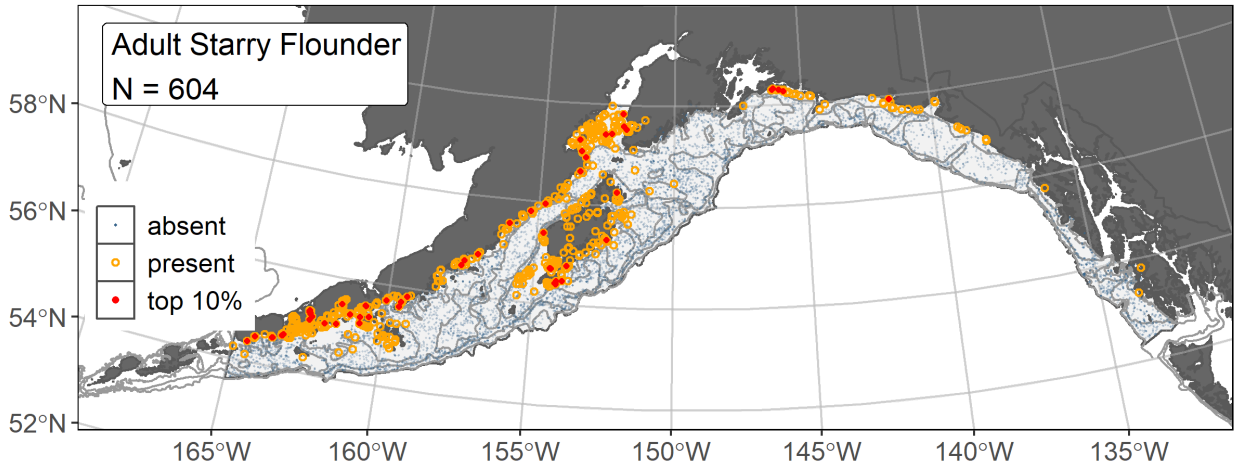

Figure 97. -- Distribution of adult starry flounder catches (N = 604) in 1993–2019 AFSC RACE-GAP summer bottom trawl surveys of the Gulf of Alaska with the 100 m, 200 m, and 700 m isobaths indicated; filled red circles indicate locations in top 10% of overall abundance, open orange circles indicate presence in remaining catches, and blue dots indicate stations sampled where the animals were not present.

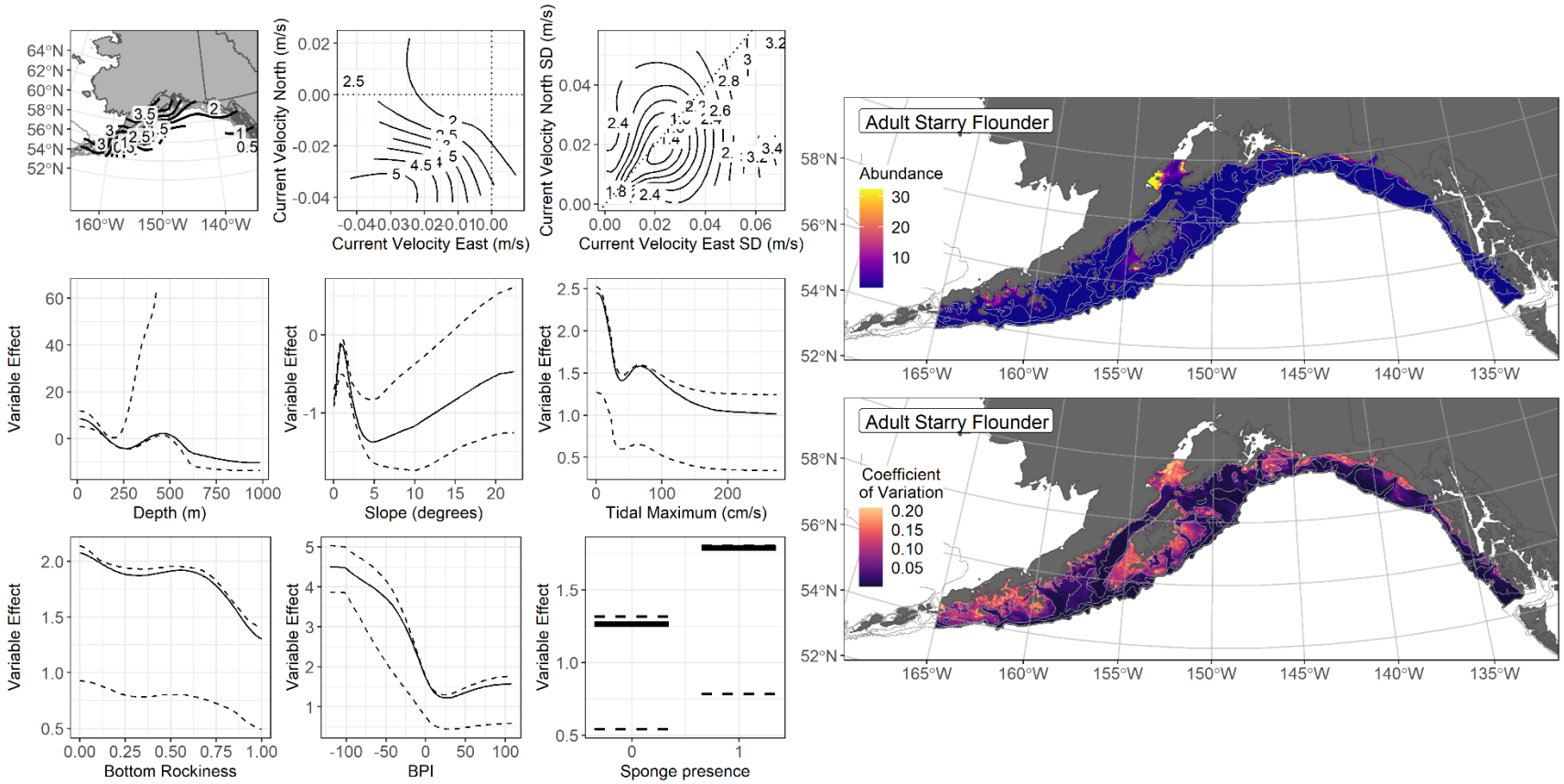

Figure 98. -- The top nine covariate effects (left panel) on ensemble-predicted adult starry flounder numerical abundance across the Gulf of Alaska (upper right panel) along with the coefficient of variation (CV) of the ensemble predictions (lower right panel).

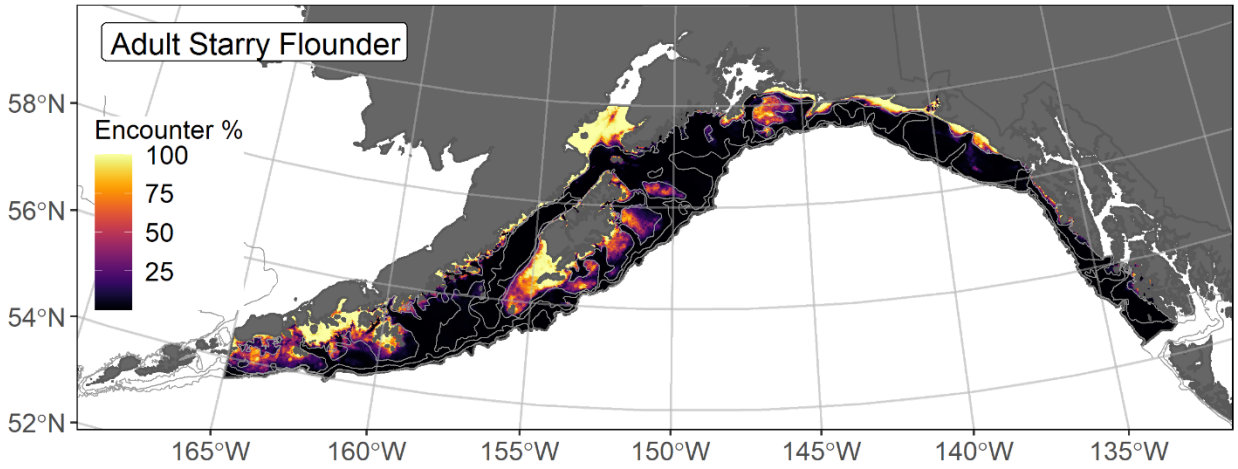

Figure 99. -- Encounter probability of adult starry flounder from AFSC RACE-GAP summer bottom trawl surveys (1993–2019) of the Gulf of Alaska with the 100 m, 200 m, and 700 m isobaths indicated.

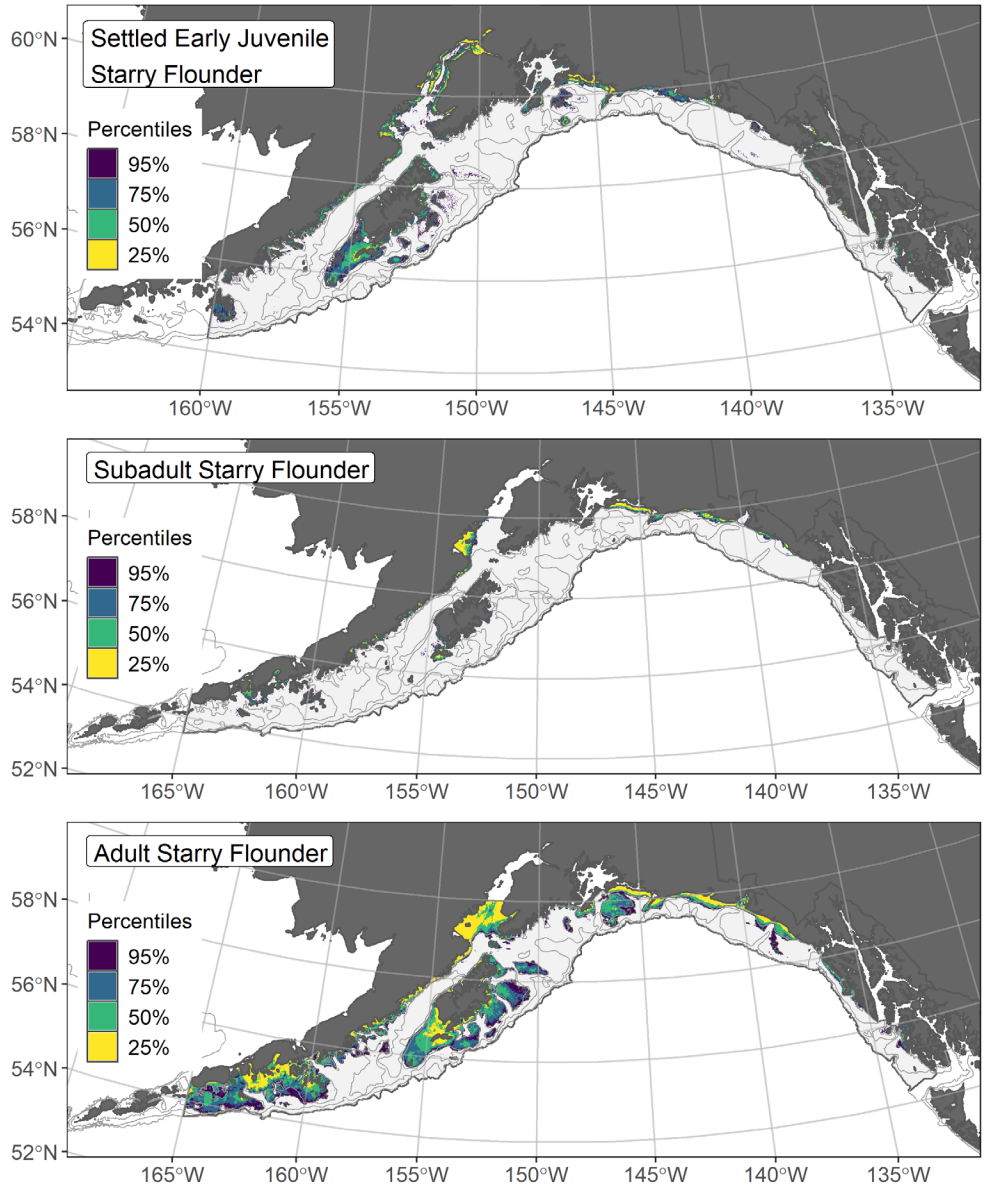

Figure 100. -- Essential fish habitat (EFH) is the area containing the top 95% of occupied habitat (defined as greater than 5% predicted probability of suitable habitat) for settled early juvenile (top panel) starry flounder from an SDM fitted to their distribution in Gulf of Alaska (GOA) mixed gear-type summer surveys (1989–2019), and for subadults (middle panel) and adults (bottom panel) is the area containing the top 95% of occupied habitat (defined as model estimated encounter probabilities greater than 5%) from an SDM ensemble fitted to starry flounder distribution and abundance in AFSC RACE-GAP GOA summer bottom trawl surveys (1993–2019) with 100 m, 200 m, and 700 m isobaths indicated; within the EFH area map are the subareas of the top 25% (EFH hot spots), top 50% (core EFH area), and top 75% (principal EFH area).

Yellowfin sole (*Limanda aspera*)

Yellowfin sole (*Limanda aspera*, YFS) in the GOA are managed in the Shallow Water Flatfish stock complex, where they are one of the five species that account for a majority of the biomass of this group (Turncock et al. 2017b). In the Gulf of Alaska, the minimum length of early juvenile stage YFS was set to the smallest mean length from beach seines (30 mm FL) (NFAA), and the maximum length was set to 140 mm FL (Yeung and Cooper 2020). The mesh size of the RACE-GAP bottom trawl is large enough that the smaller juvenile life stages may not be wholly retained in the catch[25]. Subadults and adults were separated in this study using L50 = 296 mm FL (Tenbrink and Wilderbuer 2015).

Settled early juvenile yellowfin sole distribution predicted from mixed gear-type summer surveys in the Gulf of Alaska -- Settled early juvenile YFS (N = 66) caught in mixed gear-type summer surveys (1989–2019), using large and small mesh bottom trawls and purse and beach seines, were distributed in nearshore areas of the GOA continental shelf (Fig. 101). Settled early juvenile YFS presence records from multiple surveys were combined in a habitat-related MaxEnt SDM predicting suitable habitat probabilities for this life stage in the GOA. The best model had a β-multiplier of 3.0 and an AUC of 0.94 (Table 38). Bottom depth alone accounted for 72.6% of the contribution among covariates to the deviance explained by the final SDM (Table 39). The highest predicted probabilities of suitable habitat for settled early juvenile YFS were less than 100 m depth on the GOA continental shelf (Fig. 102). The standard deviation among k-folds as a result of cross-validation for the final SDM was relatively low.

Subadult yellowfin sole abundance and distribution predicted from RACE-GAP summer bottom trawl surveys in the Gulf of Alaska -- Subadult YFS (N = 401) caught in GOA RACE-GAP summer bottom trawl surveys (1996–2019) occurred primarily inshore west of the Kenai Peninsula (Fig. 103). Three of the five SDMs considered for inclusion in the ensemble to predict numerical abundance of subadult YFS in the GOA converged (Table 40); the GAM_{nb} was eliminated by skill testing. The remaining two best-performing SDMs were weighted by RMSE in the final ensemble, which attained a good overall fit to the observed subadult YFS distribution and abundance data. The ensemble was fair at predicting high and low abundance catches (ρ = 0.38), and excellent at discriminating presence-absence (AUC = 0.98), and at explaining deviance (PDE = 0.78). Bottom depth, geographic location, and tidal maximum accounted for 83.3% of the contribution among covariates to the deviance explained by the final ensemble (Table 39). The highest abundances of subadult YFS were predicted in inshore areas of the

[25] Adding other high quality sources of data if available to future SDM ensemble EFH mapping for this species will be included as a research recommendation from the 2023 EFH 5-year Review.

central and western GOA west of the Kenai Peninsula (Fig. 104). The CV of ensemble predictions was higher at bathymetric rises on the continental shelf in the central and western GOA. The probability of encountering subadult YFS was highest in the central and western GOA and also occurred in inshore areas of the eastern GOA (Fig. 105).

Adult yellowfin sole abundance and distribution predicted from RACE-GAP summer bottom trawl surveys in the Gulf of Alaska -- Adult YFS (N = 491) caught in GOA RACE-GAP summer bottom trawl surveys (1996–2019) occurred mainly on the continental shelf of the central and western GOA west of the Kenai Peninsula (Fig. 106). Three of the five SDMs considered for inclusion in the ensemble to predict numerical abundance of adult YFS in the GOA converged (Table 40); the GAM_{nb} was eliminated by skill testing. The remaining two best-performing SDMs were weighted by RMSE in the final ensemble, which attained a good overall fit to the observed adult YFS distribution and abundance data. The ensemble was fair at predicting high and low abundance catches (ρ = 0.40), and excellent at discriminating presence-absence (AUC = 0.98) and explaining deviance (PDE = 0.79). Geographic location, bottom depth, and tidal maximum accounted for 73.1% of the contribution among covariates to the deviance explained by the final ensemble (Table 39). Similar to subadults, higher abundance of adult YFS was predicted in inshore areas of the central and western GOA west of the Kenai Peninsula (Fig. 107). The CV of ensemble predictions was higher at bathymetric rises on the continental shelf in the central and western GOA. The probability of encountering adult YFS was highest in the central and western GOA and also occurred in inshore areas of the eastern GOA (Fig. 108).

Essential Fish Habitat of three life stages of yellowfin sole in the Gulf of Alaska -- Habitat-related predictions of YFS demersal life stage distribution and abundance from summer surveys of the GOA (mixed gear-type summer surveys (1989–2019) and RACE-GAP bottom trawl surveys (1996–2019)) were mapped as EFH areas and subareas (Fig. 109). Settled early juvenile EFH occurred in inshore areas of the GOA continental shelf, with EFH hot spots inside Cook Inlet and offshore of the Copper and Bering rivers. The EFH areas for subadult and adult YFS were similar and concentrated west of the Kenai Peninsula, with some EFH area also inshore in the eastern GOA. Subadult and adult core EFH area included most of the total EFH area, and EFH hot spots were present at shallower depths on the continental shelf and in nearshore areas west of the Kenai Peninsula.

Essential Fish Habitat Level 3 habitat-related vital rates of settled early juvenile yellowfin sole in the Gulf of Alaska -- Temperature-dependent growth rate of laboratory-reared early juvenile YFS is described by the following equation (Hurst *in prep*aration):

$$GR = 0.000719 - 0.000690 * T + 0.000383 * T^2 - 0.000018 * T^3 \ ,$$

where *GR* is the growth rate (% body weight (g) per day (d)), and *T* is the temperature. The raster product of early juvenile YFS predicted probability of suitable habitat from a MaxEnt SDM, and their temperature-dependent growth is an EFH Level 3 map of habitat-related growth potential (Fig. 110). The temperature of maximum growth for early juvenile YFS is 12.8°C (Hurst *in prep*aration), which was within the range (2.9–17.5°C) of the CGOA ROMS 3 km summer bottom temperature covariate raster (2000–2019) in the SDM and to the EFH Level 3 map of habitat-related growth potential (Fig. 110). The bottom temperature range at settled early juvenile YFS catch locations in the SDM was 6.2–12.5°C (Fig. 101). In the map of temperature-dependent growth, the highest growth areas occurred inshore and along the coast, as well as on the banks and bathymetric rises on the GOA continental shelf (Fig. 110). The SDM of settled early juvenile stage YFS suitable habitat limited areas of high predicted habitat-related growth potential (Fig. 110), notably to shallower depths, suggesting that temperature was not the only driver of distribution for this life stage in the GOA. EFH subareas of core EFH area and EFH hot spots corresponded with locations of high habitat-related growth potential for settled early juvenile stage YFS, which added value in interpreting the EFH Level 1 map (Fig. 109).

Table 38. -- Maximum entropy model (MaxEnt) used to construct Essential Fish Habitat (EFH) for settled early juvenile yellowfin sole: regularization multiplier (β); *k*-fold cross-validation root-mean-square-error (RMSE), area under the receiver operating characteristic curve (AUC), and areal extent of EFH (km^2).

Model	**β**	**RMSE**	**AUC**	**EFH area (km^2)**
MaxEnt	3.0	3.25	0.94	54,600

Table 39. -- Covariates retained in the a) settled early juvenile habitat-related maximum entropy (MaxEnt) species distribution model (SDM), and b) subadult and c) adult SDM final ensembles for yellowfin sole with the percent contribution of each covariate to the deviance explained by the SDMs and the cumulative deviance explained: SD = standard deviation and BPI = bathymetric position index.

yellowfin sole	**Covariate**	**% Contribution**	**Cumulative %**
a) settled early juvenile	bottom depth	72.6	72.6
	aspect north	7.4	80.0
	tidal maximum	4.6	84.5
	curvature	3.8	88.3
	sponge presence	3.2	91.5
	aspect east	2.4	94.0
	pennatulacean presence	1.7	95.7
	BPI	1.6	97.2
	rockiness	1.5	98.8
	bottom temperature	0.9	99.6
	slope	0.3	99.9
	coral presence	0.1	100.0
b) subadult	bottom depth	33.6	33.6
	location	29.5	63.1
	tidal maximum	14.2	77.3
	BPI	6.0	83.3
	current SD	4.3	87.6
	slope	3.4	91.0
	current	3.1	94.1
	aspect east	2.1	96.2
	rockiness	1.3	97.5
	bottom temperature	0.8	98.3
	aspect north	0.8	99.1
	curvature	0.4	99.5
	sponge presence	0.2	99.7
	coral presence	0.2	99.9
	pennatulacean presence	0.1	100.0
c) adult	location	36.3	36.3
	bottom depth	24.4	60.7
	tidal maximum	12.4	73.1
	BPI	5.8	78.9
	slope	5.0	83.9
	current SD	4.3	88.2
	current	3.5	91.7
	aspect north	2.5	94.2

yellowfin sole

Covariate	% Contribution	Cumulative %
rockiness	2.4	96.6
aspect east	1.2	97.8
curvature	1.1	98.9
sponge presence	0.5	99.4
bottom temperature	0.4	99.8
coral presence	0.1	99.9

Table 40. -- Constituent species distribution models (SDMs) used to construct Essential Fish Habitat (EFH) for a) subadult and b) adult yellowfin sole: MaxEnt = Maximum entropy; paGAM = presence-absence generalized additive model; hGAM = zero-adjusted Poisson hurdle GAM; GAM_P = standard Poisson GAM; GAM_{nb} = standard negative-binomial GAM; RMSE = root mean square error; ρ (*rho*) = Spearman's rank correlation coefficient; AUC = area under the receiver operating characteristic curve; and PDE = Poisson deviance explained *. The "--" indicates that this model was not included in the final ensemble.

a) subadult yellowfin sole

Models	RMSE	Relative Weight	*P*	AUC	PDE	EFH area (km^2)
MaxEnt	--	--	--	--	--	--
paGAM	55.1	0.50	0.37	0.98	0.64	113,700
hGAM	--	--	--	--	--	--
GAM_P	55.4	0.50	0.42	0.96	0.67	57,000
GAM_{nb}	62.9	0	--	--	--	--
ensemble	46.9	1	0.38	0.98	0.78	101,600

b) adult yellowfin sole

Models	RMSE	Relative Weight	ρ	AUC	PDE	EFH area (km^2)
MaxEnt	--	--	--	--	--	--
paGAM	72.1	0.43	0.39	0.97	0.62	133,200
hGAM	--	--	--	--	--	--
GAM_P	63.0	0.57	0.43	0.96	0.74	72,900
GAM_{nb}	139.5	0	--	--	--	--
ensemble	58.0	1	0.40	0.98	0.79	118,900

* Refer to the Species Distribution Model Performance Metrics subsection within the Statistical Modeling section of the Methods for detailed descriptions of individual model performance metrics.

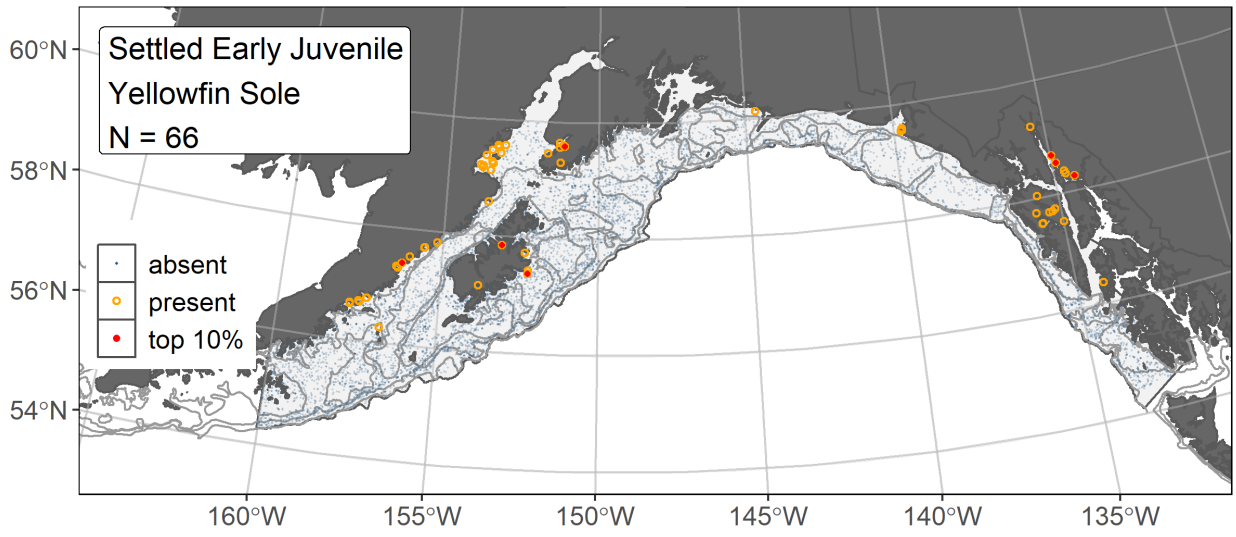

Figure 101. -- Distribution of settled early juvenile yellowfin sole catches (N = 66) in mixed gear-type summer surveys of the Gulf of Alaska (GOA) (1989–2019) with the 100 m, 200 m, and 700 m isobaths indicated; filled red circles indicate locations in top 10% of overall abundance, open orange circles indicate presence in remaining catches, and blue dots indicate stations sampled where the animals were not present.

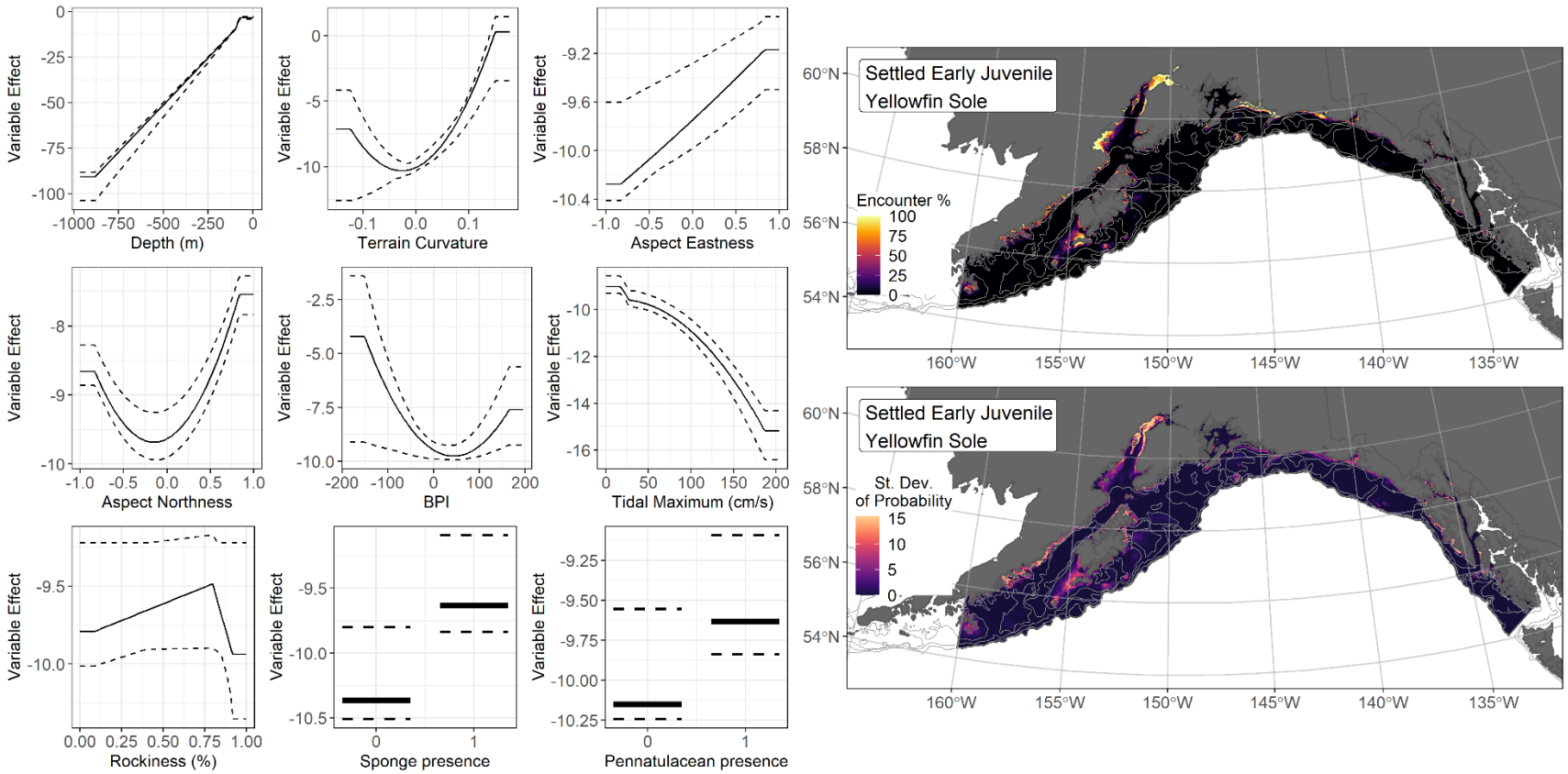

Figure 102. -- The top nine covariate effects (left panel) from a habitat-related species distribution model (MaxEnt) of settled early juvenile yellowfin sole probability of suitable habitat in the Gulf of Alaska (upper right panel) with the standard deviation of the probability predictions (lower right panel).

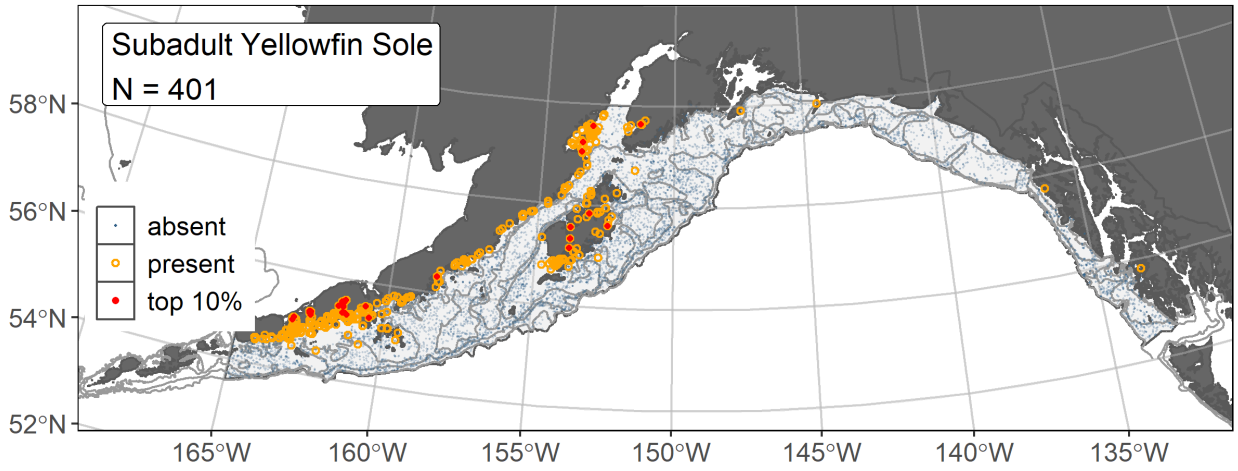

Figure 103. -- Distribution of subadult yellowfin sole catches (N = 401) in 1993–2019 AFSC RACE-GAP summer bottom trawl surveys of the Gulf of Alaska with the 100 m, 200 m, and 700 m isobaths indicated; filled red circles indicate locations in top 10% of overall abundance, open orange circles indicate presence in remaining catches, and blue dots indicate stations sampled where the animals were not present.

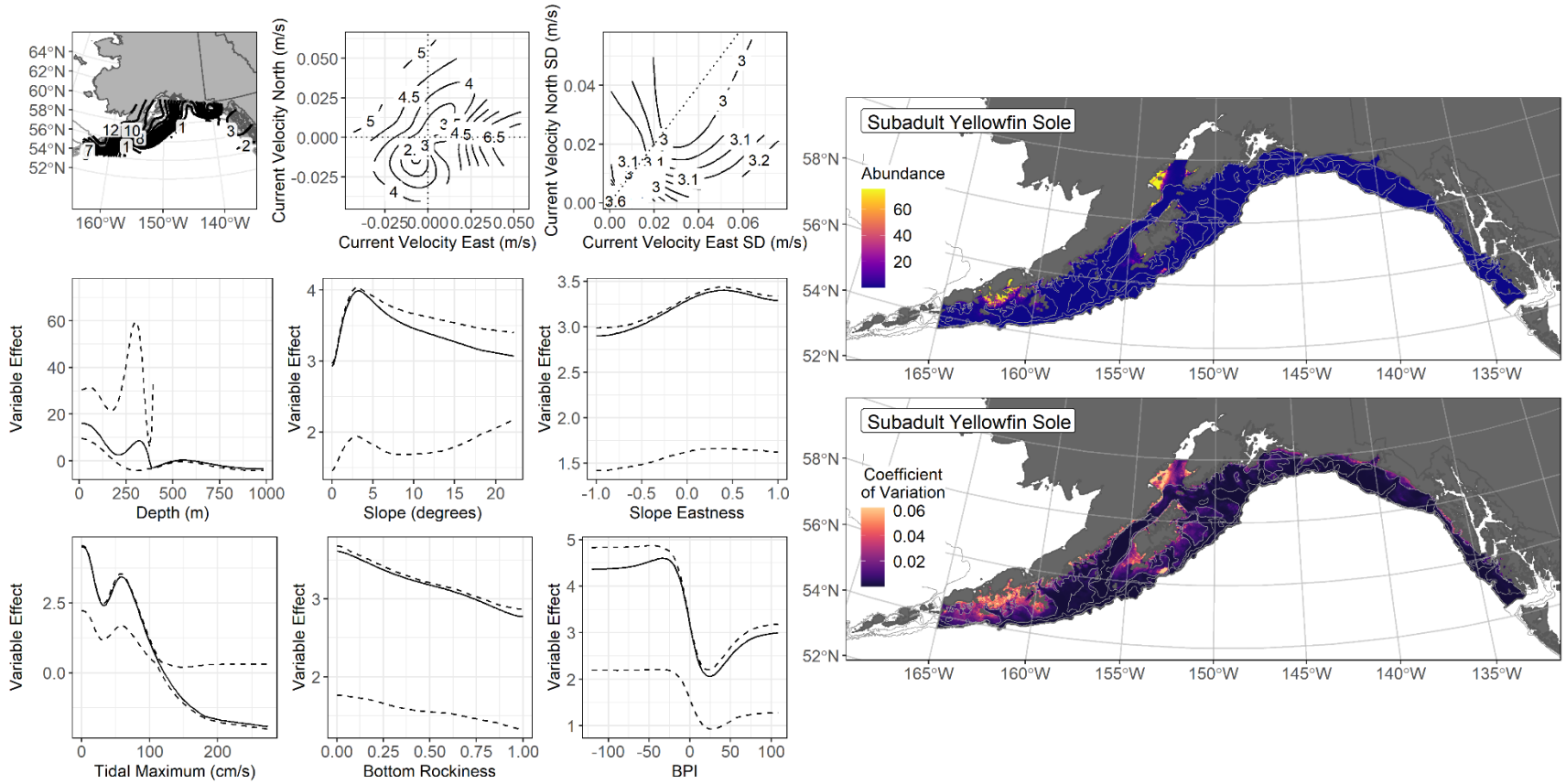

Figure 104. -- The top nine covariate effects (left panel) on ensemble-predicted subadult yellowfin sole numerical abundance across the Gulf of Alaska (upper right panel) along with the coefficient of variation (CV) of the ensemble predictions (lower right panel).

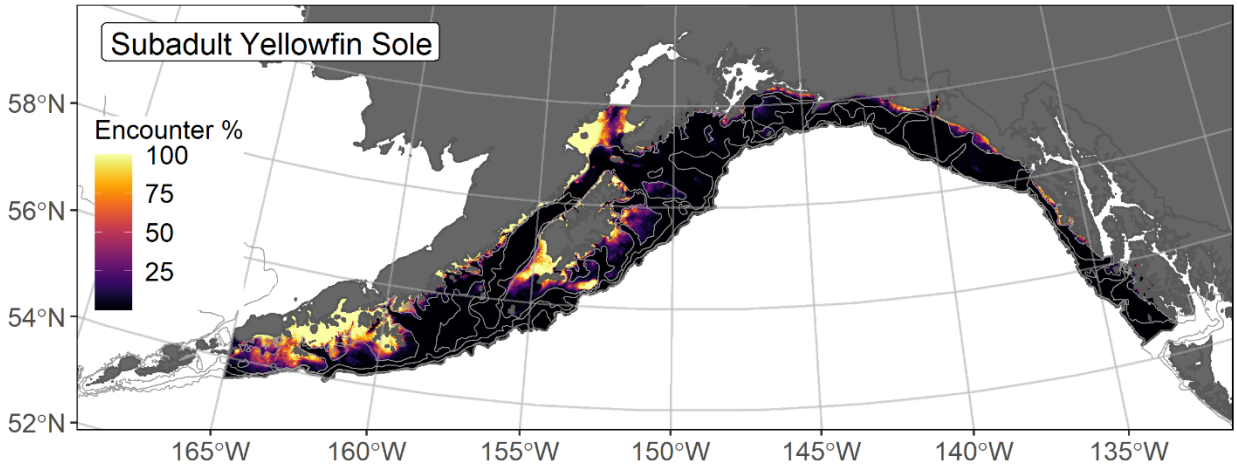

Figure 105. -- Encounter probability of subadult yellowfin sole from AFSC RACE-GAP summer bottom trawl surveys (1993–2019) of the Gulf of Alaska with the 100 m, 200 m, and 700 m isobaths indicated.

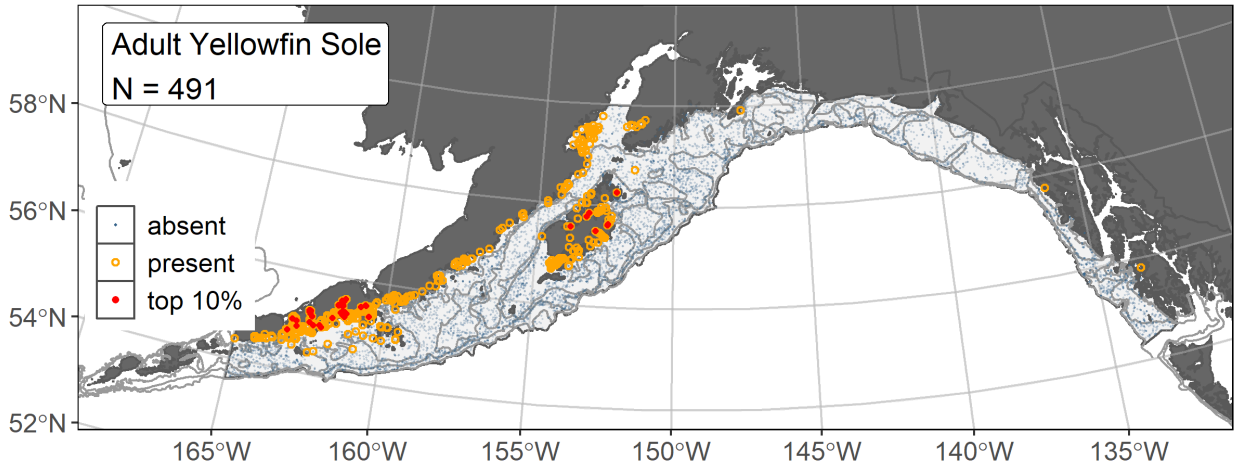

Figure 106. -- Distribution of adult yellowfin sole catches (N = 491) in 1993–2019 AFSC RACE-GAP summer bottom trawl surveys of the Gulf of Alaska with the 100 m, 200 m, and 700 m isobaths indicated; filled red circles indicate locations in top 10% of overall abundance, open orange circles indicate presence in remaining catches, and blue dots indicate stations sampled where the animals were not present.

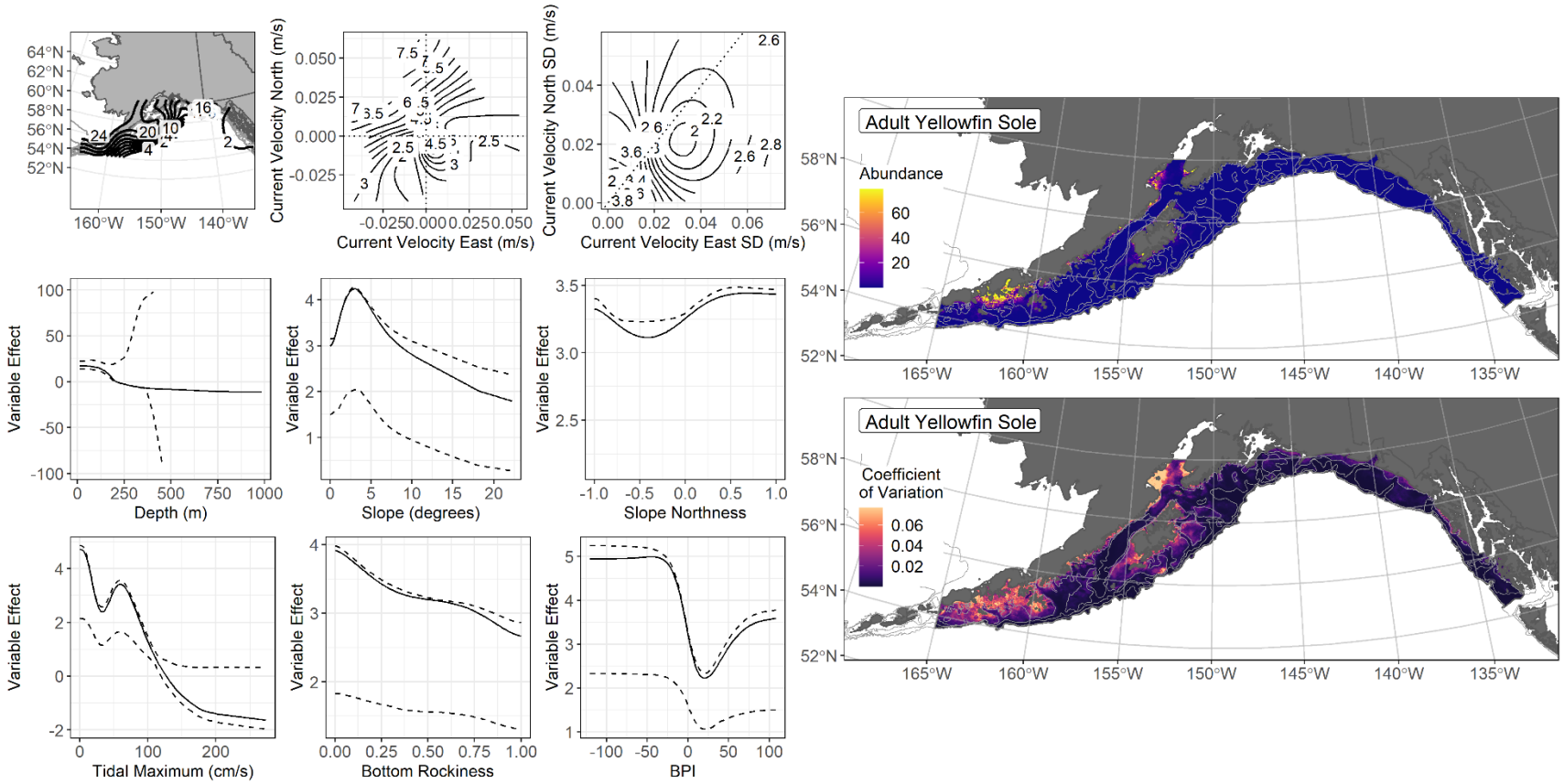

Figure 107. -- The top nine covariate effects (left panel) on ensemble-predicted adult yellowfin sole numerical abundance across the Gulf of Alaska (upper right panel) along with the coefficient of variation (CV) of the ensemble predictions (lower right panel).

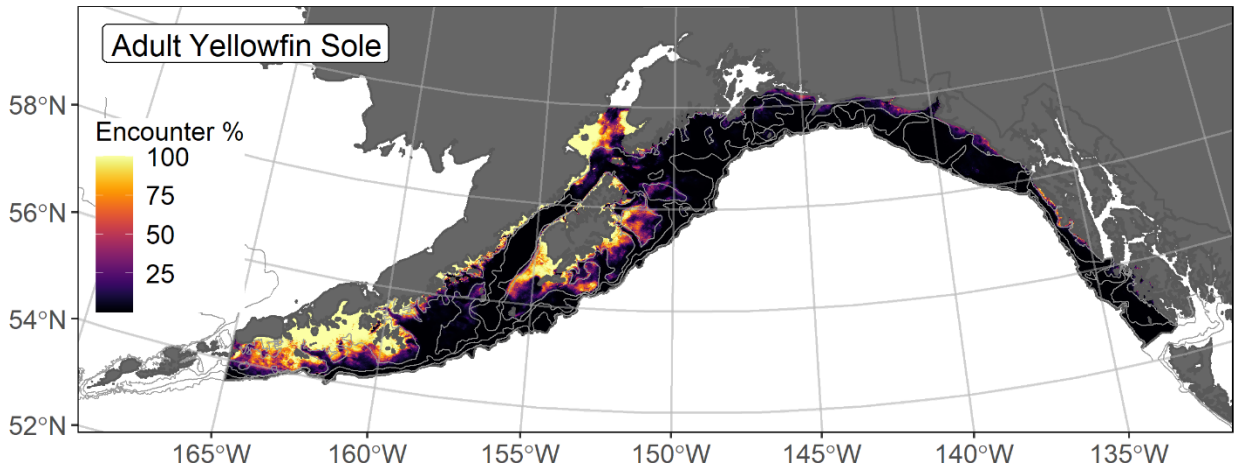

Figure 108. -- Encounter probability of adult yellowfin sole from AFSC RACE-GAP summer bottom trawl surveys (1993–2019) of the Gulf of Alaska with the 100 m, 200 m, and 700 m isobaths indicated.

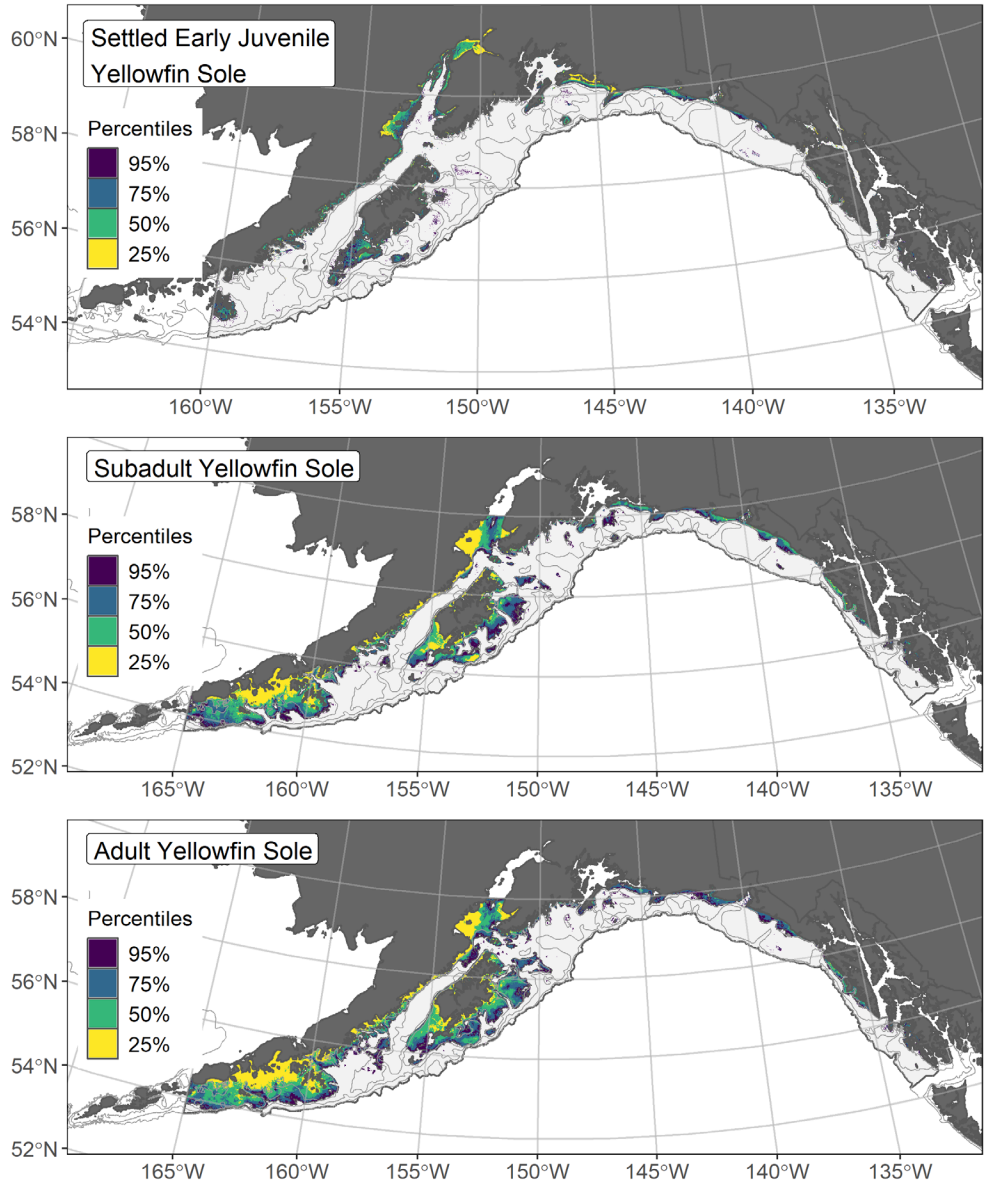

Figure 109. -- Essential fish habitat (EFH) is the area containing the top 95% of occupied habitat (defined as greater than 5% predicted probability of suitable habitat) for settled early juvenile (top panel) yellowfin sole from an SDM fitted to their distribution in Gulf of Alaska (GOA) mixed gear-type summer surveys (1989–2019), and for subadults (middle panel) and adults (bottom panel) is the area containing the top 95% of occupied habitat (defined as model estimated encounter probabilities greater than 5%) from an SDM ensemble fitted to yellowfin sole distribution and abundance in AFSC RACE-GAP GOA summer bottom trawl surveys (1993–2019) with 100 m, 200 m, and 700 m isobaths indicated; within the EFH area map are the subareas of the top 25% (EFH hot spots), top 50% (core EFH area), and top 75% (principal EFH area).

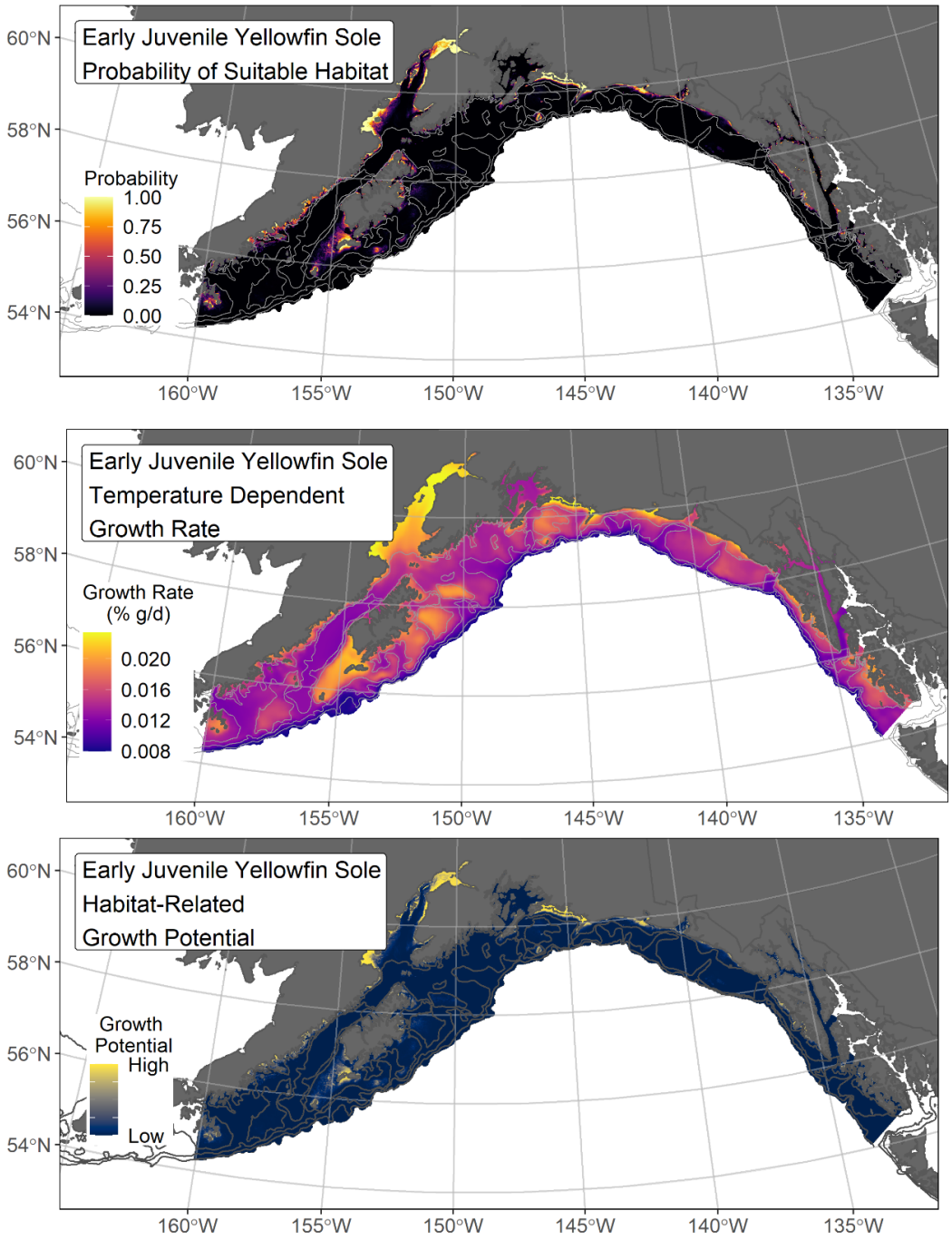

Figure 110. -- Settled early juvenile yellowfin sole predicted probability of suitable habitat from a habitat-related species distribution model fitted to their distribution in Gulf of Alaska mixed gear-type summer surveys (1989–2019; top panel), temperature-dependent growth rate ($GR = \%\ body\ weight\ (g) \cdot day^{-1}$; center panel), and EFH Level 3 map of habitat-related growth potential (bottom panel), which is the raster product of probability of suitable habitat and temperature-dependent growth rate.

Roundfishes

Atka mackerel (*Pleurogrammus monopterygius*)

Atka mackerel (*Pleurogrammus monopterygius*) is in the family of greenlings (Hexagrammidae) that is found across the northern Pacific Ocean from the Kuril Islands to the eastern GOA, with the largest concentrations found around their namesake island in the western Aleutian Islands (Lauth et al. 2007). The RACE-GAP bottom trawl survey and fishery data suggest that the Atka mackerel population in the GOA is smaller and much more patchily distributed than that in the Aleutian Islands (Lowe 2019)[26]. The maturity schedule of Atka mackerel can vary by region and growth conditions. This study uses the average length at 50% maturity in the Aleutian Islands from McDermott and Lowe (1997; L_{50} = 344 mm FL) to define the upper length limit of the subadult Atka mackerel life stage. Atka mackerel form nests in rocky habitat within nesting colonies widespread across the continental shelf of the Aleutian Island and western GOA, where males typically guard the developing eggs for several months (Lauth et al. 2007). Adult Atka mackerel are an important component in the diets of several marine mammals, particularly Steller sea lions (Sinclair et al. 2013). There has not been a directed fishery for Atka mackerel in the GOA since 1996. Steller sea lion protection measures prohibit directed fishing for Atka mackerel in the GOA. This species is presently managed as a bycatch-only fishery, with TAC levels set to provide for anticipated bycatch needs in targeted groundfish fisheries, primarily for Pacific cod, walleye pollock, and rockfishes (Lowe 2019).

Subadult Atka mackerel abundance and distribution predicted from RACE-GAP summer bottom trawl surveys in the Gulf of Alaska -- Subadult Atka mackerel (N = 87) caught in GOA RACE-GAP summer bottom trawl surveys (1993–2019) were encountered infrequently and primarily from Kodiak Island through the western GOA with the highest density catches located in the Shumagin Islands (Fig. 111). Four of the five SDMs considered for inclusion in the ensemble to predict numerical abundance of subadult Atka mackerel in the GOA converged (Table 41); the GAM_P was eliminated through skill testing. The remaining three best-performing SDMs were equally weighted by RMSE in the final ensemble. The final ensemble was a fair fit to the observed subadult Atka mackerel distribution and abundance data. The ensemble was poor at predicting high and low abundance catches (ρ = 0.15), excellent at discriminating presence-absence (AUC = 0.91), and fair to good at explaining deviance (PDE = 0.41). Bottom depth, geographic location, and sponge presence accounted for 68.5% of covariate contribution to the deviance explained by the final ensemble (Table 42). In general, higher subadult Atka

[26] The reviewing stock author raised concern about the ongoing challenges of mapping EFH for this species with patchy distribution in time and space.

mackerel ensemble-predicted numerical abundance occurred further west geographically in the study area, at shallower depths, with low presence of sponges (Fig. 112). Predicted abundance was highest in the areas around the Shumagin Islands and on the banks on the continental shelf south and west of Kodiak Island. The CV of ensemble predictions was higher in shallower areas across the GOA continental shelf. The probability of encountering subadult Atka mackerel was higher in areas of predicted high abundance (Fig. 113).

Adult Atka mackerel abundance and distribution predicted from RACE-GAP summer bottom trawl surveys in the Gulf of Alaska -- Adult Atka mackerel (N = 700) caught in GOA RACE-GAP summer bottom trawl surveys (1993–2019) occurred throughout the central and western GOA, with the highest abundance catches in the west and occasionally east of Kodiak Island (Fig. 114). Adult Atka mackerel catches also occurred in the eastern GOA. Four SDMs considered for inclusion in the ensemble to predict numerical abundance of adult Atka mackerel in the GOA converged (Table 41); the hGAM and GAM_P were eliminated by skill testing. The remaining two best-performing SDMs were weighted by RMSE in the final ensemble, which attained a fair overall fit to the observed adult Atka mackerel distribution and abundance data. The ensemble was fair at predicting high and low abundance catches ($\rho = 0.33$), good at discriminating presence-absence (AUC = 0.85), and fair at explaining deviance (PDE = 0.35). Geographic location and bottom depth contributed 75.4% among covariates to the deviance explained by the ensemble (Table 42). Higher adult Atka mackerel abundance was predicted to occur in the western GOA on bathymetric rises at depths less than 250 m (Fig. 115). The CV of ensemble predictions was also higher moving from east to west in the GOA study area. The probability of encountering adult Atka mackerel in the GOA increased from around Kayak Island through the western extent of the study area (Fig. 116).

Essential fish habitat of subadult and adult Atka mackerel in the Gulf of Alaska -- Ensemble-predicted habitat-related numerical abundance of Atka mackerel life stages collected in RACE-GAP summer bottom trawl surveys of the GOA (1993–2019) was mapped as EFH areas and subareas (Fig. 117, Fig. 13). EFH area for subadult Atka mackerel occurred at the shallower banks and areas south and west of Kodiak Island. The EFH area of adults was larger than the area for subadults. The core EFH area occurred from Kayak Island west. Highest EFH area percentiles, including EFH hot spots, increased moving west in the study area.

Table 41. -- Constituent species distribution models (SDMs) used to construct Essential Fish Habitat (EFH) for a) subadult and b) adult Atka mackerel: MaxEnt = Maximum entropy; paGAM = presence-absence generalized additive model; hGAM = zero-adjusted Poisson hurdle GAM; GAM_P = standard Poisson GAM; GAM_{nb} = standard negative-binomial GAM; RMSE = root mean square error; ρ (rho) = Spearman's rank correlation coefficient; AUC = area under the receiver-operating characteristic curve; and PDE = Poisson deviance explained *. The "--" indicates that this model was not included in the final ensemble.

a) subadult Atka mackerel

Models	RMSE	Relative Weight	ρ	AUC	PDE	EFH area (km^2)
MaxEnt	1.66	0.33	0.11	0.83	0.23	97,500
paGAM	1.66	0.33	0.14	0.87	0.29	78,100
hGAM	--	--	--	--	--	--
GAM_P	1.72	0	--	--	--	--
GAM_{nb}	1.66	0.33	0.14	0.86	0.31	55,800
ensemble	1.64	1	0.15	0.91	0.41	83,900

b) adult Atka mackerel

Models	RMSE	Relative Weight	ρ	AUC	PDE	EFH area (km^2)
paGAM	142.6	0.52	0.33	0.84	0.20	243,900
hGAM	680.5	0	--	--	--	--
GAM_P	154.2	0	--	--	--	--
GAM_{nb}	147.7	0.48	0.31	0.82	0.27	143,700
ensemble	142.5	1	0.33	0.85	0.35	233,800

* Refer to the Species Distribution Model Performance Metrics subsection within the Statistical Modeling section of the Methods for detailed descriptions of individual model performance metrics.

Table 42. -- Covariates retained in the a) subadult and b) adult Atka mackerel species distribution model (SDM) final ensembles, the percent contribution to the ensemble deviance explained by each covariate, and the cumulative deviance explained: SD = standard deviation and BPI = bathymetric position index.

Atka mackerel

	Covariate	**% Contribution**	**Cumulative %**
a) subadult	bottom depth	31.4	31.4
	location	30.1	61.4
	sponge presence	7.1	68.5
	aspect east	6.7	75.2
	current SD	6.6	81.8
	bottom temperature	5.6	87.4
	aspect north	4.2	91.6
	rockiness	2.2	93.8
	current	1.9	95.7
	tidal maximum	1.9	97.6
	BPI	1.1	98.7
	slope	1.0	99.7
	coral presence	0.2	99.9
	pennatulacean presence	0.1	100.0
b) adult	location	62.8	62.8
	bottom depth	12.6	75.4
	current	4.4	79.8
	tidal maximum	4.3	84.1
	aspect north	3.6	87.7
	aspect east	2.9	90.6
	bottom temperature	2.9	93.5
	current SD	1.9	95.4
	BPI	1.6	97.0
	rockiness	1.2	98.2
	slope	0.9	99.1
	pennatulacean presence	0.4	99.5
	coral presence	0.4	99.9
	sponge presence	0.1	100.0

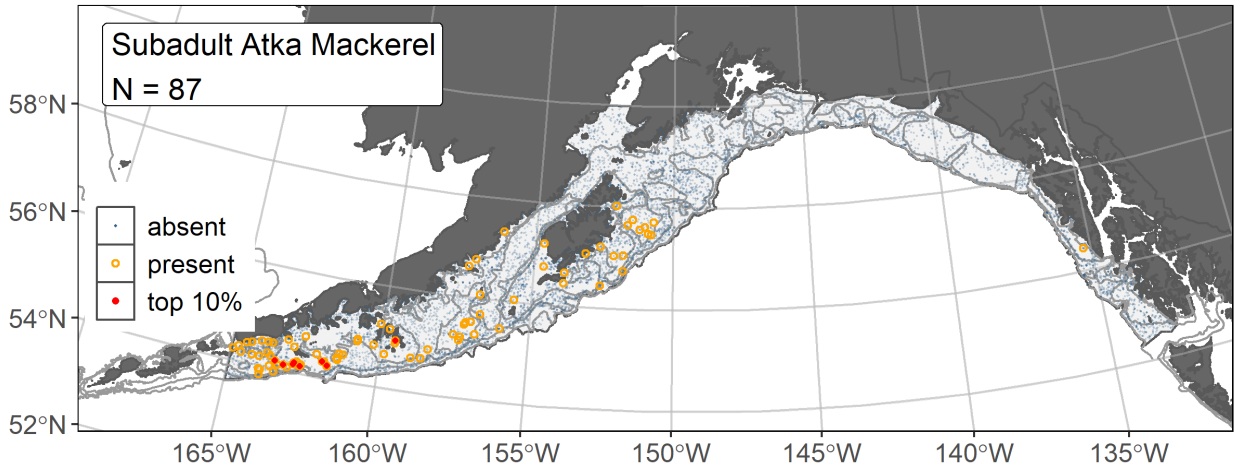

Figure 111. -- Distribution of subadult Atka mackerel catches (N = 87) in 1993–2019 AFSC RACE-GAP summer bottom trawl surveys of the Gulf of Alaska with the 100 m, 300 m, and 700 m isobaths indicated; filled red circles indicate locations in top 10% of overall abundance, open orange circles indicate presence in remaining catches, and blue dots indicate stations sampled where the animals were not present.

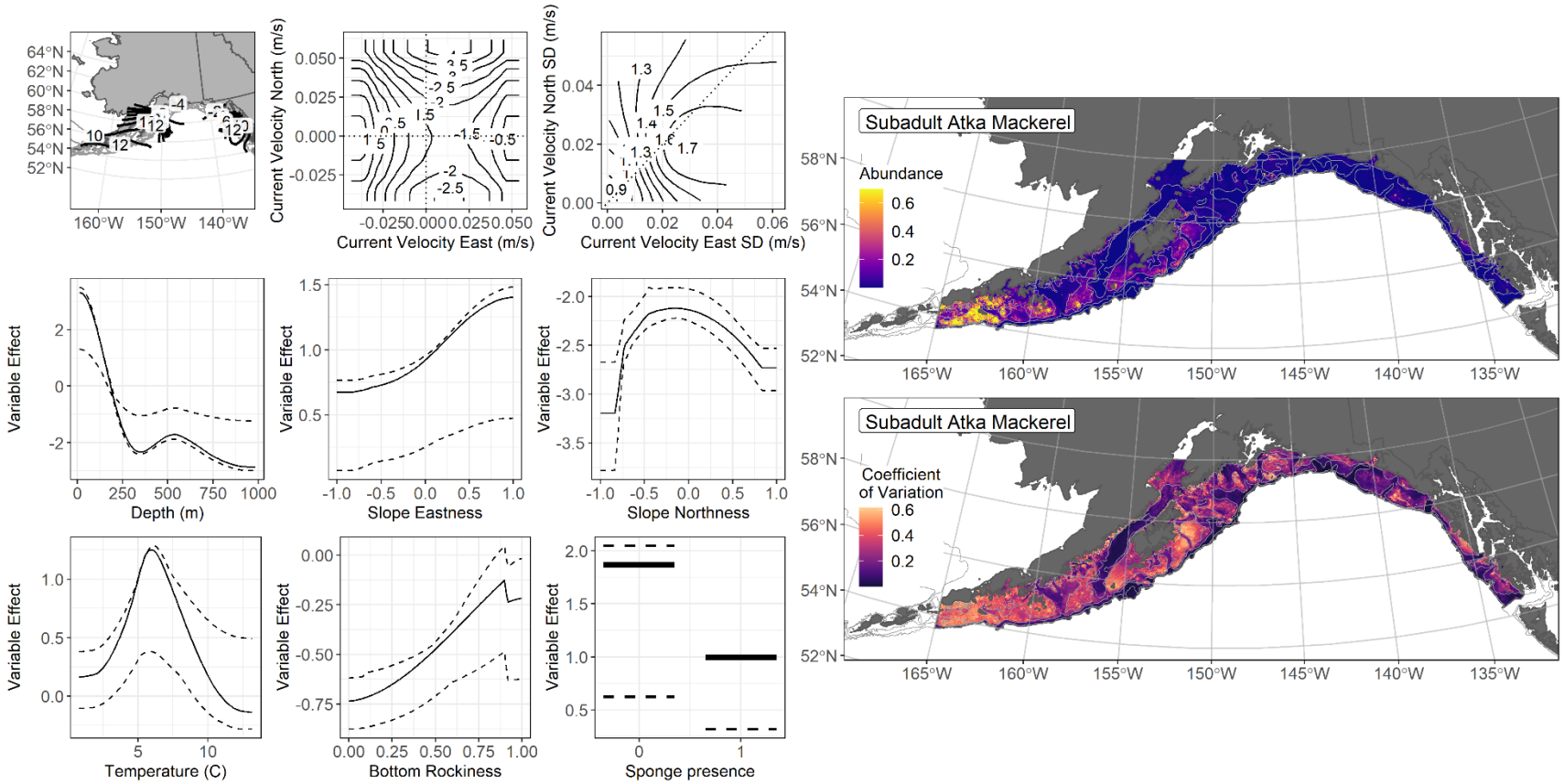

Figure 112. -- The top nine covariate effects (left panel) on ensemble-predicted subadult Atka mackerel numerical abundance across the Gulf of Alaska (upper right panel) alongside the coefficient of variation of the ensemble predictions (lower right panel).

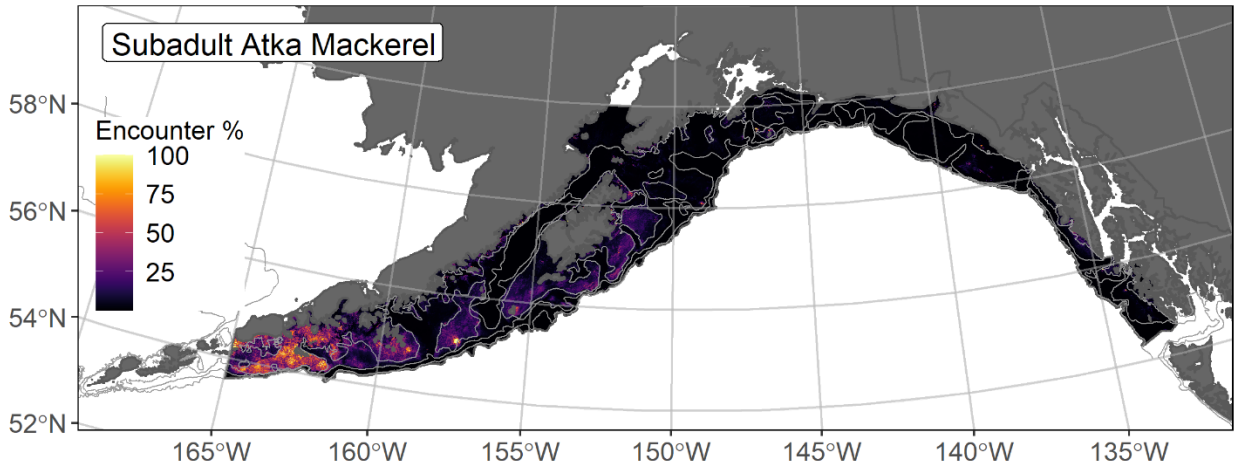

Figure 113. -- Encounter probability of subadult Atka mackerel from AFSC RACE-GAP summer bottom trawl surveys (1993–2019) of the Gulf of Alaska with the 100 m, 300 m, and 700 m isobaths indicated.

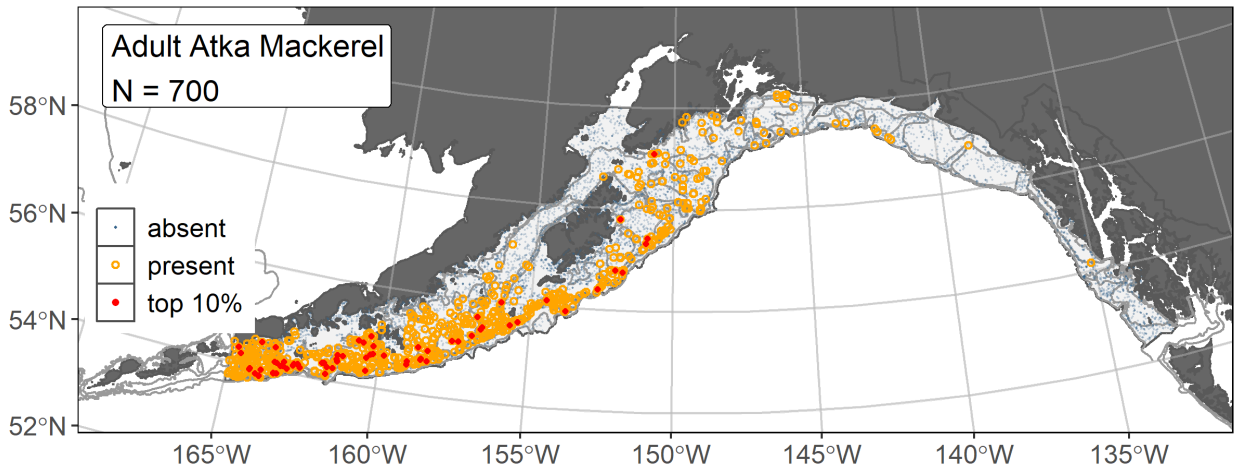

Figure 114. -- Distribution of adult Atka mackerel catches (N = 700) in 1993–2019 AFSC RACE-GAP summer bottom trawl surveys of the Gulf of Alaska with the 100 m, 300 m, and 700 m isobaths indicated; filled red circles indicate locations in top 10% of overall abundance, open orange circles indicate presence in remaining catches, and blue dots indicate stations sampled where the animals were not present.

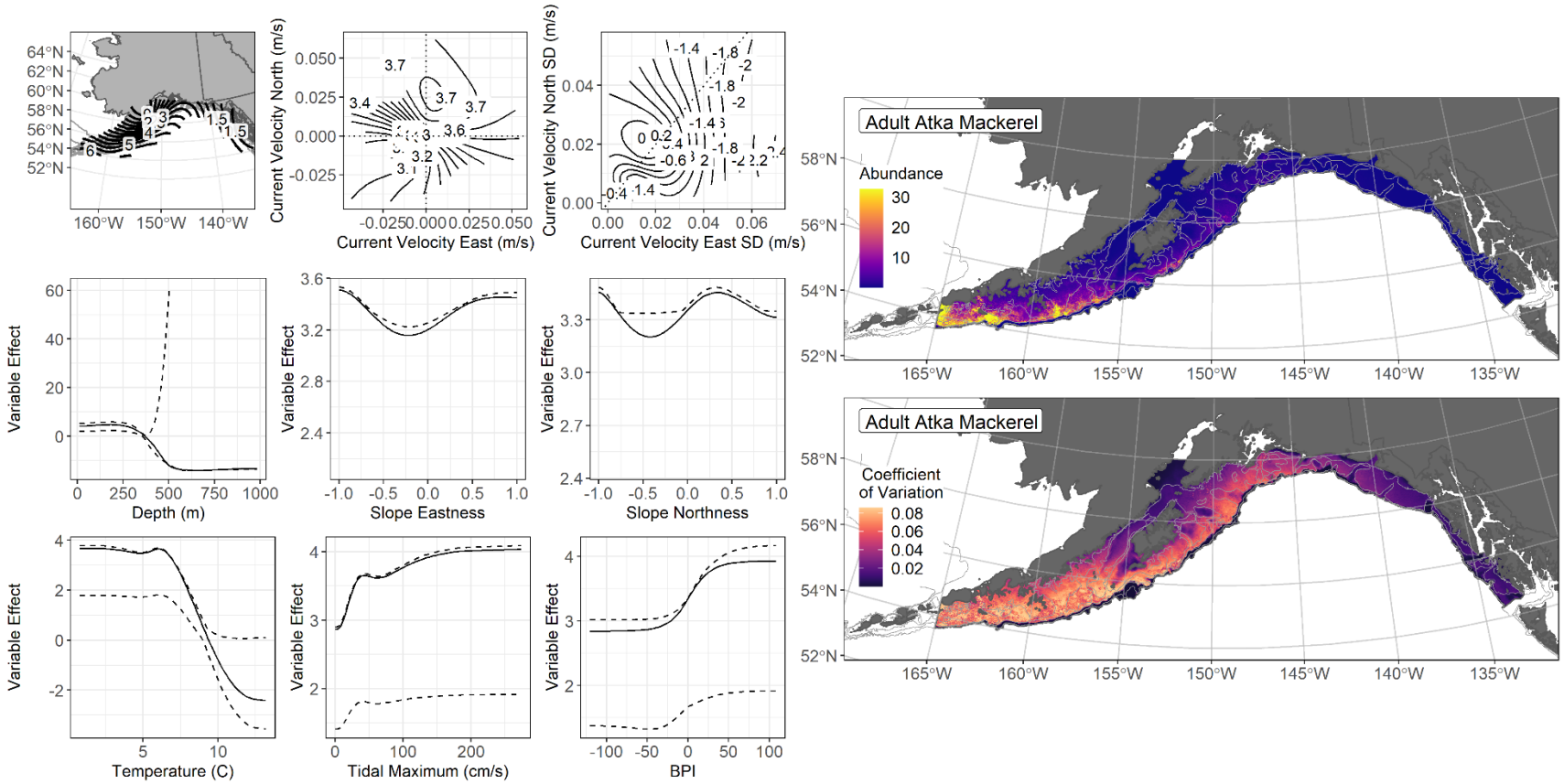

Figure 115. -- The top nine covariate effects (left panel) on ensemble-predicted adult Atka mackerel numerical abundance across the Gulf of Alaska (upper right panel) alongside the coefficient of variation of the ensemble predictions (lower right panel).

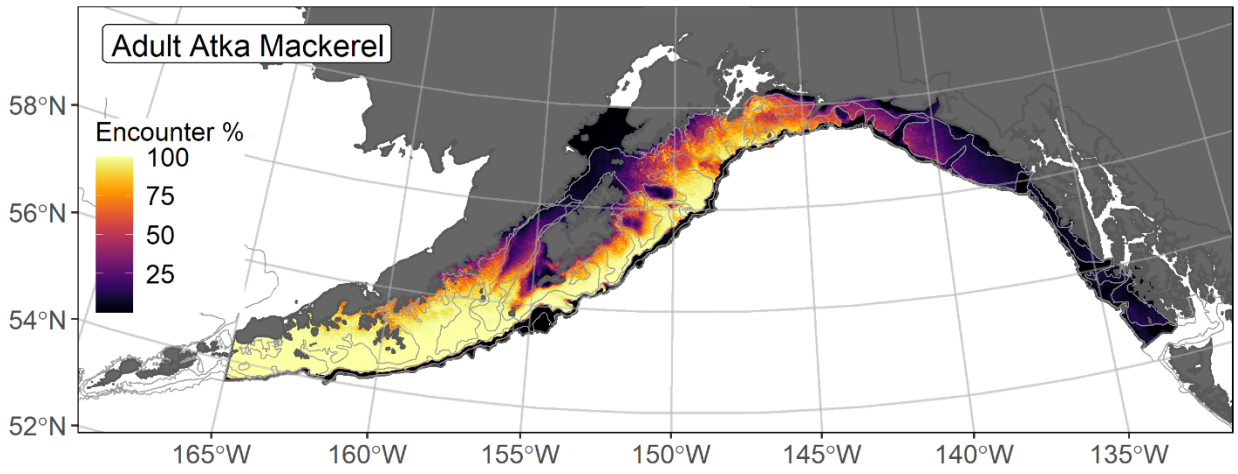

Figure 116. -- Encounter probability of adult Atka mackerel from AFSC RACE-GAP summer bottom trawl surveys (1993–2019) of the Gulf of Alaska with the 100 m, 200 m, and 700 m isobaths indicated.

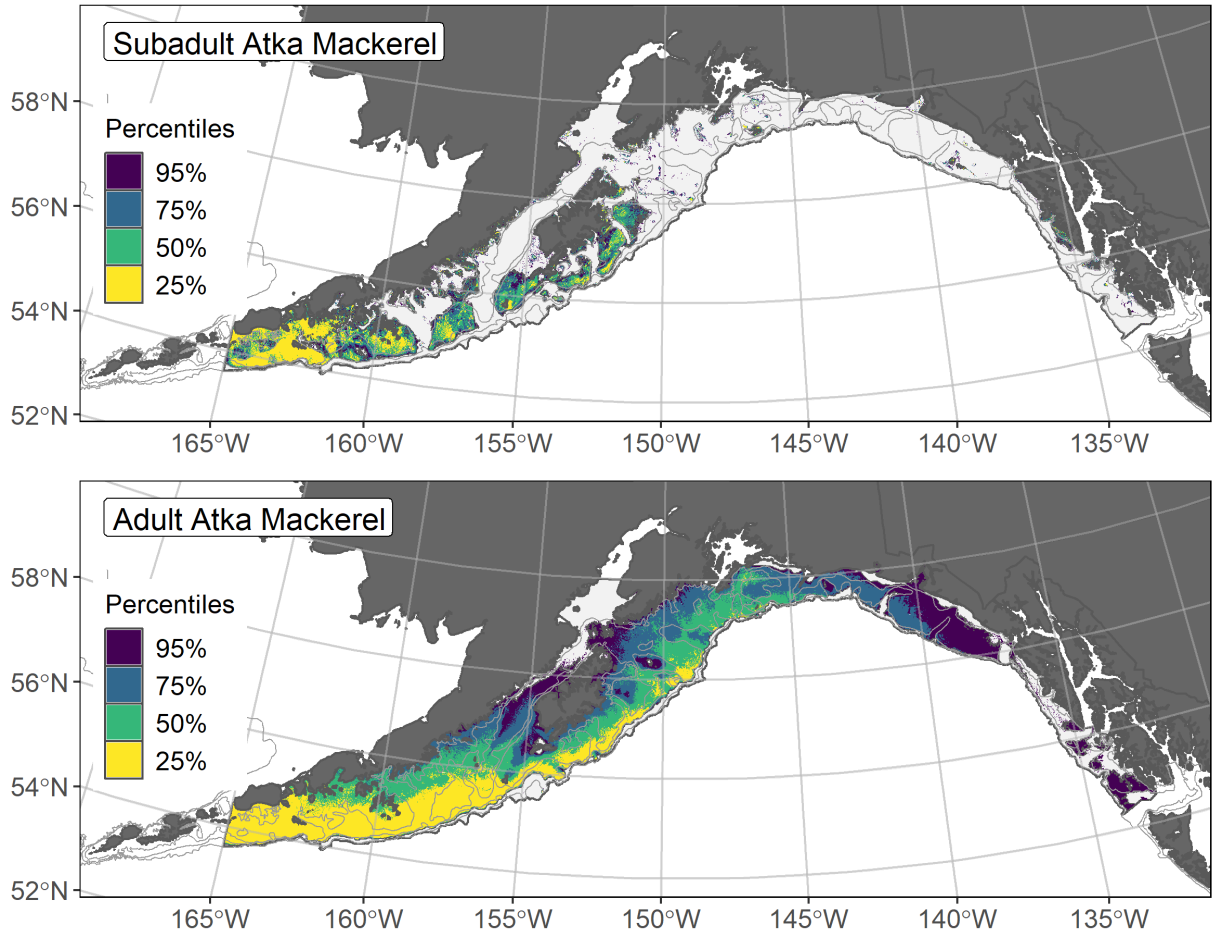

Figure 117. -- Essential fish habitat (EFH) is the area containing the top 95% of occupied habitat (defined as model estimated encounter probabilities greater than 5%) from an SDM ensemble fitted to subadult (top panel) and adult (bottom panel) Atka mackerel distribution and abundance in AFSC RACE-GAP summer bottom trawl surveys (1993–2019) with 100 m, 200 m, and 700 m isobaths indicated; within the EFH area map are the subareas of the top 25% (EFH hot spots), top 50% (core EFH area), and top 75% (principal EFH area) of habitat-related, ensemble-predicted numerical abundance.

Pacific cod (*Gadus macrocephalus*)

Pacific cod (*Gadus macrocephalus*) occur from the shoreline to 500 m depth throughout the RACE-GAP study area and support important multi-gear commercial fisheries in the GOA and BSAI (Barbeaux et al. 2020, Spies et al. 2020, Thompson et al. 2020). Pacific cod form aggregations during peak spawning season (Neidetcher et al. 2014) and lay demersal, adhesive eggs with a narrow thermal window for successful incubation (3–6°C). After hatching, pelagic larvae move downward in the water column as they grow and settle as early juveniles (40–150 mm FL; Doyle et al. 2019, Laurel et al. 2009), residing in nearshore nursery habitats (< 20 m depth) until undergoing ontogenetic migration to deeper depths (Abookire et al. 2007, Laurel et al. 2007, Pirtle et al. 2019). The mesh size of the RACE-GAP bottom trawl is large enough that these smaller life stages may not be wholly retained in the catch[27]. Length-based life stage breaks distinguish between subadults (151–503 mm FL; Laurel et al. 2009) and adults (> 503 mm FL; Stark 2007). Pacific cod growth rates are affected by water temperatures. Laboratory studies demonstrate that Pacific cod can grow two to three times faster than other boreal and Arctic gadids over a range of temperatures, yet their populations are vulnerable to the effects of marine heat waves (Laurel et al. 2016, Barbeaux et al. 2020).

Settled early juvenile Pacific cod distribution predicted from mixed gear-type summer surveys in the Gulf of Alaska -- Settled early juvenile Pacific cod (N = 354) caught in mixed gear-type summer surveys (1989–2019) were distributed primarily inshore throughout the GOA with some occurrences at shallower depths offshore on the continental shelf (Fig. 118). Settled early juvenile Pacific cod presence records from multiple surveys were combined in a habitat-related MaxEnt SDM predicting suitable habitat probabilities for this life stage in the GOA. The best model had a β-multiplier of 2.5 and an AUC of 0.95 (Table 43). Bottom depth accounted for 69.9% of covariate contribution to the deviance explained by the SDM (Table 44). The highest probabilities of suitable habitat for early juvenile Pacific cod in the GOA were predicted to occur in nearshore areas and around islands throughout the GOA (Fig. 119). The SD among k-folds as a result of cross-validation for the final SDM was generally higher at locations that were also predicted to have high probability of being suitable habitat for this life stage.

Subadult Pacific cod abundance and distribution predicted from RACE-GAP summer bottom trawl surveys in the Gulf of Alaska -- Subadult Pacific cod (N = 3,653) caught in GOA RACE-GAP summer bottom trawl surveys (1993–2019) were widely distributed across the GOA continental shelf throughout the survey area with concentrations of high abundance catches south of the Kenai

[27] Adding other high quality sources of data if available to future SDM ensemble EFH mapping for this species will be included as a research recommendation from the 2023 EFH 5-year Review.

Peninsula and west and off of southeast Alaska (Fig. 120). Five SDMs were considered for inclusion in the ensemble to predict numerical abundance of subadult Pacific cod in the GOA (Table 45); the GAM_{nb} was eliminated by skill testing. The four remaining SDMs had very similar RMSE and were weighted equally in the final ensemble, which attained a good fit to the observed subadult Pacific cod distribution and abundance data. The ensemble was good at predicting high and low abundance catches ($\rho = 0.53$) and at discriminating presence-absence (AUC = 0.79), and fair at explaining deviance (PDE = 0.30). Bottom depth, geographic location, and tidal currents provided the majority of covariate contribution (75.5%) to the deviance explained by the ensemble (Table 44). The highest subadult Pacific cod abundances were predicted west of the Kenai Peninsula on bathymetric rises in the central and western GOA, with hot spots on the banks south of Kodiak and the Shumagin islands (Fig. 121). Higher CV from cross-validating these predictions occurred in the glacial troughs and on the eastern GOA continental shelf. The probability of encountering subadult Pacific cod was high across the GOA continental shelf and low along the continental slope and in glacial troughs of the eastern GOA (Fig. 122).

Adult Pacific cod abundance and distribution predicted from RACE-GAP summer bottom trawl surveys in the Gulf of Alaska -- Adult Pacific cod (N = 4,476) were common and widely distributed across the GOA continental shelf throughout the survey area with most concentrations of high abundance catches south of the Kenai Peninsula and west (1993–2019; Fig. 123). Five SDMs were considered for inclusion in the ensemble to predict numerical abundance of adult Pacific cod in the GOA (Table 45); the GAM_P was eliminated by skill testing. The remaining four SDMs were nearly equally weighted in the final ensemble, which attained a good fit to the observed adult Pacific cod distribution and abundance data. The ensemble was good at predicting high and low abundance catches ($\rho = 0.47$) and at discriminating presence-absence (AUC = 0.75), and poor at explaining deviance (PDE = 0.25). Bottom depth, geographic location, and bottom temperature accounted for 78.1% of the covariate contribution to the deviance explained by the ensemble (Table 44). Adult Pacific cod abundance predicted from the ensemble was highest at depths less than 175 m on bathymetric rises west of the Kenai Peninsula (Fig. 124). The CV of ensemble predictions was high in the glacial troughs, along the continental slope, and in the eastern GOA. The probability of encountering adult Pacific cod was high across the continental shelf and low along the continental slope and glacial troughs in the eastern GOA (Fig. 125).

Essential fish habitat of three life stages of Pacific cod in the Gulf of Alaska -- Habitat-related predictions of Pacific cod life stage distribution and abundance from summer surveys of the GOA (mixed gear-type summer surveys (1989–2019) and RACE-GAP bottom trawl surveys (1993–2019)) were mapped as EFH areas and subareas (Fig. 126). Settled early juvenile Pacific cod EFH included nearshore areas and bathymetric rises on the continental shelf most prevalent in the central and western GOA. Core

EFH areas and EFH hot spots for settled early juveniles were generally associated with shallower nearshore areas and bathymetric rises. The EFH areas for subadult and adult Pacific cod extended from southeast Alaska to the western GOA. The core EFH area of subadults was more extensive at shallower depths on the continental shelf than for adults. EFH hot spots are most prominent on the continental shelf west of the Kenai Peninsula for both the subadult and adult life stages of Pacific cod. Pacific cod ontogenetic differences in depth distribution (e.g., Laurel et al. 2009, Pirtle et al. 2019) were reflected by the predicted EFH areas among life stages modeled, with the greatest difference between the early juveniles and older life stages.

Essential Fish Habitat Level 3 habitat-related vital rates of settled early juvenile Pacific cod in the Gulf of Alaska – Laboratory-reared early juvenile Pacific cod temperature-dependent growth rate is described by the following equation (Laurel et al. 2016):

$$GR = 0.2494 + 0.3216 * T - 0.0069 * T^2 - 0.0004 * T^3 \ ,$$

where *GR* is the growth rate (% body weight (g) per day (d)), and *T* is the temperature. The raster product of early juvenile Pacific cod predicted probability of suitable habitat from a MaxEnt SDM, and their temperature-dependent growth is an EFH Level 3 map of habitat-related growth potential (Fig. 127). The temperature of maximum growth for early juvenile Pacific cod is 11.5°C (Laurel et al. 2016), which was within the range (2.9–17.5°C) of the CGOA ROMS 3 km summer bottom temperature covariate raster (2000–2019) applied to the SDM and the EFH Level 3 map of habitat-related growth potential (Fig. 127). The bottom temperature range at settled early juvenile Pacific cod catch locations contributing to the SDM was 5.4–15.5°C (Fig. 118). In the map of temperature-dependent growth, the highest growth areas occurred inshore and along the coast, as well as on the banks and bathymetric rises on the GOA continental shelf (Fig. 127). The SDM of settled early juvenile stage Pacific cod suitable habitat limited areas of high predicted habitat-related growth potential (Fig. 127), notably to shallower depths, suggesting that temperature was not the only driver of distribution for this life stage in the GOA. EFH subareas of core EFH and hot spots corresponded with areas of high habitat-related growth potential for settled early juvenile stage Pacific cod, which added value in interpreting the EFH Level 1 map (Fig. 126).

Laboratory-reared early juvenile Pacific cod temperature-dependent lipid accumulation rate is described by the following equation (Copeman et al. 2017):

$$LAR = 6.77 \cdot exp\{-0.5 \cdot [(T_i - 10.00)/5.53]^2\} \ ,$$

where *LAR* is the lipid accumulation rate ($\%\, Lipid \cdot GR$) and *T* is the temperature. LAR is a measure of the ability of juvenile fish to accumulate lipid over time, which is an indicator of body condition. The

raster product of early juvenile Pacific cod predicted probability of suitable habitat and their temperature-dependent LAR is an EFH Level 3 map of habitat-related condition (Fig. 128). In the map of temperature-dependent LAR, the highest areas occurred inshore and along the coast, as well as on the banks and bathymetric rises on the GOA continental shelf (Fig. 128). The SDM of settled early juvenile stage Pacific cod suitable habitat limited areas of high predicted habitat-related condition in a similar pattern observed with habitat-related growth potential (Fig. 127). The EFH Level 3 maps are intended to add value in interpreting the EFH Level 1 map if settled early juvenile Pacific cod (Fig. 126). Additional research to groundtruth these relationships is needed. Mapping EFH at dynamic temporal scales will also help inform how species distributions shift as suitable habitat availability is altered due to climate change in the North Pacific region.

Table 43. -- Maximum entropy model (MaxEnt) used to construct Essential Fish Habitat (EFH) for settled early juvenile Pacific cod: regularization multiplier (β); *k*-fold cross-validation root-mean-square-error (RMSE), area under the receiver operating characteristic curve (AUC), and areal extent of EFH (km^2).

Model	**β**	**RMSE**	**AUC**	**EFH area (km^2)**
MaxEnt	2.5	112.90	0.95	124,800

Table 44. -- Covariates retained in the a) settled early juvenile habitat-related maximum entropy (MaxEnt) species distribution model (SDM), and b) subadult and c) adult SDM final ensembles for Pacific cod with the percent contribution of each covariate to the deviance explained by the SDMs and the cumulative deviance explained: SD = standard deviation and BPI = bathymetric position index.

Pacific cod			
	Covariate	**% Contribution**	**Cumulative %**
a) settled early juvenile	bottom depth	69.9	69.9
	aspect east	7.4	77.3
	BPI	5.9	83.2
	aspect north	5.2	88.5
	rockiness	3.9	92.4
	tidal maximum	3.2	95.6
	curvature	2.0	97.6
	bottom temperature	0.9	98.5
	coral presence	0.8	99.3
	sponge presence	0.7	100.0
b) subadult	bottom depth	56.2	56.2
	location	12.4	68.6
	tidal maximum	6.9	75.5
	bottom temperature	5.5	81.0
	slope	5.0	86.0
	rockiness	2.6	88.6
	aspect east	2.3	90.9
	current	2.2	93.1
	current SD	1.4	94.5
	aspect north	1.4	95.9
	BPI	1.3	97.2
	sponge presence	0.9	98.1
	curvature	0.9	99.0
	pennatulacean presence	0.7	99.7
	coral presence	0.3	100.0
c) adult	bottom depth	53.1	53.1
	location	15.6	68.7
	bottom temperature	9.4	78.1
	tidal maximum	5.7	83.7
	current	3.3	87.0
	BPI	2.9	89.9
	aspect east	2.6	92.5
	current SD	2.1	94.6
	slope	1.8	96.4
	rockiness	1.3	97.7

Pacific cod

Covariate	% Contribution	Cumulative %
sponge presence	1.1	98.8
aspect north	0.9	99.7
coral presence	0.1	99.8
pennatulacean presence	0.1	99.9
curvature	0.1	100.0

Table 45. -- Constituent species distribution models (SDMs) used to construct Essential Fish Habitat (EFH) for a) subadult and b) adult Pacific cod: MaxEnt = Maximum entropy; paGAM = presence-absence generalized additive model; hGAM = zero-adjusted Poisson hurdle GAM; GAM_P = standard Poisson GAM; GAM_{nb} = standard negative-binomial GAM; RMSE = root mean square error; ρ (*rho*) = Spearman's rank correlation coefficient; AUC = area under the receiver-operating characteristic curve; and PDE = Poisson deviance explained *. The "--" indicates that this model was not included in the final ensemble.

a) subadult Pacific cod

Models	RMSE	Relative Weight	ρ	AUC	PDE	EFH area (km^2)
MaxEnt	67.2	0.25	0.49	0.77	0.17	278,800
paGAM	67.2	0.25	0.55	0.80	0.17	258,800
hGAM	67.2	0.25	0.50	0.80	0.21	252,300
GAM_P	67.1	0.25	0.49	0.77	0.22	249,300
GAM_{nb}	67.1	0	--	--	--	--
ensemble	66.2	1	0.53	0.79	0.30	265,600

b) adult Pacific cod

Models	RMSE	Relative Weight	ρ	AUC	PDE	EFH area (km^2)
MaxEnt	71.6	0.25	0.45	0.75	0.05	272,800
paGAM	71.3	0.25	0.49	0.77	0.09	261,900
hGAM	71.1	0.25	0.40	0.77	0.18	257,500
GAM_P	71.1	--	--	--	--	--
GAM_{nb}	70.9	0.25	0.41	0.72	0.18	258,600
ensemble	70.2	1	0.47	0.75	0.25	264,700

* Refer to the Species Distribution Model Performance Metrics subsection within the Statistical Modeling section of the Methods for detailed descriptions of individual model performance metrics.

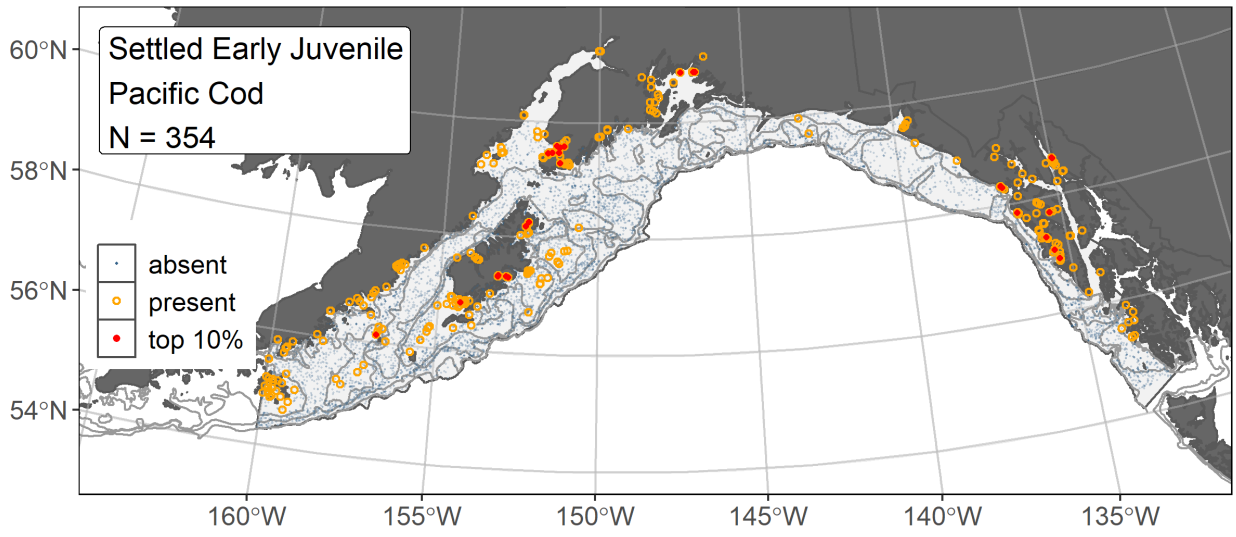

Figure 118. -- Distribution of settled early juvenile Pacific cod catches (N = 354) in mixed gear-type summer surveys of the Gulf of Alaska (1989–2019) with the 100 m, 200 m, and 700 m isobaths indicated; filled red circles indicate locations in top 10% of overall abundance, open orange circles indicate presence in remaining catches, and blue dots indicate stations sampled where the animals were not present.

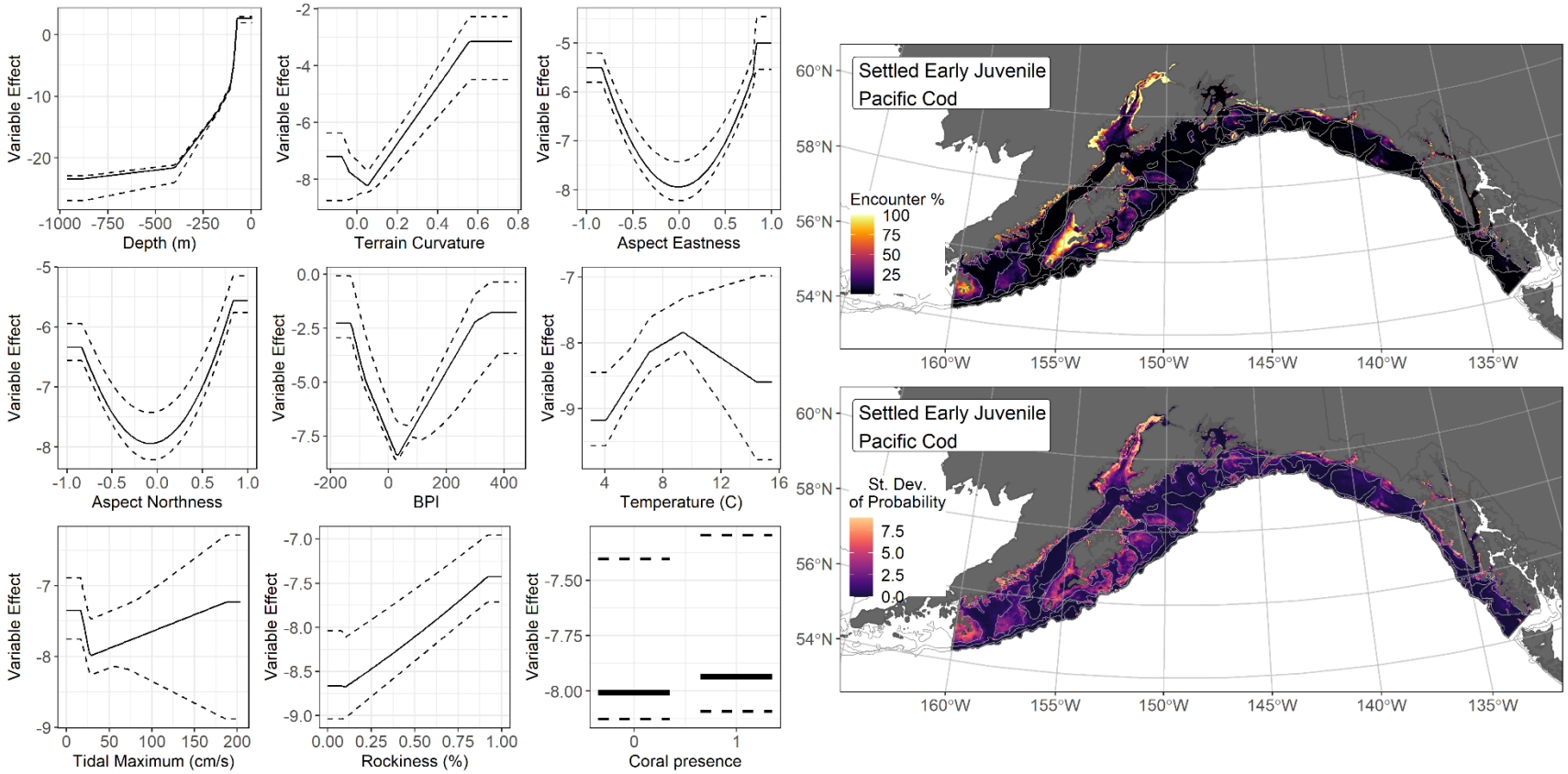

Figure 119. -- The top nine covariate effects (left panel) from a habitat-related species distribution model (MaxEnt) of settled early juvenile Pacific cod probability of suitable habitat in the Gulf of Alaska (upper right panel) with the standard deviation of the probability predictions (lower right panel).

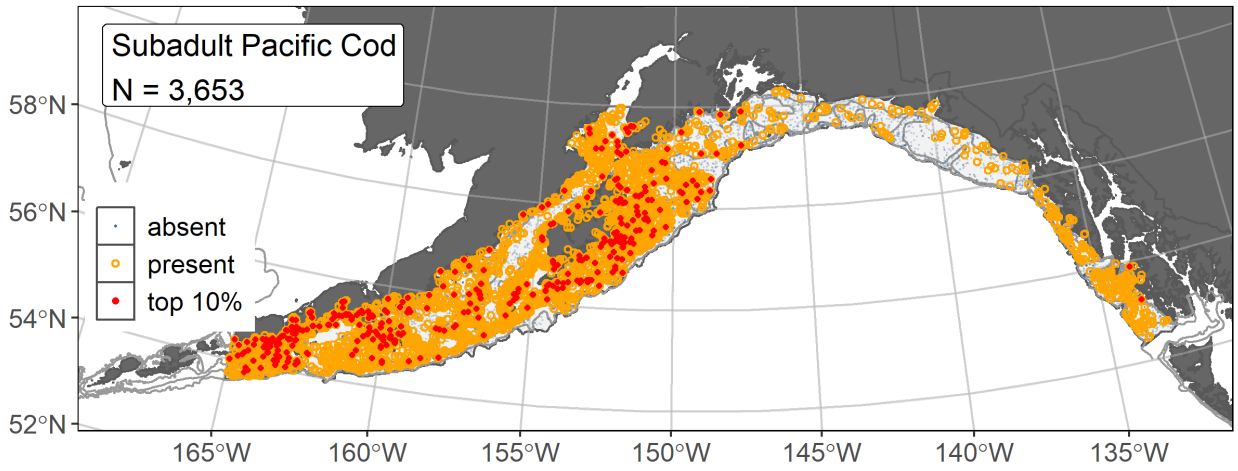

Figure 120. -- Distribution of subadult Pacific cod catches (N = 3,653) in 1993–2019 AFSC RACE-GAP summer bottom trawl surveys of the Gulf of Alaska with the 100 m, 200 m, and 700 m isobaths indicated; filled red circles indicate locations in top 10% of overall abundance, open orange circles indicate presence in remaining catches, and blue dots indicate stations sampled where the animals were not present.

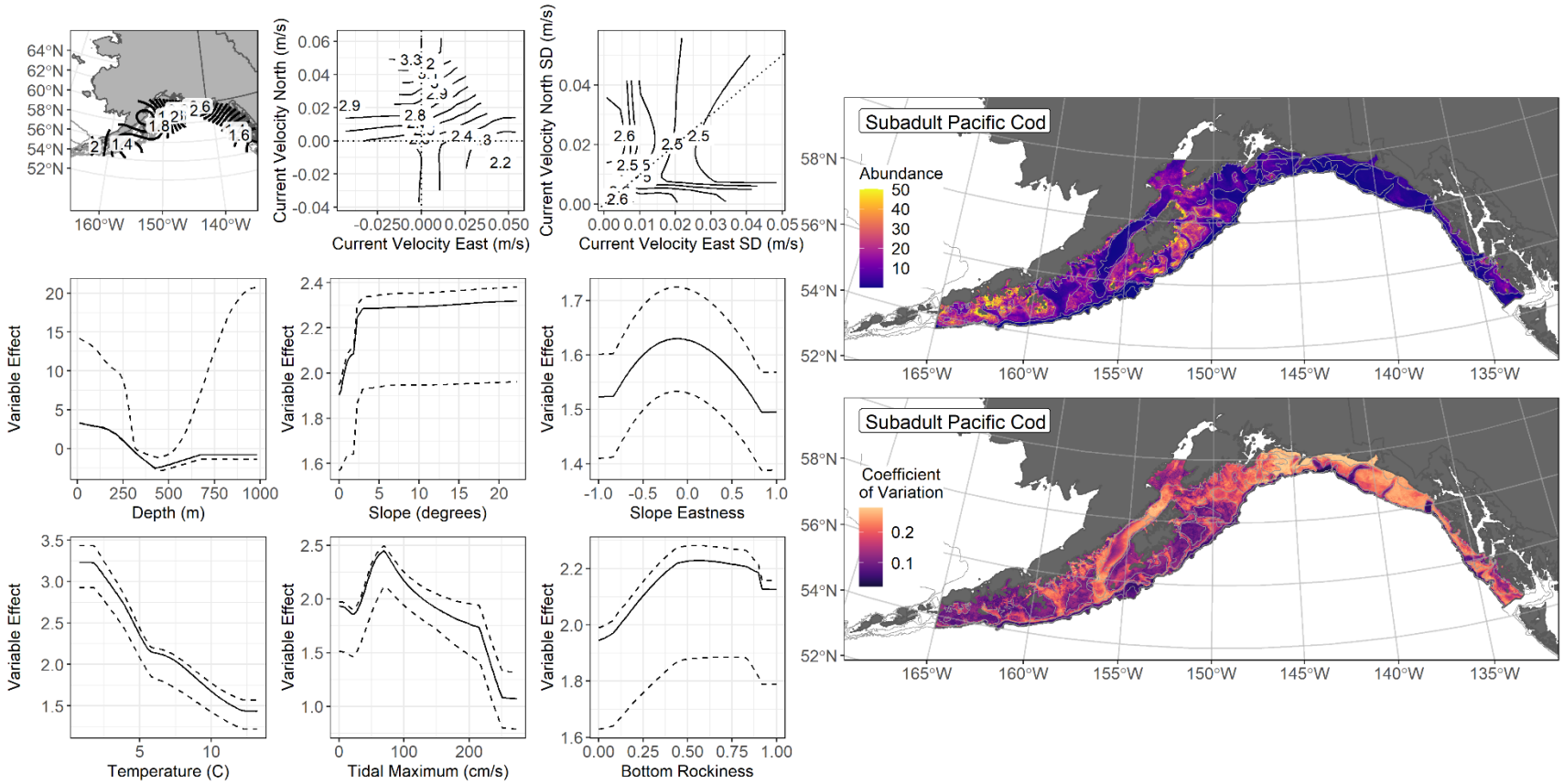

Figure 121. -- The top nine covariate effects (left panel) on ensemble-predicted subadult Pacific cod numerical abundance across the Gulf of Alaska (upper right panel) along with the coefficient of variation (CV) of the ensemble predictions (lower right panel).

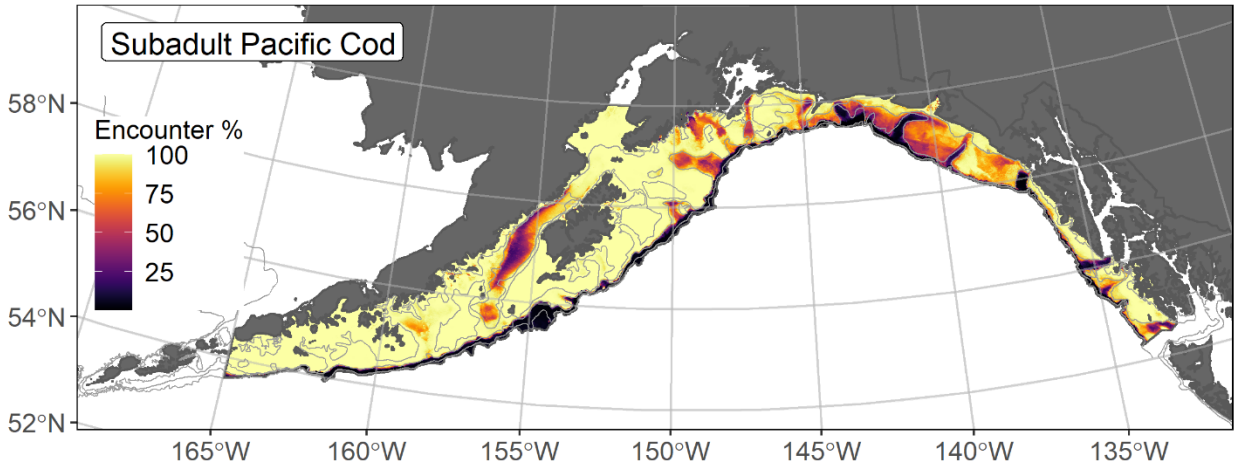

Figure 122. -- Encounter probability of subadult Pacific cod from AFSC RACE-GAP summer bottom trawl surveys (1993–2019) of the Gulf of Alaska with the 100 m, 200 m, and 700 m isobaths indicated.

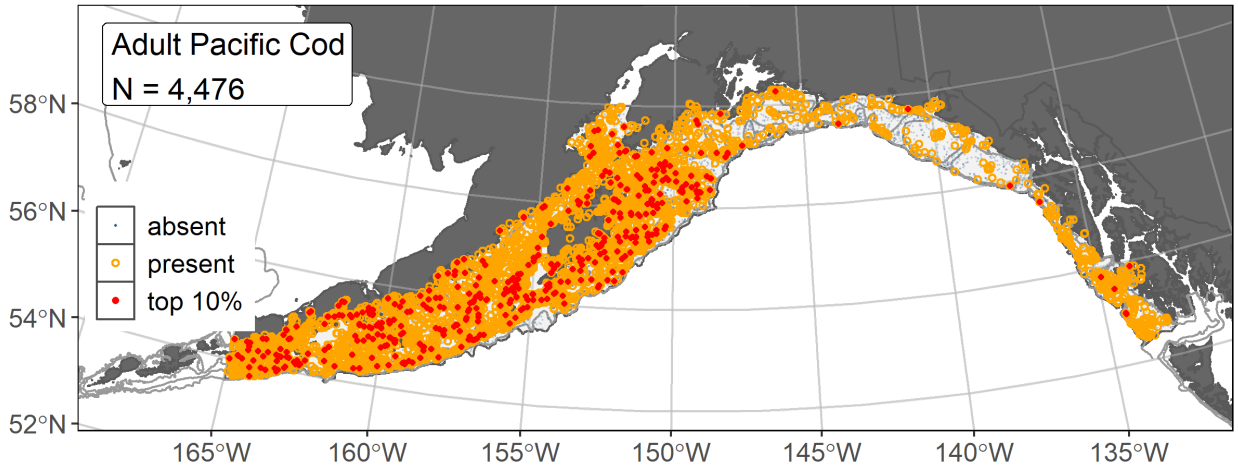

Figure 123. -- Distribution of adult Pacific cod catches (N = 4,476) in 1993–2019 AFSC RACE-GAP summer bottom trawl surveys of the Gulf of Alaska with the 100 m, 200 m, and 700 m isobaths indicated; filled red circles indicate locations in top 10% of overall abundance, open orange circles indicate presence in remaining catches, and blue dots indicate stations sampled where the animals were not present.

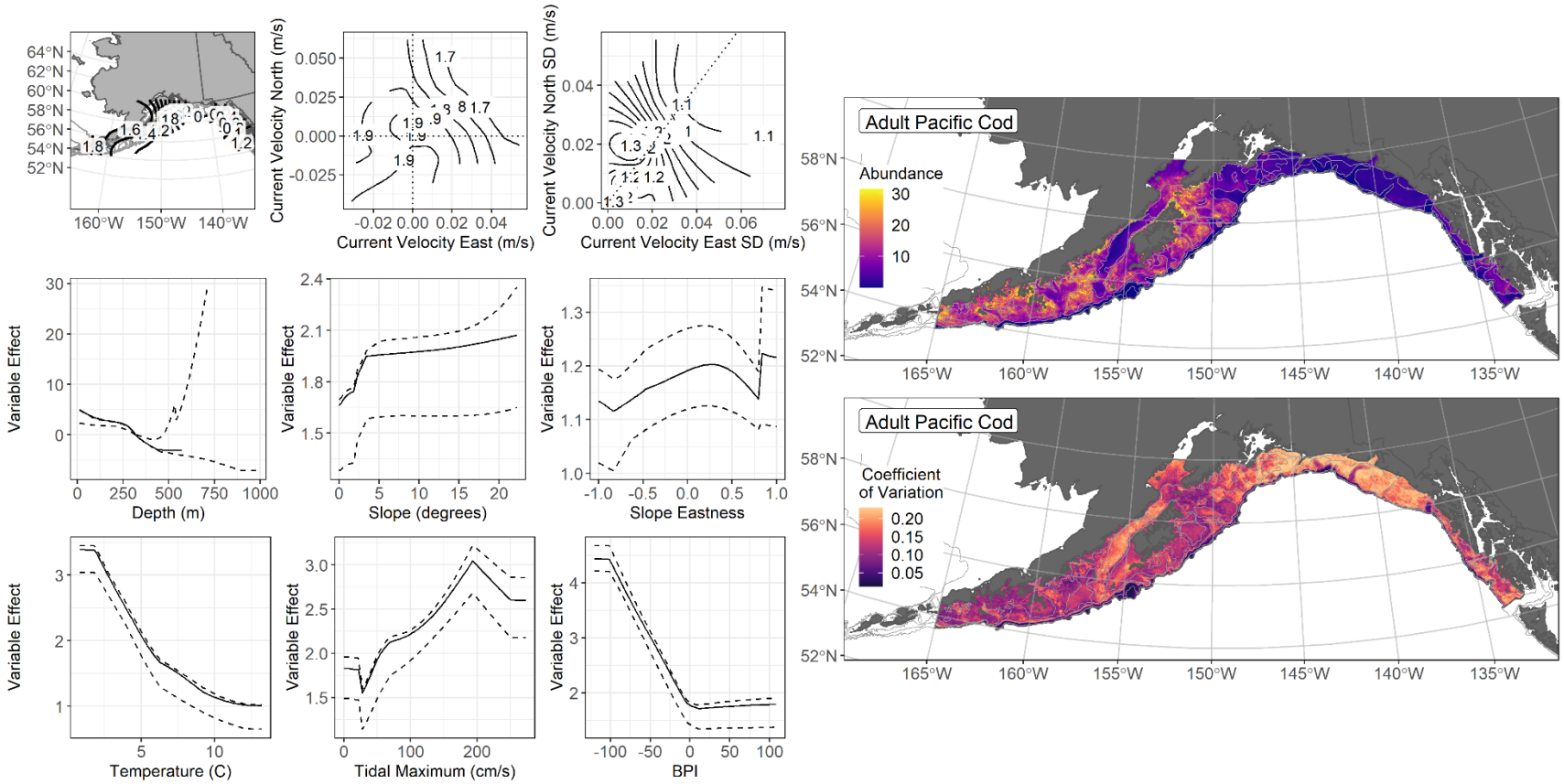

Figure 124. -- The top nine covariate effects (left panel) on ensemble-predicted adult Pacific cod numerical abundance across the Gulf of Alaska (upper right panel) along with the coefficient of variation (CV) of the ensemble predictions (lower right panel).

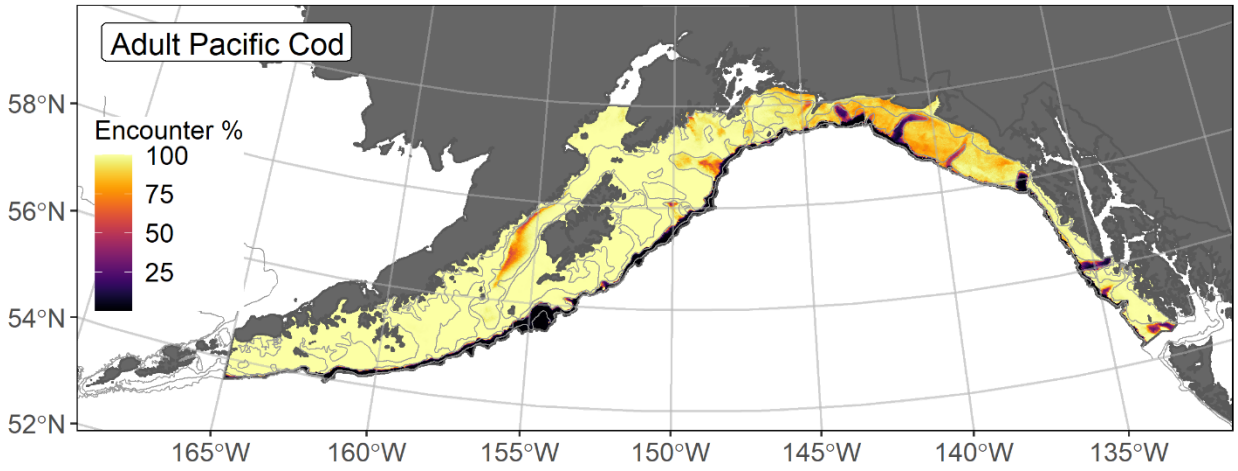

Figure 125. -- Encounter probability of adult Pacific cod from AFSC RACE-GAP summer bottom trawl surveys (1993–2019) of the Gulf of Alaska with the 100 m, 200 m, and 700 m isobaths indicated.

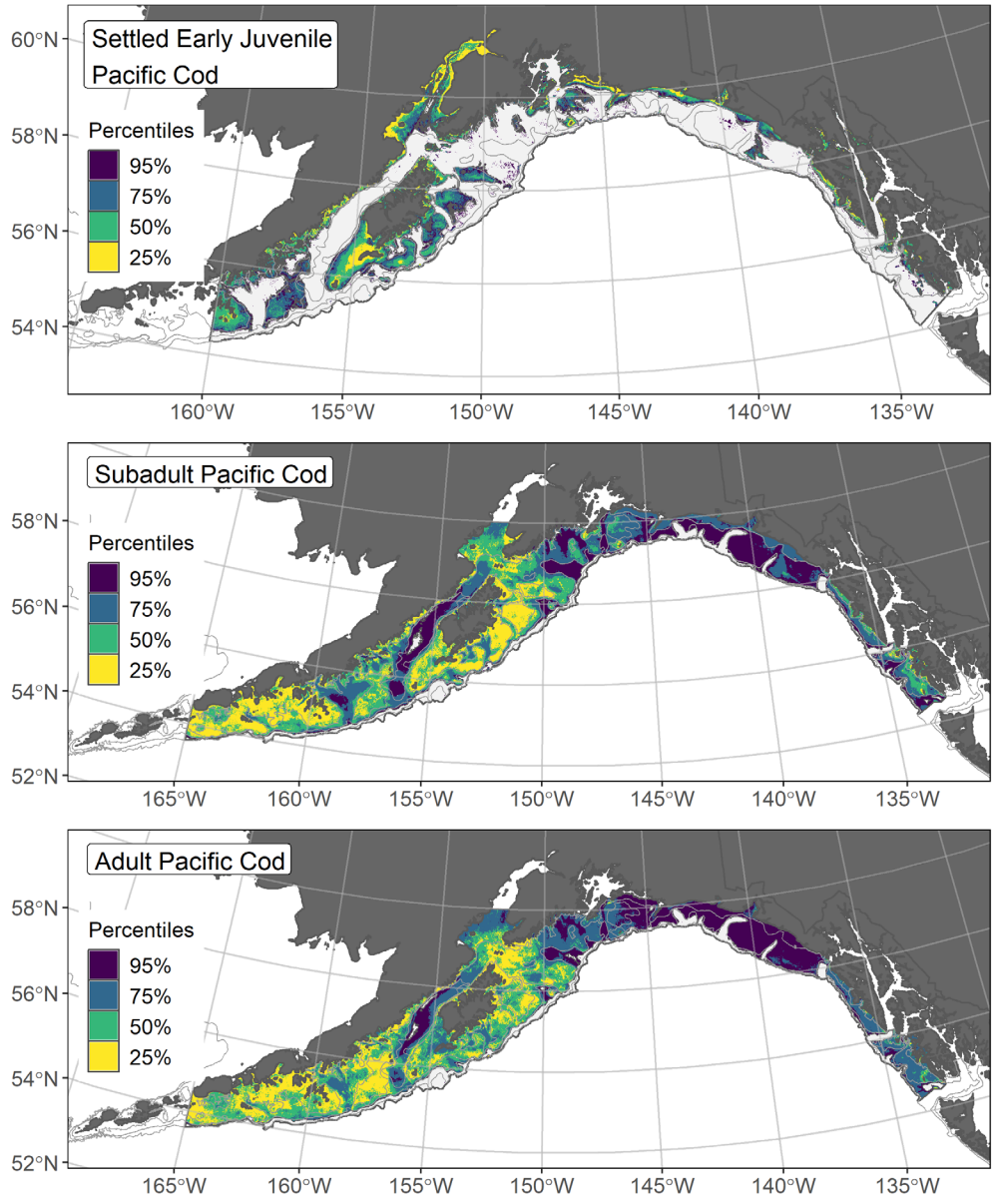

Figure 126. -- Essential fish habitat (EFH) is the area containing the top 95% of occupied habitat (defined as greater than 5% predicted probability of suitable habitat) for settled early juvenile (top panel) Pacific cod from an SDM fitted to their distribution in Gulf of Alaska (GOA) mixed gear-type summer surveys (1989–2019), and for subadults (middle panel) and adults (bottom panel) is the area containing the top 95% of occupied habitat (defined as model estimated encounter probabilities greater than 5%) from an SDM ensemble fitted to Pacific cod distribution and abundance in AFSC RACE-GAP GOA summer bottom trawl surveys (1993–2019) with 100 m, 200 m, and 700 m isobaths indicated; within the EFH area map are the subareas of the top 25% (EFH hot spots), top 50% (core EFH area), and top 75% (principal EFH area).

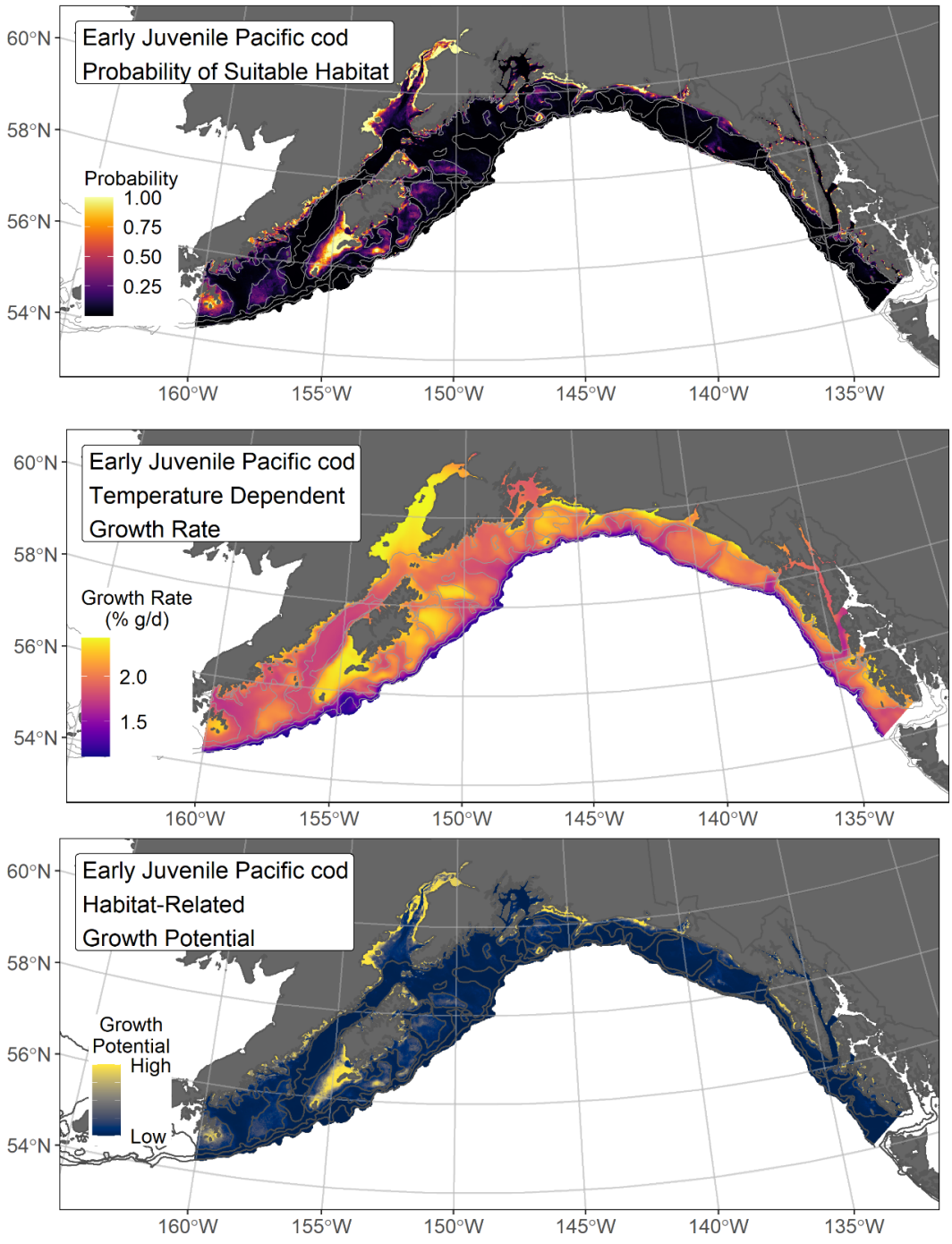

Figure 127. -- Settled early juvenile Pacific cod predicted probability of suitable habitat from a habitat-related species distribution model fitted to their distribution in Gulf of Alaska mixed gear-type summer surveys (1989–2019; top panel), temperature-dependent growth rate ($GR = \%\ body\ weight\ (g) \cdot day^{-1}$; center panel), and EFH Level 3 map of habitat-related growth potential (bottom panel), which is the raster product of probability of suitable habitat and temperature-dependent growth rate.

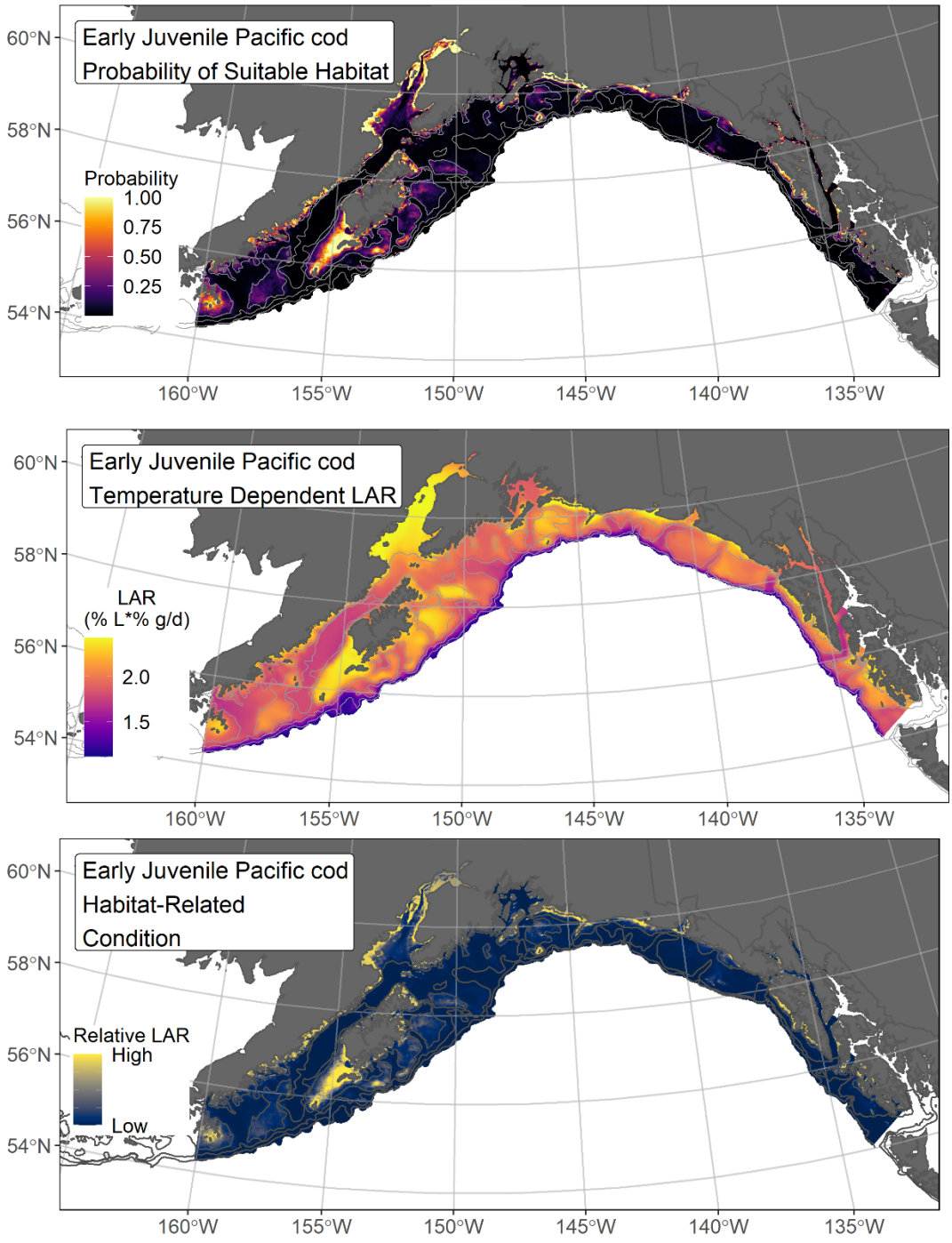

Figure 128. -- Settled early juvenile Pacific cod predicted probability of suitable habitat from a habitat-related species distribution model fitted to their distribution in Gulf of Alaska mixed gear-type summer surveys (1989–2019; top panel), temperature-dependent lipid accumulation rate ($LAR = \%\ lipid \cdot \%\ body\ weight\ (g) \cdot day^{-1}$; center panel), and EFH Level 3 map of habitat-related condition (relative LAR; bottom panel), which is the raster product of probability of suitable habitat and temperature-dependent LAR.

Sablefish (*Anoplopoma fimbria*)

Sablefish (*Anoplopoma fimbria*) support an important commercial fishery in Alaska, where they are assessed as a single stock in Federal waters due to their propensity for large-scale movements (Heifetz and Fujioka 1991, Goethel et al. 2020). Adult sablefish inhabit deeper depths between 200 and 1000 m, including deep fjords and glacial troughs on the continental shelf and along the shelf break and continental slope of the GOA (Mecklenburg et al. 2002). Spawning typically occurs in deeper waters (300–500 m) (Mason et al. 1983), with eggs developing at depth and larvae developing near the surface (Wing 1997). After a neustonic period moving inshore, early juveniles typically settle in nearshore bays (Brodeur and Pearcy 1986, Kendall and Matarese 1987, Rutecki and Varosi 1997). After overwintering in nearshore habitats, older juveniles migrate to deeper depths, reaching adult habitat in three to four years (Rutecki and Varosi 1997). For the EFH descriptions in this study, we separated the settled early juvenile (150–399 mm FL; Sasaki 1985, Pirtle et al. 2019), subadult (400–585 mm FL; Rodgveller et al. 2016, 2018), and adult life stages (> 585 mm) by length. The mesh size of the RACE-GAP bottom trawl is large enough that smaller life stages like those of the early juveniles and subadults may not be wholly retained in the catch. In addition, there is some evidence that adult sablefish may be able to avoid the trawl gear (Goethel et al. 2020). For these reasons, and because the AFSC longline surveys target adult sablefish (e.g., Siwicke et al. 2020, 2021), including longline survey data and other data sources with AFSC RACE-GAP summer bottom trawl survey data may improve future EFH mapping efforts for this species, however, doing so will require additional research[28].

Settled early juvenile sablefish distribution predicted from mixed gear-type summer surveys in the Gulf of Alaska -- Settled early juvenile sablefish (N = 959) caught in mixed gear-type summer surveys (1985–2020), using large and small mesh bottom trawls, purse and beach seines, and hook-and-line, were widely distributed across the GOA continental shelf with higher abundance concentrated inshore (Fig. 129). Settled early juvenile sablefish presence records from multiple surveys were combined in a habitat-related MaxEnt SDM predicting suitable habitat probabilities for this life stage. The best model had a β-multiplier of 3.0 and an AUC of 0.84 (Table 46). The covariates contributing the most (77%) to the deviance explained by the final SDM were tidal current speed, terrain aspect, bottom temperature, and terrain curvature (Table 47). The highest probabilities of suitable habitat for settled early juvenile sablefish were predicted to occur in nearshore areas (< 125 m depth) and also

[28] A recommendation from the stock author review to incorporate longline survey data in future SDM ensemble EFH mapping for this species will be included as a research recommendation from the 2023 EFH 5-year Review.

more extensively on the continental shelf of the eastern GOA (Fig. 130). The SD among k-folds as a result of cross-validation for the final SDM was relatively low across the study area.

Subadult sablefish abundance and distribution predicted from RACE-GAP summer bottom trawl surveys in the Gulf of Alaska -- Subadult sablefish (N = 2,812) caught in GOA RACE-GAP summer bottom trawl surveys (1993–2019) were distributed from southeast Alaska to the western GOA with concentrations in the glacial troughs on the continental shelf and along the shelf break and slope (Fig. 131). Five SDMs were considered for inclusion in the ensemble to predict numerical abundance of subadult sablefish in the GOA (Table 48); the GAM_{nb} was eliminated by skill testing. The four remaining best-performing SDMs had very similar RMSE and were weighted equally in the final ensemble, which attained a good fit to the observed subadult sablefish distribution and abundance data. The ensemble was good at predicting high and low abundance catches (ρ = 0.56) and discriminating presence-absence (AUC = 0.84), and fair at explaining deviance (PDE = 0.34). Bottom depth alone contributed 41.8% among covariates to the deviance explained by the ensemble, and bottom temperature and geographic location were also top contributors (Table 47). The highest subadult sablefish abundances were predicted to occur at > 250 m depth in the glacial troughs on the continental shelf, in particular from Shelikof Strait through the eastern GOA, and along the GOA shelf break and slope (Fig. 132). The CV of ensemble predictions was relatively even across the GOA study area. The probability of encountering subadult sablefish was highest in the deeper areas of the GOA continental shelf from Shelikof Strait east and along the outer shelf and slope (Fig. 133).

Adult sablefish abundance and distribution predicted from RACE-GAP summer bottom trawl surveys in the Gulf of Alaska -- Adult sablefish (N = 2,011) caught in GOA RACE-GAP summer bottom trawl surveys (1993–2019) were distributed from southeast Alaska to the western GOA with concentrations in the glacial troughs on the continental shelf and along the shelf break and slope (Fig. 134). Four of the five SDMs considered for inclusion in the ensemble to predict numerical abundance of adult sablefish in the GOA converged (Table 48); the GAM_{nb} was eliminated by skill testing. The remaining three best-performing SDMs were weighted by RMSE in the ensemble, which attained an excellent fit overall to the observed adult sablefish distribution and abundance data. The ensemble was excellent at predicting high and low abundance catches (ρ = 0.65) and discriminating presence-absence (AUC = 0.94), and good at explaining deviance (PDE = 0.61). Bottom depth, geographic location, and bottom current speed were the top contributing covariates (75.9%) to the deviance explained by the ensemble (Table 47). The highest adult sablefish abundances occurred at depths > 250 m in areas with relatively low bottom current exposure along the outer continental shelf and slope, with higher abundances also intruding into the seaward entrances of the glacial troughs (Fig. 135).

The CV of ensemble predictions was relatively high for adult sablefish and highest at deeper depths along the continental slope. Encounter probabilities for adult sablefish were high along the continental slope, outer shelf, and in the glacial troughs of the GOA (Fig. 136).

Essential Fish Habitat of three life stages of sablefish in the Gulf of Alaska -- Habitat-related predictions of sablefish life stage distribution and abundance from summer surveys of the GOA (mixed gear-type summer surveys (1985–2020) and RACE-GAP bottom trawl surveys (1993–2019)) were mapped as EFH areas and subareas (Fig. 137). EFH areas for all three sablefish life stages modeled was extensive from southeast Alaska to the western GOA. Early juvenile sablefish core EFH area occurred at shallower depths on the continental shelf, and EFH hot spots were concentrated in nearshore areas and along the shelf of the eastern GOA. EFH hot spots of subadults and adults occurred at deeper depths on the continental shelf and slope, particularly the glacial troughs on the shelf where adult EFH hots spots were better defined. Sablefish occupying progressively deeper depths offshore with age (e.g., Rutecki and Varosi 1997, Pirtle et al. 2019) was also apparent in the predicted EFH areas among life stages modeled, with the greatest difference between the early juveniles and older life stages.

Essential Fish Habitat Level 3 habitat-related vital rates of settled early juvenile sablefish in the Gulf of Alaska -- Temperature-dependent growth rate of laboratory reared early juvenile sablefish is described by the following equation (Krieger et al. 2019):

$$GR = 1.6034 + 0.3178 * T + 0.0138 * T^2 - 0.0008 * T^3 \ ,$$

where *GR* is the growth rate (% body weight (g) per day (d)), and *T* is the temperature. The raster product of early juvenile sablefish predicted probability of suitable habitat from a MaxEnt SDM and their temperature-dependent growth is an EFH Level 3 map of habitat-related growth potential (Fig. 138). The temperature of maximum growth for early juvenile sablefish is 15.1°C (Krieger et al. 2019), which was within the range (2.9–17.5°C) of the CGOA ROMS 3 km summer bottom temperature covariate raster (2000–2019) applied to the SDM and the EFH Level 3 map of habitat-related growth potential (Fig. 138). The bottom temperature range at settled early juvenile sablefish catch locations in the SDM was 4.5–12.1°C (Fig. 129). In the map of temperature-dependent growth, the highest growth areas occurred inshore and along the coast at the shallowest depths (Fig. 138). The SDM of settled early juvenile sablefish suitable habitat limited areas of high predicted habitat-related growth potential (Fig. 138), notably to shallower depths, suggesting that temperature was not the only driver of distribution for this life stage in the GOA.

Table 46. -- Maximum entropy model (MaxEnt) used to construct Essential Fish Habitat (EFH) for settled early juvenile sablefish: regularization multiplier (β); *k*-fold cross-validation root-mean-square-error (RMSE), area under the receiver operating characteristic curve (AUC), and areal extent of EFH (km^2).

Model	**β**	**RMSE**	**AUC**	**EFH area (km^2)**
MaxEnt	3.0	36.48	0.84	235,800

Table 47. -- Covariates retained in the a) settled early juvenile habitat-related maximum entropy (MaxEnt) species distribution model (SDM), and b) subadult and c) adult SDM final ensembles for sablefish with the percent contribution of each covariate to the deviance explained by the SDMs and the cumulative deviance explained: SD = standard deviation and BPI = bathymetric position index.

sablefish	**Covariate**	**% Contribution**	**Cumulative %**
a) settled early juvenile	tidal maximum	25.7	25.7
	aspect north	15.1	40.8
	bottom temperature	14.1	54.9
	curvature	12.7	67.6
	aspect east	9.2	76.8
	rockiness	7.2	84.0
	bottom depth	5.5	89.6
	BPI	4.9	94.4
	slope	4.2	98.6
	pennatulacean presence	1.0	99.6
	sponge presence	0.4	100.0
b) subadult	bottom depth	41.8	41.8
	bottom temperature	14.3	56.1
	location	11.1	67.2
	slope	7.7	74.9
	current SD	6.6	81.5
	current	5.5	87.0
	aspect north	3.1	90.1
	BPI	2.9	93.0
	rockiness	2.1	95.1
	aspect east	1.6	96.7
	sponge presence	1.5	98.2
	tidal maximum	1.2	99.4
	curvature	0.5	99.9
	coral presence	0.1	100.0
c) adult	bottom depth	36.6	36.6
	location	31.4	68.0
	current	7.9	75.9
	tidal maximum	6.6	82.5
	current SD	3.3	85.8
	aspect north	2.7	88.5
	bottom temperature	2.4	90.9
	pennatulacean presence	2.2	93.1
	aspect east	2.0	95.1
	rockiness	1.7	96.8

sablefish

Covariate	% Contribution	Cumulative %
BPI	1.3	98.1
slope	1.3	99.4
curvature	0.4	99.8
sponge presence	0.2	100.0

Table 48. -- Constituent species distribution models (SDMs) used to construct Essential Fish Habitat (EFH) for a) subadult and b) adult sablefish: MaxEnt = Maximum entropy; paGAM = presence-absence generalized additive model; hGAM = zero-adjusted Poisson hurdle GAM; GAM_P = standard Poisson GAM; GAM_{nb} = standard negative-binomial GAM; RMSE = root mean square error; ρ (*rho*) = Spearman's rank correlation coefficient; AUC = area under the receiver-operating characteristic curve; and PDE = Poisson deviance explained *. The "--" indicates that this model was not included in the final ensemble.

a) subadult sablefish

Models	**RMSE**	**Relative Weight**	**ρ**	**AUC**	**PDE**	**EFH area (km^2)**
MaxEnt	49.0	0.25	0.58	0.86	0.01	259,400
paGAM	48.8	0.25	0.58	0.86	0.13	281,300
hGAM	48.8	0.25	0.43	0.86	0.18	270,200
GAM_P	48.9	0.25	0.42	0.75	0.14	269,400
GAM_{nb}	49.0	0	--	--	--	--
ensemble	47.0	1	0.56	0.84	0.34	278,400

b) adult sablefish

Models	**RMSE**	**Relative Weight**	**ρ**	**AUC**	**PDE**	**EFH area (km^2)**
MaxEnt	--	--	--	--	--	--
paGAM	32.0	0.16	0.55	0.95	0.20	216,800
hGAM	19.4	0.43	0.65	0.95	0.58	192,600
GAM_P	19.8	0.41	0.64	0.93	0.55	229,800
GAM_{nb}	25.1	0	--	--	--	--
ensemble	18.9	1	0.65	0.94	0.61	216,700

* Refer to the Species Distribution Model Performance Metrics subsection within the Statistical Modeling section of the Methods for detailed descriptions of individual model performance metrics.

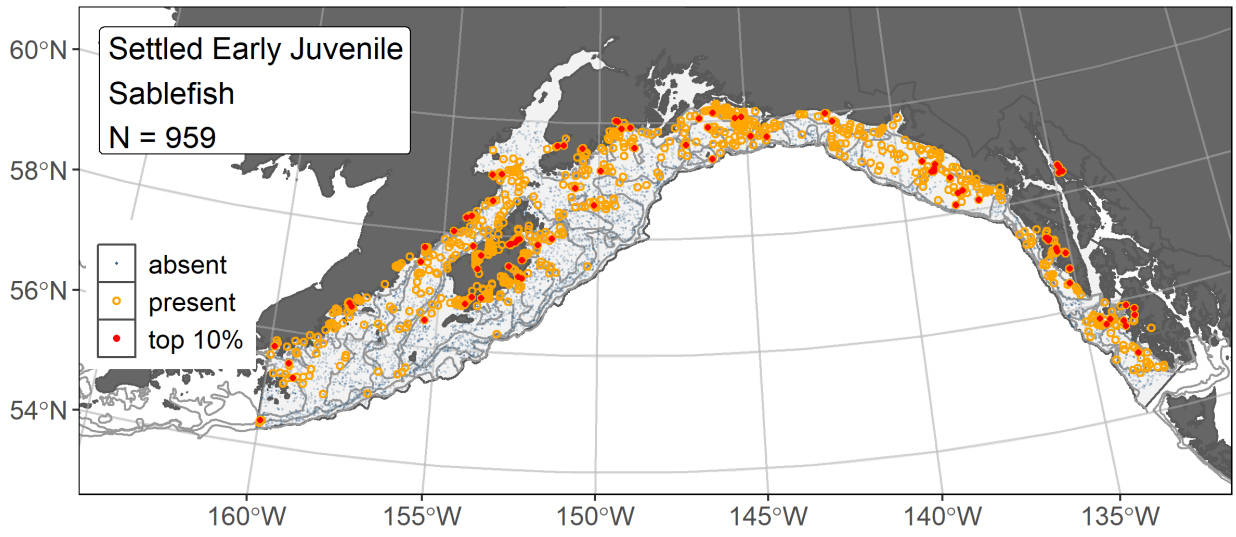

Figure 129. -- Distribution of settled early juvenile sablefish catches (N = 959) in mixed gear-type summer surveys of the Gulf of Alaska (1985–2020) with the 100 m, 200 m, and 700 m isobaths indicated; filled red circles indicate locations in top 10% of overall abundance, open orange circles indicate presence in remaining catches, and blue dots indicate stations sampled where the animals were not present.

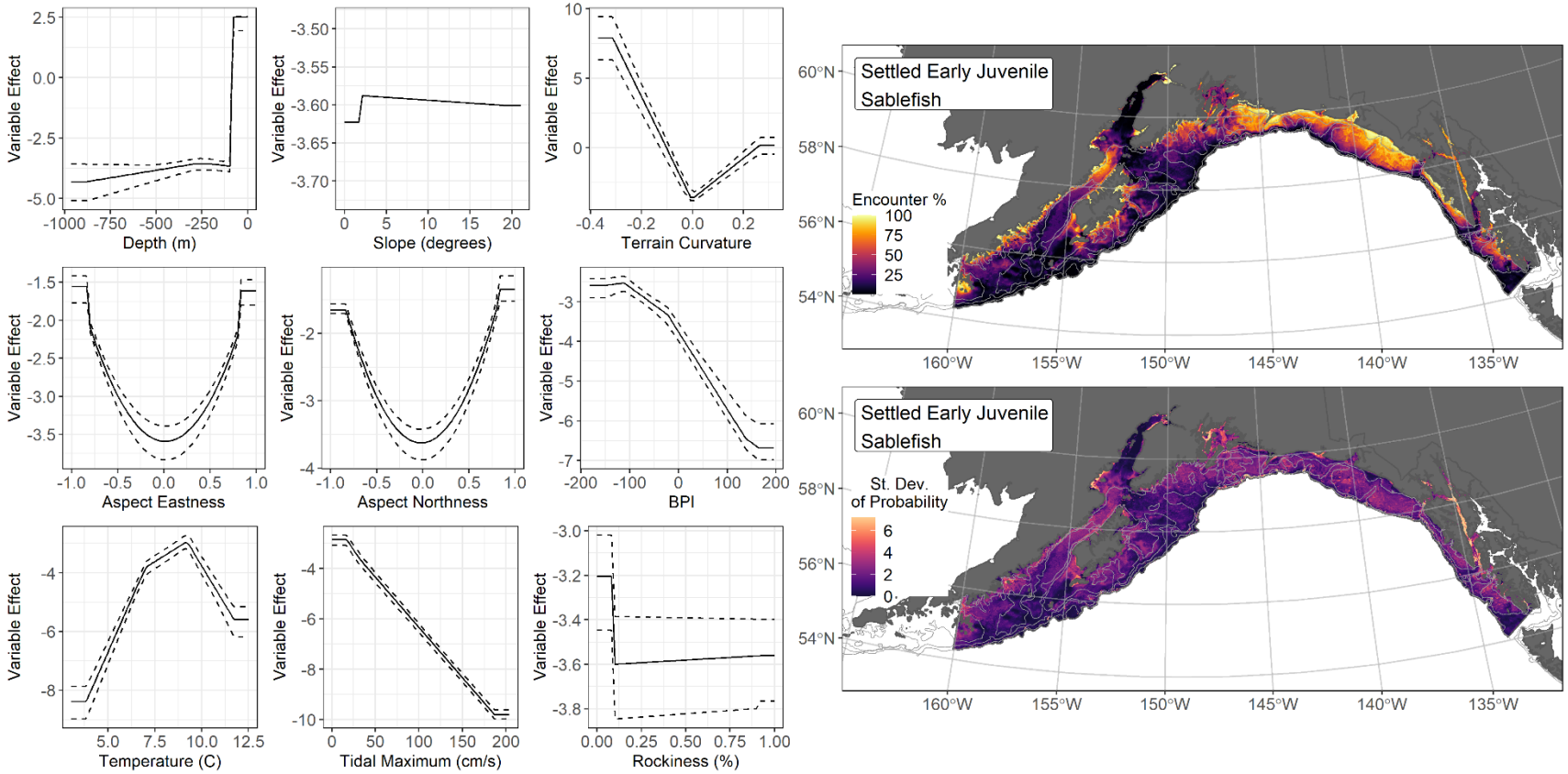

Figure 130. -- The top nine covariate effects (left panel) from a habitat-related species distribution model (MaxEnt) of settled early juvenile sablefish probability of suitable habitat in the Gulf of Alaska (upper right panel) with the standard deviation of the probability predictions (lower right panel).

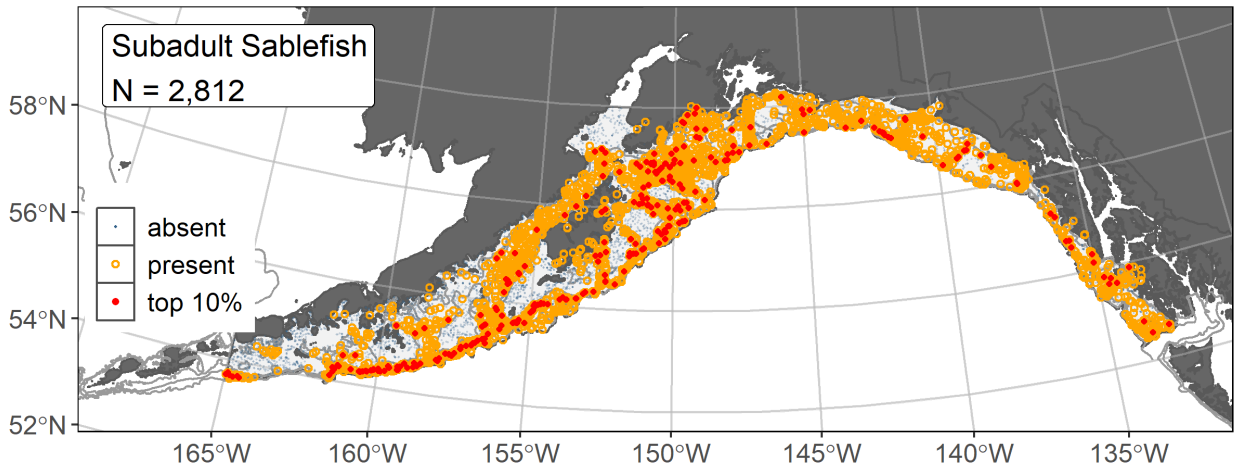

Figure 131. -- Distribution of subadult sablefish catches (N = 2,812) in 1993–2019 AFSC RACE-GAP summer bottom trawl surveys of the Gulf of Alaska with the 100 m, 200 m, and 700 m isobaths indicated; filled red circles indicate locations in top 10% of overall abundance, open orange circles indicate presence in remaining catches, and blue dots indicate stations sampled where the animals were not present.

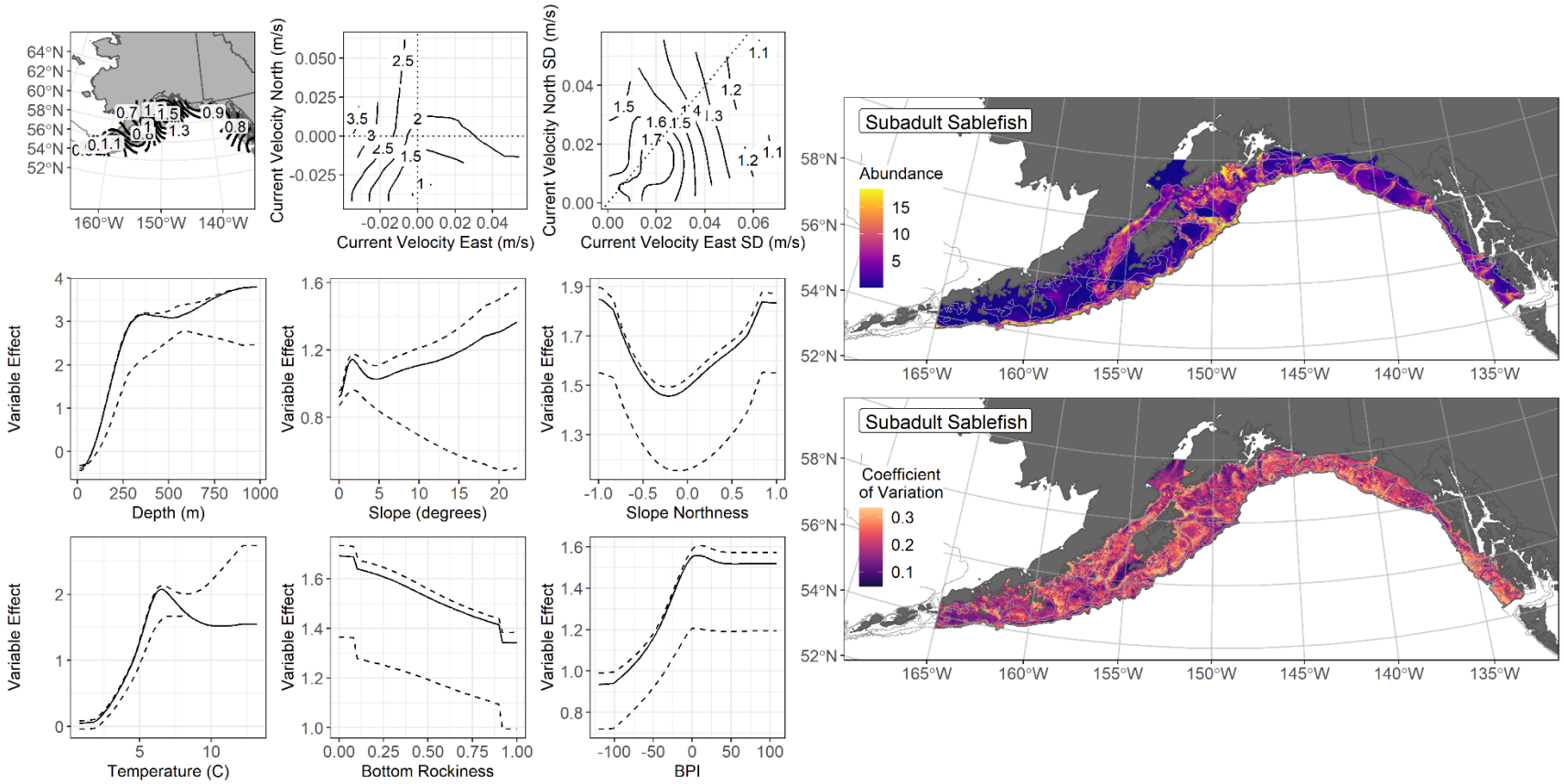

Figure 132. -- The top nine covariate effects (left panel) on ensemble-predicted subadult sablefish numerical abundance across the Gulf of Alaska (upper right panel) along with the coefficient of variation (CV) of the ensemble predictions (lower right panel).

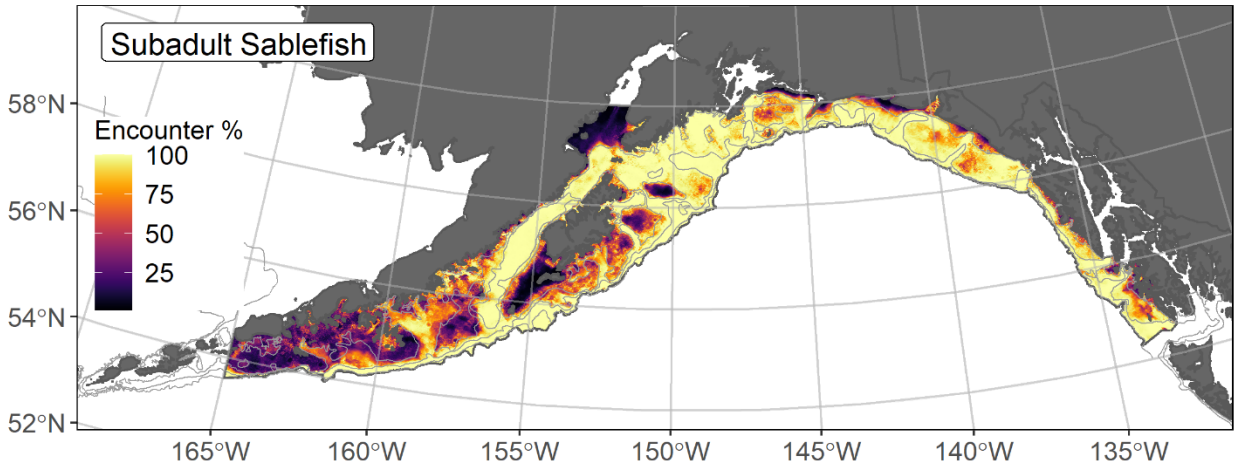

Figure 133. -- Encounter probability of subadult sablefish from AFSC RACE-GAP summer bottom trawl surveys (1993–2019) of the Gulf of Alaska with the 100 m, 200 m, and 700 m isobaths indicated.

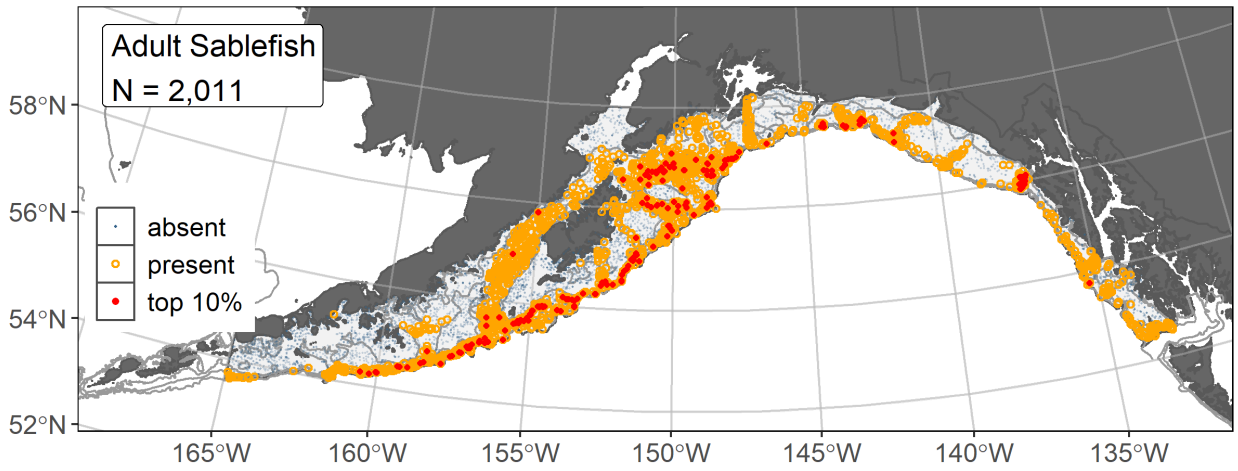

Figure 134. -- Distribution of adult sablefish catches (N = 2,011) in 1993–2019 AFSC RACE-GAP summer bottom trawl surveys of the Gulf of Alaska with the 100 m, 200 m, and 700 m isobaths indicated; filled red circles indicate locations in top 10% of overall abundance, open orange circles indicate presence in remaining catches, and blue dots indicate stations sampled where the animals were not present.

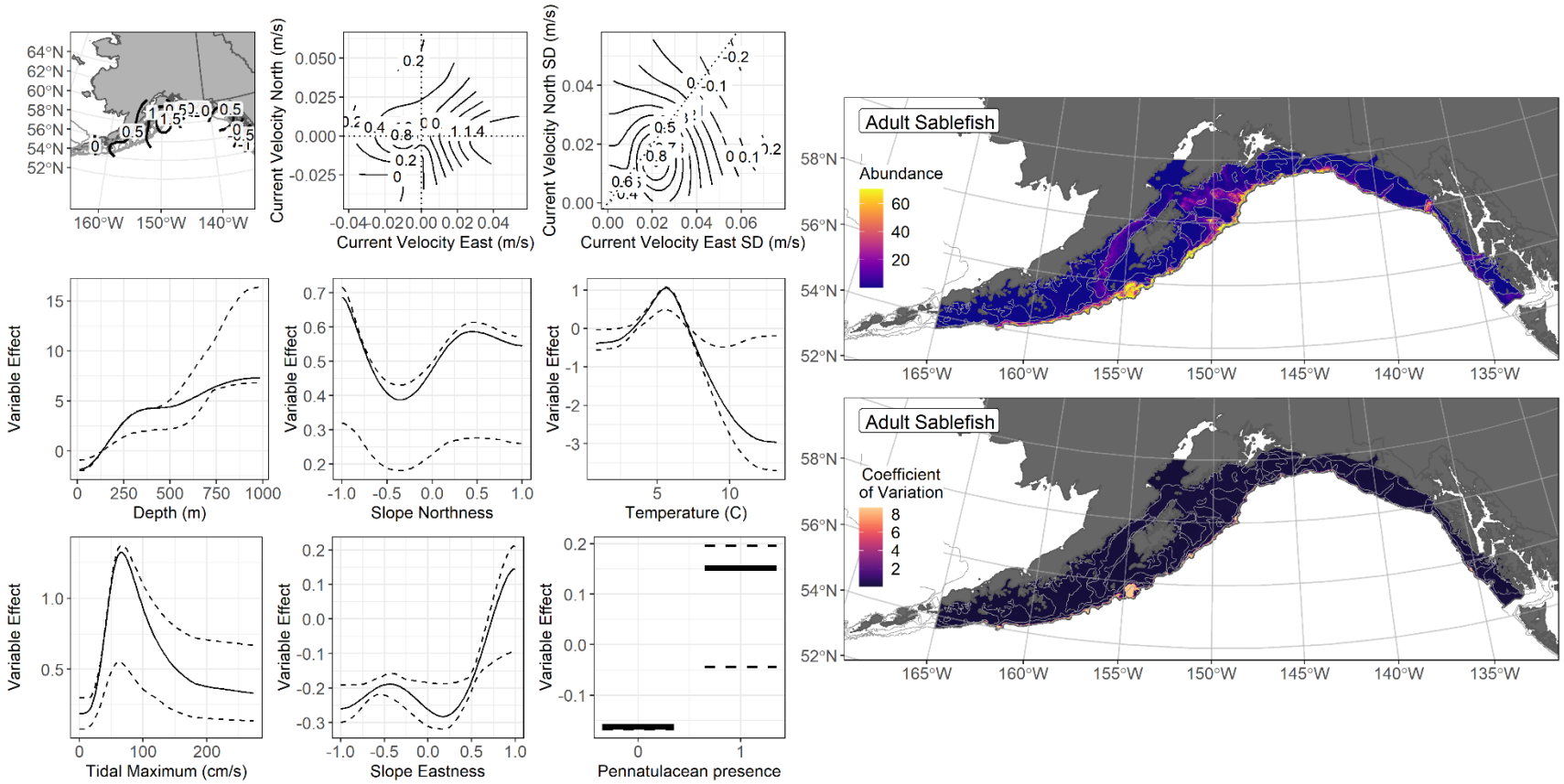

Figure 135. -- The top nine covariate effects (left panel) on ensemble-predicted adult sablefish numerical abundance across the Gulf of Alaska (upper right panel) along with the coefficient of variation (CV) of the ensemble predictions (lower right panel).

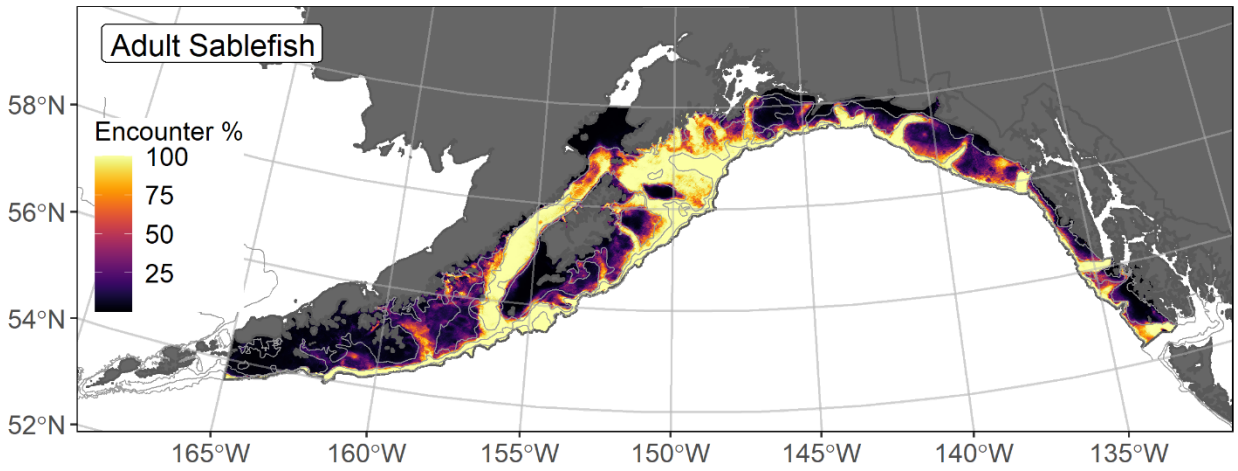

Figure 136. -- Encounter probability of adult sablefish from AFSC RACE-GAP summer bottom trawl surveys (1993–2019) of the Gulf of Alaska with the 100 m, 200 m, and 700 m isobaths indicated.

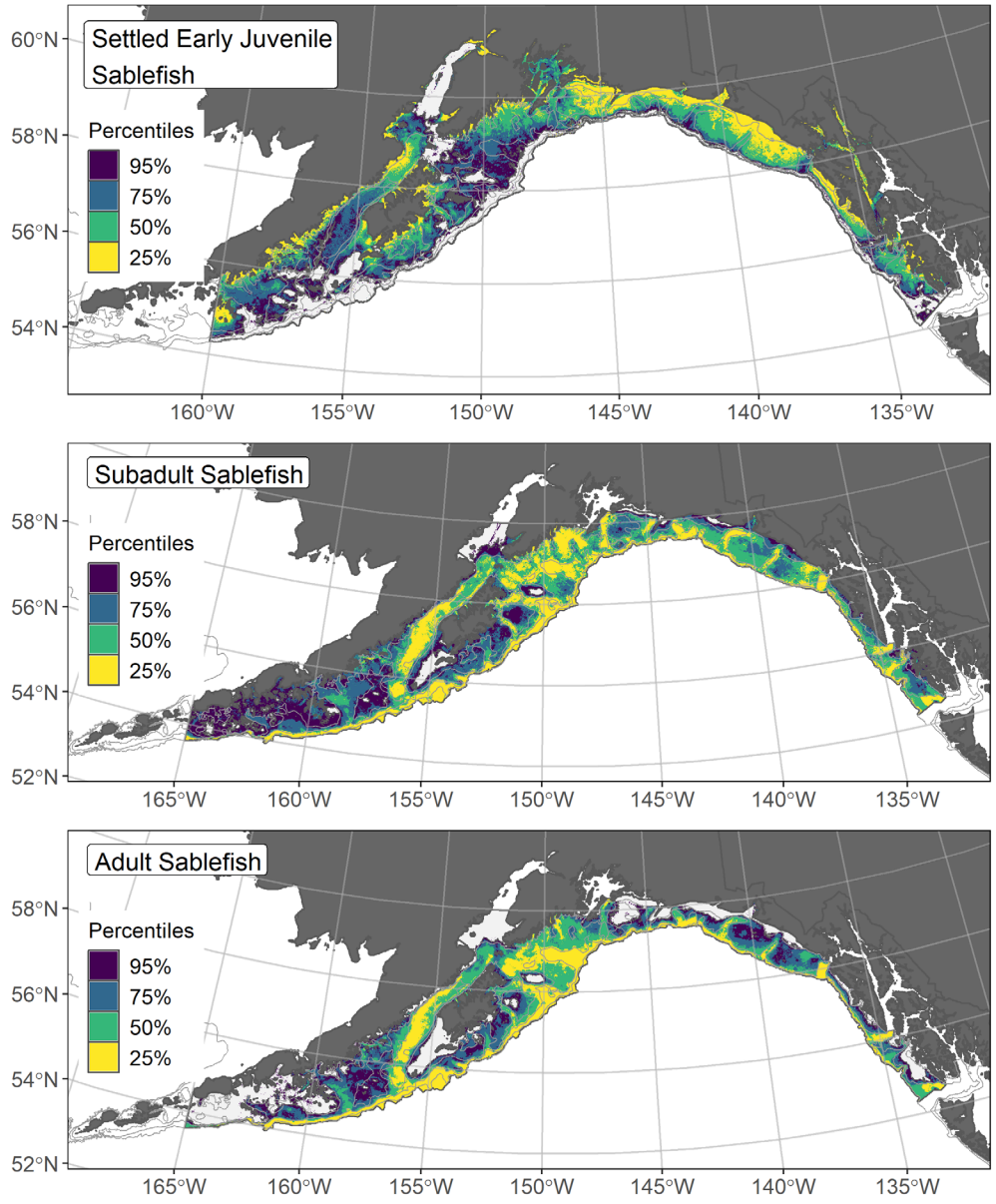

Figure 137. -- Essential fish habitat (EFH) is the area containing the top 95% of occupied habitat (defined as greater than 5% predicted probability of suitable habitat) for settled early juvenile (top panel) sablefish from an SDM fitted to their distribution in Gulf of Alaska (GOA) mixed gear-type summer surveys (1985–2020), and for subadults (middle panel) and adults (bottom panel) is the area containing the top 95% of occupied habitat (defined as model estimated encounter probabilities greater than 5%) from an SDM ensemble fitted to sablefish distribution and abundance in AFSC RACE-GAP GOA summer bottom trawl surveys (1993–2019) with 100 m, 200 m, and 700 m isobaths indicated; within the EFH area map are the subareas of the top 25% (EFH hot spots), top 50% (core EFH area), and top 75% (principal EFH area).

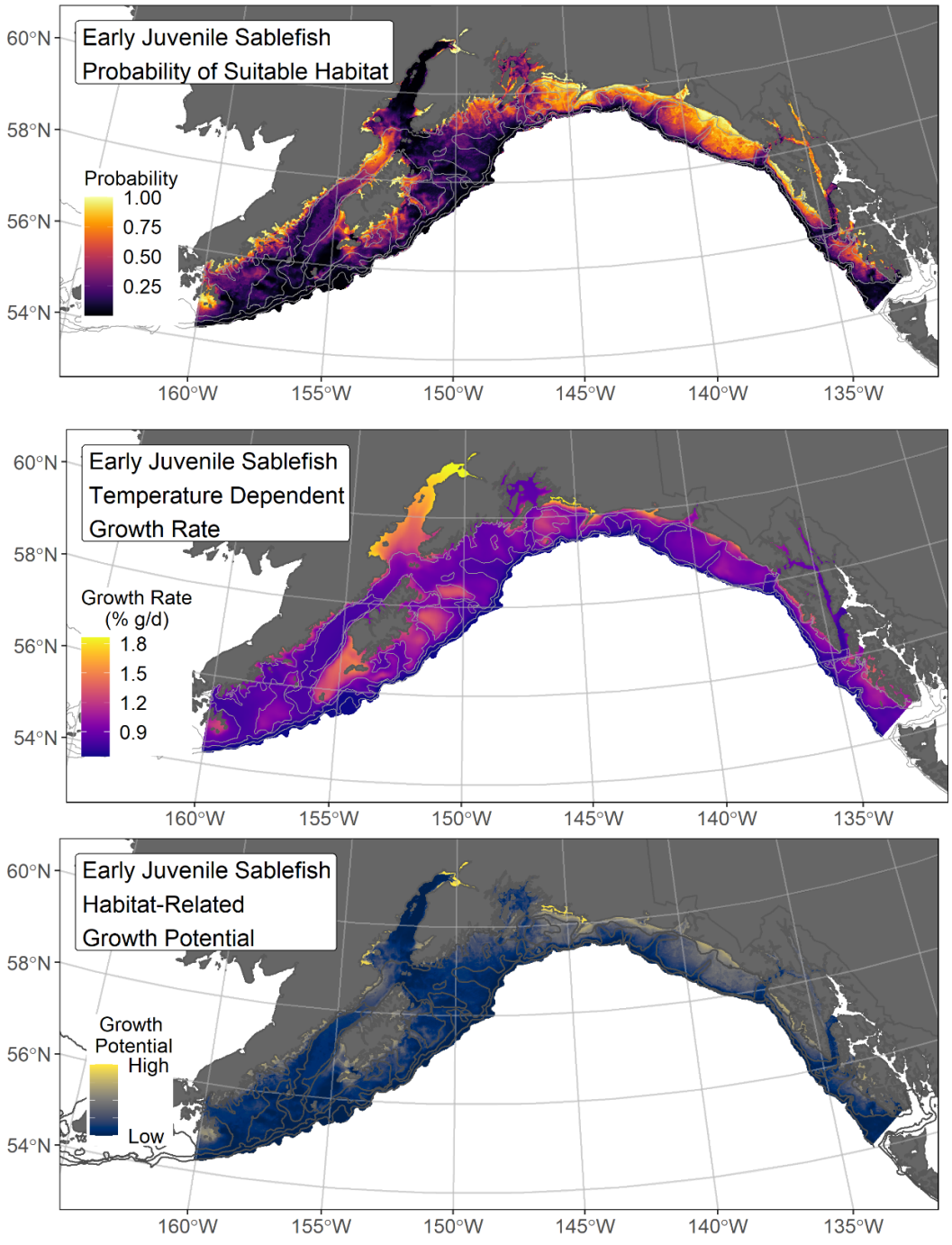

Figure 138. -- Settled early juvenile sablefish predicted probability of suitable habitat from a habitat-related species distribution model fitted to their distribution in Gulf of Alaska mixed gear-type summer surveys (1985–2020; top panel), temperature-dependent growth rate ($GR = \%\ body\ weight\ (g) \cdot day^{-1}$; center panel), and EFH Level 3 map of habitat-related growth potential (bottom panel), which is the raster product of probability of suitable habitat and temperature-dependent growth rate.

Walleye pollock (*Gadus chalcogrammus*)

Walleye pollock (*Gadus chalcogrammus*; hereafter referred to as pollock) is a semi-pelagic schooling fish widely distributed in the North Pacific Ocean. Pollock in the central and western GOA are managed as a single stock independently of pollock in the EBS, which is supported by analysis of spawning locations and larval drift patterns (Bailey et al. 1997, Dorn et al. 2020). Pollock are an ecologically important member of the groundfish community that support a shore-based commercial fishery in the GOA, using primarily pelagic trawls. Young-of-the-year pollock feed on plankton (Ciannelli et al. 2004) and provide forage for piscivores in the system (Yang and Livingston 1986, Barnes et al. 2020). Length-based life stage breaks distinguish between pollock settled early juveniles (40–140 mm FL) (Doyle et al. 2019, NFAA), subadults (141–410 mm FL), and adults (> 410 mm FL) (Williams
et al. 2016).

Settled early juvenile walleye pollock distribution predicted from mixed gear-type summer surveys in the Gulf of Alaska -- Settled early juvenile pollock (N = 2,958) caught in mixed gear-type summer surveys (1989–2019), using large and small mesh bottom trawls, purse and beach seines, were fairly common and widely distributed across the continental shelf throughout the GOA with higher abundance catches centered near Kodiak Island, Shelikof Strait, and the Shumagin Islands (Fig. 139). For these early juvenile pollock, presence records from multiple surveys were combined in a habitat-related MaxEnt SDM predicting suitable habitat probabilities for this life stage in the GOA. The best model had a β-multiplier of 3.0 and an AUC of 0.83 (Table 49). Bathymetric position index (BPI), bottom depth, and terrain aspect covariates contributed 71.2% to the deviance explained by the final SDM (Table 50). The highest probabilities of suitable habitat for early juvenile pollock in the GOA were predicted to occur < 125 m depth, inshore, and on the continental shelf (Fig. 140). Suitable habitat for this life stage included bathymetric lows (i.e., BPI lows) such as Shelikof Strait and to a lesser extent other glacial troughs on the GOA continental shelf. Relatively low SD among k-folds resulted from cross-validation for the final SDM.

Subadult walleye pollock abundance and distribution predicted from RACE-GAP summer bottom trawl surveys in the Gulf of Alaska -- Subadult pollock (N = 4,599) caught in GOA RACE-GAP summer bottom trawl surveys (1993–2019) were widely distributed across the study area (Fig. 141). Five SDMs were considered for inclusion in the ensemble to predict numerical abundance of subadult pollock in the GOA (Table 51); the GAM_{nb} was eliminated by skill testing. The remaining four best-performing SDMs had similar RMSE and were weighted nearly equally in the final ensemble, which attained a fair overall fit to the data. The ensemble was fair to good at predicting high and low abundance

catches (ρ = 0.41) and discriminating presence-absence (AUC = 0.70), and fair at explaining deviance (PDE = 0.21). Bottom depth, geographic location, and tidal current speed contributed 62.3% of the contribution among covariates to the deviance explained by the ensemble (Table 50). The highest subadult pollock abundances were predicted relatively inshore in the RACE-GAP GOA survey area (Fig. 142). The CV of ensemble predictions was relatively even across the GOA study area. The probability of encountering subadult pollock was higher across the GOA continental shelf and lower along the continental slope (Fig. 143).

Adult walleye pollock abundance and distribution predicted from RACE-GAP summer bottom trawl surveys in the Gulf of Alaska -- Adult pollock (N = 4,351) caught in GOA RACE-GAP summer bottom trawl surveys (1993–2019) were also widely distributed across the GOA study area with the highest abundance catches near Kodiak Island and west (Fig. 144). Adult catches were less evenly distributed across the GOA than subadult catches, with greater concentration in the glacial troughs. Five SDMs were considered for inclusion in the ensemble to predict numerical abundance of adult pollock in the GOA (Table 51); the GAM_{nb} was eliminated by skill testing. The remaining four best-performing SDMs were weighted by RMSE in the final ensemble, which attained a good fit overall to the observed adult pollock distribution and abundance data. The ensemble was good at predicting high and low abundance catches (ρ = 0.49) and discriminating presence-absence (AUC = 0.74), and fair at explaining deviance (PDE = 0.23). Bottom depth, geographic location, and rockiness accounted for 73.8% of the covariate contribution to the deviance explained by the ensemble (Table 50). Adult pollock abundance was predicted to be highest near 250 m depth in the glacial troughs (BPI lows), including Shelikof Strait (Fig. 145). The CV of ensemble predictions was higher in areas of predicted higher abundance. The probability of encountering adult pollock was high across the continental shelf and low along the continental slope (Fig. 146).

Essential Fish Habitat of three life stages of walleye pollock in the Gulf of Alaska -- Habitat-related predictions of pollock life stage distribution and abundance from summer surveys of the GOA (mixed gear-type summer surveys (1989–2019) and RACE-GAP bottom trawl surveys (1993–2019)) were mapped as EFH areas and additional subareas (Fig. 147). Settled early juvenile pollock EFH was extensive throughout the GOA continental shelf, excluding deeper depths. Core EFH areas and EFH hot spots for settled early juveniles increased inshore and were also prevalent in the glacial troughs. The EFH areas for subadult and adult pollock extended from southeast Alaska to the western GOA. The core EFH areas and EFH hot spots of subadults were shallower and extended further into southeast Alaska than did that of adults. For both the subadult and adult life stages of pollock, EFH hot spots were prominent in Shelikof Strait. However, adult EFH hot spots are better defined in the glacial troughs. The ontogenetic

migration of pollock to deeper depths over the continental shelf with greater size and age is apparent in the EFH maps.

Essential Fish Habitat Level 3 habitat-related vital rates of settled early juvenile walleye pollock in the Gulf of Alaska -- Laboratory reared early juvenile pollock temperature-dependent growth rate is described by the following equation (Laurel et al. 2016):

$$GR = 0.2023 + 0.0992 * T + 0.0335 * T^2 - 0.0019 * T^3 \ ,$$

where *GR* is the growth rate (% body weight (g) per day (d)), and *T* is the temperature. The raster product of early juvenile pollock predicted probability of suitable habitat from a MaxEnt SDM and their temperature-dependent growth is an EFH Level 3 map of habitat-related growth potential (Fig. 148). The temperature of maximum growth for early juvenile pollock is 13.0°C (Laurel et al. 2016), which is within the range (2.9–17.5°C) of the CGOA ROMS 3 km summer bottom temperature covariate raster (2000–2019) applied to the SDM and the EFH Level 3 map of habitat-related growth potential (Fig. 10). The bottom temperature range at settled early juvenile pollock catch locations contributing to the SDM was 3.0–12.5°C (Fig. 139). In the map of temperature-dependent growth, the highest growth areas occurred inshore and along the coast, as well as in the glacial troughs on the GOA continental shelf, such as Shelikof Strait (Fig. 148). The SDM of settled early juvenile stage walleye pollock suitable habitat somewhat limited the spatial extent of areas of high predicted habitat-related growth potential (Fig. 148), notably to inshore areas, although Shelikof Strait and the continental shelf off some of the major river systems in the central and eastern GOA remain, suggesting that temperature was not the only driver of distribution for this life stage in the GOA. Areas of EFH hot spots correspond with areas of high predicted habitat-related growth potential for settled early juvenile stage pollock, which added value in interpreting the EFH Level 1 map (Fig. 147).

Laboratory-reared early juvenile pollock temperature-dependent lipid accumulation rate is described by the following equation (Copeman et al. 2017):

$$LAR = 11.60 \cdot exp\{-0.5 \cdot [(\mathrm{T_i} - 14.37)/6.39]^2\} \ ,$$

where *LAR* is the lipid accumulation rate (*% Lipid · GR*) and *T* is the temperature. LAR is a measure of the ability of juvenile fish to accumulate lipid over time, which is an indicator of body condition. The raster product of early juvenile pollock predicted probability of suitable habitat and their temperature-dependent LAR is an EFH Level 3 map of habitat-related condition (Fig. 149). In the map of temperature-dependent LAR, the highest areas occurred inshore and along the coast, as well as in the glacial troughs on the GOA continental shelf, such as Shelikof Strait (Fig. 149), similar to the pattern observed with

growth potential. The EFH Level 3 maps are intended to add value in interpreting the EFH Level 1 map of settled early juvenile pollock (Fig. 147). Additional research to groundtruth these relationships is needed. Mapping EFH at dynamic temporal scales will also help inform how species distributions shift as suitable habitat availability is altered due to climate change in the North Pacific region.

Table 49. -- Maximum entropy model (MaxEnt) used to construct Essential Fish Habitat (EFH) for settled early juvenile walleye pollock: regularization multiplier (β); *k*-fold cross-validation root-mean-square-error (RMSE), area under the receiver operating characteristic curve (AUC), and areal extent of EFH (km^2).

Model	**β**	**RMSE**	**AUC**	**EFH area (km^2)**
MaxEnt	3.0	819.12	0.82	254,200

Table 50. -- Covariates retained in the a) settled early juvenile habitat-related maximum entropy (MaxEnt) species distribution model (SDM), and b) subadult and c) adult SDM final ensembles for walleye pollock with the percent contribution of each covariate to the deviance explained by the SDMs and the cumulative deviance explained: SD = standard deviation and BPI = bathymetric position index.

walleye pollock	**Covariate**	**% Contribution**	**Cumulative %**
a) settled early juvenile	BPI	26.1	26.1
	bottom depth	18.8	45.0
	aspect east	13.9	58.9
	aspect north	13.1	72.0
	tidal maximum	9.0	80.9
	rockiness	7.5	88.5
	bottom temperature	4.8	93.2
	pennatulacean presence	3.8	97.0
	curvature	1.4	98.5
	sponge presence	1.1	99.6
	slope	0.4	100.0
b) subadult	bottom depth	35.4	35.4
	location	16.6	52.0
	tidal maximum	10.3	62.3
	BPI	8.8	71.1
	current	5.2	76.4
	curvature	5.2	81.6
	current SD	5.0	86.6
	bottom temperature	3.9	90.5
	slope	3.4	93.9
	rockiness	3.1	97.0
	sponge presence	1.0	98.0
	aspect east	0.7	98.7
	pennatulacean presence	0.7	99.4
	aspect north	0.4	99.8
	coral presence	0.2	100.0
c) adult	bottom depth	34.9	34.9
	location	30.0	64.8
	rockiness	9.0	73.8
	BPI	7.2	81.0
	current	5.3	86.3
	current SD	2.7	89.0
	tidal maximum	2.6	91.6
	slope	2.0	93.6
	sponge presence	1.7	95.3

walleye pollock

Covariate	% Contribution	Cumulative %
aspect east	1.2	96.5
curvature	1.1	97.6
aspect north	1.0	98.6
bottom temperature	0.8	99.4
coral presence	0.5	99.9
pennatulacean presence	0.1	100.0

Table 51. -- Constituent species distribution models (SDMs) used to construct Essential Fish Habitat (EFH) for a) subadult and b) adult walleye pollock: MaxEnt = Maximum entropy; paGAM = presence-absence generalized additive model; hGAM = zero-adjusted Poisson hurdle GAM; GAM_P = standard Poisson GAM; GAM_{nb} = standard negative-binomial GAM; RMSE = root mean square error; ρ (*rho*) = Spearman's rank correlation coefficient; AUC = area under the receiver-operating characteristic curve; and PDE = Poisson deviance explained *. The "--" indicates that this model was not included in the final ensemble.

a) subadult walleye pollock

Models	**RMSE**	**Relative Weight**	**ρ**	**AUC**	**PDE**	**EFH area (km^2)**
MaxEnt	309.2	0.24	0.45	0.75	0.01	275,000
paGAM	305.2	0.25	0.46	0.75	0.01	281,800
hGAM	305.0	0.25	0.24	0.75	0.05	271,000
GAM_P	305.1	0.25	0.26	0.62	0.05	271,000
GAM_{nb}	306.3	0	--	--	--	--
ensemble	298.1	1	0.40	0.70	0.21	281,700

b) adult walleye pollock

Models	**RMSE**	**Relative Weight**	**ρ**	**AUC**	**PDE**	**EFH area (km^2)**
MaxEnt	387.1	0.11	0.55	0.80	0.25	277,400
paGAM	243.1	0.28	0.56	0.81	0.02	281,800
hGAM	235.9	0.30	0.33	0.81	0.20	278,500
GAM_P	236.7	0.30	0.30	0.63	0.19	265,900
GAM_{nb}	241.6	0	--	--	--	--
ensemble	237.4	1	0.49	0.74	0.23	281,800

* Refer to the Species Distribution Model Performance Metrics subsection within the Statistical Modeling section of the Methods for detailed descriptions of individual model performance metrics.

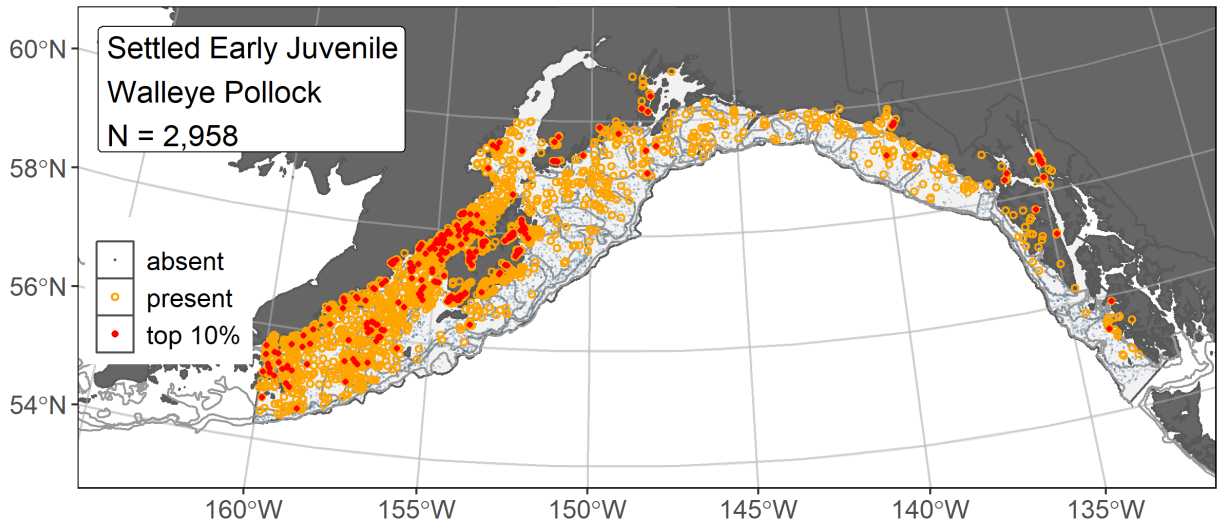

Figure 139. -- Distribution of settled early juvenile walleye pollock catches (N = 2,958) in mixed gear-type summer surveys of the Gulf of Alaska (1989–2019) with the 100 m, 200 m, and 700 m isobaths indicated; filled red circles indicate locations in top 10% of overall abundance, open orange circles indicate presence in remaining catches, and blue dots indicate stations sampled where the animals were not present.

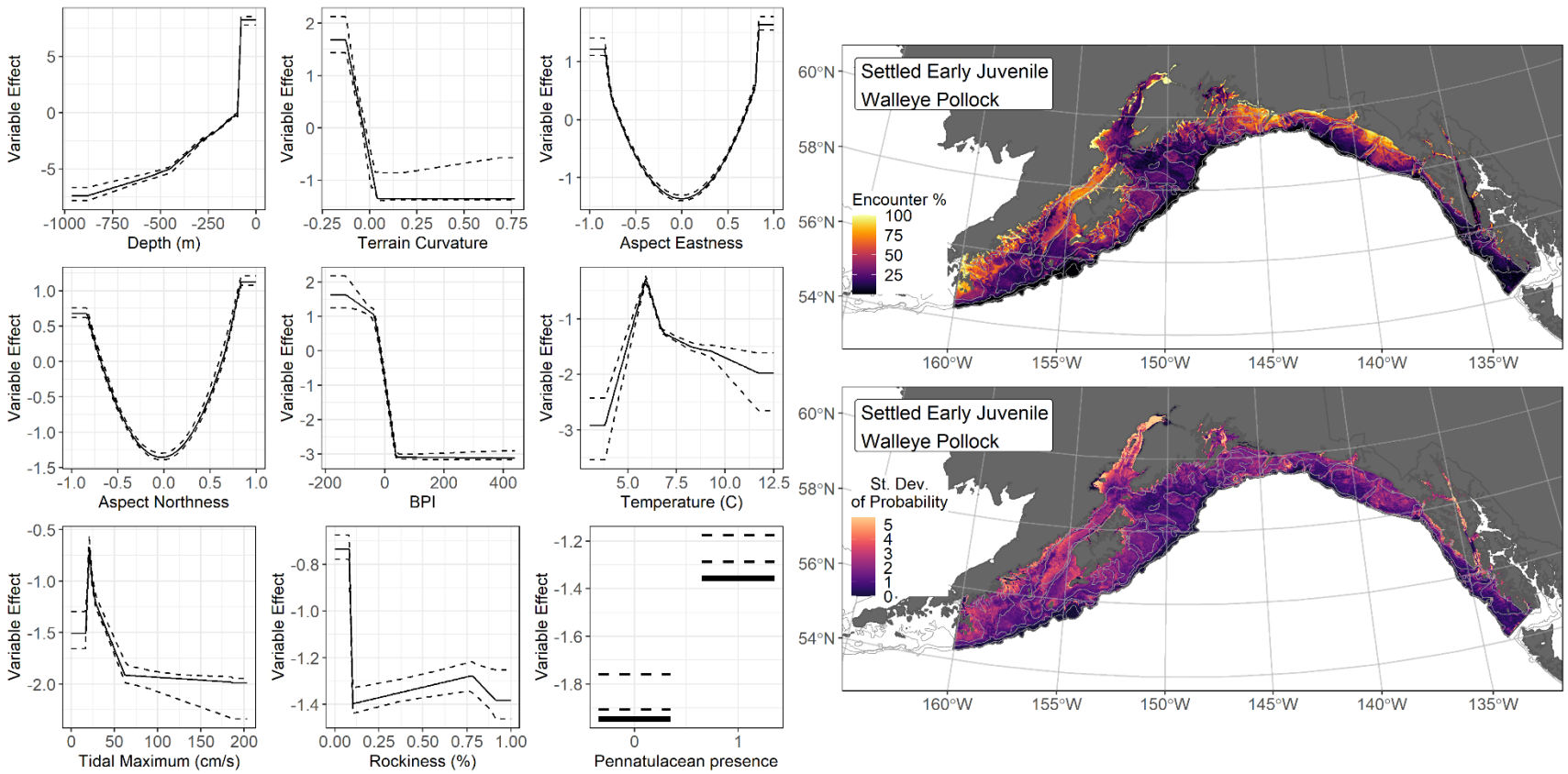

Figure 140. -- The top nine covariate effects (left panel) from a habitat-related species distribution model (MaxEnt) of settled early juvenile walleye pollock probability of suitable habitat in the Gulf of Alaska (upper right panel) with the standard deviation of the probability predictions (lower right panel).

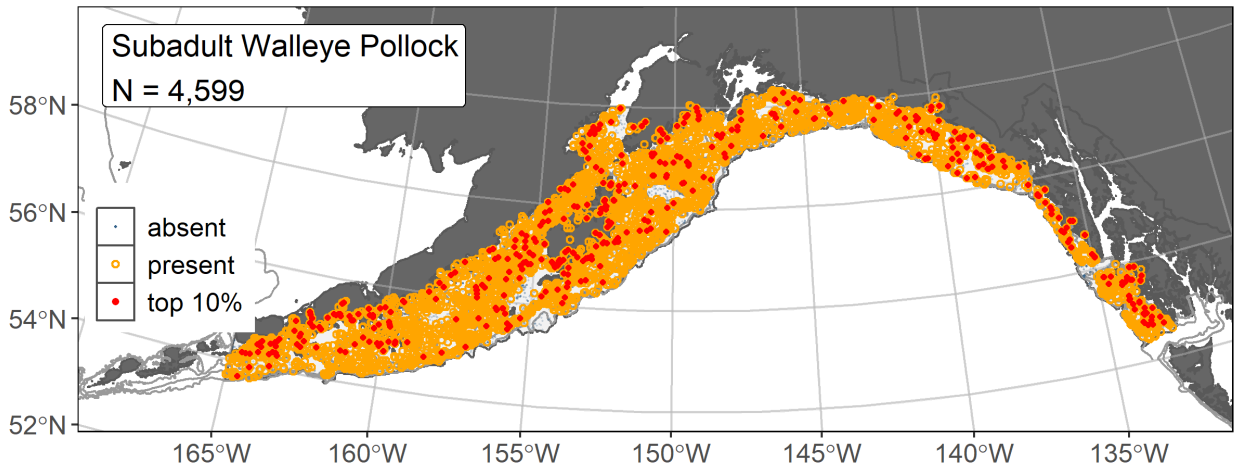

Figure 141. -- Distribution of subadult walleye pollock catches (N = 4,599) in 1993–2019 AFSC RACE-GAP summer bottom trawl surveys of the Gulf of Alaska with the 100 m, 200 m, and 700 m isobaths indicated; filled red circles indicate locations in top 10% of overall abundance, open orange circles indicate presence in remaining catches, and blue dots indicate stations sampled where the animals were not present.

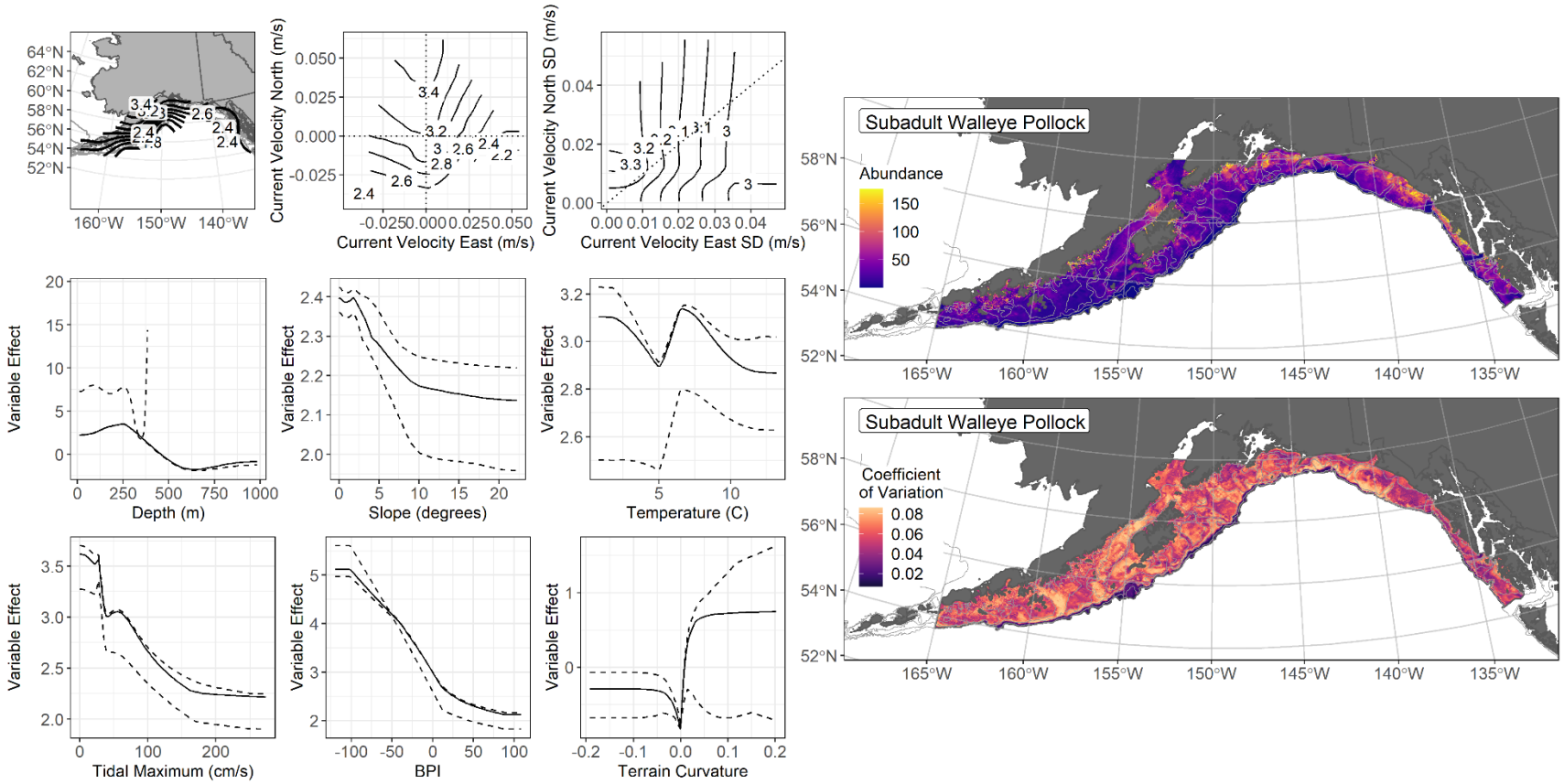

Figure 142. -- The top nine covariate effects (left panel) on ensemble-predicted subadult walleye pollock numerical abundance across the Gulf of Alaska (upper right panel) along with the coefficient of variation (CV) of the ensemble predictions (lower right panel).

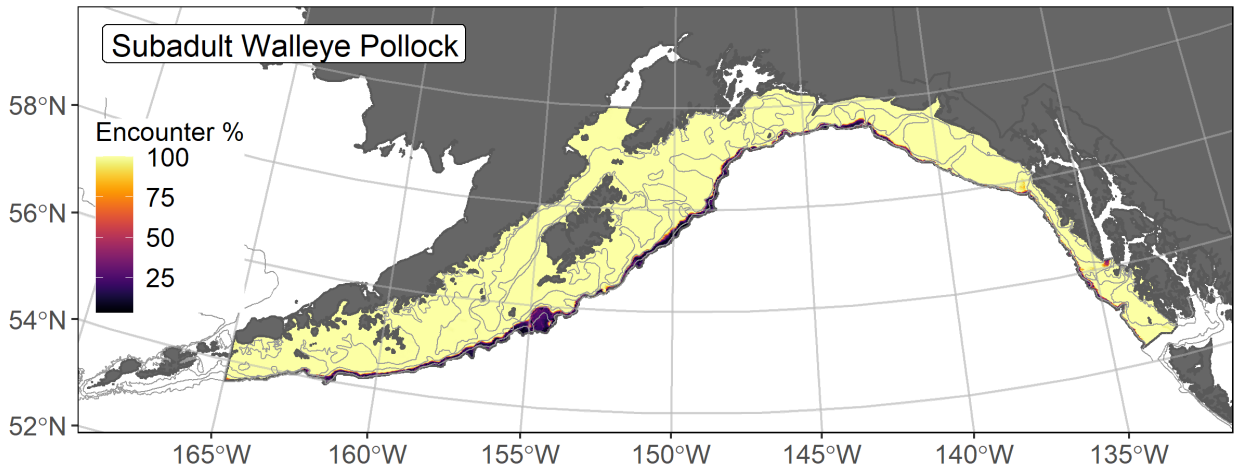

Figure 143. -- Encounter probability of subadult walleye pollock from AFSC RACE-GAP summer bottom trawl surveys (1993–2019) of the Gulf of Alaska with the 100 m, 200 m, and 700 m isobaths indicated.

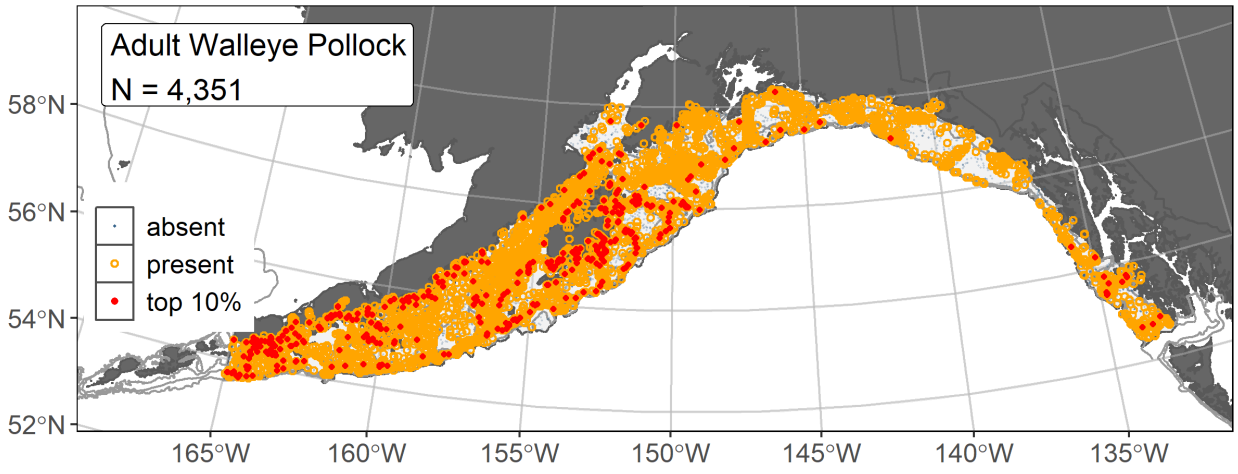

Figure 144. -- Distribution of adult walleye pollock catches (N = 4,351) in 1993–2019 AFSC RACE-GAP summer bottom trawl surveys of the Gulf of Alaska with the 100 m, 200 m, and 700 m isobaths indicated; filled red circles indicate locations in top 10% of overall abundance, open orange circles indicate presence in remaining catches, and blue dots indicate stations sampled where the animals were not present.

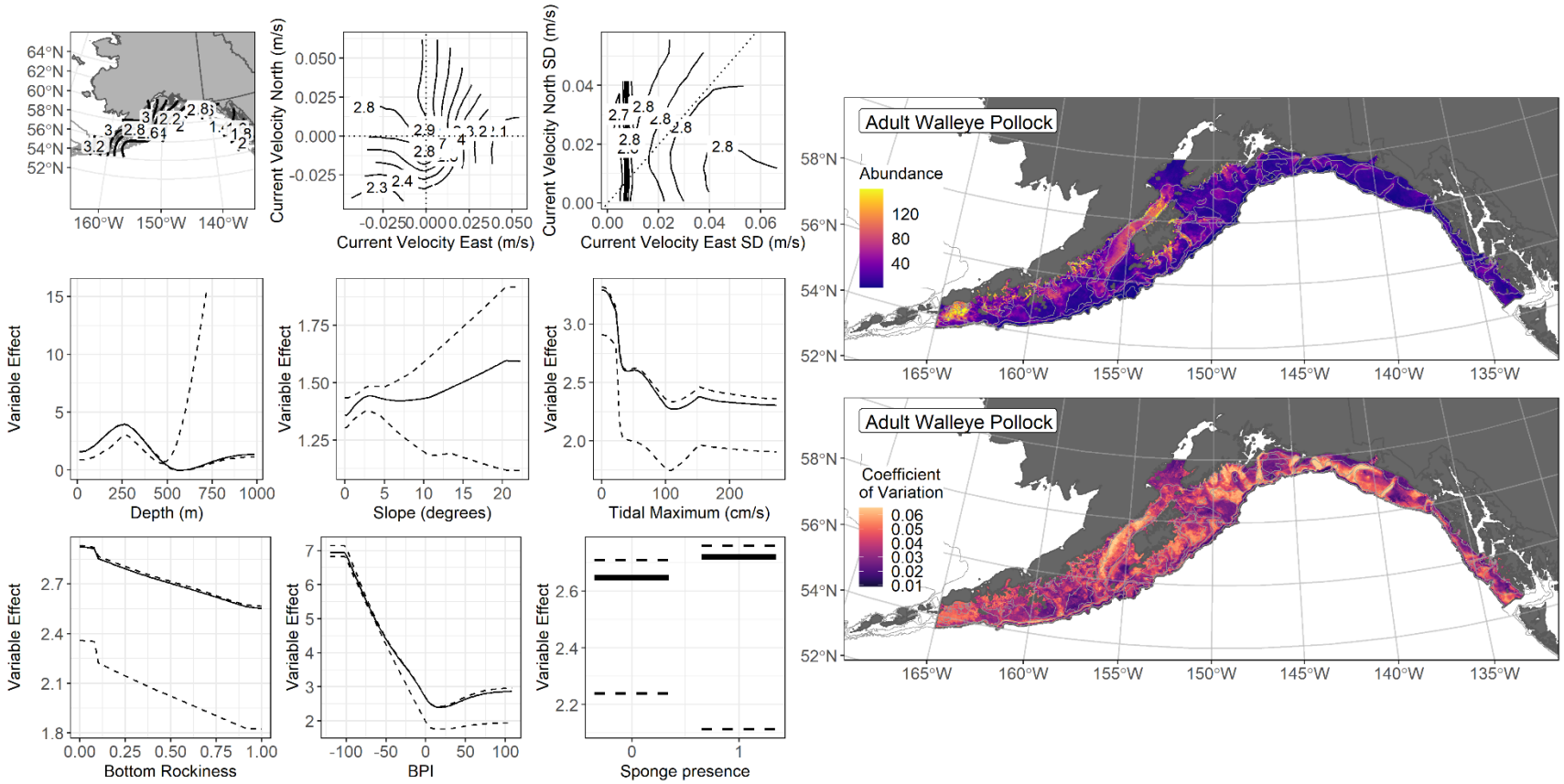

Figure 145. -- The top nine covariate effects (left panel) on ensemble-predicted adult walleye pollock numerical abundance across the Gulf of Alaska (upper right panel) along with the coefficient of variation (CV) of the ensemble predictions (lower right panel).

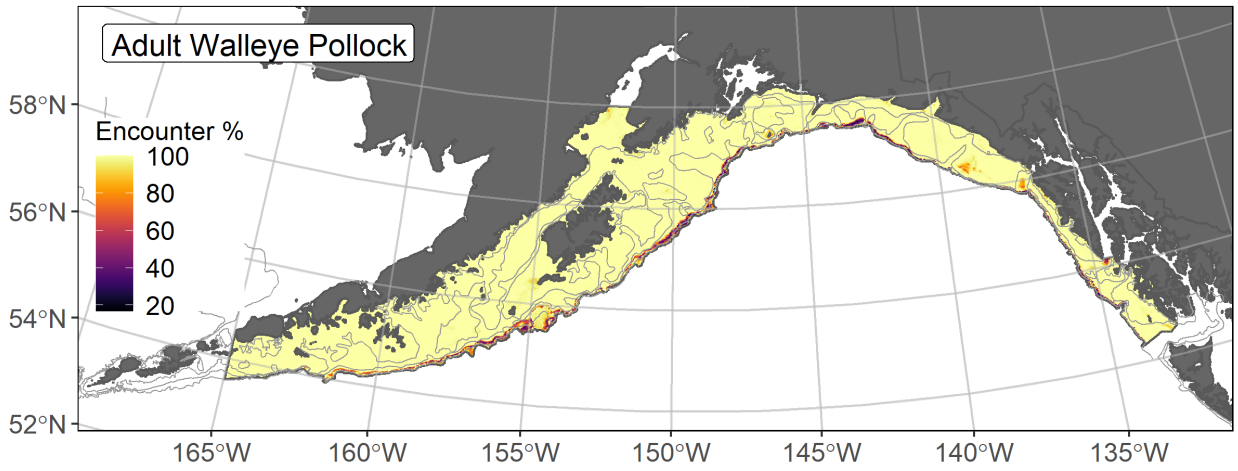

Figure 146. -- Encounter probability of adult walleye pollock from AFSC RACE-GAP summer bottom trawl surveys (1993–2019) of the Gulf of Alaska with the 100 m, 200 m, and 700 m isobaths indicated.

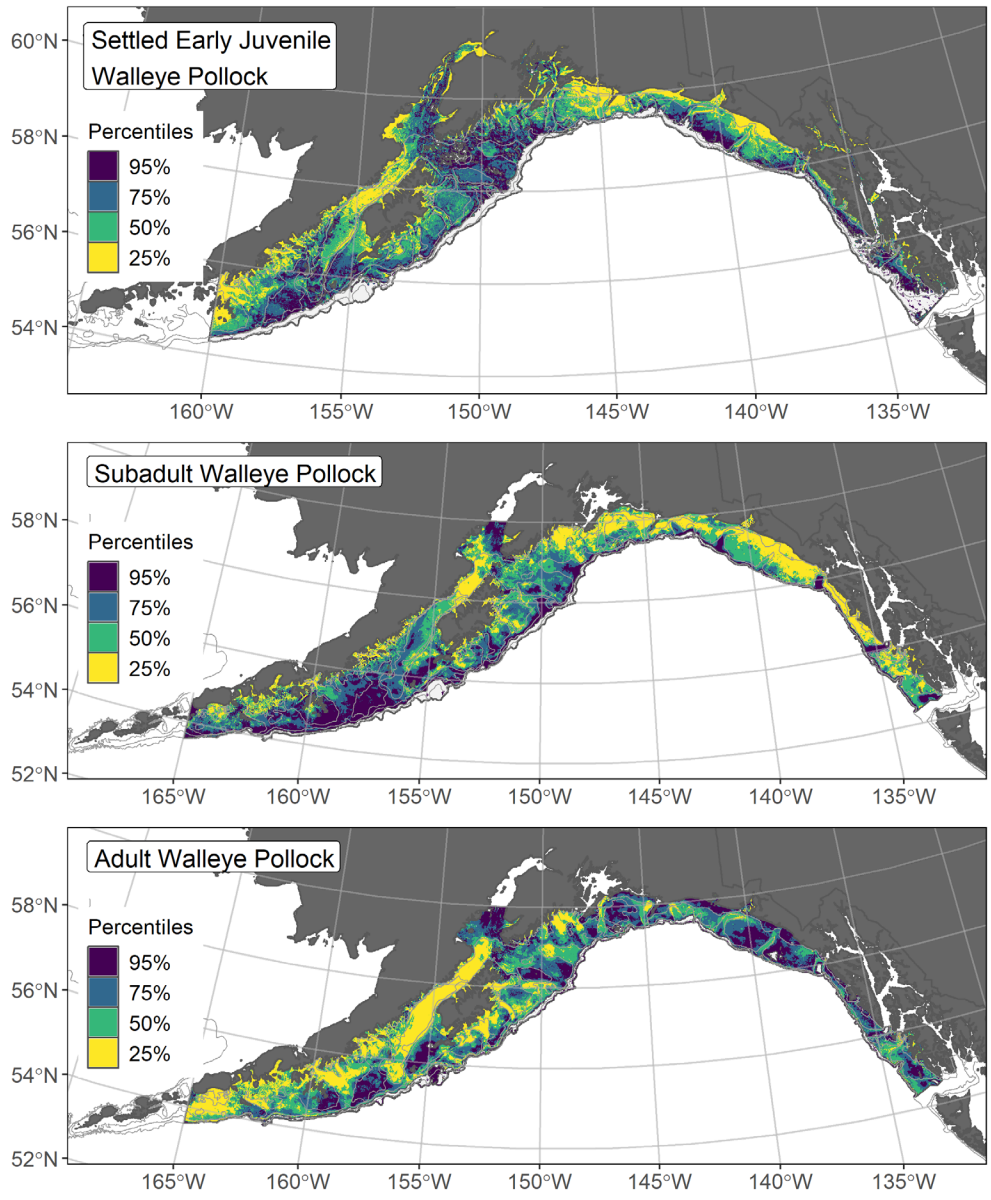

Figure 147. -- Essential fish habitat (EFH) is the area containing the top 95% of occupied habitat (defined as greater than 5% predicted probability of suitable habitat) for settled early juvenile (top panel) walleye pollock from an SDM fitted to their distribution in Gulf of Alaska (GOA) mixed gear-type summer surveys (1989–2019), and for subadults (middle panel) and adults (bottom panel) is the area containing the top 95% of occupied habitat (defined as model estimated encounter probabilities greater than 5%) from an SDM ensemble fitted to walleye pollock distribution and abundance in AFSC RACE-GAP GOA summer bottom trawl surveys (1993–2019) with 100 m, 200 m, and 700 m isobaths indicated; within the EFH area map are the subareas of the top 25% (EFH hot spots), top 50% (core EFH area), and top 75% (principal EFH area).

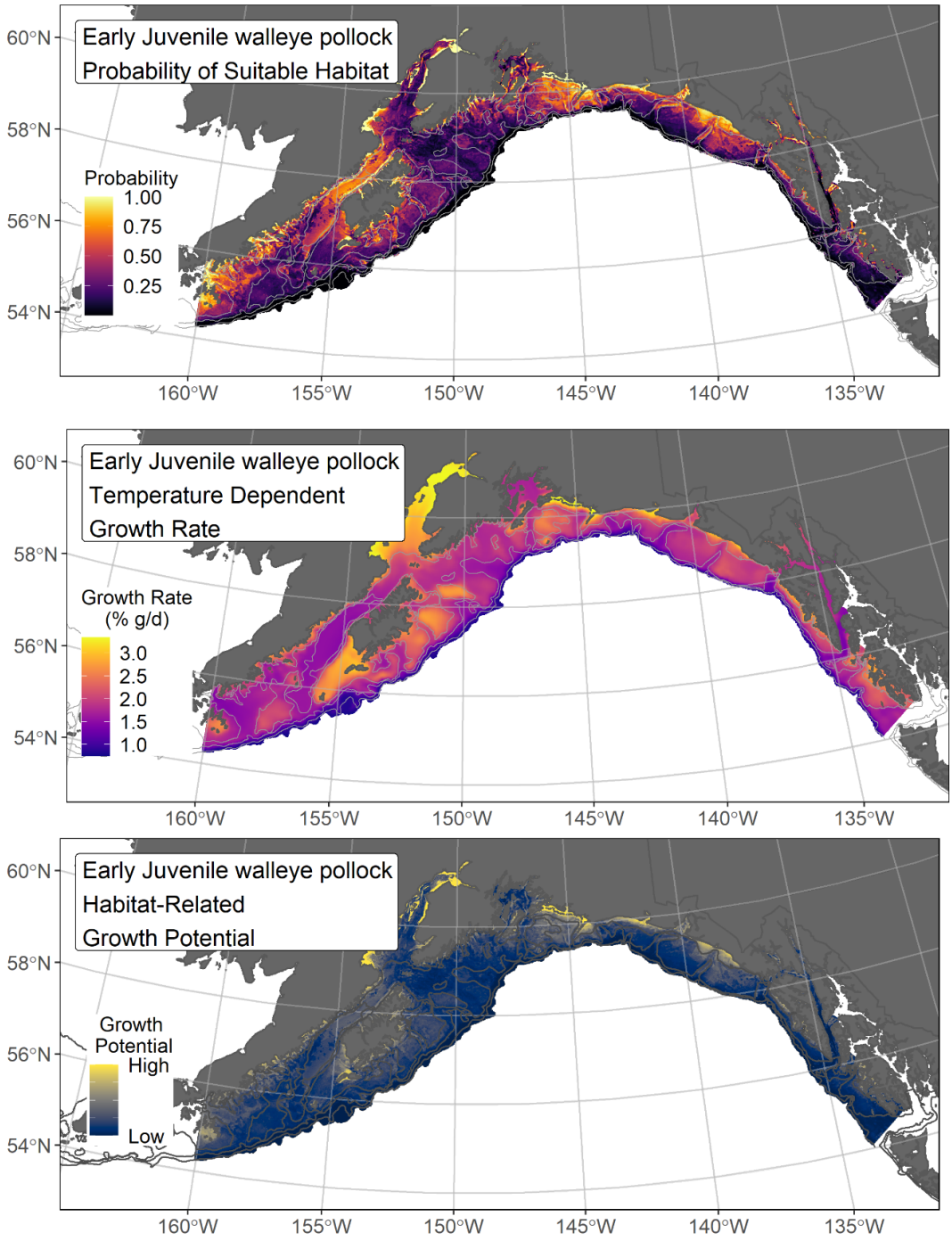

Figure 148. -- Settled early juvenile walleye pollock predicted probability of suitable habitat from a habitat-related species distribution model fitted to their distribution in Gulf of Alaska mixed gear-type summer surveys (1989–2019; top panel), temperature-dependent growth rate ($GR = \%\ body\ weight\ (g) \cdot day^{-1}$; center panel), and EFH Level 3 map of habitat-related growth potential (bottom panel), which is the raster product of probability of suitable habitat and temperature-dependent growth rate.

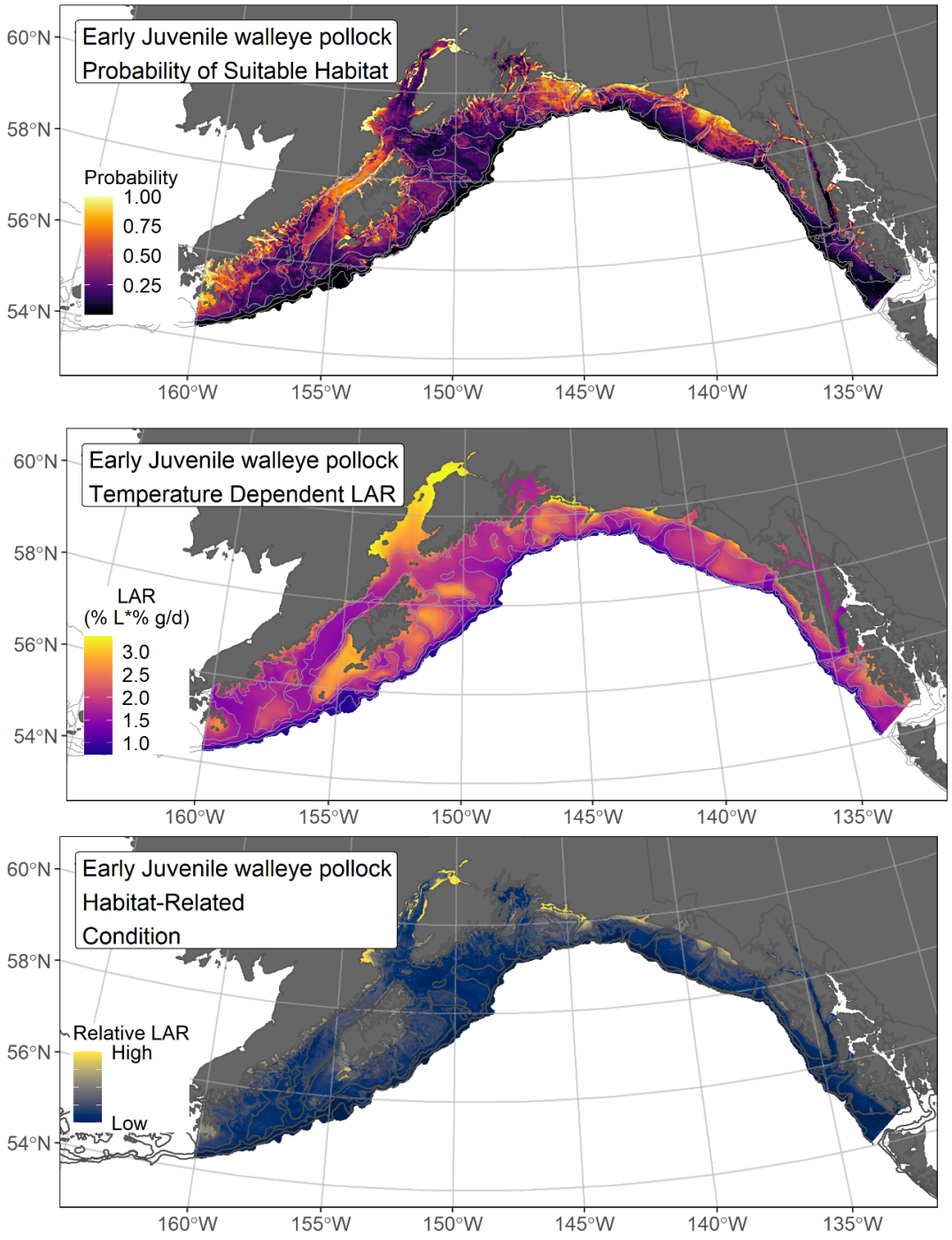

Figure 149. -- Settled early juvenile walleye pollock predicted probability of suitable habitat from a habitat-related species distribution model fitted to their distribution in Gulf of Alaska mixed gear-type summer surveys (1989–2019; top panel), temperature-dependent lipid accumulation rate ($LAR = \%\ lipid \cdot \%\ body\ weight\ (g) \cdot day^{-1}$; center panel), and EFH Level 3 map of habitat-related condition (relative LAR; bottom panel), which is the raster product of probability of suitable habitat and temperature-dependent LAR.

Rockfishes

Dusky Rockfish (*Sebastes variabilis*)

Dusky rockfish (*Sebastes variabilis*) range from southern British Columbia north to the Bering Sea and west to Hokkaido Island, Japan (Orr and Blackburn 2004). Dusky rockfish is one of the more common rockfish species in the GOA where it is managed as a single species stock (Fenske et al. 2020). A moderately large rockfish species, duskies become mature around 365 mm and can grow as large as 590 mm (Chilton 2010). Prior to 1996, dusky rockfish were often mixed with catches of the dark rockfish (*S. ciliatus*), and these species were recorded as "light dusky" or "dark dusky," which allowed for the true species to be retroactively determined from the RACE-GAP survey data after the species were officially described by Orr and Blackburn (2004). Dusky rockfish are caught by the RACE-GAP survey around banks and gullies in the GOA (Fenske et al. 2020). Other studies have observed this species in rocky, untrawlable habitats in association with habitat-forming sponges and corals (Krieger and Wing 2002, Rooper et al. 2012a, Jones et al. 2021)[29].

Subadult dusky rockfish abundance and distribution predicted from RACE-GAP summer bottom trawl surveys in the Gulf of Alaska -- Subadult dusky rockfish (N = 315) caught in GOA RACE-GAP summer bottom trawl surveys (1993–2019) occurred from south of the Kenai Peninsula to the western extent of the GOA study area at 165° W (Fig. 150). Four of the five SDMs considered for inclusion in the ensemble to predict numerical abundance of subadult dusky rockfish in the GOA converged (Table 52); the GAM_P was eliminated by skill testing. The remaining three best-performing SDMs were weighted nearly equally by RMSE in the final ensemble, which attained a fair overall fit to the observed subadult dusky rockfish distribution and abundance data. The ensemble was fair at predicting high and low abundance catches (ρ = 0.21), good at discriminating presence-absence (AUC = 0.80), and fair at explaining deviance (PDE = 0.27).) Bottom depth, geographic location, tidal current speed, and sponge presence accounted for 68.1% of the covariate contribution to the deviance explained by the final ensemble (Table 53). Higher subadult dusky rockfish abundance was predicted at less than 250 m depth with low occurrence of sponges, including the banks and glacial trough edges on the continental shelf and upper slope of the GOA from Portlock Bank and west (Fig. 151). The CV of ensemble predictions was higher across most of the GOA continental shelf. The probability of encountering subadult dusky rockfish was higher in areas of predicted high abundance and increased further west (Fig. 152).

[29] Incorporating high quality sources of data from untrawlable habitats in future SDM ensemble EFH mapping for this species will be included as a research recommendation from the 2023 EFH 5-year Review.

Adult dusky rockfish abundance and distribution predicted from RACE-GAP summer bottom trawl surveys in the Gulf of Alaska -- Adult dusky rockfish (N = 1,061) caught in GOA RACE-GAP summer bottom trawl surveys (1993–2019) were distributed from southern southeast Alaska to the western extent of the GOA study area at 165° W, where highest abundance catches were most prevalent in the central GOA south of the Kenai Peninsula and west (Fig. 153). The five SDMs considered for inclusion in the ensemble to predict numerical abundance of adult dusky rockfish in the GOA converged (Table 52); the GAM_{nb} was eliminated by skill testing. The remaining four best-performing SDMs were weighted by RMSE in the final ensemble, which attained a fair overall fit to the observed adult dusky rockfish distribution and abundance data. The ensemble was fair at predicting high and low abundance catches (ρ = 0.40), good at discriminating presence-absence (AUC = 0.83), and fair at explaining deviance (PDE = 0.28). Bottom depth, rockiness, and geographic location accounted for 62.5% of the covariate contribution to the deviance explained by the ensemble (Table 53). Higher adult dusky rockfish abundance was predicted at < 250 m depth with rocky substrate present, including on the banks along the continental shelf and in areas of the outer continental shelf and upper slope from Portlock Bank and west, with some areas of higher abundance at the Fairweather Grounds in the eastern GOA (Fig. 154). The CV of ensemble predictions was relatively even across the GOA study area. Adult Dusky rockfish encounter probability is high across most of the GOA continental shelf (Fig. 155).

Essential Fish Habitat of subadult and adult dusky rockfish in the Gulf of Alaska -- Ensemble-predicted habitat-related numerical abundance of dusky rockfish life stages collected in RACE-GAP summer bottom trawl surveys of the GOA (1993–2019) was mapped as EFH areas and subareas (Fig. 156). Subadult dusky rockfish EFH area included the GOA continental shelf and upper slope from southeast Alaska through the western GOA, excluding the glacial troughs. Core EFH area and EFH hot spots for subadults were prevalent from south of the Kenai Peninsula through the western GOA, although some EFH hot spots were predicted to occur off southeast Alaska. Adult dusky rockfish EFH, including core EFH area, was more extensive than subadult EFH. Similar to subadults, adult EFH occurred on the continental shelf and upper slope of the GOA. However, adult EFH also included the glacial troughs west of Kayak Island.

Table 52. -- Constituent species distribution models (SDMs) used to construct Essential Fish Habitat (EFH) for a) subadult and b) adult dusky rockfish: MaxEnt = Maximum entropy; paGAM = presence-absence generalized additive model; hGAM = zero-adjusted Poisson hurdle GAM; GAM_P = standard Poisson GAM; GAM_{nb} = standard negative-binomial GAM; RMSE = root mean square error; ρ (rho) = Spearman's rank correlation coefficient; AUC = area under the receiver-operating characteristic curve; and PDE = Poisson deviance explained *. The "--" indicates that this model was not included in the final ensemble.

a) subadult dusky rockfish

Models	RMSE	Relative Weight	ρ	AUC	PDE	EFH area (km^2)
MaxEnt	17.8	0.33	0.18	0.76	0.14	240,700
paGAM	17.8	0.33	0.20	0.79	0.17	226,100
hGAM	--	--	--	--	--	--
GAM_P	18.3	0	--	--	--	--
GAM_{nb}	17.9	0.33	0.18	0.76	0.02	176,200
ensemble	17.7	1	0.21	0.80	0.27	235,200

b) adult dusky rockfish

Models	RMSE	Relative Weight	ρ	AUC	PDE	EFH area (km^2)
MaxEnt	54.2	0.26	0.40	0.83	0.17	259,400
paGAM	54.3	0.26	0.40	0.83	0.12	261,700
hGAM	60.9	0.21	0.29	0.83	0.01	241,900
GAM_P	54.4	0.26	0.31	0.75	0.08	210,500
GAM_{nb}	115.3	0	--	--	--	--
ensemble	53.1	1	0.40	0.83	0.28	264,000

* Refer to the Species Distribution Model Performance Metrics subsection within the Statistical Modeling section of the Methods for detailed descriptions of individual model performance metrics.

Table 53. -- Covariates retained in the a) subadult and b) adult dusky rockfish species distribution model (SDM) final ensembles, the percent contribution to the ensemble deviance explained by each covariate, and the cumulative deviance explained: SD = standard deviation and BPI = bathymetric position index.

dusky rockfish			
	Covariate	**% Contribution**	**Cumulative %**
a) subadult	bottom depth	31.7	31.7
	location	15.2	46.9
	tidal maximum	10.8	57.7
	sponge presence	10.4	68.1
	rockiness	8.8	76.9
	BPI	5.3	82.2
	aspect north	4.2	86.4
	bottom temperature	3.1	89.5
	current	3.0	92.5
	aspect east	2.9	95.4
	coral presence	2.7	98.1
	current SD	1.0	99.1
	slope	0.7	99.8
	pennatulacean presence	0.2	100.0
b) adult	bottom depth	44.3	44.3
	rockiness	9.7	53.9
	location	8.6	62.5
	current	7.7	70.2
	tidal maximum	6.0	76.2
	BPI	5.7	81.9
	current SD	3.9	85.8
	aspect north	3.2	89.0
	aspect east	3.0	92.0
	coral presence	2.2	94.2
	bottom temperature	1.8	96.0
	slope	1.3	97.3
	sponge presence	1.0	98.3
	pennatulacean presence	1.0	99.3
	curvature	0.7	100.0

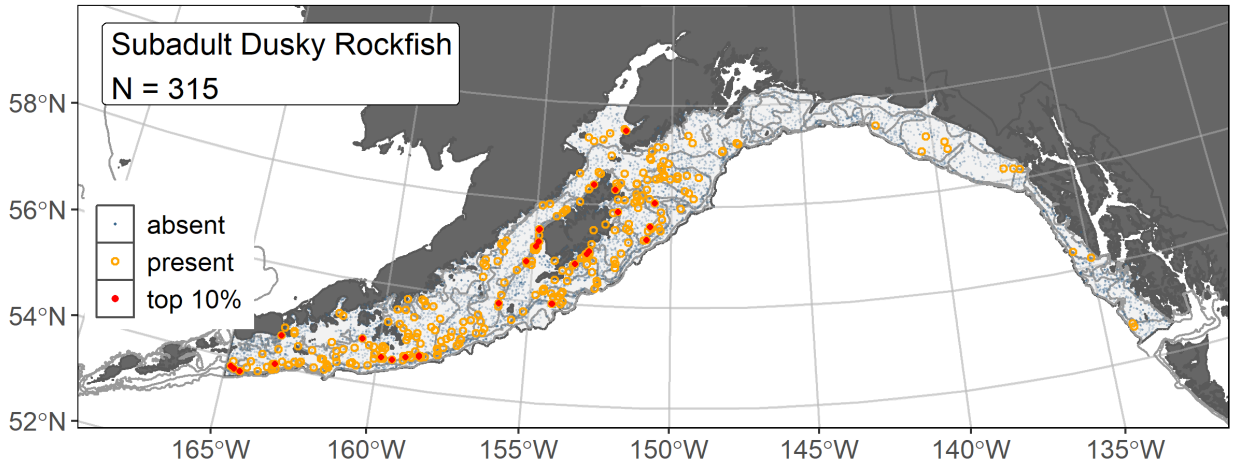

Figure 150. -- Distribution of subadult dusky rockfish catches (N = 315) in 1993–2019 AFSC RACE-GAP summer bottom trawl surveys of the Gulf of Alaska with the 100 m, 300 m, and 700 m isobaths indicated; filled red circles indicate locations in top 10% of overall abundance, open orange circles indicate presence in remaining catches, and blue dots indicate stations sampled where the animals were not present.

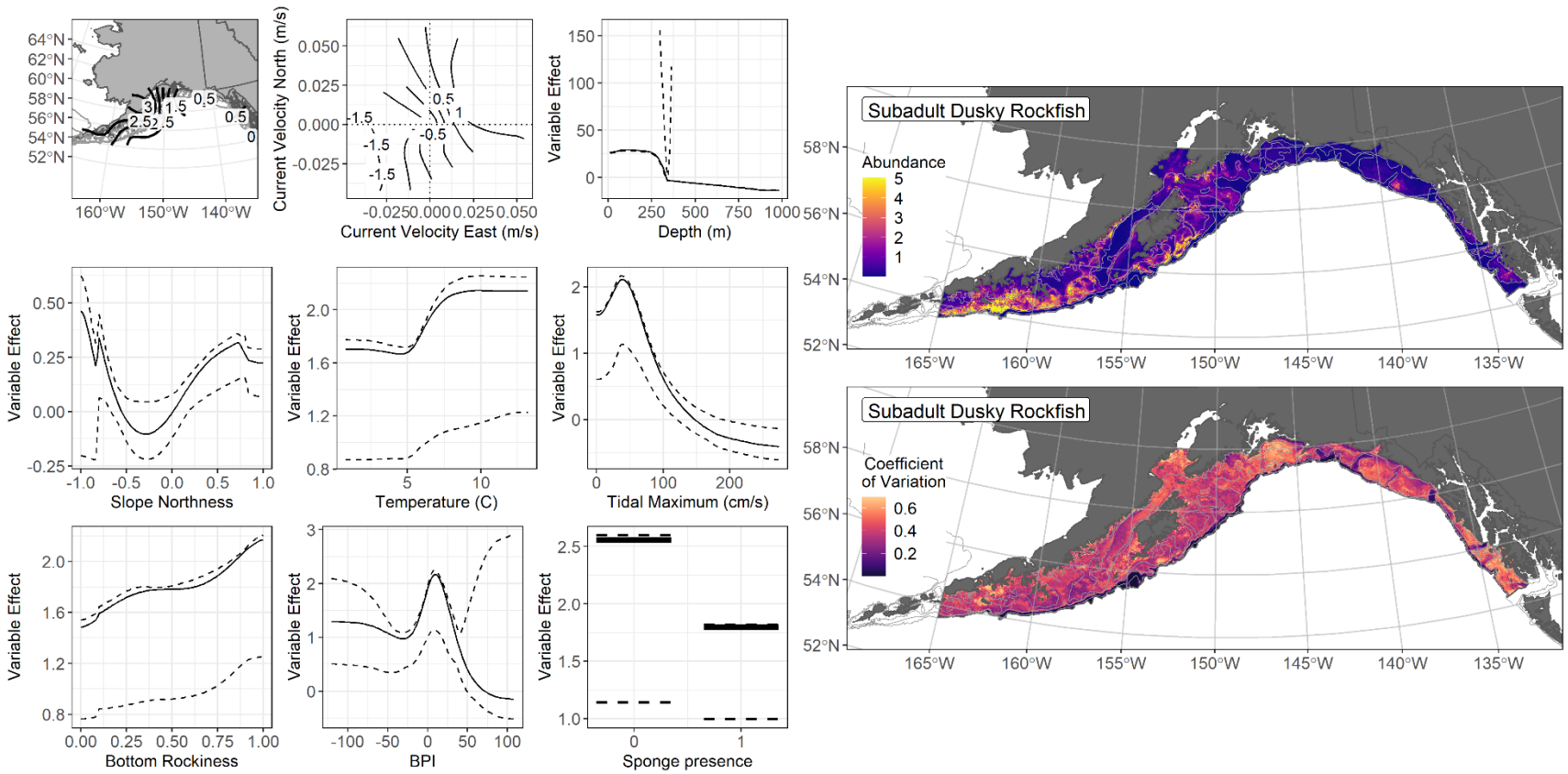

Figure 151. -- The top nine covariate effects (left panel) on ensemble-predicted subadult dusky rockfish numerical abundance across the Gulf of Alaska (upper right panel) alongside the coefficient of variation of the ensemble predictions (lower right panel).

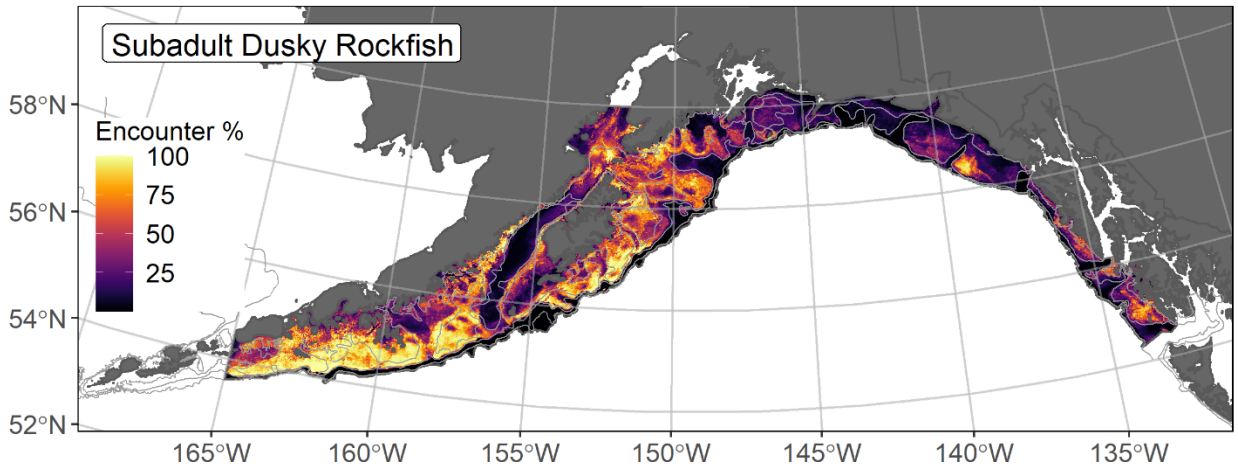

Figure 152. -- Encounter probability of subadult dusky rockfish from AFSC RACE-GAP summer bottom trawl surveys (1993–2019) of the Gulf of Alaska with the 100 m, 300 m, and 700 m isobaths indicated.

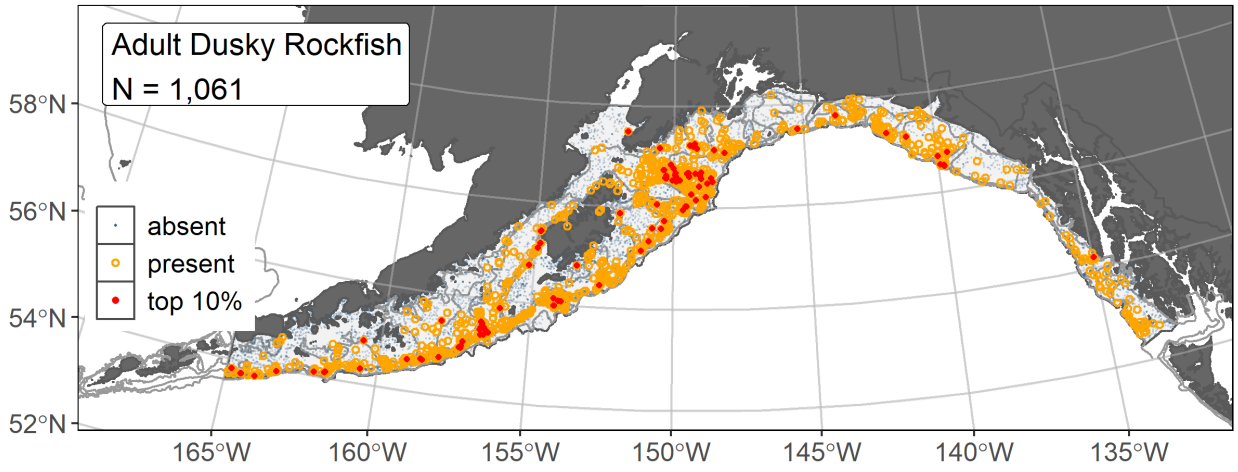

Figure 153. -- Distribution of adult dusky rockfish catches (N = 1,061) in 1993–2019 AFSC RACE-GAP summer bottom trawl surveys of the Gulf of Alaska with the 100 m, 300 m, and 700 m isobaths indicated; filled red circles indicate locations in top 10% of overall abundance, open orange circles indicate presence in remaining catches, and blue dots indicate stations sampled where the animals were not present.

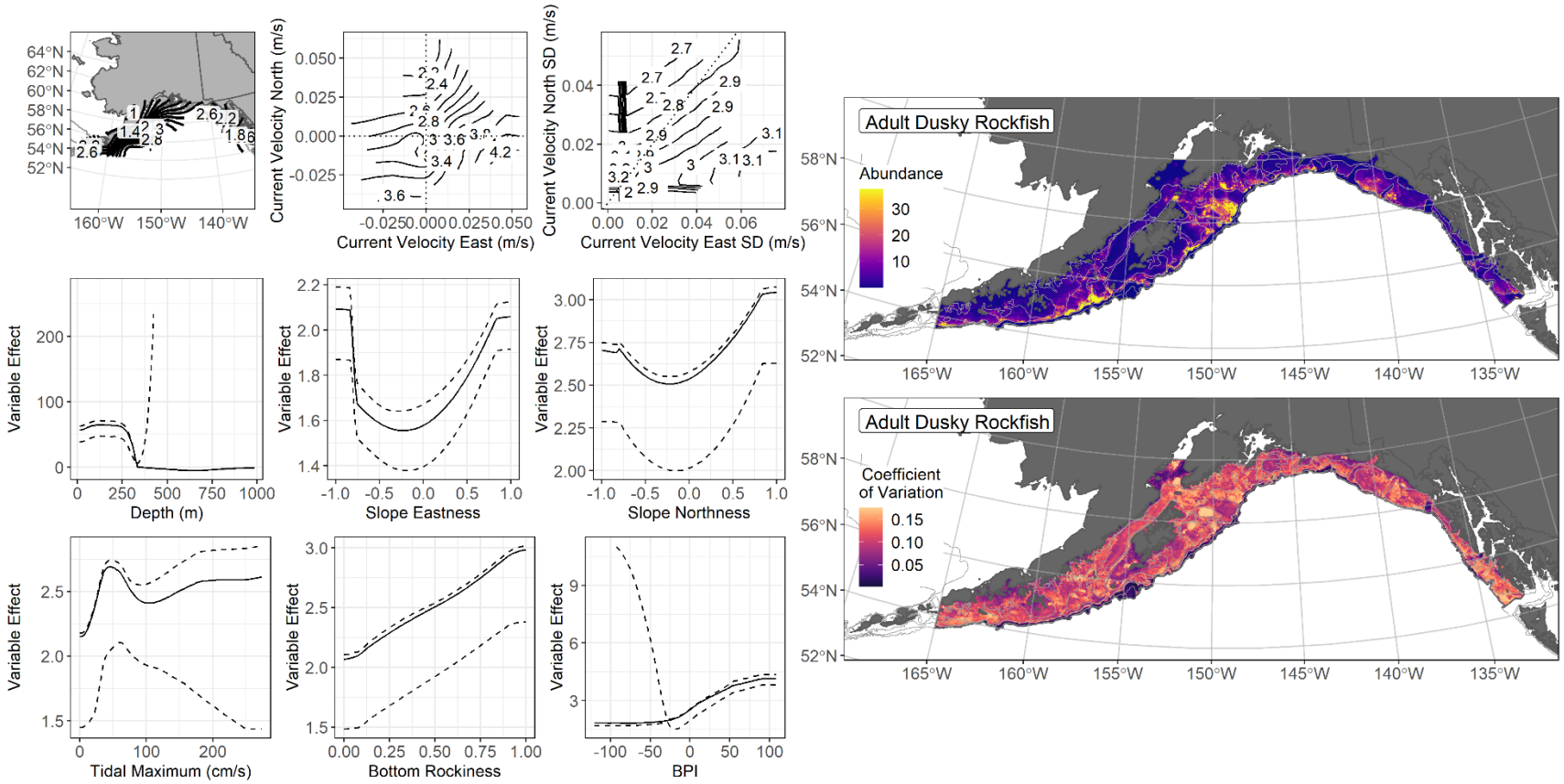

Figure 154. -- The top nine covariate effects (left panel) on ensemble-predicted adult dusky rockfish numerical abundance across the Gulf of Alaska (upper right panel) alongside the coefficient of variation of the ensemble predictions (lower right panel).

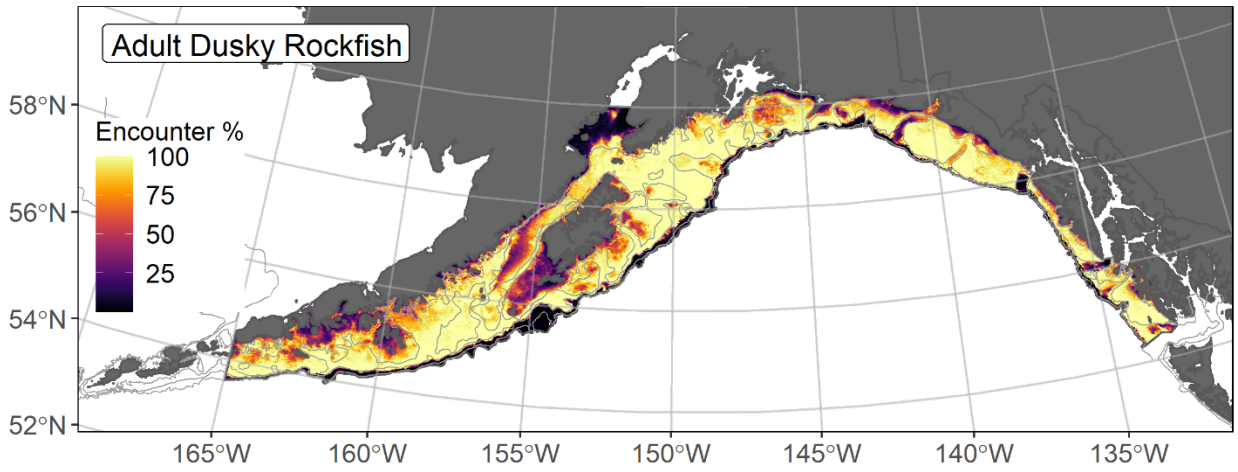

Figure 155. -- Encounter probability of adult dusky rockfish from AFSC RACE-GAP summer bottom trawl surveys (1993–2019) of the Gulf of Alaska with the 100 m, 300 m, and 700 m isobaths indicated.

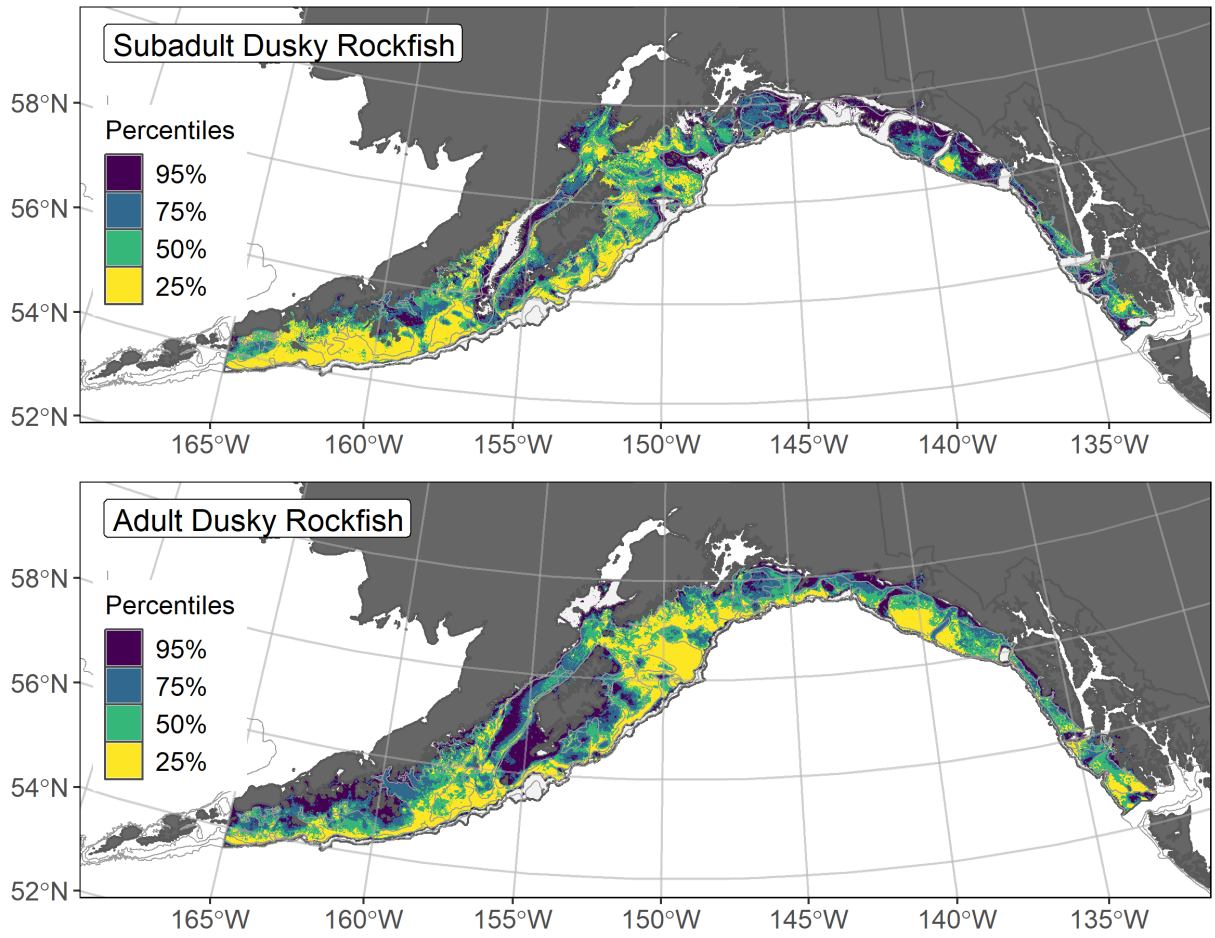

Figure 156. -- Essential fish habitat (EFH) is the area containing the top 95% of occupied habitat (defined as model estimated encounter probabilities greater than 5%) from an SDM ensemble fitted to subadult (top panel) and adult (bottom panel) dusky rockfish distribution and abundance in AFSC RACE-GAP summer bottom trawl surveys (1993–2019) with 100 m, 200 m, and 700 m isobaths indicated; within the EFH area map are the subareas of the top 25% (EFH hot spots), top 50% (core EFH area), and top 75% (principal EFH area) of habitat-related, ensemble-predicted numerical abundance.

Northern Rockfish (*Sebastes polyspinis*)

Northern rockfish (*Sebastes polyspinis*) range from British Columbia to the Kuril Islands and Kamchatka Peninsula (Allen and Smith 1988) and are most common in Alaska waters from Portlock Bank in the central GOA to the western Aleutian Islands (Clausen and Heifetz 2002). There is regional variation in northern rockfish growth and maturation, with GOA specimens reaching L_{50} at around 310 mm and a maximum age at 67 years (Chilton 2007), although Aleutian specimens reach L_{50} around 277 mm and live longer with a maximum age of 72 years (Tenbrink and Spencer 2013). Northern rockfish are managed as a single species stock in the GOA (Williams et al. 2020) and are also part of the Other Rockfish Slope Sub-Group in the eastern GOA (Tribuzio and Echave 2019). Little information is available on the habitat of northern rockfish settled early juveniles (Williams et al. 2020), which is a common life history information gap among rockfishes (Love et al. 2002). However, subadults (>200 mm) are frequently caught inshore of adults by the RACE-GAP GOA bottom trawl survey (Williams et al. 2020). Adults are commonly caught on bathymetric rises and banks on the continental shelf around depths of 75-150 m (Clausen and Heifetz 2002). Northern rockfish subadults and adults are strongly associated with the seafloor in both trawlable and rocky, rugged untrawlable habitats with sponges and corals (Clausen and Heifetz 2002, Rooper et al. 2012, Jones et al. 2021)[30].

Subadult northern rockfish abundance and predicted distribution from RACE-GAP summer bottom trawl surveys in the Gulf of Alaska -- Subadult northern rockfish (N = 522) caught in GOA RACE-GAP summer bottom trawl surveys (1993–2019) were distributed from south of the Kenai Peninsula to the western extent of the GOA study area at 165° W (Fig. 157). Five SDMs considered for inclusion in the ensemble to predict numerical abundance of subadult northern rockfish in the GOA converged (Table 54); the GAM_{nb} was eliminated by skill testing. The remaining four best-performing SDMs were weighted by RMSE in the final ensemble, which attained a good overall fit to the observed subadult northern rockfish distribution and abundance data. The ensemble was fair at predicting high and low abundance catches (ρ = 0.30), and good at discriminating presence-absence (AUC = 0.86) and explaining deviance (PDE = 0.42). Bottom depth, geographic location, and rockiness were the three most influential covariates, accounting for 60.6% of the covariate contribution to the deviance explained by the ensemble (Table 55). Subadult northern rockfish abundance was generally higher at depths less than 250 m in areas with rocky substrate (Fig. 158). Predicted abundance was highest on the banks on the continental shelf of the GOA from Portlock Bank west through the Shumagin Islands. The CV of

[30] Incorporating high quality sources of data from untrawlable habitats in future SDM ensemble EFH mapping for this species will be included as a research recommendation from the 2023 EFH 5-year Review.

ensemble predictions was highest off of southern southeast Alaska; this life stage rarely occurred in survey catches east of Kayak Island. The probability of encountering subadult northern rockfish was highest on bathymetric rises south of the Kenai Peninsula and west in the GOA (Fig. 159).

Adult northern rockfish abundance and predicted distribution from RACE-GAP summer bottom trawl surveys in the Gulf of Alaska -- Adult northern rockfish (N = 1,141) caught in GOA RACE-GAP summer bottom trawl surveys (1993–2019) occurred from the outer continental shelf in the vicinity of Yakutat trough to the western extent of the GOA study area at 165° W, with catches of highest abundance most prevalent on the outer continental shelf of the central GOA south of the Kenai Peninsula and west (Fig. 160). Four of the five SDMs considered for inclusion in the ensemble to predict numerical abundance of adult northern rockfish in the GOA converged (Table 54); the GAM_P was eliminated by skill testing. The remaining three best-performing SDMs were weighted by RMSE in the final ensemble, which attained a good overall fit to the observed adult northern rockfish distribution and abundance data. The ensemble was good at predicting high and low abundance catches ($\rho = 0.46$) and discriminating presence-absence (AUC = 0.89), and fair at explaining deviance (PDE = 0.32). Bottom depth, geographic location, bottom current, and rockiness accounted for 70.4% of the covariate contribution to the deviance explained by the ensemble (Table 55). Higher adult northern rockfish abundance peaked at 190 m depth on bathymetric rises with rocky substrate and moderate bottom current exposure, including at Portlock Bank and along the outer continental shelf from Kodiak Island through the western GOA (Fig. 161). The CV ensemble predictions were relatively even across the GOA study area, except for inshore areas and glacial troughs where this species is not expected to occur. Adult Northern rockfish encounter probability was high across most of the GOA continental shelf west of 148° W (Fig. 162).

Essential Fish Habitat of subadult and adult northern rockfish in the Gulf of Alaska -- Ensemble-predicted habitat-related numerical abundance of northern rockfish life stages collected in RACE-GAP summer bottom trawl surveys of the GOA (1993–2019) was mapped as EFH areas and subareas (Fig. 163). Subadult northern rockfish EFH area extended across the GOA continental shelf west of Kayak Island and included some areas of the eastern GOA where the RACE-GAP survey has not encountered this species. Core EFH area and EFH hot spots for subadults were prevalent from south of the Kenai Peninsula through the western GOA. Adult northern rockfish EFH area was more extensive than subadult EFH area. Adult EFH included the eastern GOA, although the RACE-GAP survey has not encountered this species southeast of the Fairweather Grounds. Adult core EFH area and EFH hot spots were concentrated west of Kayak Island on the continental shelf.

Table 54. -- Constituent species distribution models (SDMs) used to construct Essential Fish Habitat (EFH) for a) subadult and b) adult northern rockfish: MaxEnt = Maximum entropy; paGAM = presence-absence generalized additive model; hGAM = zero-adjusted Poisson hurdle GAM; GAM_P = standard Poisson GAM; GAM_{nb} = standard negative-binomial GAM; RMSE = root mean square error; ρ (rho) = Spearman's rank correlation coefficient; AUC = area under the receiver-operating characteristic curve; and PDE = Poisson deviance explained *. The "--" indicates that this model was not included in the final ensemble.

a) subadult northern rockfish

Models	RMSE	Relative Weight	ρ	AUC	PDE	EFH area (km^2)
MaxEnt	8.56	0.26	0.26	0.81	0.25	232,900
paGAM	8.55	0.26	0.29	0.85	0.26	184,600
hGAM	9.23	0.23	0.23	0.85	0.42	138,200
GAM_P	8.85	0.25	0.26	0.81	0.23	119,200
GAM_{nb}	9.02	0	--	--	--	--
ensemble	8.32	1	0.30	0.86	0.42	215,600

b) adult northern rockfish

Models	RMSE	Relative Weight	ρ	AUC	PDE	EFH area (km^2)
MaxEnt	274.5	0.35	0.44	0.87	0.31	252,800
paGAM	276.6	0.34	0.45	0.88	0.24	249,300
hGAM	--	--	--	--	--	--
GAM_P	291.0	0	--	--	--	--
GAM_{nb}	289.5	0.31	0.43	0.86	0.25	169,200
ensemble	276.3	1	0.46	0.89	0.32	261,100

* Refer to the Species Distribution Model Performance Metrics subsection within the Statistical Modeling section of the Methods for detailed descriptions of individual model performance metrics.

Table 55. -- Covariates retained in the a) subadult and b) adult northern rockfish species distribution model (SDM) final ensembles, the percent contribution to the ensemble deviance explained by each covariate, and the cumulative deviance explained: SD = standard deviation and BPI = bathymetric position index.

northern rockfish

	Covariate	% Contribution	Cumulative %
a) subadult	bottom depth	32.7	32.7
	location	17.5	50.2
	rockiness	10.4	60.6
	current	8.2	68.8
	current SD	4.7	73.5
	sponge presence	4.7	78.1
	tidal maximum	3.8	81.9
	BPI	3.7	85.6
	bottom temperature	3.0	88.6
	coral presence	2.9	91.5
	slope	2.6	94.1
	aspect east	2.3	96.4
	aspect north	2.1	98.5
	curvature	1.2	99.7
	pennatulacean presence	0.3	100.0
b) adult	bottom depth	24.2	24.2
	location	24.2	48.4
	current	11.7	60.0
	rockiness	10.4	70.4
	bottom temperature	6.8	77.2
	tidal maximum	6.0	83.2
	current SD	4.4	87.6
	aspect north	3.1	90.7
	BPI	3.1	93.8
	aspect east	2.2	96.0
	sponge presence	1.9	97.9
	slope	1.1	99.0
	pennatulacean presence	0.5	99.5
	coral presence	0.3	99.8
	curvature	0.2	100.0

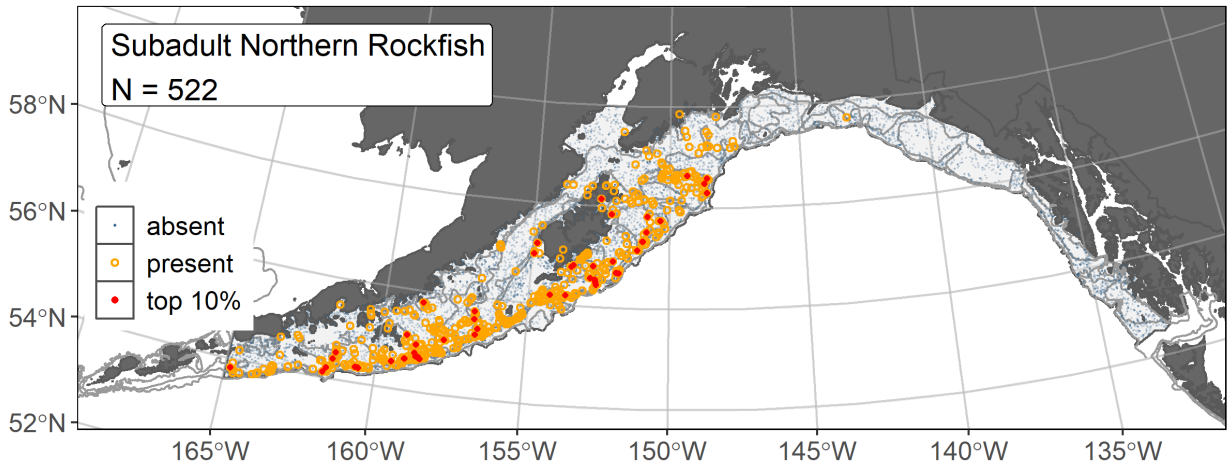

Figure 157. -- Distribution of subadult northern rockfish catches (N = 522) in 1993–2019 AFSC RACE-GAP summer bottom trawl surveys of the Gulf of Alaska with the 100 m, 300 m, and 700 m isobaths indicated; filled red circles indicate locations in top 10% of overall abundance, open orange circles indicate presence in remaining catches, and blue dots indicate stations sampled where the animals were not present.

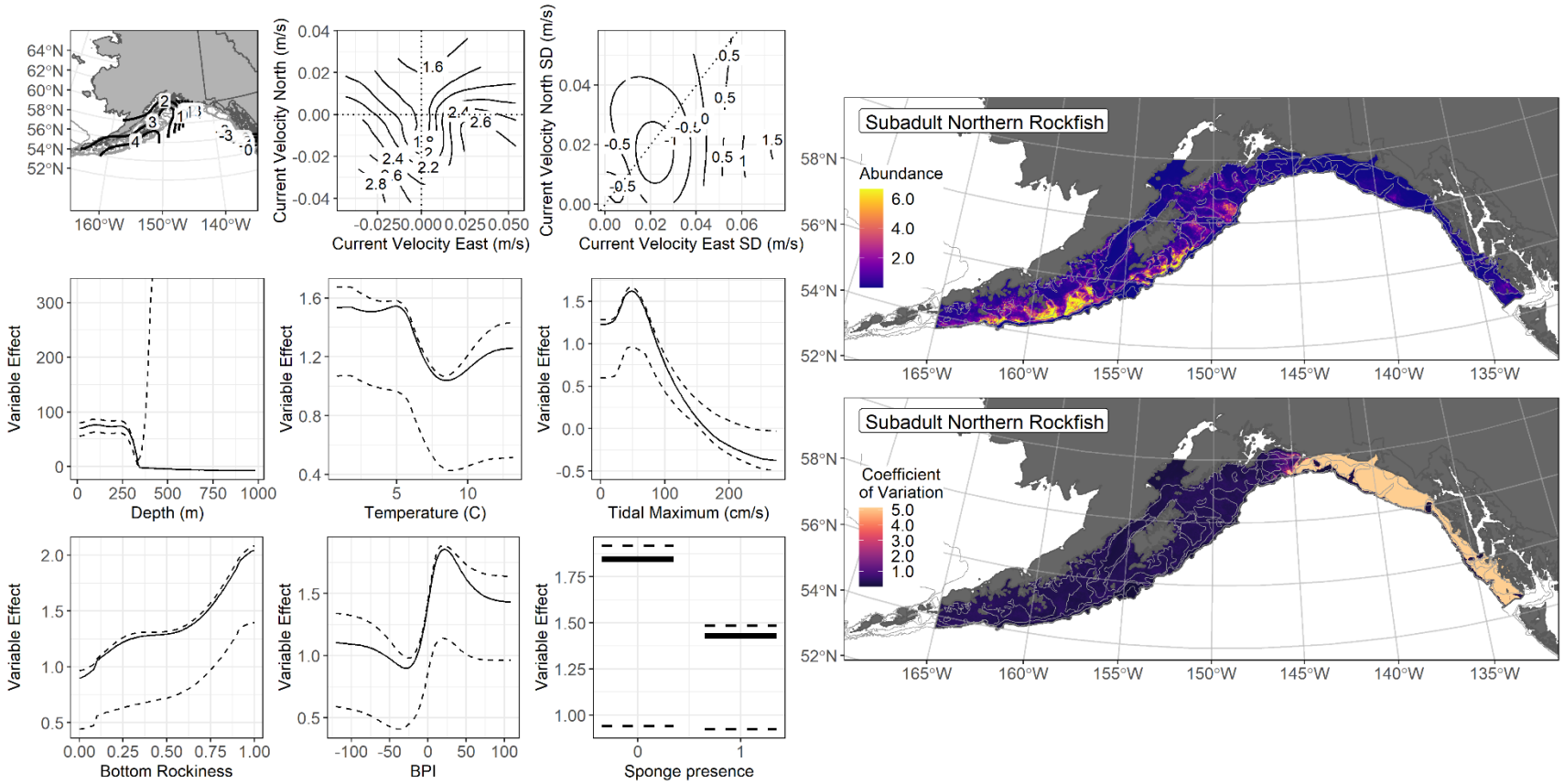

Figure 158. -- The top nine covariate effects (left panel) on ensemble-predicted subadult northern rockfish numerical abundance across the Gulf of Alaska (upper right panel) alongside the coefficient of variation (CV) of the ensemble predictions (lower right panel).

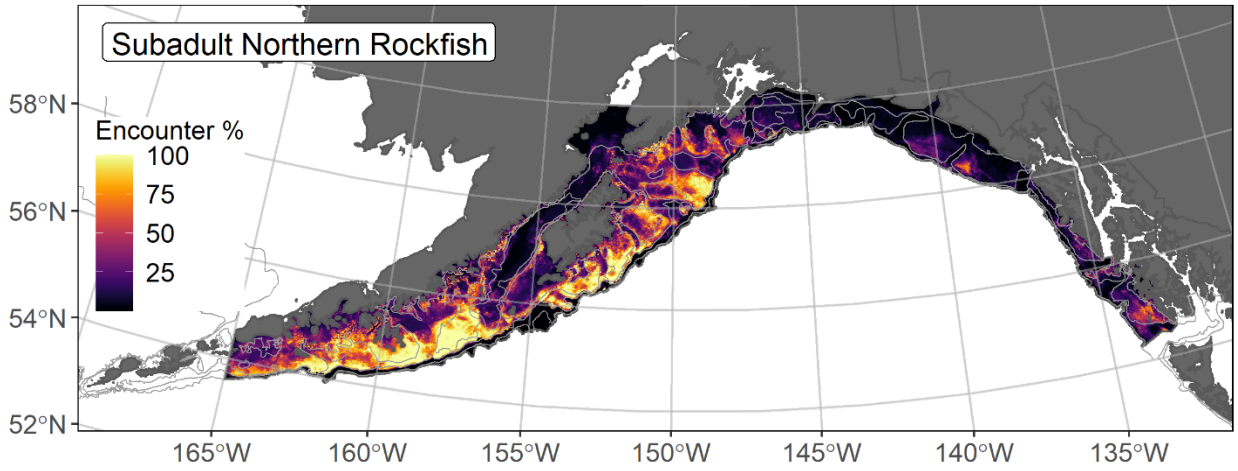

Figure 159. -- Encounter probability of subadult northern rockfish from AFSC RACE-GAP summer bottom trawl surveys (1993–2019) of the Gulf of Alaska with the 100 m, 300 m, and 700 m isobaths indicated.

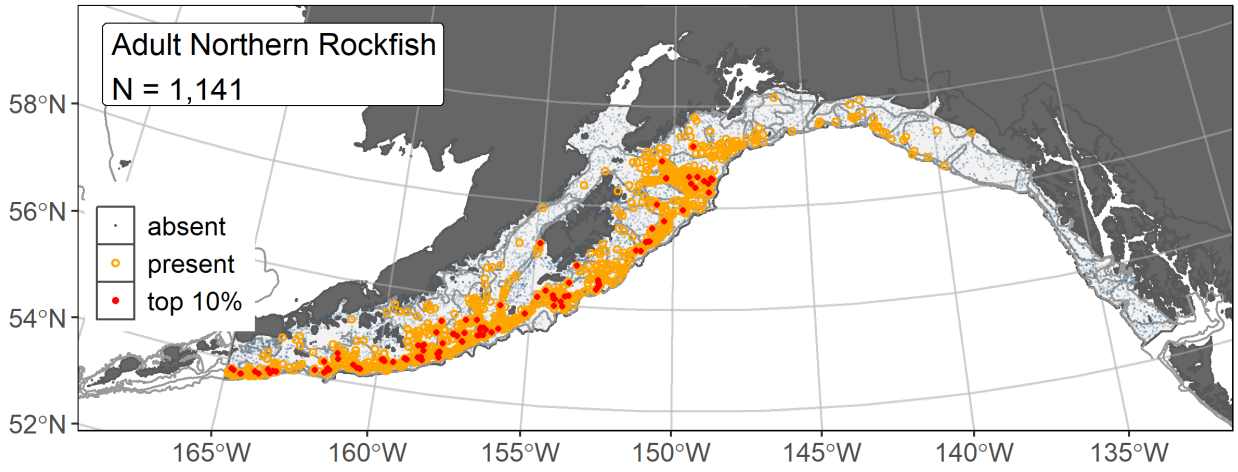

Figure 160. -- Distribution of adult northern rockfish catches (N = 1,141) in 1993–2019 AFSC RACE-GAP summer bottom trawl surveys of the Gulf of Alaska with the 100 m, 300 m, and 700 m isobaths indicated; filled red circles indicate locations in top 10% of overall abundance, open orange circles indicate presence in remaining catches, and blue dots indicate stations sampled where the animals were not present.

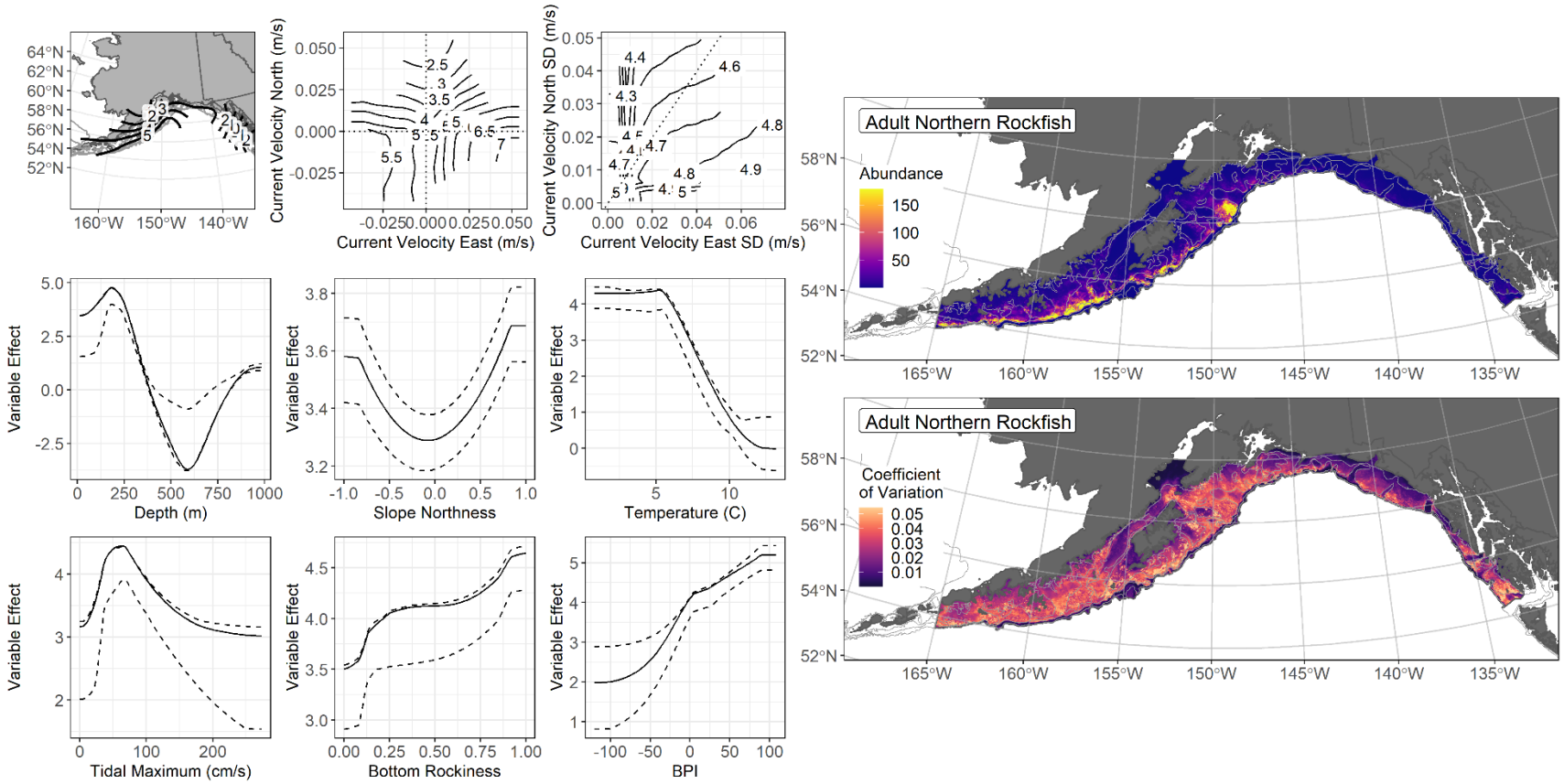

Figure 161. -- The top nine covariate effects (left panel) on ensemble-predicted adult northern rockfish numerical abundance across the Gulf of Alaska (upper right panel) alongside the coefficient of variation (CV) of the ensemble predictions (lower right panel).

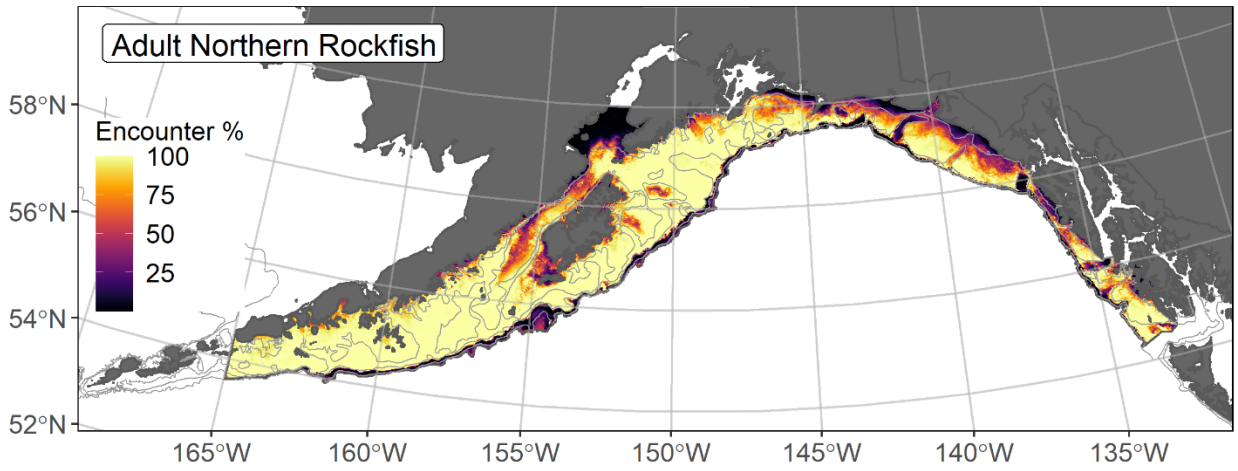

Figure 162. -- Encounter probability of adult northern rockfish from AFSC RACE-GAP summer bottom trawl surveys (1993–2019) of the Gulf of Alaska with the 100 m, 300 m, and 700 m isobaths indicated.

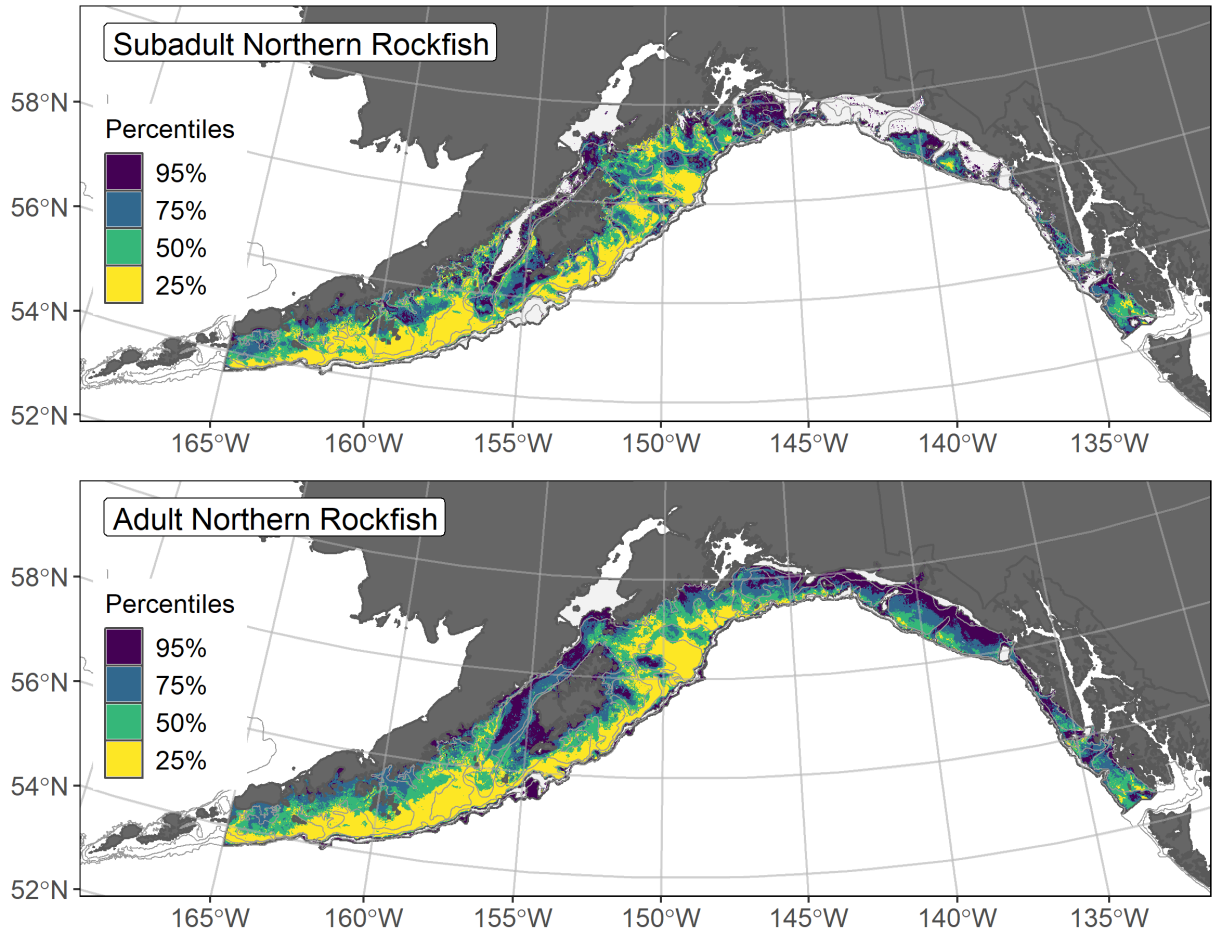

Figure 163. -- Essential fish habitat (EFH) is the area containing the top 95% of occupied habitat (defined as model estimated encounter probabilities greater than 5%) from an SDM ensemble fitted to subadult (top panel) and adult (bottom panel) northern rockfish distribution and abundance in AFSC RACE-GAP summer bottom trawl surveys (1993–2019) with 100 m, 200 m, and 700 m isobaths indicated; within the EFH area map are the subareas of the top 25% (EFH hot spots), top 50% (core EFH area), and top 75% (principal EFH area) of habitat-related, ensemble-predicted numerical abundance.

Pacific ocean perch (*Sebastes alutus*)

Pacific ocean perch (*Sebastes alutus*, POP) are widely distributed across the North Pacific, ranging from Baja California to Japan, including the Gulf of Alaska (Mecklenburg et al. 2002). Seasonal differences in depth distributions were noted by Love et al. (2002) and compare favorably with the depths where POP are typically encountered on RACE-GAP summer bottom trawl surveys of the GOA (150–300 m). Adults inhabit deeper depths (300–420 m) in fall and winter until around May. Juveniles have been found in shallow (37 m) inshore waters, gradually moving to deeper habitats with age (Carlson and Straty 1981). These rockfish display pronounced diel vertical movements (Brodeur 2001) and often form dense, localized schools off bottom (Hanselman et al. 2001, Hulson et al. 2020). Species in the genus *Sebastes* are ovoviviparous, with internal fertilization and the release of live young. Settled early juvenile POP can be up to 200 mm FL and may be found in habitats not sampled by the RACE-GAP bottom trawl survey and subadult (201–250 mm FL) and adult POP (> 250 mm FL) are also postulated to occupy different habitats (Carlson and Straty 1981, Rooper et al. 2007, Rooper 2008). The mesh size of the RACE-GAP bottom trawl is large enough that smaller life stages like settled early juveniles may not be wholly retained in the catch[31]. Pacific ocean perch are managed as an individual, single-species stock in the GOA (Hulson et al. 2020).

Settled early juvenile Pacific ocean perch distribution predicted from mixed gear-type summer surveys in the Gulf of Alaska -- Settled early juvenile POP (N = 1,552) caught in multiple mixed gear-type GOA summer surveys (1989–2019), using large and small mesh bottom trawls, purse and beach seines, were distributed from nearshore areas out to the edge of the continental shelf with more high abundance catches of this life stage occurring in southeastern Alaska (Fig. 164). For these early juvenile POP, presence records from multiple surveys were combined in a MaxEnt SDM predicting suitable habitat probabilities for this life stage. The best model had a β-multiplier of 3.0 and an AUC of 0.81 (Table 56). The covariates contributing the most to the final SDM (66%) were bottom depth, bottom temperature, tidal current speed, and BPI (Table 57). The highest probabilities of suitable habitat for early juvenile POP in the GOA were predicted in offshore waters at depths around 250 m, with bottom temperatures around 6°C, lower tidal current exposure, on bathymetric highs (BPI) (Fig. 165). The areas with the highest error around the MaxEnt predictions for settled early juvenile suitable habitat were typically mapped to nearshore areas.

[31] Incorporating high quality sources of data from untrawlable habitats in future SDM ensemble EFH mapping for this species will be included as a research recommendation from the 2023 EFH 5-year Review.

Subadult Pacific ocean perch abundance and distribution predicted from RACE-GAP summer bottom trawl surveys in the Gulf of Alaska -- Subadult POP (N = 1,686) caught in GOA RACE-GAP summer bottom trawl surveys (1993–2019) were distributed across the continental shelf domain and onto the upper slope with concentrations of higher abundance catches in southeast Alaska (Fig. 166). Five SDMs were considered for inclusion in the ensemble to predict numerical abundance of subadult POP in the GOA (Table 58); the GAM_{nb} was eliminated by skill testing. The remaining four best-performing SDMs had similar RMSE and were weighted nearly equally in the final ensemble, which attained a good overall fit to the observed subadult POP distribution and abundance data. The ensemble was good at predicting high and low abundance catches (ρ = 0.49) and discriminating presence-absence (AUC = 0.85), and fair at explaining deviance (PDE = 0.39). Bottom depth, geographic location, and rockiness were the top contributors (66.9%) among covariates to the deviance explained by the ensemble (Table 57). The highest abundances of subadult POP were predicted to occur at depths around 250 m over increasingly rocky bottom (Fig. 167). The CV of ensemble predictions was high throughout the GOA with exceptions of very low values in southern Cook Inlet, the nearshore of the Yakutat management area, and off the continental shelf edge. Similarly, the probability of encountering subadult POP was high across the region but near zero in Cook Inlet, in the nearshore areas of Yakutat, and off the continental shelf (Fig. 168).

Adult Pacific ocean perch abundance and distribution predicted from RACE-GAP summer bottom trawl surveys in the Gulf of Alaska -- Adult POP (N = 2,992) caught in GOA RACE-GAP summer bottom trawl surveys (1993–2019) were distributed from nearshore areas and across the continental shelf to the slope edge throughout the GOA survey area with concentrations of higher abundance catches along the 300 m isobaths and in glacial troughs (Fig. 169). Five SDMs were considered for inclusion in the ensemble to predict numerical abundance of adult POP in the GOA (Table 58); the GAM_{nb} was eliminated by skill testing. The remaining four best-performing SDMs were weighted by RMSE in the final ensemble, which attained a good overall fit to the observed adult POP distribution and abundance data. The ensemble was excellent at predicting high and low abundance catches (ρ = 0.65), good at discriminating presence-absence (AUC = 0.81), and fair at explaining deviance (PDE = 0.39). Bottom depth, geographic location, tidal current speed, and BPI accounted for 76.3% of the contribution among covariates to the deviance explained by the ensemble (Table 57), which predicted the highest adult POP abundances along the edge of the continental shelf in depths around 250 m over seafloor features of increasing vertical relief (Fig. 170). The CV of ensemble predictions was high throughout the GOA, with exceptions in southern Cook Inlet and nearshore zones of the Yakutat and southeast Alaska management areas. The probability of encountering adult POP was high throughout the

GOA study area, with exceptions in southern Cook Inlet, southwest of Kodiak Island, and in nearshore areas off of the Yakutat management area (Fig. 171).

Essential Fish Habitat of three life stages of Pacific ocean perch in the Gulf of Alaska -- Habitat-related predictions of POP life stage distribution and abundance from summer surveys of the GOA (mixed gear-type summer surveys (1989–2019) and RACE-GAP bottom trawl surveys (1993–2019)) were mapped as EFH areas and subareas (Fig. 172). The spatial extent of EFH area for all three life stages overlapped throughout the GOA and extended from the southernmost portion of the southeast Alaska management area to the western extent of the study area. Similarly, core EFH areas and EFH hot spots for the three life stages modeled overlapped throughout their range, with most EFH hot spots overlapping in the Yakutat and southeast Alaska management areas. For adult POP, and to a lesser extent subadults, there were prominent EFH hot spots in the western GOA in the Chirikof management area.

Essential Fish Habitat Level 3 habitat-related vital rates of settled early juvenile Pacific ocean perch in the Gulf of Alaska -- A Wisconsin bioenergetics model was parameterized for juvenile POP by Rooper et al. (2012b). The model used diet, energetics, and growth data sampled in the field and in laboratory experiments from several studies funded in the eastern Aleutian Islands by the Alaska EFH Research Plan (e.g., Sigler et al. 2017). The bioenergetics model was driven by monthly mean temperatures derived from relationships between satellite-derived sea-surface temperature (SST) and RACE-GAP bottom trawl survey data. The model also incorporated the duration of the growing season inferred from continuous plankton recorder data from the central Gulf of Alaska. The model was run for 1987-2010, and growth predicted by the bioenergetics model was found to accurately predict growth measured in the field in the 2003-2008 Aleutian Islands EFH projects. Full details of the bioenergetics model and growth predictions are found in Rooper et al. (2012b).

The raster product of early juvenile POP predicted probability of suitable habitat from a MaxEnt SDM and the spatially explicit calculation of growth potential ($GP = body\ weight\ (g) \cdot day^{-1}$) for the GOA from Rooper et al. (2012b) is an EFH Level 3 map of habitat-related growth potential (Fig. 173). Growth potential for settled early juvenile POP was highest in the eastern GOA (where water temperatures are generally higher in the summer) and lowest westward of Kodiak. This spatial pattern was consistent across most individual years examined by the Rooper et al. (2012b) study, but they found that the temporal pattern across years was highly variable. The bottom temperature range at settled early juvenile POP catch locations in the SDM was 3.6–9.7°C. Mapping EFH Level 3 information for species' life stages annually may be informative of the influence of environmental change on habitat-related growth potential, with implications for understanding the connection between the North Pacific marine environment and population productivity. EFH subareas of core EFH and EFH hot spots corresponded

with areas of high habitat-related growth potential for settled early juvenile POP in the eastern GOA, which added value in interpreting the EFH Level 1 map (Fig. 172).

Table 56. -- Maximum entropy model (MaxEnt) used to construct Essential Fish Habitat (EFH) for settled early juvenile Pacific ocean perch: regularization multiplier (β); *k*-fold cross-validation root-mean-square-error (RMSE), area under the receiver operating characteristic curve (AUC), and areal extent of EFH (km^2).

Model	**β**	**RMSE**	**AUC**	**EFH area (km^2)**
MaxEnt	3.0	58.3	0.81	212,500

Table 57. -- Covariates retained in the a) settled early juvenile habitat-related maximum entropy (MaxEnt) species distribution model (SDM), and b) subadult and c) adult SDM final ensembles for Pacific ocean perch with the percent contribution of each covariate to the deviance explained by the SDMs and the cumulative deviance explained: SD = standard deviation and BPI = bathymetric position index.

Pacific ocean perch			
	Covariate	**% Contribution**	**Cumulative %**
a) settled early juvenile	bottom depth	24.3	24.3
	bottom temperature	21.3	45.6
	tidal maximum	18.6	64.2
	BPI	15.2	79.4
	rockiness	8.9	88.3
	sponge presence	4.5	92.8
	coral presence	2.9	95.7
	aspect east	1.5	97.2
	slope	1.4	98.6
	aspect north	1.4	100.0
b) subadult	bottom depth	31.9	31.9
	location	28.7	60.7
	rockiness	6.2	66.9
	sponge presence	4.2	71.1
	aspect north	4.0	75.0
	slope	3.9	78.9
	tidal maximum	3.9	82.8
	current SD	3.8	86.6
	bottom temperature	2.9	89.5
	coral presence	2.9	92.4
	current	2.8	95.2
	aspect east	2.5	97.7
	BPI	1.7	99.4
	curvature	0.4	99.8
	pennatulacean presence	0.2	100.0
c) adult	bottom depth	44.8	44.8
	location	17.3	62.1
	tidal maximum	7.5	69.6
	BPI	6.7	76.3
	current	5.4	81.7
	slope	3.9	85.6
	rockiness	3.1	88.7
	sponge presence	3.1	91.8
	bottom temperature	2.4	94.2
	current SD	2.0	96.2

Pacific ocean perch

Covariate	% Contribution	Cumulative %
aspect north	1.3	97.5
aspect east	1.1	98.6
curvature	1.0	99.6
coral presence	0.4	100.0

Table 58. -- Constituent species distribution models (SDMs) used to construct Essential Fish Habitat (EFH) for a) subadult and b) adult Pacific ocean perch: MaxEnt = Maximum entropy; paGAM = presence-absence generalized additive model; hGAM = zero-adjusted Poisson hurdle GAM; GAM_P = standard Poisson GAM; GAM_{nb} = standard negative-binomial GAM; RMSE = root mean square error; ρ (*rho*) = Spearman's rank correlation coefficient; AUC = area under the receiver-operating characteristic curve; and PDE = Poisson deviance explained *. The "--" indicates that this model was not included in the final ensemble.

a) subadult Pacific ocean perch

Models	**RMSE**	**Relative Weight**	**ρ**	**AUC**	**PDE**	**EFH area (km^2)**
MaxEnt	50.2	0.25	0.47	0.84	0.20	244,200
paGAM	49.9	0.25	0.49	0.85	0.28	253,100
hGAM	50.9	0.24	0.46	0.85	0.28	230,800
GAM_P	50.2	0.25	0.45	0.82	0.31	231,000
GAM_{nb}	51.4	0	--	--	--	--
ensemble	48.6	1	0.49	0.85	0.39	253,400

b) adult Pacific ocean perch

Models	**RMSE**	**Relative Weight**	**ρ**	**AUC**	**PDE**	**EFH area (km^2)**
MaxEnt	729.5	0.24	0.64	0.87	0.22	279,400
paGAM	725.5	0.25	0.65	0.88	0.25	281,800
hGAM	713.5	0.25	0.58	0.88	0.34	276,200
GAM_P	711.5	0.26	0.57	0.78	0.34	274,400
GAM_{nb}	874.2	0	--	--	--	--
ensemble	691.7	1	0.65	0.81	0.39	281,500

* Refer to the Species Distribution Model Performance Metrics subsection within the Statistical Modeling section of the Methods for detailed descriptions of individual model performance metrics.

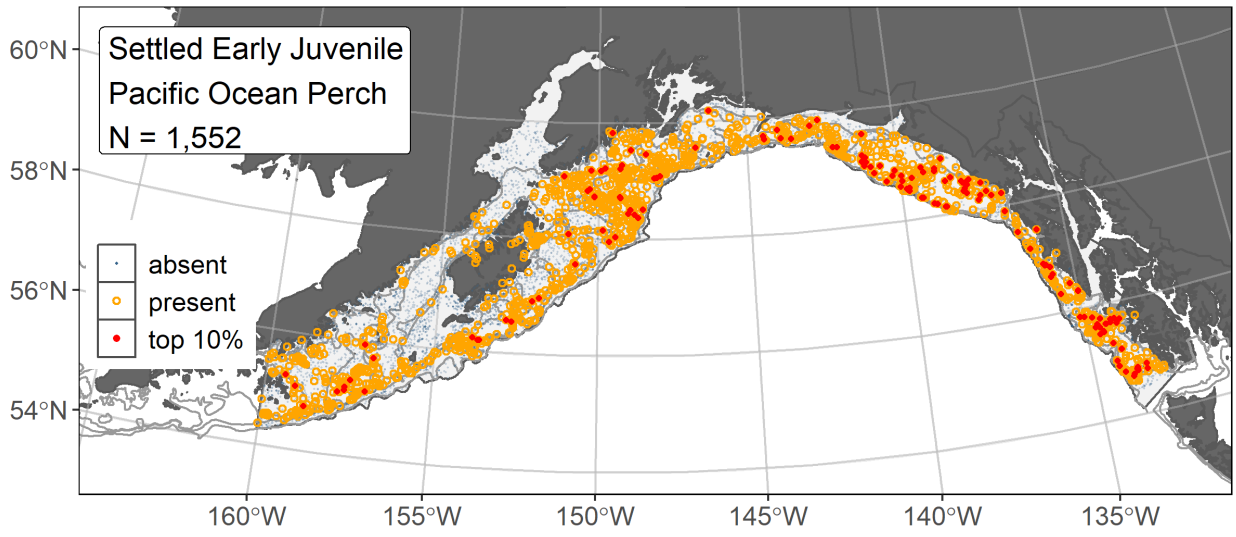

Figure 164. -- Distribution of settled early juvenile Pacific ocean perch catches (N = 1,552) in mixed gear-type summer surveys of the Gulf of Alaska (1989–2019) with the 100 m, 200 m, and 700 m isobaths indicated; filled red circles indicate locations in top 10% of overall abundance, open orange circles indicate presence in remaining catches, and blue dots indicate stations sampled where the animals were not present.

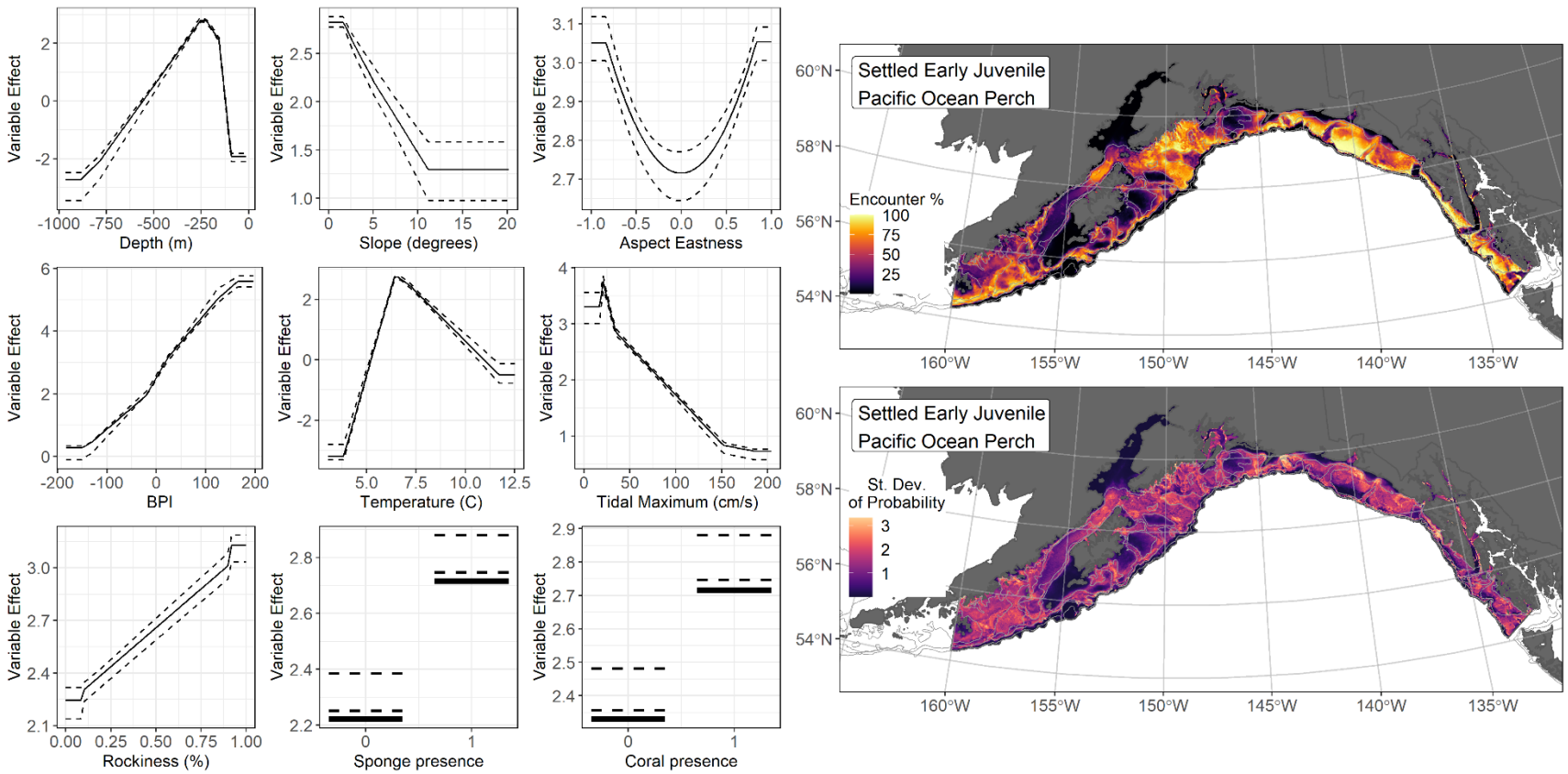

Figure 165. -- The top nine covariate effects (left panel) from a habitat-related species distribution model (MaxEnt) of settled early juvenile Pacific ocean perch probability of suitable habitat in the Gulf of Alaska (upper right panel) with the standard deviation of the probability predictions (lower right panel).

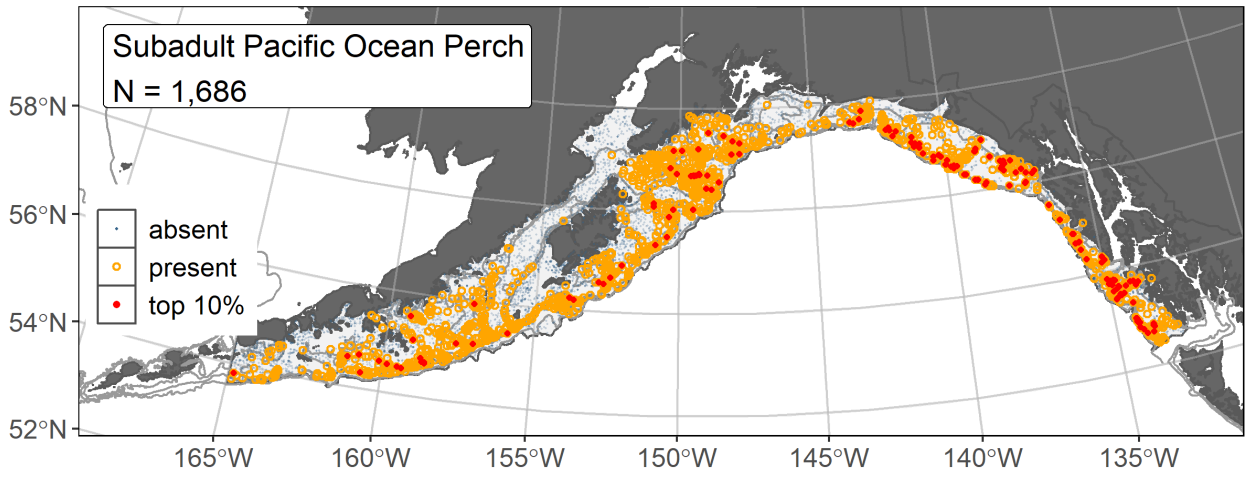

Figure 166. -- Distribution of subadult Pacific ocean perch catches (N = 1,686) in 1993–2019 AFSC RACE-GAP summer bottom trawl surveys of the Gulf of Alaska with the 100 m, 200 m, and 700 m isobaths indicated; filled red circles indicate locations in top 10% of overall abundance, open orange circles indicate presence in remaining catches, and blue dots indicate stations sampled where the animals were not present.

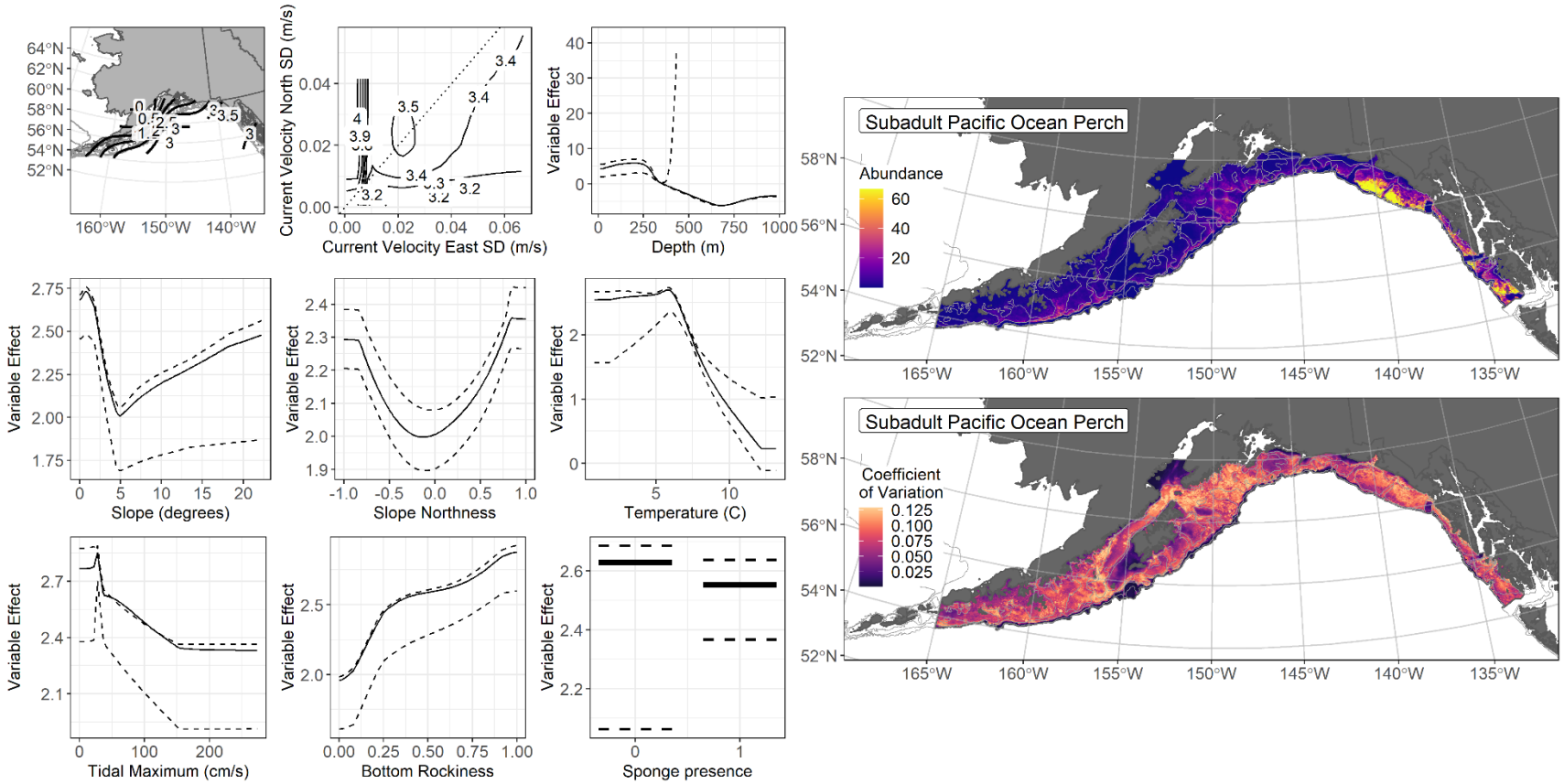

Figure 167. -- The top nine covariate effects (left panel) on ensemble-predicted subadult Pacific ocean perch numerical abundance across the Gulf of Alaska (upper right panel) along with the coefficient of variation (CV) of the ensemble predictions (lower right panel).

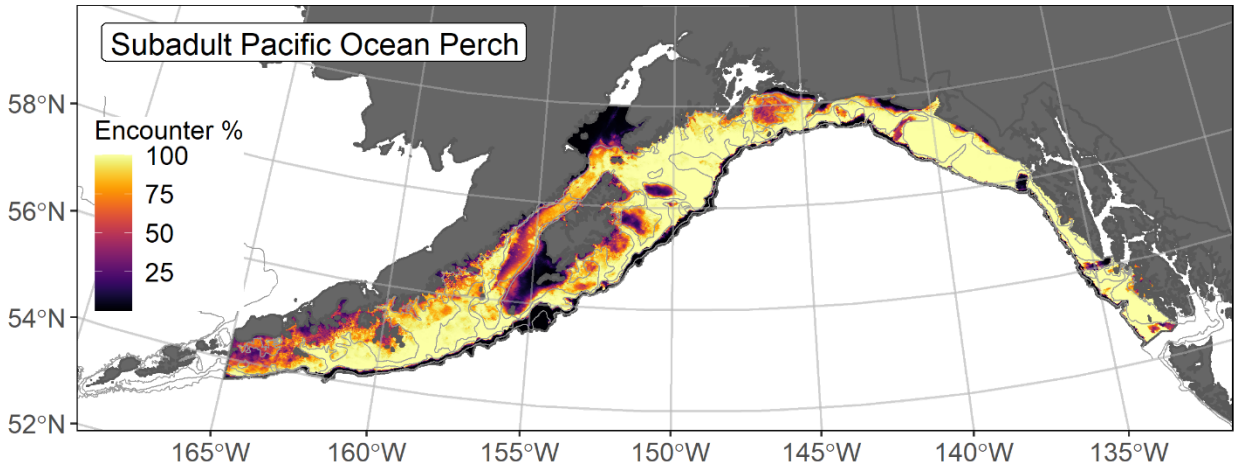

Figure 168. -- Encounter probability of subadult Pacific ocean perch from AFSC RACE-GAP summer bottom trawl surveys (1993–2019) of the Gulf of Alaska with the 100 m, 200 m, and 700 m isobaths indicated.

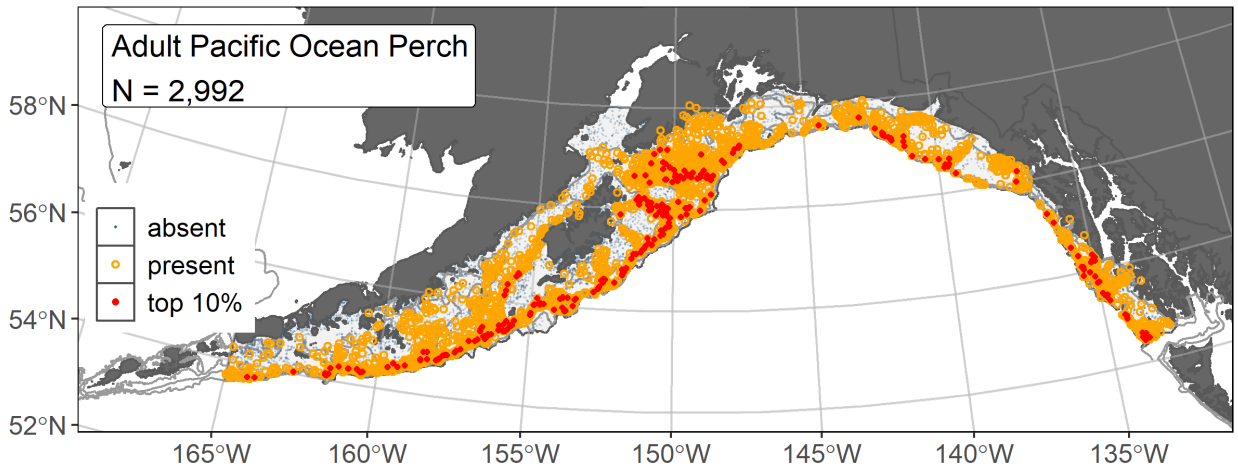

Figure 169. -- Distribution of adult Pacific ocean perch catches (N = 2,992) in 1993–2019 AFSC RACE-GAP summer bottom trawl surveys of the Gulf of Alaska with the 100 m, 200 m, and 700 m isobaths indicated; filled red circles indicate locations in top 10% of overall abundance, open orange circles indicate presence in remaining catches, and blue dots indicate stations sampled where the animals were not present.

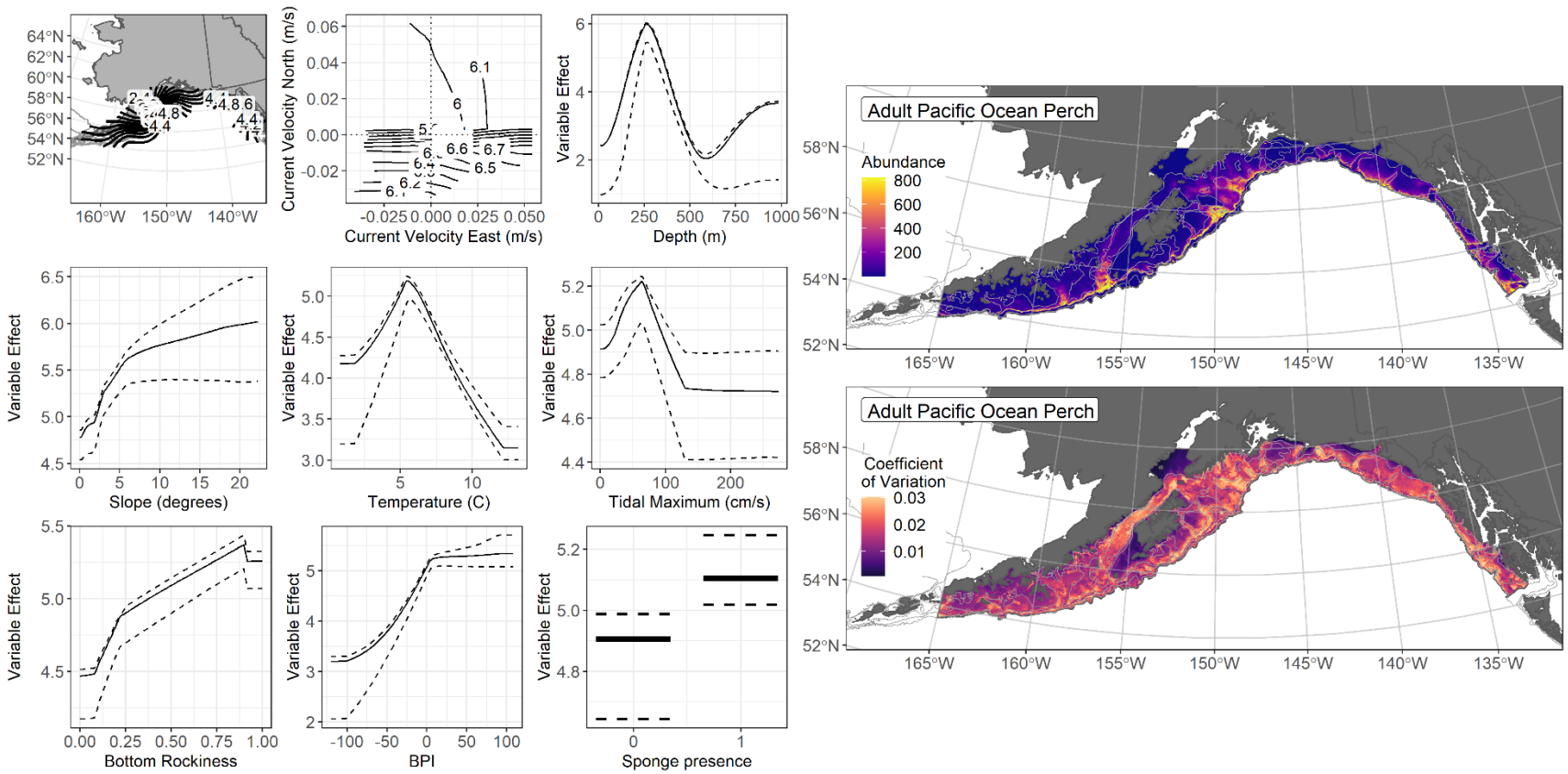

Figure 170. -- The top nine covariate effects (left panel) on ensemble-predicted adult Pacific ocean perch numerical abundance across the Gulf of Alaska (upper right panel) along with the coefficient of variation (CV) of the ensemble predictions (lower right panel).

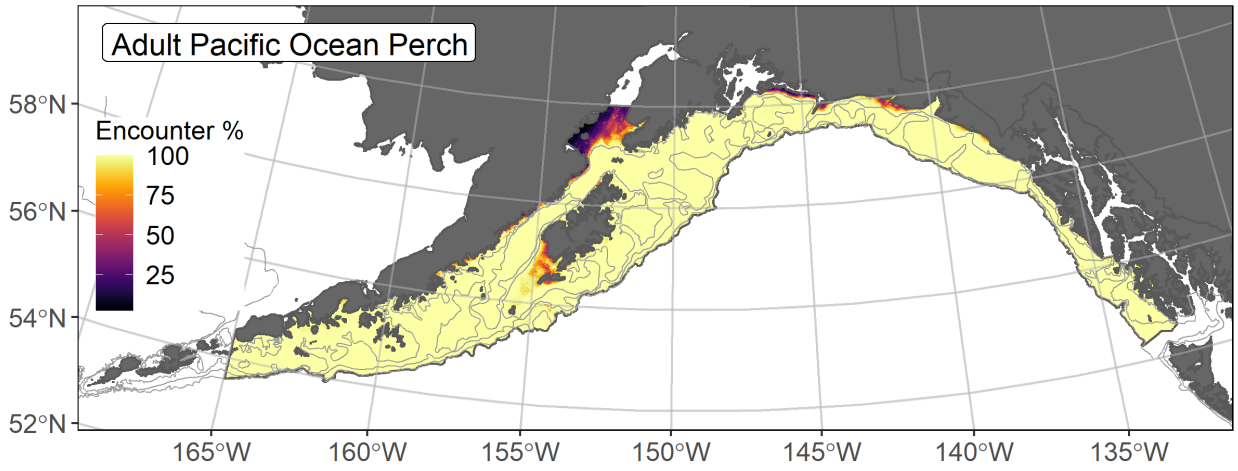

Figure 171. -- Encounter probability of adult Pacific ocean perch from AFSC RACE-GAP summer bottom trawl surveys (1993–2019) of the Gulf of Alaska with the 100 m, 200 m, and 700 m isobaths indicated.

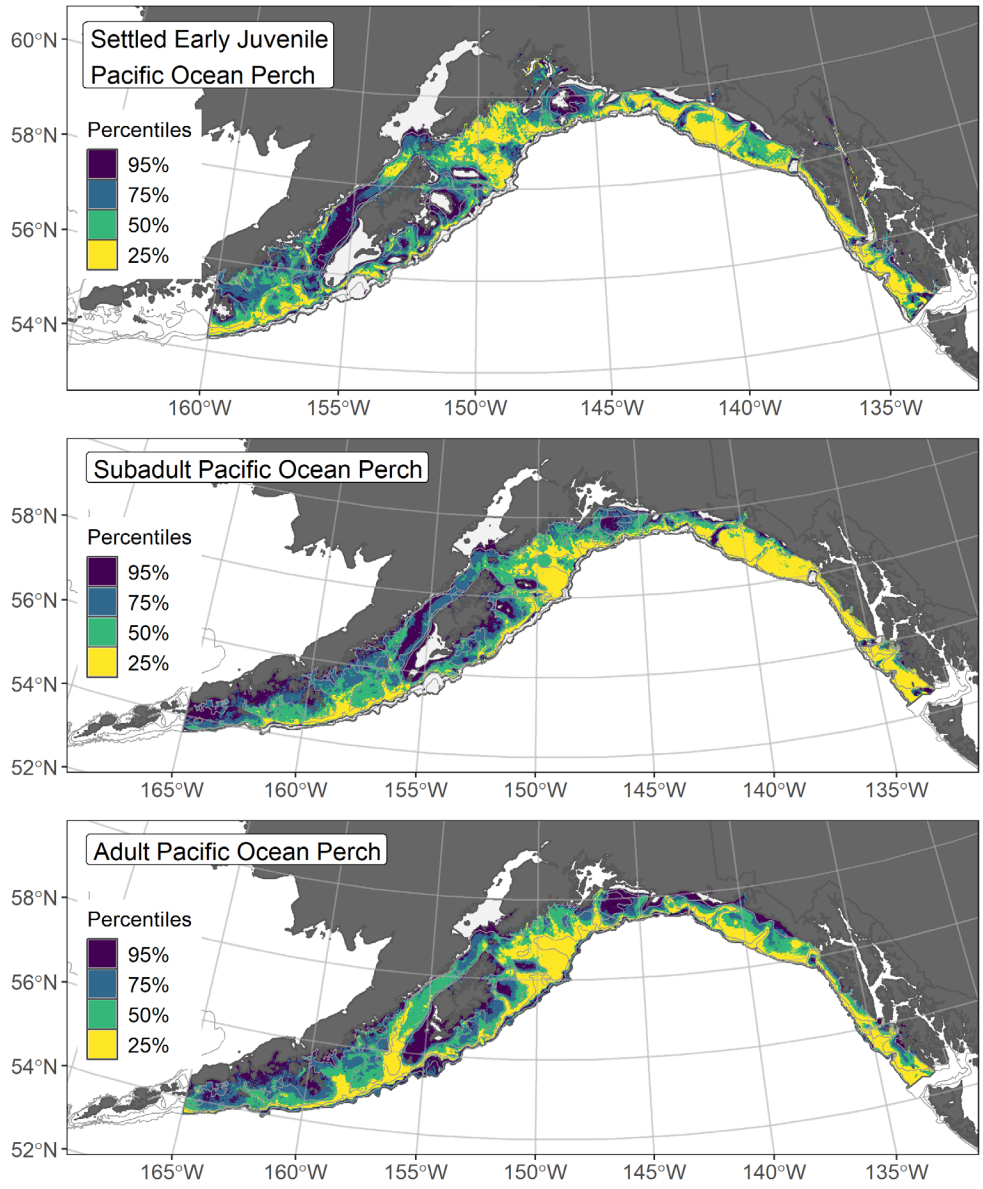

Figure 172. -- Essential fish habitat (EFH) is the area containing the top 95% of occupied habitat (defined as greater than 5% predicted probability of suitable habitat) for settled early juvenile (top panel) Pacific ocean perch (POP) from an SDM fitted to their distribution in Gulf of Alaska (GOA) mixed gear-type summer surveys (1989–2019), and for subadults (middle panel) and adults (bottom panel) is the area containing the top 95% of occupied habitat (defined as model estimated encounter probabilities greater than 5%) from an SDM ensemble fitted to POP distribution and abundance in AFSC RACE-GAP GOA summer bottom trawl surveys (1993–2019) with 100 m, 200 m, and 700 m isobaths indicated; within the EFH area map are the subareas of the top 25% (EFH hot spots), top 50% (core EFH area), and top 75% (principal EFH area).

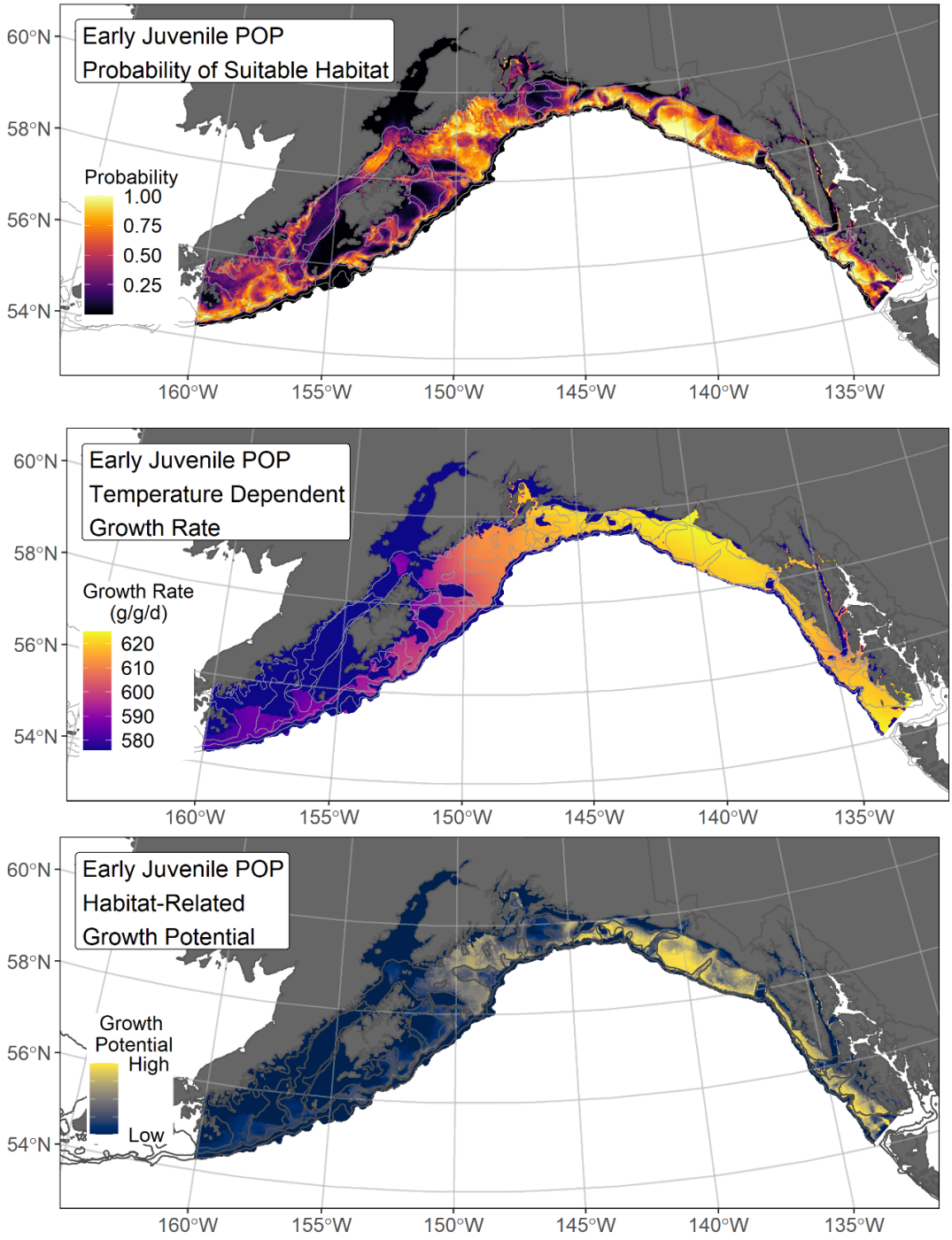

Figure 173. -- Settled early juvenile Pacific ocean perch predicted probability of suitable habitat from a habitat-related species distribution model fitted to their distribution in Gulf of Alaska mixed gear-type summer surveys (1989–2019; top panel), temperature-dependent growth rate ($GR = \%\ body\ weight\ (g) \cdot day^{-1}$; center panel), and EFH Level 3 map of habitat-related growth potential (bottom panel), which is the raster product of probability of suitable habitat and temperature-dependent growth rate.

Shortraker rockfish (*Sebastes borealis*)

Shortraker rockfish (*Sebastes borealis*) range from Japan to California, including the Bering Sea (Allen and Smith 1988, Love et al. 2002, Mecklenburg et al. 2002). This species is one of the largest and longest-lived rockfishes, reaching maturity in the GOA at 499 mm (Conrath 2017) and attaining a maximum length of 1,200 mm and age greater than 150 years (Mecklenberg et al. 2002), though no data exist on the timing of early juvenile settlement into demersal habitats and few individuals less than 350 mm have been caught in the GOA (Echave and Hulson 2019). Adults are most abundant in the GOA between 300 and 500 m depth and occur infrequently from 25 to 1,200 m depth (Ito 1999, Mecklenburg et al. 2002). This species likely prefers habitats of steeply sloping terrain with boulders, where they associate with structure, including *Primnoa* spp. corals (Krieger and Ito 1999, Krieger and Wing 2002, Rooper and Martin 2012)[32]. Shortraker rockfish have been managed as a single species stock in the GOA groundfish FMP since 2010 (Echave and Hulson 2019).

Subadult shortraker rockfish abundance and predicted distribution from RACE-GAP summer bottom trawl surveys in the Gulf of Alaska -- Subadult shortraker rockfish (N = 316) caught in GOA RACE-GAP summer bottom trawl surveys (1993–2019) occurred from Yakutat Trough through the western GOA (Fig. 174). Four of the five SDMs considered for inclusion in the ensemble to predict numerical abundance of subadult shortraker rockfish in the GOA converged (Table 59); the GAM_P was eliminated by skill testing. The remaining three best-performing constituent SDMs were weighted by RMSE in the final ensemble, which attained an excellent overall fit to the observed subadult shortraker rockfish distribution and abundance data. The ensemble was good at predicting high and low abundance catches (ρ = 0.45), and excellent at discriminating presence-absence (AUC = 0.99) and explaining deviance (PDE = 0.77). Bottom depth alone accounted for 70.3% of the covariate contribution to the deviance explained by the final ensemble, although other covariates contributed (Table 60). Higher subadult shortraker rockfish abundance was predicted to peak around 375 m depth, occurring over a relatively narrow depth range that included the outer extent of glacial troughs on the continental shelf and areas along the continental slope of the GOA (Fig. 175). The CV of ensemble predictions was higher in glacial troughs on the GOA continental shelf and areas along the continental slope. The probability of encountering subadult shortraker rockfish was highest along the GOA continental slope (Fig. 176).

Adult shortraker rockfish abundance and predicted distribution from RACE-GAP summer bottom trawl surveys in the Gulf of Alaska -- Adult shortraker rockfish (N = 679) caught in GOA

[32] A recommendation from the stock author review to incorporate longline survey data in future SDM ensemble EFH mapping for this species will be included as a research recommendation from the 2023 EFH 5-year Review.

RACE-GAP summer bottom trawl surveys (1993–2019) were distributed from southeast Alaska through the western GOA (Fig. 177). Five SDMs considered for inclusion in the ensemble to predict numerical abundance of adult shortraker rockfish in the GOA converged (Table 59); the GAM_{nb} was eliminated by skill testing. The remaining four best-performing constituent SDMs were weighted by RMSE in the final ensemble, which attained an excellent overall fit to the observed adult shortraker rockfish distribution and abundance data. The ensemble was good at predicting high and low abundance catches ($\rho = 0.47$), and excellent at discriminating presence-absence (AUC = 0.97) and explaining deviance (PDE = 0.73). Bottom depth, bottom current speed, and geographic location accounted for 78.5% of the covariate contribution to the deviance explained by the final ensemble (Table 60). Higher adult shortraker rockfish abundance was predicted to peak around 375 m depth along increasingly sloping terrain with relatively moderate bottom current exposure, within a relatively narrow depth range that included the outer extent of glacial troughs on the continental shelf and areas along the continental slope of the GOA (Fig. 178), similar to subadults. The CV of ensemble predictions was higher in glacial troughs on the GOA continental shelf and areas along the continental slope. Areas with the greatest predicted encounter probability were very similar to areas of predicted high abundance (Fig. 179).

Essential Fish Habitat of subadult and adult shortraker rockfish in the Gulf of Alaska -- Ensemble-predicted habitat-related numerical abundance of shortraker rockfish life stages collected in RACE-GAP summer bottom trawl surveys of the GOA (1993–2019) was mapped as EFH areas and subareas (Fig. 180). Shortraker rockfish EFH for subadults and adults occurred primarily within a relatively narrow depth range along the continental slope of the GOA. EFH was also within the glacial troughs on the continental shelf, particularly for adults. Core EFH area and EFH hot spots were extensive throughout the total EFH area for this species.

Table 59. -- Constituent species distribution models (SDMs) used to construct Essential Fish Habitat (EFH) for a) subadult and b) adult shortraker rockfish: MaxEnt = Maximum entropy; paGAM = presence-absence generalized additive model; hGAM = zero-adjusted Poisson hurdle GAM; GAM_P = standard Poisson GAM; GAM_{nb} = standard negative-binomial GAM; RMSE = root mean square error; ρ (rho) = Spearman's rank correlation coefficient; AUC = area under the receiver-operating characteristic curve; and PDE = Poisson deviance explained *. The "--" indicates that this model was not included in the final ensemble.

a) subadult shortraker rockfish

Models	RMSE	Relative Weight	ρ	AUC	PDE	EFH area (km^2)
MaxEnt	--	--	--	--	--	--
paGAM	1.47	0.36	0.43	0.98	0.69	25,700
hGAM	1.56	0.32	0.45	0.98	0.66	25,300
GAM_P	1.58	0	--	--	--	--
GAM_{nb}	1.58	0.32	0.47	0.98	0.66	19,700
ensemble	1.39	1	0.45	0.99	0.77	24,800

b) adult shortraker rockfish

Models	RMSE	Relative Weight	ρ	AUC	PDE	EFH area (km^2)
MaxEnt	9.64	0.24	0.51	0.97	0.54	38,100
paGAM	8.58	0.31	0.45	0.97	0.62	79,700
hGAM	11.96	0.16	0.41	0.97	0.35	57,100
GAM_P	8.72	0.30	0.47	0.96	0.60	58,200
GAM_{nb}	12.03	0	--	--	--	--
ensemble	7.62	1	0.47	0.97	0.73	65,200

* Refer to the Species Distribution Model Performance Metrics subsection within the Statistical Modeling section of the Methods for detailed descriptions of individual model performance metrics.

Table 60. -- Covariates retained in the a) subadult and b) adult shortraker rockfish species distribution model (SDM) final ensembles, the percent contribution to the ensemble deviance explained by each covariate, and the cumulative deviance explained: SD = standard deviation and BPI = bathymetric position index.

shortraker rockfish

	Covariate	% Contribution	Cumulative %
a) subadult	bottom depth	70.3	70.3
	location	6.7	77.0
	current	6.0	83.0
	current SD	4.0	87.0
	aspect north	3.2	90.2
	aspect east	2.4	92.6
	BPI	1.8	94.4
	bottom temperature	1.7	96.1
	tidal maximum	1.2	97.3
	sponge presence	0.7	98.0
	slope	0.6	98.6
	coral presence	0.6	99.2
	curvature	0.6	99.8
	pennatulacean presence	0.2	100.0
b) adult	bottom depth	64.4	64.4
	current	8.7	73.1
	location	5.4	78.5
	slope	5.1	83.6
	tidal maximum	4.5	88.1
	current SD	4.0	92.1
	BPI	2.0	94.1
	bottom temperature	1.4	95.5
	aspect north	1.1	96.6
	aspect east	1.0	97.6
	rockiness	0.8	98.4
	curvature	0.6	99.0
	coral presence	0.4	99.4
	sponge presence	0.4	99.8
	pennatulacean presence	0.2	100.0

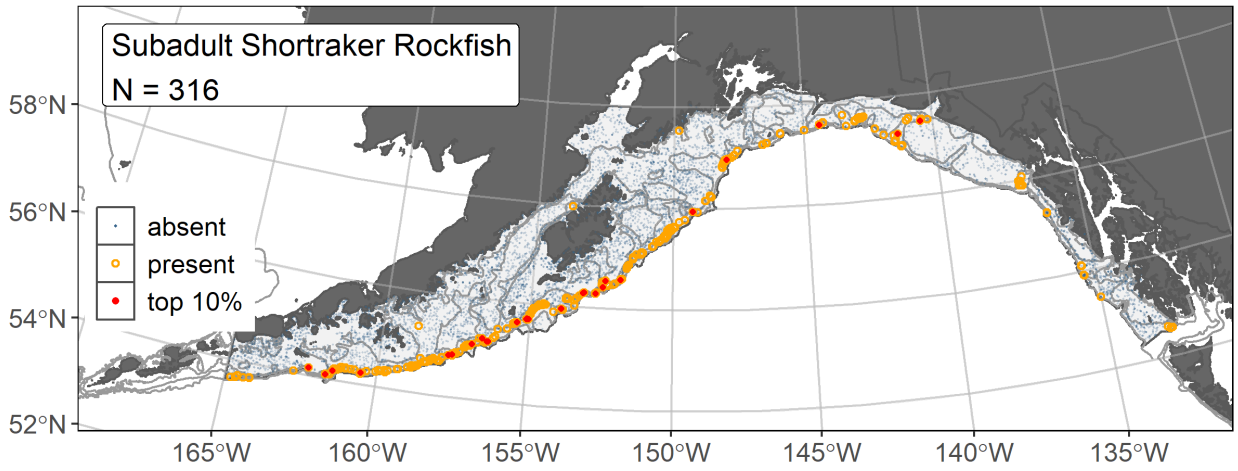

Figure 174. -- Distribution of subadult shortraker rockfish catches (N = 316) in 1993–2019 AFSC RACE-GAP summer bottom trawl surveys of the Gulf of Alaska with the 100 m, 300 m, and 700 m isobaths indicated; filled red circles indicate locations in top 10% of overall abundance, open orange circles indicate presence in remaining catches, and blue dots indicate stations sampled where the animals were not present.

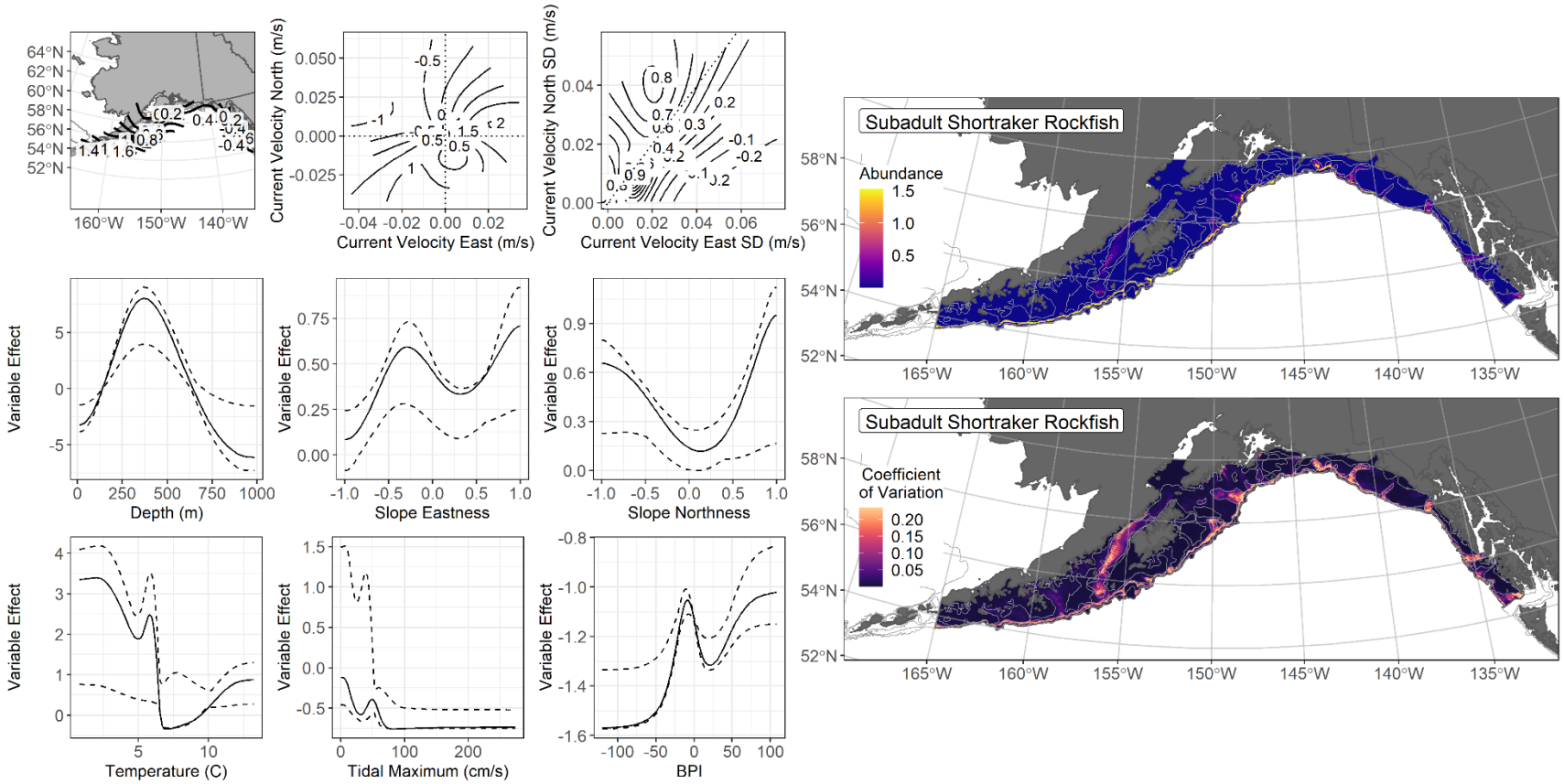

Figure 175. -- The top nine covariate effects (left panel) on ensemble-predicted subadult shortraker rockfish numerical abundance across the Gulf of Alaska (upper right panel) alongside the coefficient of variation (CV) of the ensemble predictions (lower right panel).

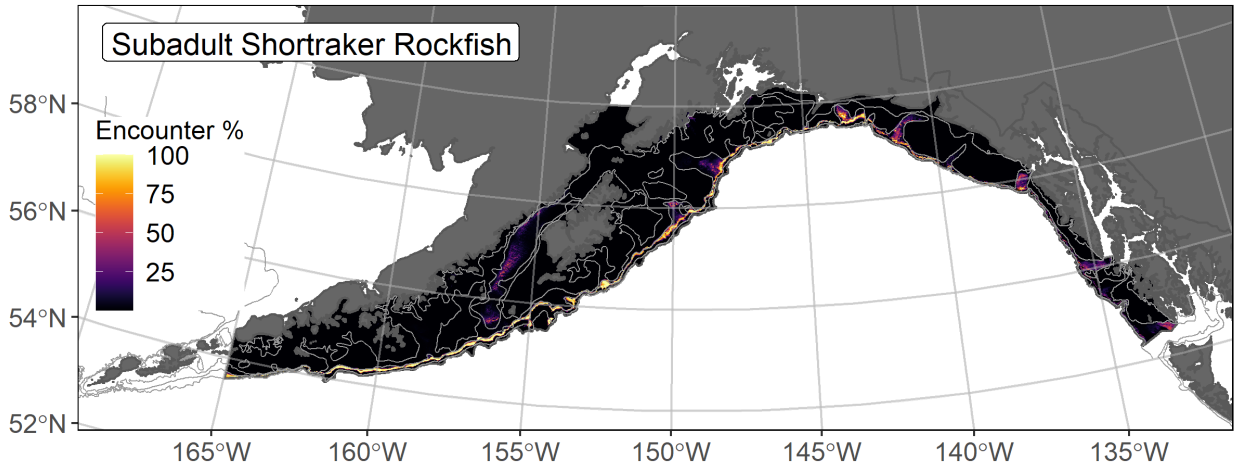

Figure 176. -- Encounter probability of subadult shortraker rockfish from AFSC RACE-GAP summer bottom trawl surveys (1993–2019) of the Gulf of Alaska with the 100 m, 300 m, and 700 m isobaths indicated.

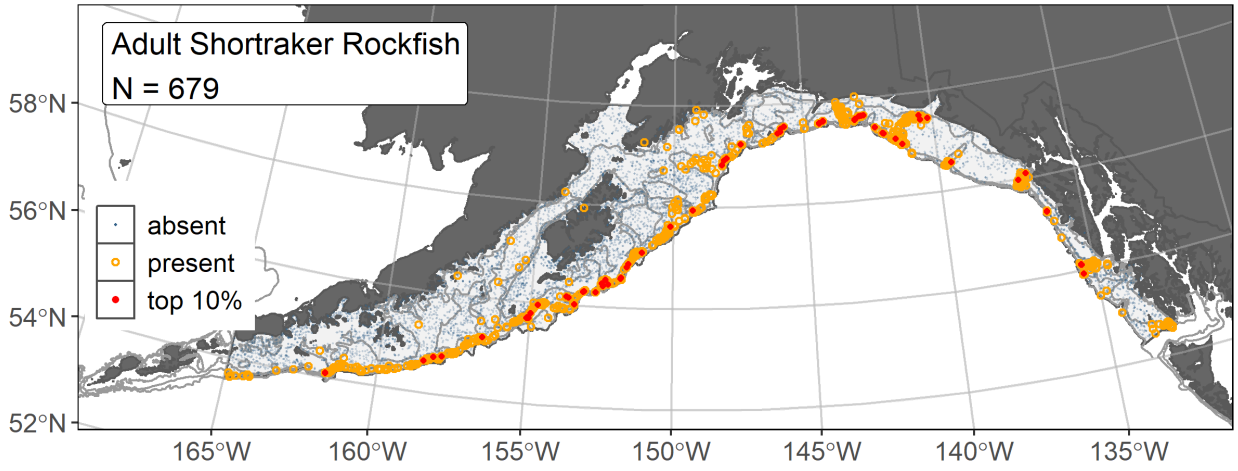

Figure 177. -- Distribution of adult shortraker rockfish catches (N = 679) in 1993–2019 AFSC RACE-GAP summer bottom trawl surveys of the Gulf of Alaska with the 100 m, 300 m, and 700 m isobaths indicated; filled red circles indicate locations in top 10% of overall abundance, open orange circles indicate presence in remaining catches, and blue dots indicate stations sampled where the animals were not present.

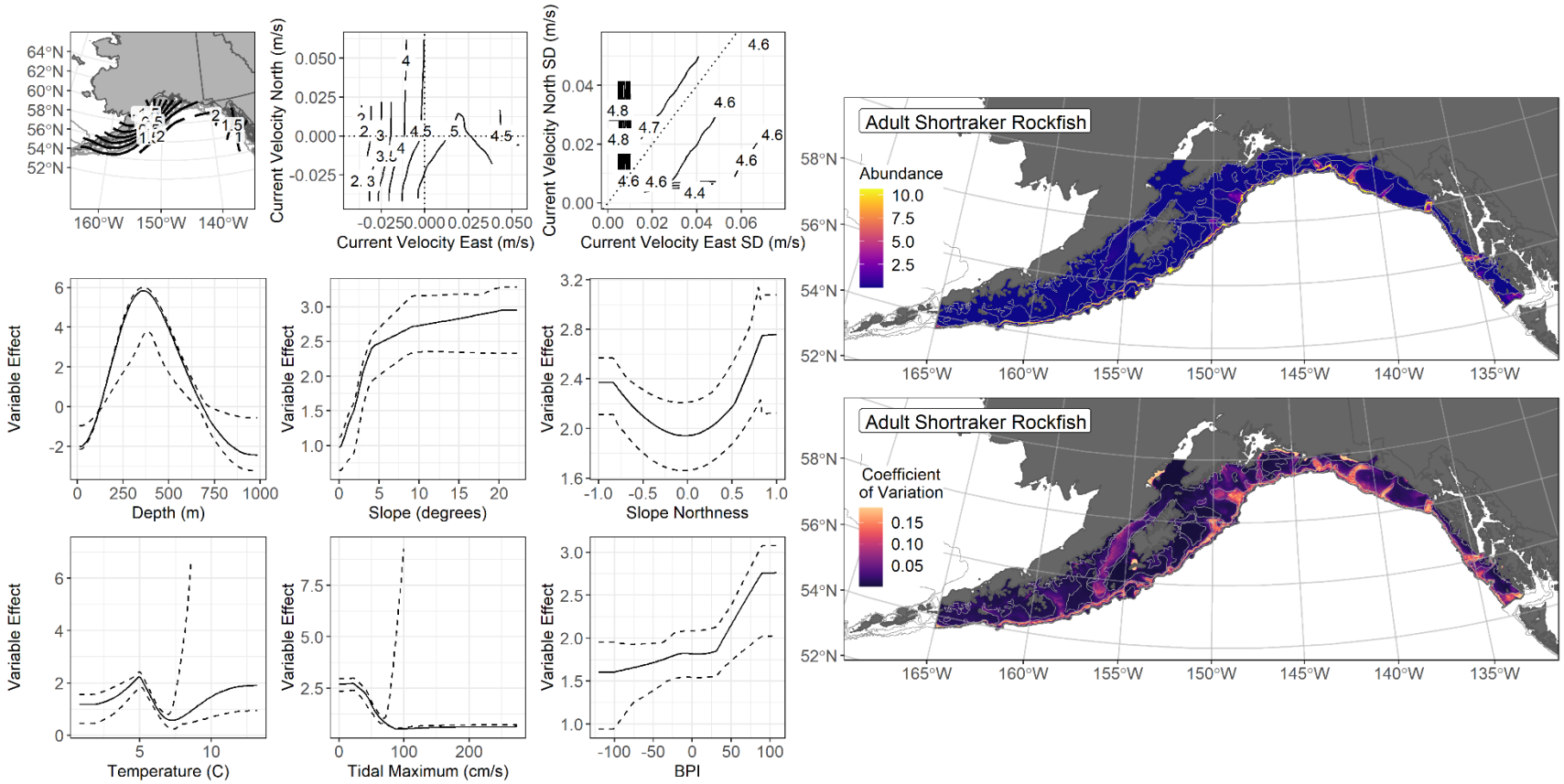

Figure 178. -- The top nine covariate effects (left panel) on ensemble-predicted adult shortraker rockfish numerical abundance across the Gulf of Alaska (upper right panel) alongside the coefficient of variation (CV) of the ensemble predictions (lower right panel).

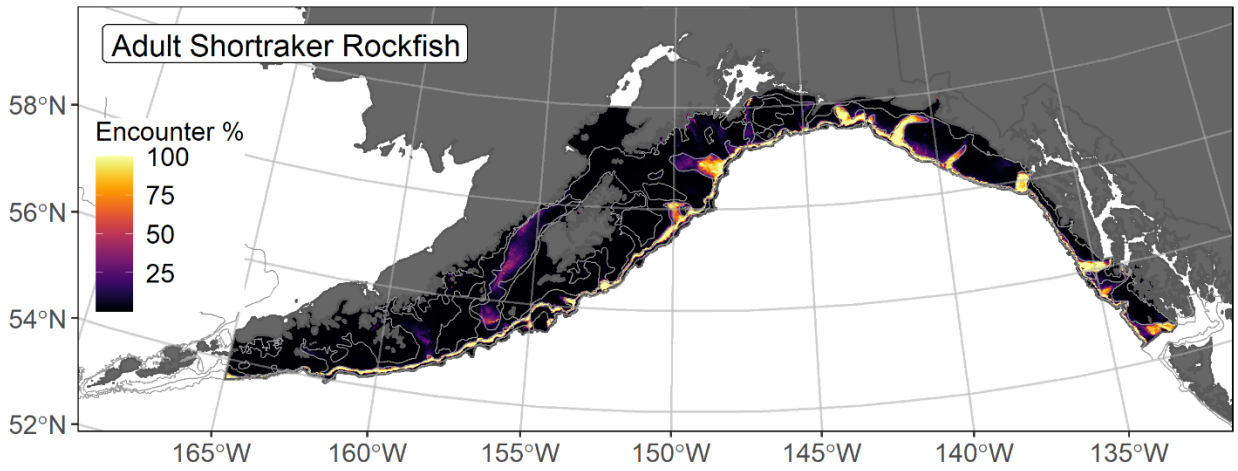

Figure 179. -- Encounter probability of adult shortraker rockfish from AFSC RACE-GAP summer bottom trawl surveys (1993–2019) of the Gulf of Alaska with the 100 m, 300 m, and 700 m isobaths indicated.

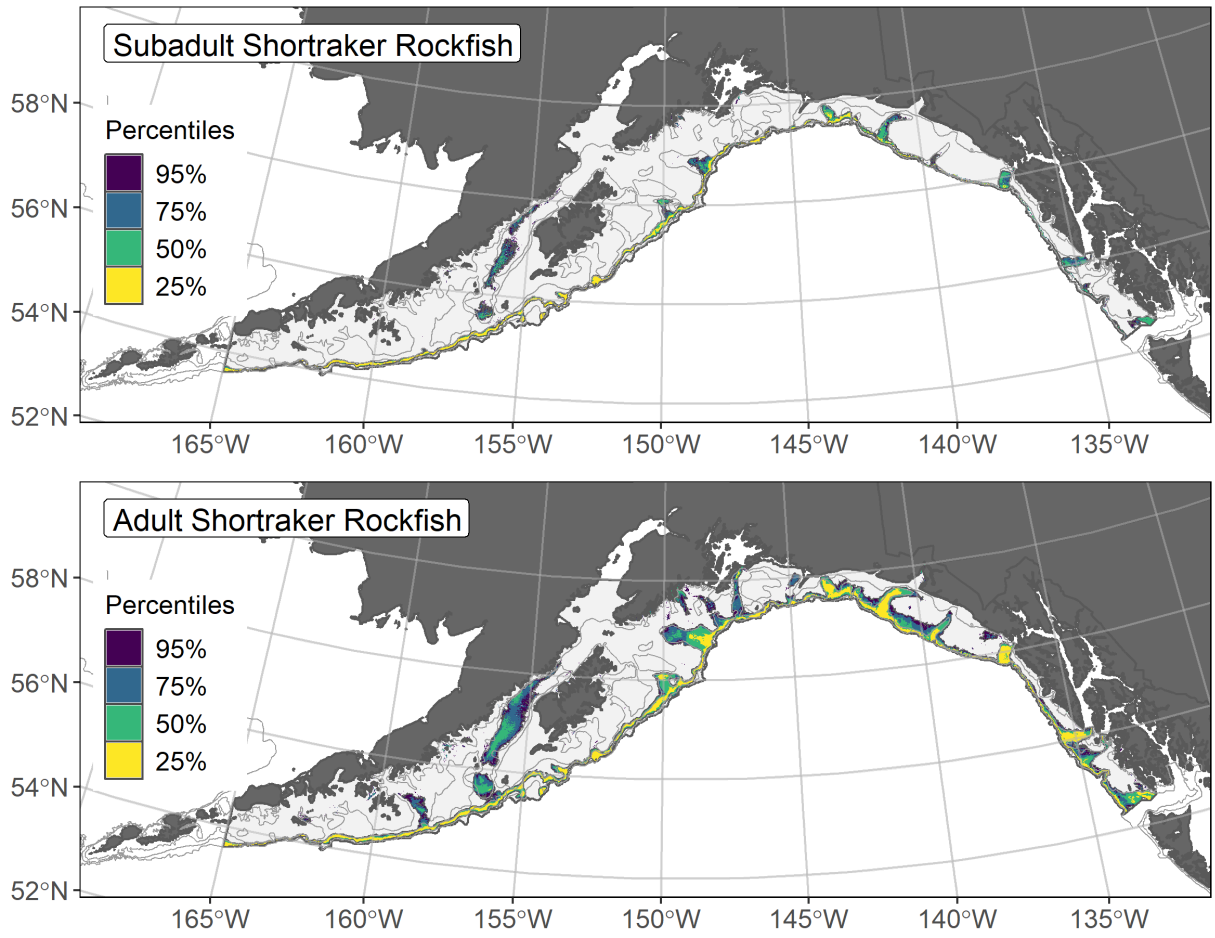

Figure 180. -- Essential fish habitat (EFH) is the area containing the top 95% of occupied habitat (defined as model estimated encounter probabilities greater than 5%) from an SDM ensemble fitted to subadult (top panel) and adult (bottom panel) shortraker rockfish distribution and abundance in AFSC RACE-GAP summer bottom trawl surveys (1993–2019) with 100 m, 200 m, and 700 m isobaths indicated; within the EFH area map are the subareas of the top 25% (EFH hot spots), top 50% (core EFH area), and top 75% (principal EFH area) of habitat-related, ensemble-predicted numerical abundance.

Rougheye / blackspotted rockfish complex

Rougheye rockfish (*Sebastes aleutianus*) and blackspotted rockfish (*S. melanostictus*) are distributed along the outer continental shelf and upper continental slope of the northeastern Pacific across the North Pacific from Japan to Point Conception, California and including the Bering Sea (Kramer and O'Connell 1988). The two species co-occur throughout their range and overlap extensively (Gharrett et al. 2005) though blackspotted rockfish extend farther into the western Aleutian Islands in Alaska (Orr and Hawkins 2008) than rougheye. Adults of these species co-inhabit a narrow depth band (300–500 m) along the upper continental slope in the Gulf of Alaska (Ito 1999)[33]. Recent work in the GOA allows us to separately model subadult and adult life stages of these two species using length at 50% maturity (L_{50} for blackspotted = 453 mm and L_{50} for rougheye = 450 mm; Conrath 2017). Due to high field misidentification rates, these two close congeners are presently managed as a two-species complex in the BSAI and GOA regions (Shotwell and Hanselman 2019).

Subadult rougheye / blackspotted rockfish complex abundance and distribution predicted from RACE-GAP summer bottom trawl surveys in the Gulf of Alaska -- Subadults of the rougheye / blackspotted rockfish complex (N = 2,178) caught in GOA RACE-GAP summer bottom trawl surveys (1993–2019) were distributed primarily from southeast Alaska through the western GOA (Fig. 181). Five SDMs considered for inclusion in the ensemble to predict numerical abundance of subadults in the GOA converged (Table 61); the GAM_{nb} was eliminated by skill testing. The remaining four best-performing SDMs were weighted by RMSE in the final ensemble, which attained an excellent overall fit to the observed subadult distribution and abundance data. The ensemble was excellent at predicting high and low abundance catches (ρ = 0.62) and discriminating presence-absence (AUC = 0.90), and good at explaining deviance (PDE = 0.57). Bottom depth, geographic location, and seafloor slope accounted for 77.4% of the covariate contribution to the deviance explained by the final ensemble (Table 62). Higher subadult abundance peaked around 300 m depth, including the glacial troughs on the continental shelf and a narrow depth range along the slope (Fig. 182). The CV of ensemble predictions was higher in the deeper areas of the GOA continental shelf and upper slope. Areas with higher predicted encounter probability were similar to areas of predicted high abundance in the GOA (Fig. 183).

[33] A recommendation from the stock author review to incorporate additional high quality sources of data (e.g., from longline surveys) in future SDM ensemble EFH mapping for this species will be included as a research recommendation from the 2023 EFH 5-year Review.

Adult rougheye / blackspotted rockfish complex abundance and distribution predicted from RACE-GAP summer bottom trawl surveys in the Gulf of Alaska -- Adults of the rougheye / blackspotted rockfish complex (N = 878) caught in GOA RACE-GAP summer bottom trawl surveys (1993–2019) were distributed from southeast Alaska through the western GOA, where the highest abundance catches occurred along the outer continental shelf and slope (Fig. 184). Five SDMs were considered for inclusion in the ensemble to predict numerical abundance of adults in the GOA (Table 61); the GAM_P was eliminated by skill testing. The remaining four best-performing SDMs were weighted nearly equally by RMSE in the final ensemble, which attained an excellent overall fit to the observed adult distribution and abundance data. The ensemble was good at predicting high and low abundance catches (ρ = 0.46), and excellent at discriminating presence-absence (AUC = 0.93) and explaining deviance (PDE = 0.70). Bottom depth, seafloor slope, and geographic location accounted for 84.1% of the covariate contribution to the deviance explained by the final ensemble, although other covariates contributed (Table 62). Higher adult abundance for these species was predicted to peak around 375 m depth and within a relatively small depth range that included the glacial troughs on the continental shelf and areas along the outer continental shelf and slope of the GOA (Fig. 185). The CV of ensemble predictions was higher in glacial troughs on the GOA continental shelf and areas along the continental slope. Areas with the greatest predicted encounter probability were very similar to areas of predicted high abundance (Fig. 186).

Essential Fish Habitat of rougheye / blackspotted rockfish complex in the Gulf of Alaska -- Ensemble-predicted habitat-related numerical abundance of rougheye / blackspotted rockfish life stages collected in RACE-GAP summer bottom trawl surveys of the GOA (1993–2019) was mapped as EFH areas and subareas Fig. 187). EFH area, including core EFH, for subadults was extensive throughout the GOA study area. Subadult EFH hot spots were prevalent in the glacial troughs on the GOA continental shelf and along the upper slope. Adult EFH area was smaller overall and limited to the glacial troughs, outer shelf, and upper slope of the GOA. EFH was also within the glacial troughs on the continental shelf, in particular for adults.

Table 61. -- Constituent species distribution models (SDMs) used to construct Essential Fish Habitat (EFH) for a) subadult and b) adult rougheye / blackspotted rockfish complex: MaxEnt = Maximum entropy; paGAM = presence-absence generalized additive model; hGAM = zero-adjusted Poisson hurdle GAM; GAM_P = standard Poisson GAM; GAM_{nb} = standard negative-binomial GAM; RMSE = root mean square error; ρ (rho) = Spearman's rank correlation coefficient; AUC = area under the receiver-operating characteristic curve; and PDE = Poisson deviance explained *. The "--" indicates that this model was not included in the final ensemble.

a) subadult rougheye / blackspotted rockfish complex

Models	RMSE	Relative Weight	ρ	AUC	PDE	EFH area (km^2)
MaxEnt	24.3	0.22	0.60	0.89	0.38	218,900
paGAM	23.3	0.24	0.61	0.90	0.47	268,700
hGAM	21.9	0.27	0.59	0.90	0.52	237,900
GAM_P	21.6	0.28	0.58	0.88	0.51	254,300
GAM_{nb}	48.8	0	--	--	--	--
ensemble	20.4	1	0.62	0.90	0.57	258,000

b) adult rougheye / blackspotted rockfish complex

Models	RMSE	Relative Weight	ρ	AUC	PDE	EFH area (km^2)
MaxEnt	10.9	0.25	0.45	0.93	0.62	127,500
paGAM	11.0	0.25	0.46	0.93	0.58	173,700
hGAM	11.0	0.25	0.45	0.93	0.63	88,700
GAM_P	10.9	0	--	--	--	--
GAM_{nb}	10.8	0.26	0.46	0.93	0.64	93,900
ensemble	9.9	1	0.46	0.93	0.70	128,700

* Refer to the Species Distribution Model Performance Metrics subsection within the Statistical Modeling section of the Methods for detailed descriptions of individual model performance metrics.

Table 62. -- Covariates retained in the a) subadult and b) adult rougheye / blackspotted rockfish complex species distribution model (SDM) final ensembles, the percent contribution to the ensemble deviance explained by each covariate, and the cumulative deviance explained: SD = standard deviation and BPI = bathymetric position index.

rougheye / blackspotted rockfish complex	**Covariate**	**% Contribution**	**Cumulative %**
a) subadult	bottom depth	48.1	48.1
	location	21.7	69.9
	slope	7.5	77.4
	current SD	4.4	81.8
	tidal maximum	4.0	85.8
	rockiness	3.0	88.8
	current	2.7	91.5
	aspect north	2.3	93.8
	coral presence	2.0	95.8
	sponge presence	1.1	96.9
	curvature	0.9	97.8
	aspect east	0.7	98.5
	bottom temperature	0.7	99.2
	BPI	0.7	99.9
	pennatulacean presence	0.1	100.0
b) adult	bottom depth	71.4	71.4
	slope	7.4	78.8
	location	5.3	84.1
	current	2.7	86.8
	rockiness	2.5	89.3
	current SD	2.4	91.7
	bottom temperature	2.0	93.7
	aspect east	1.2	94.9
	aspect north	1.2	96.1
	BPI	1.2	97.3
	curvature	1.1	98.4
	coral presence	0.6	99.0
	tidal maximum	0.5	99.5
	sponge presence	0.4	99.9
	pennatulacean presence	0.1	100.0

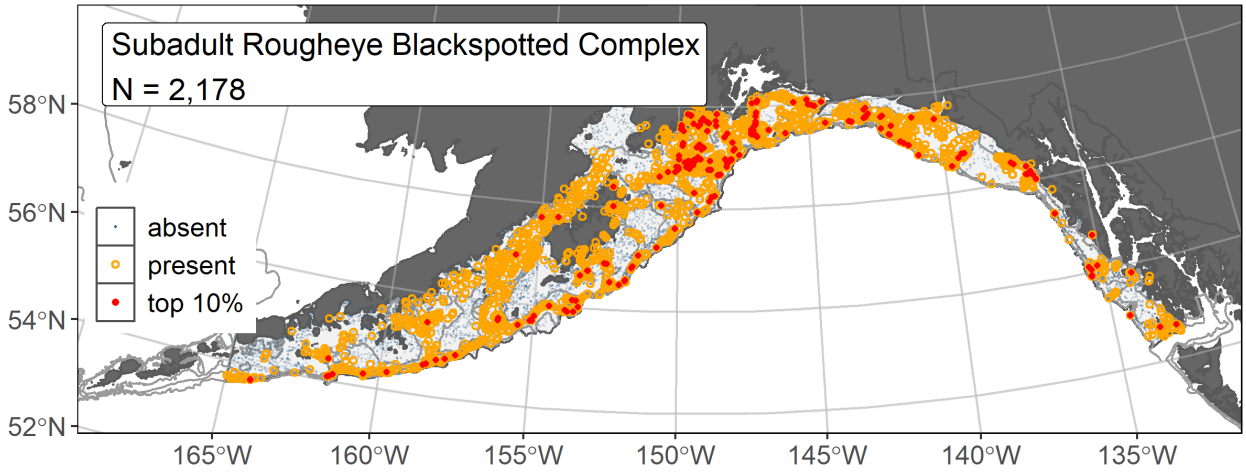

Figure 181. -- Distribution of subadult rougheye / blackspotted rockfish complex catches (N = 2,178) in 1993–2019 AFSC RACE-GAP summer bottom trawl surveys of the Gulf of Alaska with the 100 m, 300 m, and 700 m isobaths indicated; filled red circles indicate locations in top 10% of overall abundance, open orange circles indicate presence in remaining catches, and blue dots indicate stations sampled where the animals were not present.

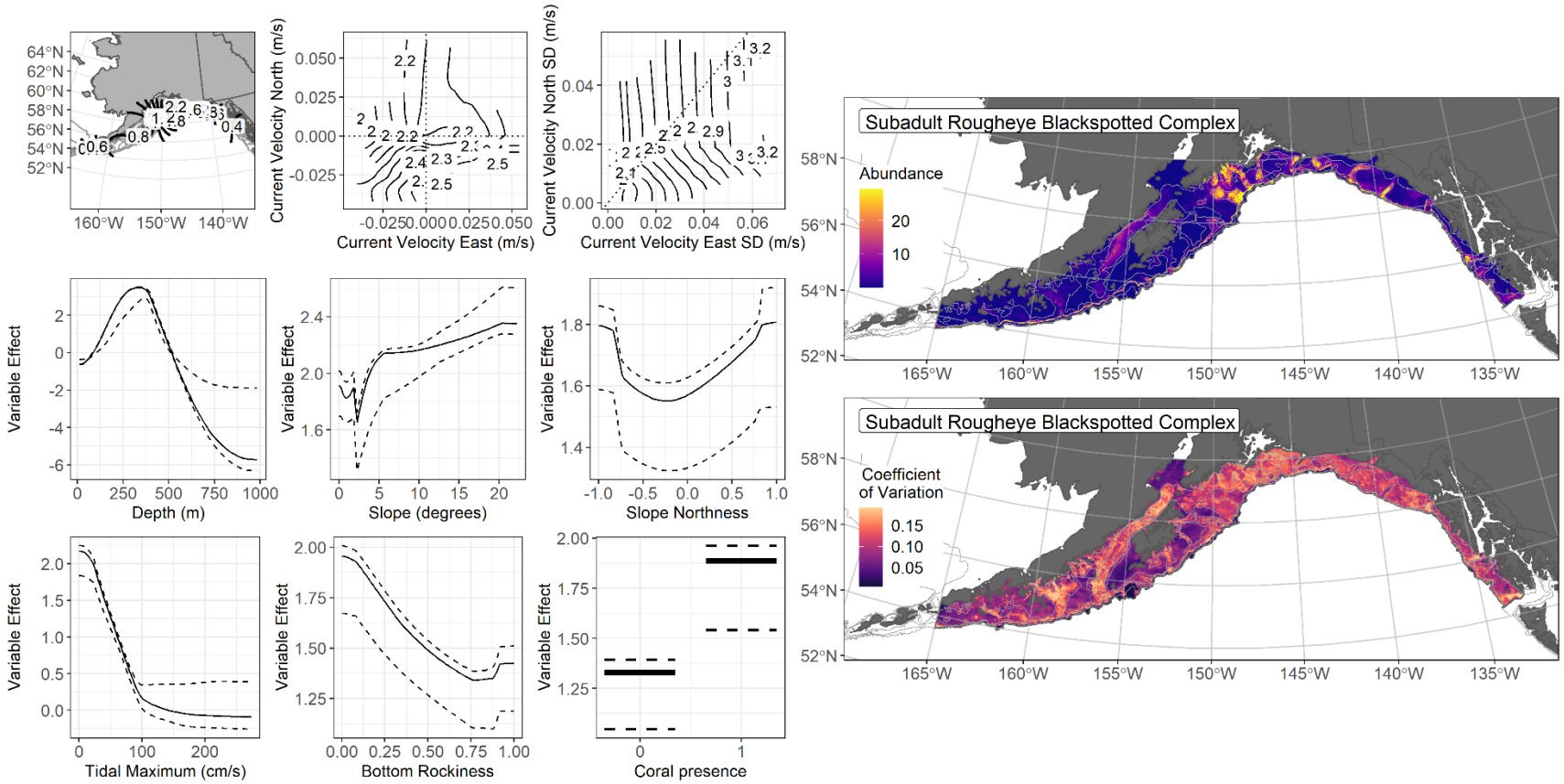

Figure 182. -- The top nine covariate effects (left panel) on ensemble-predicted subadult rougheye / blackspotted rockfish complex numerical abundance across the Gulf of Alaska (upper right panel) alongside the coefficient of variation of the ensemble predictions (lower right panel).

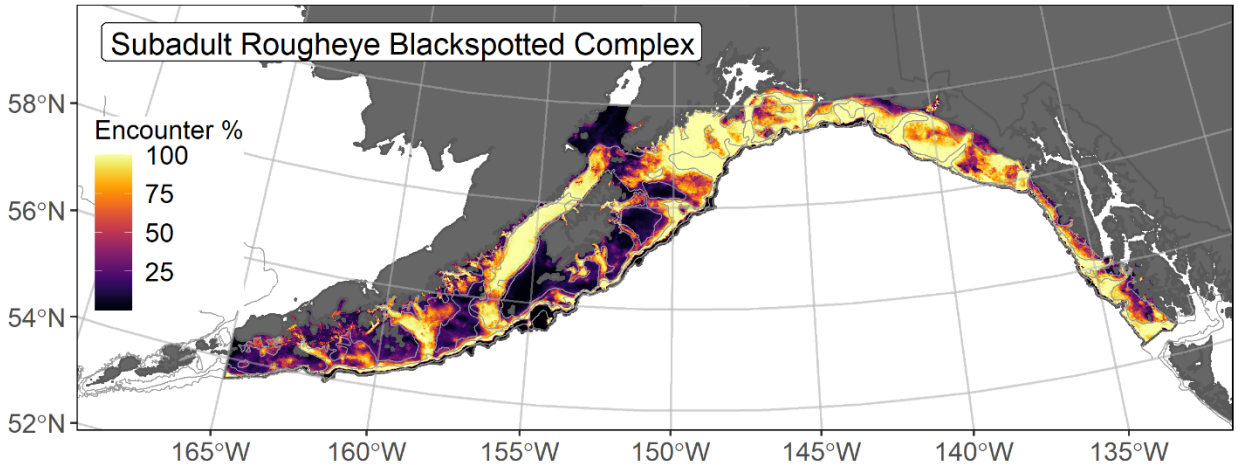

Figure 183. -- Encounter probability of subadult rougheye / blackspotted rockfish complex from AFSC RACE-GAP summer bottom trawl surveys (1993–2019) of the Gulf of Alaska with the 100 m, 300 m, and 700 m isobaths indicated.

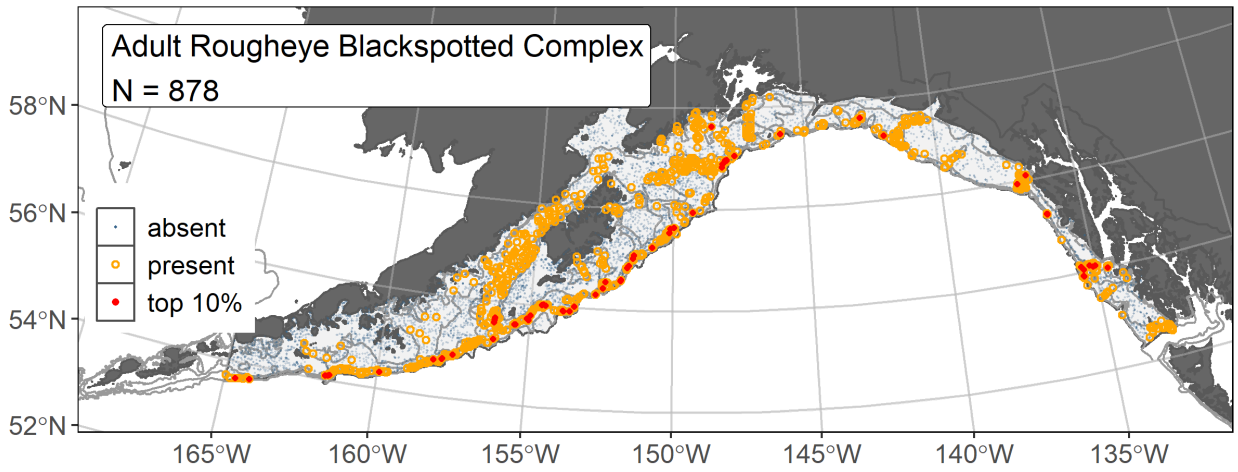

Figure 184. -- Distribution of adult rougheye / blackspotted rockfish complex catches (N = 878) in 1993–2019 AFSC RACE-GAP summer bottom trawl surveys of the Gulf of Alaska with the 100 m, 300 m, and 700 m isobaths indicated; filled red circles indicate locations in top 10% of overall abundance, open orange circles indicate presence in remaining catches.

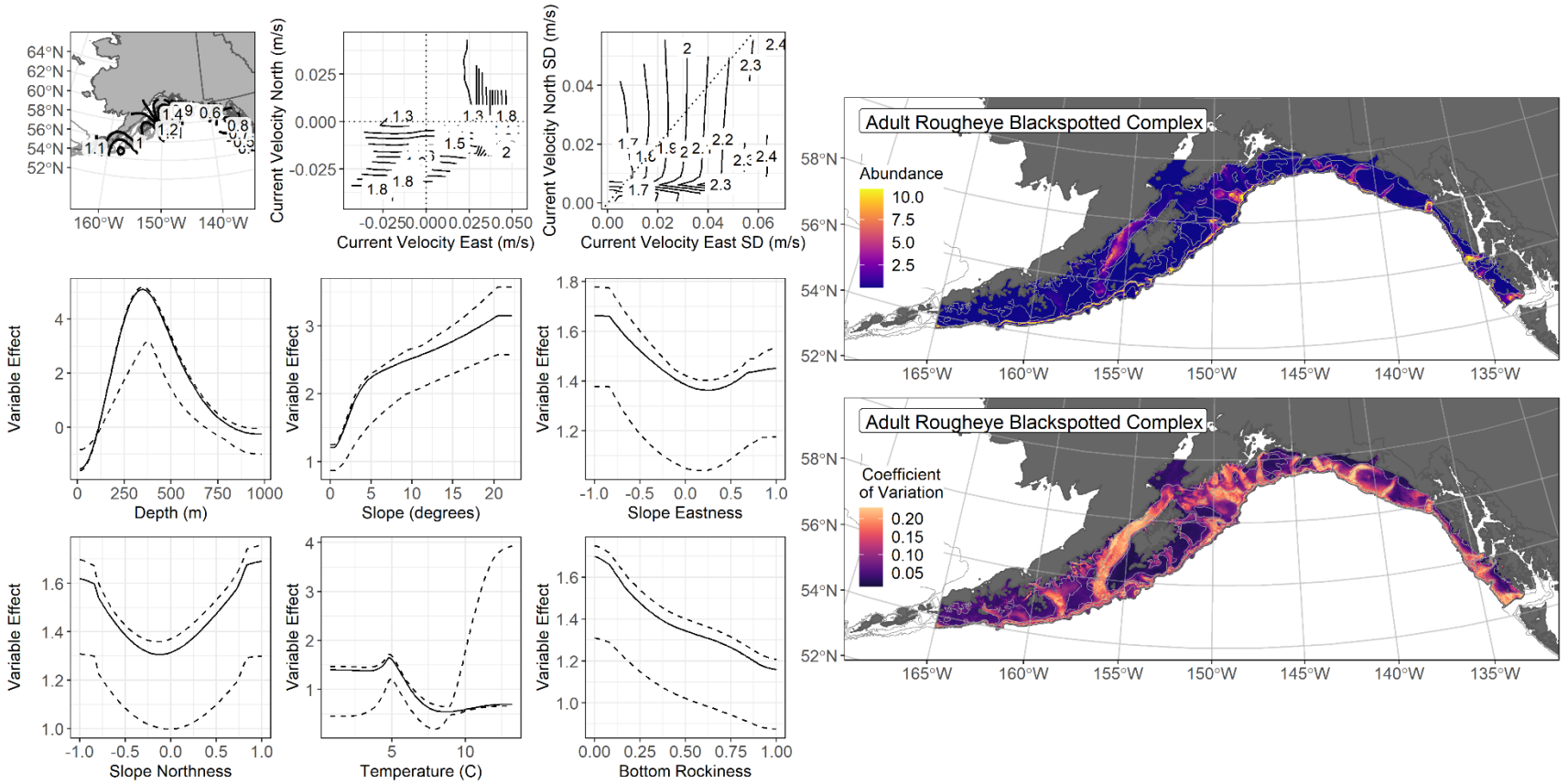

Figure 185. -- The top nine covariate effects (left panel) on ensemble-predicted adult rougheye / blackspotted rockfish complex numerical abundance across the Gulf of Alaska (upper right panel) alongside the coefficient of variation of the ensemble predictions (lower right panel).

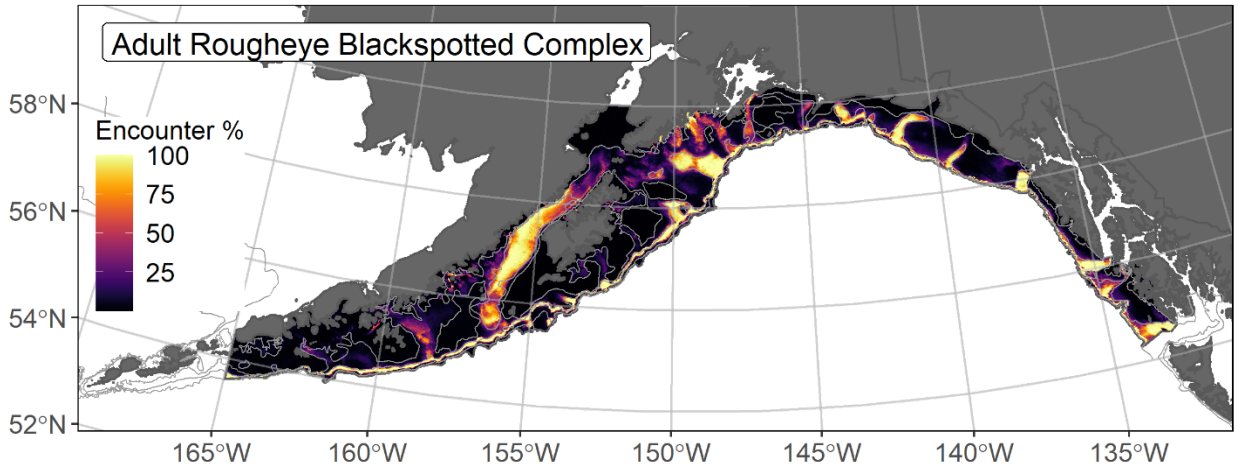

Figure 186. -- Encounter probability of adult rougheye / blackspotted rockfish complex from AFSC RACE-GAP summer bottom trawl surveys (1993–2019) of the Gulf of Alaska with the 100 m, 300 m, and 700 m isobaths indicated.

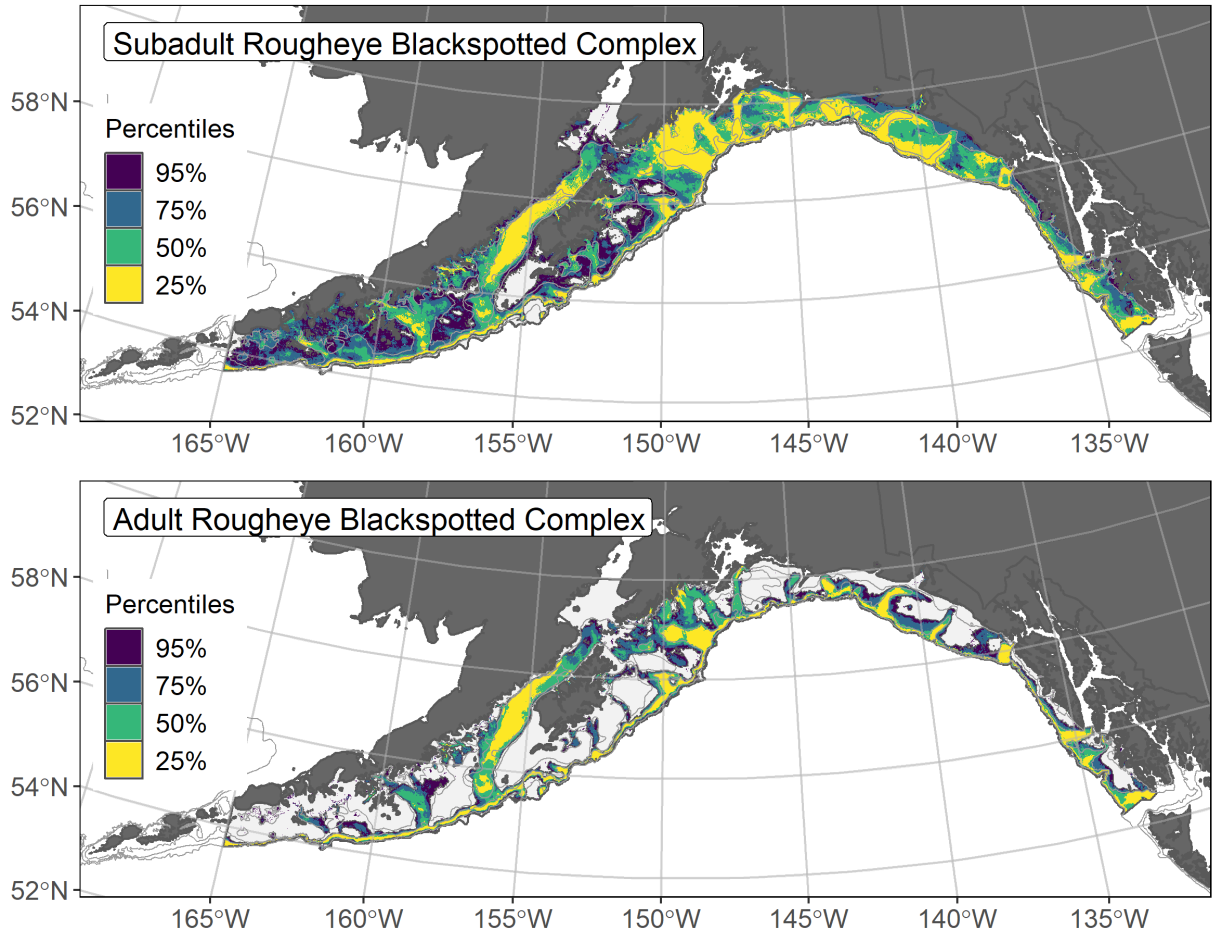

Figure 187. -- Essential fish habitat (EFH) is the area containing the top 95% of occupied habitat (defined as model estimated encounter probabilities greater than 5%) from an SDM ensemble fitted to subadult (top panel) and adult (bottom panel) rougheye / blackspotted rockfish complex distribution and abundance in AFSC RACE-GAP summer bottom trawl surveys (1993–2019) with 100 m, 200 m, and 700 m isobaths indicated; within the EFH area map are the subareas of the top 25% (EFH hot spots), top 50% (core EFH area), and top 75% (principal EFH area) of habitat-related, ensemble-predicted numerical abundance.

Other rockfish complex demersal sub-group

In the GOA, the Other Rockfish (OR) stock complex includes the demersal sub-group comprised of canary, China, copper, quillback, rosethorn, tiger, and yelloweye rockfishes (Tribuzio and Echave 2019). These seven species are managed as the Demersal Shelf Rockfish complex in some regions of the GOA and as the OR complex demersal sub-group in all other GOA management areas. While stocks are managed differently depending on the species (either across regions or at smaller scales), EFH is designated and mapped for each FMP species[34]. EFH of the demersal sub-group is mapped to the extent of the GOA-wide management area for the purpose of this study. In GOA RACE-GAP summer bottom trawl survey catches (1993–2019), quillback, rosethorn, and yelloweye rockfishes were common enough ($N > 50$) to support individual species life stage SDMs of habitat-related abundance to map EFH[35]. To map EFH of the demersal sub-group, the SDMs of the three species were combined to generate an additive composite maps of habitat-related abundance and EFH, which represents the EFH of sub-group species where an individual EFH map was not possible due to insufficient data[36].

Other rockfish complex demersal sub-group abundance and distribution predicted from RACE-GAP summer bottom trawl surveys in the Gulf of Alaska -- Habitat-related, ensemble-predicted numerical abundance was combined for the subadult and adult life stages of the three rockfish species to represent the demersal sub-group in the GOA and mapped along with the combined encounter probability and EFH (Fig. 188). The composite, ensemble-predicted abundance of the demersal sub-group reflects the higher abundance catches of these three species on the continental shelf of the eastern GOA. Encounter probabilities for the sub-group were higher in areas of predicted high abundance in the eastern GOA. The influence of yelloweye rockfish occurring further west is reflected as slightly elevated encounter probabilities for the sub-group in the central GOA south of the Kenai Peninsula and westward along the continental shelf break south of Kodiak and the Shumagin Islands.

Essential fish habitat of the other rockfish complex demersal sub-group in the Gulf of Alaska -- EFH of the demersal sub-group includes a large extent of the continental shelf of the eastern GOA with additional, patchy areas in the central GOA south of the Kenai Peninsula, Kodiak Island, and the Shumagin Islands (Fig. 188). Core EFH encompassed most of the total EFH area, and EFH hot spots primarily occur in the eastern and central GOA for the demersal sub-group.

---

[34] 50 CFR 600.815(a)(1)(i)
[35] A recommenation from the stock author review to incorporate additional high quality sources of data (e.g., from ROV surveys of untrawlable habitats) in future SDM ensemble EFH mapping for these species will be included as a research recommendation from the 2023 EFH 5-year Review.
[36] 50 CFR 600.815(a)(1)(iv)(E)

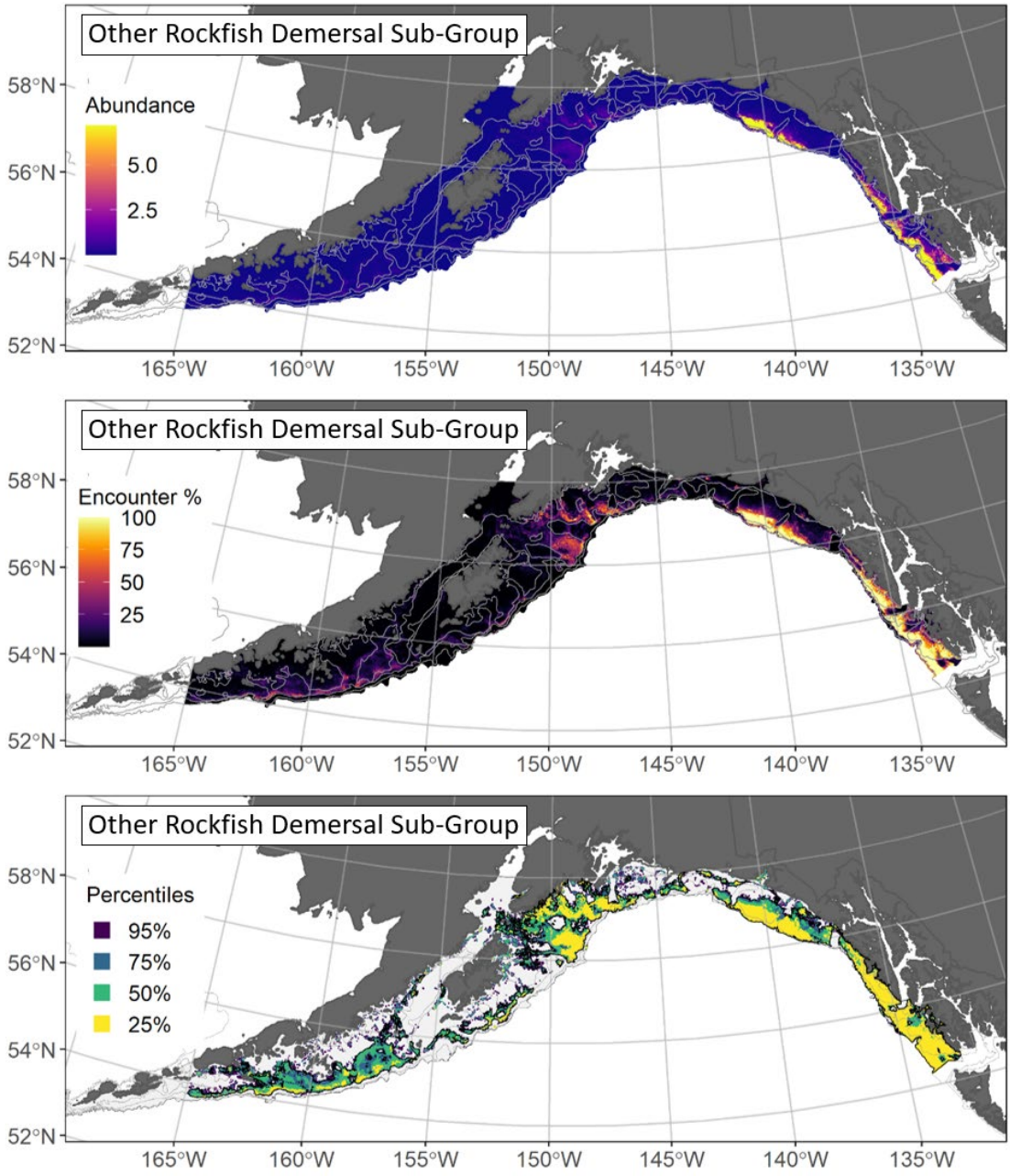

Figure 188. -- Composite habitat-related, ensemble-predicted numerical abundance (top panel), encounter probability (middle panel), and essential fish habitat (EFH) (the area containing the top 95% of occupied habitat defined as model estimated encounter probabilities greater than 5%) (bottom panel) of the Other Rockfish complex demersal sub-group from the Gulf of Alaska in AFSC RACE-GAP summer bottom trawl surveys (1993–2019) with 100 m, 200 m, and 700 m isobaths indicated; within the EFH area map are the subareas of the top 25% (EFH hot spots), top 50% (core EFH area), and top 75% (principal EFH area) of habitat-related, ensemble-predicted numerical abundance.

Quillback rockfish (*Sebastes mailger*)

Quillback rockfish (*Sebastes maliger*) are distributed from Anacapa Passage in southern California to the central GOA, and are most common from southeast Alaska to northern California (Love et al. 2002). Quillback rockfish is managed as part of the Other Rockfish (OR) stock complex in the GOA, where they are part of the Demersal Sub-group. Life history data for this species is based on studies from waters off Alaska and British Columbia, where quillback are reported mature at 290 mm length and 11 years age and live to a maximum of 95 years (Munk 2001, Love et al. 2002, Rooper 2008). Quillback rockfish are associated with the seafloor and prefer rocky, high-relief habitats with kelp cover, where they form a home site association (Love et al. 2002)[37].

Adult quillback rockfish distribution and predicted abundance from RACE-GAP summer bottom trawl surveys in the Gulf of Alaska -- Adult quillback rockfish (N = 73) caught in GOA RACE-GAP summer bottom trawl surveys (1993–2019) were infrequent and occurred primarily in southeast Alaska and near the Kenai Peninsula in the central GOA (Fig. 189). Of the five SDMs considered for inclusion in the ensemble to predict numerical abundance of adult quillback rockfish in the GOA, only the MaxEnt converged and attained a fair fit overall to the observed distribution and abundance data. The MaxEnt was poor at predicting high and low abundance catches (ρ = 0.17), excellent at discriminating presence-absence (AUC = 0.96), and good at explaining deviance (PDE = 0.51) (Table 63). Bottom depth, bottom temperature, and bottom current speed accounted for 59.0% of the covariate contribution to the deviance explained by the SDM (Table 64). In general, higher abundance of adult quillback rockfish occurred at shallow depths (Fig. 190). Predicted abundance was highest in southeast Alaska with patches of high abundance throughout their range in the GOA. The CV of SDM predictions tended to be higher in shallower areas across the GOA continental shelf. Areas with the greatest predicted encounter probability were very similar to the areas of predicted high abundance in southeast Alaska (Fig. 191).

Essential Fish Habitat of adult quillback rockfish in the Gulf of Alaska -- Ensemble-predicted habitat-related numerical abundance of adult quillback rockfish collected in RACE-GAP summer bottom trawl surveys of the GOA (1993–2019) was mapped as EFH area and subareas (Fig. 192). The EFH area, including EFH hot spots, for adult quillback rockfish mainly occurs on the continental shelf and inshore areas of the southeastern GOA. Otherwise, EFH for adult quillback rockfish is patchy throughout their range in the GOA.

[37] A recommendation from the stock author review to incorporate additional high quality sources of data (e.g., from ROV surveys untrawlable habitats) in future SDM ensemble EFH mapping efforts for this species will be included as a research recommendation from the 2023 EFH 5-year Review.

Table 63. -- Constituent species distribution models (SDMs) used to construct Essential Fish Habitat (EFH) for adult quillback rockfish: MaxEnt = Maximum entropy; paGAM = presence-absence generalized additive model; hGAM = zero-adjusted Poisson hurdle GAM; GAM_P = standard Poisson GAM; GAM_{nb} = standard negative-binomial GAM; RMSE = root mean square error; ρ (*rho*) = Spearman's rank correlation coefficient; AUC = area under the receiver-operating characteristic curve; and PDE = Poisson deviance explained *. The "--" indicates that this model was not included in the final ensemble.

adult quillback rockfish

Models	**RMSE**	**Relative Weight**	**ρ**	**AUC**	**PDE**	**EFH area (km^2)**
MaxEnt	0.45	1	0.17	0.96	0.51	17,700
paGAM	--	--	--	--	--	--
hGAM	--	--	--	--	--	--
GAM_P	--	--	--	--	--	--
GAM_{nb}	--	--	--	--	--	--
ensemble	1.36	1	0.45	0.99	0.78	24,700

* Refer to the Species Distribution Model Performance Metrics subsection within the Statistical Modeling section of the Methods for detailed descriptions of individual model performance metrics.

Table 64. -- Covariates retained in the adult quillback rockfish species distribution model (SDM) final ensembles, the percent contribution to the ensemble deviance explained by each covariate, and the cumulative deviance explained: SD = standard deviation and BPI = bathymetric position index.

quillback rockfish	**Covariate**	**% Contribution**	**Cumulative %**
adult	bottom depth	27.8	27.8
	bottom temperature	19.1	46.9
	current	12.1	59.0
	tidal maximum	11.1	70.1
	current SD	9.7	79.8
	rockiness	7.2	87.0
	aspect north	5.7	92.7
	sponge presence	2.3	95.0
	aspect east	1.9	96.9
	slope	1.3	98.2
	BPI	0.9	99.1
	pennatulacean presence	0.6	99.7
	coral presence	0.2	99.9
	curvature	0.1	100.0

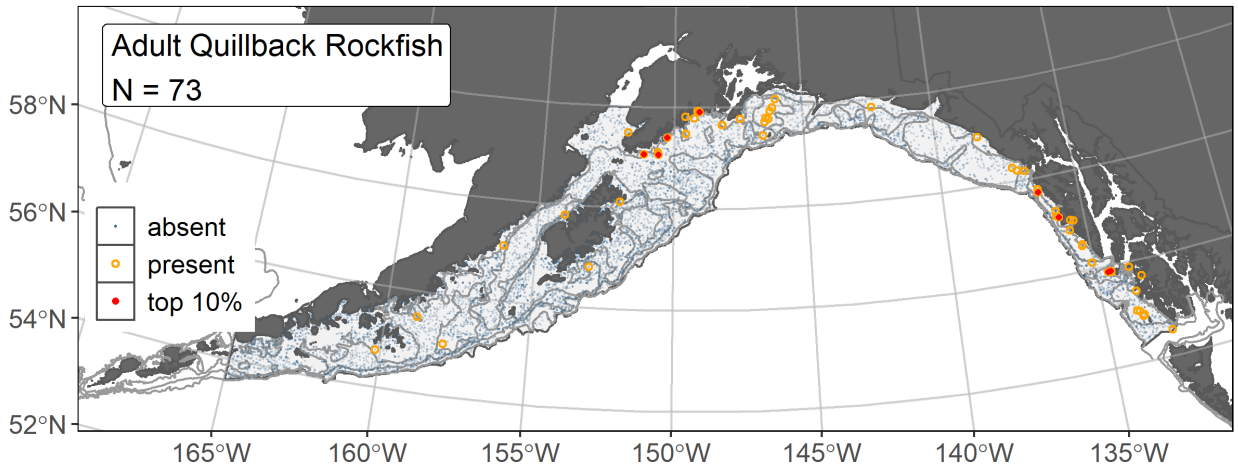

Figure 189. -- Distribution of adult quillback rockfish catches (N = 73) in 1993–2019 AFSC RACE-GAP summer bottom trawl surveys of the Gulf of Alaska with the 100 m, 200 m, and 700 m isobaths indicated; filled red circles indicate locations in top 10% of overall abundance, open orange circles indicate presence in remaining catches, and blue dots indicate stations sampled where the animals were not present.

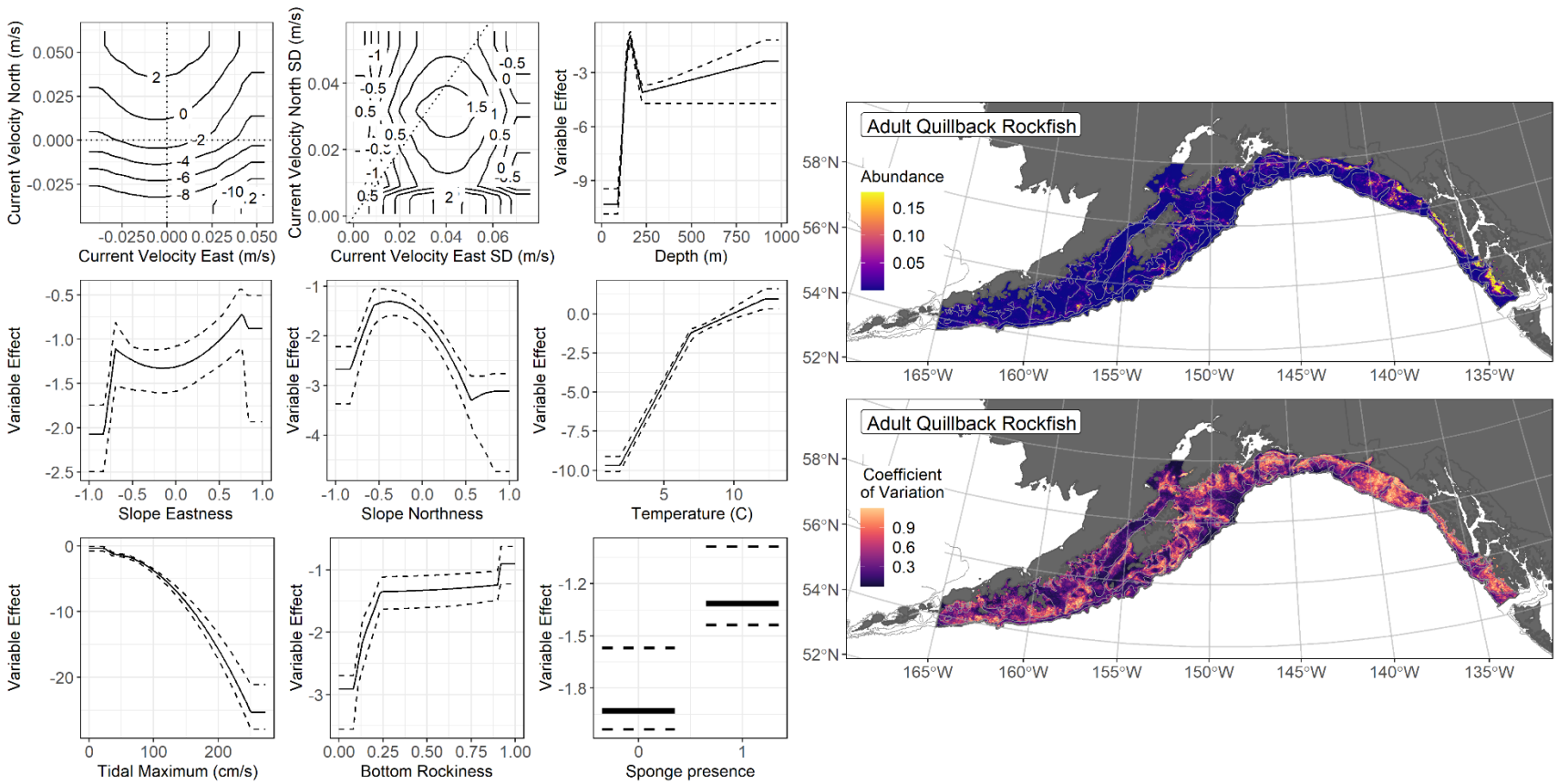

Figure 190. -- The top nine covariate effects (left panel) on ensemble-predicted adult quillback rockfish numerical abundance across the Gulf of Alaska (upper right panel) alongside the coefficient of variation (CV) of the ensemble predictions (lower right panel).

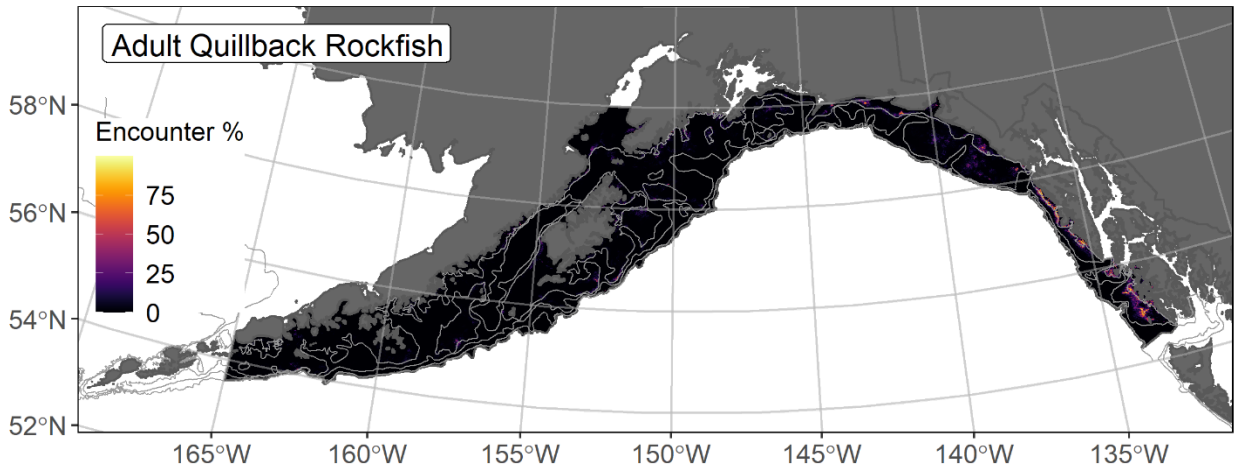

Figure 191. -- Encounter probability of adult quillback rockfish from AFSC RACE-GAP summer bottom trawl surveys (1993–2019) of the Gulf of Alaska with the 100 m, 300 m, and 700 m isobaths indicated.

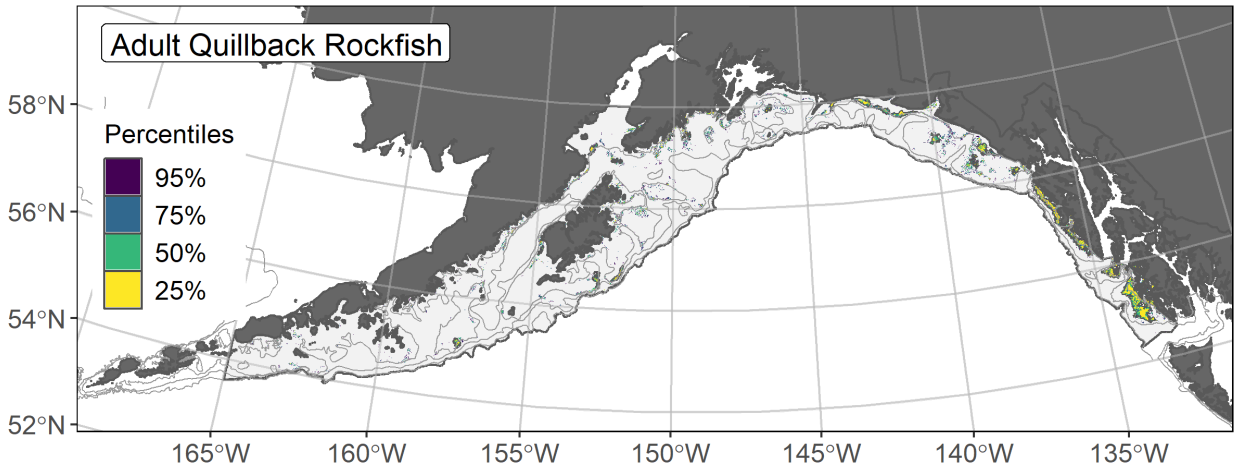

Figure 192. -- Essential fish habitat (EFH) is the area containing the top 95% of occupied habitat (defined as model estimated encounter probabilities greater than 5%) from an SDM ensemble fitted to adult quillback rockfish distribution and abundance from AFSC RACE-GAP Gulf of Alaska (GOA) summer bottom trawl surveys (1993–2019) with 100 m, 200 m, and 700 m isobaths indicated; within the EFH area map are the subareas of the top 25% (EFH hot spots), top 50% (core EFH area), and top 75% (principal EFH area) of habitat-related, ensemble-predicted numerical abundance.

Rosethorn rockfish (*Sebastes helvomaculatus*)

Rosethorn rockfish (*Sebastes helvomaculatus*) are distributed from Baja California to near Sitkinak Island in the western GOA (Love et al. 2002). Rosethorn rockfish are managed as part of the Other Rockfish (OR) stock complex in the GOA, where they are part of the Demersal Sub-group. Life history data for this species is based on studies from waters off Alaska and British Columbia, where rosethorn rockfish are reported to mature at 215 mm length, living to a maximum age of 87 years (Munk 2001, Love et al. 2002, Rooper 2008). Rosethorn rockfish associate with seafloor structure, often in transitions between habitats of soft unconsolidated and rocky substrates (Love et al. 2002)[38].

Subadult rosethorn rockfish abundance and distribution predicted from RACE-GAP summer bottom trawl surveys in the Gulf of Alaska -- Subadult rosethorn rockfish (N = 132) caught in GOA RACE-GAP summer bottom trawl surveys (1993–2019) were infrequent and concentrated on the outer continental shelf in the eastern GOA (Fig. 193). Three of five SDMs considered for inclusion in the ensemble to predict numerical abundance of subadult rosethorn rockfish in the GOA converged (Table 65). The three best-performing SDMs were weighted by RMSE in the final ensemble, which attained a good overall fit to the observed subadult rosethorn rockfish distribution and abundance data. The ensemble was fair at predicting high and low abundance catches (ρ = 0.30), and excellent at discriminating presence-absence (AUC = 0.99) and explaining deviance (PDE = 0.77). Geographic location, bottom depth, bottom temperature, and sponge presence accounted for 80% of the covariate contribution to the deviance explained by the final ensemble (Table 66). Higher abundance of subadult rosethorn rockfish occurred along the outer continental shelf of the eastern GOA in depths around 250 m in areas of low sponge presence (Fig. 194). The CV of ensemble predictions was higher in the eastern GOA and generally higher at deeper depths. Areas with the highest probability of encounter were very similar to the areas of predicted high abundance (Fig. 195).

Adult rosethorn rockfish abundance and distribution predicted from RACE-GAP summer bottom trawl surveys in the Gulf of Alaska -- Adult rosethorn rockfish (N = 186) caught in GOA RACE-GAP summer bottom trawl surveys (1993–2019) were infrequent and concentrated on the outer continental shelf in the eastern GOA, similar to the subadults (Fig. 196). Three of five SDMs considered for inclusion in the ensemble to predict numerical abundance of adult rosethorn rockfish in the GOA converged (Table 65); the GAM_{nb} was eliminated by skill testing. The two remaining models were

[38] A recommendation from the stock author review to incorporate additional high quality sources of data (e.g., from ROV surveys of untrawlable habitats) in future SDM ensemble EFH mapping for this species will be included as a research recommendation from the 2023 EFH 5-year Review.

weighted by RMSE in the final ensemble that attained a good overall fit the observed adult rosethorn rockfish distribution and abundance data. The ensemble was fair at predicting high and low abundance catches (ρ = 0.40), and excellent at discriminating presence-absence (AUC = 0.99) and explaining deviance (PDE = 0.82). Geographic location, bottom current, bottom temperature, and sponge presence accounted for 77.9% of the covariate contribution to the deviance explained by the final ensemble (Table 66). In a pattern very similar to subadults, a higher abundance of adult rosethorn rockfish was predicted along the outer continental shelf of the eastern GOA at depths around 250 m in areas of low sponge presence (Fig. 197). The CV of ensemble predictions was higher in the central and eastern GOA. The probability of encountering adult rosethorn rockfish is highest on the outer continental shelf in the eastern GOA (Fig. 198).

Essential Fish Habitat of subadult and adult rosethorn rockfish in the Gulf of Alaska -- Ensemble-predicted habitat-related numerical abundance of rosethorn rockfish life stages collected in RACE-GAP summer bottom trawl surveys of the GOA (1993–2019) was mapped as EFH areas and subareas (Fig. 199). The EFH areas for subadult and adult rosethorn rockfish were very similar, mainly occurring on bathymetric rises along the outer continental shelf of the GOA east of Kayak Island. EFH for this species was patchy west of Kayak Island, including southeast of the Kenai Peninsula on the continental shelf in an area known for the presence of boulder fields resulting from glacial retreat (Carlson et al. 1982). EFH core areas and hot spots mainly occurred in the eastern GOA, with greater predominance in southeast Alaska.

Table 65. -- Constituent species distribution models (SDMs) used to construct Essential Fish Habitat (EFH) for a) subadult and b) adult rosethorn rockfish: MaxEnt = Maximum entropy; paGAM = presence-absence generalized additive model; hGAM = zero-adjusted Poisson hurdle GAM; GAM_P = standard Poisson GAM; GAM_{nb} = standard negative-binomial GAM; RMSE = root mean square error; ρ (*rho*) = Spearman's rank correlation coefficient; AUC = area under the receiver-operating characteristic curve; and PDE = Poisson deviance explained *. The "--" indicates that this model was not included in the final ensemble.

a) subadult rosethorn rockfish

Models	RMSE	Relative Weight	ρ	AUC	PDE	EFH area (km^2)
MaxEnt	1.03	0.31	0.24	0.98	0.61	33,900
paGAM	0.94	0.37	0.39	0.99	0.74	22,800
hGAM	--	--	--	--	--	--
GAM_P	--	--	--	--	--	--
GAM_{nb}	1.00	0.32	0.43	0.99	0.73	13,600
ensemble	0.93	1	0.30	0.99	0.76	25,900

b) adult rosethorn rockfish

Models	RMSE	Relative Weight	ρ	AUC	PDE	EFH area (km^2)
MaxEnt	--	--	--	--	--	--
paGAM	2.99	0.53	0.36	0.99	0.71	31,900
hGAM	--	--	--	--	--	--
GAM_P	3.20	0.47	0.46	0.98	0.76	21,900
GAM_{nb}	3.38	0	--	--	--	--
ensemble	2.48	1	0.40	0.99	0.82	29,600

* Refer to the Species Distribution Model Performance Metrics subsection within the Statistical Modeling section of the Methods for detailed descriptions of individual model performance metrics.

Table 66. -- Covariates retained in the a) settled early juvenile habitat-related maximum entropy (MaxEnt) species distribution model (SDM), and b) subadult and c) adult SDM final ensembles for rosethorn rockfish with the percent contribution of each covariate to the deviance explained by the SDMs and the cumulative deviance explained: SD = standard deviation and BPI = bathymetric position index.

rosethorn rockfish			
	Covariate	**% Contribution**	**Cumulative %**
a) subadult	location	44.4	44.4
	bottom depth	13.3	57.6
	bottom temperature	12.5	70.1
	sponge presence	9.9	80.0
	current	4.7	84.7
	rockiness	4.4	89.1
	tidal maximum	3.1	92.2
	BPI	3.0	95.2
	aspect east	1.8	97.0
	aspect north	1.3	98.3
	current SD	1.1	99.4
	slope	0.4	99.8
	coral presence	0.1	99.9
	pennatulacean presence	0.1	100.0
b) adult	location	46.9	46.9
	current	11.4	58.2
	bottom temperature	10.4	68.6
	sponge presence	9.3	77.9
	bottom depth	4.3	82.2
	rockiness	4.0	86.1
	current SD	3.8	89.9
	tidal maximum	3.4	93.3
	slope	3.1	96.4
	BPI	1.1	97.5
	coral presence	0.7	98.2
	aspect north	0.7	98.9
	aspect east	0.5	99.4
	curvature	0.5	99.9
	pennatulacean presence	0.1	100.0

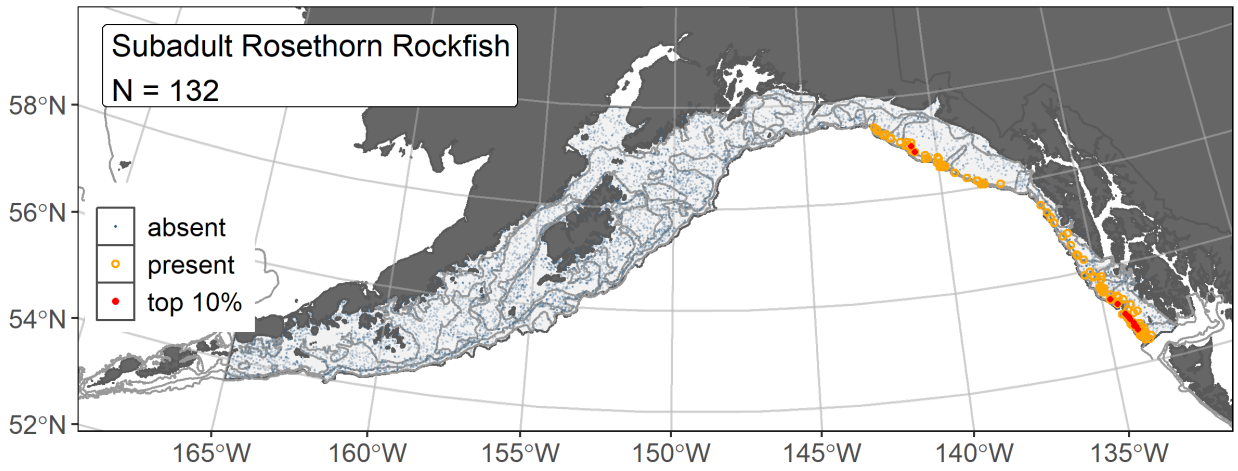

Figure 193. -- Distribution of subadult rosethorn rockfish catches (N = 132) in 1993–2019 AFSC RACE-GAP summer bottom trawl surveys of the Gulf of Alaska with the 100 m, 200 m, and 700 m isobaths indicated; filled red circles indicate locations in top 10% of overall abundance, open orange circles indicate presence in remaining catches, and blue dots indicate stations sampled where the animals were not present.

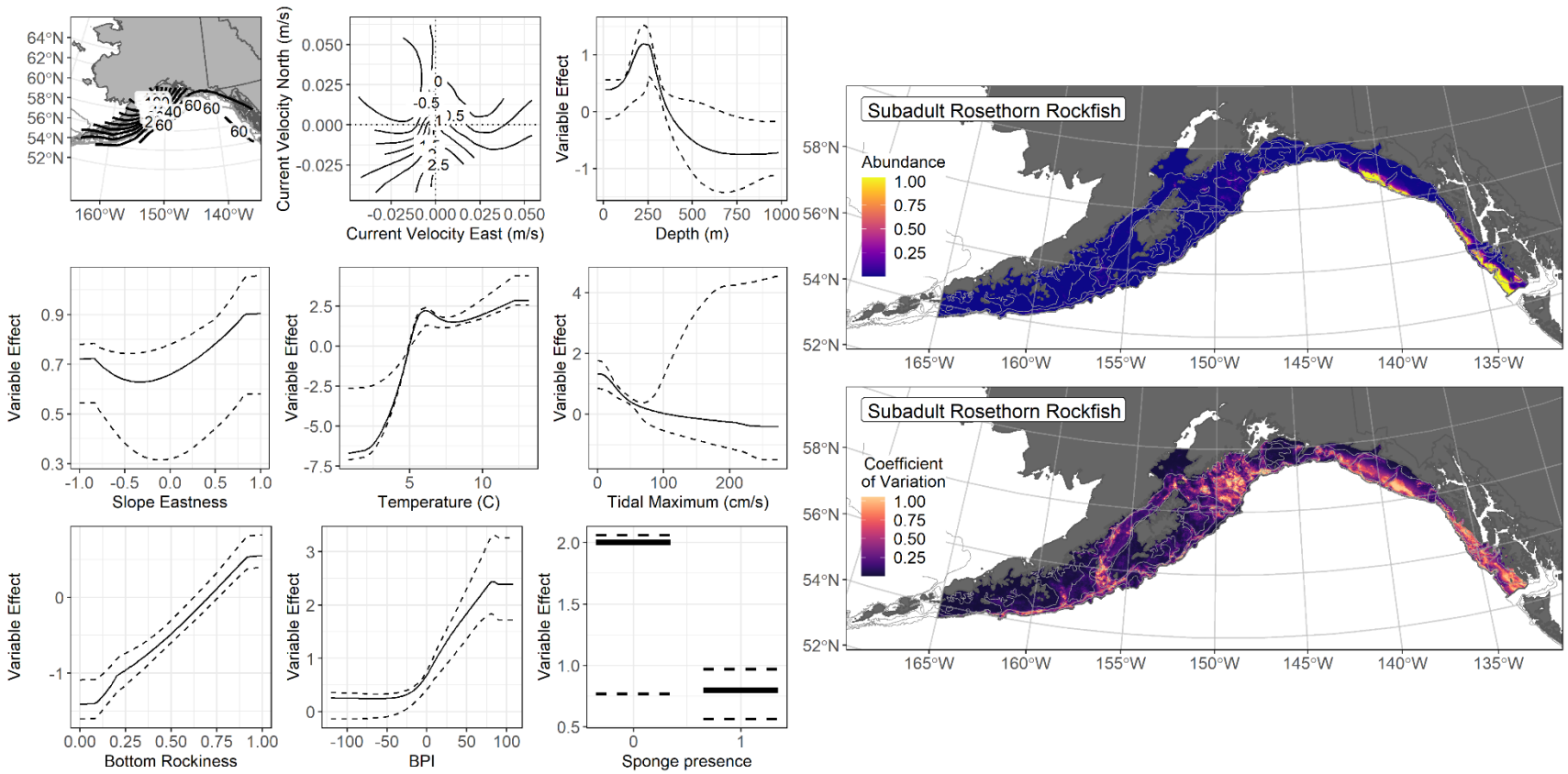

Figure 194. -- The top nine covariate effects (left panel) on ensemble-predicted subadult rosethorn rockfish numerical abundance across the Gulf of Alaska (upper right panel) alongside the coefficient of variation (CV) of the ensemble predictions (lower right panel).

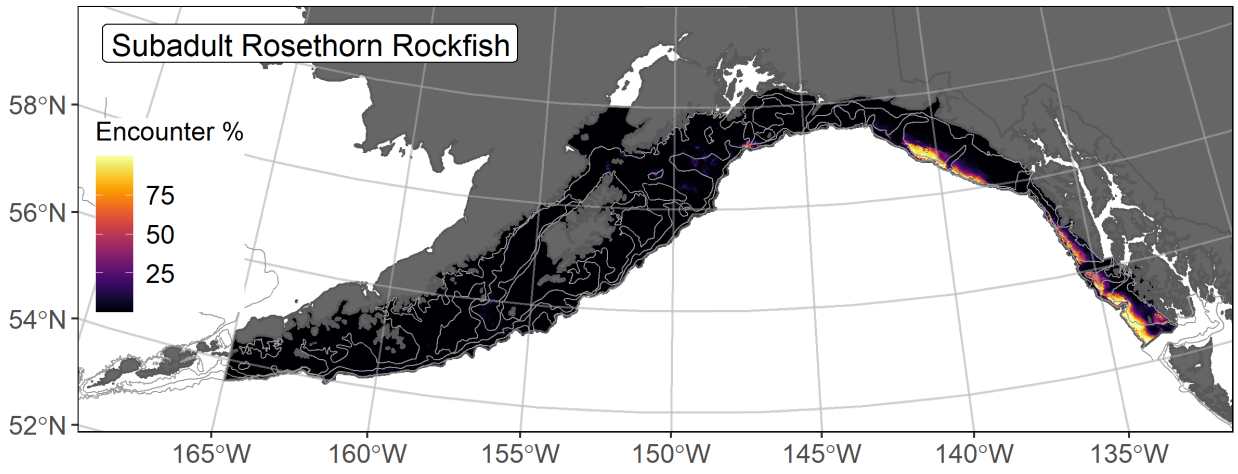

Figure 195. -- Encounter probability of subadult rosethorn rockfish from AFSC RACE-GAP summer bottom trawl surveys (1993–2019) of the Gulf of Alaska with the 100 m, 300 m, and 700 m isobaths indicated.

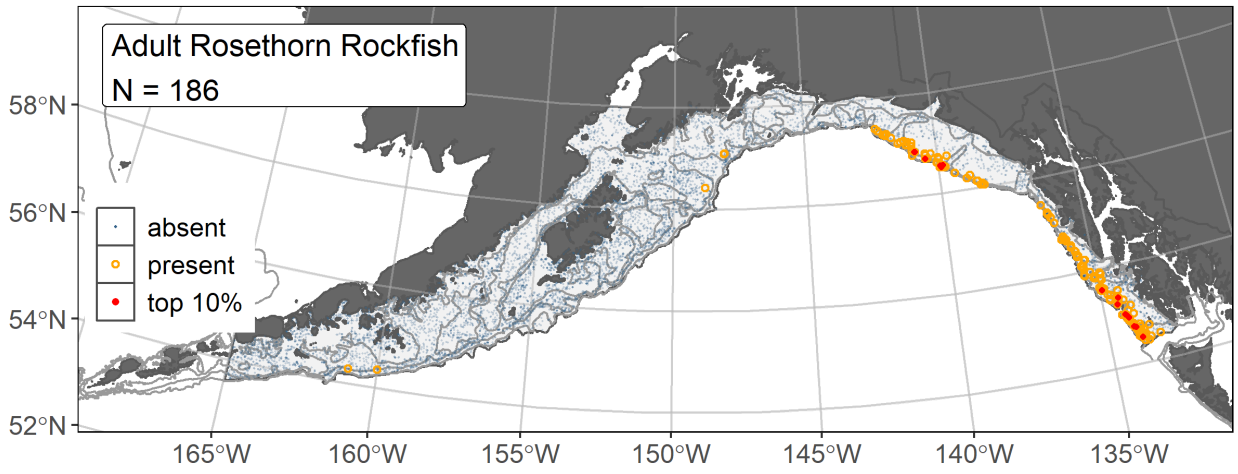

Figure 196. -- Distribution of adult rosethorn rockfish catches (N = 186) in 1993–2019 AFSC RACE-GAP summer bottom trawl surveys of the Gulf of Alaska with the 100 m, 300 m, and 700 m isobaths indicated; filled red circles indicate locations in top 10% of overall abundance, open orange circles indicate presence in remaining catches, and blue dots indicate stations sampled where the animals were not present.

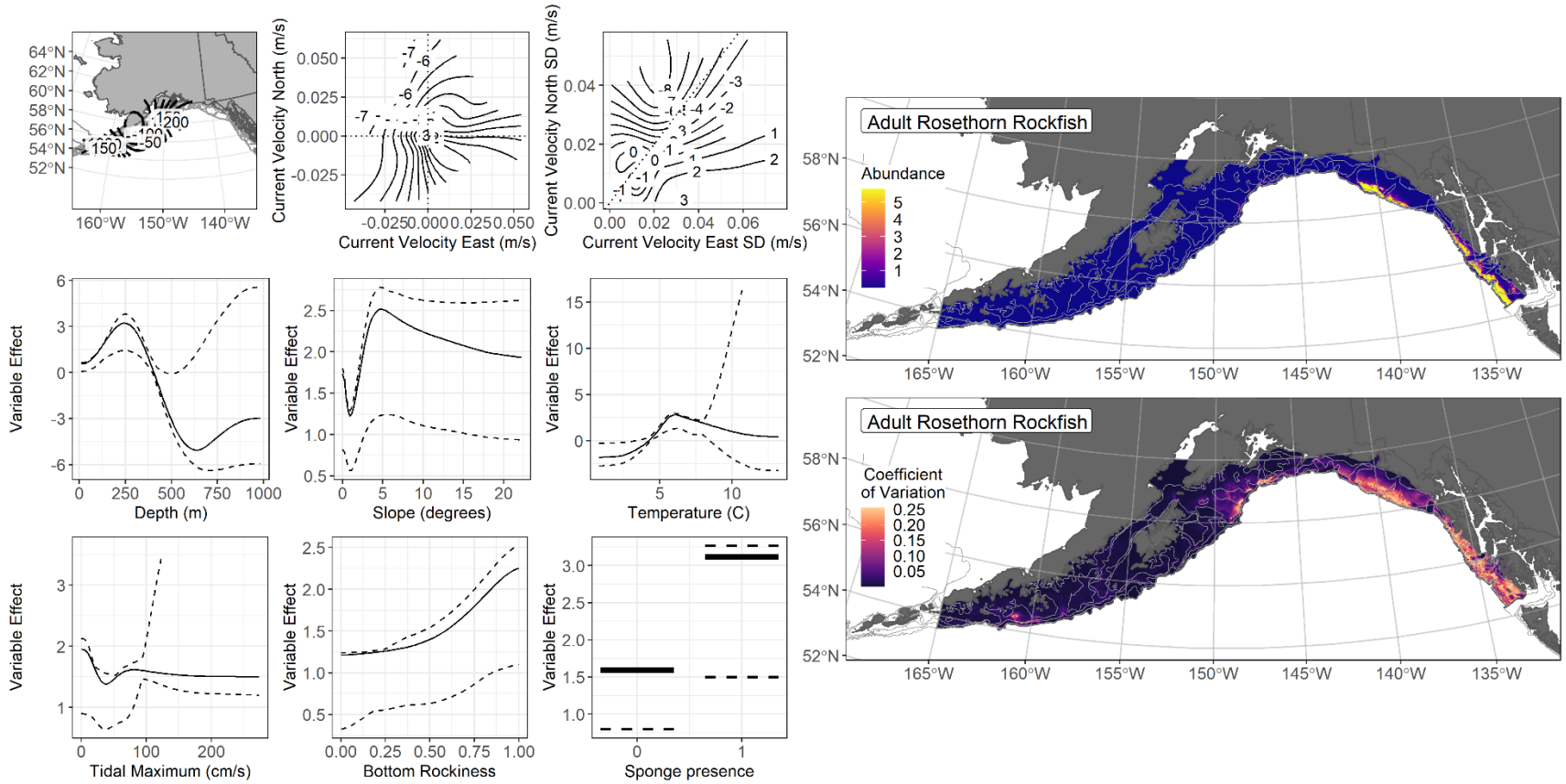

Figure 197. -- The top nine covariate effects (left panel) on ensemble-predicted adult rosethorn rockfish numerical abundance across the Gulf of Alaska (upper right panel) alongside the coefficient of variation (CV) of the ensemble predictions (lower right panel).

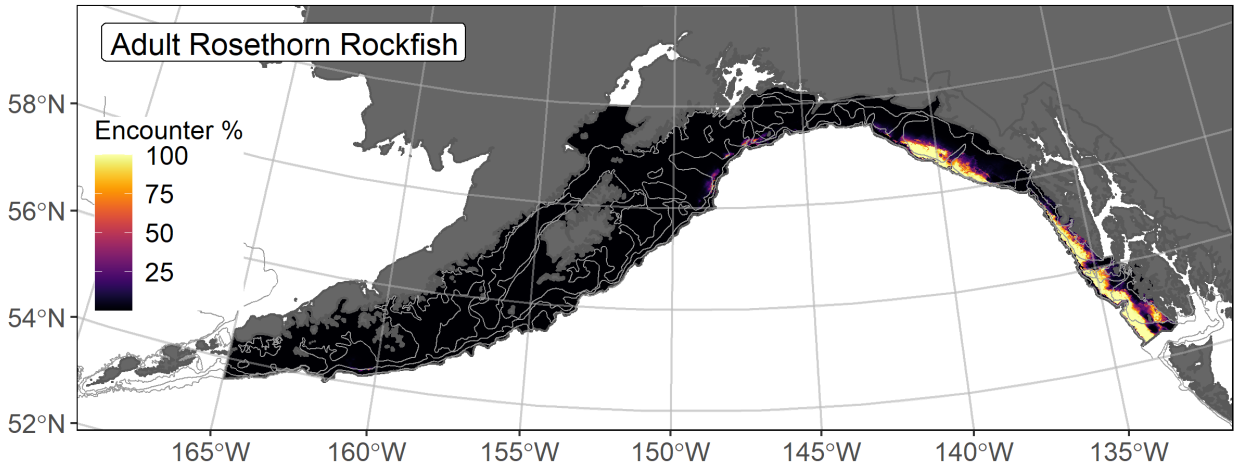

Figure 198. -- Encounter probability of adult rosethorn rockfish from AFSC RACE-GAP summer bottom trawl surveys (1993–2019) of the Gulf of Alaska with the 100 m, 300 m, and 700 m isobaths indicated.

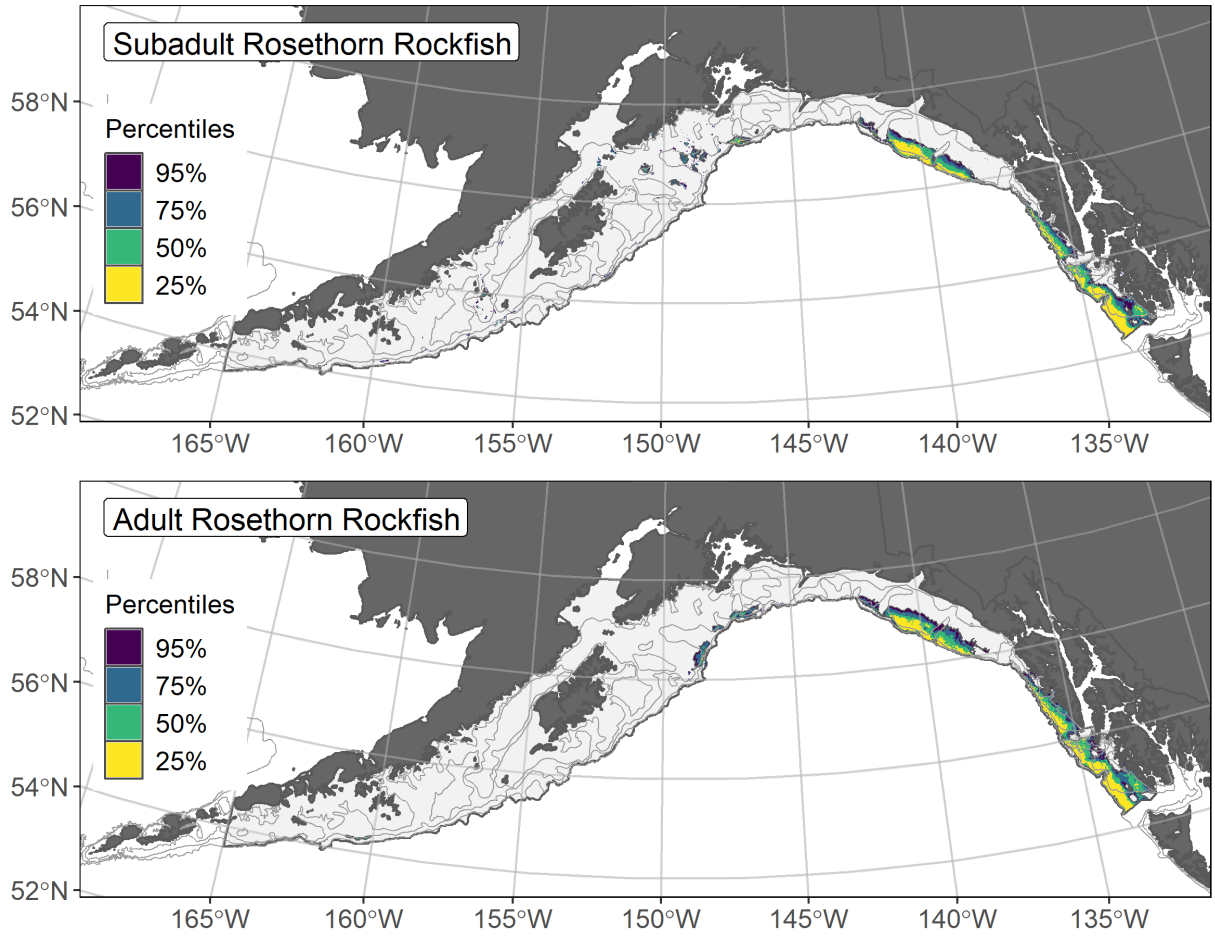

Figure 199. -- Essential fish habitat (EFH) is the area containing the top 95% of occupied habitat (defined as model estimated encounter probabilities greater than 5%) from an SDM ensemble fitted to subadult (top panel) and adult (bottom panel) rosethorn rockfish distribution and abundance in AFSC RACE-GAP summer bottom trawl surveys (1993–2019) with 100 m, 200 m, and 700 m isobaths indicated; within the EFH area map are the subareas of the top 25% (EFH hot spots), top 50% (core EFH area), and top 75% (principal EFH area) of habitat-related, ensemble-predicted numerical abundance.

Yelloweye rockfish (*Sebastes ruberrimus*)

Yelloweye rockfish (*Sebastes ruberrimus*) are distributed from northern Baja California to Umnak and Unalaska Islands in the Aleutian Islands region and are abundant from southeast Alaska to central California (Love et al. 2002). Yelloweye rockfish are managed as part of the Other Rockfish (OR) stock complex in the GOA, where they are part of the Demersal Sub-group and one of the six most common OR species by survey catch or biomass (Tribuzio and Echave 2019). Yelloweye are one of the largest and most recognizable rockfishes. Life history data collected in waters off Alaska describes yelloweye becoming mature at 450 mm length and 22 years, with a maximum reported size of 910 mm and living as long as 118 years (O'Connell and Funk 1987, Love et al. 2002, Tribuzio and Echave 2019). Yelloweye rockfish are closely associated with the seafloor in rocky habitats with biogenic structure (Love et al. 2002) and are not commonly encountered by the GOA RACE-GAP bottom trawl survey (Tribuzio and Echave 2019)[39]. In a productivity-susceptibility analysis of 39 species in the GOA, yelloweye rockfish were the most vulnerable species (Ormseth and Spencer 2011).

Subadult yelloweye rockfish distribution and predicted abundance from RACE-GAP summer bottom trawl surveys in the Gulf of Alaska -- Subadult yelloweye rockfish (N = 79) caught in GOA RACE-GAP summer bottom trawl surveys (1993–2019) were infrequent and occurred throughout the GOA survey area (Fig. 200). Five SDMs considered for inclusion in the ensemble to predict numerical abundance of subadult yelloweye rockfish in the GOA converged (Table 67); the GAM_{nb} was eliminated by skill testing. The remaining four best-performing SDMs were weighted by RMSE in the final ensemble, which attained a fair overall fit to the observed subadult yelloweye rockfish distribution and abundance data. The ensemble was poor at predicting high and low abundance catches ($\rho = 0.16$), and excellent at discriminating presence-absence (AUC = 0.92), and fair to good at explaining deviance (PDE = 0.39). Bottom depth, sponge presence, geographic position, and BPI accounted for 73.1% of the covariate contribution to the deviance explained by the final ensemble (Table 68). Higher abundance of subadult yelloweye was predicted around 125 m depth on bathymetric rises (BPI highs) in areas of low sponge presence on the GOA continental shelf (Fig. 201). The CV of ensemble predictions was relatively high across the GOA continental shelf. Predicted encounter probability was around 25% or less throughout the GOA RACE-GAP survey area, with the exception of southern southeast Alaska where encounters are likely more frequent (Fig. 202).

[39] A recommendation from the stock author review to incorporate additional high quality sources of data (e.g., from ROV surveys of untrawlable habitats) in future SDM ensemble EFH mapping for this species will be included as a research recommendation from the 2023 EFH 5-year Review.

Adult yelloweye rockfish distribution and predicted abundance from RACE-GAP summer bottom trawl surveys in the Gulf of Alaska -- Adult yelloweye rockfish (N = 186) caught in GOA RACE-GAP summer bottom trawl surveys (1993–2019) were infrequent throughout the GOA RACE-GAP survey area (Fig. 203). Five SDMs were considered for inclusion in the ensemble to predict numerical abundance of adult yelloweye rockfish in the GOA (Table 67); the GAM_{nb} was eliminated by skill testing. The remaining four best-performing SDMs were weighted nearly equally by RMSE in the final ensemble, which attained a good overall fit to the observed adult yelloweye rockfish distribution and abundance data. The ensemble was fair at predicting high and low abundance catches (ρ = 0.22), and excellent at discriminating presence-absence (AUC = 0.91), and good at explaining deviance (PDE = 0.43). Bottom depth, geographic location, and seafloor rockiness accounted for 59.3% of the covariate contribution to the deviance explained by the final ensemble (Table 68). In a pattern very similar to subadults, higher abundance of adult yelloweye rockfish in the GOA was predicted around 125 m depth on bathymetric rises (BPI highs) with rocky substrate present (Fig. 204). The CV of ensemble predictions was also relatively high across the GOA continental shelf. Predicted encounter probability was around 25% or less throughout the GOA RACE-GAP survey area, with the exception of patchy areas throughout the GOA where encounters are likely more frequent (Fig. 205).

Essential Fish Habitat of subadult and adult yelloweye rockfish in the Gulf of Alaska -- Ensemble-predicted habitat-related numerical abundance of yelloweye rockfish life stages collected in RACE-GAP summer bottom trawl surveys of the GOA (1993–2019) was mapped as EFH areas and subareas s (Fig. 206). The total EFH area for subadult yelloweye rockfish was smaller than the total area predicted for adults. EFH for both life stages occurs in patchy areas of the GOA continental shelf, notably along rocky bathymetric rises.

Table 67. -- Constituent species distribution models (SDMs) used to construct Essential Fish Habitat (EFH) for a) subadult and b) adult yelloweye rockfish: MaxEnt = Maximum entropy; paGAM = presence-absence generalized additive model; hGAM = zero-adjusted Poisson hurdle GAM; GAM_P = standard Poisson GAM; GAM_{nb} = standard negative-binomial GAM; RMSE = root mean square error; ρ (rho) = Spearman's rank correlation coefficient; AUC = area under the receiver-operating characteristic curve; and PDE = Poisson deviance explained *. The "--" indicates that this model was not included in the final ensemble.

a) subadult yelloweye rockfish

Models	RMSE	Relative Weight	ρ	AUC	PDE	EFH area (km^2)
MaxEnt	0.18	0.25	0.13	0.87	0.21	21,000
paGAM	0.18	0.25	0.17	0.90	0.25	27,700
hGAM	0.18	0.25	0.14	0.89	0.22	29,200
GAM_P	0.18	0.25	0.16	0.88	0.20	27,200
GAM_{nb}	0.18	0	--	--	--	--
ensemble	0.17	1	0.16	0.92	0.39	27,100

b) adult yelloweye rockfish

Models	RMSE	Relative Weight	ρ	AUC	PDE	EFH area (km^2)
MaxEnt	0.49	0.25	0.19	0.87	0.26	66,900
paGAM	0.48	0.26	0.21	0.89	0.34	66,400
hGAM	0.50	0.24	0.20	0.89	0.30	61,500
GAM_P	0.48	0.26	0.21	0.88	0.30	55,900
GAM_{nb}	0.50	0	--	--	--	--
ensemble	0.46	1	0.22	0.91	0.43	64,500

* Refer to the Species Distribution Model Performance Metrics subsection within the Statistical Modeling section of the Methods for detailed descriptions of individual model performance metrics.

Table 68. -- Covariates retained in the a) subadult and b) adult yelloweye rockfish species distribution model (SDM) final ensembles, the percent contribution to the ensemble deviance explained by each covariate, and the cumulative deviance explained: SD = standard deviation and BPI = bathymetric position index.

yelloweye rockfish

	Covariate	**% Contribution**	**Cumulative %**
a) subadult	bottom depth	28.9	28.9
	sponge presence	15.7	44.6
	location	15.1	59.7
	BPI	13.4	73.1
	current	6.2	79.3
	tidal maximum	4.2	83.5
	aspect north	3.6	87.1
	slope	3.4	90.5
	rockiness	3.4	93.9
	current SD	2.6	96.5
	coral presence	1.7	98.2
	bottom temperature	1.2	99.4
	curvature	0.5	99.9
	aspect east	0.1	100.0
b) adult	bottom depth	29.0	29.0
	location	21.2	50.1
	rockiness	9.2	59.3
	current	8.4	67.7
	sponge presence	8.1	75.8
	current SD	5.4	81.2
	BPI	5.2	86.4
	aspect east	3.3	89.7
	slope	3.1	92.8
	coral presence	2.7	95.5
	bottom temperature	1.6	97.1
	aspect north	1.5	98.6
	tidal maximum	1.2	99.8
	curvature	0.2	100.0

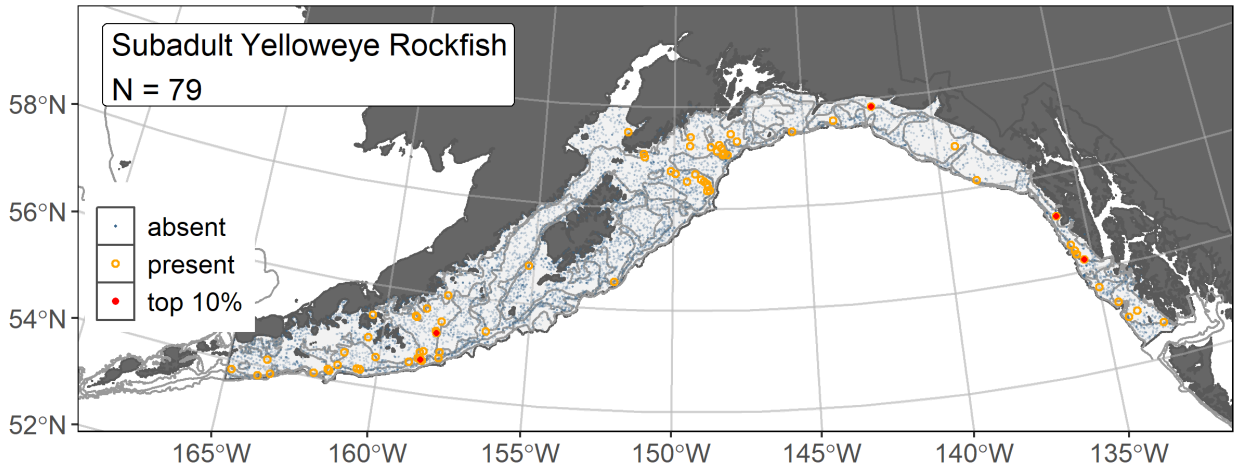

Figure 200. -- Distribution of subadult yelloweye rockfish catches (N = 79) in 1993–2019 AFSC RACE-GAP summer bottom trawl surveys of the Gulf of Alaska with the 100 m, 200 m, and 700 m isobaths indicated; filled red circles indicate locations in top 10% of overall abundance, open orange circles indicate presence in remaining catches, and blue dots indicate stations sampled where the animals were not present.

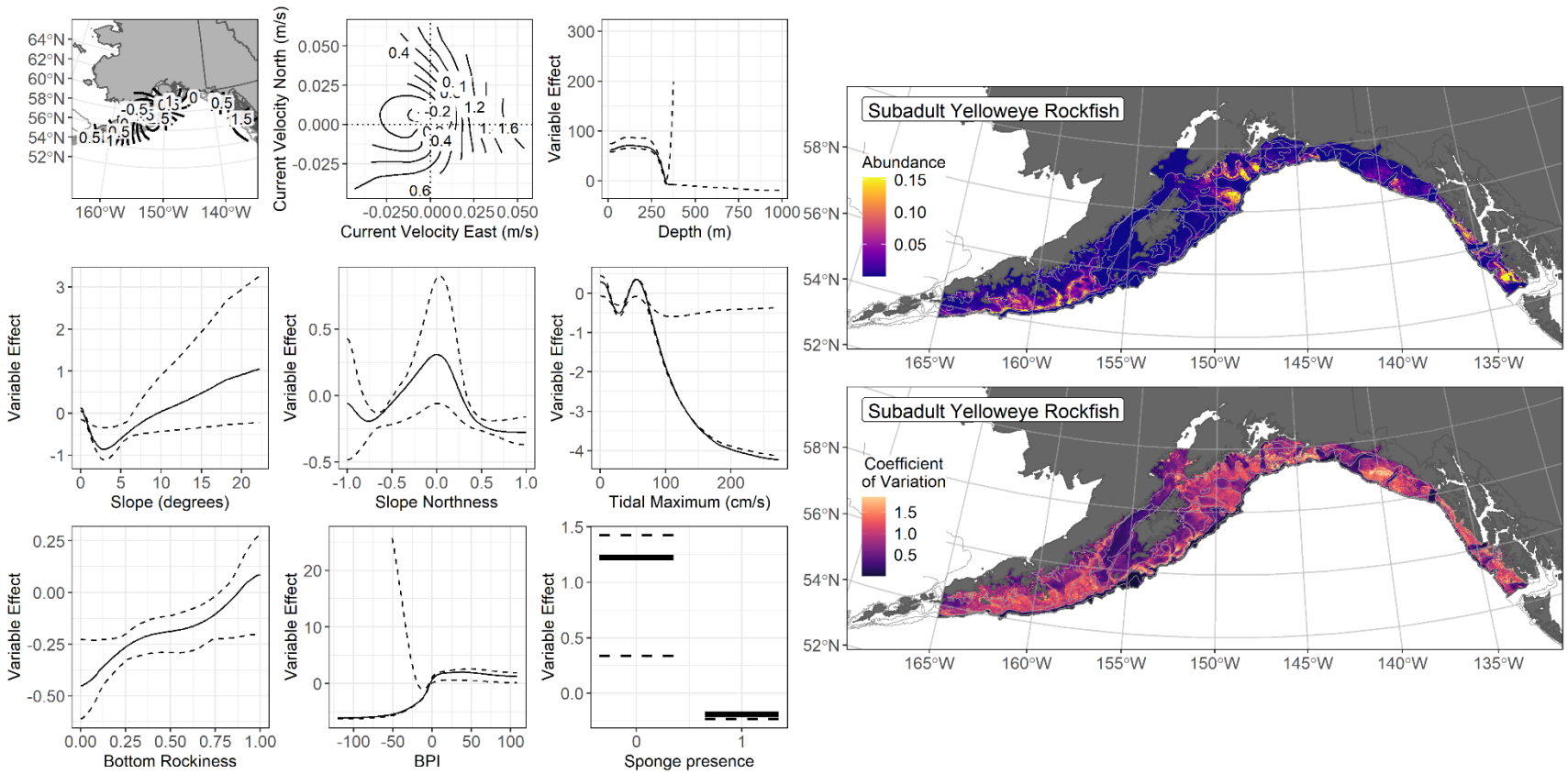

Figure 201. -- The top nine covariate effects (left panel) on ensemble-predicted subadult yelloweye rockfish numerical abundance across the Gulf of Alaska (upper right panel) alongside the coefficient of variation (CV) of the ensemble predictions (lower right panel).

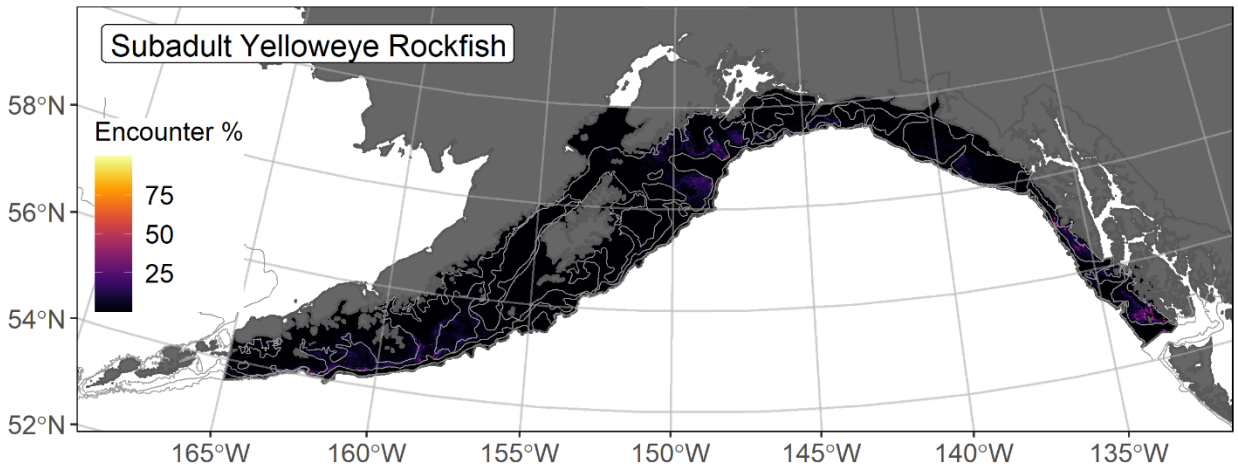

Figure 202. -- Encounter probability of subadult yelloweye rockfish from AFSC RACE-GAP summer bottom trawl surveys (1993–2019) of the Gulf of Alaska with the 100 m, 300 m, and 700 m isobaths indicated.

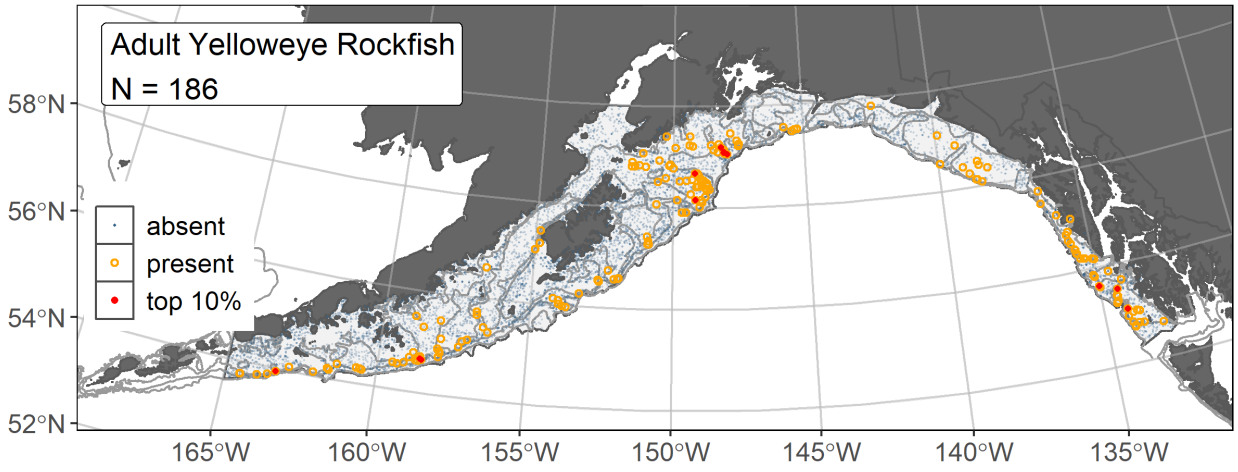

Figure 203. -- Distribution of adult yelloweye rockfish catches (N = 186) in 1993–2019 AFSC RACE-GAP summer bottom trawl surveys of the Gulf of Alaska with the 100 m, 300 m, and 700 m isobaths indicated; filled red circles indicate locations in top 10% of overall abundance, open orange circles indicate presence in remaining catches, and blue dots indicate stations sampled where the animals were not present.

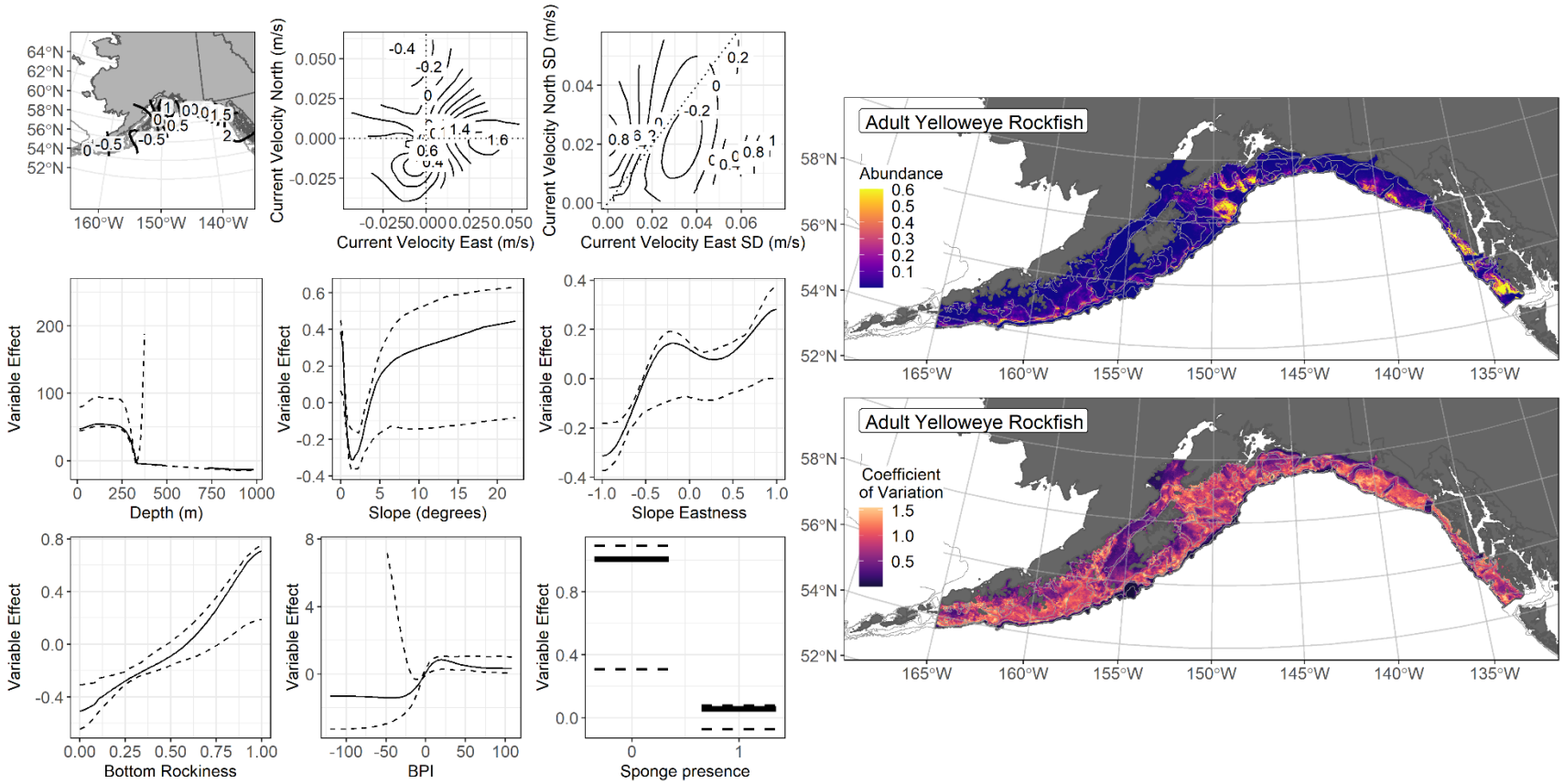

Figure 204. -- The top nine covariate effects (left panel) on ensemble-predicted adult yelloweye rockfish numerical abundance across the Gulf of Alaska (upper right panel) alongside the coefficient of variation (CV) of the ensemble predictions (lower right panel).

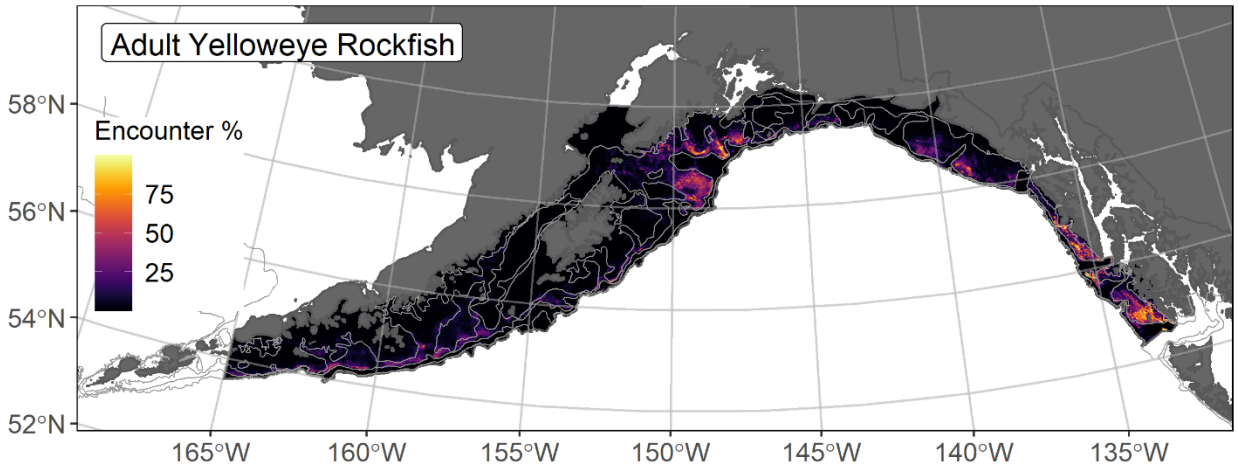

Figure 205. -- Encounter probability of adult yelloweye rockfish from AFSC RACE-GAP summer bottom trawl surveys (1993–2019) of the Gulf of Alaska with the 100 m, 300 m, and 700 m isobaths indicated.

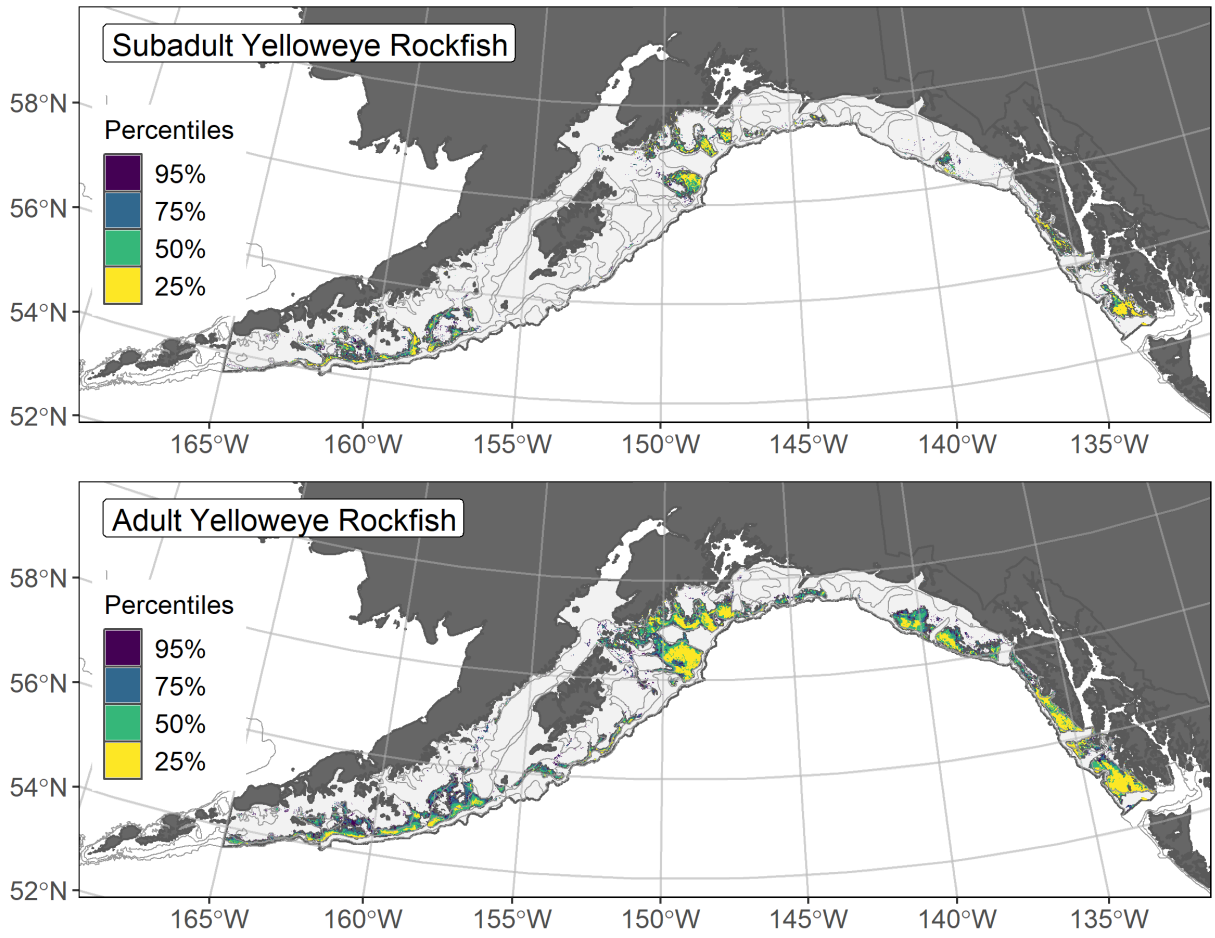

Figure 206. -- Essential fish habitat (EFH) is the area containing the top 95% of occupied habitat (defined as model estimated encounter probabilities greater than 5%) from an SDM ensemble fitted to subadult (top panel) and adult (bottom panel) yelloweye rockfish distribution and abundance in AFSC RACE-GAP summer bottom trawl surveys (1993–2019) with 100 m, 200 m, and 700 m isobaths indicated; within the EFH area map are the subareas of the top 25% (EFH hot spots), top 50% (core EFH area), and top 75% (principal EFH area) of habitat-related, ensemble-predicted numerical abundance.

Other rockfish complex slope sub-group

In the GOA, the Other Rockfish (OR) stock complex includes the slope sub-group with the following species: aurora, blackgill, darkblotched, greenstriped, harlequin, northern, pygmy, redbanded, redstripe, sharpchin, shortbelly, silvergray, splitnose, stripetail, vermilion, widow, yellowmouth, yellowtail rockfishes, boccacio, and chilipepper (Tribuzio and Echave 2019). Northern rockfish are only included in this complex in the eastern GOA, and their EFH is described and mapped separately from the GOA OR complex. While stocks are managed differently depending on the species (either across regions or at smaller scales), EFH is designated and mapped for each FMP species[40]. Slope sub-group species, including greenstriped, harlequin, pygmy, redbanded, redstripe, sharpchin, and silvergray rockfishes were common enough (N > 50) in GOA RACE-GAP summer bottom trawl survey catches (1993–2019) to support individual species life stage SDMs of habitat-related abundance to map EFH[41]. To map EFH of the slope sub-group, the SDM ensemble predictions of the seven species were combined to generate additive composite maps of habitat-related abundance and EFH, which represents the EFH of slope sub-group species where an individual EFH map was not possible due to insufficient data[42].

Other rockfish complex slope sub-group abundance and distribution predicted from RACE-GAP summer bottom trawl surveys in the Gulf of Alaska -- Habitat-related, ensemble-predicted numerical abundance was combined for the subadult and adult life stages of the seven rockfish species to represent the slope sub-group in the GOA and mapped along with the combined encounter probability and EFH (Fig. 207). The composite, ensemble-predicted abundance of the slope sub-group reflects the higher abundance catches of these seven species on the outer continental shelf and upper slope of the eastern GOA, with higher abundances also present on the continental shelf south of the Kenai Peninsula and lower abundance moving westward along the outer continental shelf and upper slope. Predicted encounter probabilities for the slope sub-group by the GOA RACE-GAP were higher across the GOA continental shelf and upper slope.

Essential fish habitat of the other rockfish slope sub-group in the Gulf of Alaska -- EFH of the slope sub-group included most of the GOA RACE-GAP survey area (Fig. 207). Core EFH area was extensive within the total EFH area. EFH hot spots were primarily along a large extent of the eastern and

[40] 50 CFR 600.815(a)(1)(i)
[41] A recommendation from the stock author review to incorporate additional high quality data sources in future SDM ensemble EFH mapping for these species will be included as a future research recommendation from the 2023 EFH 5-year Review.
[42] 50 CFR 600.815(a)(1)(iv)(E)

central GOA continental shelf and extended west along the outer continental shelf and upper slope to 165° W longitude.

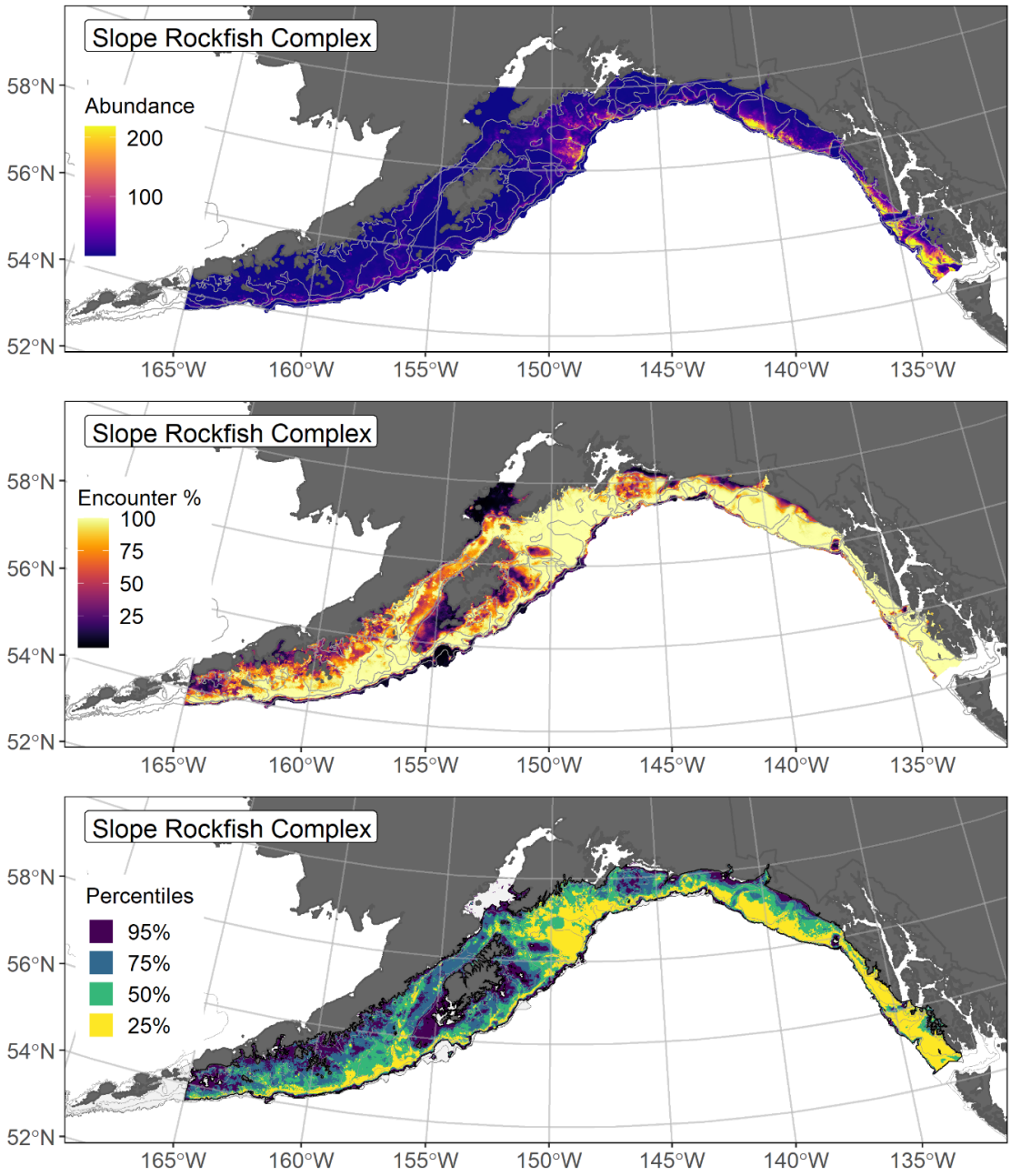

Figure 207. -- Composite habitat-related, ensemble-predicted numerical abundance (top panel), encounter probability (middle panel), and essential fish habitat (EFH) (the area containing the top 95% of occupied habitat defined as model estimated encounter probabilities greater than 5%) (bottom panel) of the Other Rockfish stock complex Slope Sub-group from the Gulf of Alaska in AFSC RACE-GAP summer bottom trawl surveys (1993–2019) with 100 m, 200 m, and 700 m isobaths indicated; within the EFH area map are the subareas of the top 25% (EFH hot spots), top 50% (core EFH area), and top 75% (principal EFH area) of habitat-related, ensemble-predicted numerical abundance.

Greenstriped rockfish (*Sebastes elongatus*)

Greenstriped rockfish (*Sebastes elongatus*) are distributed from southern California to Chirikof Island in the western GOA (Love et al. 2002). Greenstriped rockfish are managed as part of the Other Rockfish (OR) stock complex in the GOA, where they are part of the Slope Sub-group. Life history data for this species is based on studies from waters off Washington and Oregon, indicating that greenstriped rockfish reach maturity at 220 mm length and live up to 54 years (Love et al. 2002). Greenstriped rockfish move to deeper depths with age and associate with a variety of benthic habitats, where they are often observed solitary and resting on the seafloor (Love et al. 2002). In GOA RACE-GAP summer bottom trawl survey catches (1993–2019) greenstriped rockfish adults were common enough (N > 50) to support individual species life stage SDMs of habitat-related abundance to map EFH[43].

Adult greenstriped rockfish distribution and predicted abundance from RACE-GAP summer bottom trawl surveys in the Gulf of Alaska -- Adult greenstriped rockfish (N = 120) caught in GOA RACE-GAP summer survey were infrequent and concentrated in the eastern GOA off southeast Alaska (Fig. 208). Four of five SDMs considered for inclusion in the ensemble to predict numerical abundance of adult greenstriped rockfish in the GOA converged (Table 1); the GAM_{nb} was eliminated by skill testing. The remaining three best-performing SDMs were weighted by RMSE in the final ensemble, which attained a good overall fit to the observed adult greenstriped rockfish distribution and abundance data. The ensemble was fair at predicting high and low abundance catches ($\rho = 0.30$), and excellent at discriminating presence-absence (AUC = 0.99) and explaining deviance (PDE = 0.86). Geographic location, bottom depth, and bottom temperature accounted for 72.3% of the covariate contribution to the deviance explained by the final ensemble (Table 2). Higher abundance of adult greenstriped rockfish was predicted to occur on the eastern GOA continental shelf off southeast Alaska with peaks at depths < 200 m (Fig. 209). The CV of ensemble predictions was highest in the eastern and central GOA. The probability of encountering adult greenstriped rockfish is higher in areas of the eastern GOA continental shelf off southeast Alaska (Fig. 210). This species was not caught by the survey west of Kayak Island.

Essential Fish Habitat of adult greenstriped rockfish in the Gulf of Alaska -- Ensemble-predicted habitat-related numerical abundance of northern rockfish life stages collected in RACE-GAP summer bottom trawl surveys of the GOA (1993–2019) was mapped as EFH areas and subareas (Fig.

[43] A recommendation from the stock author review to incorporate additional sources of data (e.g., from longline surveys and fishery observers) in future SDM ensemble EFH mapping for this species will be included as a research recommendation from the 2023 EFH 5-year Review.

211). The EFH area for adult greenstriped rockfish occurred along the continental shelf of the eastern GOA off southeast Alaska.

Table 69. -- Constituent species distribution models (SDMs) used to construct Essential Fish Habitat (EFH) for a) subadult and b) adult greenstriped rockfish: MaxEnt = Maximum entropy; paGAM = presence-absence generalized additive model; hGAM = zero-adjusted Poisson hurdle GAM; GAM_P = standard Poisson GAM; GAM_{nb} = standard negative-binomial GAM; RMSE = root mean square error; ρ (rho) = Spearman's rank correlation coefficient; AUC = area under the receiver-operating characteristic curve; and PDE = Poisson deviance explained *. The "--" indicates that this model was not included in the final ensemble.

adult greenstriped rockfish

Models	RMSE	Relative Weight	ρ	AUC	PDE	EFH area (km^2)
MaxEnt	2.74	0.17	0.24	0.99	0.64	28,000
paGAM	1.75	0.41	0.40	0.99	0.75	17,600
hGAM	--	--	--	--	--	--
GAM_P	1.74	0.42	0.45	0.99	0.70	13,200
GAM_{nb}	1.88	0	--	--	--	--
ensemble	1.41	1	0.30	1.00	0.86	19,300

* Refer to the Species Distribution Model Performance Metrics subsection within the Statistical Modeling section of the Methods for detailed descriptions of individual model performance metrics.

Table 70. -- Covariates retained in the adult greenstriped rockfish species distribution model (SDM) final ensembles, the percent contribution to the ensemble deviance explained by each covariate, and the cumulative deviance explained: SD = standard deviation and BPI = bathymetric position index.

greenstriped rockfish			
	Covariate	**% Contribution**	**Cumulative %**
adult	location	40.2	40.2
	bottom depth	20.2	60.4
	bottom temperature	11.9	72.3
	current	6.3	78.7
	rockiness	3.9	82.6
	BPI	3.4	86.0
	sponge presence	3.4	89.4
	current SD	3.3	92.7
	tidal maximum	2.8	95.5
	aspect east	1.3	96.8
	slope	1.2	98.0
	curvature	1.0	99.0
	aspect north	0.6	99.6
	coral presence	0.3	99.9
	pennatulacean presence	0.1	100.0

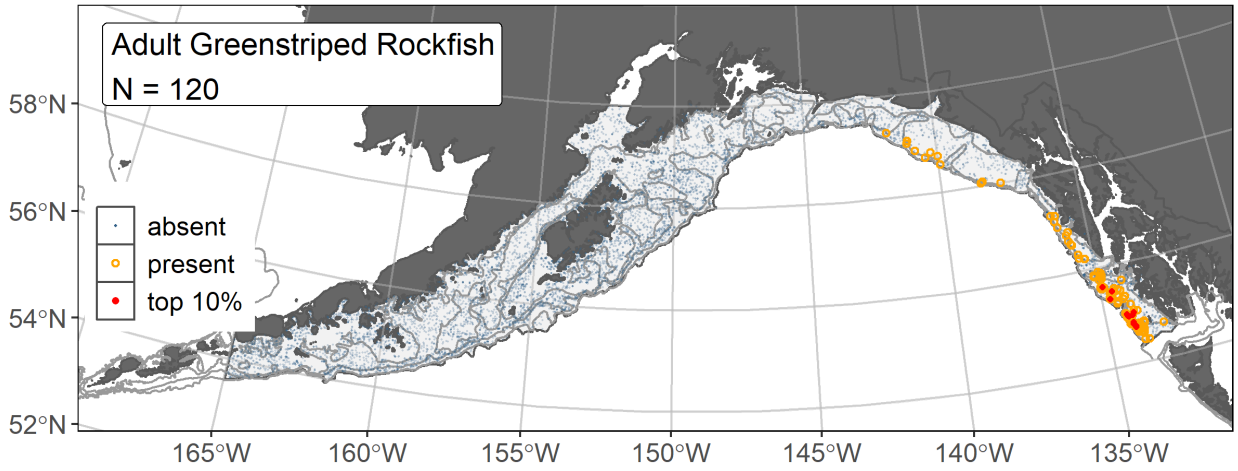

Figure 208. -- Distribution of adult greenstriped rockfish catches (N = 120) in 1993–2019 AFSC RACE-GAP summer bottom trawl surveys of the Gulf of Alaska with the 100 m, 300 m, and 700 m isobaths indicated; filled red circles indicate locations in top 10% of overall abundance, open orange circles indicate presence in remaining catches, and blue dots indicate stations sampled where the animals were not present.

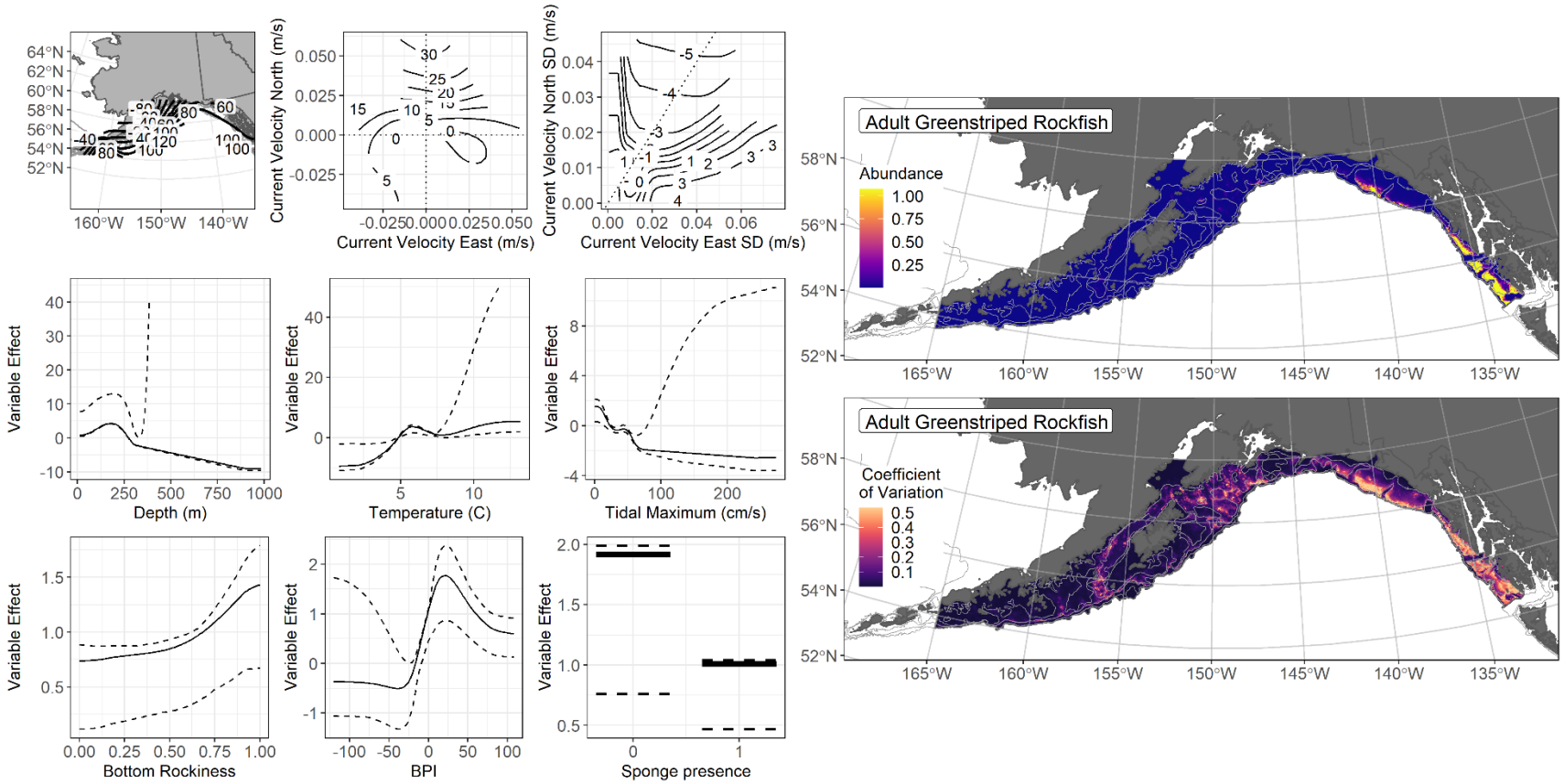

Figure 209. -- The top nine covariate effects (left panel) on ensemble-predicted adult greenstriped rockfish numerical abundance across the Gulf of Alaska (upper right panel) alongside the coefficient of variation (CV) of the ensemble predictions (lower right panel).

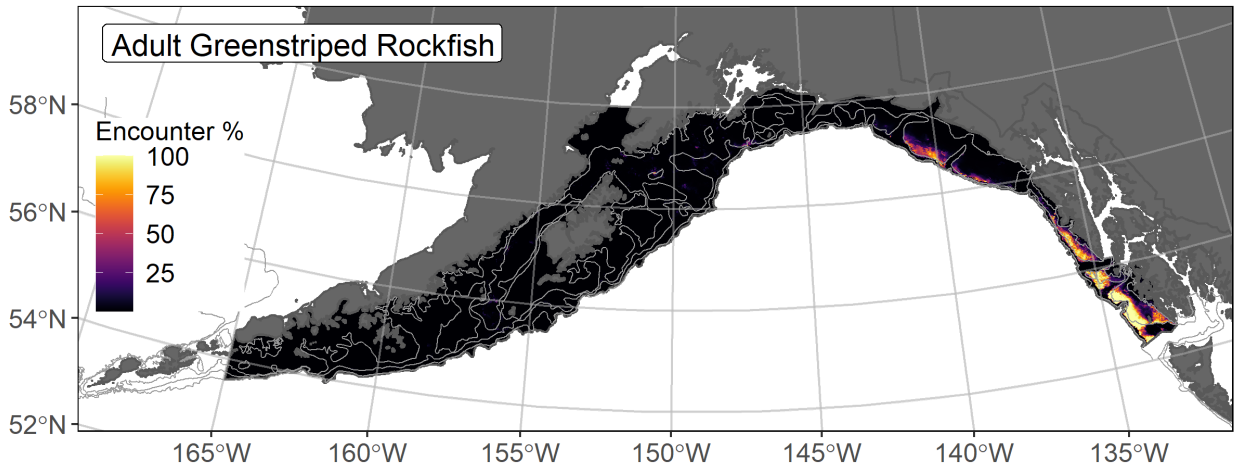

Figure 210. -- Encounter probability of adult greenstriped rockfish from AFSC RACE-GAP summer bottom trawl surveys (1993–2019) of the Gulf of Alaska with the 100 m, 300 m, and 700 m isobaths indicated.

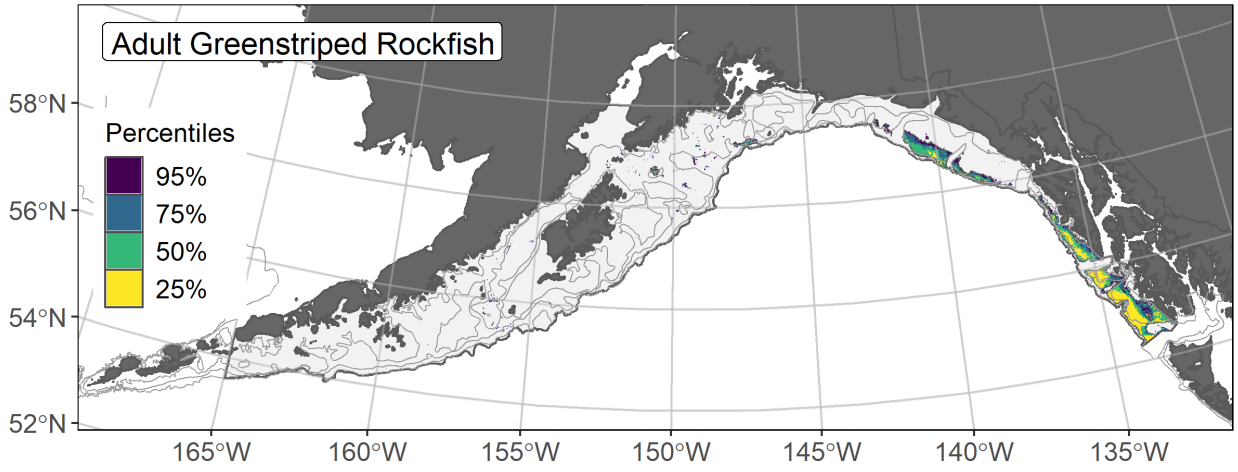

Figure 211. -- Essential fish habitat (EFH) is the area containing the top 95% of occupied habitat (defined as model estimated encounter probabilities greater than 5%) from an SDM ensemble fitted to adult greenstriped rockfish distribution and abundance in AFSC RACE-GAP summer bottom trawl surveys (1993–2019) with 100 m, 200 m, and 700 m isobaths indicated; within the EFH area map are the subareas of the top 25% (EFH hot spots), top 50% (core EFH area), and top 75% (principal EFH area) of habitat-related, ensemble-predicted numerical abundance.

Harlequin rockfish (*Sebastes variegatus*)

Harlequin rockfish (*Sebastes variegatus*) are found from the Oregon coast to the western Aleutian Islands (Love et al. 2002). Harlequin rockfish is managed as part of the Other Rockfish (OR) stock complex in both the GOA and BSAI. In the GOA, they are part of the Slope Sub-group and one of the six most common OR species by survey catch or biomass, although uncommon in the BSAI (Tribuzio and Echave 2019, Sullivan et al. 2020). Life history data collected in waters off Alaska describes harlequin rockfish as one of the smaller OR species, becoming mature at a length of 188 mm and at a relatively young age for rockfishes (4.5 years), but still living as long as 72 years (Tribuzio and Echave 2019, Tenbrink and Helser 2021). Harlequin rockfish associate with the seafloor in trawlable and untrawlable habitats; they have a high affinity for rocky and rugged habitats (Rooper et al. 2012a, Jones et al. 2021)[44].

Subadult harlequin rockfish abundance and predicted distribution from RACE-GAP summer bottom trawl surveys in the Gulf of Alaska -- Subadult harlequin rockfish (N = 102) caught in GOA RACE-GAP summer bottom trawl surveys (1993–2019) were distributed primarily in the eastern and central GOA with some occurrences on the outer continental shelf south of Kodiak Island through the western GOA (Fig. 212). Highest abundance catches occurred east of Kodiak Island. Three of five SDMs considered for inclusion in the ensemble to predict numerical abundance of subadult harlequin rockfish in the GOA converged (Table 71). The three best-performing SDMs were equally weighted by RMSE in the final ensemble, which attained a fair overall fit to the observed subadult harlequin rockfish distribution and abundance data. The ensemble was poor at predicting high and low abundance catches ($\rho = 0.16$), excellent at discriminating presence-absence (AUC = 0.92), and good at explaining deviance (PDE = 0.52). Geographic location, bottom depth, and sponge presence accounted for 54.6% of the covariate contribution to the deviance explained by the final ensemble (Fig. 213). Subadult harlequin rockfish abundance was higher in the central and eastern GOA at shallower depths on the continental shelf, where the CV of ensemble predictions was also higher (Fig. 213). The probability of encountering subadult harlequin rockfish corresponded with areas of predicted higher abundance, including Portlock bank and the Fairweather grounds (Fig. 214).

Adult harlequin rockfish abundance and predicted distribution from RACE-GAP summer bottom trawl surveys in the Gulf of Alaska -- Adult harlequin rockfish (N = 514) caught in GOA RACE-GAP summer bottom trawl surveys (1993–2019) were distributed along the outer continental shelf and upper slope with highest abundance catches scattered throughout the survey area (Fig. 215). Three of

[44] A recommendation from the stock author review to incorporate additional sources of data (e.g., from fishery observers) in future SDM ensemble EFH mapping for this species will be included as a research recommendation from the 2023 EFH 5-year Review.

five SDMs considered for inclusion in the ensemble to predict numerical abundance of adult harlequin rockfish in the GOA converged (Table 71). The three best-performing SDMs were nearly equally weighted by RMSE in the final ensemble, which attained a good overall fit to the observed adult harlequin rockfish distribution and abundance data. The ensemble was fair at predicting high and low abundance catches ($\rho = 0.31$), and good at discriminating presence-absence (AUC = 0.88) and explaining deviance (PDE = 0.44). Bottom depth, geographic location, and seafloor rockiness accounted for 51.3% of the covariate contribution to the deviance explained by the ensemble (Table 72). Adult harlequin rockfish abundance was higher around 200 m depth with rocky substrate present along the outer continental shelf and upper slope in the eastern and central GOA and west of Kodiak Island (Fig. 216). The CV of ensemble predictions was relatively low across the survey area compared to subadults. The probability of encountering adult harlequin rockfish was most likely on the outer continental shelf and upper slope throughout the GOA (Fig. 217).

Essential Fish Habitat of subadult and adult harlequin rockfish in the Gulf of Alaska -- Ensemble-predicted habitat-related numerical abundance of harlequin rockfish life stages collected in RACE-GAP summer bottom trawl surveys of the GOA (1993–2019) was mapped as EFH areas and subareas (Fig. 218). EFH area of subadult harlequin rockfish occurred on the continental shelf and upper slope primarily in the central and eastern GOA. The EFH area of adults was more extensive than that of subadults in the GOA study area.

Table 71. -- Constituent species distribution models (SDMs) used to construct Essential Fish Habitat (EFH) for a) subadult and b) adult harlequin rockfish: MaxEnt = Maximum entropy; paGAM = presence-absence generalized additive model; hGAM = zero-adjusted Poisson hurdle GAM; GAM_P = standard Poisson GAM; GAM_{nb} = standard negative-binomial GAM; RMSE = root mean square error; ρ (rho) = Spearman's rank correlation coefficient; AUC = area under the receiver-operating characteristic curve; and PDE = Poisson deviance explained *. The "--" indicates that this model was not included in the final ensemble.

a) subadult harlequin rockfish

Models	RMSE	Relative Weight	ρ	AUC	PDE	EFH area (km^2)
MaxEnt	15.0	0.33	0.12	0.81	0.03	193,500
paGAM	14.9	0.34	0.15	0.89	0.20	155,000
hGAM	--	--	--	--	--	--
GAM_P	--	--	--	--	--	--
GAM_{nb}	14.9	0.33	0.16	0.89	0.32	81,600
ensemble	14.6	1	0.16	0.92	0.50	170,600

b) adult harlequin rockfish

Models	RMSE	Relative Weight	ρ	AUC	PDE	EFH area (km^2)
MaxEnt	75.2	0.34	0.30	0.87	0.21	232,300
paGAM	75.1	0.34	0.31	0.87	0.21	258,000
hGAM	--	--	--	--	--	--
GAM_P	77.2	0.32	0.22	0.76	0.14	158,900
GAM_{nb}	--	--	--	--	--	--
ensemble	71.3	1	0.31	0.88	0.44	254,800

* Refer to the Species Distribution Model Performance Metrics subsection within the Statistical Modeling section of the Methods for detailed descriptions of individual model performance metrics.

Table 72. -- Covariates retained in the a) subadult and b) adult harlequin rockfish species distribution model (SDM) final ensembles, the percent contribution to the ensemble deviance explained by each covariate, and the cumulative deviance explained: SD = standard deviation and BPI = bathymetric position index.

harlequin rockfish

	Covariate	% Contribution	Cumulative %
a) subadult	location	32.4	32.4
	bottom depth	11.5	43.9
	sponge presence	10.8	54.6
	bottom temperature	8.7	63.3
	current SD	7.8	71.1
	current	7.2	78.3
	aspect east	4.7	83.0
	rockiness	4.6	87.6
	slope	4.3	91.9
	BPI	3.0	94.9
	tidal maximum	2.4	97.3
	aspect north	1.3	98.6
	coral presence	0.6	99.2
	curvature	0.5	99.7
	pennatulacean presence	0.3	100.0
b) adult	bottom depth	21.4	21.4
	location	16.6	38.0
	rockiness	13.3	51.3
	current	10.3	61.6
	sponge presence	8.8	70.4
	aspect east	6.6	77.0
	bottom temperature	6.2	83.2
	current SD	4.5	87.7
	BPI	4.2	91.9
	coral presence	2.3	94.2
	aspect north	2.0	96.2
	tidal maximum	1.9	98.1
	curvature	1.2	99.3
	slope	0.4	99.7
	pennatulacean presence	0.3	100.0

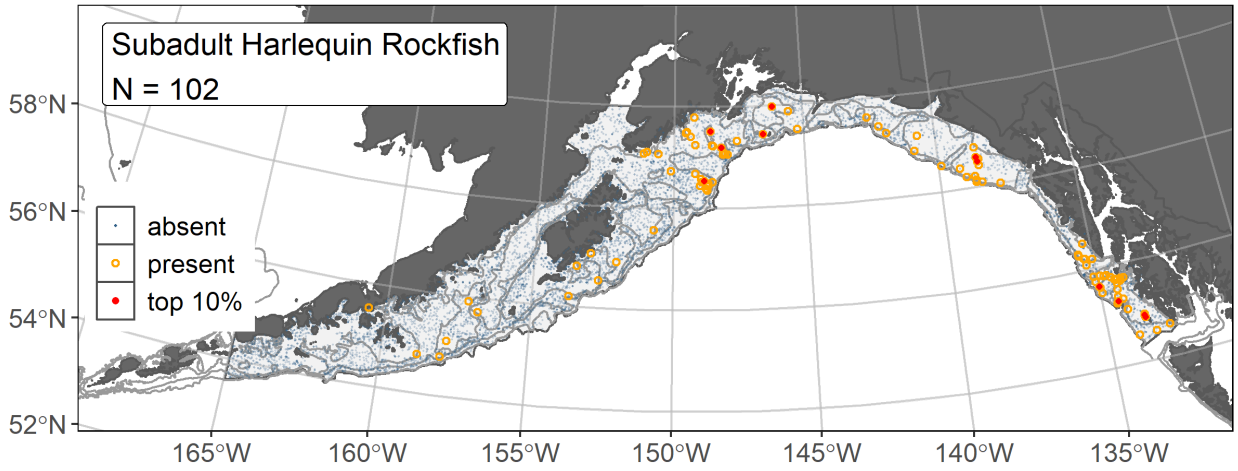

Figure 212. -- Distribution of subadult harlequin rockfish catches (N = 102) in 1993–2019 AFSC RACE-GAP summer bottom trawl surveys of the Gulf of Alaska with the 100 m, 300 m, and 700 m isobaths indicated; filled red circles indicate locations in top 10% of overall abundance, open orange circles indicate presence in remaining catches, and blue dots indicate stations sampled where the animals were not present.

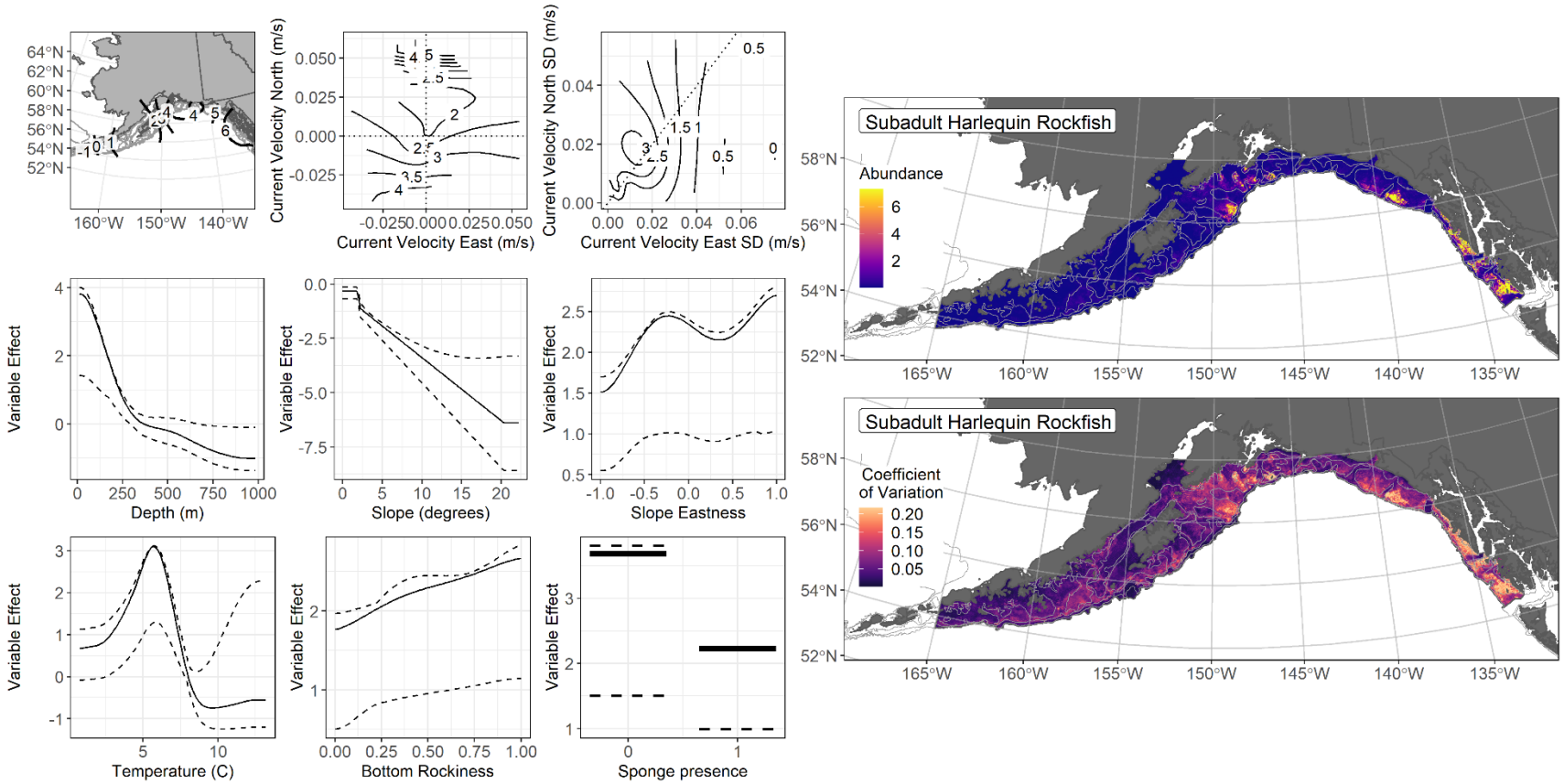

Figure 213. -- The top nine covariate effects (left panel) on ensemble-predicted subadult harlequin rockfish numerical abundance across the Gulf of Alaska (upper right panel) alongside the coefficient of variation (CV) of the ensemble predictions (lower right panel).

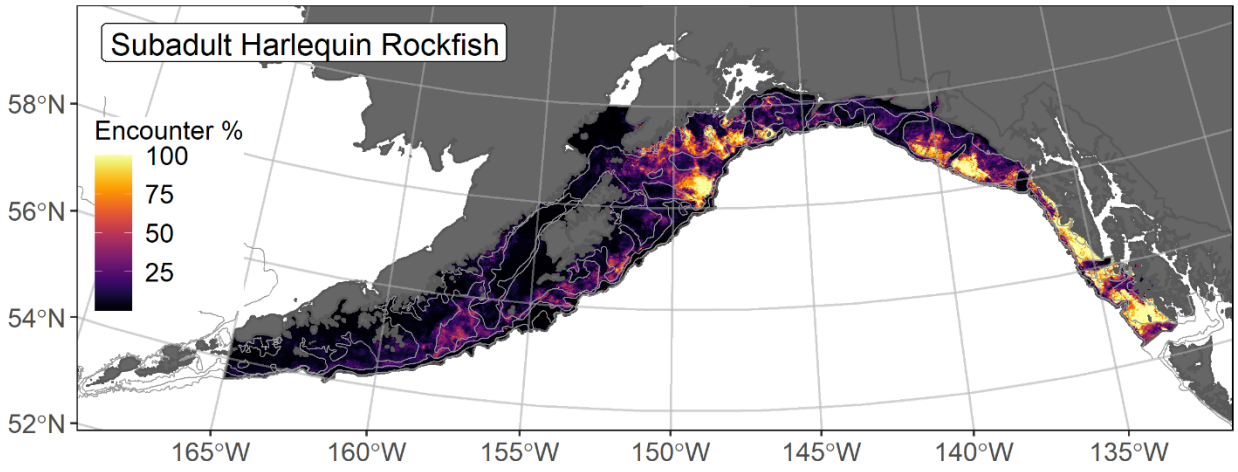

Figure 214. -- Encounter probability of subadult harlequin rockfish from AFSC RACE-GAP summer bottom trawl surveys (1993–2019) of the Gulf of Alaska with the 100 m, 300 m, and 700 m isobaths indicated.

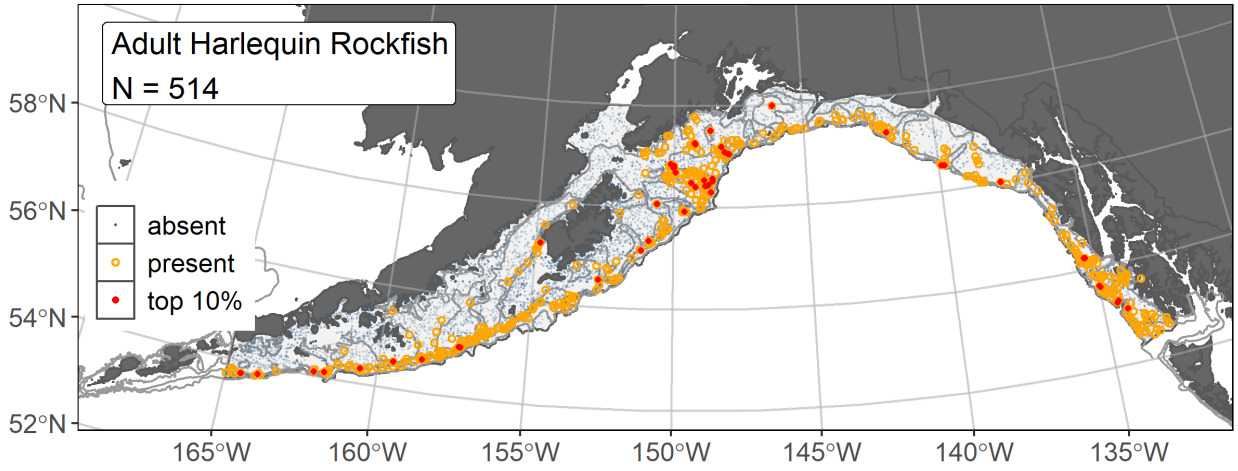

Figure 215. -- Distribution of adult harlequin rockfish catches (N = 514) in 1993–2019 AFSC RACE-GAP summer bottom trawl surveys of the Gulf of Alaska with the 100 m, 300 m, and 700 m isobaths indicated; filled red circles indicate locations in top 10% of overall abundance, open orange circles indicate presence in remaining catches, and blue dots indicate stations sampled where the animals were not present.

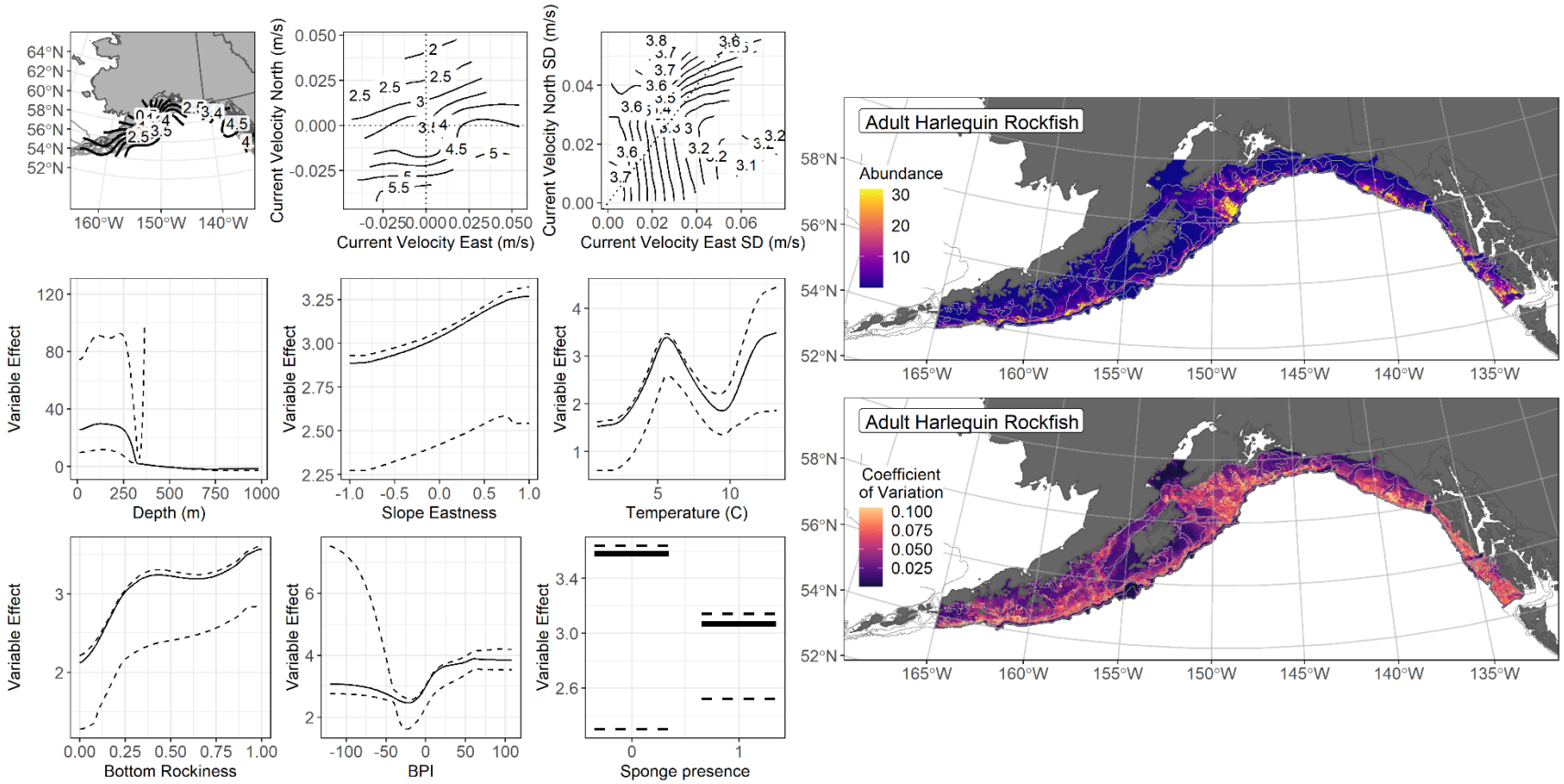

Figure 216. -- The top nine covariate effects (left panel) on ensemble-predicted adult harlequin rockfish numerical abundance across the Gulf of Alaska (upper right panel) alongside the coefficient of variation (CV) of the ensemble predictions (lower right panel).

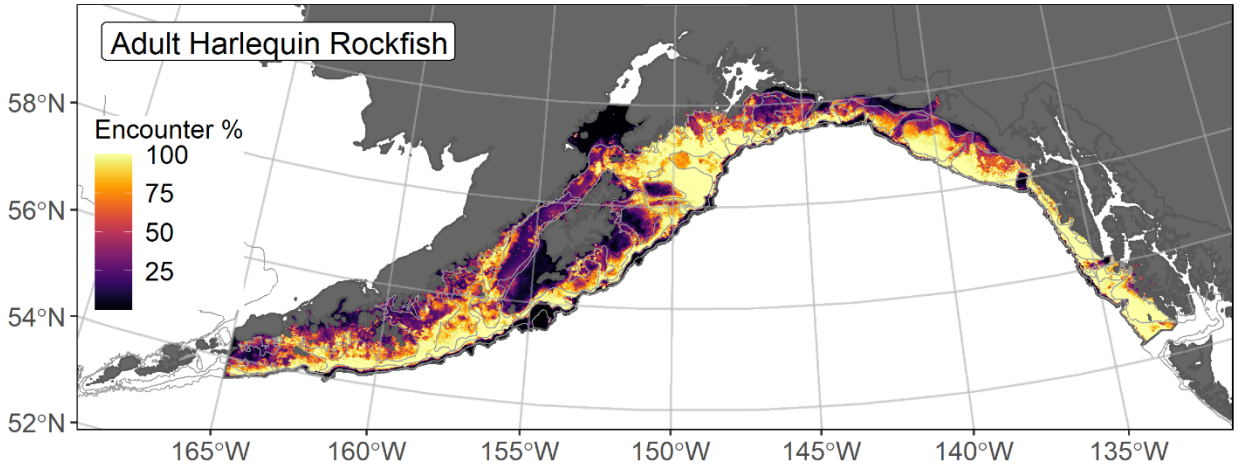

Figure 217. -- Encounter probability of adult harlequin rockfish from AFSC RACE-GAP summer bottom trawl surveys (1993–2019) of the Gulf of Alaska with the 100 m, 300 m, and 700 m isobaths indicated.

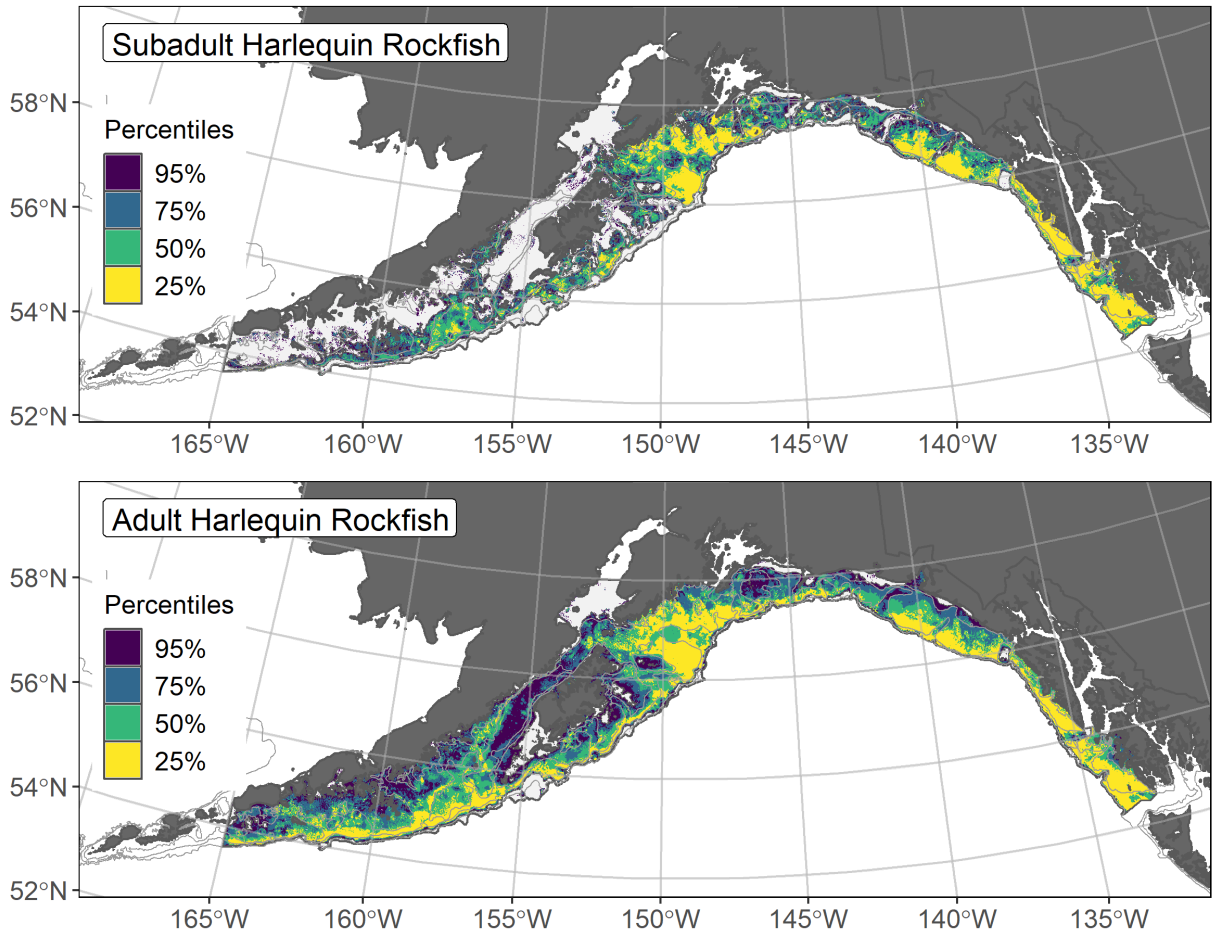

Figure 218. -- Essential fish habitat (EFH) is the area containing the top 95% of occupied habitat (defined as model estimated encounter probabilities greater than 5%) from an SDM ensemble fitted to subadult (top panel) and adult (bottom panel) harlequin rockfish distribution and abundance in AFSC RACE-GAP summer bottom trawl surveys (1993–2019) with 100 m, 200 m, and 700 m isobaths indicated; within the EFH area map are the subareas of the top 25% (EFH hot spots), top 50% (core EFH area), and top 75% (principal EFH area) of habitat-related, ensemble-predicted numerical abundance.

Pygmy rockfish (*Sebastes wilsoni*)

Pygmy rockfish (*Sebastes wilsoni*) are distributed from southern California to the central GOA (Love et al. 2002). Pygmy rockfish are managed as part of the Other Rockfish (OR) stock complex in the GOA, where they are part of the Slope Sub-group. Life history data for this small rockfish species is not well known, with a maximum observed size of 260 mm and a maximum age of 26 years based on studies south of Alaska (Love et al. 2002). Pygmy rockfish are thought to be most closely related to harlequin and Puget Sound rockfishes, with lengths at maturity of 190 mm and 130 mm, respectively. Without length at maturity information to separate subadults and adults, all pygmy rockfish in GOA RACE-GAP summer bottom trawl survey catches (1993–2019) were combined in SDMs of habitat-related abundance to map EFH. This species is often observed in large schools over rocky habitat and closely associated with structural invertebrate cover such as crinoids, sponges, and soft corals (Love et al. 2002, Pirtle 2005)[45].

Pygmy rockfish abundance and predicted distribution from RACE-GAP summer bottom trawl surveys in the Gulf of Alaska -- Pygmy rockfish (N = 63) catches in GOA RACE-GAP summer bottom trawl surveys (1993–2019) were infrequent and occurred primarily east of Kodiak Island (Fig. 219). Three of five SDMs considered for inclusion in the ensemble to predict numerical abundance of pygmy rockfish in the GOA converged (Table 73). The three best-performing SDMs were weighted by RMSE in the final ensemble, which attained a fair overall fit to the observed pygmy rockfish distribution and abundance data. The ensemble was poor at predicting high and low abundance catches ($\rho = 0.14$), excellent at discriminating presence-absence (AUC = 0.96), and fair at explaining deviance (PDE = 0.40). Seafloor rockiness, geographic location, and sponge presence accounted for 58.3% of the covariate contribution to the deviance explained by the final ensemble (Table 74). Pygmy rockfish abundance was higher at depths < 250 m with rocky substrate present and low sponge presence on the continental shelf of the eastern GOA off southeast Alaska and some higher abundance areas in the central GOA (Fig. 220). The CV of ensemble predictions was higher east of Kodiak Island (Fig. 220). The probability of encountering pygmy rockfish was high in areas of predicted high abundance (Fig. 221).

Essential Fish Habitat of pygmy rockfish in the Gulf of Alaska -- Ensemble-predicted habitat-related numerical abundance of pygmy rockfish life stages collected in RACE-GAP summer bottom trawl surveys of the GOA (1993–2019) was mapped as EFH areas and subareas (Fig. 222). The EFH area for pygmy rockfish mainly occurred on the continental shelf east of Kodiak Island, with some patchy EFH

[45] A recommendation from the stock author review to incorporate additional sources of data if available (e.g., from untrawlable habitats) in future SDM ensemble EFH mapping for this species will be included as a research recommendation from the 2023 EFH 5-year Review.

areas farther west. Core EFH area and EFH hot spots were concentrated on the continental shelf south of the Kenai Peninsula, Portlock bank, the Fairweather grounds, and off southeast Alaska.

Table 73. -- Constituent species distribution models (SDMs) used to construct Essential Fish Habitat (EFH) for pygmy rockfish: MaxEnt = Maximum entropy; paGAM = presence-absence generalized additive model; hGAM = zero-adjusted Poisson hurdle GAM; GAM_P = standard Poisson GAM; GAM_{nb} = standard negative-binomial GAM; RMSE = root mean square error; ρ (rho) = Spearman's rank correlation coefficient; AUC = area under the receiver-operating characteristic curve; and PDE = Poisson deviance explained *. The "--" indicates that this model was not included in the final ensemble.

pygmy rockfish

Models	RMSE	Relative Weight	ρ	AUC	PDE	EFH area (km^2)
MaxEnt	2.98	0.40	0.12	0.91	0.32	77,500
paGAM	2.98	0.40	0.14	0.92	0.29	74,800
hGAM	--	--	--	--	--	--
GAM_P	--	--	--	--	--	--
GAM_{nb}	4.11	0.21	0.19	0.96	0.34	31,600
ensemble	3.02	1	0.14	0.96	0.40	74,900

* Refer to the Species Distribution Model Performance Metrics subsection within the Statistical Modeling section of the Methods for detailed descriptions of individual model performance metrics.

Table 74. -- Covariates retained in the pygmy rockfish species distribution model (SDM) final ensembles, the percent contribution to the ensemble deviance explained by each covariate, and the cumulative deviance explained: SD = standard deviation and BPI = bathymetric position index.

pygmy rockfish

Covariate	% Contribution	Cumulative %
rockiness	23.4	23.4
location	22.7	46.1
sponge presence	12.2	58.3
bottom temperature	7.8	66.1
bottom depth	7.5	73.6
current	7.3	80.9
slope	6.2	87.1
BPI	4.9	92.0
tidal maximum	4.6	96.6
current SD	1.7	98.3
curvature	1.0	99.3
aspect north	0.4	99.7
aspect east	0.2	99.9
coral presence	0.1	100.0

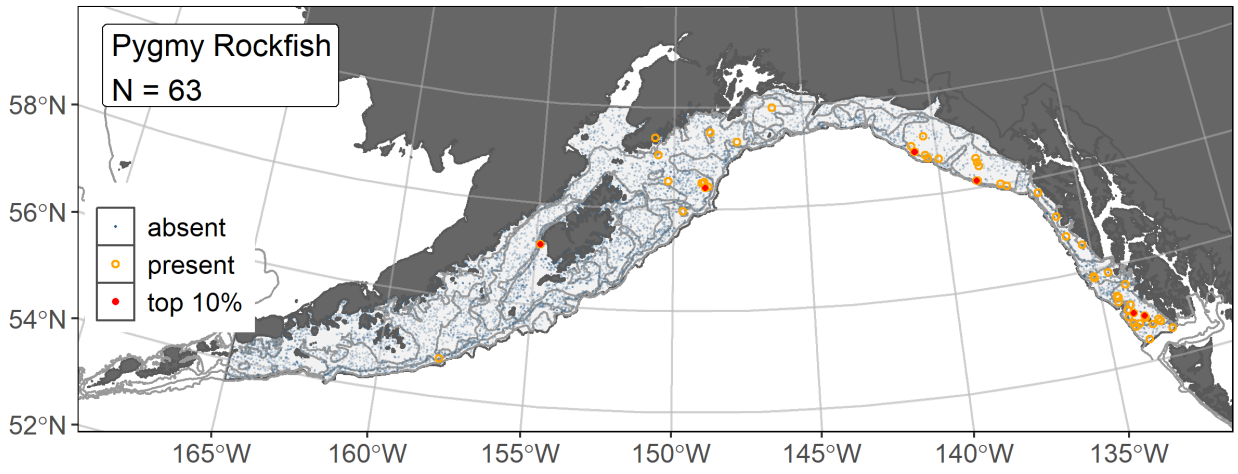

Figure 219. -- Distribution of pygmy rockfish catches (N = 63) in 1993–2019 AFSC RACE-GAP summer bottom trawl surveys of the Gulf of Alaska with the 100 m, 300 m, and 700 m isobaths indicated; filled red circles indicate locations in top 10% of overall abundance, open orange circles indicate presence in remaining catches, and blue dots indicate stations sampled where the animals were not present.

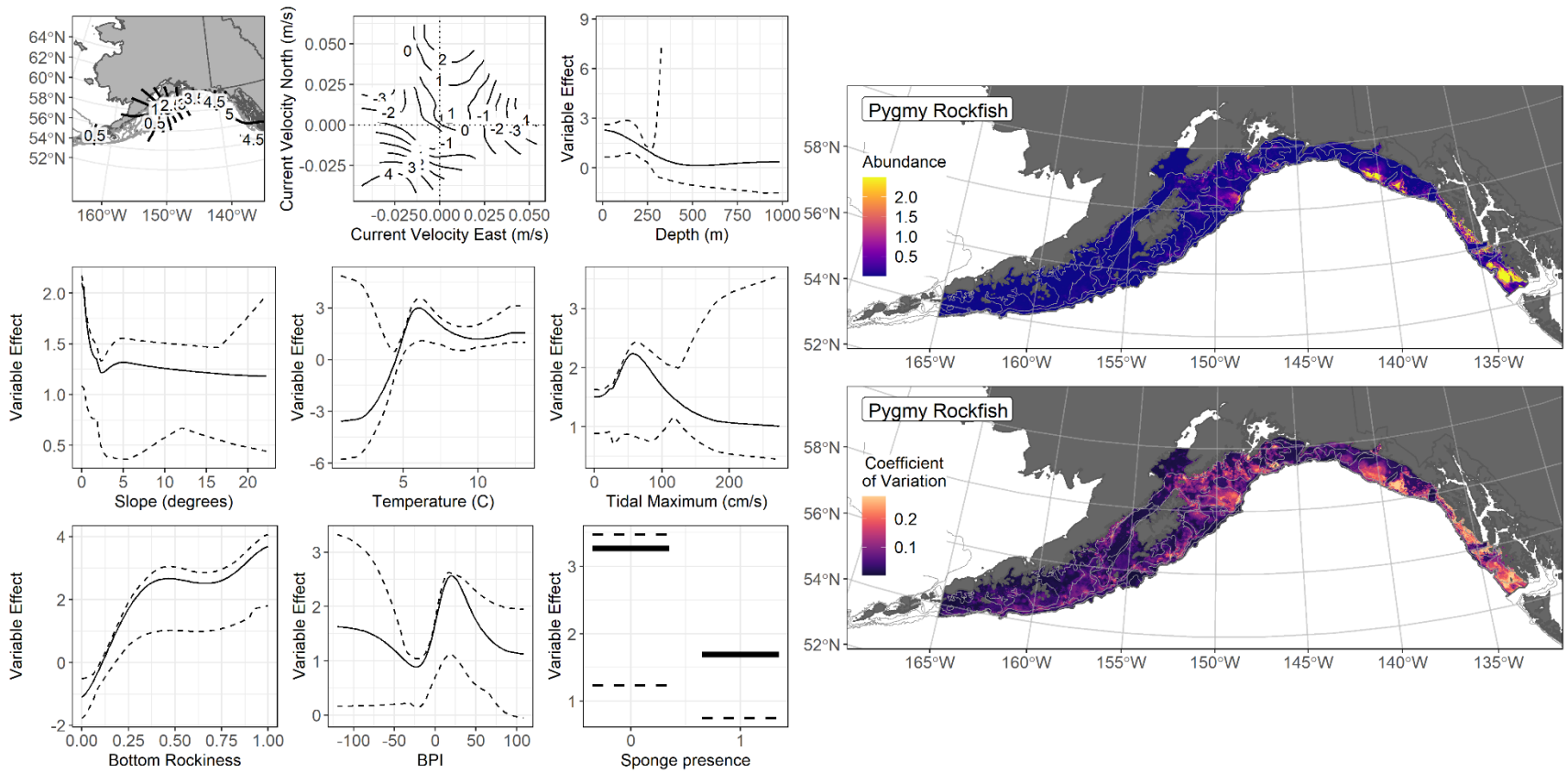

Figure 220. -- The top nine covariate effects (left panel) on ensemble-predicted pygmy rockfish numerical abundance across the Gulf of Alaska (upper right panel) alongside the coefficient of variation (CV) of the ensemble predictions (lower right panel).

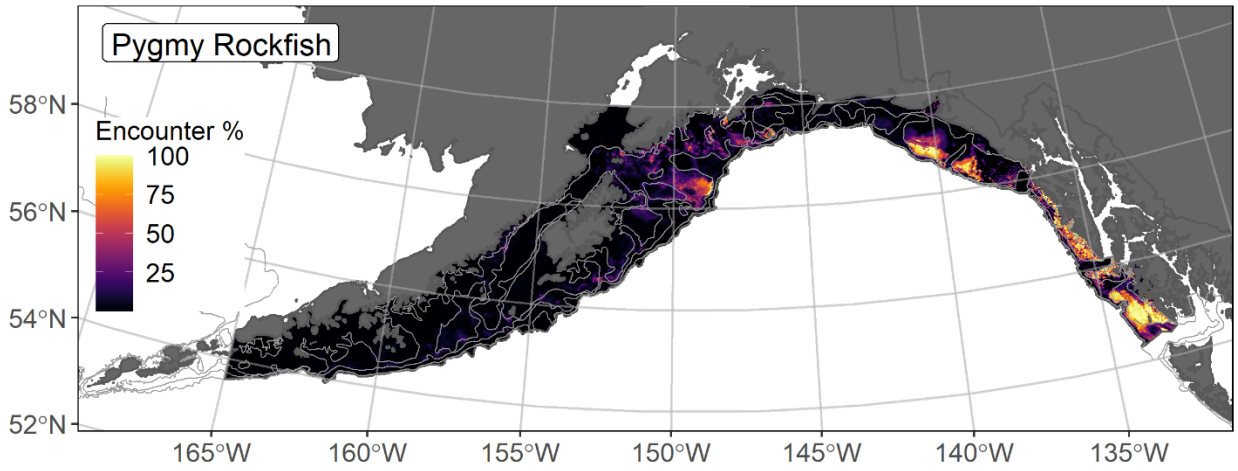

Figure 221. -- Encounter probability of pygmy rockfish from AFSC RACE-GAP summer bottom trawl surveys (1993–2019) of the Gulf of Alaska with the 100 m, 300 m, and 700 m isobaths indicated.

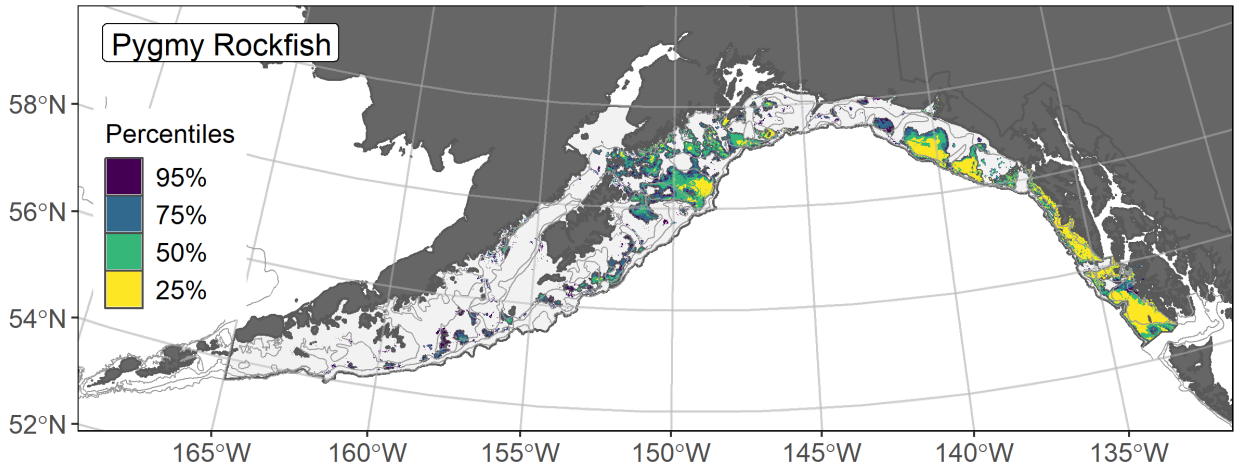

Figure 222. -- Essential fish habitat (EFH) is the area containing the top 95% of occupied habitat (defined as model estimated encounter probabilities greater than 5%) from an SDM ensemble fitted to pygmy rockfish distribution and abundance in AFSC RACE-GAP summer bottom trawl surveys (1993–2019) with 100 m, 200 m, and 700 m isobaths indicated; within the EFH area map are the subareas of the top 25% (EFH hot spots), top 50% (core EFH area), and top 75% (principal EFH area) of habitat-related, ensemble-predicted numerical abundance.

Redbanded rockfish (*Sebastes babcocki*)

Redbanded rockfish (*Sebastes babcocki*) are distributed from southern California to the Aleutian Islands and Bering Sea canyons (Love et al. 2002). Life history data collected in waters off Alaska and elsewhere describes redbanded rockfish becoming mature at a length of 420 mm and 19 years age and living as long as 106 years (Love et al. 2002, Munk 2001, Tribuzio and Echave 2019). Redbanded rockfish are managed as part of the Other Rockfish (OR) stock complex in the GOA, where they are part of the Slope Sub-group and one of the six most common OR species by survey catch or biomass (Tribuzio and Echave 2019). This species associates with the seafloor in rocky or mixed substrate type habitats (Love et al. 2002)[46].

Subadult redbanded rockfish abundance and predicted distribution from RACE-GAP summer bottom trawl surveys in the Gulf of Alaska -- Subadult redbanded rockfish (N = 829) catches in the RACE-GAP summer survey occurred throughout the GOA with most of the highest abundance catches in the eastern GOA and off southeast Alaska (Fig. 223). Four of five SDMs considered for inclusion in the ensemble to predict numerical abundance of subadult redbanded rockfish in the GOA converged (Table 75); the GAM_{nb} was eliminated by skill testing. The remaining three best-performing SDMs were weighted by RMSE in the final ensemble, which attained an excellent overall fit to the observed subadult redbanded rockfish distribution and abundance data. The ensemble was good at predicting high and low abundance catches (ρ = 0.46), and excellent at discriminating presence-absence (AUC = 0.94) and explaining deviance (PDE = 0.63). Bottom depth, geographic location, slope, and seafloor rockiness accounted for 79.9% of the covariate contribution to the deviance explained by the ensemble (Table 76). Subadult redbanded rockfish abundance was higher around 250 m depth in and around glacial troughs and along the outer continental shelf and upper slope of the eastern GOA (Fig. 224). The CV of ensemble predictions was highest along the continental slope. Subadult redbanded rockfish are likely to be encountered by the RACE-GAP survey in glacial troughs and along the outer continental shelf and upper slope throughout the GOA (Fig. 225).

Adult redbanded rockfish abundance and predicted distribution from RACE-GAP summer bottom trawl surveys in the Gulf of Alaska -- Adult redbanded rockfish (N = 321) catches from the RACE-GAP summer survey were present from southeast Alaska to the western GOA with the highest abundance catches located from Kodiak Islands and east (Fig. 226). Five SDMs considered for inclusion in the ensemble to predict numerical abundance of adult redbanded rockfish in the GOA converged

[46] A recommendation from the stock author review to incorporate additional sources of data (e.g., from longline surveys) in future SDM ensemble EFH mapping for this species will be included as a research recommendation from the 2023 EFH 5-year Review.

(Table 75); the GAM_{nb} was eliminated by skill testing. The remaining four best-performing SDMs were weighted nearly equally by RMSE in the final ensemble, which attained a good overall fit to the observed adult redbanded rockfish distribution and abundance data. The ensemble was fair at predicting high and low abundance catches ($\rho = 0.29$), excellent at discriminating presence-absence (AUC = 0.93), and good at explaining deviance (PDE = 0.49). Bottom depth, geographic position, and bottom temperature accounted for 68.7% of the covariate contribution to the deviance explained by the final ensemble (Table 76). Adult redbanded rockfish abundance was higher around 250 m depth with moderate current exposure in the eastern GOA off southeast Alaska in and around glacial troughs and on the outer continental shelf and upper slope throughout the study area (Fig. 227). The CV of ensemble predictions was highest in Shelikof Strait. The probability of encountering adult redbanded rockfish is highest in the eastern GOA off southeast Alaska and in the glacial troughs and along the continental slope (Fig. 228).

Essential Fish Habitat of subadult and adult redbanded rockfish in the Gulf of Alaska -- Ensemble-predicted habitat-related numerical abundance of northern rockfish life stages collected in RACE-GAP summer bottom trawl surveys of the GOA (1993–2019) was mapped as EFH areas and subareas (Fig. 229). EFH of subadult and adult redbanded rockfish occurred in the glacial troughs and along the outer continental shelf and upper slope of the GOA.

Table 75. -- Constituent species distribution models (SDMs) used to construct Essential Fish Habitat (EFH) for a) subadult and b) adult redbanded rockfish: MaxEnt = Maximum entropy; paGAM = presence-absence generalized additive model; hGAM = zero-adjusted Poisson hurdle GAM; GAM_P = standard Poisson GAM; GAM_{nb} = standard negative-binomial GAM; RMSE = root mean square error; ρ (rho) = Spearman's rank correlation coefficient; AUC = area under the receiver-operating characteristic curve; and PDE = Poisson deviance explained *. The "--" indicates that this model was not included in the final ensemble.

a) subadult redbanded rockfish

Models	RMSE	Relative Weight	ρ	AUC	PDE	EFH area (km^2)
MaxEnt	--	--	--	--	--	--
paGAM	2.18	0.34	0.46	0.94	0.59	119,800
hGAM	2.20	0.33	0.46	0.94	0.60	111,500
GAM_P	2.23	0.33	0.45	0.93	0.59	111,900
GAM_{nb}	2.52	0	--	--	--	--
ensemble	2.06	1	0.46	0.94	0.63	116,600

b) adult redbanded rockfish

Models	RMSE	Relative Weight	ρ	AUC	PDE	EFH area (km^2)
MaxEnt	1.71	0.26	0.27	0.90	0.37	98,400
paGAM	1.69	0.26	0.28	0.92	0.41	85,400
hGAM	1.78	0.24	0.27	0.92	0.34	76,600
GAM_P	1.74	0.25	0.27	0.90	0.36	73,100
GAM_{nb}	1.76	0	--	--	--	--
ensemble	1.61	1	0.29	0.93	0.49	98,800

* Refer to the Species Distribution Model Performance Metrics subsection within the Statistical Modeling section of the Methods for detailed descriptions of individual model performance metrics.

Table 76. -- Covariates retained in the a) subadult and b) adult redbanded rockfish species distribution model (SDM) final ensembles, the percent contribution to the ensemble deviance explained by each covariate, and the cumulative deviance explained: SD = standard deviation and BPI = bathymetric position index.

redbanded rockfish			
	Covariate	**% Contribution**	**Cumulative %**
a) subadult	bottom depth	40.4	40.4
	location	28.4	68.9
	slope	6.9	75.8
	rockiness	4.1	79.9
	sponge presence	3.8	83.7
	current SD	2.8	86.5
	bottom temperature	2.8	89.3
	aspect north	2.4	91.7
	tidal maximum	2.3	94.0
	current	1.9	95.9
	BPI	1.7	97.6
	coral presence	1.4	99.0
	aspect east	0.6	99.6
	curvature	0.3	99.9
	pennatulacean presence	0.1	100.0
b) adult	bottom depth	34.2	34.2
	location	27.6	61.8
	bottom temperature	6.9	68.7
	current	6.1	74.8
	current SD	6.0	80.8
	rockiness	4.1	84.9
	tidal maximum	3.5	88.4
	slope	3.2	91.6
	BPI	3.0	94.6
	aspect north	2.0	96.6
	sponge presence	1.5	98.1
	aspect east	0.9	99.0
	coral presence	0.8	99.8
	curvature	0.2	100.0

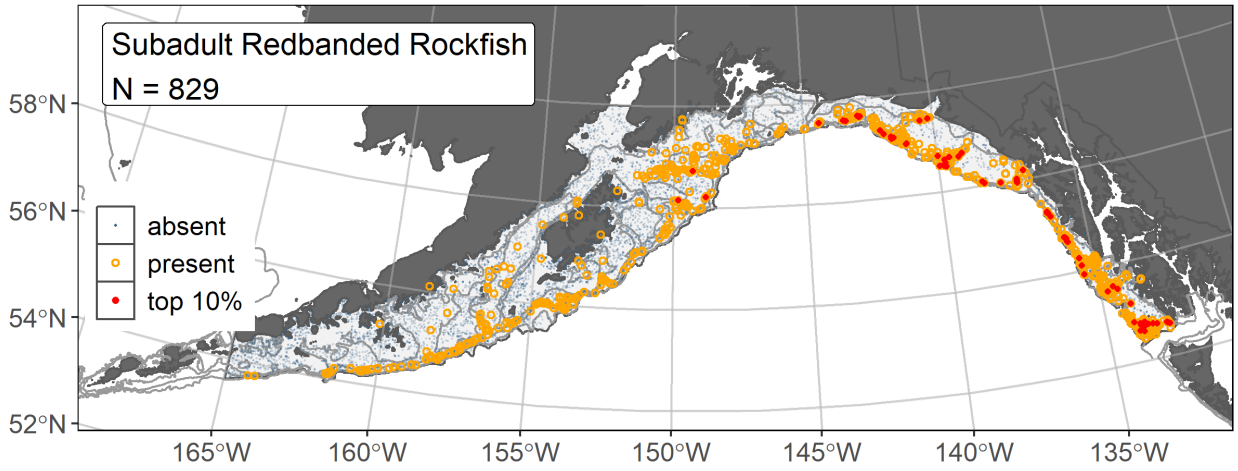

Figure 223. -- Distribution of subadult redbanded rockfish catches (N = 829) in 1993–2019 AFSC RACE-GAP summer bottom trawl surveys of the Gulf of Alaska with the 100 m, 300 m, and 700 m isobaths indicated; filled red circles indicate locations in top 10% of overall abundance, open orange circles indicate presence in remaining catches, and blue dots indicate stations sampled where the animals were not present.

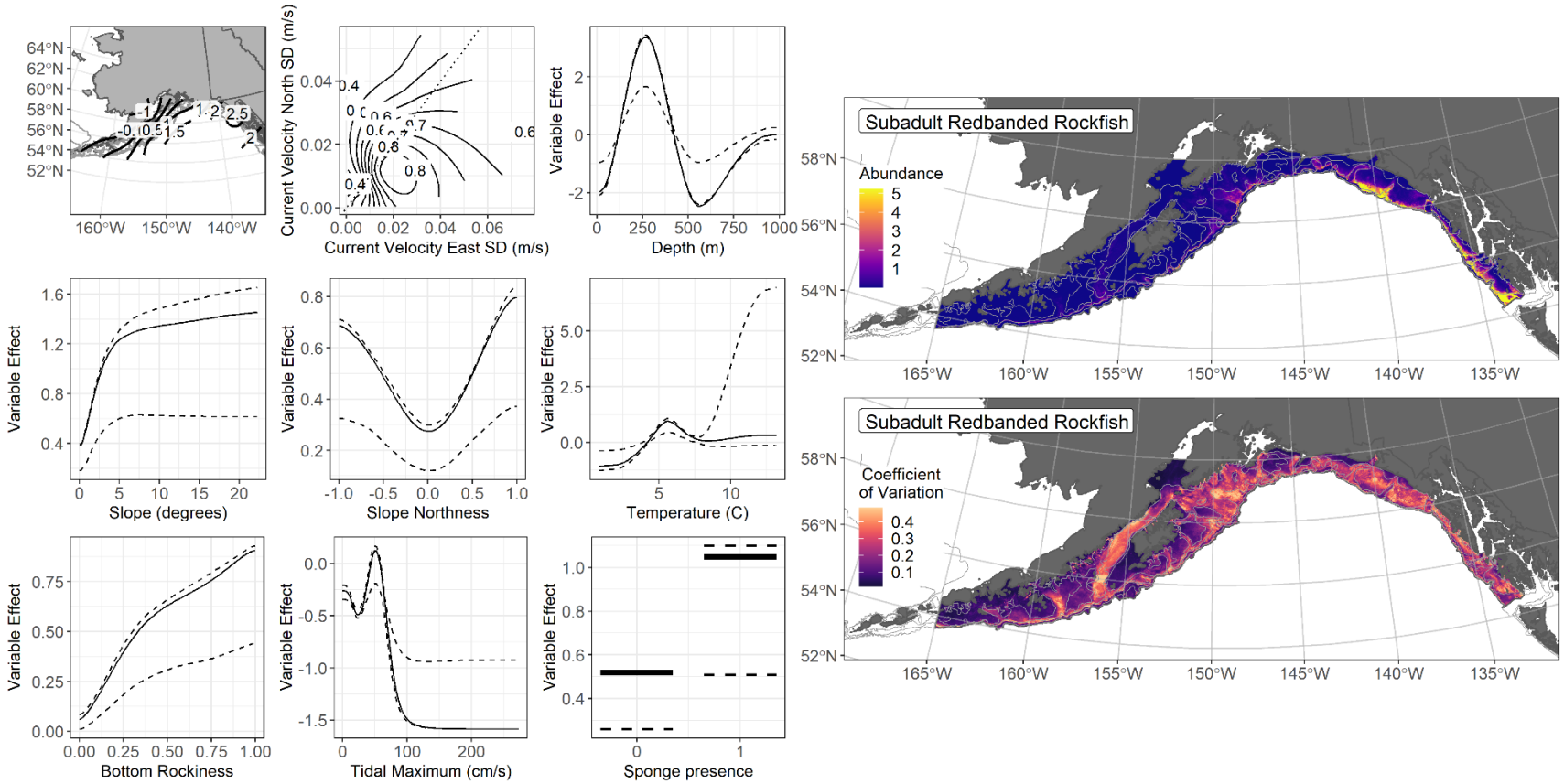

Figure 224. -- The top nine covariate effects (left panel) on ensemble-predicted subadult redbanded rockfish numerical abundance across the Gulf of Alaska (upper right panel) alongside the coefficient of variation (CV) of the ensemble predictions (lower right panel).

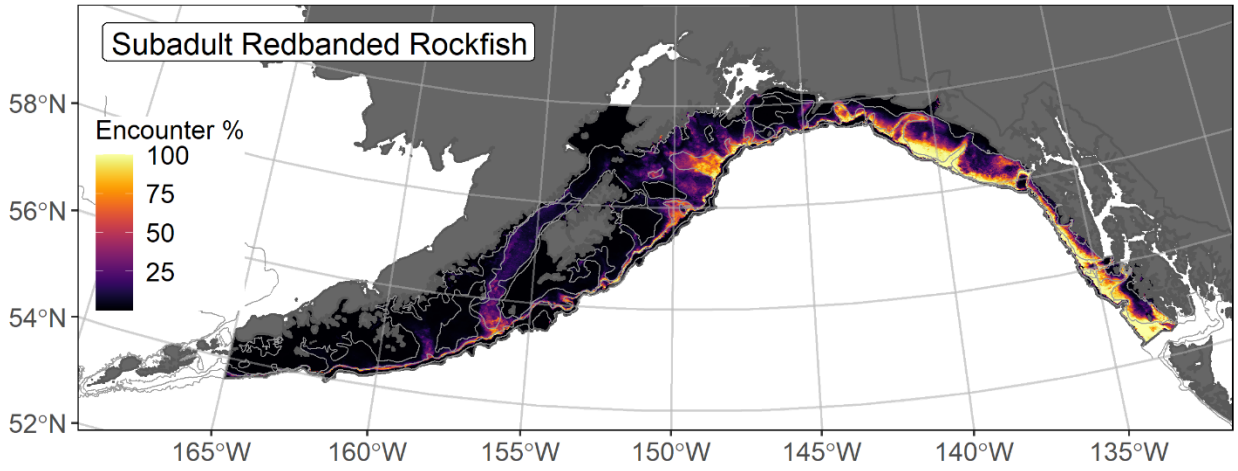

Figure 225. -- Encounter probability of subadult redbanded rockfish from AFSC RACE-GAP summer bottom trawl surveys (1993–2019) of the Gulf of Alaska with the 100 m, 300 m, and 700 m isobaths indicated.

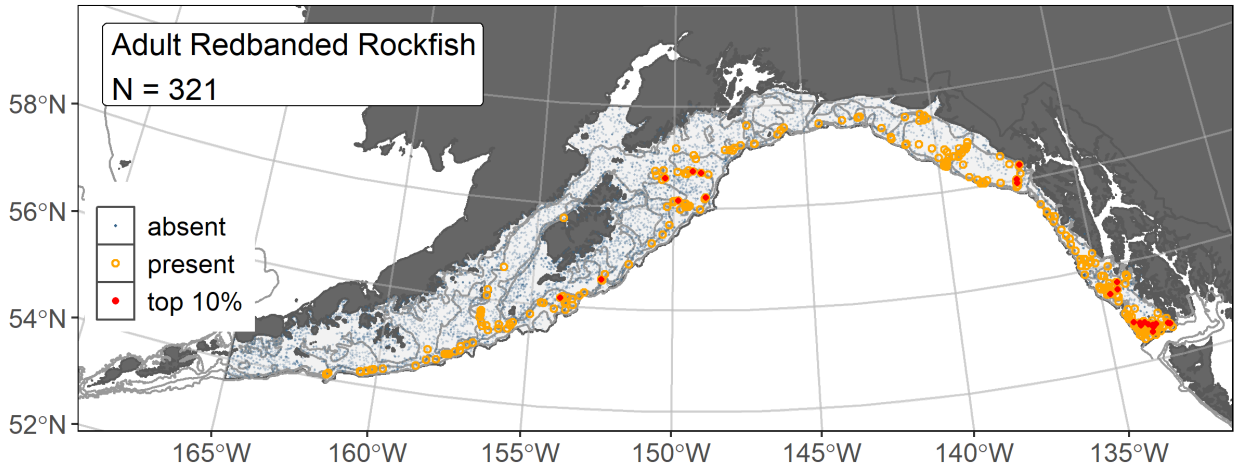

Figure 226. -- Distribution of adult redbanded rockfish catches (N = 321) in 1993–2019 AFSC RACE-GAP summer bottom trawl surveys of the Gulf of Alaska with the 100 m, 300 m, and 700 m isobaths indicated; filled red circles indicate locations in top 10% of overall abundance, open orange circles indicate presence in remaining catches, and blue dots indicate stations sampled where the animals were not present.

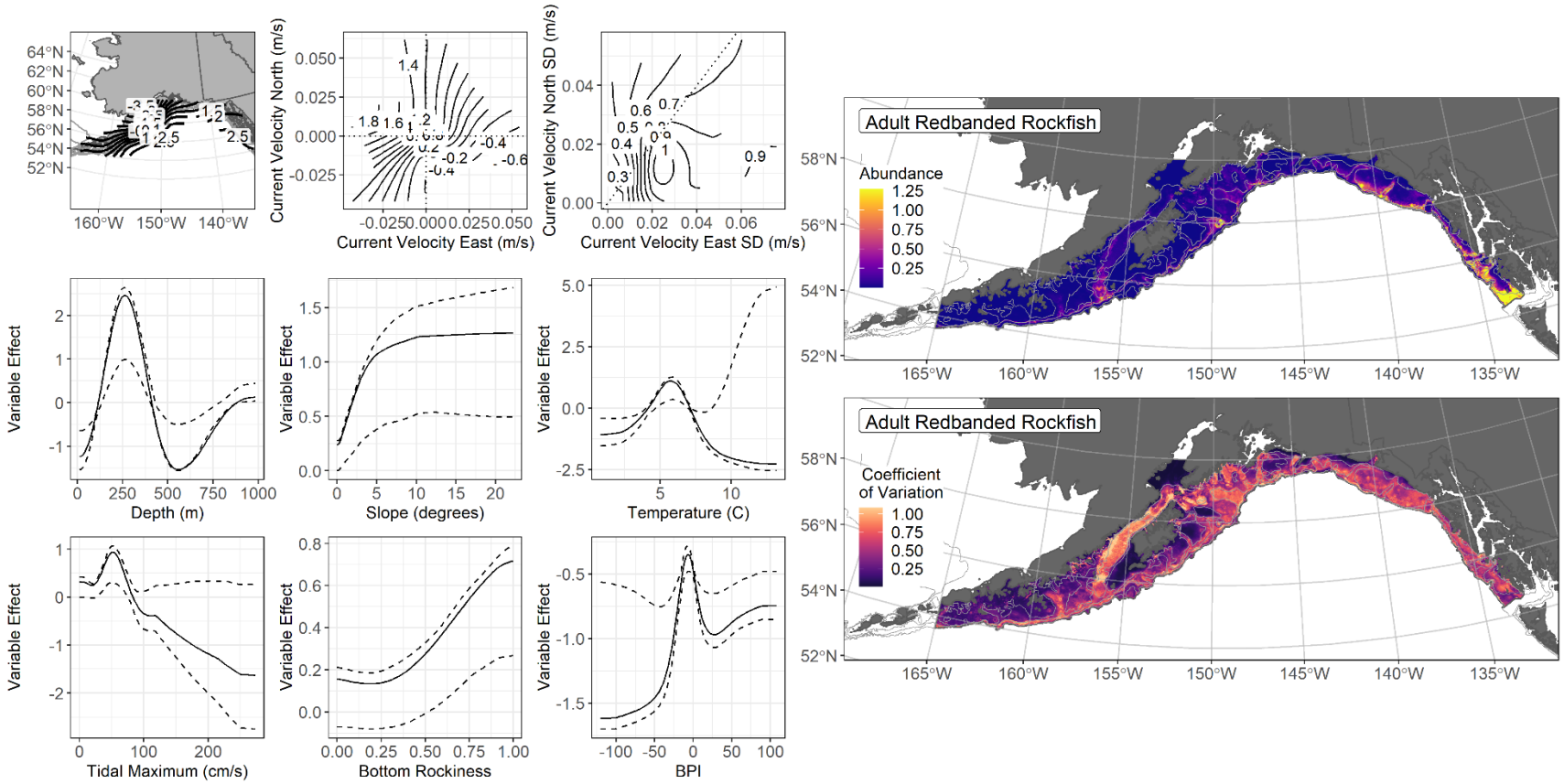

Figure 227. -- The top nine covariate effects (left panel) on ensemble-predicted adult redbanded rockfish numerical abundance across the Gulf of Alaska (upper right panel) alongside the coefficient of variation (CV) of the ensemble predictions (lower right panel).

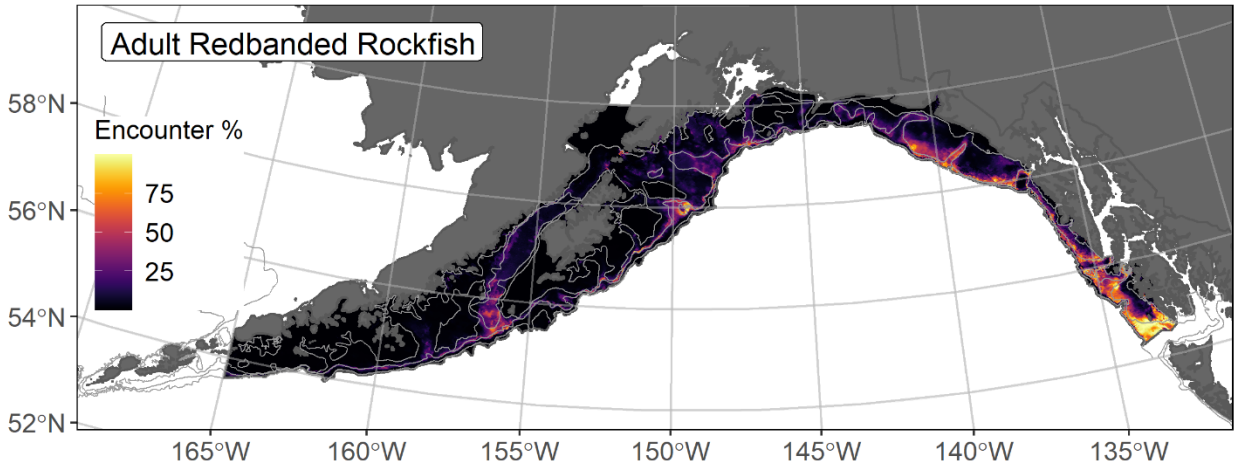

Figure 228. -- Encounter probability of adult redbanded rockfish from AFSC RACE-GAP summer bottom trawl surveys (1993–2019) of the Gulf of Alaska with the 100 m, 300 m, and 700 m isobaths indicated.

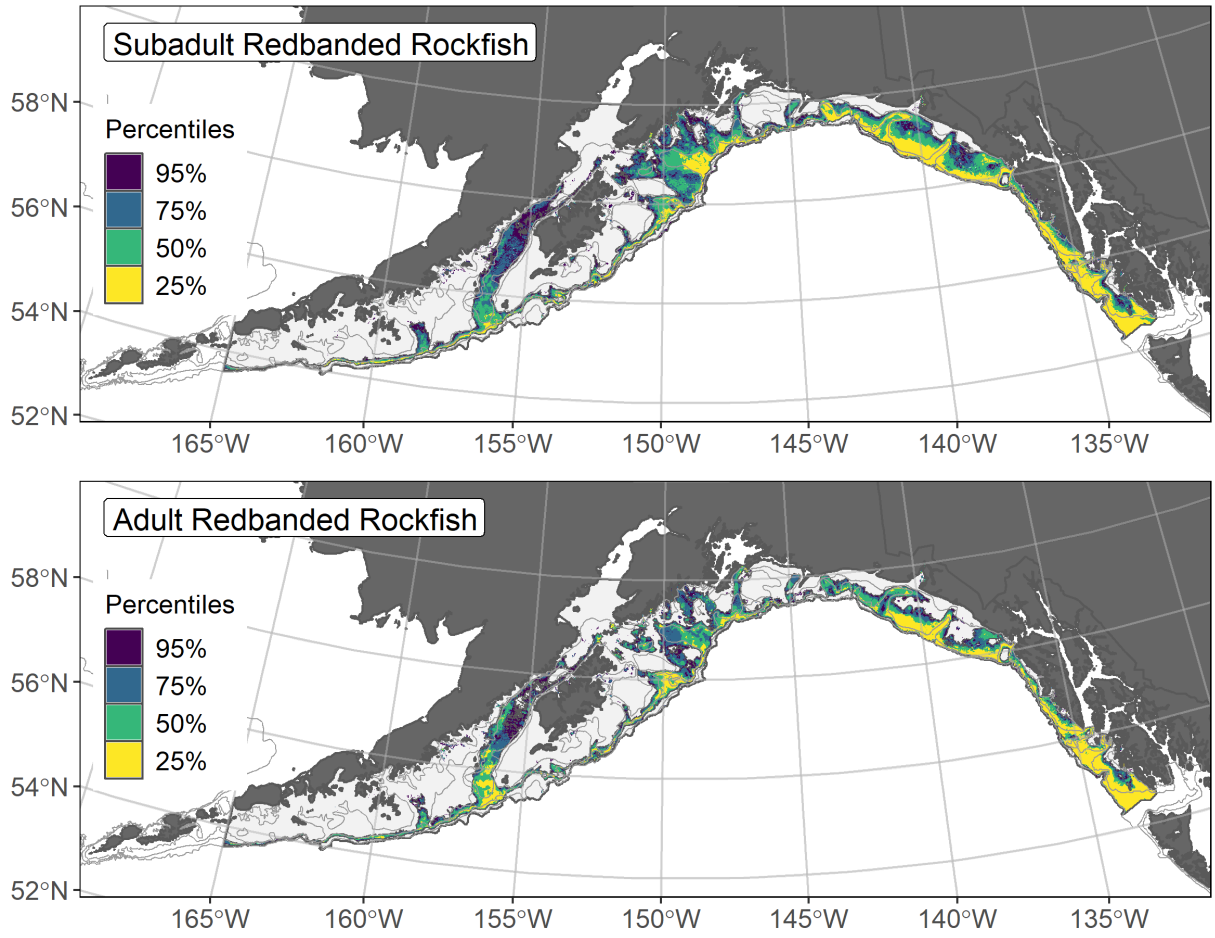

Figure 229. -- Essential fish habitat (EFH) is the area containing the top 95% of occupied habitat (defined as model estimated encounter probabilities greater than 5%) from an SDM ensemble fitted to subadult (top panel) and adult (bottom panel) redbanded rockfish distribution and abundance in AFSC RACE-GAP summer bottom trawl surveys (1993–2019) with 100 m, 200 m, and 700 m isobaths indicated; within the EFH area map are the subareas of the top 25% (EFH hot spots), top 50% (core EFH area), and top 75% (principal EFH area) of habitat-related, ensemble-predicted numerical abundance.

Redstripe rockfish (*Sebastes proriger*)

Redstripe rockfish (*Sebastes proriger*) are distributed from southern California to the western Aleutian Islands and to Pribilof Island in the Bering Sea (Love et al. 2002). This species is managed as part of the Other Rockfish (OR) stock complex in the GOA, where they are part of the Slope Sub-group and one of the six most common OR species by survey catch or biomass (Tribuzio and Echave 2019). Life history data collected in waters off Alaska and British Columbia report redstripe rockfish maximum juvenile length is 290 mm (females) (Rooper 2008), and maximum age is 41 years (Tribuzio and Echave 2019). Redstripe rockfish usually associate with high-relief and rugged seafloor habitats, where they associate with complex physical and biogenic structure (Love et al. 2002)[47].

Subadult redstripe rockfish abundance and predicted distribution from RACE-GAP summer bottom trawl surveys in the Gulf of Alaska -- Subadult redstripe rockfish (N = 133) catches in the GOA RACE-GAP summer bottom trawl surveys (1993–2019) were distributed from southeast Alaska to the western GOA with the highest abundance catches off southeast Alaska and in the central GOA (Fig. 230). Four of five SDMs considered for inclusion in the ensemble to predict numerical abundance of subadult redstripe rockfish in the GOA converged (Table 77); the GAM_P was eliminated by skill testing. The remaining three best-performing SDMs were weighted by RMSE in the final ensemble, which attained a good overall fit to the observed subadult redstripe rockfish distribution and abundance data. The ensemble was fair at predicting high and low abundance catches (ρ = 0.20), excellent at discriminating presence-absence (AUC = 0.95), and good at explaining deviance (PDE = 0.52). Geographic position, bottom depth, and rockiness accounted for 64.7% of the covariate contribution to the deviance explained by the ensemble (Table 78). Subadult redstripe rockfish abundance was higher around 200 m depth with rocky substrate present on the continental shelf of the southeastern GOA (Fig. 231). However, patchy areas of high abundance were also predicted to occur in the central GOA south of the Kenai Peninsula and areas on the outer continental shelf further west. The CV of ensemble predictions was highest on the continental shelf of the southeastern and central GOA. The probability of encountering subadult redstripe rockfish was higher on the continental shelf in the southeastern GOA, in patchy areas south of the Kenai Peninsula in the central GOA, and along the outer continental shelf in areas of the western GOA (Fig. 232).

[47] A recommendation from the stock author review to incorporate additional sources of data (e.g., from fishery observers) in future SDM ensemble EFH mapping for this species will be included as a research recommendation from the 2023 EFH 5-year Review.

Adult redstripe rockfish abundance and predicted distribution from RACE-GAP summer bottom trawl surveys in the Gulf of Alaska -- Adult redstripe rockfish (N = 234) catches in the GOA RACE-GAP summer bottom trawl surveys (1993–2019) were distributed from southeast Alaska to the western GOA with the highest concentration of high abundance catches off southeast Alaska (Fig. 233). Three of five SDMs considered for inclusion in the ensemble to predict numerical abundance of adult redstripe rockfish in the GOA converged (Table 77). The three best-performing SDMs were weighted by RMSE in the final ensemble, which attained a good overall fit to the observed adult redstripe rockfish distribution and abundance data. The ensemble was fair at predicting high and low abundance catches (ρ = 0.25), and excellent at discriminating presence-absence (AUC = 0.94) and explaining deviance (PDE = 0.66). Geographic location, bottom depth, and rockiness accounted for 59.1% of the covariate contribution to the deviance explained by the ensemble (Table 78). Adult redstripe rockfish abundance was higher around 200 m depth with rocky substrate present on the continental shelf of the southeastern GOA (Fig. 234). However, patchy areas of high abundance occurred in the central GOA south of the Kenai Peninsula and areas on the outer continental shelf of the western GOA. The CV of ensemble predictions was highest on the continental shelf of the southeastern and central GOA. The probability of encountering adult redstripe rockfish was high on the outer continental shelf off southeast Alaska and the eastern GOA, south of the Kenai Peninsula, and along the outer continental shelf south of Kodiak Islands and west, including southwest Shelikof Strait (Fig. 235).

Essential Fish Habitat of subadult and adult redstripe rockfish in the Gulf of Alaska -- Ensemble-predicted habitat-related numerical abundance of redstripe rockfish life stages collected in RACE-GAP summer bottom trawl surveys of the GOA (1993–2019) was mapped as EFH areas and subareas (Fig. 236). EFH of subadult redstripe rockfish occurred on the continental shelf in the eastern GOA, central GOA south of the Kenai Peninsula, and in the western GOA. Subadult core EFH area was extensive throughout the total EFH area, and EFH hot spots were most prevalent in the eastern GOA. EFH of adult redstripe rockfish included most of the RACE-GAP survey area in the GOA and core EFH area was extensive throughout. Adult EFH hot spots were most prevalent on the outer continental shelf of the eastern GOA, central GOA south of the Kenai Peninsula, and areas of the western GOA.

Table 77. -- Constituent species distribution models (SDMs) used to construct Essential Fish Habitat (EFH) for a) subadult and b) adult redstripe rockfish: MaxEnt = Maximum entropy; paGAM = presence-absence generalized additive model; hGAM = zero-adjusted Poisson hurdle GAM; GAM_P = standard Poisson GAM; GAM_{nb} = standard negative-binomial GAM; RMSE = root mean square error; ρ (rho) = Spearman's rank correlation coefficient; AUC = area under the receiver-operating characteristic curve; and PDE = Poisson deviance explained *. The "--" indicates that this model was not included in the final ensemble.

a) subadult redstripe rockfish

Models	RMSE	Relative Weight	ρ	AUC	PDE	EFH area (km^2)
MaxEnt	7.28	0.34	0.17	0.90	0.35	113,900
paGAM	7.18	0.35	0.20	0.94	0.50	83,800
hGAM	--	--	--	--	--	--
GAM_P	7.93	0	--	--	--	--
GAM_{nb}	7.67	0.31	0.25	0.94	0.36	37,100
ensemble	7.18	1	0.20	0.95	0.52	95,400

b) adult redstripe rockfish

Models	RMSE	Relative Weight	ρ	AUC	PDE	EFH area (km^2)
MaxEnt	54.5	0.34	0.23	0.91	0.34	216,800
paGAM	54.0	0.35	0.24	0.93	0.36	214,100
hGAM	--	--	--	--	--	--
GAM_P	56.8	0.31	0.23	0.84	0.14	61,600
GAM_{nb}	--	--	--	--	--	--
ensemble	47.9	1	0.25	0.94	0.65	214,500

* Refer to the Species Distribution Model Performance Metrics subsection within the Statistical Modeling section of the Methods for detailed descriptions of individual model performance metrics.

Table 78. -- Covariates retained in the a) subadult and b) adult redstripe rockfish species distribution model (SDM) final ensembles, the percent contribution to the ensemble deviance explained by each covariate, and the cumulative deviance explained: SD = standard deviation and BPI = bathymetric position index.

redstripe rockfish

	Covariate	% Contribution	Cumulative %
a) subadult	location	34.1	34.1
	bottom depth	18.4	52.5
	rockiness	12.2	64.7
	current SD	7.3	72.0
	current	6.9	78.8
	BPI	5.9	84.7
	sponge presence	3.3	88.0
	bottom temperature	2.3	90.3
	tidal maximum	2.2	92.5
	aspect north	1.9	94.4
	coral presence	1.4	95.8
	slope	1.3	97.1
	aspect east	1.3	98.4
	pennatulacean presence	1.1	99.5
	curvature	0.5	100.0
b) adult	location	23.7	23.7
	bottom depth	21.8	45.5
	rockiness	13.6	59.1
	current	9.7	68.8
	current SD	8.7	77.5
	BPI	7.1	84.6
	bottom temperature	4.7	89.3
	aspect north	3.8	93.1
	slope	2.5	95.6
	aspect east	1.4	97.0
	sponge presence	0.9	97.9
	pennatulacean presence	0.7	98.6
	tidal maximum	0.6	99.2
	coral presence	0.6	99.8
	curvature	0.2	100.0

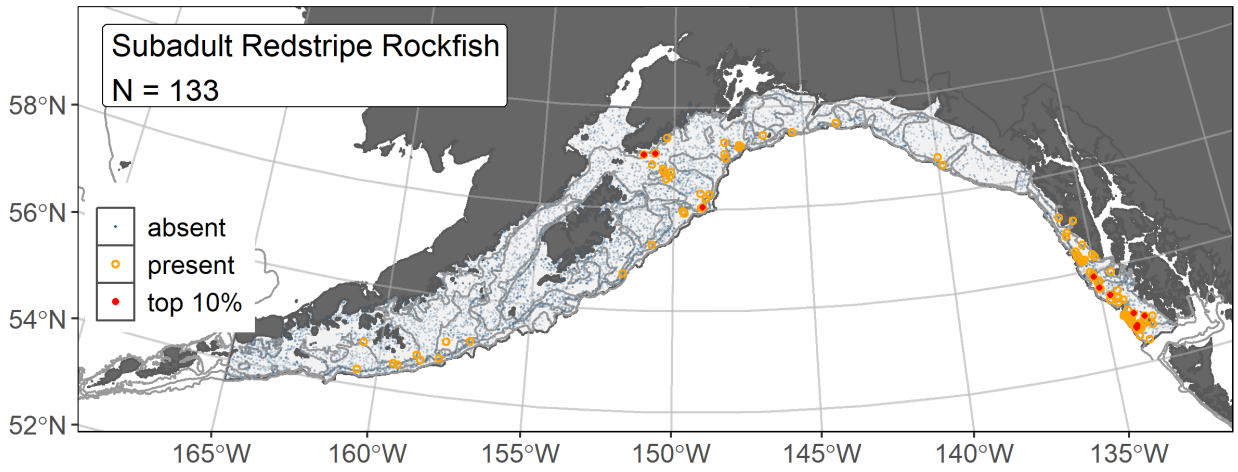

Figure 230. -- Distribution of subadult redstripe rockfish catches (N = 133) in 1993–2019 AFSC RACE-GAP summer bottom trawl surveys of the Gulf of Alaska with the 100 m, 300 m, and 700 m isobaths indicated; filled red circles indicate locations in top 10% of overall abundance, open orange circles indicate presence in remaining catches, and blue dots indicate stations sampled where the animals were not present.

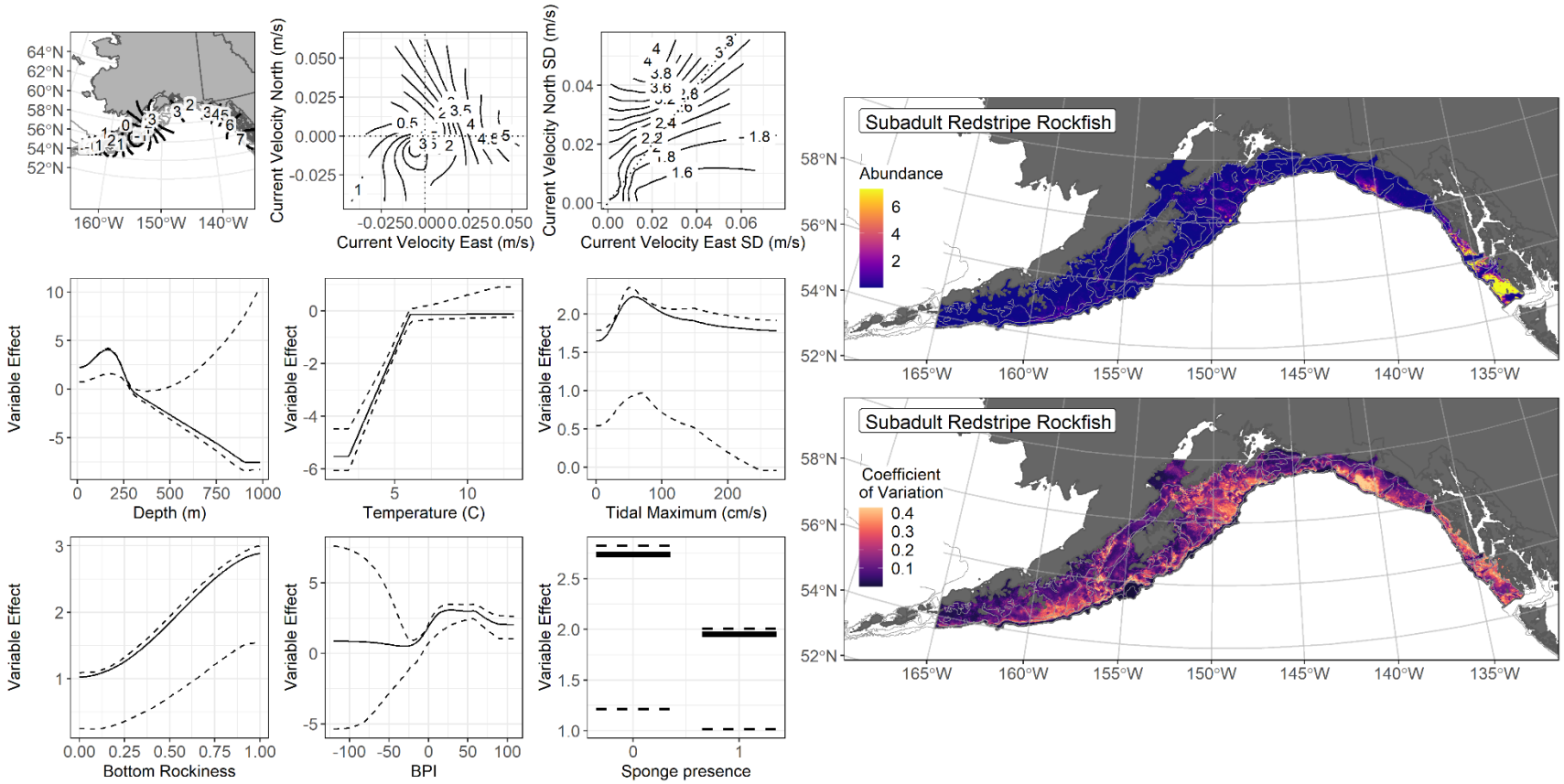

Figure 231. -- The top nine covariate effects (left panel) on ensemble-predicted subadult redstripe rockfish numerical abundance across the Gulf of Alaska (upper right panel) alongside the coefficient of variation (CV) of the ensemble predictions (lower right panel).

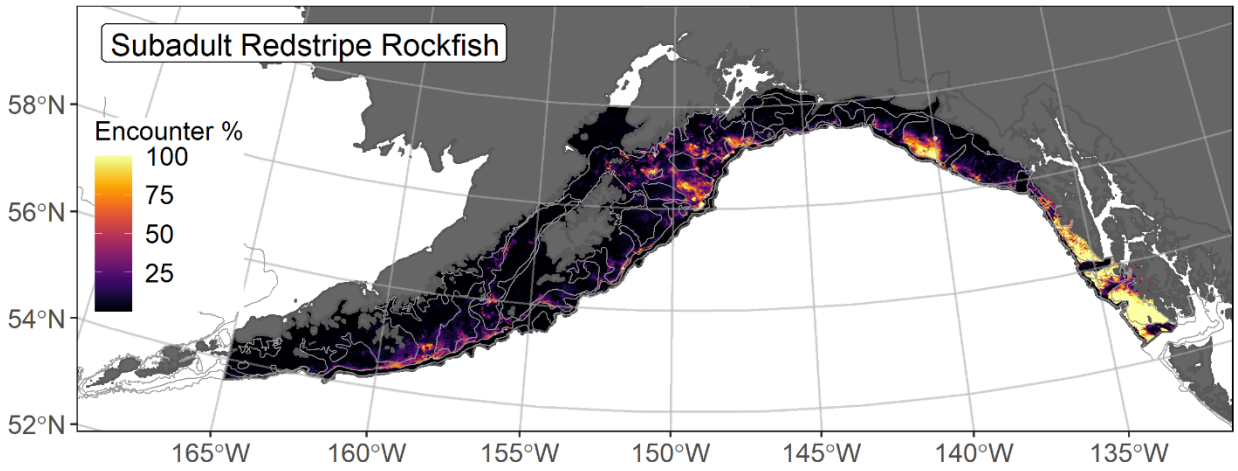

Figure 232. -- Encounter probability of subadult redstripe rockfish from AFSC RACE-GAP summer bottom trawl surveys (1993–2019) of the Gulf of Alaska with the 100 m, 300 m, and 700 m isobaths indicated.

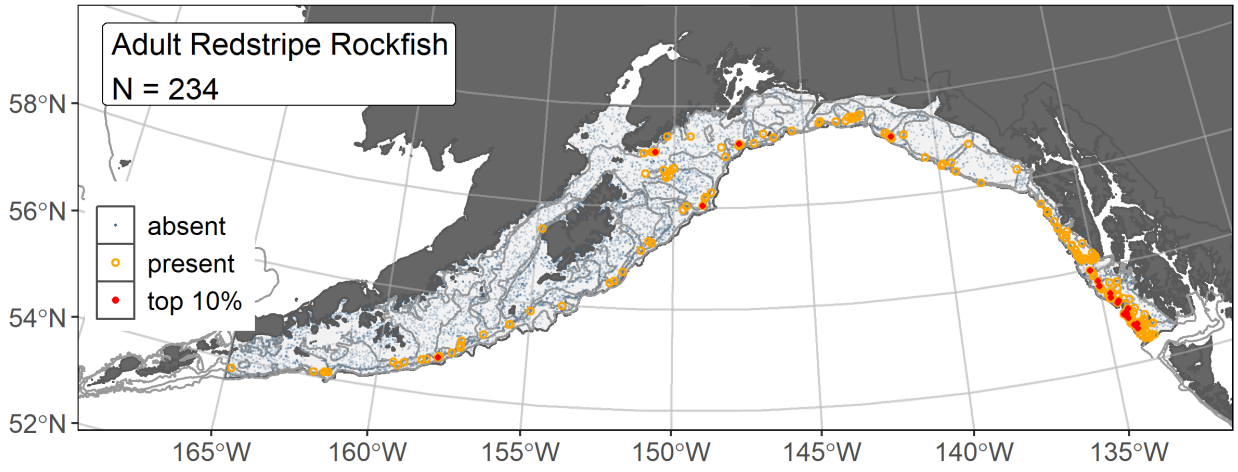

Figure 233. -- Distribution of adult redstripe rockfish catches (N = 234) in 1993–2019 AFSC RACE-GAP summer bottom trawl surveys of the Gulf of Alaska with the 100 m, 300 m, and 700 m isobaths indicated; filled red circles indicate locations in top 10% of overall abundance, open orange circles indicate presence in remaining catches, and blue dots indicate stations sampled where the animals were not present.

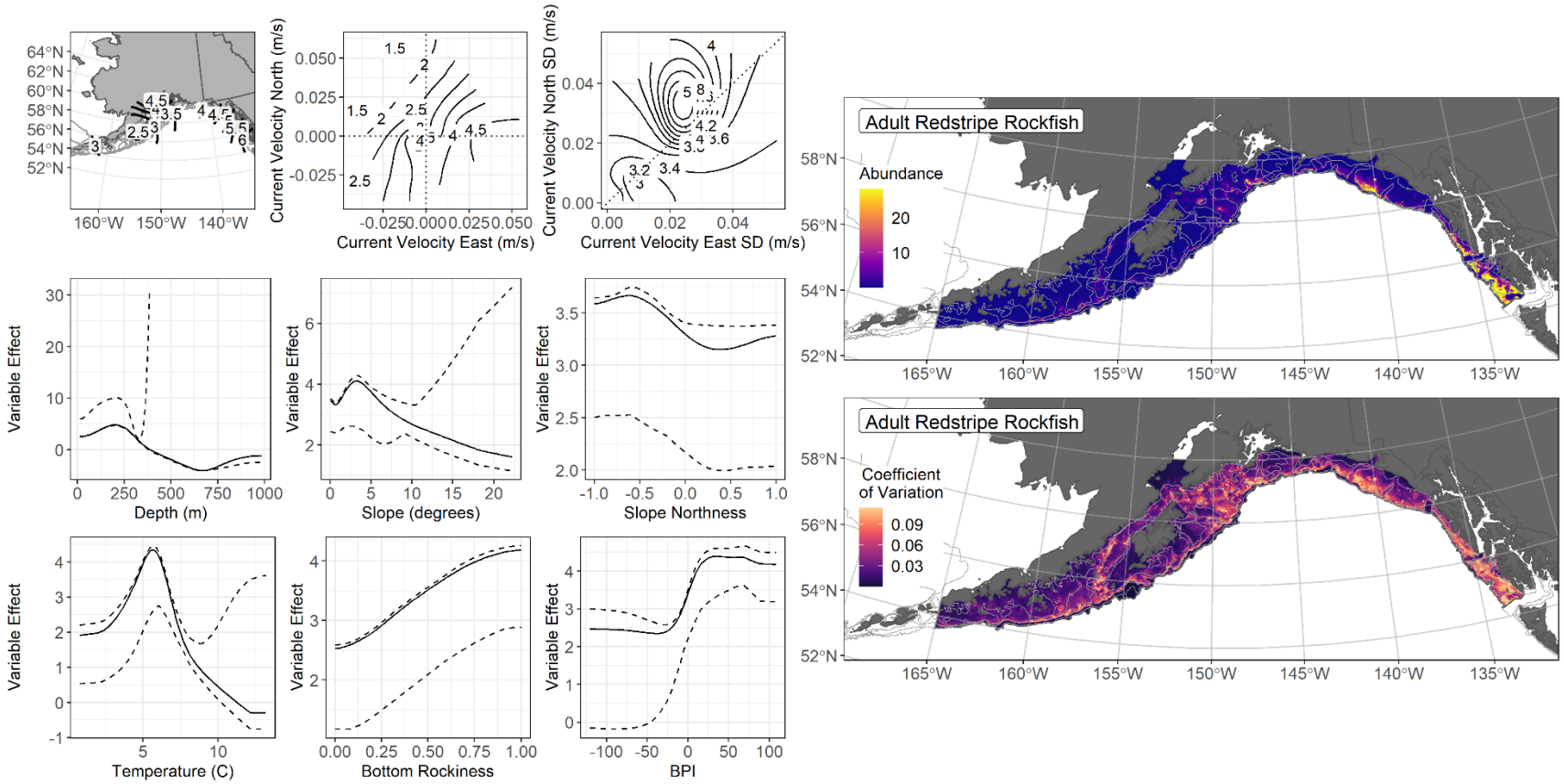

Figure 234. -- The top nine covariate effects (left panel) on ensemble-predicted adult redstripe rockfish numerical abundance across the Gulf of Alaska (upper right panel) alongside the coefficient of variation (CV) of the ensemble predictions (lower right panel).

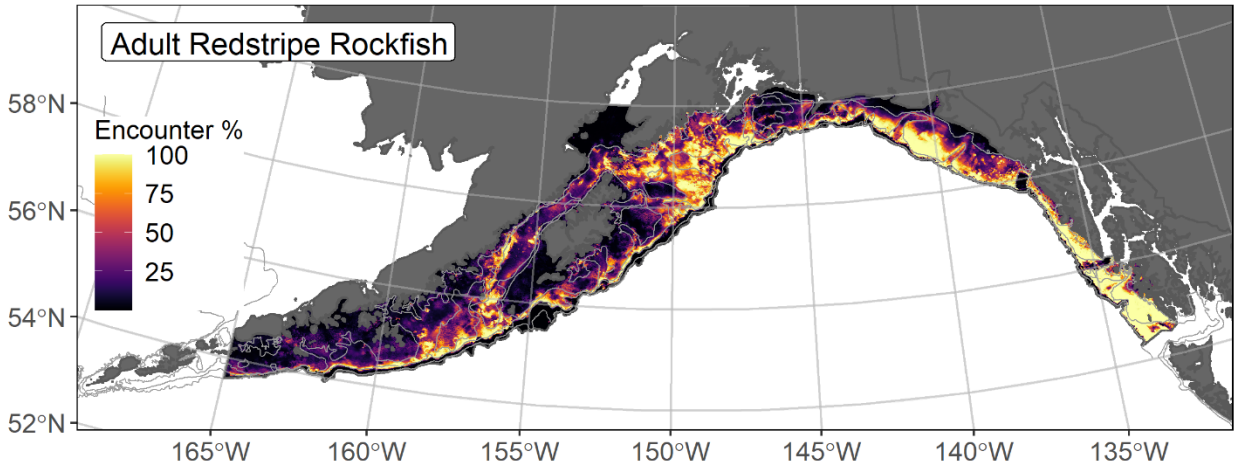

Figure 235. -- Encounter probability of adult redstripe rockfish from AFSC RACE-GAP summer bottom trawl surveys (1993–2019) of the Gulf of Alaska with the 100 m, 300 m, and 700 m isobaths indicated.

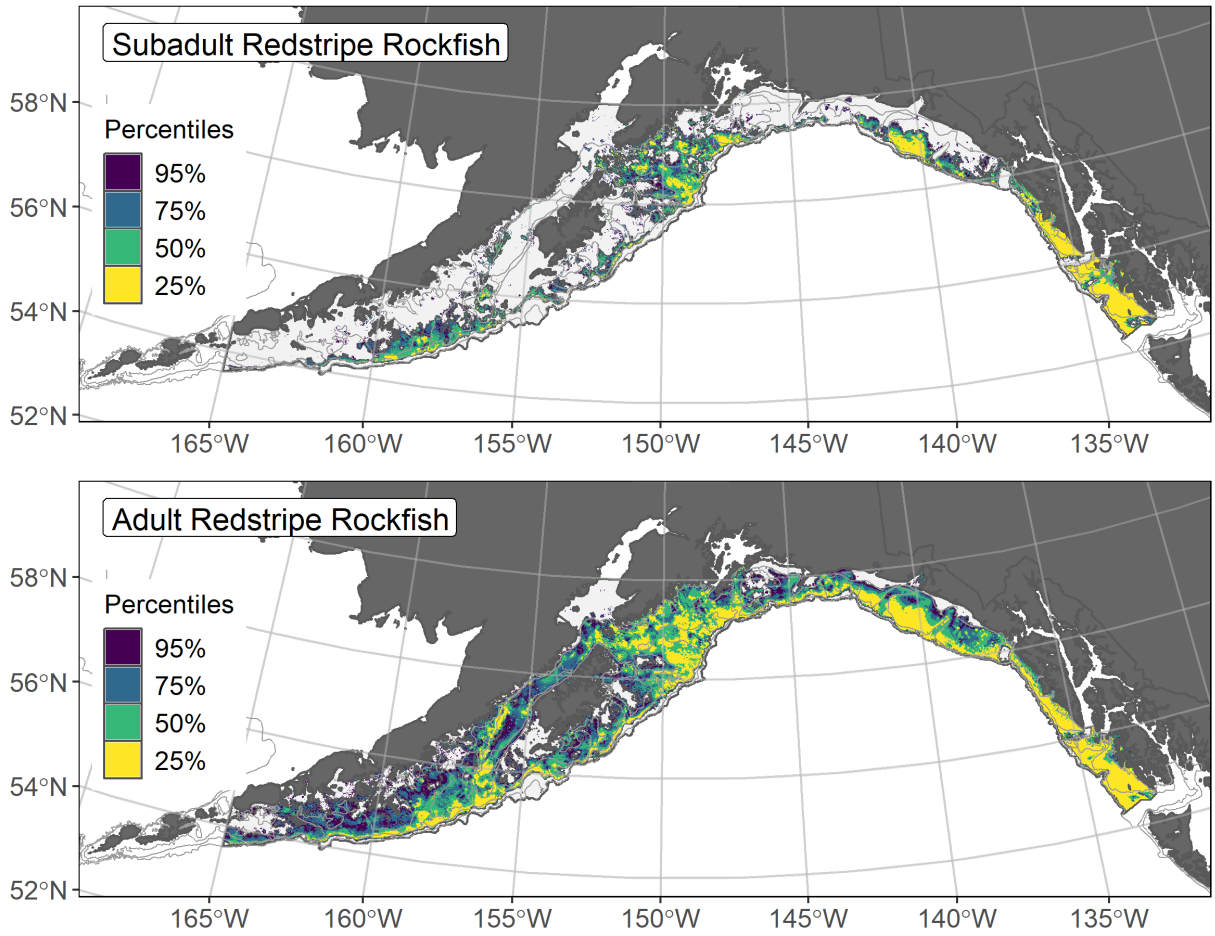

Figure 236. -- Essential fish habitat (EFH) is the area containing the top 95% of occupied habitat (defined as model estimated encounter probabilities greater than 5%) from an SDM ensemble fitted to subadult (top panel) and adult (bottom panel) redstripe rockfish distribution and abundance in AFSC RACE-GAP summer bottom trawl surveys (1993–2019) with 100 m, 200 m, and 700 m isobaths indicated; within the EFH area map are the subareas of the top 25% (EFH hot spots), top 50% (core EFH area), and top 75% (principal EFH area) of habitat-related, ensemble-predicted numerical abundance.

Sharpchin rockfish (*Sebastes zacentrus*)

Sharpchin rockfish (*Sebastes zacentrus*) are distributed from southern California to the western Aleutian Islands and to Pribilof Island in the Bering Sea (Love et al. 2002). This species is managed as part of the Other Rockfish (OR) stock complex in the GOA, where they are part of the Slope Sub-group and one of the six most common OR species by survey catch or biomass (Tribuzio and Echave 2019). Life history data collected in waters off Alaska describes sharpchin rockfish becoming mature at 265 mm and 10 years of age, living as long as 58 years (Malecha et al. 2007, Tribuzio and Echave 2019). Sharpchin rockfish are often observed in groups within sponge-covered boulder fields and habitats of scattered cobbles and boulders with sponges (Love et al. 2002, Pirtle 2005)[48].

Subadult sharpchin rockfish abundance and predicted distribution from RACE-GAP summer bottom trawl surveys in the Gulf of Alaska -- Subadult sharpchin rockfish (N = 498) catches in the GOA RACE-GAP summer bottom trawl surveys were primarily distributed in the eastern and central GOA with some occurrences on the outer continental shelf south of Kodiak Island and to the west (Fig. 237). Four of the five SDMs considered for inclusion in the ensemble to predict numerical abundance of subadult sharpchin rockfish in the GOA converged (Table 79); the GAM_{nb} was eliminated by skill testing. The remaining three best-performing SDMs were weighted by RMSE in the final ensemble, which attained a good overall fit to the observed subadult sharpchin rockfish distribution and abundance data. The ensemble was fair at predicting high and low abundance catches ($\rho = 0.37$), and excellent at discriminating presence-absence (AUC = 0.96) and explaining deviance (PDE = 0.69). Geographic location, bottom depth, sponge presence, and rockiness accounted for 68.4% of the covariate contribution to the deviance explained by the final ensemble (Table 80). Subadult sharpchin rockfish abundance was higher around 200 m depth with rocky substrate and low presence of sponges on the outer continental shelf of the GOA east of Kodiak Island (Fig. 238). The CV of ensemble predictions was higher throughout the central and eastern GOA. The probability of encountering subadult sharpchin rockfish was highest on the continental shelf of the central and eastern GOA and in patchy areas to the west (Fig. 239).

Adult sharpchin rockfish abundance and predicted distribution from RACE-GAP summer bottom trawl surveys in the Gulf of Alaska -- Adult sharpchin rockfish (N = 425) catches in the GOA RACE-GAP summer bottom trawl surveys were primarily distributed in the eastern and central GOA

[48] A recommendation from the stock author review to incorporate additional sources of data (e.g., from fishery observers) in future SDM ensemble EFH mapping for this species will be included as a research recommendation from the 2023 EFH 5-year Review.

with some occurrences on the outer continental shelf south of Kodiak Island and to the west (Fig. 240). Teo of the five SDMs considered for inclusion in the ensemble to predict numerical abundance of adult sharpchin rockfish in the GOA converged (Table 79). The SDM attained a good overall fit to the observed adult sharpchin rockfish distribution and abundance data. The SDM was fair at predicting high and low abundance catches (ρ = 0.34), excellent at discriminating presence-absence (AUC = 0.95), and good at explaining deviance (PDE = 0.54). Bottom depth, geographic location, and rockiness accounted for 60.1% of the covariate contribution to the deviance explained by the final ensemble (Table 80). Adult sharpchin rockfish abundance was highest at around 200 m depth on the outer continental shelf of the GOA east of Kodiak Island (Fig. 241). The CV of ensemble predictions was relatively even across the GOA continental shelf in the study area. The probability of encountering adult sharpchin rockfish was higher in the eastern and central GOA and on the outer continental shelf from Kodiak Island west (Fig. 242).

Essential Fish Habitat of subadult and adult sharpchin rockfish in the Gulf of Alaska -- Ensemble-predicted habitat-related numerical abundance of sharpchin rockfish life stages collected in RACE-GAP summer bottom trawl surveys of the GOA (1993–2019) was mapped as EFH areas and subareas (Fig. 243). EFH area of subadult and adult sharpchin rockfish was very similar, with core EFH areas and EFH hot spots extending progressively deeper throughout the total EFH area. EFH hot spots for both life stages were most prevalent on the continental shelf east of Kodiak Island and along the outer continental shelf of the western GOA.

Table 79. -- Constituent species distribution models (SDMs) used to construct Essential Fish Habitat (EFH) for a) subadult and b) adult sharpchin rockfish: MaxEnt = Maximum entropy; paGAM = presence-absence generalized additive model; hGAM = zero-adjusted Poisson hurdle GAM; GAM_P = standard Poisson GAM; GAM_{nb} = standard negative-binomial GAM; RMSE = root mean square error; ρ (rho) = Spearman's rank correlation coefficient; AUC = area under the receiver-operating characteristic curve; and PDE = Poisson deviance explained *. The "--" indicates that this model was not included in the final ensemble.

a) subadult sharpchin rockfish

Models	RMSE	Relative Weight	ρ	AUC	PDE	EFH area (km^2)
MaxEnt	53.8	0.34	0.35	0.93	0.39	179,900
paGAM	52.7	0.35	0.37	0.95	0.52	192,500
hGAM	--	--	--	--	--	--
GAM_P	55.4	0.32	0.41	0.93	0.47	78,400
GAM_{nb}	70.6	0	--	--	--	--
ensemble	47.0	1	0.37	0.96	0.69	191,800

b) adult sharpchin rockfish

Models	RMSE	Relative Weight	ρ	AUC	PDE	EFH area (km^2)
MaxEnt	99.6	0.49	0.33	0.94	0.51	204,900
paGAM	98.4	0.51	0.34	0.95	0.51	211,000
hGAM	--	--	--	--	--	--
GAM_P	--	--	--	--	--	--
GAM_{nb}	--	--	--	--	--	--
ensemble	97.9	1	0.34	0.95	0.54	218,600

* Refer to the Species Distribution Model Performance Metrics subsection within the Statistical Modeling section of the Methods for detailed descriptions of individual model performance metrics.

Table 80. -- Covariates retained in the a) subadult and b) adult sharpchin rockfish species distribution model (SDM) final ensembles, the percent contribution to the ensemble deviance explained by each covariate, and the cumulative deviance explained: SD = standard deviation and BPI = bathymetric position index.

sharpchin rockfish

	Covariate	% Contribution	Cumulative %
a) subadult	location	24.4	24.4
	bottom depth	21.9	46.3
	sponge presence	11.7	57.9
	rockiness	10.5	68.4
	current	9.8	78.2
	bottom temperature	7.8	86.0
	current SD	3.1	89.1
	BPI	2.6	91.7
	aspect east	2.5	94.2
	aspect north	2.4	96.6
	tidal maximum	1.9	98.5
	slope	1.0	99.5
	curvature	0.3	99.8
	pennatulacean presence	0.2	100.0
b) adult	bottom depth	32.7	32.7
	position	14.3	47.0
	rockiness	13.2	60.1
	current	9.1	69.2
	sponge presence	8.9	78.1
	bottom temperature	6.2	84.3
	BPI	5.3	89.6
	slope	4.3	93.9
	aspect north	1.7	95.6
	tidal maximum	1.6	97.2
	current SD	1.5	98.7
	aspect east	0.6	99.3
	coral presence	0.5	99.8
	pennatulacean presence	0.2	100.0

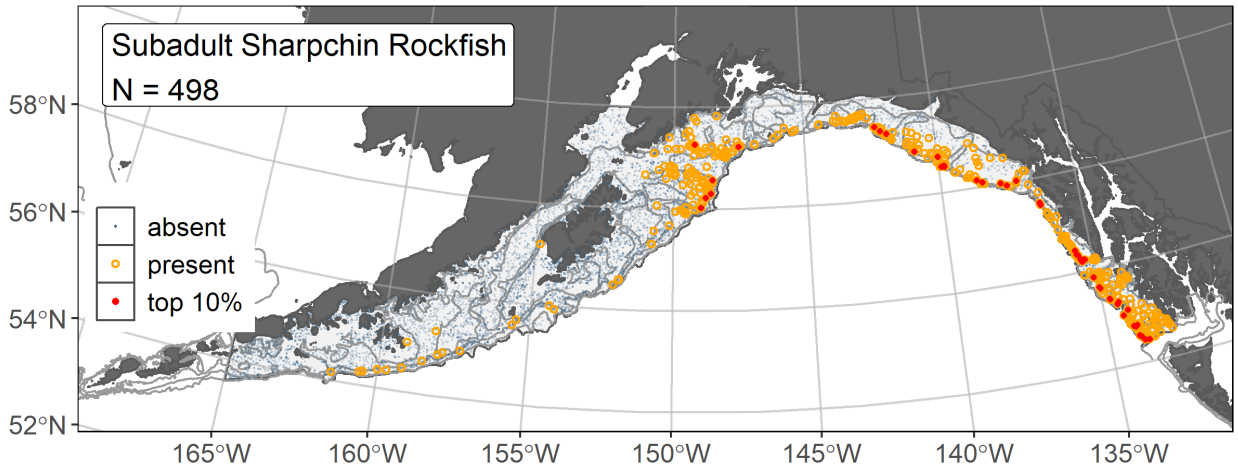

Figure 237. -- Distribution of subadult sharpchin rockfish catches (N = 498) in 1993–2019 AFSC RACE-GAP summer bottom trawl surveys of the Gulf of Alaska with the 100 m, 300 m, and 700 m isobaths indicated; filled red circles indicate locations in top 10% of overall abundance, open orange circles indicate presence in remaining catches, and blue dots indicate stations sampled where the animals were not present.

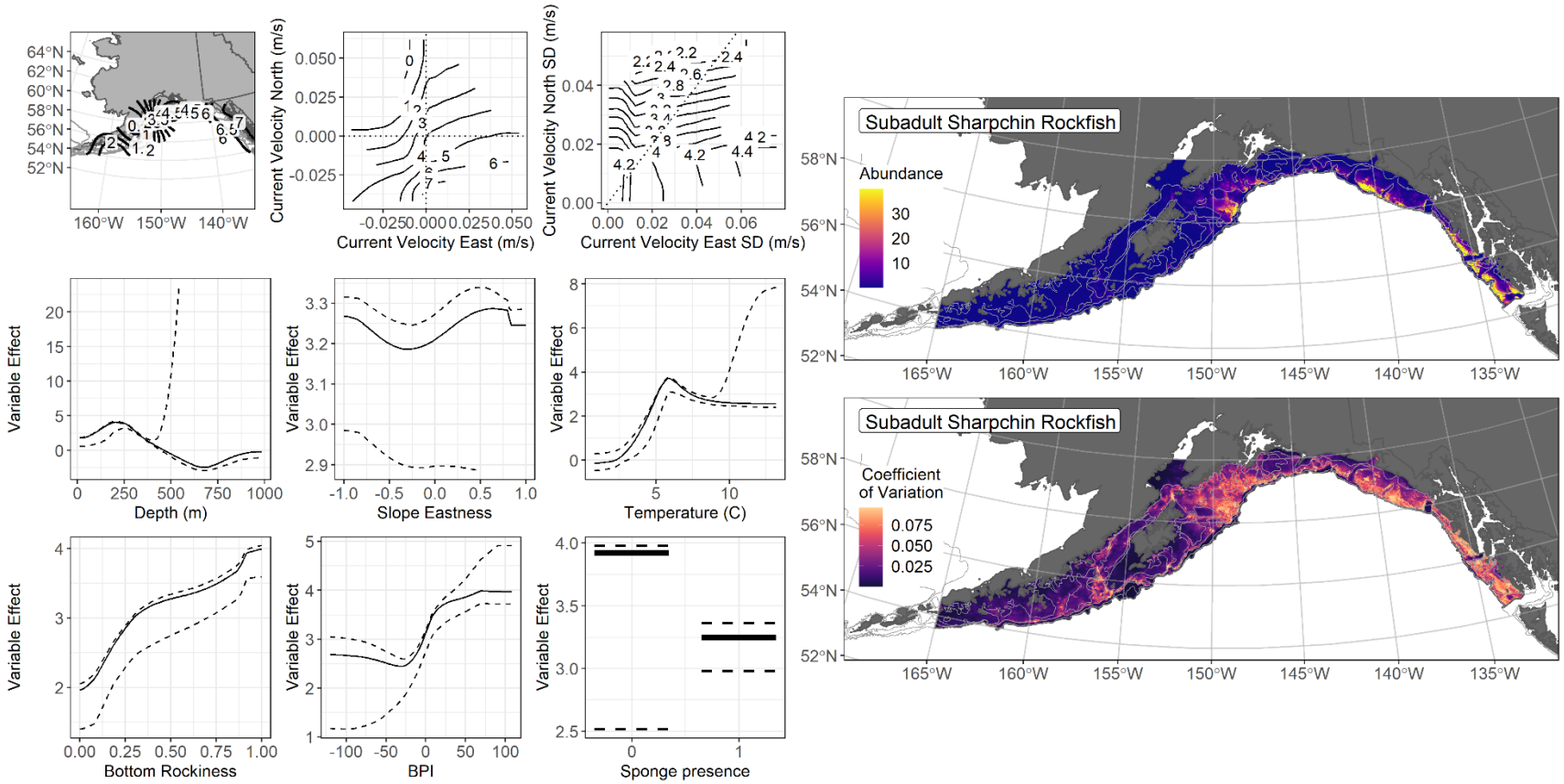

Figure 238. -- The top nine covariate effects (left panel) on ensemble-predicted subadult sharpchin rockfish numerical abundance across the Gulf of Alaska (upper right panel) alongside the coefficient of variation (CV) of the ensemble predictions (lower right panel).

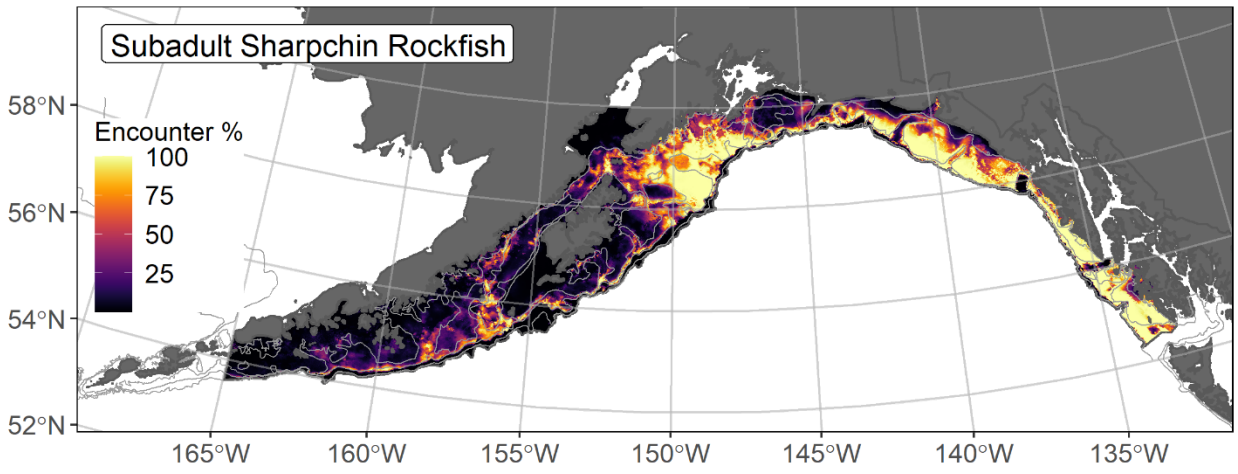

Figure 239. -- Encounter probability of subadult sharpchin rockfish from AFSC RACE-GAP summer bottom trawl surveys (1993–2019) of the Gulf of Alaska with the 100 m, 300 m, and 700 m isobaths indicated.

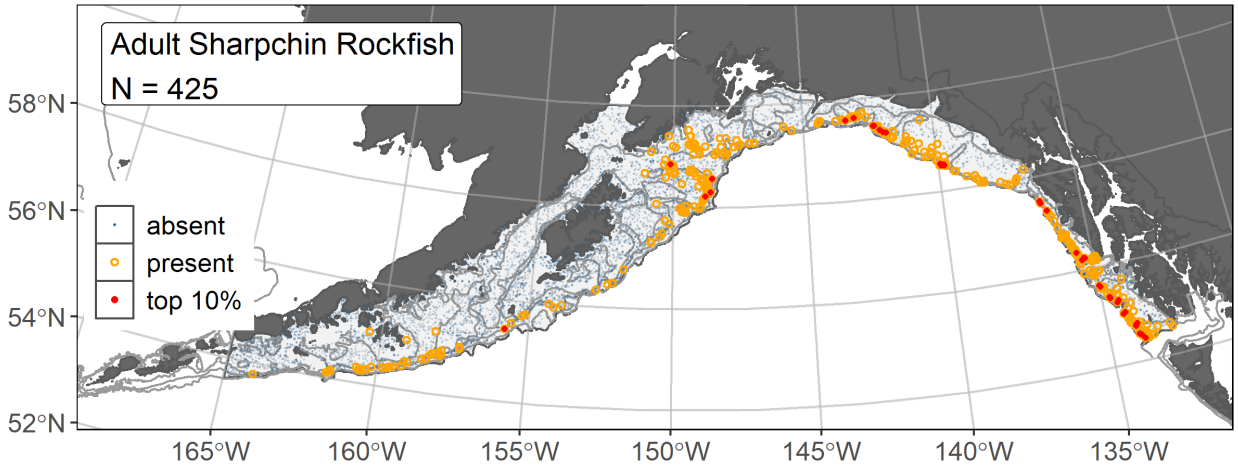

Figure 240. -- Distribution of adult sharpchin rockfish catches (N = 425) in 1993–2019 AFSC RACE-GAP summer bottom trawl surveys of the Gulf of Alaska with the 100 m, 300 m, and 700 m isobaths indicated; filled red circles indicate locations in top 10% of overall abundance, open orange circles indicate presence in remaining catches, and blue dots indicate stations sampled where the animals were not present.

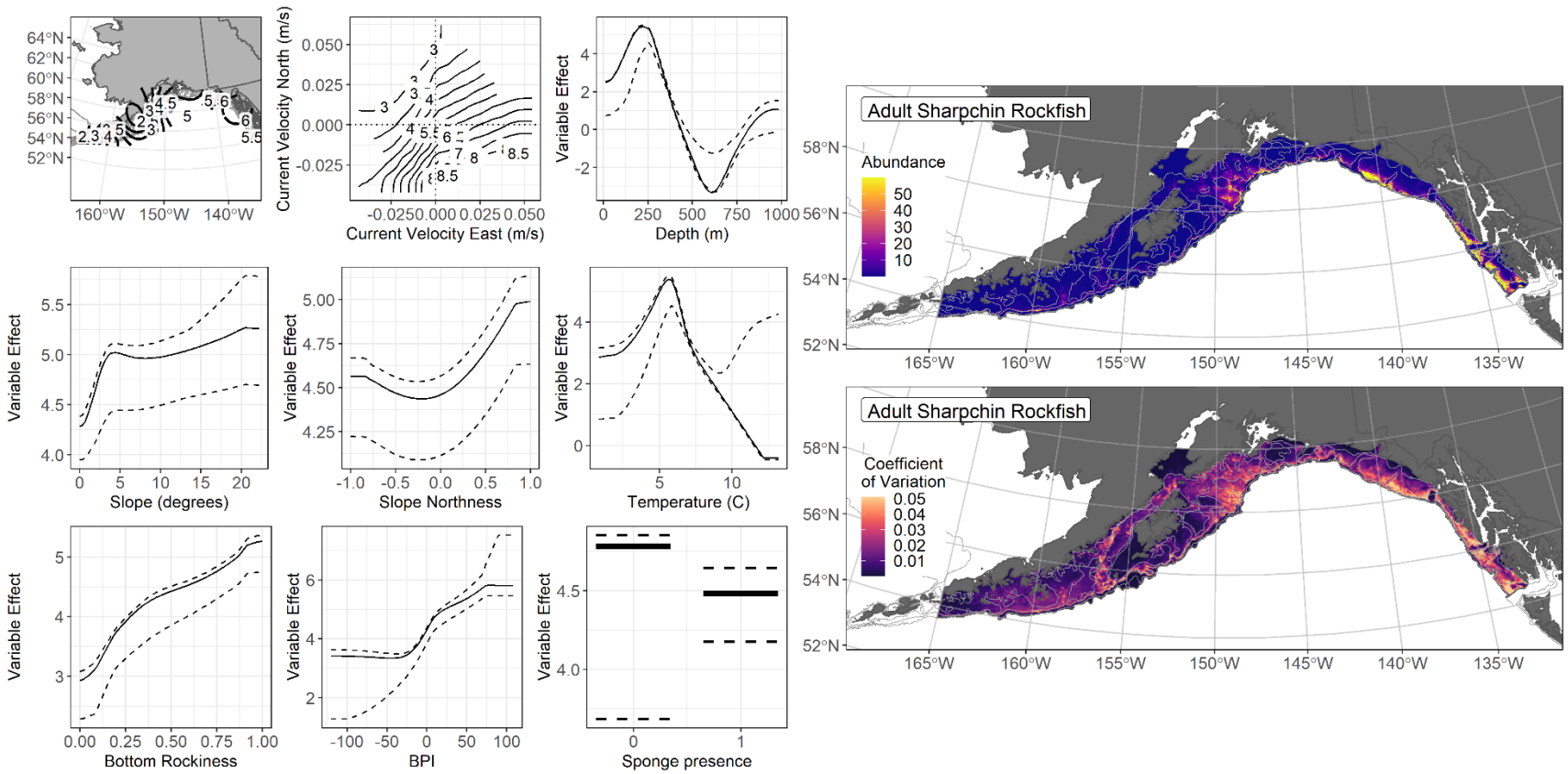

Figure 241. -- The top nine covariate effects (left panel) on ensemble-predicted adult sharpchin rockfish numerical abundance across the Gulf of Alaska (upper right panel) alongside the coefficient of variation (CV) of the ensemble predictions (lower right panel).

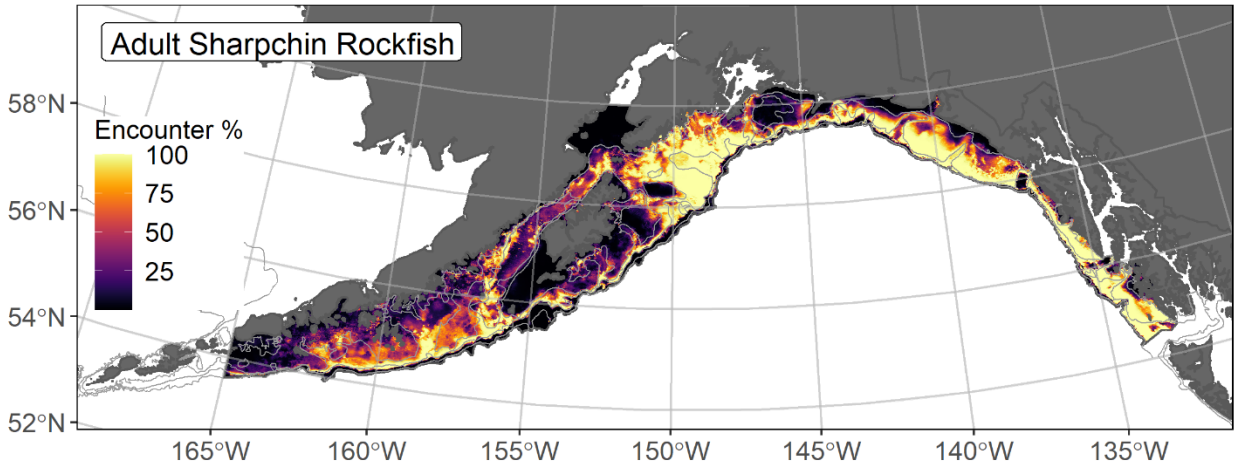

Figure 242. -- Encounter probability of adult sharpchin rockfish from AFSC RACE-GAP summer bottom trawl surveys (1993–2019) of the Gulf of Alaska with the 100 m, 300 m, and 700 m isobaths indicated.

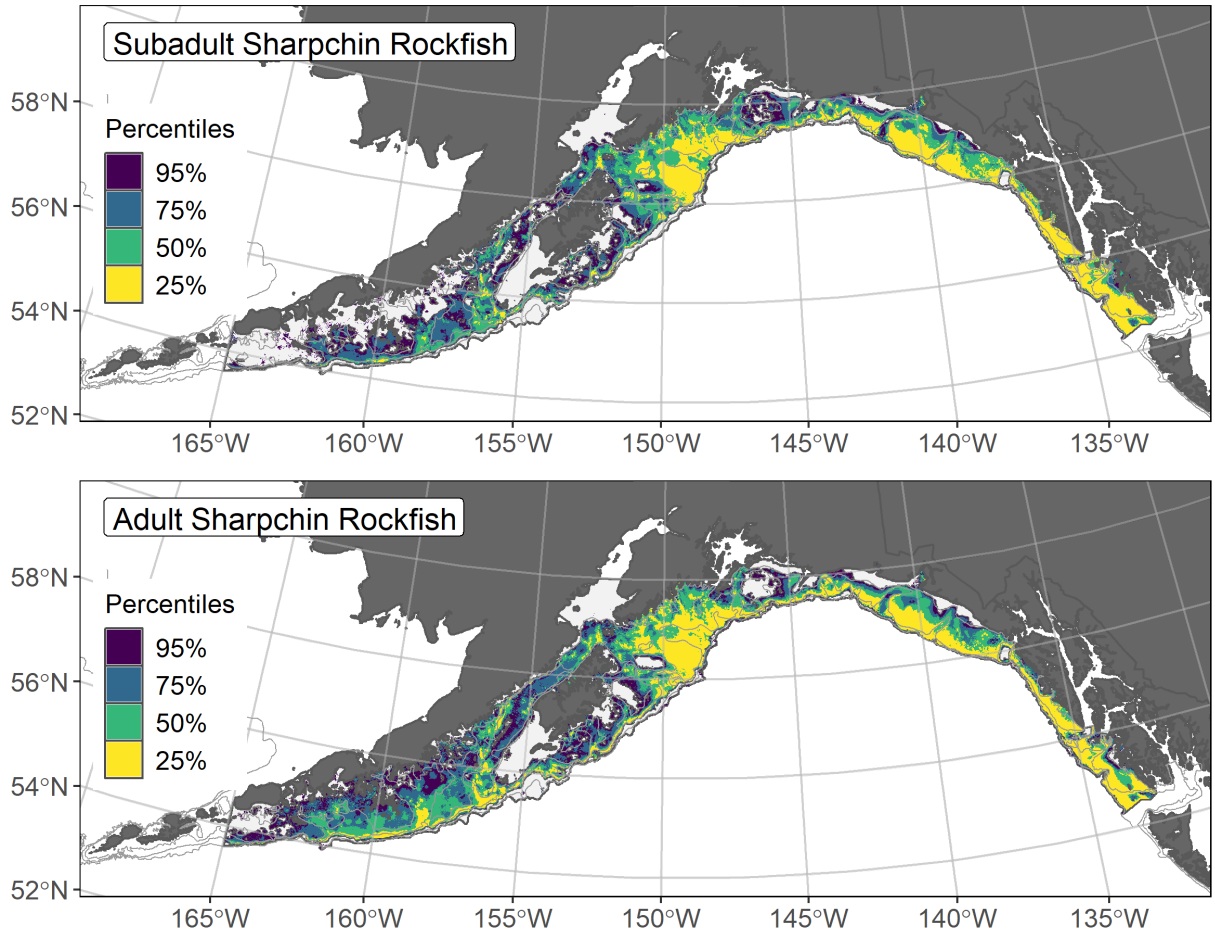

Figure 243. -- Essential fish habitat (EFH) is the area containing the top 95% of occupied habitat (defined as model estimated encounter probabilities greater than 5%) from an SDM ensemble fitted to subadult (top panel) and adult (bottom panel) sharpchin rockfish distribution and abundance in AFSC RACE-GAP summer bottom trawl surveys (1993–2019) with 100 m, 200 m, and 700 m isobaths indicated; within the EFH area map are the subareas of the top 25% (EFH hot spots), top 50% (core EFH area), and top 75% (principal EFH area) of habitat-related, ensemble-predicted numerical abundance.

Silvergray rockfish (*Sebastes brevispinis*)

Silvergray rockfish (*Sebastes brevispinis*) are found from Baja California to around Sanak Island in the western GOA (Love et al. 2002). Silvergray rockfish is managed as part of the Other Rockfish (OR) stock complex in the GOA, where they are part of the Slope Sub-group and one of the six most common OR species by survey catch or biomass (Tribuzio and Echave 2019). Life history data collected in waters off Alaska describes silvergray rockfish with an average maximum juvenile length of 405 mm and living as long as 75 years (Rooper 2008, Tribuzio and Echave 2019). Silvergray rockfish associate with various high-relief and rugged rocky habitats generally off the seafloor and are often observed with species that have similar behavior, such as canary, dusky, widow, and yellowtail rockfishes (Love et al. 2002, Bosley et al. 2004, Jones et al. 2012)[49].

Subadult silvergray rockfish abundance and predicted distribution from RACE-GAP summer bottom trawl surveys in the Gulf of Alaska -- Subadult silvergray rockfish (N = 159) catches in GOA RACE-GAP summer bottom trawl surveys were infrequent and occurred from southeast Alaska west to the Shumagin Islands (Fig. 244). The highest abundance catches were scattered across the survey area. Four of the five SDMs considered for inclusion in the ensemble to predict numerical abundance of subadult silvergray rockfish in the GOA converged (Table 81); the GAM_P was eliminated by skill testing. The remaining three best-performing SDMs were weighted by RMSE in the final ensemble, which attained a fair overall fit to the observed subadult silvergray rockfish distribution and abundance data. The ensemble was poor at predicting high and low abundance catches (ρ = 0.18), good at discriminating presence-absence (AUC = 0.88), and fair at explaining deviance (PDE = 0.21). Geographic location, bottom depth, and rockiness accounted for 60.7% of the covariate contribution to the deviance explained by the final ensemble (Table 82). Subadult silvergray rockfish abundance was highest around 200 m depth in areas with rocky substrate present in the eastern GOA off southeast Alaska (Fig. 245). The CV of ensemble predictions was relatively high across most of the GOA continental shelf except larger glacial troughs (Fig. 245). The probability of encountering subadult silvergray rockfish was highest in the eastern GOA (Fig. 246).

Adult silvergray rockfish abundance and predicted distribution from RACE-GAP summer bottom trawl surveys in the Gulf of Alaska -- Adult silvergray rockfish (N = 557) catches in GOA RACE-GAP summer bottom trawl surveys were present from southeast Alaska west to the Shumagin Islands, with the highest abundance catches located off southeast Alaska (Fig. 247). Five SDMs were

[49] A recommendation from the stock author review to incorporate additional sources of data (e.g., from longline surveys and fishery observers) in future SDM ensemble EFH mapping for this species will be included as a research recommendation from the 2023 EFH 5-year Review.

considered for inclusion in the ensemble to predict numerical abundance of adult silvergray rockfish in the GOA (Table 81); the GAM_{nb} was eliminated by skill testing. The four best-performing SDMs were equally weighted by RMSE in the final ensemble, which attained a good overall fit to the observed adult silvergray rockfish distribution and abundance data. The ensemble was fair at predicting high and low abundance catches ($\rho = 0.37$), and excellent at discriminating presence-absence (AUC = 0.93) and explaining deviance (PDE = 0.63). Geographic location, bottom depth, and bottom current variability accounted for 65.0% of the covariate contribution to the total deviance explained by the ensemble (Table 82). Higher adult silvergray rockfish abundance occurred around 200 m depth in the eastern GOA off southern southeast Alaska (Fig. 248). The CV of ensemble predictions was higher in the eastern GOA. The probability of encountering adult silvergray rockfish was highest in the eastern GOA (Fig. 249).

Essential Fish Habitat of subadult and adult silvergray rockfish in the Gulf of Alaska -- Ensemble-predicted habitat-related numerical abundance of silvergray rockfish life stages collected in RACE-GAP summer bottom trawl surveys of the GOA (1993–2019) was mapped as EFH areas and subareas (Fig. 250). Subadult silvergray rockfish EFH area was primarily east of Kodiak Island, with hot spots concentrated off southeast Alaska. Adult silvergray rockfish EFH was more extensive than the area of subadult EFH. Adult EFH occurred on the continental shelf and upper slope east of the Shumagin Islands, with core EFH area and EFH hot spots increasing east of Kodiak Island through the eastern GOA to the southern extent of the survey area.

Table 81. -- Constituent species distribution models (SDMs) used to construct Essential Fish Habitat (EFH) for a) subadult and b) adult silvergray rockfish: MaxEnt = Maximum entropy; paGAM = presence-absence generalized additive model; hGAM = zero-adjusted Poisson hurdle GAM; GAM_P = standard Poisson GAM; GAM_{nb} = standard negative-binomial GAM; RMSE = root mean square error; ρ (rho) = Spearman's rank correlation coefficient; AUC = area under the receiver-operating characteristic curve; and PDE = Poisson deviance explained *. The "--" indicates that this model was not included in the final ensemble.

a) subadult silvergray rockfish

Models	RMSE	Relative Weight	ρ	AUC	PDE	EFH area (km^2)
MaxEnt	1.94	0.21	0.16	0.84	0.06	108,500
paGAM	1.42	0.40	0.15	0.83	0.09	109,900
hGAM	--	--	--	--	--	--
GAM_P	1.44	0	--	--	--	--
GAM_{nb}	1.44	0.39	0.15	0.82	0.02	88,000
ensemble	1.44	1	0.18	0.88	0.21	104,500

b) adult silvergray rockfish

Models	RMSE	Relative Weight	ρ	AUC	PDE	EFH area (km^2)
MaxEnt	36.6	0.25	0.35	0.90	0.28	194,700
paGAM	36.2	0.25	0.38	0.94	0.44	187,400
hGAM	36.3	0.25	0.36	0.94	0.45	108,300
GAM_P	36.2	0.25	0.36	0.89	0.46	102,500
GAM_{nb}	39.0	0	--	--	--	--
ensemble	33.3	1	0.37	0.93	0.63	184,300

* Refer to the Species Distribution Model Performance Metrics subsection within the Statistical Modeling section of the Methods for detailed descriptions of individual model performance metrics.

Table 82. -- Covariates retained in the a) subadult and b) adult silvergray rockfish species distribution model (SDM) final ensembles, the percent contribution to the ensemble deviance explained by each covariate, and the cumulative deviance explained: SD = standard deviation and BPI = bathymetric position index.

silvergray rockfish			
	Covariate	**% Contribution**	**Cumulative %**
a) subadult	location	32.9	32.9
	bottom depth	18.6	51.4
	rockiness	9.3	60.7
	current SD	6.6	67.3
	bottom temperature	5.4	72.7
	BPI	5.2	77.9
	current	4.2	82.1
	aspect east	3.9	86.0
	slope	3.2	89.2
	sponge presence	2.9	92.1
	tidal maximum	2.3	94.4
	curvature	2.1	96.5
	pennatulacean presence	1.8	98.3
	aspect north	1.7	100.0
b) adult	location	30.8	30.8
	bottom depth	21.2	52.0
	current SD	13.0	65.0
	current	8.3	73.3
	bottom temperature	8.3	81.7
	rockiness	4.0	85.7
	BPI	3.6	89.3
	aspect east	2.5	91.8
	slope	2.2	94.0
	aspect north	2.1	96.1
	sponge presence	1.6	97.7
	tidal maximum	1.1	98.8
	curvature	0.9	99.7
	pennatulacean presence	0.2	99.9
	coral presence	0.1	100.0

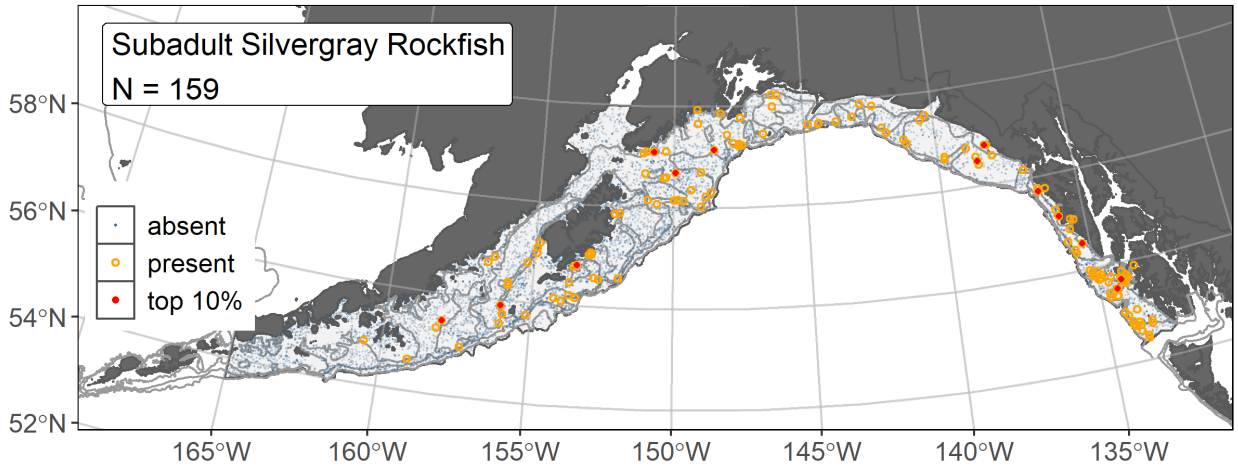

Figure 244. -- Distribution of subadult silvergray rockfish catches (N = 159) in 1993–2019 AFSC RACE-GAP summer bottom trawl surveys of the Gulf of Alaska with the 100 m, 300 m, and 700 m isobaths indicated; filled red circles indicate locations in top 10% of overall abundance, open orange circles indicate presence in remaining catches, and blue dots indicate stations sampled where the animals were not present.

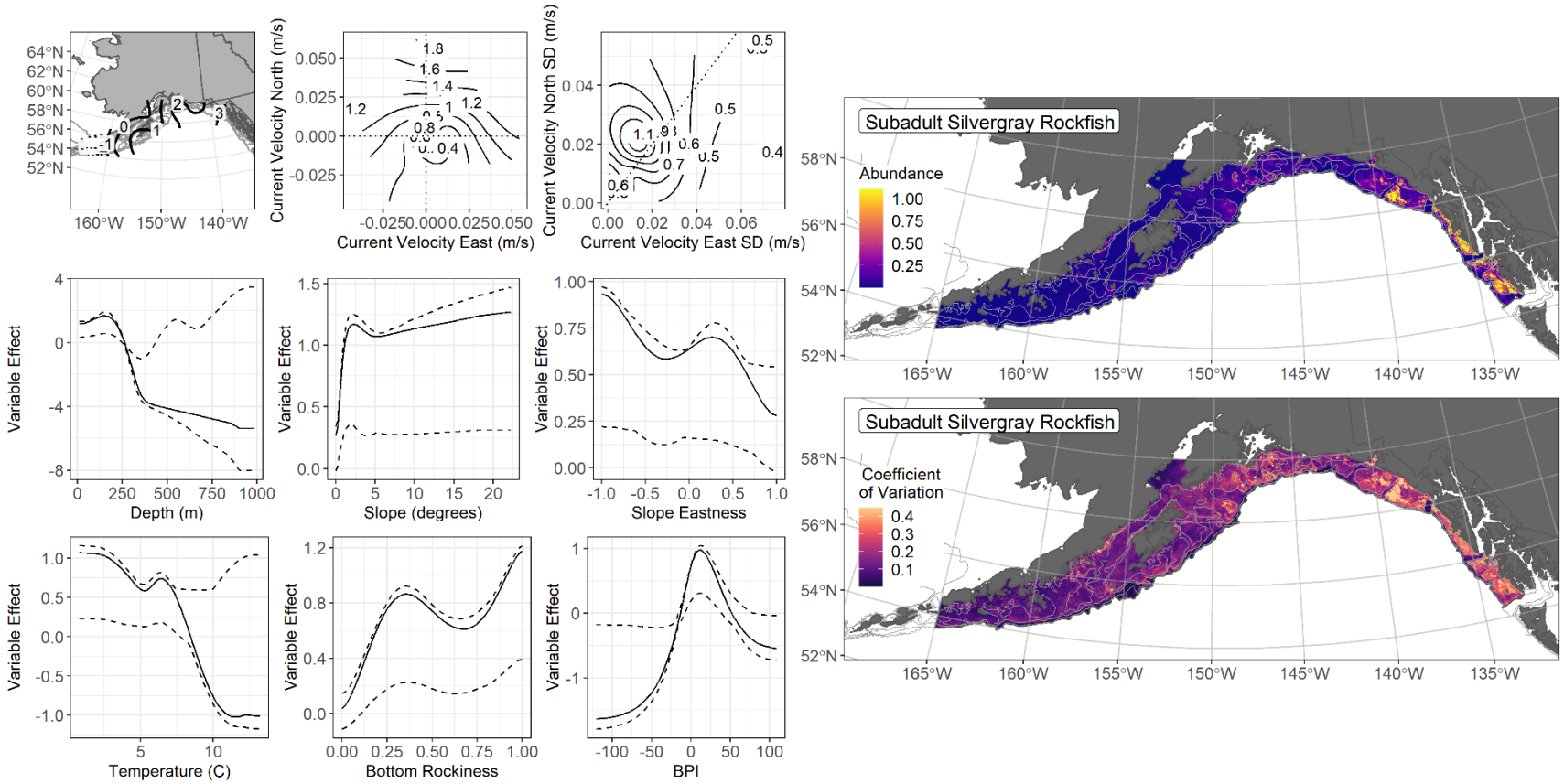

Figure 245. -- The top nine covariate effects (left panel) on ensemble-predicted subadult silvergray rockfish numerical abundance across the Gulf of Alaska (upper right panel) alongside the coefficient of variation (CV) of the ensemble predictions (lower right panel).

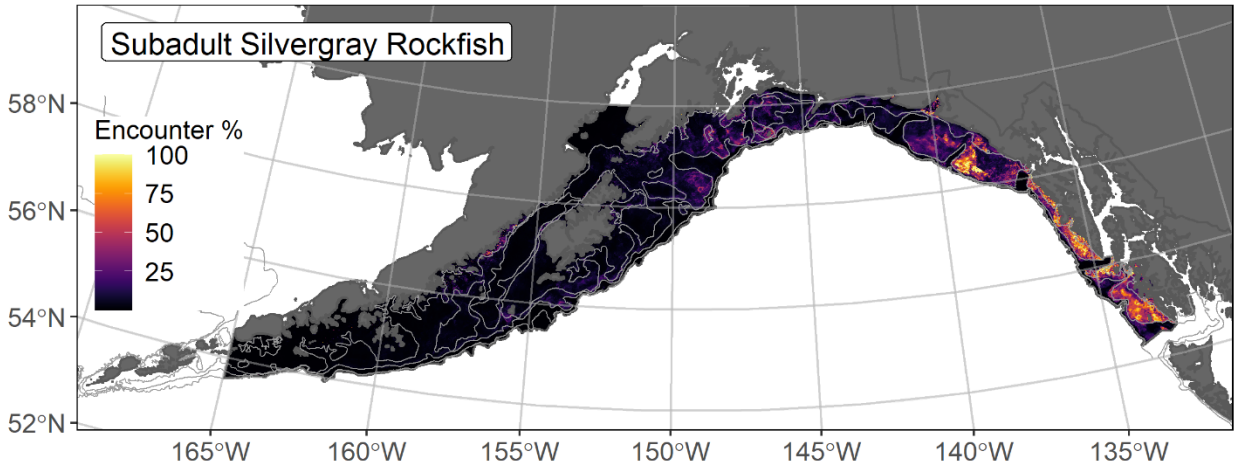

Figure 246. -- Encounter probability of subadult silvergray rockfish from AFSC RACE-GAP summer bottom trawl surveys (1993–2019) of the Gulf of Alaska with the 100 m, 300 m, and 700 m isobaths indicated.

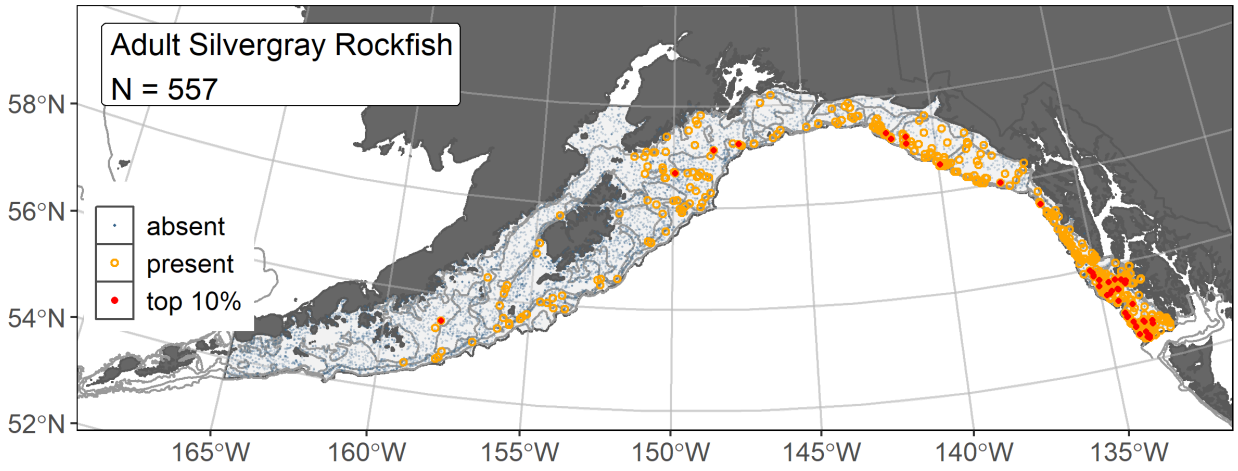

Figure 247. -- Distribution of adult silvergray rockfish catches (N = 557) in 1993–2019 AFSC RACE-GAP summer bottom trawl surveys of the Gulf of Alaska with the 100 m, 300 m, and 700 m isobaths indicated; filled red circles indicate locations in top 10% of overall abundance, open orange circles indicate presence in remaining catches, and blue dots indicate stations sampled where the animals were not present.

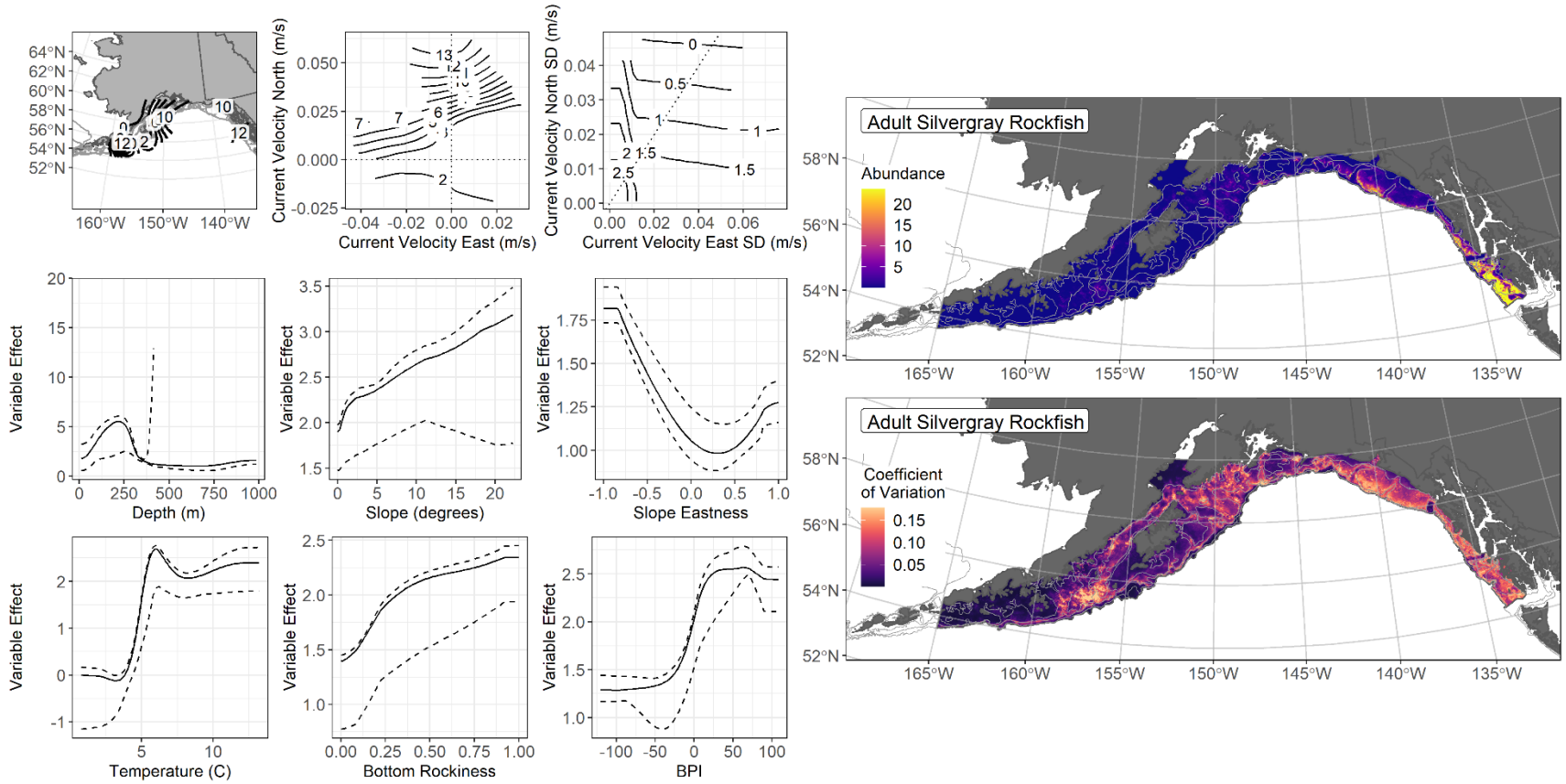

Figure 248. -- The top nine covariate effects (left panel) on ensemble-predicted adult silvergray rockfish numerical abundance across the Gulf of Alaska (upper right panel) alongside the coefficient of variation (CV) of the ensemble predictions (lower right panel).

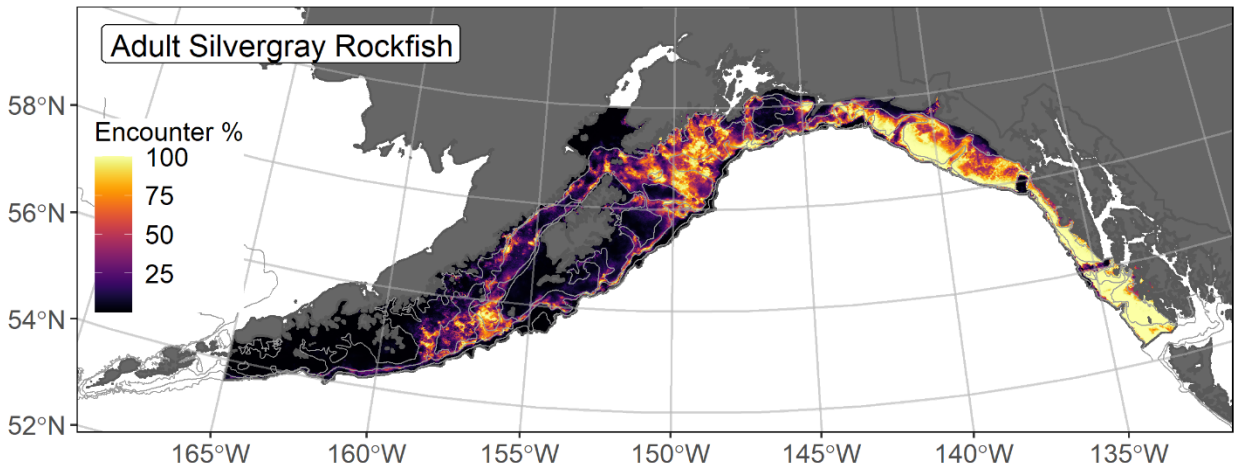

Figure 249. -- Encounter probability of adult silvergray rockfish from AFSC RACE-GAP summer bottom trawl surveys (1993–2019) of the Gulf of Alaska with the 100 m, 300 m, and 700 m isobaths indicated.

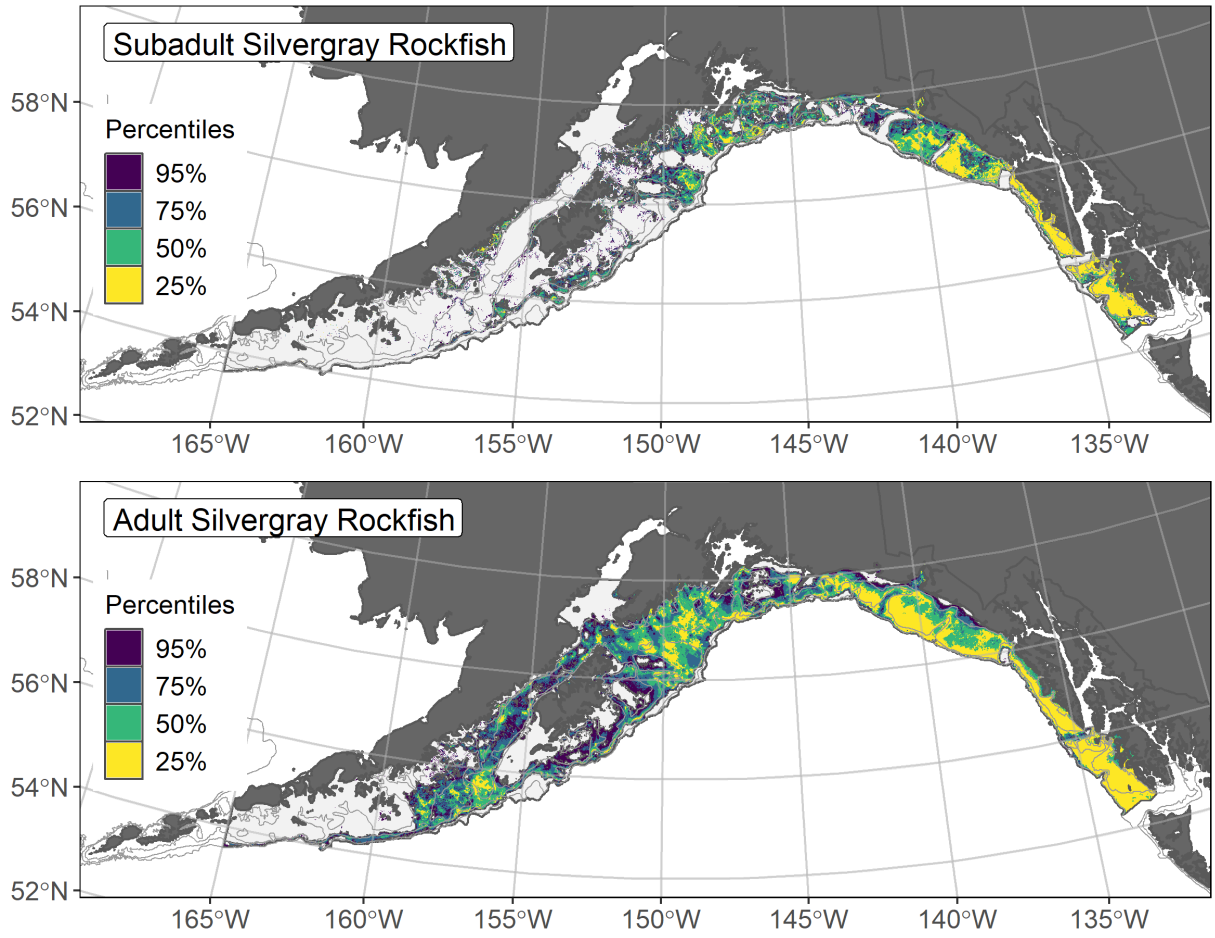

Figure 250. -- Essential fish habitat (EFH) is the area containing the top 95% of occupied habitat (defined as model estimated encounter probabilities greater than 5%) from an SDM ensemble fitted to subadult (top panel) and adult (bottom panel) silvergray rockfish distribution and abundance in AFSC RACE-GAP summer bottom trawl surveys (1993–2019) with 100 m, 200 m, and 700 m isobaths indicated; within the EFH area map are the subareas of the top 25% (EFH hot spots), top 50% (core EFH area), and top 75% (principal EFH area) of habitat-related, ensemble-predicted numerical abundance.

Shortspine thornyhead (*Sebastolobus alascanus*)

The GOA Thornyhead Rockfish complex is composed of shortspine thornyhead (*Sebastolobus alascanus*) and longspine thornyhead (*S. altivelis*) and has been managed as a single stock since 1980 (Echave et al. 2020). Shortspine thornyhead represent EFH of Thornyhead Rockfish complex, since longspine thornyhead were not sufficiently prevalent (> 50 catches) to parameterize SDMs for the subadult and adult life stages. Shortspine thornyhead are encountered from Russia and Japan to the NBS (Navarin Canyon) and through the Aleutian Islands to Baja California (Love et al. 2002, Mecklenburg et al. 2002). They are common throughout the GOA, inhabiting a wide band of depths throughout their range (20–1,500 m) but are most abundant between 150 and 450 m. Their larvae have a prolonged pelagic phase of up to 15 months, and juveniles are often found over mud bottoms in relatively shallow water (100–600 m), migrating into deeper depths as they mature[50]. Length at 50% maturity has been reported as 215 mm for both sexes (Pearson and Gunderson 2003), and we used this length to separate the subadult and adult life stages for this study.

Subadult shortspine thornyhead abundance and predicted distribution from RACE-GAP summer bottom trawl surveys in the Gulf of Alaska -- Subadult shortspine thornyhead (N = 1,634) caught in GOA RACE-GAP summer bottom trawl surveys (1993–2019) occurred from southern southeast Alaska through the western GOA (Fig. 251). Four of the five SDMs considered for inclusion in the ensemble to predict numerical abundance of subadult shortspine thornyhead in the GOA converged (Table 83); the GAM_{nb} was eliminated by skill testing. The remaining three best-performing SDMs were weighted by RMSE in the final ensemble, which attained an excellent overall fit to the observed subadult distribution and abundance data. The ensemble was excellent at predicting high and low abundance catches (ρ = 0.65), discriminating presence-absence (AUC = 0.97), and explaining deviance (PDE = 0.76). Bottom depth, geographic location, and sponge presence accounted for 73.9% of the covariate contribution to the deviance explained by the final ensemble (Table 84). Higher subadult shortspine thornyhead abundance was predicted to peak around 375 m depth with a low presence of sponges (Fig. 252). Predicted abundance was highest within a relatively small depth range that included the outer extent of glacial troughs on the continental shelf and areas along the continental slope of the GOA. The CV of ensemble predictions was higher in glacial troughs on the GOA continental shelf and

[50] A recommendation from the stock author review to incorporate longline survey data in future SDM ensemble EFH mapping for this species will be included as a research recommendation from the 2023 EFH 5-year Review.

areas along the continental slope. Areas with the greatest predicted encounter probability occurred within glacial troughs and along the continental slope of the GOA (Fig. 253).

Adult shortspine thornyhead abundance and predicted distribution from RACE-GAP summer bottom trawl surveys in the Gulf of Alaska -- Adult shortspine thornyhead (N = 1,998) caught in GOA RACE-GAP summer bottom trawl surveys (1993–2019) occurred from southern southeast Alaska through the western GOA (Fig. 254). Three models produced results, though the GAM_{nb} was removed through skill testing (Table 83). Three of the five SDMs considered for inclusion in the ensemble to predict numerical abundance of adult shortspine thornyhead in the GOA converged (Table 83); the GAM_{nb} was eliminated by skill testing. The remaining two best-performing SDMs were weighted by RMSE in the final ensemble, which attained an excellent overall fit to the observed adult distribution and abundance data. The ensemble was excellent at predicting high and low abundance catches (ρ = 0.70), discriminating presence-absence (AUC = 0.96), and explaining deviance (PDE = 0.82). Bottom depth, geographic location, and bottom current accounted for 83.5% of the covariate contribution to the deviance explained by the final ensemble (Table 84). Higher adult shortspine thornyhead abundance was predicted to peak around 300 m depth with relatively low bottom current exposure within a relatively small depth range, including glacial troughs on the continental shelf and areas along the continental slope of the GOA (Fig. 255). The CV of ensemble predictions was higher in areas with predicted higher abundance. Areas with the highest predicted encounter probability were similar to areas of predicted high abundance, yet more spatially extensive inshore (Fig. 256).

Essential fish habitat of subadult and adult shortspine thornyhead in the Gulf of Alaska -- Ensemble-predicted habitat-related numerical abundance of shortspine thornyhead life stages collected in RACE-GAP summer bottom trawl surveys of the GOA (1993–2019) was mapped as EFH areas and subareas (Fig. 257). EFH for subadults and adults was similar and occurs within glacial troughs on the continental shelf and along the outer shelf and continental slope of the GOA. Core EFH area was extensive throughout the total EFH area, and EFH hot spots were restricted to the main glacial troughs, outer continental shelf, and slope for this species.

Table 83. -- Constituent species distribution models (SDMs) used to construct Essential Fish Habitat (EFH) for a) subadult and b) adult shortspine thornyhead: MaxEnt = Maximum entropy; paGAM = presence-absence generalized additive model; hGAM = zero-adjusted Poisson hurdle GAM; GAMP = standard Poisson GAM; GAMnb = standard negative-binomial GAM; RMSE = root mean square error; ρ (rho) = Spearman's rank correlation coefficient; AUC = area under the receiver-operating characteristic curve; and PDE = Poisson deviance explained *. The "-- " indicates that this model was not included in the final ensemble.

a) subadult shortspine thornyhead

Models	RMSE	Relative Weight	ρ	AUC	PDE	EFH area (km^2)
MaxEnt	--	--	--	--	--	--
paGAM	30.1	0.27	0.66	0.98	0.66	190,000
hGAM	25.5	0.37	0.65	0.98	0.75	153,700
GAM_P	26.0	0.36	0.64	0.97	0.73	194,000
GAM_{nb}	36.3	0	--	--	--	--
ensemble	24.4	1	0.65	0.97	0.76	186,900

b) adult shortspine thornyhead

Models	RMSE	Relative Weight	ρ	AUC	PDE	EFH area (km^2)
MaxEnt	--	--	--	--	--	--
paGAM	--	--	--	--	--	--
hGAM	45.9	0.53	0.70	0.97	0.81	186,400
GAM_P	48.4	0.47	0.70	0.96	0.79	236,900
GAM_{nb}	67.1	0	--	--	--	--
ensemble	44.4	1	0.70	0.96	0.82	229,200

* Refer to the Species Distribution Model Performance Metrics subsection within the Statistical Modeling section of the Methods for detailed descriptions of individual model performance metrics.

Table 84. -- Covariates retained in the a) subadult and b) adult shortspine thornyhead species distribution model (SDM) final ensembles, the percent contribution to the ensemble deviance explained by each covariate, and the cumulative deviance explained: SD = standard deviation and BPI = bathymetric position index.

shortspine thornyhead	**Covariate**	**% Contribution**	**Cumulative %**
a) subadult	bottom depth	48.8	48.8
	location	19.4	68.3
	sponge presence	5.6	73.9
	current	5.1	79.0
	rockiness	3.6	82.6
	aspect north	3.3	85.9
	bottom temperature	2.8	88.7
	slope	2.7	91.4
	tidal maximum	2.2	93.6
	current SD	2.0	95.6
	aspect east	2.0	97.6
	pennatulacean presence	1.1	98.7
	BPI	0.6	99.3
	coral presence	0.4	99.7
	curvature	0.3	100.0
b) adult	bottom depth	59.9	59.9
	location	16.4	76.3
	current	7.2	83.5
	slope	5.1	88.6
	bottom temperature	2.4	91.0
	sponge presence	2.3	93.3
	tidal maximum	1.8	95.1
	aspect north	1.5	96.6
	BPI	1.2	97.8
	current SD	0.6	98.4
	rockiness	0.6	99.0
	aspect east	0.5	99.5
	curvature	0.4	99.9
	coral presence	0.1	100.0

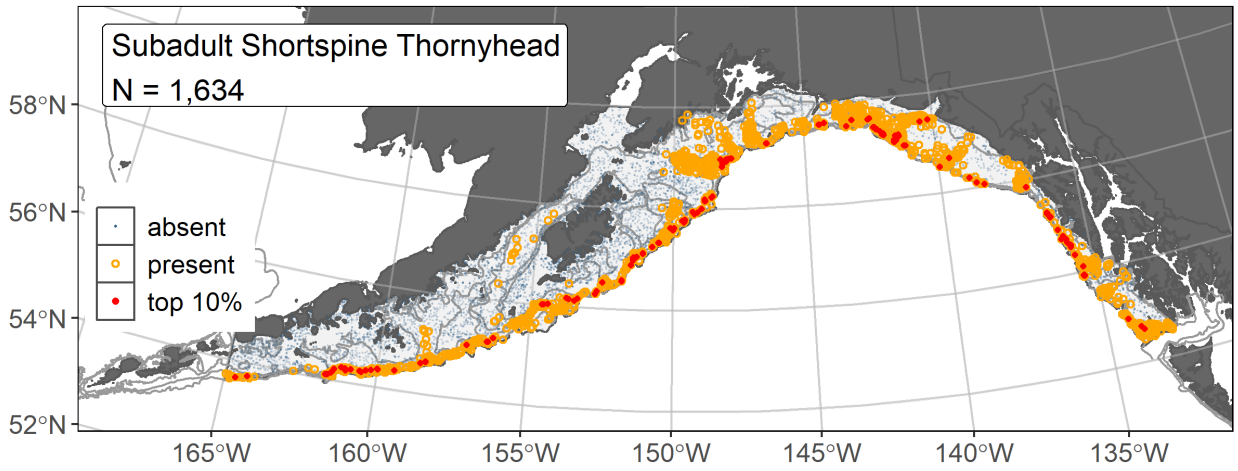

Figure 251. -- Distribution of subadult shortspine thornyhead catches (N = 1,634) in 1993–2019 AFSC RACE-GAP summer bottom trawl surveys of the Gulf of Alaska with the 100 m, 200 m, and 700 m isobaths indicated; filled red circles indicate locations in top 10% of overall abundance, open orange circles indicate presence in remaining catches, and blue dots indicate stations sampled where the animals were not present.

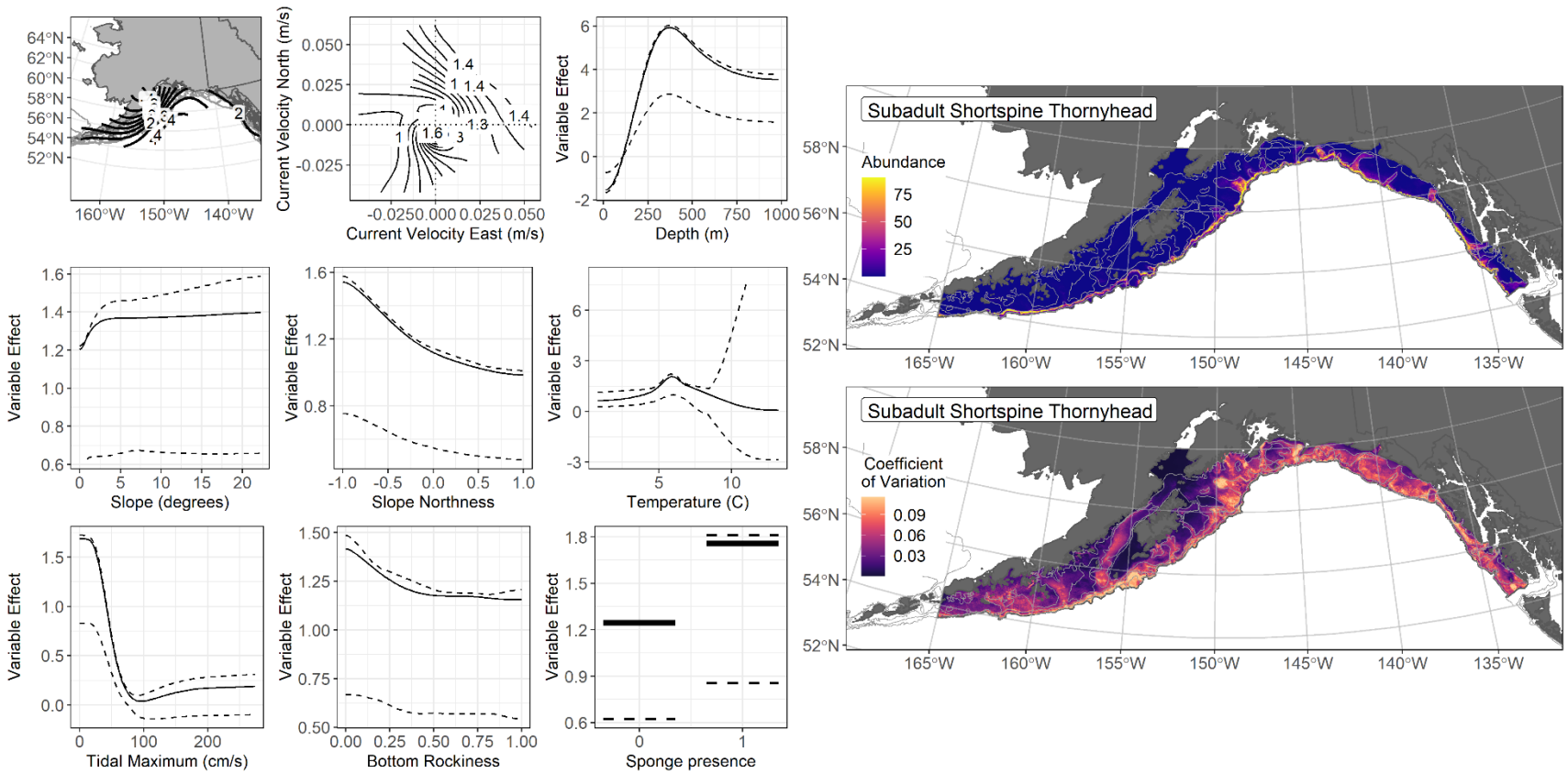

Figure 252. -- The top nine covariate effects (left panel) on ensemble-predicted subadult shortspine thornyhead numerical abundance across the Gulf of Alaska (upper right panel) along with the coefficient of variation (CV) of the ensemble predictions (lower right panel).

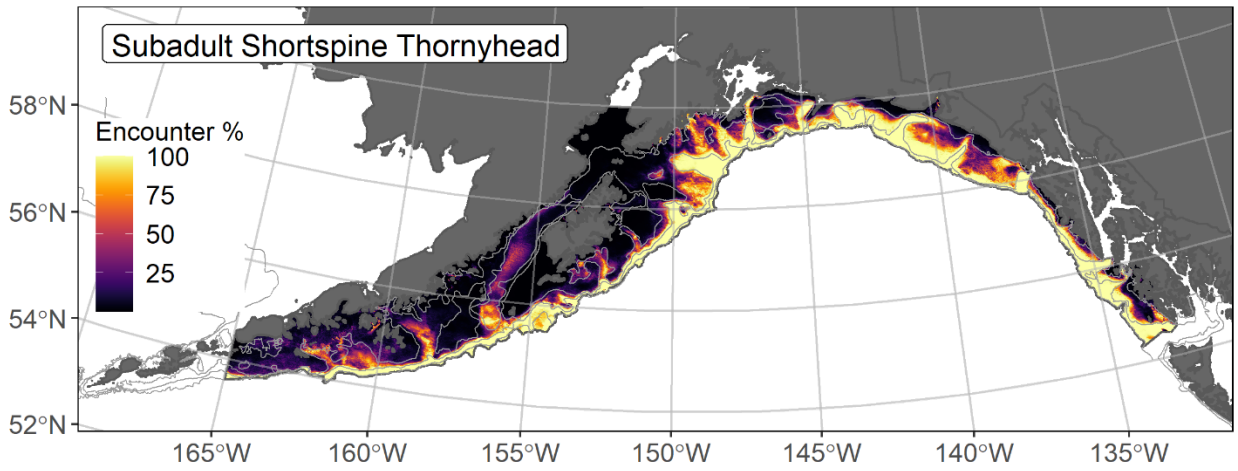

Figure 253. -- Encounter probability of subadult shortspine thornyhead from AFSC RACE-GAP summer bottom trawl surveys (1993–2019) of the Gulf of Alaska with the 100 m, 300 m, and 700 m isobaths indicated.

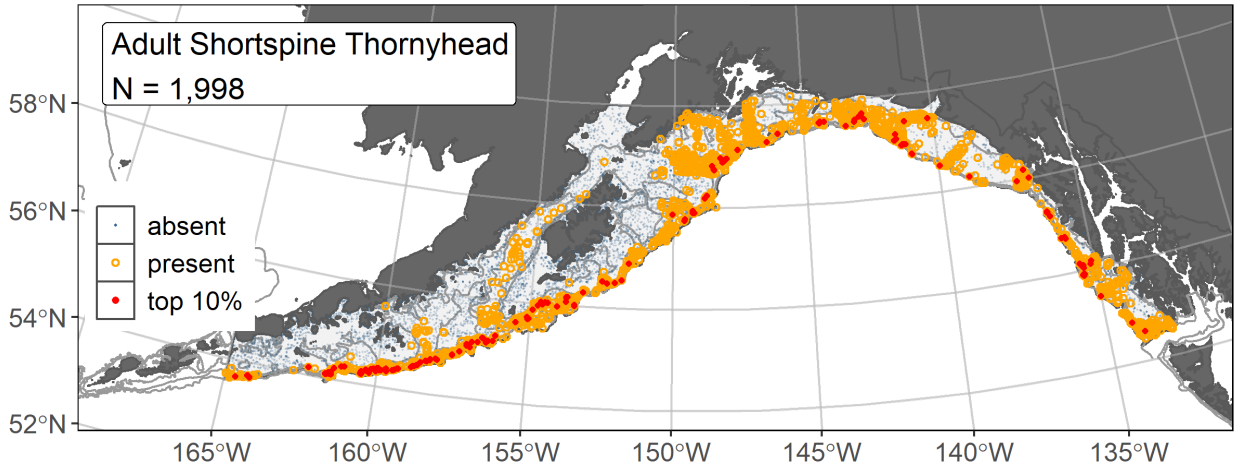

Figure 254. -- Distribution of adult shortspine thornyhead catches (N = 1,998) in 1993–2019 AFSC RACE-GAP summer bottom trawl surveys of the Gulf of Alaska with the 100 m, 200 m, and 700 m isobaths indicated; filled red circles indicate locations in top 10% of overall abundance, open orange circles indicate presence in remaining catches, and blue dots indicate stations sampled where the animals were not present.

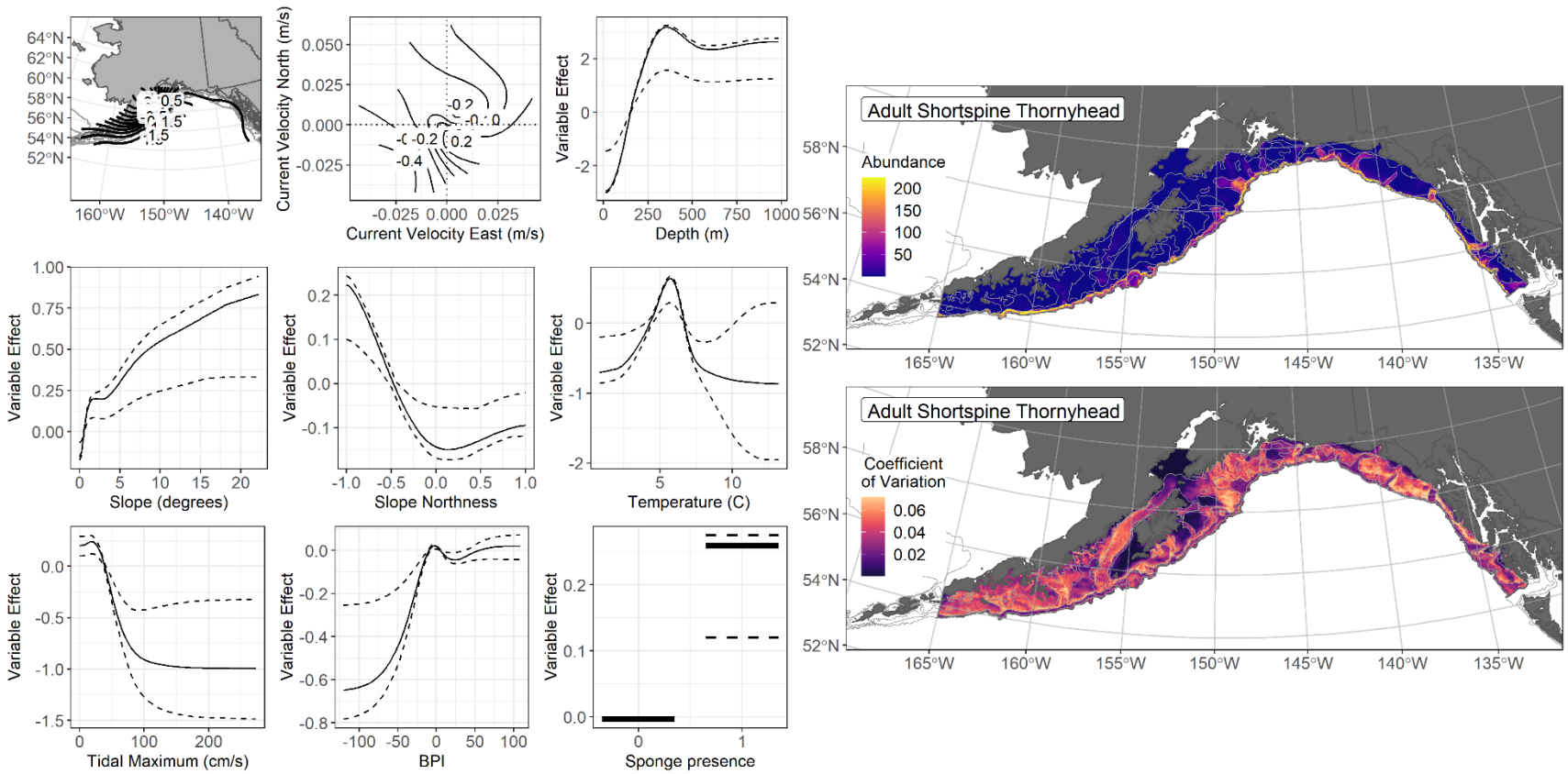

Figure 255. -- The top nine covariate effects (left panel) on ensemble-predicted adult shortspine thornyhead numerical abundance across the Gulf of Alaska (upper right panel) alongside the coefficient of variation (CV) of the ensemble predictions (lower right panel).

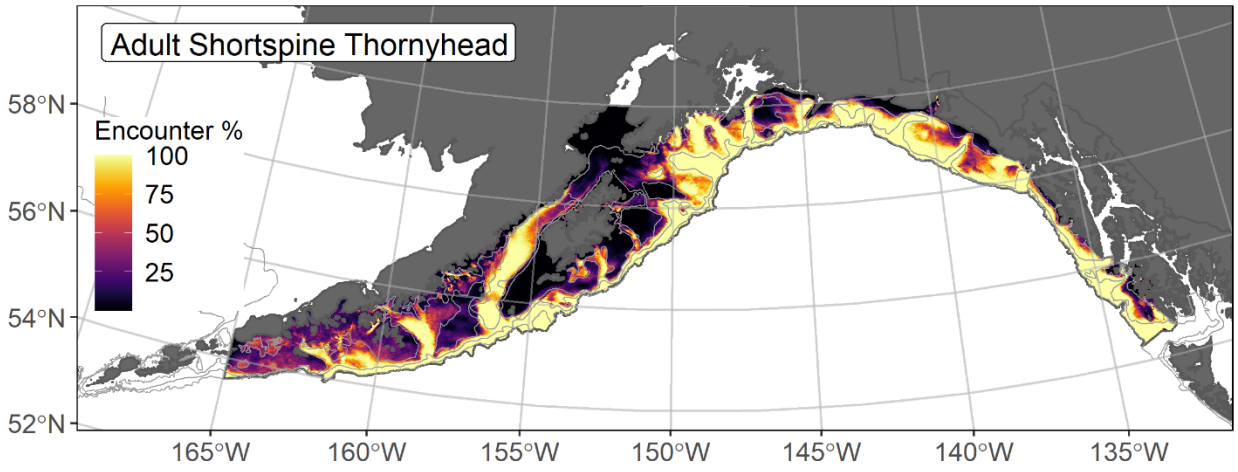

Figure 256. -- Encounter probability of adult shortspine thornyhead from AFSC RACE-GAP summer bottom trawl surveys (1993–2019) of the Gulf of Alaska with the 100 m, 300 m, and 700 m isobaths indicated.

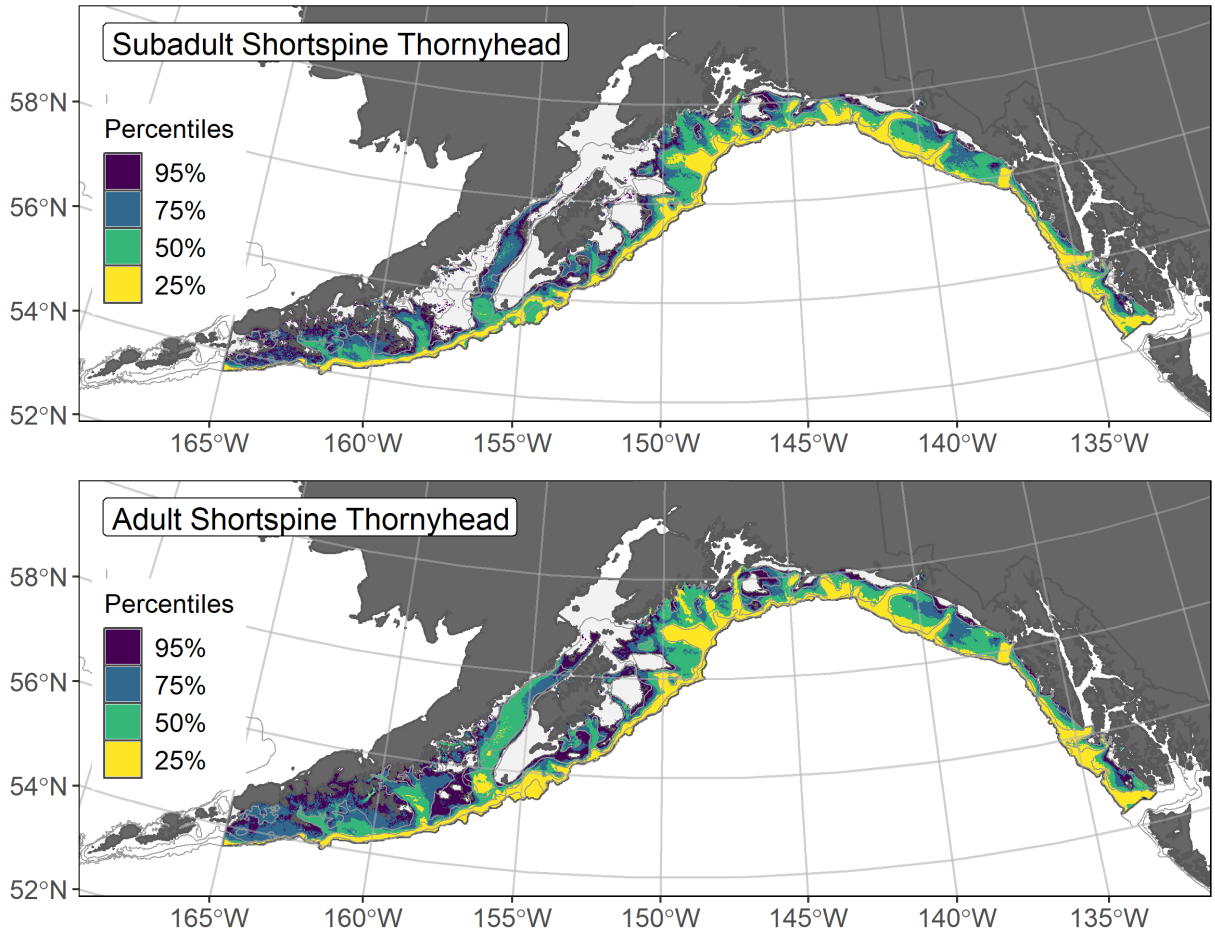

Figure 257. -- Essential fish habitat (EFH) is the area containing the top 95% of occupied habitat (defined as model estimated encounter probabilities greater than 5%) from an SDM ensemble fitted to subadult (top panel) and adult (bottom panel) shortspine thornyhead distribution and abundance in AFSC RACE-GAP summer bottom trawl surveys (1993–2019) with 100 m, 200 m, and 700 m isobaths indicated; within the EFH area map are the subareas of the top 25% (EFH hot spots), top 50% (core EFH area), and top 75% (principal EFH area) of habitat-related, ensemble-predicted numerical abundance.

Sharks and skates

Spiny dogfish (*Squalus suckleyi*)

Spiny dogfish (*Squalus suckelyi*) are a member of the shark complex (spiny dogfish, Pacific sleeper shark, salmon shark, and other/unidentified sharks) in the GOA (Tribuzio et al. 2020). Spiny dogfish EFH was not mapped in the 2017 EFH 5-year Review, nor was the EFH for any other shark complex species. The spiny dogfish is a small shark species common in sub-tropical and sub-arctic waters ranging in the North Pacific from the eastern Chukchi Sea through the Bering Sea and into the Gulf of California (Mecklenberg et al. 2002). Spiny dogfish, recently re-described as a distinct species from the circumboreal *S. acanthias* (Ebert et al. 2010), is not a targeted species in the GOA (Tribuzio et al. 2020). This species is considered to be a single population in the eastern North Pacific Ocean (Ebert et al. 2010). Tribuzio and Kruse (2012) reported that in the GOA, most females were mature at L_{50} = 973 mm TL setting the upper limit for the subadult length range and the lower limit for adults in the present study. Due to data limitation concerns for the adult spiny dogfish the subadult and adult life stages were combined in an SDM ensemble to map the summer distribution EFH in the GOA. Since the longline surveys also catch spiny dogfish, including additional data from these surveys may be helpful in future SDM EFH mapping for this species[51].

Spiny dogfish abundance and distribution predicted from RACE-GAP summer bottom trawl surveys in the Gulf of Alaska -- Subadult spiny dogfish (N = 1,291) caught in GOA RACE-GAP summer bottom trawl surveys (1993–2019) were distributed across the GOA continental shelf from Dixon Entrance in the southeast to Unimak Pass in the west, but were most common in the central and southeast GOA and were particularly abundant east of Kodiak Island (Fig. 258). Five SDMs were considered for inclusion in the ensemble to predict numerical abundance of subadult spiny dogfish in the GOA (Table 85); the GAM_{nb} was eliminated by skill testing. The remaining four best-performing SDMs were weighted based on RMSE in the final ensemble, which was a good overall fit to the observed spiny dogfish distribution and abundance data. The ensemble was good at predicting high and low abundance catches (ρ = 0.42), discriminating presence-absence (AUC = 0.83), and explaining deviance (PDE = 0.48). Geographic location, bottom temperature, and bottom current velocity accounted for 66.6% of the covariate contribution to the deviance explained by the final ensemble (Table 86). Higher abundance of spiny dogfish was predicted to occur in southern Cook Inlet, east of Kodiak Island, and areas of the central and eastern GOA (Fig. 259). The CVs of ensemble predictions were relatively even

[51] A recommendation from the stock author review to incorporate longline survey data in future SDM ensemble EFH mapping for this species will be included as a research recommendation from the 2023 EFH 5-year Review.

across the survey area. Encounter probabilities of spiny dogfish were higher east of Kodiak Island (Fig. 260).

Essential Fish Habitat of spiny dogfish in the Gulf of Alaska -- Ensemble-predicted habitat-related numerical abundance of spiny dogfish life stages collected in RACE-GAP summer bottom trawl surveys of the GOA (1993–2019) was mapped as EFH area and subareas (Fig. 261). Spiny dogfish EFH spanned most of the GOA survey area, with core EFH extending from the eastern side of Kodiak Island into southeast Alaska. EFH hotspots occurred in Cook Inlet and were extensive throughout the central GOA to Baranof Island off southeast Alaska.

Table 85. -- Constituent species distribution models (SDMs) used to construct Essential Fish Habitat (EFH) for spiny dogfish: MaxEnt = Maximum entropy; paGAM = presence-absence generalized additive model; hGAM = zero-adjusted Poisson hurdle GAM; GAM_P = standard Poisson GAM; GAM_{nb} = standard negative-binomial GAM; RMSE = root mean square error; ρ (rho) = Spearman's rank correlation coefficient; AUC = area under the receiver-operating characteristic curve; and PDE = Poisson deviance explained *. The "--" indicates that this model was not included in the final ensemble.

spiny dogfish

Models	RMSE	Relative Weight	ρ	AUC	PDE	EFH area (km^2)
MaxEnt	10.8	0.28	0.36	0.78	0.24	280,100
paGAM	10.8	0.28	0.41	0.82	0.33	268,300
hGAM	14.3	0.16	0.39	0.82	0.29	185,300
GAM_P	10.7	0.28	0.39	0.81	0.40	176,900
GAM_{nb}	10.6	0	--	--	--	--
ensemble	10.0	1	0.42	0.84	0.48	273,900

* Refer to the Species Distribution Model Performance Metrics subsection within the Statistical Modeling section of the Methods for detailed descriptions of individual model performance metrics.

Table 86. -- Covariates retained in the spiny dogfish species distribution model (SDM) final ensemble, the percent contribution to the ensemble deviance explained by each covariate, and the cumulative deviance explained: SD = standard deviation and BPI = bathymetric position index.

spiny dogfish

Covariate	% Contribution	Cumulative %
location	37.5	37.5
bottom temperature	19.1	56.6
current	10.0	66.6
bottom depth	7.4	74.0
current SD	5.7	79.7
tidal maximum	4.3	84.0
aspect north	3.7	87.7
rockiness	3.6	91.3
BPI	3.3	94.6
aspect east	2.6	97.2
curvature	1.3	98.5
slope	0.7	99.2
pennatulacean presence	0.7	99.9
coral presence	0.1	100.0

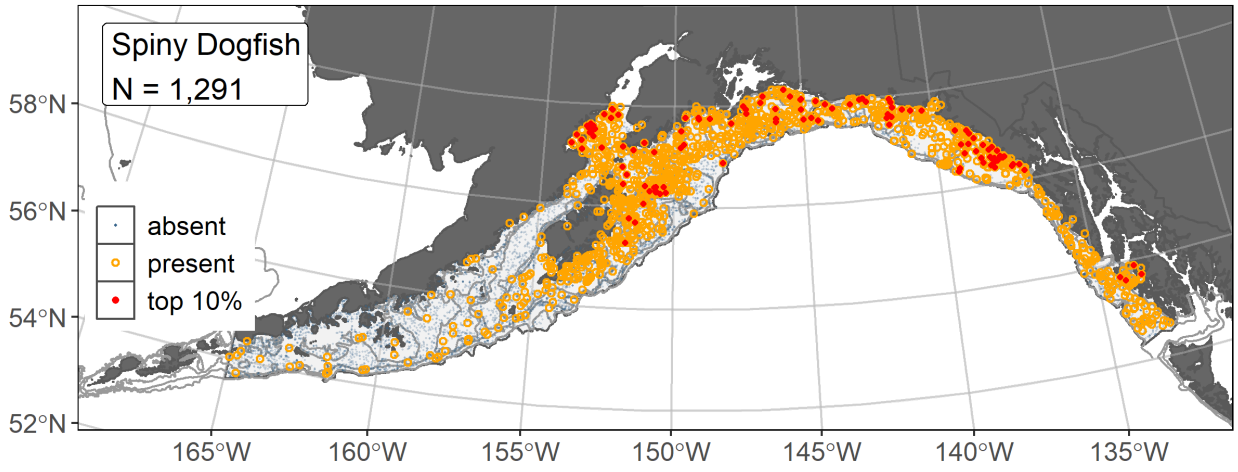

Figure 258. -- Distribution of spiny dogfish catches (N = 1,291) in 1993–2019 AFSC RACE-GAP summer bottom trawl surveys of the Gulf of Alaska with the 100 m, 200 m, and 700 m isobaths indicated; filled red circles indicate locations in top 10% of overall abundance, open orange circles indicate presence in remaining catches, and blue dots indicate stations sampled where the animals were not present.

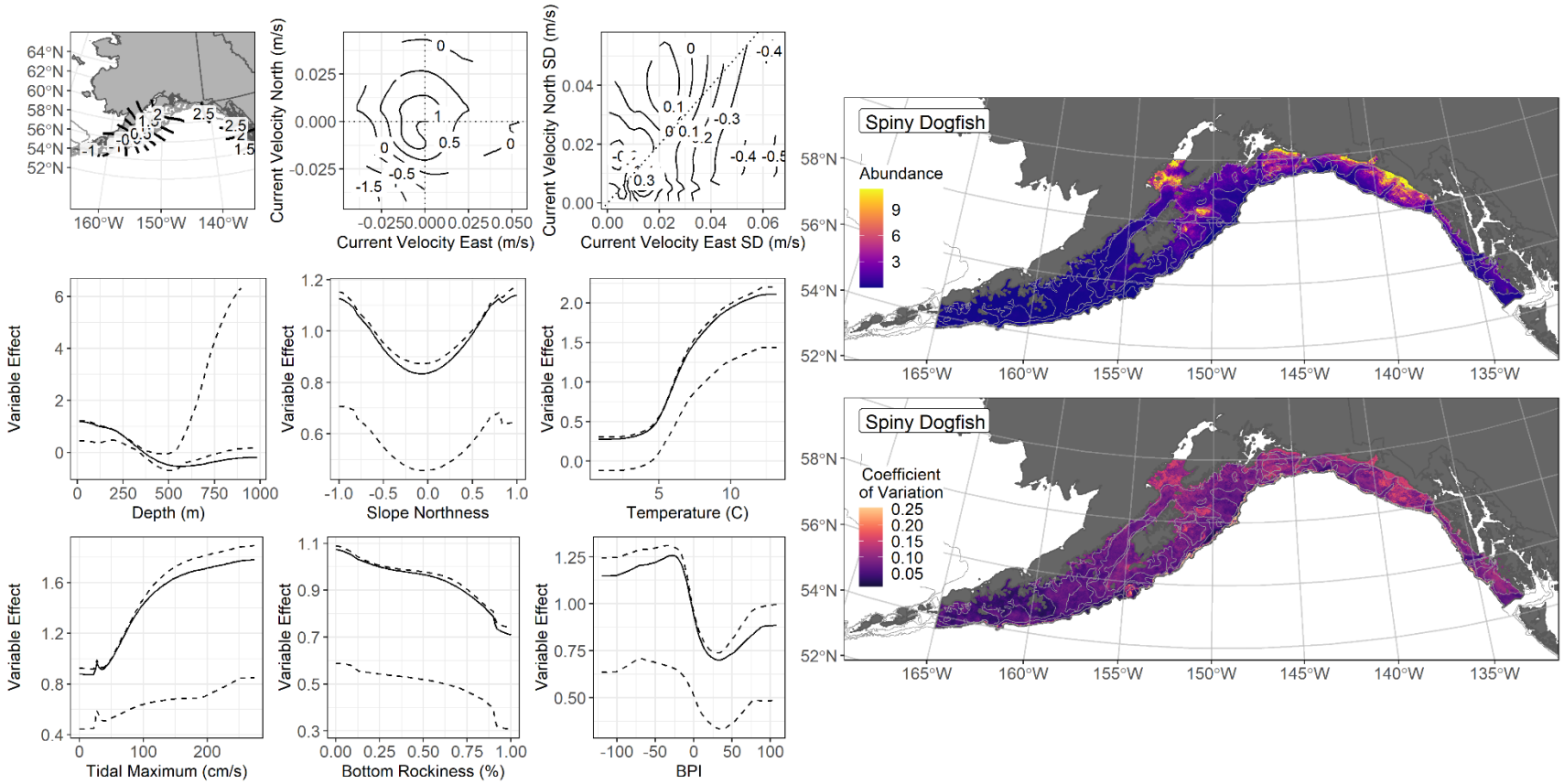

Figure 259. -- The top nine covariate effects (left panel) on ensemble-predicted spiny dogfish numerical abundance across the Gulf of Alaska (upper right panel) and the coefficient of variation (CV) of the ensemble predictions (lower right panel).

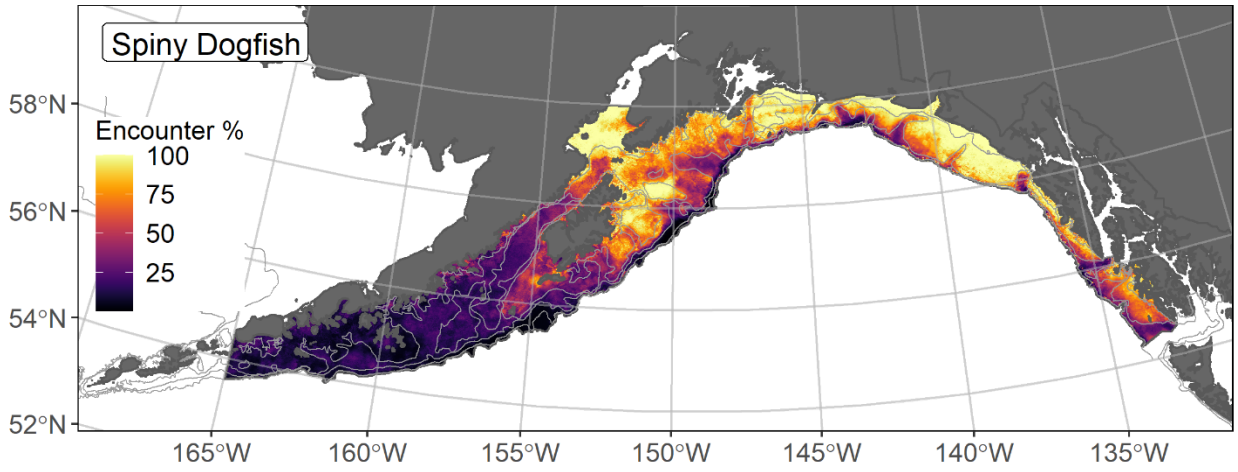

Figure 260. -- Encounter probability of spiny dogfish from AFSC RACE-GAP summer bottom trawl surveys (1993–2019) of the Gulf of Alaska with the 100 m, 200 m, and 700 m isobaths indicated.

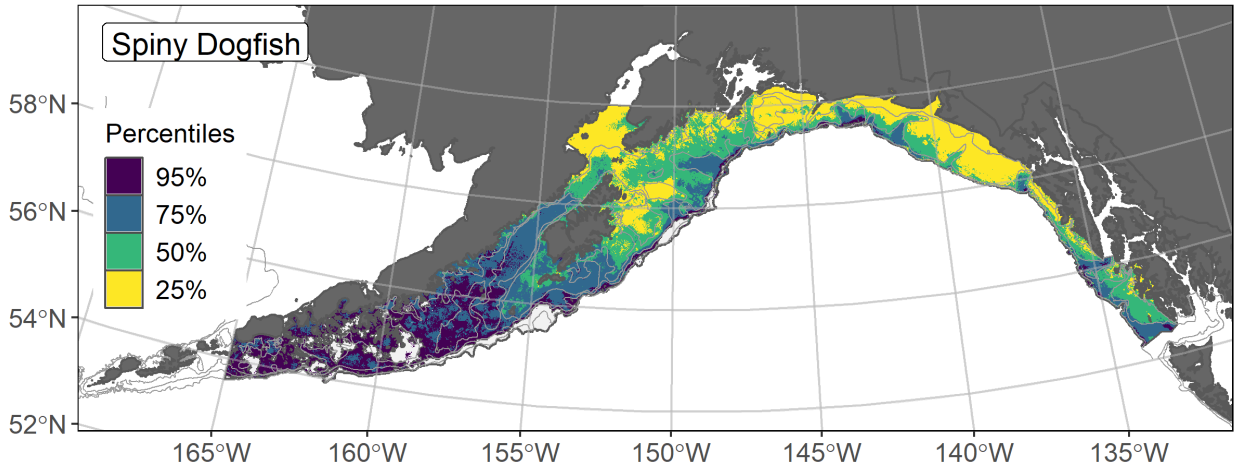

Figure 261. -- Essential fish habitat (EFH) is the area containing the top 95% of occupied habitat (defined as model estimated encounter probabilities greater than 5%) from an SDM ensemble fitted to subadult and adult spiny dogfish distribution and abundance in AFSC RACE-GAP summer bottom trawl surveys (1993–2019) with 100 m, 200 m, and 700 m isobaths indicated; within the EFH area map are the subareas of the top 25% (EFH hot spots), top 50% (core EFH area), and top 75% (principal EFH area) of habitat-related, ensemble-predicted numerical abundance.

Skate stock complex

In the GOA, the Skate stock complex is managed as three units with big skate and longnose skate each having separate harvest specifications, and all remaining skates are managed as an "other skates" group (Ormseth 2019). The three most abundant species in the "other skates" group are Aleutian skate, Bering skate, and Alaska skate. Five skate species, including big, longnose, Aleutian, Bering, and Alaska, were sufficiently prevalent in RACE-GAP GOA bottom trawl survey catches (N > 50) to support SDMs of habitat-related abundance to map EFH for each species[52]. To map the EFH of the skate complex, the SDMs of these species were combined separately for subadults and adults to generate additive composite maps of habitat-related abundance and EFH, representing the EFH of member species' life stages where an EFH map was not possible due to insufficient data[53].

Subadult skate abundance and distribution predicted from RACE-GAP summer bottom trawl surveys in the Gulf of Alaska -- Habitat-related, ensemble-predicted numerical abundance was combined for the subadults of five skate species to represent the skate complex in the GOA and mapped along with the combined encounter probability and EFH area (Fig. 262). The composite, ensemble-predicted abundance of subadult skates reflected contributions of the more common and abundant species: Aleutian skate, Bering skate, and big skate. The Aleutian and Bering skates were common and abundant in the vicinity of Chirikof Straight, while the big skate was common in nearshore areas along the mainland in the Kodiak and Yakutat regions. The probability of encounter for subadult skates also reflected these distribution and abundance patterns.

Adult skate abundance and distribution predicted from RACE-GAP summer bottom trawl surveys in the Gulf of Alaska -- Habitat-related, ensemble-predicted numerical abundance was combined for the adults of five skate species to represent the skate complex in the GOA and mapped along with the combined encounter probability and EFH area (Fig. 263). The composite, ensemble-predicted abundance of adult skates showed high abundance in Shelikof Strait, throughout the central GOA, and into shallower waters in the Kodiak and Yakutat regions. The high prevalence of adult longnose skate in these areas and the complementary distribution of big skate in nearshore areas, Cook Inlet, and west of the Shumagin Islands combined to be some of the stronger influences on the resulting maps. Adult skate encounter probabilities followed a similar pattern with high encounter rates in Shelifkof Straight and through the central GOA into the Yakutat region.

---

[52] Incorporating other high quality sources of data if available in future SDM ensemble EFH mapping for this species will be included as a research recommendation from the 2023 EFH 5-year Review.
[53] 50 CFR 600.815(a)(1)(iv)(E)

Essential fish habitat of skate complex subadults and adults in the Gulf of Alaska -- EFH of subadult skates included most of the GOA study area from southeast Alaska to Unimak Pass (Fig. 262). Core EFH areas and EFH hot spots primarily reflected the distribution and abundance of Aleutian, Bering, and big skates in the central GOA. EFH of adults also included most of the GOA study area (Fig. 263). Core EFH area for adults extends from the Chirikof region in the western GOA through the central GOA to the southeast Alaska region. Adult EFH hot spots, which dominated Shelikof Strait, lower Cook Inlet, and the Kodiak region to the west, reflected the high prevalence and abundance of Bering and longnose skates in the Shelikof Strait and Kodiak regions, as well as the complementary distribution of big skate abundance in Cook Inlet and other nearshore areas around Kodiak Island and the Yakutat region.

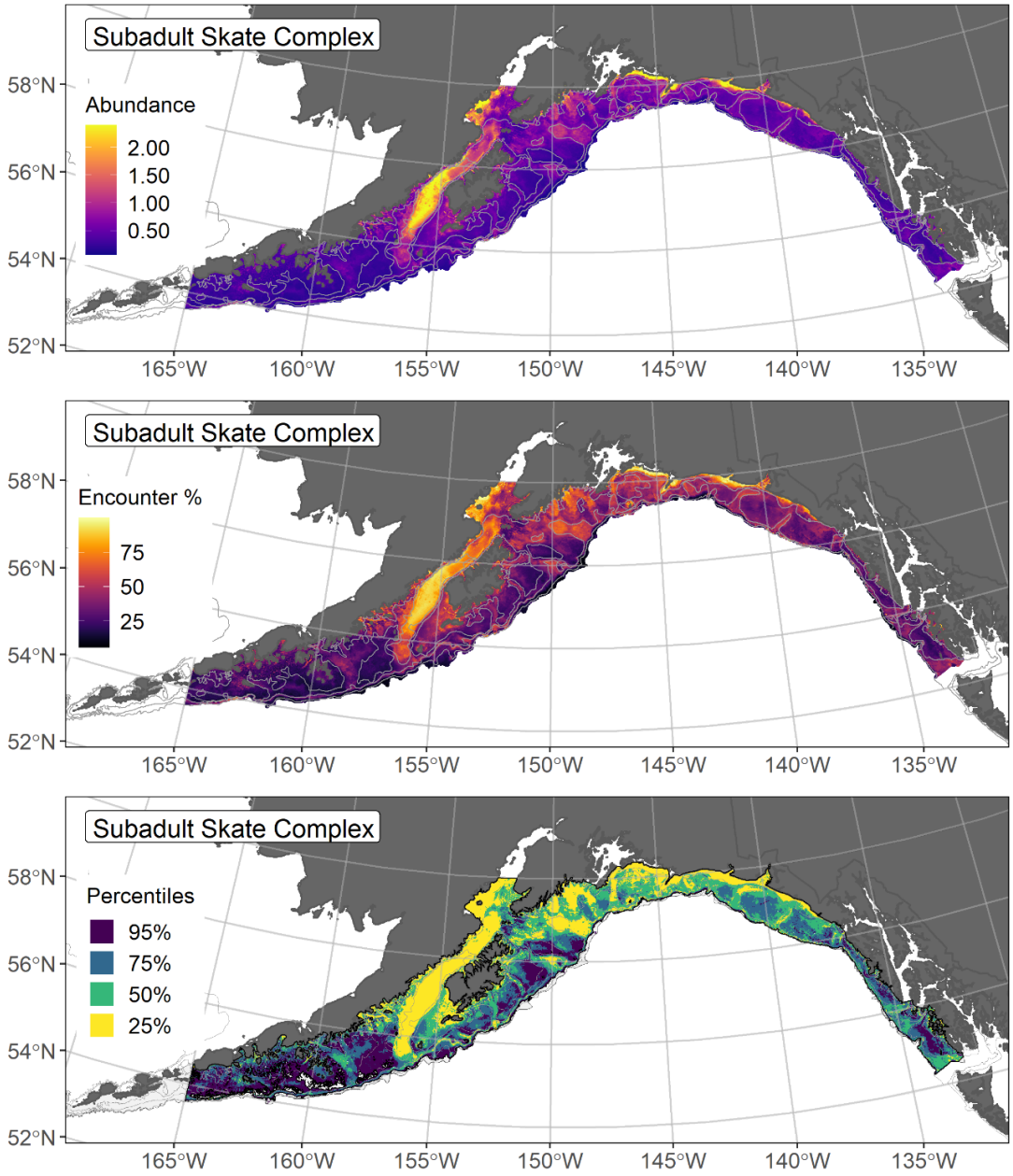

Figure 262. -- Composite habitat-related, ensemble-predicted numerical abundance (top panel), encounter probability (middle panel), and essential fish habitat (EFH) (the area containing the top 95% of occupied habitat defined as model estimated encounter probabilities greater than 5%) (bottom panel) of subadults of the Skate stock complex from the Gulf of Alaska in AFSC RACE-GAP summer bottom trawl surveys (1993–2019) with 100 m, 200 m, and 700 m isobaths indicated; within the EFH area map are the subareas of the top 25% (EFH hot spots), top 50% (core EFH area), and top 75% (principal EFH area) of habitat-related, ensemble-predicted numerical abundance.

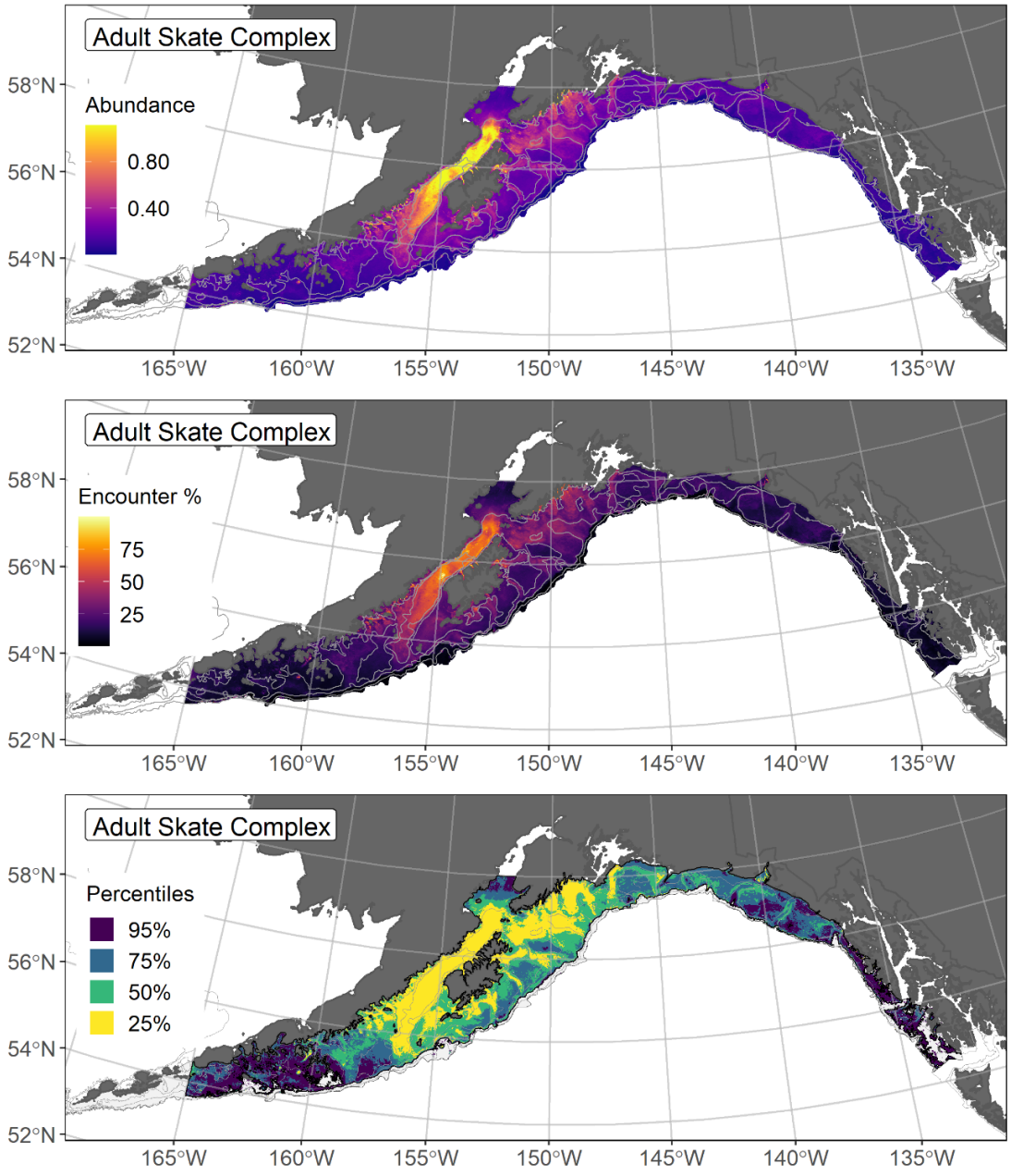

Figure 263. -- Composite habitat-related, ensemble-predicted numerical abundance (top panel), encounter probability (middle panel), and essential fish habitat (EFH) (the area containing the top 95% of occupied habitat defined as model estimated encounter probabilities greater than 5%) (bottom panel) of adults of the Skate stock complex from the Gulf of Alaska in AFSC RACE-GAP summer bottom trawl surveys (1993–2019) with 100 m, 200 m, and 700 m isobaths indicated; within the EFH area map are the subareas of the top 25% (EFH hot spots), top 50% (core EFH area), and top 75% (principal EFH area) of habitat-related, ensemble-predicted numerical abundance.

Alaska skate (*Bathyraja parmifera*)

The Alaska skate (*Bathyraja parmifera*) is a large, shallow water skate (Ebert 2005, Stevenson et al. 2007) that ranges from the eastern Bering Sea and Aleutian Islands to the eastern Gulf of Alaska (Mecklenberg et al. 2002). Subadult Alaska skates (≤ 920 mm TL) were distinguished from adults (> 920 mm TL) in the present study based on length a 50% maturity (L_{50}, Matta and Gunderson 2007) and modeled separately[54]. Although directed fishing for skates in the Gulf is prohibited, incidental catches of skates in other fisheries are sufficiently high that they are considered "in the fishery" and require harvest specifications (Ormseth 2019). Alaska skate are managed within the GOA Skate stock complex as part of the other skates group, with Gulf-wide harvest specifications; big and longnose skates are managed separately within the complex.

Subadult Alaska skate abundance and distribution predicted from RACE-GAP summer bottom trawl surveys in the Gulf of Alaska -- Subadult Alaska skate (N = 103) caught in GOA RACE-GAP summer bottom trawl surveys (1993–2019) were distributed throughout the GOA from Dixon Entrance to Unimak Pass and were most abundant in the central and western GOA (Fig. 264). Five constituent SDMs were considered for inclusion in the ensemble predicting numerical abundance of subadult Alaska skate in the GOA (Table 87); the GAM_{nb} was eliminated by skill testing. The remaining four best-performing SDMs were weighted by RMSE in the final ensemble, which attained a fair overall fit to the observed subadult Alaska skate distribution and abundance data. The ensemble was poor at predicting high and low abundance catches ($\rho = 0.13$), good at discriminating presence-absence (AUC = 0.82), and fair at explaining deviance (PDE = 0.21). Geographic location, bottom depth, and BPI accounted for 62.9% of the covariate contribution to the deviance explained by the final ensemble (Table 88). The highest abundances of subadult Alaska skate were predicted in the central GOA in Shelikof Strait and near the western end of the Alaska Peninsula at depths around 250 m (Fig. 268). The CV of ensemble predictions was lower where subadult Alaska skate were more abundant. The probability of encountering subadult Alaska skate mirrored their predicted abundance distribution and was high in association with Shelikof Strait and the western end of the Alaska Peninsula but was low elsewhere in the Gulf (Fig. 266).

Adult Alaska skate abundance and distribution predicted from RACE-GAP summer bottom trawl surveys in the Gulf of Alaska -- Adult Alaska skate (N = 78) caught in GOA RACE-GAP summer bottom trawl surveys (1993–2019) occurred from Yakutat west to the Shumagin Islands

[54] Incorporating other high quality sources of data if available in future SDM ensemble EFH mapping for this species will be included as a research recommendation from the 2023 EFH 5-year Review.

(Fig. 267). Four of the five SDMs considered for inclusion in the ensemble to predict numerical abundance of adult Alaska skate in the GOA converged (Table 87); the GAM_{nb} was eliminated by skill testing. The remaining three best-performing SDMs were equally weighted in the final ensemble, which was a fair fit overall to the observed adult Alaska skate distribution and abundance data. The ensemble was poor at predicting high and low abundance catches (ρ = 0.13), good at discriminating presence-absence (AUC = 0.85), and fair at explaining deviance (PDE = 0.25). Geographic location, bottom depth, and bottom current velocity variability accounted for 76.5% of the covariate contribution to the deviance explained by the final ensemble (Table 88). Their predicted numerical abundance was higher in the western half of GOA (Fig. 268). The CV of ensemble predictions were highest off the southwestern end of Kodiak Island and on the upper continental slope. The highest probability of encountering adult Alaska skates was in Shelikof Strait and along the south side of Kodiak Island (Fig. 269).

Essential Fish Habitat of subadult and adult Alaska skate in the Gulf of Alaska -- Habitat-related ensemble-predicted numerical abundance of Alaska skate life stages collected in RACE-GAP summer bottom trawl surveys of the GOA (1993–2019) were mapped as EFH areas and subareas (Fig. 273). The EFH area for both subadults and adults was primarily in the Shelikof Strait, along the southwestern coast of Kodiak Island, and near Unimak Pass in the west. Areas of core EFH and hot spots were similarly located for both Alaska skate life stages.

Table 87. -- Constituent species distribution models (SDMs) used to construct Essential Fish Habitat (EFH) for a) subadult and b) adult Alaska skate: MaxEnt = Maximum entropy; paGAM = presence-absence generalized additive model; hGAM = zero-adjusted Poisson hurdle GAM; GAM_P = standard Poisson GAM; GAM_{nb} = standard negative-binomial GAM; RMSE = root mean square error; ρ (rho) = Spearman's rank correlation coefficient; AUC = area under the receiver-operating characteristic curve; and PDE = Poisson deviance explained *. The "--" indicates that this model was not included in the final ensemble.

a) subadult Alaska skate

Models	RMSE	Relative Weight	ρ	AUC	PDE	EFH area (km^2)
MaxEnt	0.21	0.25	0.07	0.70	0.06	5,200
paGAM	0.21	0.25	0.11	0.76	0.10	19,600
hGAM	0.21	0.25	0.11	0.76	-Inf	16,600
GAM_P	0.21	0.25	0.10	0.74	0.07	20,400
GAM_{nb}	0.21	0	--	--	--	--
ensemble	0.21	1	0.13	0.82	0.21	14,600

b) adult Alaska skate

Models	RMSE	Relative Weight	ρ	AUC	PDE	EFH area (km^2)
MaxEnt	--	--	--	--	--	--
paGAM	0.15	0.37	0.11	0.81	0.17	11,700
hGAM	0.18	0.27	0.08	0.79	0.01	14,500
GAM_P	0.15	0.37	0.11	0.81	0.17	12,900
GAM_{nb}	0.15	0	--	--	--	--
ensemble	0.15	1	0.13	0.85	0.25	13,300

* Refer to the Species Distribution Model Performance Metrics subsection within the Statistical Modeling section of the Methods for detailed descriptions of individual model performance metrics.

Table 88. -- Covariates retained in the a) subadult and b) adult Alaska skate species distribution model (SDM) final ensembles, the percent contribution to the ensemble deviance explained by each covariate, and the cumulative deviance explained: SD = standard deviation and BPI = bathymetric position index.

Alaska skate			
	Covariate	**% Contribution**	**Cumulative %**
a) subadult	location	40.8	40.8
	bottom depth	13.0	53.9
	BPI	9.0	62.9
	bottom temperature	8.6	71.5
	current	8.2	79.7
	aspect east	3.8	83.5
	tidal maximum	3.8	87.3
	aspect north	3.5	90.8
	current SD	3.4	94.2
	coral presence	2.9	97.1
	rockiness	1.2	98.3
	pennatulacean presence	1.2	99.5
	curvature	0.3	99.8
	slope	0.1	99.9
	sponge presence	0.1	100.0
b) adult	location	59.6	59.6
	bottom temperature	8.7	68.3
	current SD	8.2	76.5
	current	8.0	84.5
	curvature	4.9	89.4
	pennatulacean presence	3.8	93.2
	bottom depth	3.1	96.3
	sponge presence	1.9	98.2
	tidal maximum	1.8	100.0

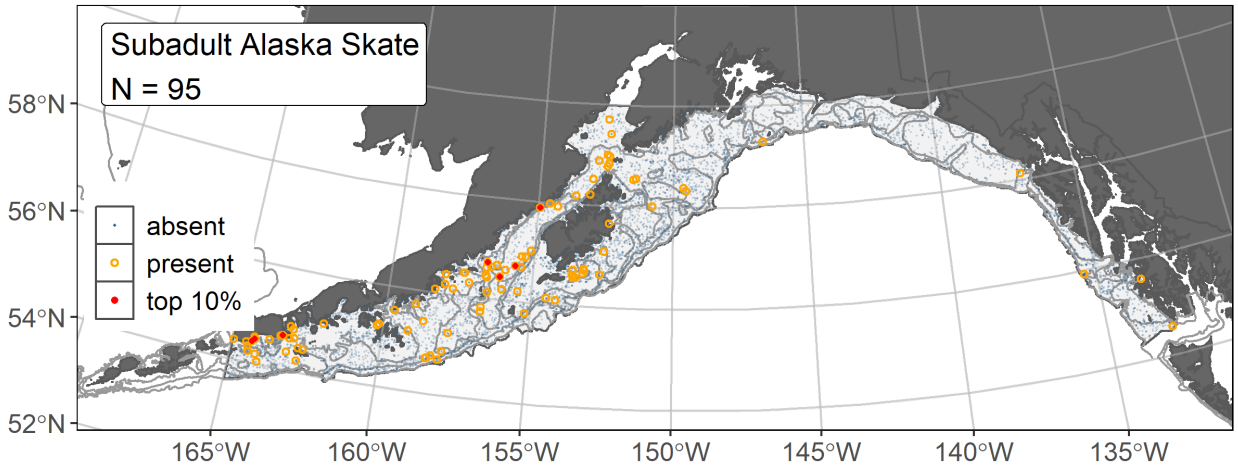

Figure 264. -- Distribution of subadult Alaska skate catches (N = 103) in 1993–2019 AFSC RACE-GAP summer bottom trawl surveys of the Gulf of Alaska with the 100 m, 200 m, and 700 m isobaths indicated; filled red circles indicate locations in top 10% of overall abundance, open orange circles indicate presence in remaining catches, and blue dots indicate stations sampled where the animals were not present.

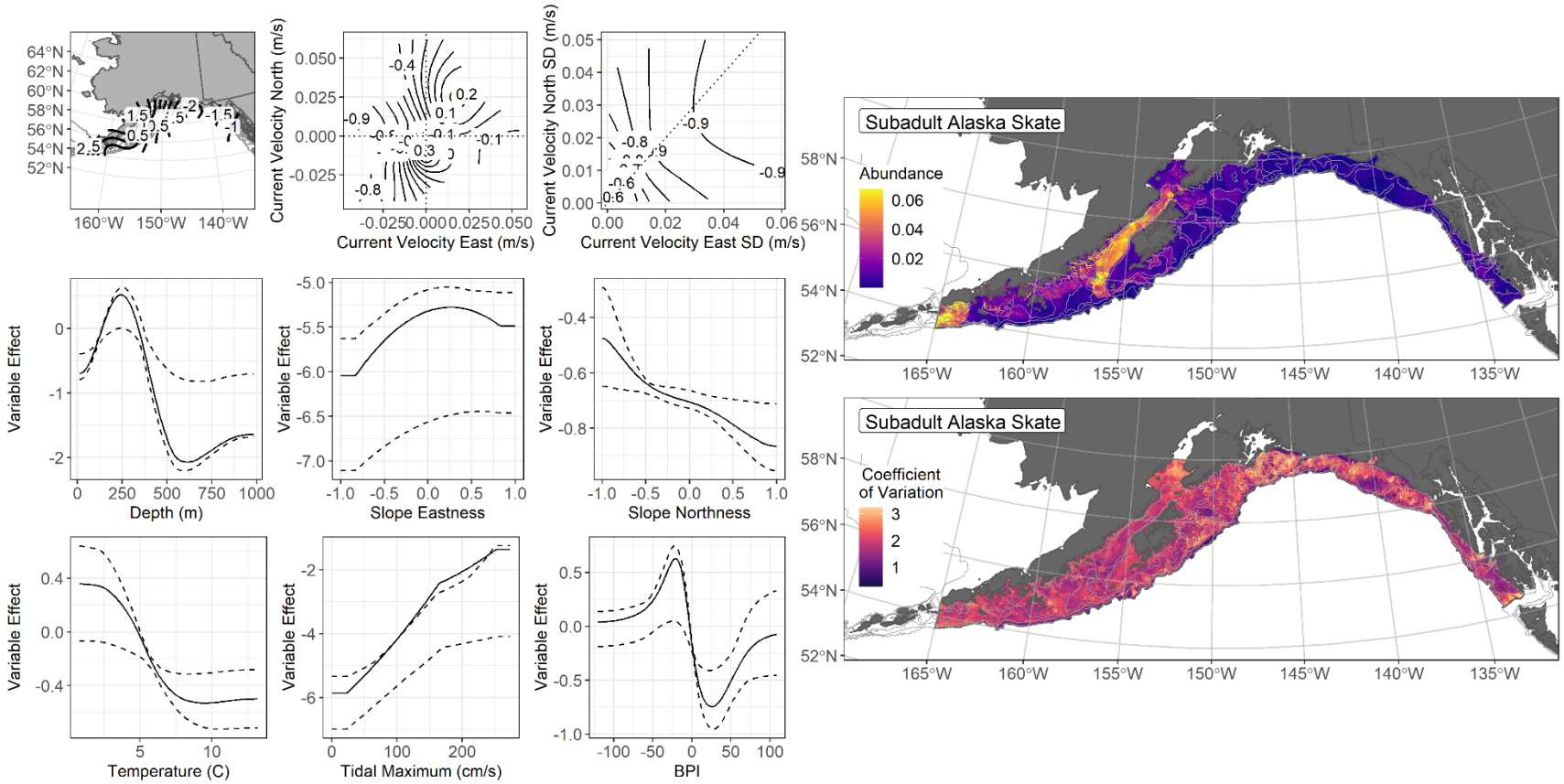

Figure 265. -- The top nine covariate effects (left panel) on ensemble-predicted subadult Alaska skate numerical abundance across the Gulf of Alaska (upper right panel) and the coefficient of variation (CV) of the ensemble predictions (lower right panel)

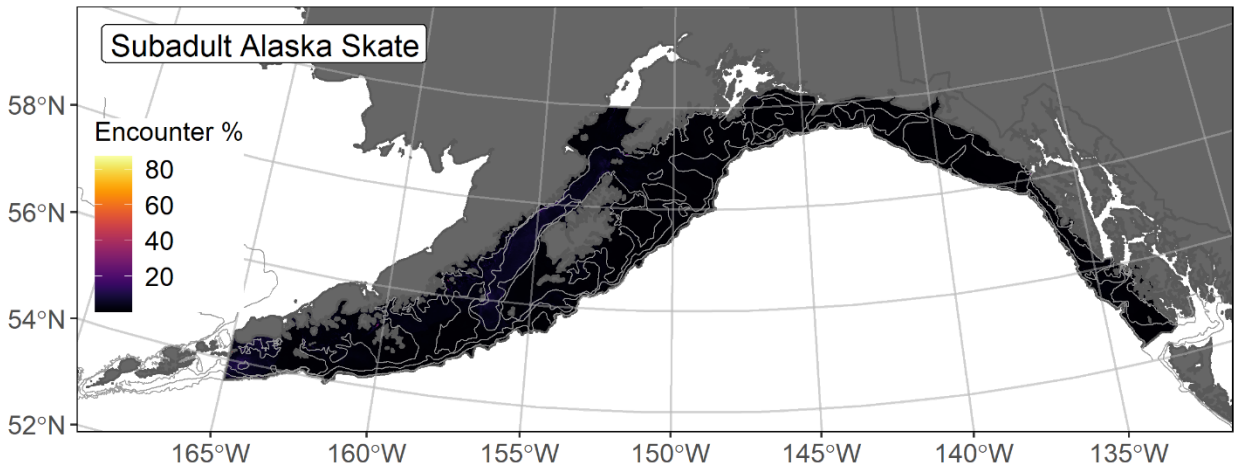

Figure 266. -- Encounter probability of subadult Alaska skate from AFSC RACE-GAP summer bottom trawl surveys (1993–2019) of the Gulf of Alaska with the 100 m, 200 m, and 700 m isobaths indicated.

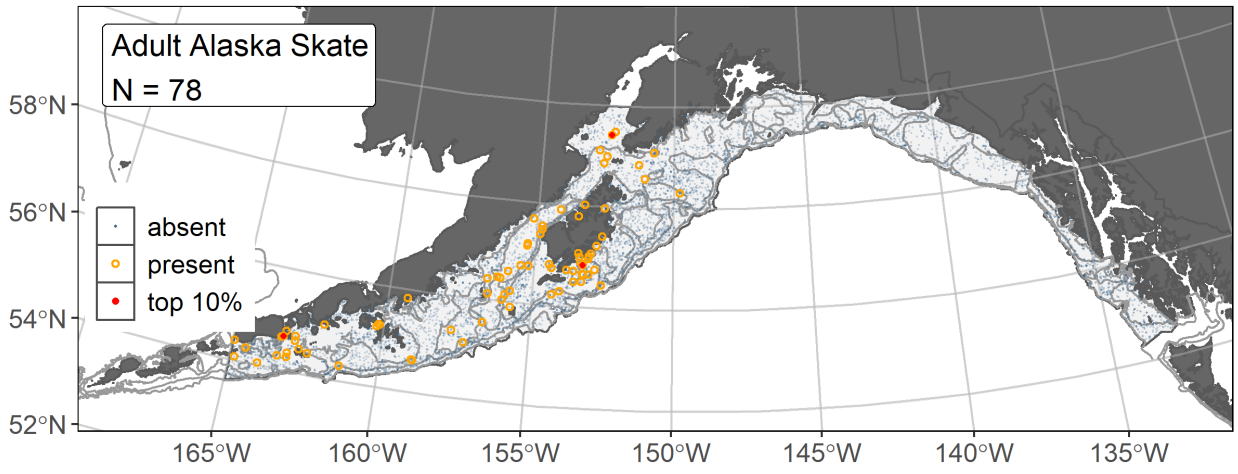

Figure 267. -- Distribution of adult Alaska skate catches (N = 78) in 1993–2019 AFSC RACE-GAP summer bottom trawl surveys of the Gulf of Alaska with the with the 100 m, 200 m, and 700 m isobaths indicated; filled red circles indicate locations in top 10% of overall abundance, open orange circles indicate presence in remaining catches, and blue dots indicate stations sampled where the animals were not present.

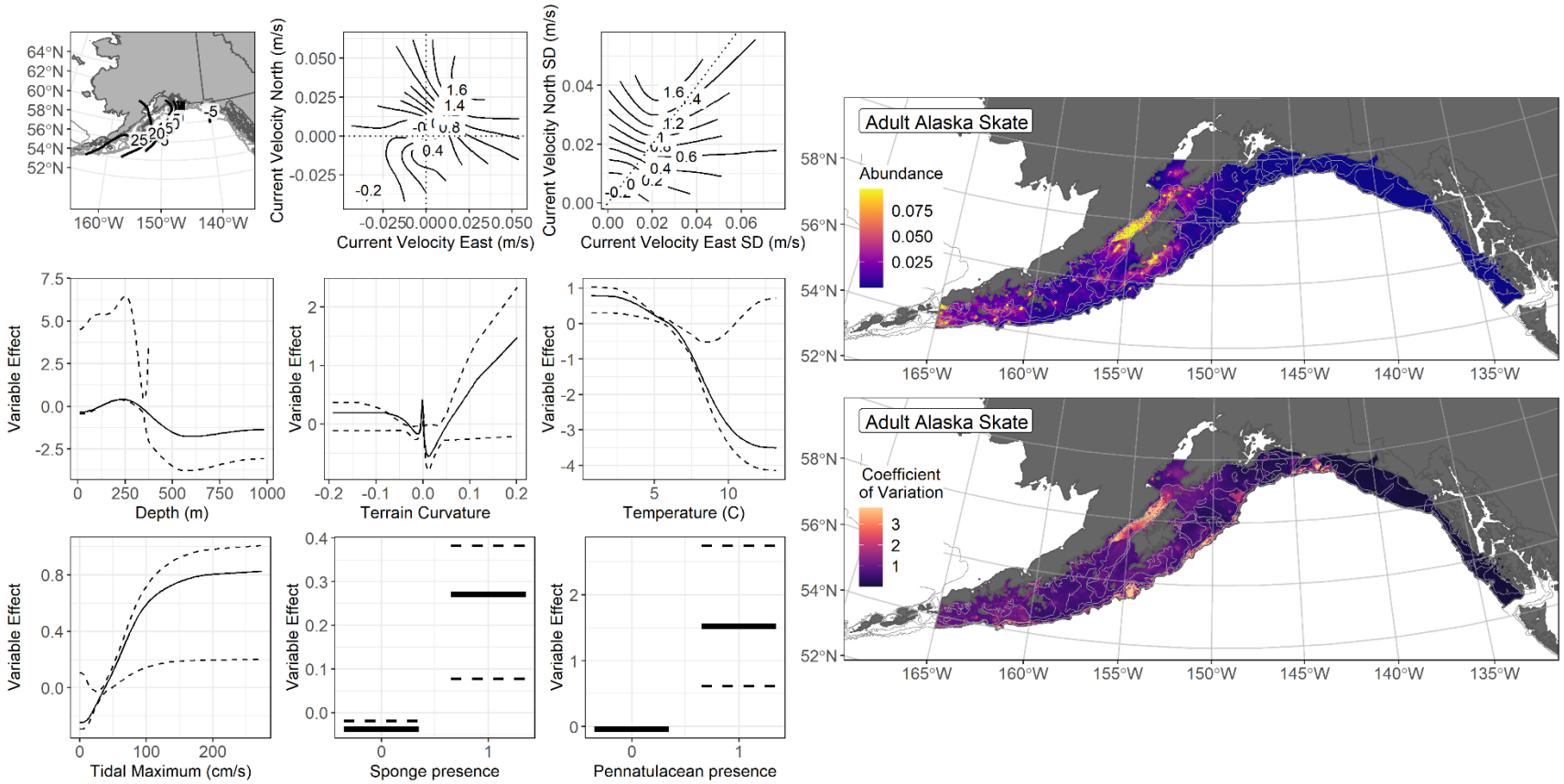

Figure 268. -- The top nine covariate effects (left panel) on ensemble-predicted adult Alaska skate numerical abundance across the Gulf of Alaska (upper right panel) and the coefficient of variation (CV) of the ensemble predictions (lower right panel).

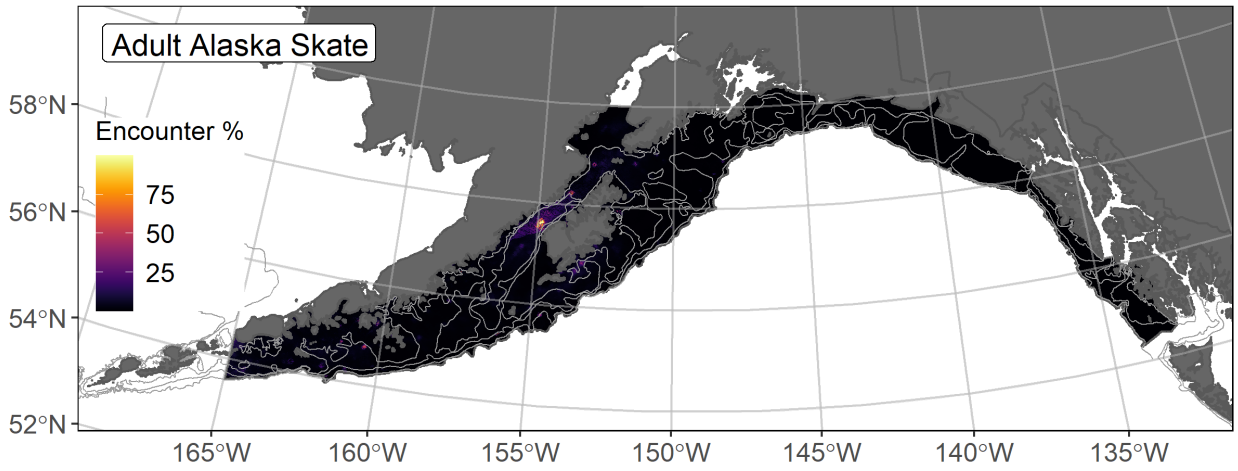

Figure 269. -- Encounter probability of adult Alaska skate from AFSC RACE-GAP summer bottom trawl surveys (1993–2019) of the Gulf of Alaska with the 100 m, 200 m, and 700 m isobaths indicated.

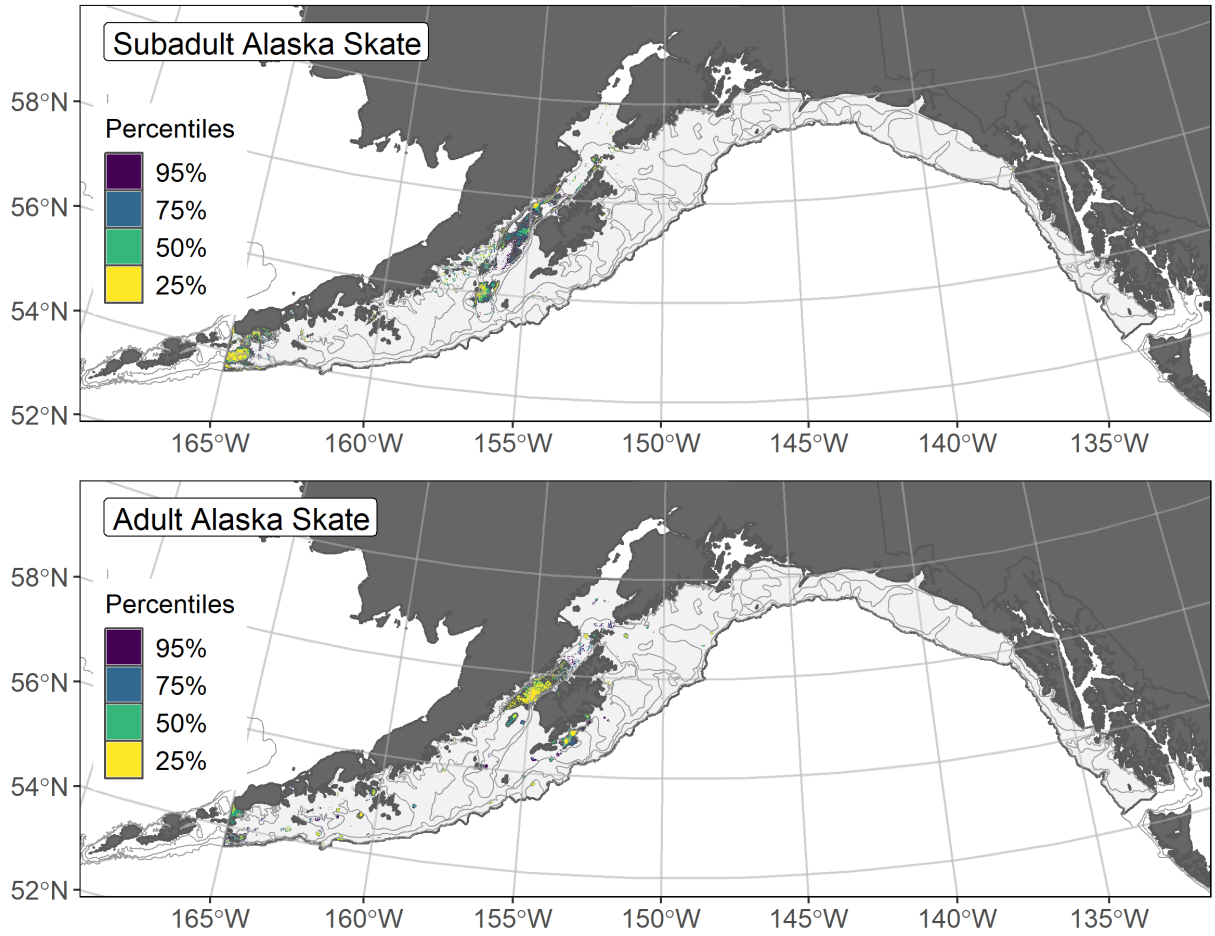

Figure 270. -- Essential fish habitat (EFH) is the area containing the top 95% of occupied habitat (defined as model estimated encounter probabilities greater than 5%) from an SDM ensemble fitted to subadult (top panel) and adult (bottom panel) Alaska skate distribution and abundance in AFSC RACE-GAP summer bottom trawl surveys (1993–2019) with 100 m, 200 m, and 700 m isobaths indicated; within the EFH area map are the subareas of the top 25% (EFH hot spots), top 50% (core EFH area), and top 75% (principal EFH area) of habitat-related, ensemble-predicted numerical abundance.

Aleutian skate (*Bathyraja aleutica*)

The Aleutian skate (*Bathyraja aleutica*) is a large species (1,500 mm TL maximum length) that ranges from the Bering Sea and Aleutian Islands into the Gulf of Alaska over a wide range of depths (29–950 m; Stevenson et al. 2007). In RACE-GAP summer bottom trawl surveys of the GOA, they are generally found in the outer domain on the GOA shelf (> 200 m depths) and on the upper continental slope (Hoff 2009)[55]. The spatial distribution of subadult (≤ 1,320 mm TL) and adult (> 1,320 mm TL) life stages (Ebert et al. 2007, Haas et al. 2016) overlaps in the GOA. Aleutian skates are among the most abundant skates in RACE-GAP GOA bottom trawl surveys and are managed in aggregate as part of the GOA Skates stock complex across the region (Ormseth 2019).

Subadult Aleutian skate abundance and distribution predicted from RACE-GAP summer bottom trawl surveys in the Gulf of Alaska -- Subadults Aleutian skate (N = 631) caught in GOA RACE-GAP summer bottom trawl surveys (1993–2019) were distributed throughout the GOA over the continental shelf but were particularly abundant in Shelikof Strait and the Chirikof region (Fig. 271). Five SDMs were considered for inclusion in the ensemble to predict numerical abundance of subadult Aleutian skate in the GOA (Table 89); the GAM_{nb} was eliminated by skill testing. The remaining four best-performing SDMs were weighted by RMSE in the final ensemble, which was a fair fit overall to the observed subadult Aleutian skate distribution and abundance data. The ensemble was fair at predicting high and low abundance catches (ρ = 0.28), good at discriminating presence-absence (AUC = 0.78), and fair at explaining deviance (PDE = 0.30). Bottom depth, geographic location, and bottom temperature accounted for the majority (75%) of the covariate contribution to the deviance explained by the final ensemble (Table 90). Higher subadult Aleutian skate abundance occurred in Shelikof Strait and to the southwest in depths around 300 m (Fig. 272). The CV of ensemble predictions was highest in areas where this life stage was less common. Encounter probabilities of subadult Aleutian skate were high where their predicted abundance was high in the vicinity of Shelikof Strait and southwest into the Chirikof region (Fig. 273).

Adult Aleutian skate abundance and distribution predicted from RACE-GAP summer bottom trawl surveys in the Gulf of Alaska -- Adult Aleutian skate (N = 147) caught in GOA RACE-GAP summer bottom trawl surveys (1993–2019) were scattered across the continental shelf from Unimak Pass into the Yakutat region with their highest abundance catches in the Chirikof region west of Kodiak Island (Fig. 274). Five SDMs were considered for inclusion in the ensemble to predict numerical

[55] Incorporating other high quality sources of data if available in future SDM ensemble EFH mapping for this species will be included as a research recommendation from the 2023 EFH 5-year Review.

abundance of adult Aleutian skate in the GOA (Table 89); the GAM_{nb} was eliminated by skill testing. The remaining four best-performing SDMs were weighted by RMSE in the final ensemble, which was a fair fit overall to the observed adult Aleutian skate distribution and abundance data. The ensemble was poor at predicting high and low abundance catches ($\rho = 0.17$), good at discriminating presence-absence (AUC = 0.83), and fair at explaining deviance (PDE = 0.25). Geographic location, bottom depth, and bottom temperature accounted for 73.8% of the covariate contribution to the deviance explained by the final ensemble (Table 90), which predicted adult Aleutian skate abundance to be highest in the Shelikof Strait and into the Chirikof region in depths around 250 m (Fig. 275). The CV of ensemble predictions was higher in Cook Inlet and along the continental shelf, where adult Aleutian skates were less common. Encounter probabilities of adult Aleutian skate were low throughout the study area except Shelikof Strait (Fig. 276).

Essential fish habitat of subadult and adult Aleutian skate in the Gulf of Alaska -- Ensemble-predicted habitat-related numerical abundance of Aleutian skate life stages collected in RACE-GAP summer bottom trawl surveys of the GOA (1993–2019) was mapped as EFH areas and subareas (Fig. 277). The subadult EFH area was widespread across the GOA continental shelf, while EFH of adult Aleutian skate was more tightly associated with the Shelikof Strait. Core EFH for subadults was scattered across much of the GOA continental shelf, with the main EFH hotspots occurring in the Shelikof Strait and Chirikof region. For adults, core EFH and EFH hot spots were primarily constrained to the Shelikof Strait and Chirikof region.

Table 89. -- Constituent species distribution models (SDMs) used to construct Essential Fish Habitat (EFH) for a) subadult and b) adult Aleutian skate: MaxEnt = Maximum entropy; paGAM = presence-absence generalized additive model; hGAM = zero-adjusted Poisson hurdle GAM; GAM_P = standard Poisson GAM; GAM_{nb} = standard negative-binomial GAM; RMSE = root mean square error; ρ (rho) = Spearman's rank correlation coefficient; AUC = area under the receiver-operating characteristic curve; and PDE = Poisson deviance explained *. The "--" indicates that this model was not included in the final ensemble.

a) subadult Aleutian skate

Models	RMSE	Relative Weight	ρ	AUC	PDE	EFH area (km^2)
MaxEnt	0.57	0.23	0.24	0.74	0.20	164,900
paGAM	0.55	0.26	0.26	0.77	0.28	169,500
hGAM	0.55	0.26	0.26	0.77	0.28	150,400
GAM_P	0.54	0.26	0.26	0.77	0.28	148,100
GAM_{nb}	0.54	0	--	--	--	--
ensemble	0.54	1	0.28	0.78	0.30	165,800

b) adult Aleutian skate

Models	RMSE	Relative Weight	ρ	AUC	PDE	EFH area (km^2)
MaxEnt	0.27	0.14	0.14	0.78	0.13	17,500
paGAM	0.19	0.29	0.15	0.81	0.20	33,500
hGAM	0.19	0.29	0.15	0.80	0.19	31,400
GAM_P	0.19	0.29	0.15	0.80	0.19	31,400
GAM_{nb}	0.19	0	--	--	--	--
ensemble	0.19	1	0.17	0.83	0.25	30,600

* Refer to the Species Distribution Model Performance Metrics subsection within the Statistical Modeling section of the Methods for detailed descriptions of individual model performance metrics.

Table 90. -- Covariates retained in the a) subadult and b) adult Aleutian skate species distribution model (SDM) final ensembles, the percent contribution to the ensemble deviance explained by each covariate, and the cumulative deviance explained: SD = standard deviation and BPI = bathymetric position index.

Aleutian skate			
	Covariate	**% Contribution**	**Cumulative %**
a) subadult	bottom depth	37.1	37.1
	location	35.4	72.4
	bottom temperature	7.4	79.9
	rockiness	6.5	86.4
	tidal maximum	4.6	91.0
	aspect east	2.4	93.4
	current	2.3	95.7
	aspect north	1.7	97.4
	current SD	1.5	98.9
	BPI	0.5	99.4
	pennatulacean presence	0.3	99.7
	sponge presence	0.2	99.9
	slope	0.1	100.0
	bottom depth	37.1	37.1
b) adult	location	49.2	49.2
	bottom depth	16.7	65.9
	bottom temperature	7.9	73.8
	BPI	5.9	79.7
	tidal maximum	4.5	84.2
	aspect east	4.4	88.6
	rockiness	4.1	92.7
	curvature	3.2	95.9
	current	1.6	97.5
	aspect north	1.1	98.6
	current SD	0.4	99.0
	slope	0.3	99.3
	coral presence	0.3	99.6
	sponge presence	0.2	99.8
	pennatulacean presence	0.2	100.0

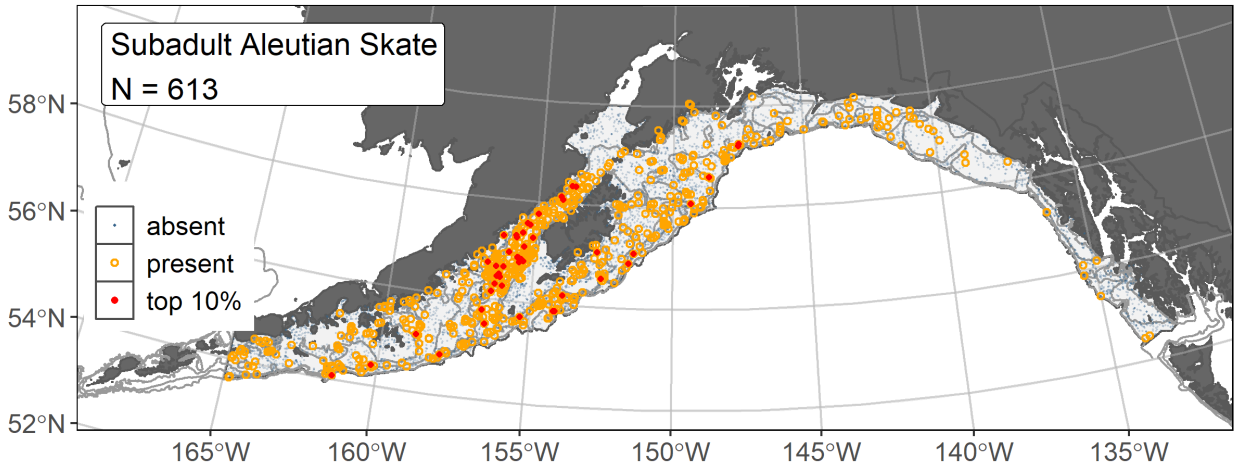

Figure 271. -- Distribution of subadult Aleutian skate catches (N = 631) in 1993–2019 AFSC RACE-GAP summer bottom trawl surveys of the Gulf of Alaska with the 100 m, 200 m, and 700 m isobaths indicated; filled red circles indicate locations in top 10% of overall abundance, open orange circles indicate presence in remaining catches, and blue dots indicate stations sampled where the animals were not present.

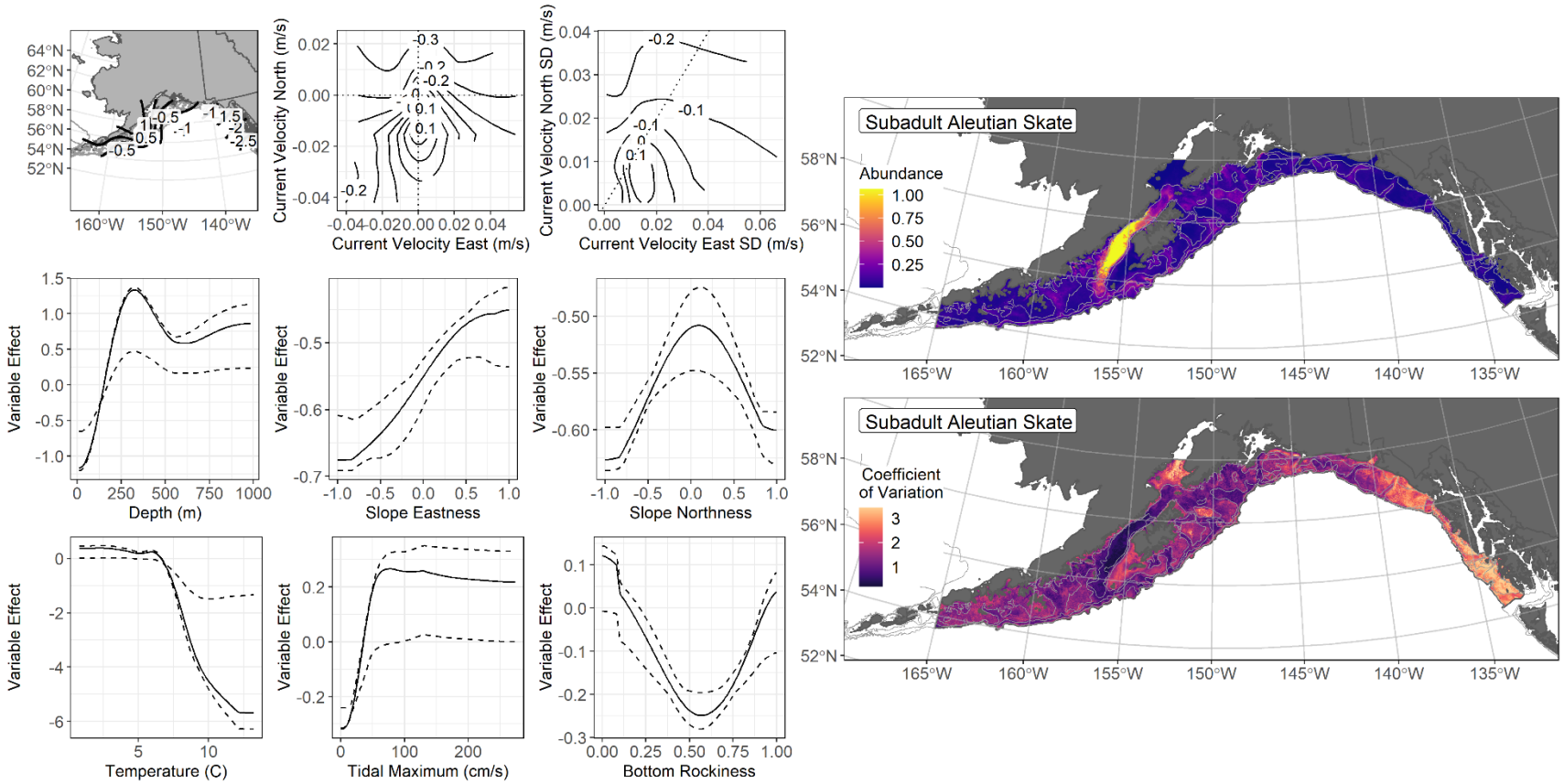

Figure 272. -- The top nine covariate effects (left panel) on ensemble-predicted subadult Aleutian skate numerical abundance across the Gulf of Alaska (upper right panel) and the coefficient of variation (CV) of the ensemble predictions (lower right panel).

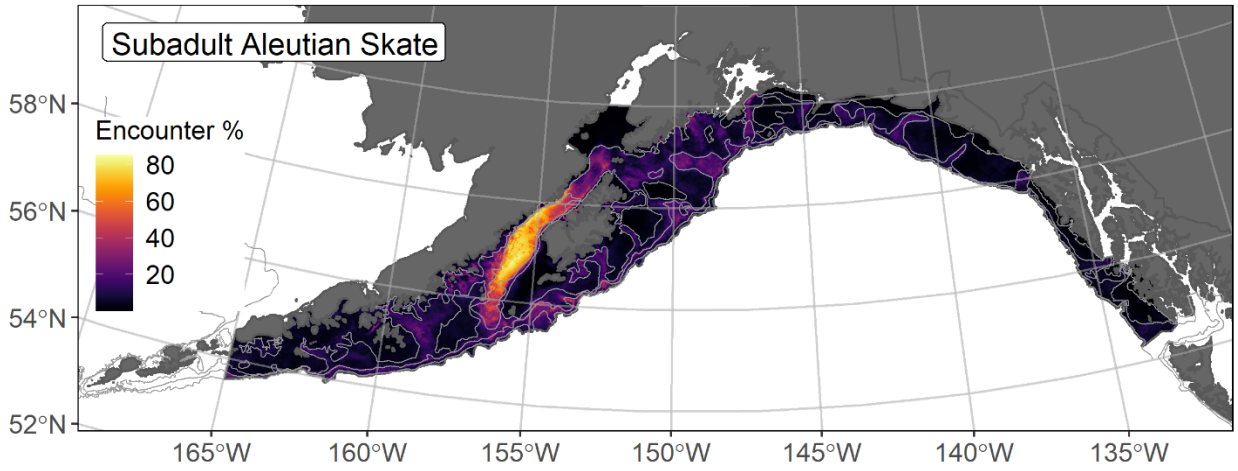

Figure 273. -- Encounter probability of subadult Aleutian skate from AFSC RACE-GAP summer bottom trawl surveys (1993–2019) of the Gulf of Alaska with the 100 m, 200 m, and 700 m isobaths indicated.

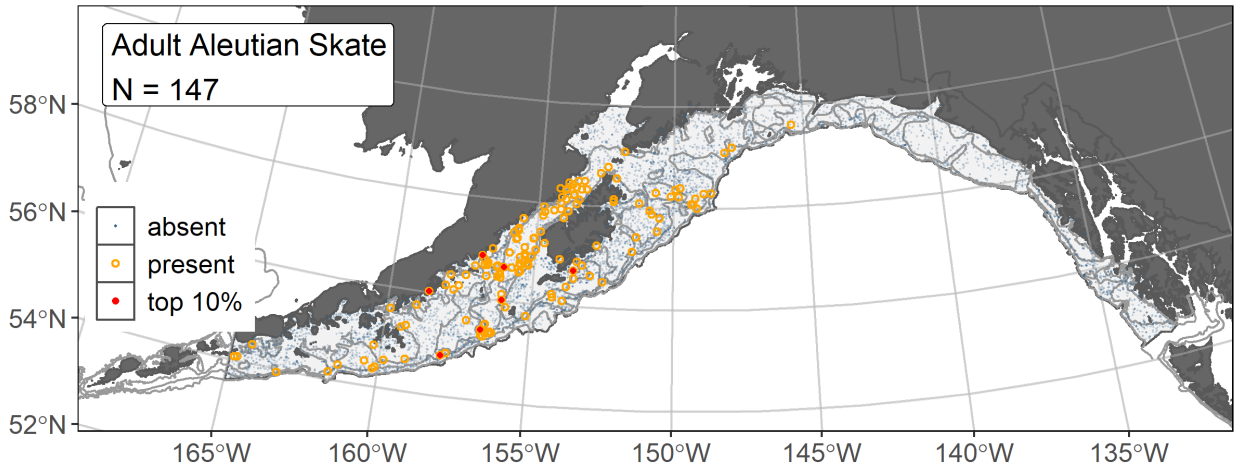

Figure 274. -- Distribution of adult Aleutian skate catches (N = 147) in 1993–2019 AFSC RACE-GAP summer bottom trawl surveys of the Gulf of Alaska with the with the 100 m, 200 m, and 700 m isobaths indicated; filled red circles indicate locations in top 10% of overall abundance, open orange circles indicate presence in remaining catches, and blue dots indicate stations sampled where the animals were not present.

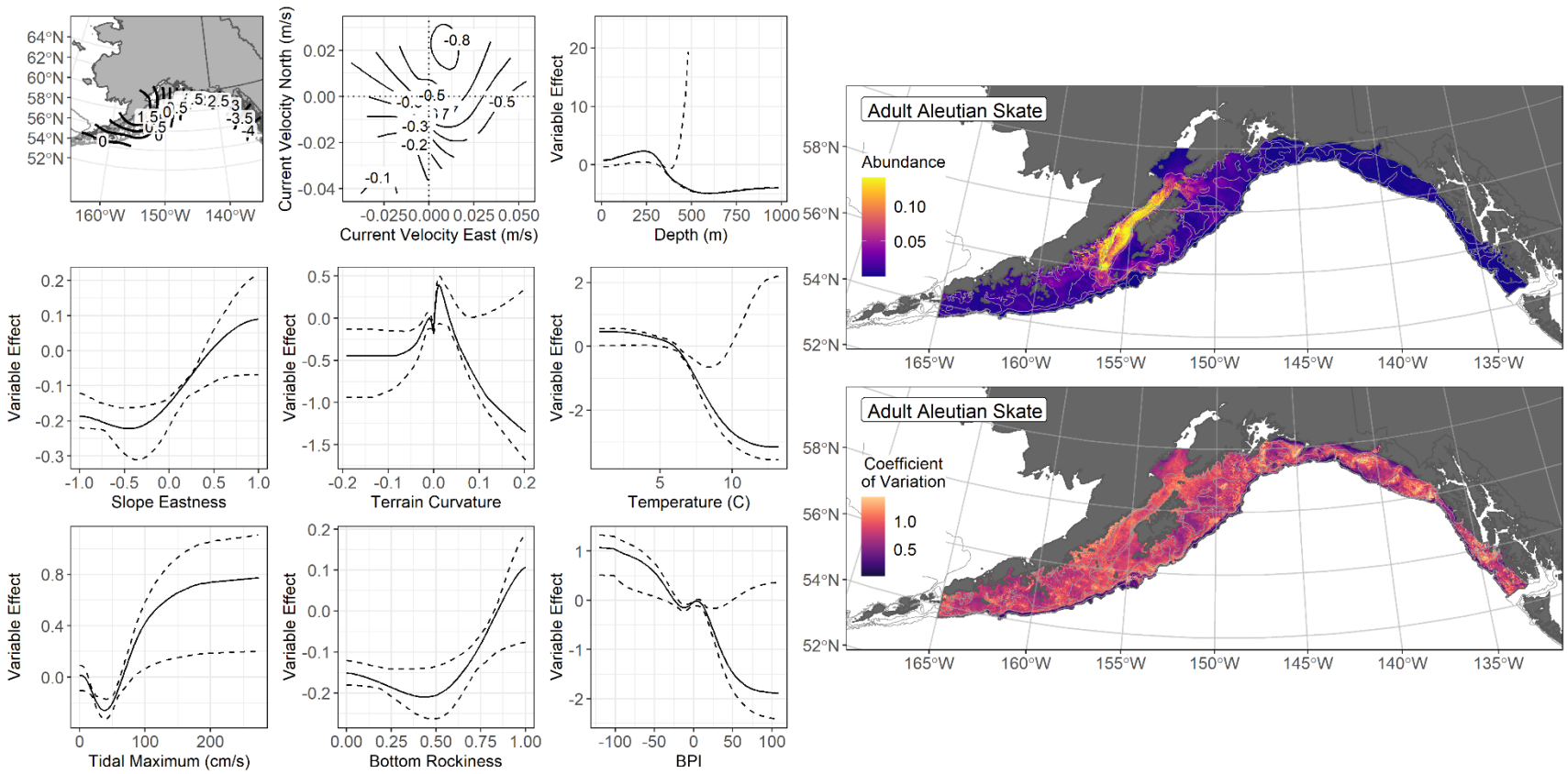

Figure 275. -- The top nine covariate effects (left panel) on ensemble-predicted adult Aleutian skate numerical abundance across the Gulf of Alaska (upper right panel) and the coefficient of variation (CV) of the ensemble predictions (lower right panel).

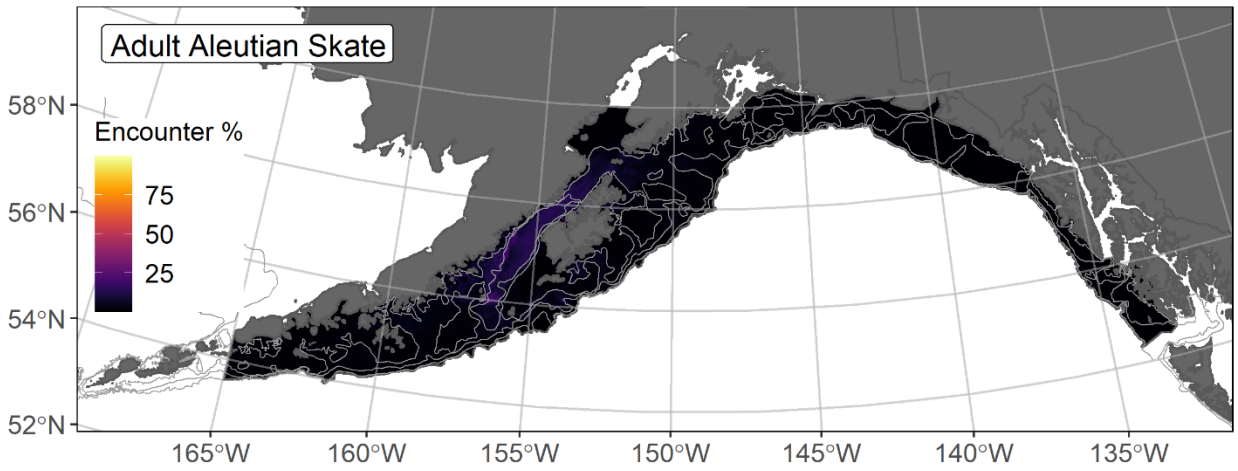

Figure 276. -- Encounter probability of adult Aleutian skate from AFSC RACE-GAP summer bottom trawl surveys (1993–2019) of the Gulf of Alaska with the 100 m, 200 m, and 700 m isobaths indicated.

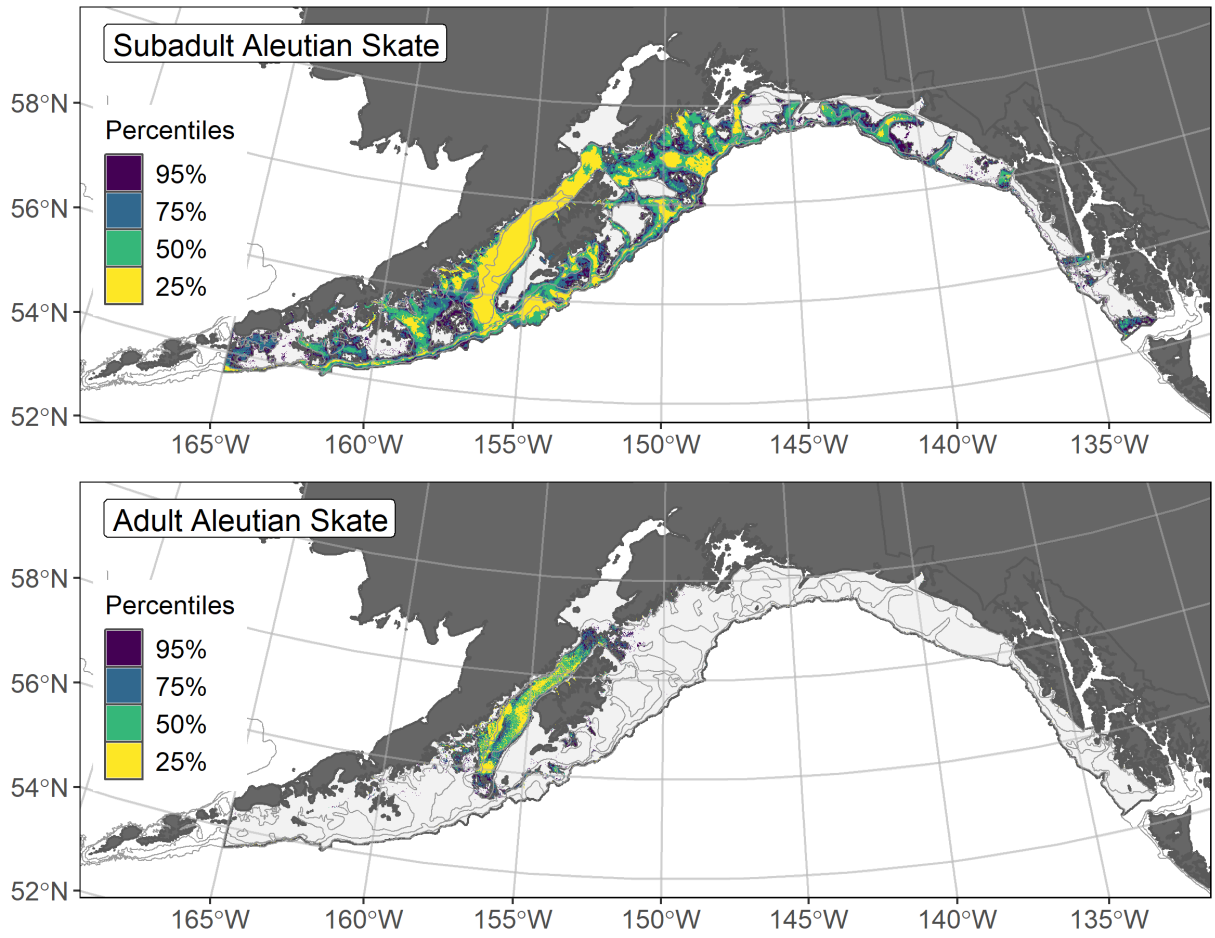

Figure 277. -- Essential fish habitat (EFH) is the area containing the top 95% of occupied habitat (defined as model estimated encounter probabilities greater than 5%) from an SDM ensemble fitted to subadult (top panel) and adult (bottom panel) Aleutian skate distribution and abundance in AFSC RACE-GAP summer bottom trawl surveys (1993–2019) with 100 m, 200 m, and 700 m isobaths indicated; within the EFH area map are the subareas of the top 25% (EFH hot spots), top 50% (core EFH area), and top 75% (principal EFH area) of habitat-related, ensemble-predicted numerical abundance.

Bering skate (Bathyraja interrupta)

The Bering skate (*Bathyraja interrupta*) is distributed from California to the Bering Sea over a wide range of depths (37–1372 m; Mecklenberg et al. 2002) and reaches a maximum length of 800 mm TL (Stevenson et al. 2007). Bering skate are managed as part of the GOA Skate stock complex (Ormseth 2019). Bering skate subadult (≤ 690 mm TL) and adult (> 690 mm TL) life stages (Ainsley et al. 2011) were modeled separately in the present study[56].

Subadult Bering skate abundance and distribution predicted from RACE-GAP summer bottom trawl surveys in the Gulf of Alaska -- Subadult Bering skate (N = 429) caught in GOA RACE-GAP summer bottom trawl surveys (1993–2019) were distributed across the GOA continental shelf from Dixon Entrance in the southeast to Unimak Pass in the west, but were particularly abundant in Shelikof Strait and the adjacent Chirikof region (Fig. 278). Five SDMs were considered for inclusion in the ensemble to predict numerical abundance subadult Bering skate in the GOA (Table 91); the GAM_{nb} was eliminated by skill testing. The remaining four best-fitting SDMs received equal weights in the final ensemble, which was a fair overall fit to the observed subadult Bering skate distribution and abundance data. The ensemble was fair at predicting high and low abundance catches (ρ = 0.27), good at discriminating presence-absence (AUC = 0.84), and fair at explaining deviance (PDE = 0.28). Geographic location, bottom depth, and bottom temperature accounted for 72% of the covariate contribution to the deviance explained by the final ensemble (Table 92). Higher abundances of subadult Bering skate occurred in Shelikof Strait and to the southwest in depths around 300 m (Fig. 279). The CV of ensemble predictions was higher in areas where this life stage was less common. Encounter probabilities of subadult Bering skate were high in the vicinity of Shelikof Strait (Fig. 280).

Adult Bering skate abundance and distribution predicted from RACE-GAP summer bottom trawl surveys in the Gulf of Alaska -- Adult Bering skate (N = 408) caught in GOA RACE-GAP summer bottom trawl surveys (1993–2019) were more common from the Yakutat region into the central and western Gulf with their highest abundance catches occurring around Kodiak Island (Fig. 281). Five SDMs were considered for inclusion in the ensemble to predict numerical abundance of adult Bering skate in the GOA (Table 91); the GAM_{P} was eliminated by skill testing. The remaining four best-fitting SDMs received were weighted by RMSE in the final ensemble, which was a fair overall fit to the observed adult Bering skate distribution and abundance data. The ensemble was fair at predicting high and low abundance catches (ρ = 0.28), good at discriminating presence-absence (AUC = 0.84), and fair at

[56] Incorporating other high quality sources of data if available in future SDM ensemble EFH mapping for this species will be included as a research recommendation from the 2023 EFH 5-year Review.

explaining deviance (PDE = 0.31). Geographic location, bottom depth, and bottom temperature accounted for 73.3% of covariate contribution to the deviance explained by the final ensemble (Table 92). Adult Bering skate abundance was highest in Shelikof Strait in depths around 250 m with relatively little bottom current (Fig. 282). The CV of ensemble predictions was higher in southeast Alaska, where adult Bering skates were less common. Encounter probabilities of adult Bering skate were low throughout the study area, except Shelikof Strait (Fig. 283).

Essential fish habitat of subadult and adult Bering skate in the Gulf of Alaska -- Ensemble-predicted habitat-related numerical abundance of Bering skate life stages collected in RACE-GAP summer bottom trawl surveys of the GOA (1993–2019) was mapped as EFH areas and subareas (Fig. 284). Subadult and adult Bering skate EFH area was primarily in the Chirikof and Kodiak regions of the GOA in association with glacial troughs and with the subadult EFH extending further into southeast Alaska than that of adults. Similarly, core EFH areas and EFH hot spots for subadults were more widespread across the GOA continental shelf than adults, though the largest EFH hot spot was in Shelikof Strait. Adult Bering skate core EFH was constrained to the Chirikof and Kodiak regions, while EFH hot spots for this life stage were primarily associated with Shelikof Strait.

Table 91. -- Constituent species distribution models (SDMs) used to construct Essential Fish Habitat (EFH) for a) subadult and b) adult Bering skate: MaxEnt = Maximum entropy; paGAM = presence-absence generalized additive model; hGAM = zero-adjusted Poisson hurdle GAM; GAM_P = standard Poisson GAM; GAM_{nb} = standard negative-binomial GAM; RMSE = root mean square error; ρ (rho) = Spearman's rank correlation coefficient; AUC = area under the receiver-operating characteristic curve; and PDE = Poisson deviance explained *. The "--" indicates that this model was not included in the final ensemble.

a) subadult Bering skate

Models	RMSE	Relative Weight	ρ	AUC	PDE	EFH area (km^2)
MaxEnt	0.34	0.25	0.24	0.79	0.20	117,900
paGAM	0.34	0.25	0.25	0.81	0.23	107,300
hGAM	0.34	0.25	0.25	0.81	0.23	109,400
GAM_P	0.34	0.25	0.25	0.81	0.23	106,200
GAM_{nb}	0.34	0	--	--	--	--
ensemble	0.33	1	0.27	0.84	0.28	113,600

b) adult Bering skate

Models	RMSE	Relative Weight	ρ	AUC	PDE	EFH area (km^2)
MaxEnt	0.34	0.24	0.21	0.76	0.17	113,000
paGAM	0.32	0.25	0.27	0.83	0.28	91,600
hGAM	0.32	0.26	0.27	0.83	0.29	89,000
GAM_P	0.32	0	--	--	--	--
GAM_{nb}	0.32	0.26	0.27	0.83	0.28	89,200
ensemble	0.32	1	0.28	0.84	0.31	94,700

* Refer to the Species Distribution Model Performance Metrics subsection within the Statistical Modeling section of the Methods for detailed descriptions of individual model performance metrics.

Table 92. -- Covariates retained in the a) subadult and b) adult Bering skate species distribution model (SDM) final ensembles, the percent contribution to the ensemble deviance explained by each covariate, and the cumulative deviance explained: SD = standard deviation and BPI = bathymetric position index.

Bering skate	**Covariate**	**% Contribution**	**Cumulative %**
a) subadult	location	37.3	37.3
	bottom depth	25.0	62.2
	bottom temperature	9.8	72.0
	current	8.3	80.3
	tidal maximum	4.4	84.7
	BPI	2.9	87.6
	current SD	2.4	90.0
	aspect east	2.3	92.3
	slope	1.5	93.8
	aspect north	1.5	95.3
	rockiness	1.5	96.8
	pennatulacean presence	1.4	98.2
	curvature	0.7	98.9
	sponge presence	0.6	99.5
	coral presence	0.5	100.0
b) adult	location	52.6	52.6
	bottom depth	14.1	66.7
	bottom temperature	6.6	73.3
	rockiness	6.5	79.9
	current	6.2	86.1
	slope	3.4	89.5
	BPI	3.2	92.7
	tidal maximum	2.4	95.1
	sponge presence	1.3	96.4
	aspect north	1.2	97.6
	aspect east	0.9	98.5
	current SD	0.5	99.0
	curvature	0.5	99.5
	coral presence	0.5	100.0

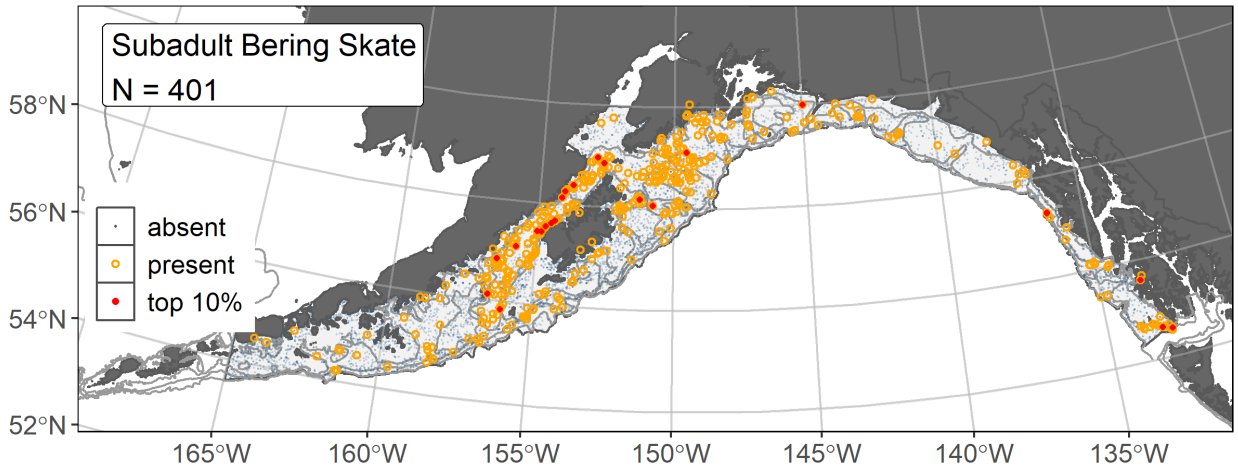

Figure 278. -- Distribution of subadult Bering skate catches (N = 429) in 1993–2019 AFSC RACE-GAP summer bottom trawl surveys of the Gulf of Alaska with the 100 m, 200 m, and 700 m isobaths indicated; filled red circles indicate locations in top 10% of overall abundance, open orange circles indicate presence in remaining catches, and blue dots indicate stations sampled where the animals were not present.

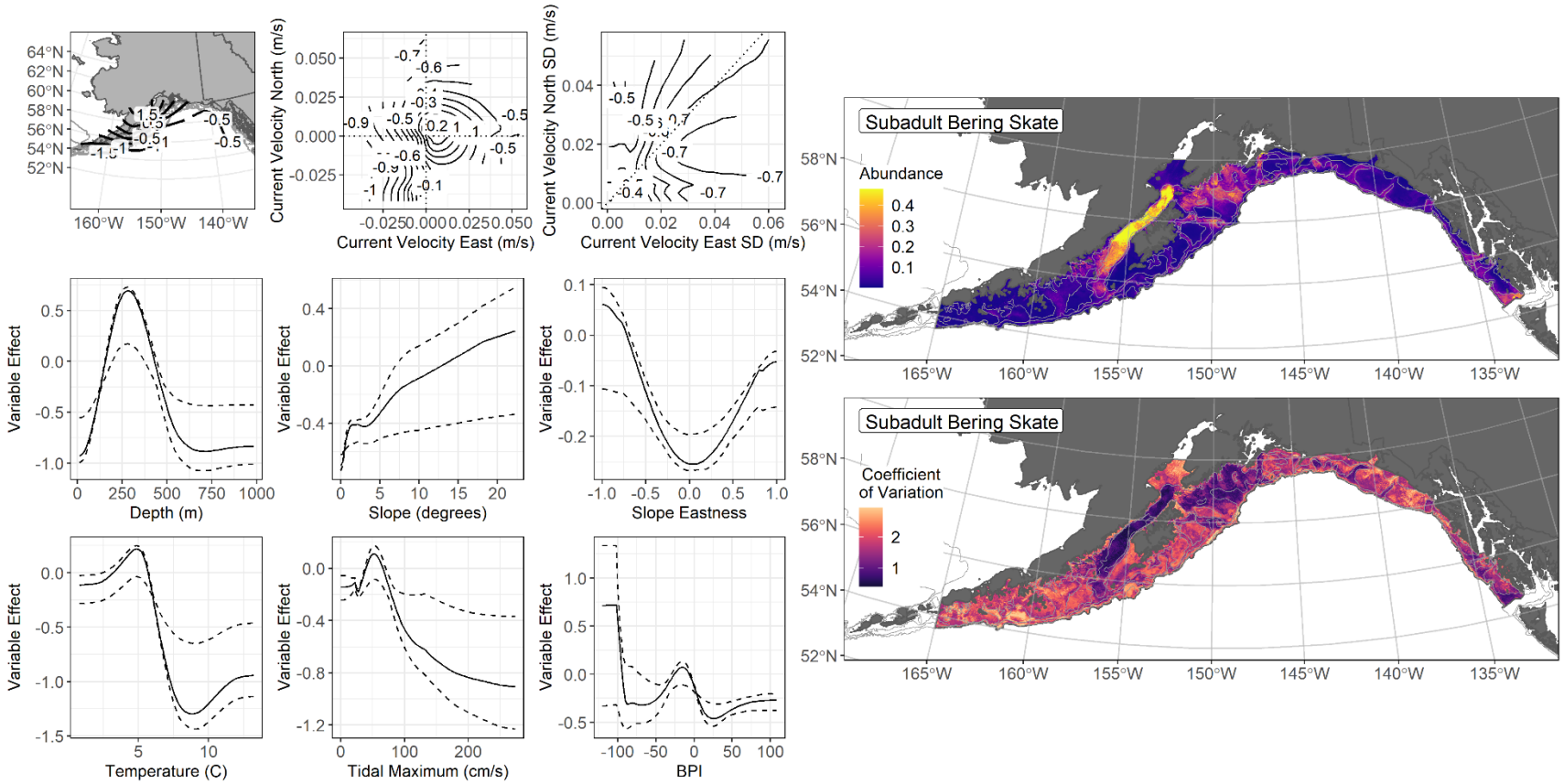

Figure 279. -- The top nine covariate effects (left panel) on ensemble-predicted subadult Bering skate numerical abundance across the Gulf of Alaska (upper right panel) and the coefficient of variation (CV) of the ensemble predictions (lower right panel).

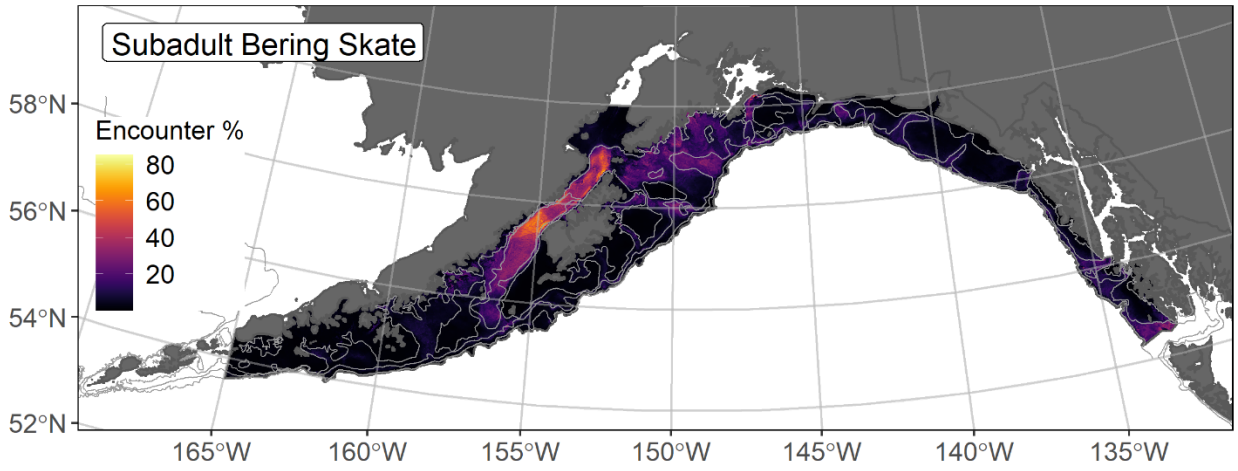

Figure 280. -- Encounter probability of subadult Bering skate from AFSC RACE-GAP summer bottom trawl surveys (1993–2019) of the Gulf of Alaska with the 100 m, 200 m, and 700 m isobaths indicated.

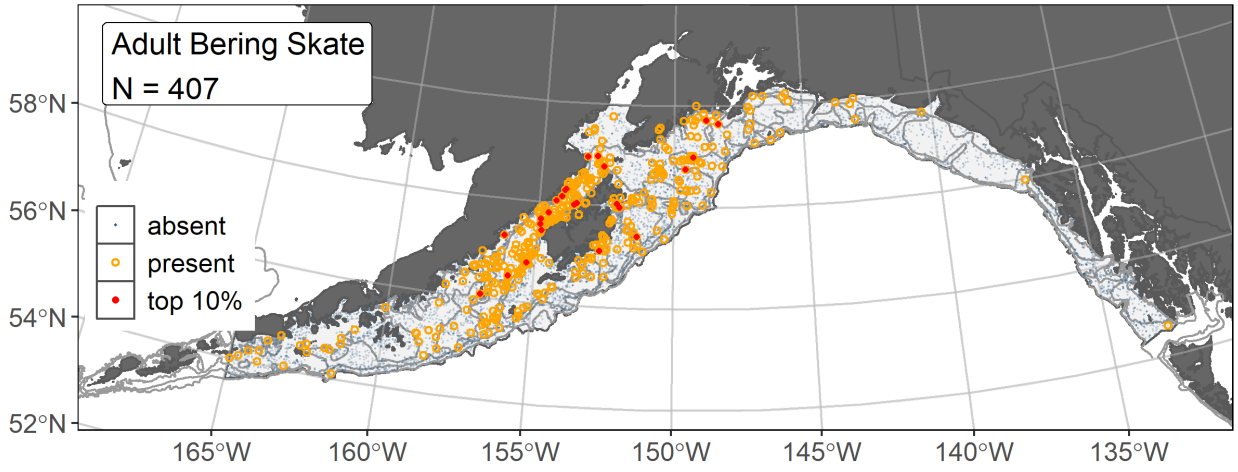

Figure 281. -- Distribution of adult Bering skate catches (N = 408) in 1993–2019 AFSC RACE-GAP summer bottom trawl surveys of the Gulf of Alaska with the with the 100 m, 200 m, and 700 m isobaths indicated; filled red circles indicate locations in top 10% of overall abundance, open orange circles indicate presence in remaining catches, and blue dots indicate stations sampled where the animals were not present.

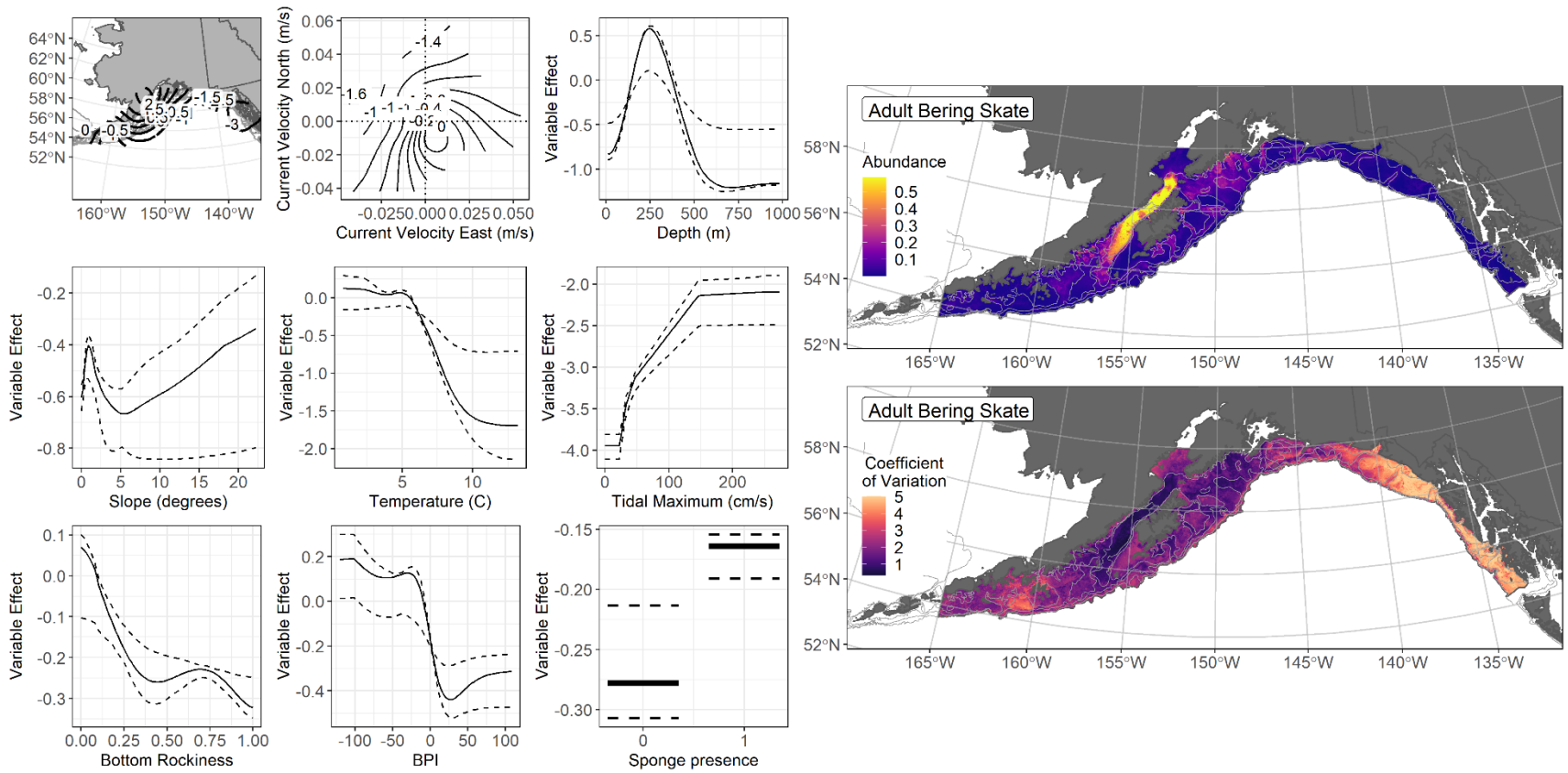

Figure 282. -- The top nine covariate effects (left panel) on ensemble-predicted adult Bering skate numerical abundance across the Gulf of Alaska (upper right panel) and the coefficient of variation (CV) of the ensemble predictions (lower right panel).

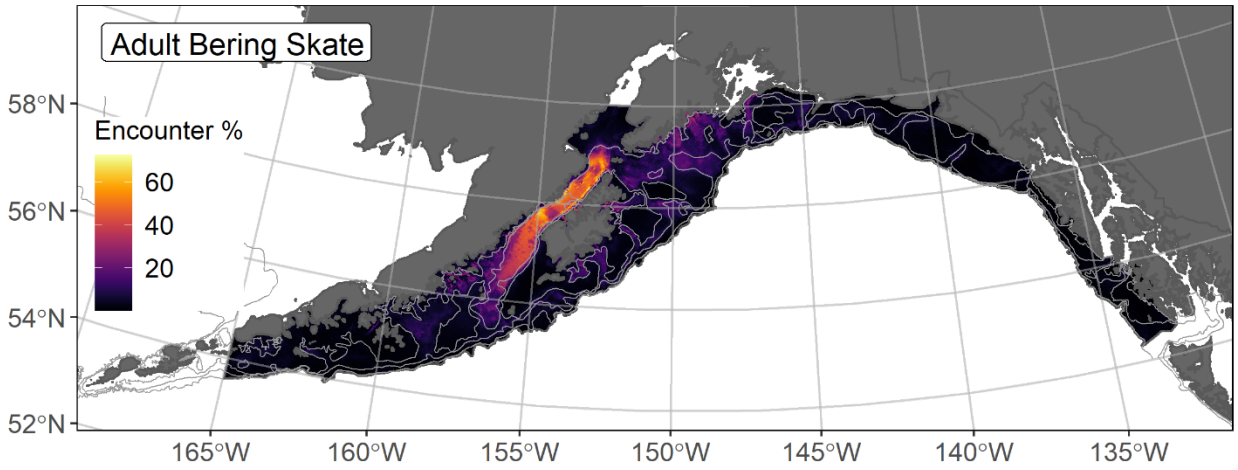

Figure 283. -- Encounter probability of adult Bering skate from AFSC RACE-GAP summer bottom trawl surveys (1993–2019) of the Gulf of Alaska with the 100 m, 200 m, and 700 m isobaths indicated.

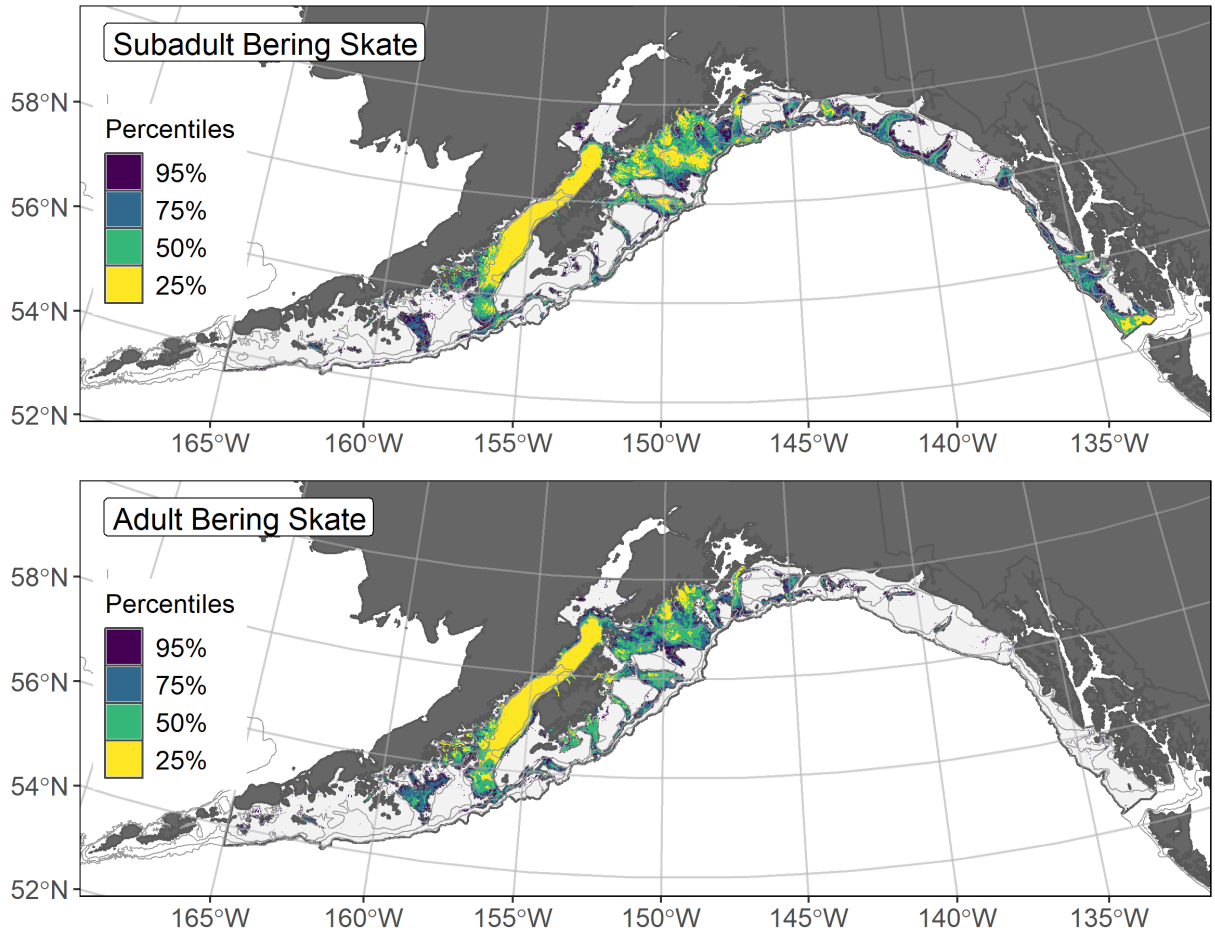

Figure 284. -- Essential fish habitat (EFH) is the area containing the top 95% of occupied habitat (defined as model estimated encounter probabilities greater than 5%) from an SDM ensemble fitted to subadult (top panel) and adult (bottom panel) Bering skate distribution and abundance in AFSC RACE-GAP summer bottom trawl surveys (1993–2019) with 100 m, 200 m, and 700 m isobaths indicated; within the EFH area map are the subareas of the top 25% (EFH hot spots), top 50% (core EFH area), and top 75% (principal EFH area) of habitat-related, ensemble-predicted numerical abundance.

Big skate (Beringraja binoculata)

The big skate (*Beringraja binoculata*) is a large skate (maximum reported TL ~ 2.4 m) that ranges from the eastern Bering Sea and Aleutians Islands to Baja California though rarely south of Point Conception (Mecklenberg et al. 2002). They inhabit a wide depth range (3–800 m) but are more commonly encountered in the GOA in waters shallower than 200 m[57]. Big skate are managed in the GOA Skate complex, although they have separate harvest specifications (Ormseth 2019). For the present work, we separated the big skate subadult and adult life stages using L_{50} = 1,486 mm (Ebert et al. 2008).

Subadult big skate abundance and distribution predicted from RACE-GAP summer bottom trawl surveys in the Gulf of Alaska -- Subadult big skate (N = 594) caught in GOA RACE-GAP summer bottom trawl surveys (1993–2019) were distributed in shallower waters of the GOA continental shelf from southeast Alaska to Unimak Pass in the west and were particularly abundant in shallow, nearshore waters in the Yakutat region (Fig. 285). Five SDMs were considered for inclusion in the ensemble to predict numerical abundance of subadult big skate in the GOA (Table 93); the GAM_{nb} was eliminated by skill testing. The four remaining best-performing SDMs were similarly weighted by RMSE in the final ensemble, which attained a good overall all fit to the observed subadult big skate distribution and abundance data. The ensemble was fair at predicting high and low abundance catches (ρ = 0.31), good at discriminating presence-absence (AUC = 0.85) and explaining deviance (PDE = 0.44). Bottom depth, BPI, and geographic location accounted for 74.7% of the covariate contribution to the deviance explained by the final ensemble (Table 94). Subadult big skate abundance was highest in shallower depths (< 100 m) over high bathymetric rises in the Yakutat region, Cook Inlet, and around Kodiak Island (Fig. 286). The CV of ensemble predictions was higher in areas where this life stage was less common. Encounter probabilities of subadult big skate were high in the vicinity of Shelikof Strait (Fig. 287).

Adult big skate abundance and distribution predicted from RACE-GAP summer bottom trawl surveys in the Gulf of Alaska -- Adult big skate (N = 195) caught in GOA RACE-GAP summer bottom trawl surveys (1993–2019) were widely distributed across the region with concentrations of catches around Kodiak Island and in Cook Inlet with the highest abundance catches come from those areas as well (Fig. 288). Five SDMs were considered for inclusion in the ensemble to predict numerical abundance of adult big skate in the GOA (Table 93); the GAM_{nb} was eliminated by skill testing. The four remaining best-performing SDMs were equally weighted in the final ensemble, which attained a fair

[57] Incorporating other high quality sources of data if available in future SDM ensemble EFH mapping for this species will be included as a research recommendation from the 2023 EFH 5-year Review.

overall fit to the observed adult big skate distribution and abundance data. The ensemble was poor at predicting high and low abundance catches (ρ = 0.19), good at discriminating presence-absence (AUC = 0.86), and fair at explaining deviance (PDE = 0.27). Bottom depth, geographic location, and bottom temperature accounted for 67.9% of the covariate contribution to the deviance explained by the final ensemble (Table 94). Adult big skate abundance was highest in Cook Inlet and off southwestern Kodiak Island in the Chirikof region at shallower depths and warmer bottom temperatures (Fig. 289). The CV of ensemble predictions was higher in areas where adult big skates were distributed. The probability of encountering adult big skate in GOA bottom trawls was highest off southwestern Kodiak in the Chirikof region, in southern Cook Inlet, and in the shallow, inshore waters of the Yakutat region (Fig. 290).

Essential Fish Habitat of subadult and adult big skate in the Gulf of Alaska -- Ensemble-predicted habitat-related numerical abundance of big skate life stages collected in RACE-GAP summer bottom trawl surveys of the GOA (1993–2019) was mapped as EFH areas and subareas (Fig. 291). Subadult and adult big skate EFH was generally located at shallower depths on the continental shelf and in coastal areas of the GOA, although the subadult EFH area was more extensive.

Table 93. -- Constituent species distribution models (SDMs) used to construct Essential Fish Habitat (EFH) for a) subadult and b) adult big skate: MaxEnt = Maximum entropy; paGAM = presence-absence generalized additive model; hGAM = zero-adjusted Poisson hurdle GAM; GAM_P = standard Poisson GAM; GAM_{nb} = standard negative-binomial GAM; RMSE = root mean square error; ρ (rho) = Spearman's rank correlation coefficient; AUC = area under the receiver-operating characteristic curve; and PDE = Poisson deviance explained *. The "--" indicates that this model was not included in the final ensemble.

a) subadult big skate

Models	RMSE	Relative Weight	ρ	AUC	PDE	EFH area (km^2)
MaxEnt	1.19	0.28	0.31	0.85	0.37	170,400
paGAM	1.19	0.28	0.30	0.84	0.35	170,300
hGAM	1.65	0.15	0.18	0.84	0.27	140,200
GAM_P	1.16	0.29	0.29	0.83	0.36	130,200
GAM_{nb}	1.18	0	--	--	--	--
ensemble	1.09	1	0.31	0.85	0.44	158,500

b) adult big skate

Models	RMSE	Relative Weight	ρ	AUC	PDE	EFH area (km^2)
MaxEnt	0.21	0.25	0.17	0.82	0.20	42,900
paGAM	0.21	0.25	0.18	0.83	0.23	37,400
hGAM	0.21	0.25	0.17	0.83	0.23	35,100
GAM_P	0.21	0.25	0.17	0.82	0.22	34,000
GAM_{nb}	0.21	0	--	--	--	--
ensemble	0.20	1	0.19	0.86	0.27	37,300

* Refer to the Species Distribution Model Performance Metrics subsection within the Statistical Modeling section of the Methods for detailed descriptions of individual model performance metrics.

Table 94. -- Covariates retained in the a) subadult and b) adult big skate species distribution model (SDM) final ensembles, the percent contribution to the ensemble deviance explained by each covariate, and the cumulative deviance explained: SD = standard deviation and BPI = bathymetric position index.

big skate	**Covariate**	**% Contribution**	**Cumulative %**
a) subadult	bottom depth	49.6	49.6
	BPI	14.3	63.9
	location	10.8	74.7
	bottom temperature	9.9	84.5
	rockiness	3.7	88.2
	current	2.6	90.8
	current SD	2.3	93.1
	tidal maximum	1.4	94.5
	aspect east	1.2	95.7
	curvature	1.1	96.8
	slope	1.0	97.8
	coral presence	1.0	98.8
	sponge presence	0.6	99.4
	aspect north	0.4	99.8
	pennatulacean presence	0.2	100.0
b) adult	bottom depth	27.3	27.3
	location	25.5	52.9
	bottom temperature	15.0	67.9
	BPI	10.3	78.1
	tidal maximum	8.3	86.4
	current	3.3	89.7
	rockiness	2.5	92.2
	current SD	2.1	94.3
	slope	2.0	96.3
	curvature	1.0	97.3
	sponge presence	1.0	98.3
	aspect east	0.7	99.0
	aspect north	0.6	99.6
	coral presence	0.4	100.0

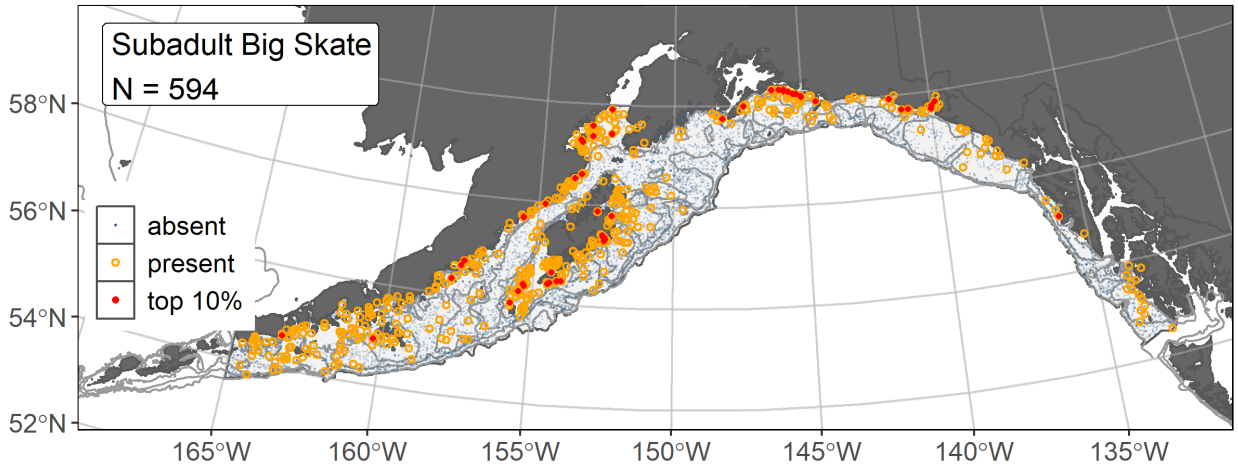

Figure 285. -- Distribution of subadult big skate catches (N = 594) in 1993–2019 AFSC RACE-GAP summer bottom trawl surveys of the Gulf of Alaska with the 100 m, 200 m, and 700 m isobaths indicated; filled red circles indicate locations in top 10% of overall abundance, open orange circles indicate presence in remaining catches, and blue dots indicate stations sampled where the animals were not present.

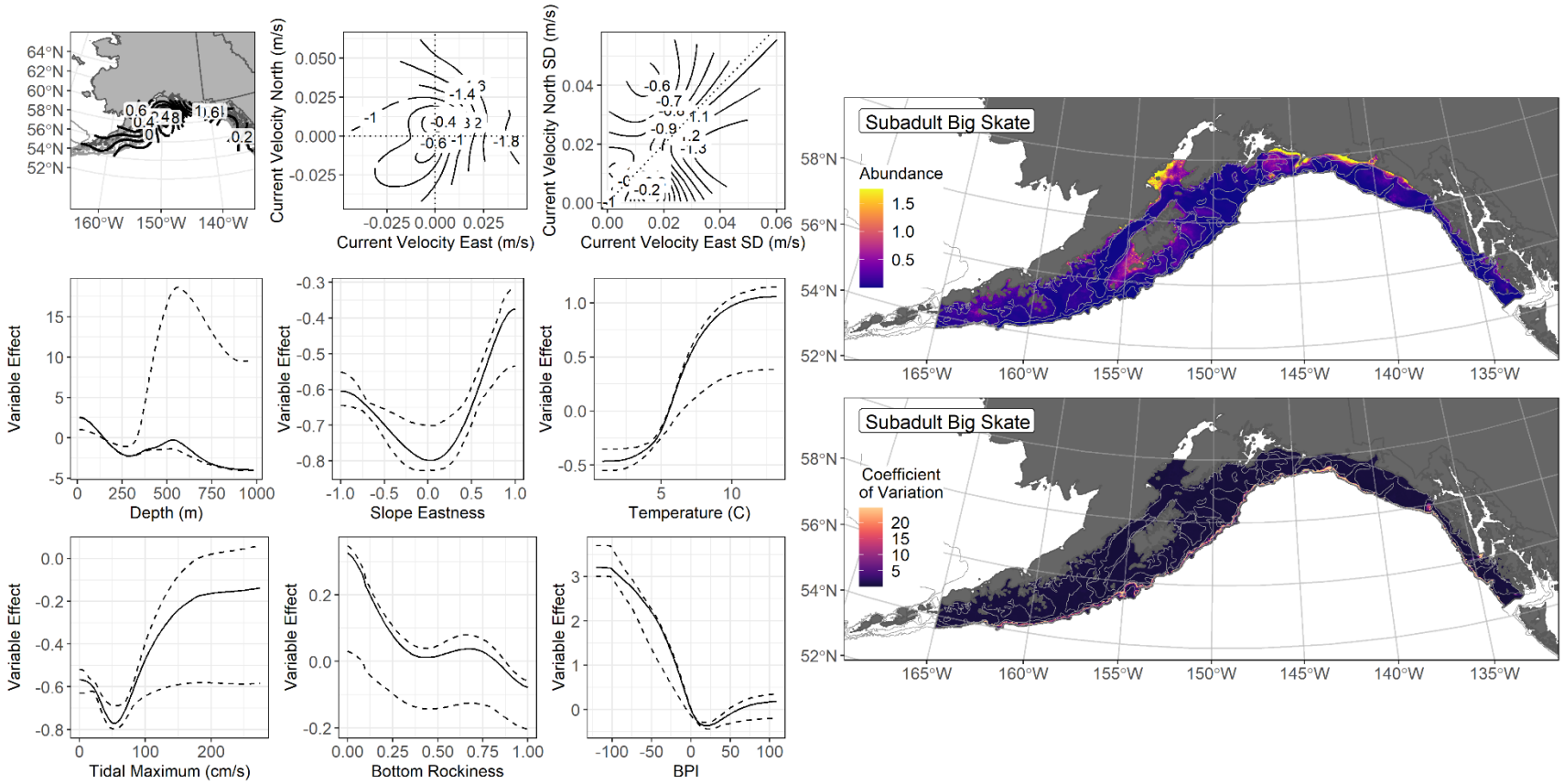

Figure 286. -- The top nine covariate effects (left panel) on ensemble-predicted subadult big skate numerical abundance across the Gulf of Alaska (upper right panel) and the coefficient of variation (CV) of the ensemble predictions (lower right panel).

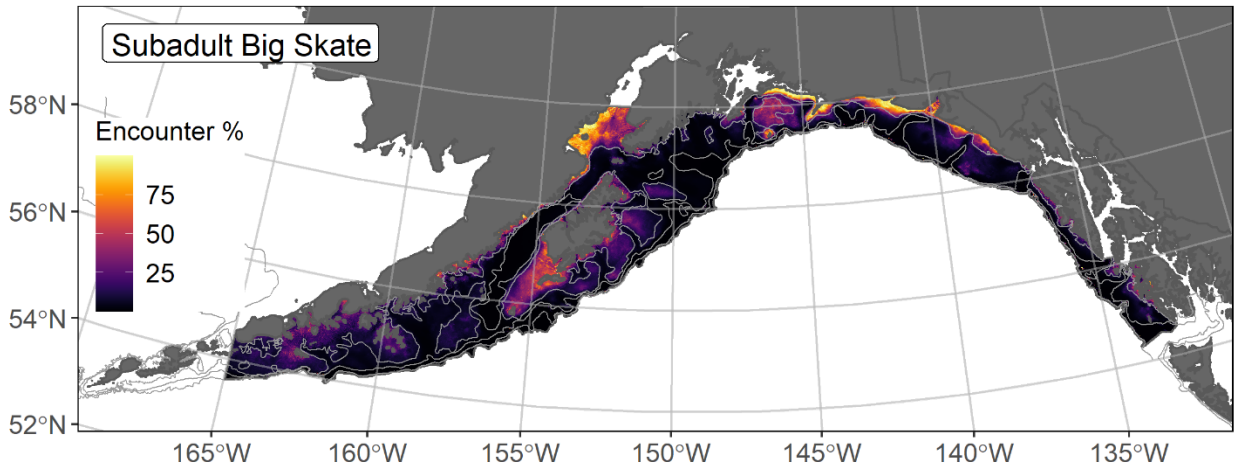

Figure 287. -- Encounter probability of subadult big skate from AFSC RACE-GAP summer bottom trawl surveys (1993–2019) of the Gulf of Alaska with the 100 m, 200 m, and 700 m isobaths indicated.

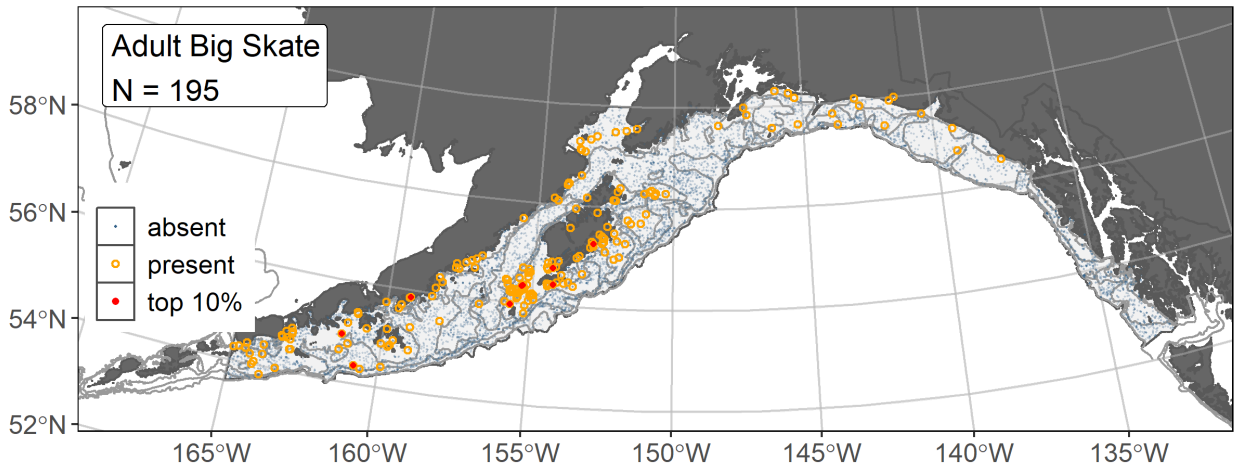

Figure 288. -- Distribution of adult big skate catches (N = 195) in 1993–2019 AFSC RACE-GAP summer bottom trawl surveys of the Gulf of Alaska with the with the 100 m, 200 m, and 700 m isobaths indicated; filled red circles indicate locations in top 10% of overall abundance, open orange circles indicate presence in remaining catches, and blue dots indicate stations sampled where the animals were not present.

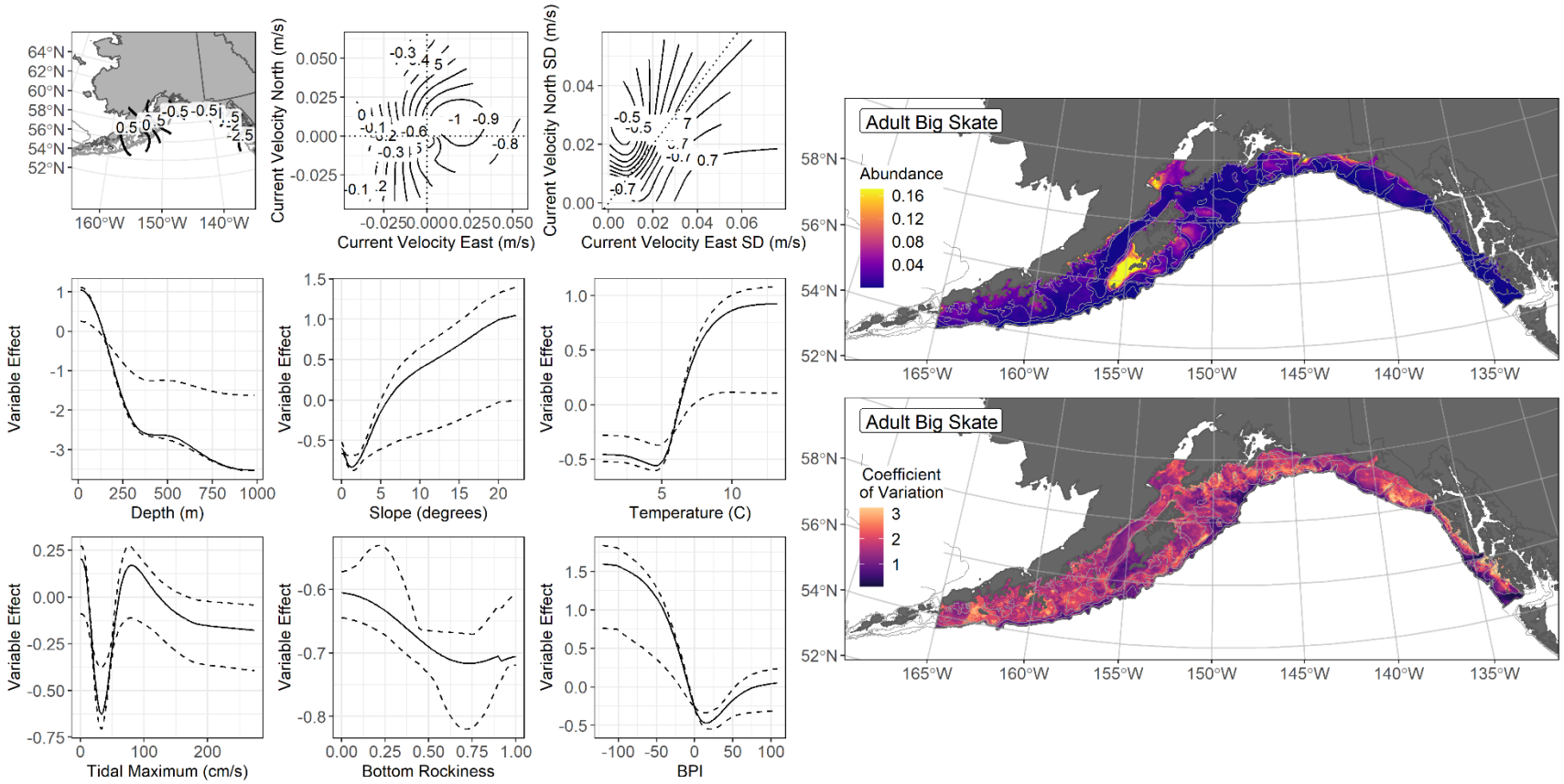

Figure 289. -- The top nine covariate effects (left panel) on ensemble-predicted adult big skate numerical abundance across the Gulf of Alaska (upper right panel) and the coefficient of variation (CV) of the ensemble predictions (lower right panel).

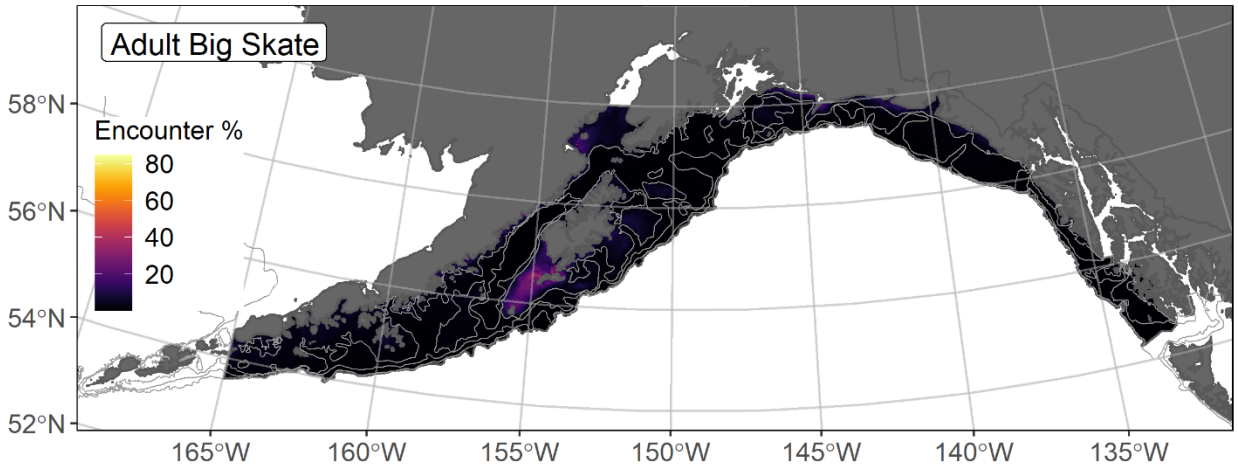

Figure 290. -- Encounter probability of adult big skate from AFSC RACE-GAP summer bottom trawl surveys (1993–2019) of the Gulf of Alaska with the 100 m, 200 m, and 700 m isobaths indicated.

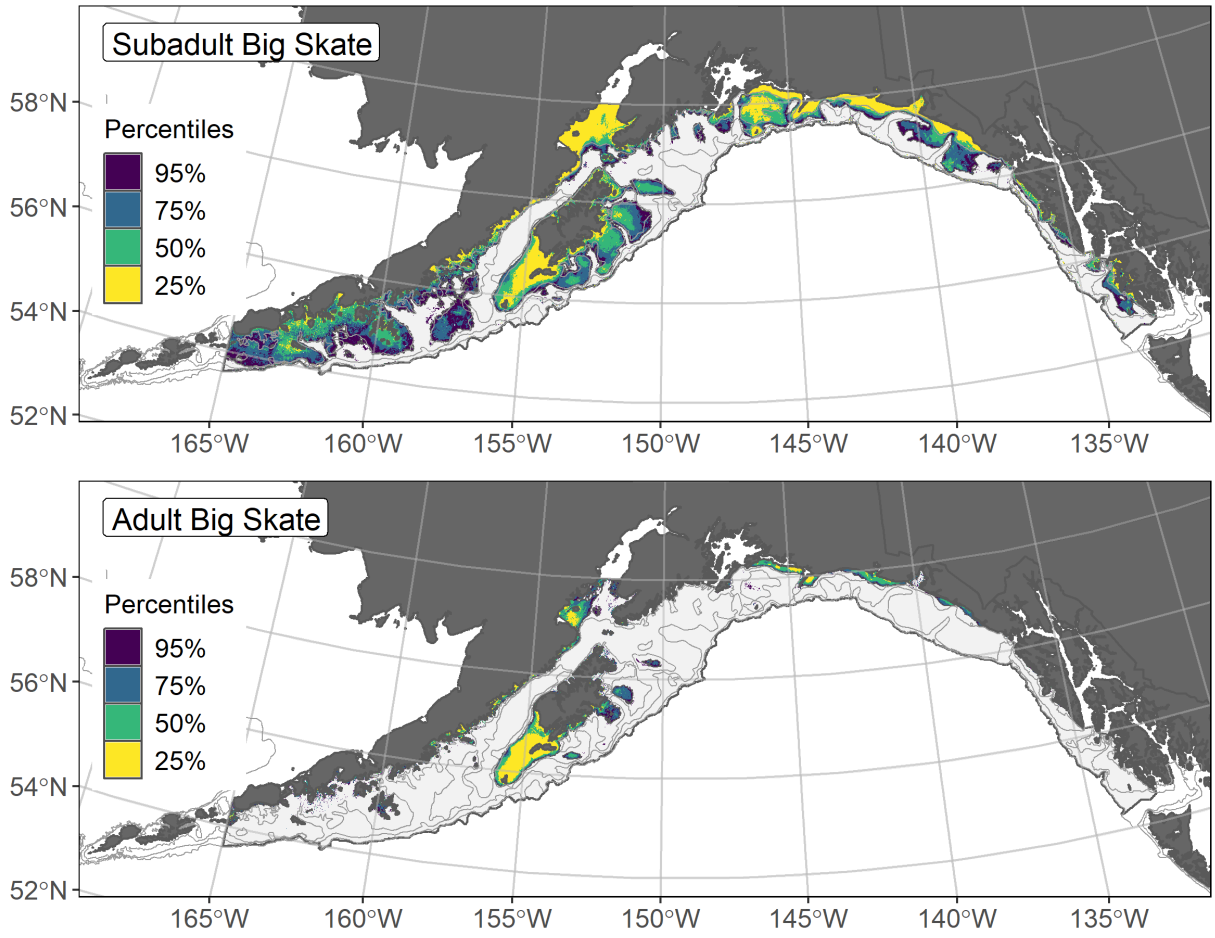

Figure 291. -- Essential fish habitat (EFH) is the area containing the top 95% of occupied habitat (defined as model estimated encounter probabilities greater than 5%) from an SDM ensemble fitted to subadult (top panel) and adult (bottom panel) big skate distribution and abundance in AFSC RACE-GAP summer bottom trawl surveys (1993–2019) with 100 m, 200 m, and 700 m isobaths indicated; within the EFH area map are the subareas of the top 25% (EFH hot spots), top 50% (core EFH area), and top 75% (principal EFH area) of habitat-related, ensemble-predicted numerical abundance.

Longnose skate (*Raja rhina*)

The longnose skate (*Raja rhina*) is a relatively large skate (maximum reported TL ~ 1.4 m) that ranges from the southeastern Bering Sea through the eastern Pacific Ocean to Baja California at depths of 20 m to more than 600 m (Mecklenberg et al. 2002). Longnose skate are managed in the GOA Skate complex, although they have separate harvest specifications (Ormseth 2019). For the present work, we separated longnose skate subadult and adult life stages using female length at the onset of maturity (1,331 mm TL; Ebert et al. 2008)[58].

Subadult longnose skate abundance and distribution predicted from RACE-GAP summer bottom trawl surveys in the Gulf of Alaska -- Subadult longnose skate (N = 1,058) caught in GOA RACE-GAP summer bottom trawl surveys (1993–2019) were distributed from the Shumagin region into southeast Alaska with most high abundance catches coming from around Kodiak Island (Fig. 292). Five SDMs were considered for inclusion in the ensemble to predict numerical abundance of subadult longnose skate in the GOA (Table 95); the GAM_P was eliminated by skill testing. The four remaining best-performing SDMs were weighted by RMSE in the final ensemble, which was a fair overall fit to the observed subadult longnose skate distribution and abundance data. The ensemble was fair at predicting high and low abundance catches (ρ = 0.28), good at discriminating presence-absence (AUC = 0.74), and poor at explaining deviance (PDE = 0.15). Bottom depth, geographic location, and bottom temperature accounted for 68.8% of the covariate contribution to the deviance explained by the final ensemble (Table 96). Subadult longnose skate abundance was highest in the Kodiak and Yakutat regions in depths around 250 m in the glacial troughs (Fig. 293). The CV of ensemble predictions was higher at shallower depths. Encounter probabilities of subadult longnose skate were highest in the central GOA (Fig. 294).

Adult longnose skate abundance and distribution predicted from RACE-GAP summer bottom trawl surveys in the Gulf of Alaska -- Adult longnose skate (N = 845) caught in GOA RACE-GAP summer bottom trawl surveys (1993–2019) were widely distributed over the GOA continental shelf from southeast Alaska to Unimak Pass with high abundance catches scattered across this range (Fig. 295). Five SDMs were considered for inclusion in the ensemble to predict numerical abundance of adult longnose skate in the GOA (Table 95); the GAM_P was eliminated by skill testing. The four remaining best-performing SDMs were weighted equally in the final ensemble, which was a fair overall fit to the observed adult longnose skate distribution and abundance data. The ensemble was fair at predicting high and low abundance catches (ρ = 0.25), good at discriminating presence-absence (AUC = 0.74), and poor

[58] Incorporating other high quality sources of data if available in future SDM ensemble EFH mapping for this species will be included as a research recommendation from the 2023 EFH 5-year Review.

at explaining deviance (PDE = 0.15). Geographic location, bottom depth, and BPI accounted for 74.1% of the covariate contribution to the deviance explained by the final ensemble (Table 96). Adult longnose skate abundance was highest in the northern portion of Shelikof Strait and the eastern portion of the Kodiak region over depths around 250 m in the glacial troughs (Fig. 296). The CV of ensemble predictions was highest in the western and eastern GOA, where adult longnose skate were less common. The probability of encountering adult longnose skate in GOA bottom trawls was higher in Shelikof Strait and the central GOA (Fig. 297).

Essential Fish Habitat of subadult and adult longnose skate in the Gulf of Alaska -- Ensemble-predicted habitat-related numerical abundance of longnose skate life stages collected in RACE-GAP summer bottom trawl surveys of the GOA (1993–2019) was mapped as EFH area and subareas (Fig. 298). Subadult and adult longnose skate EFH areas extend from the Shumagin Islands to southeast Alaska. The largest EFH hot spots for this species included Shelikof Strait and the glacial troughs.

Table 95. -- Constituent species distribution models (SDMs) used to construct Essential Fish Habitat (EFH) for a) subadult and b) adult longnose skate: MaxEnt = Maximum entropy; paGAM = presence-absence generalized additive model; hGAM = zero-adjusted Poisson hurdle GAM; GAM_P = standard Poisson GAM; GAM_{nb} = standard negative-binomial GAM; RMSE = root mean square error; ρ (rho) = Spearman's rank correlation coefficient; AUC = area under the receiver-operating characteristic curve; and PDE = Poisson deviance explained *. The "--" indicates that this model was not included in the final ensemble.

a) subadult longnose skate

Models	RMSE	Relative Weight	ρ	AUC	PDE	EFH area (km^2)
MaxEnt	0.63	0.26	0.26	0.73	0.13	216,900
paGAM	0.64	0.25	0.25	0.72	0.12	227,000
hGAM	0.65	0.24	0.24	0.72	0.10	229,300
GAM_P	0.64	0	--	--	--	--
GAM_{nb}	0.64	0.25	0.25	0.72	0.12	228,800
ensemble	0.63	1	0.28	0.74	0.15	233,800

b) adult longnose skate

Models	RMSE	Relative Weight	ρ	AUC	PDE	EFH area (km^2)
MaxEnt	0.47	0.25	0.20	0.69	0.08	219,000
paGAM	0.47	0.25	0.23	0.72	0.12	198,900
hGAM	0.47	0.25	0.22	0.72	0.11	197,000
GAM_P	0.47	0	--	--	--	--
GAM_{nb}	0.47	0.25	0.23	0.72	0.13	197,800
ensemble	0.46	1	0.25	0.74	0.15	209,100

* Refer to the Species Distribution Model Performance Metrics subsection within the Statistical Modeling section of the Methods for detailed descriptions of individual model performance metrics.

Table 96. -- Covariates retained in the a) subadult and b) adult longnose skate species distribution model (SDM) final ensembles, the percent contribution to the ensemble deviance explained by each covariate, and the cumulative deviance explained: SD = standard deviation and BPI = bathymetric position index.

longnose skate			
	Covariate	**% Contribution**	**Cumulative %**
a) subadult	bottom depth	32.4	32.4
	location	24.9	57.3
	bottom temperature	11.5	68.8
	current	7.6	76.4
	tidal maximum	6.7	83.1
	rockiness	4.4	87.5
	BPI	4.0	91.5
	aspect north	2.4	93.9
	slope	1.9	95.8
	current SD	1.7	97.5
	aspect east	1.0	98.5
	curvature	0.7	99.2
	sponge presence	0.4	99.6
	coral presence	0.4	100.0
b) adult	location	49.0	49.0
	bottom depth	16.5	65.4
	BPI	8.7	74.1
	bottom temperature	7.3	81.4
	current	6.4	87.8
	tidal maximum	2.3	90.1
	current SD	2.2	92.3
	aspect north	2.2	94.5
	aspect east	1.8	96.3
	slope	1.4	97.7
	rockiness	1.3	99.0
	coral presence	0.6	99.6
	sponge presence	0.4	100.0

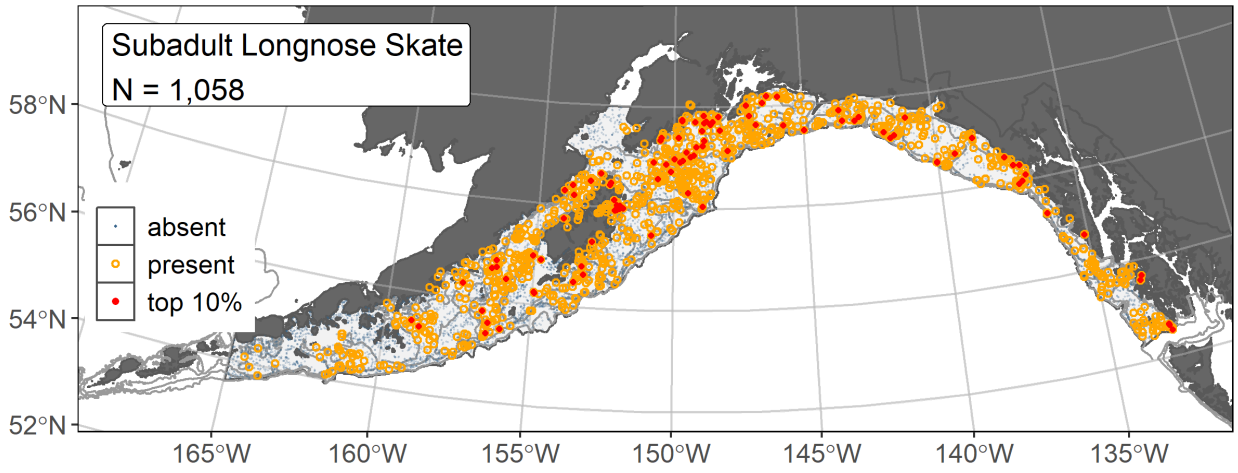

Figure 292. -- Distribution of subadult longnose skate catches (N = 1,058) in 1993–2019 AFSC RACE-GAP summer bottom trawl surveys of the Gulf of Alaska with the 100 m, 200 m, and 700 m isobaths indicated; filled red circles indicate locations in top 10% of overall abundance, open orange circles indicate presence in remaining catches, and blue dots indicate stations sampled where the animals were not present.

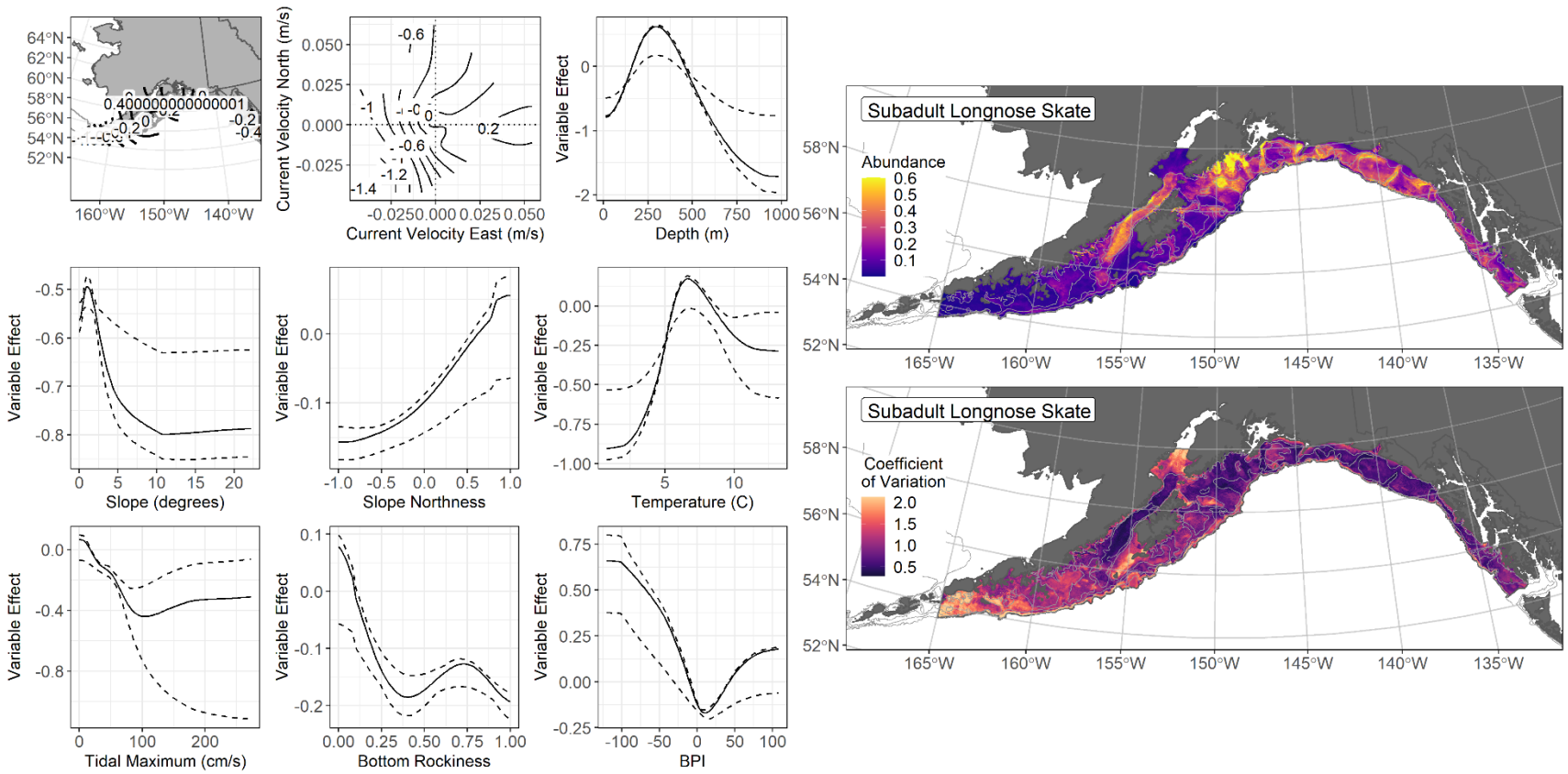

Figure 293. -- The top nine covariate effects (left panel) on ensemble-predicted subadult longnose skate numerical abundance across the Gulf of Alaska (upper right panel) and the coefficient of variation (CV) of the ensemble predictions (lower right panel).

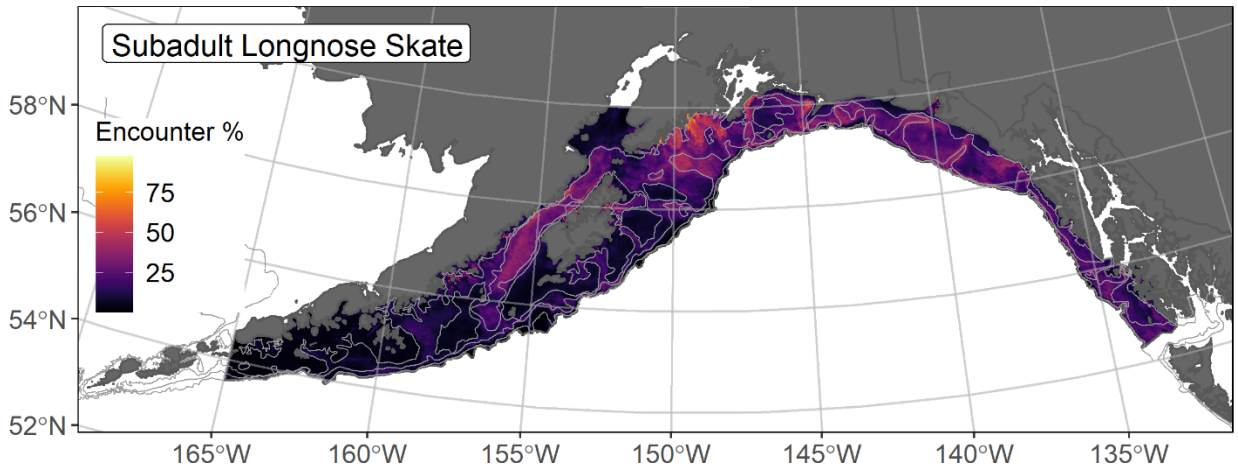

Figure 294. -- Encounter probability of subadult longnose skate from AFSC RACE-GAP summer bottom trawl surveys (1993–2019) of the Gulf of Alaska with the 100 m, 200 m, and 700 m isobaths indicated.

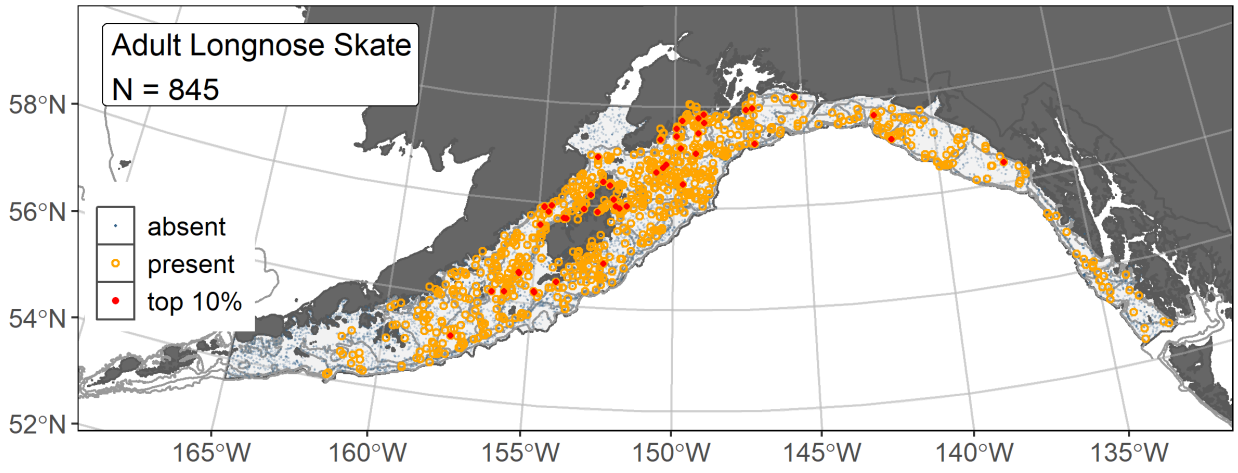

Figure 295. -- Distribution of adult longnose skate catches (N = 845) in 1993–2019 AFSC RACE-GAP summer bottom trawl surveys of the Gulf of Alaska with the with the 100 m, 200 m, and 700 m isobaths indicated; filled red circles indicate locations in top 10% of overall abundance, open orange circles indicate presence in remaining catches, and blue dots indicate stations sampled where the animals were not present.

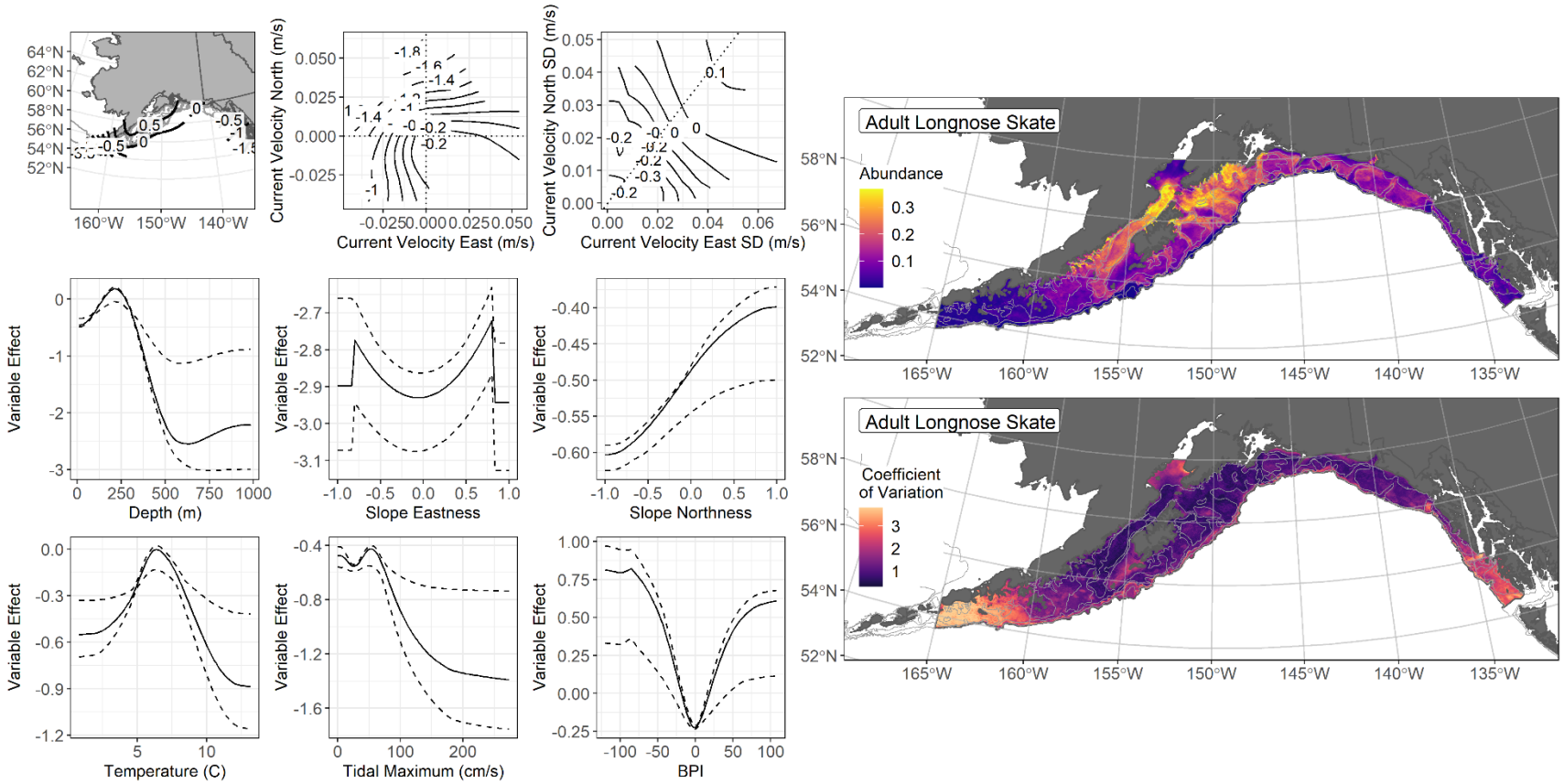

Figure 296. -- The top nine covariate effects (left panel) on ensemble-predicted adult longnose skate numerical abundance across the Gulf of Alaska (upper right panel) and the coefficient of variation (CV) of the ensemble predictions (lower right panel).

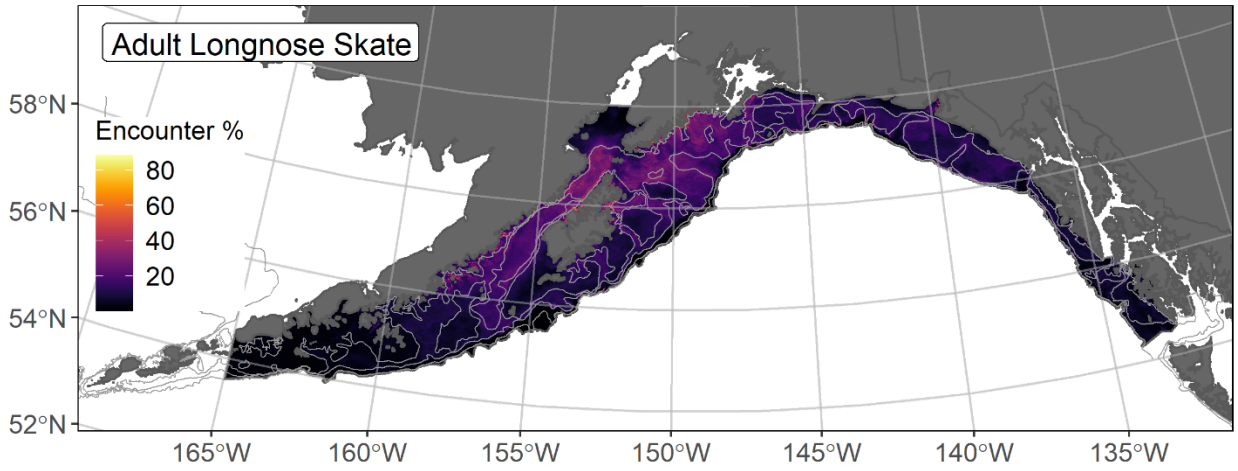

Figure 297. -- Encounter probability of adult longnose skate from AFSC RACE-GAP summer bottom trawl surveys (1993–2019) of the Gulf of Alaska with the 100 m, 200 m, and 700 m isobaths indicated.

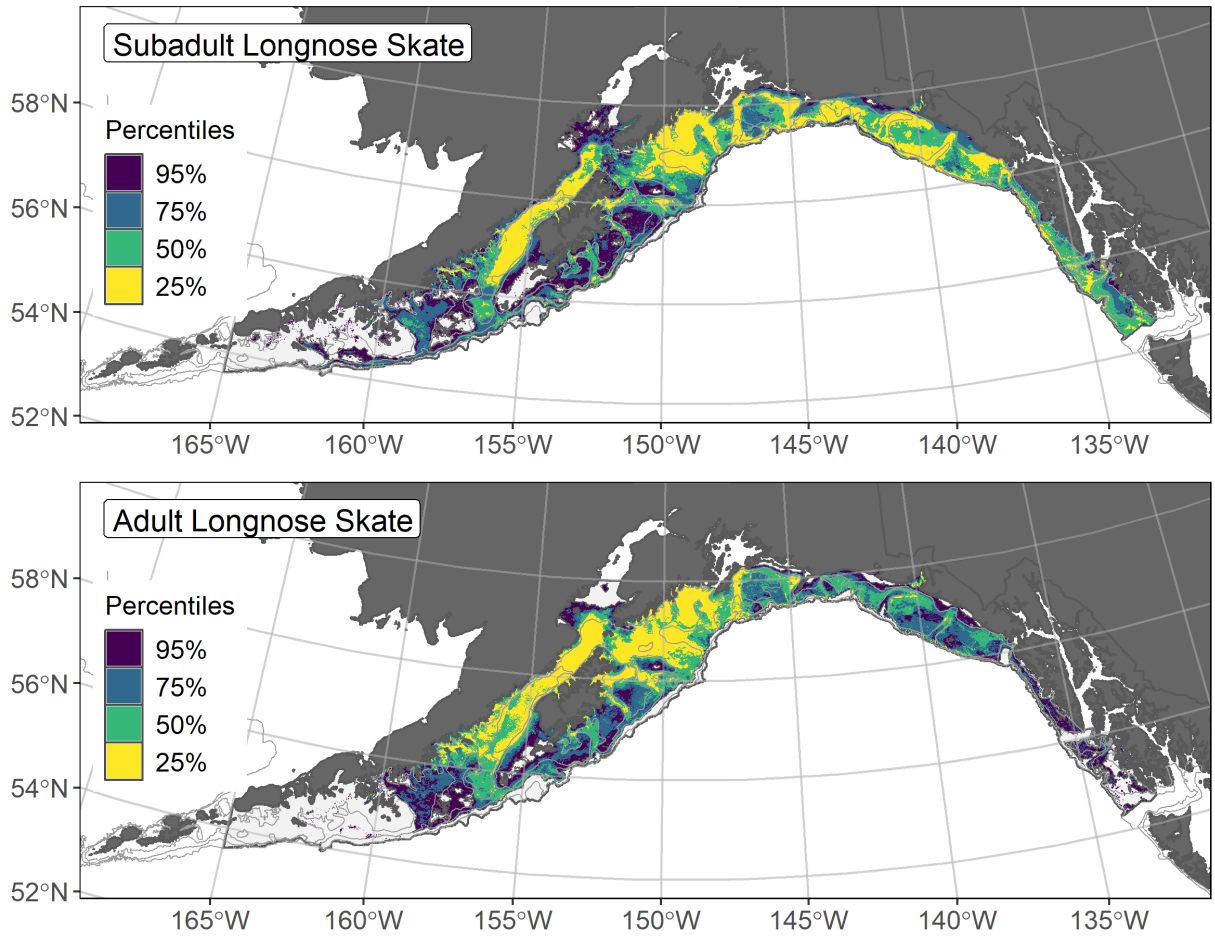

Figure 298. -- Essential fish habitat (EFH) is the area containing the top 95% of occupied habitat (defined as model estimated encounter probabilities greater than 5%) from an SDM ensemble fitted to subadult (top panel) and adult (bottom panel) longnose skate distribution and abundance in AFSC RACE-GAP summer bottom trawl surveys (1993–2019) with 100 m, 200 m, and 700 m isobaths indicated; within the EFH area map are the subareas of the top 25% (EFH hot spots), top 50% (core EFH area), and top 75% (principal EFH area) of habitat-related, ensemble-predicted numerical abundance.

Giant Pacific octopus (*Enteroctopus dofleini*)

The giant Pacific octopus (*Enteroctopus dofleini*) is the most common octopod encountered in the RACE-GAP summer bottom trawl survey of the GOA, where very low numbers of at least six other species have been found (Ormseth et al. 2019). True to its name, this species is the largest species of octopus in the world and can weigh over 25 kg. Giant Pacific octopus are terminal spawners that die after mating (males) and hatching of eggs (females; Jorgensen 2009). Peak spawning occurs in the winter and early spring (Brewer 2016), and females release between 40,000 to 240,000 eggs (Conrath and Conners 2014). While weight at 50% maturity is available for this species (Brewer and Norcross 2012), all life stages are combined for this project. Data on sex-specific octopus weights are not regularly collected in commercial fisheries or the RACE-GAP bottom trawl surveys, and estimates of octopus biomass are considered unreliable at this time (Ormseth et al. 2019). In 2011, the GOA FMP was amended to provide separate management for octopuses that were previously included in the "other species" complex managed in GOA through 2010 (Ormseth et al. 2019).

Giant Pacific octopus abundance and distribution predicted from RACE-GAP summer bottom trawl surveys in the Gulf of Alaska -- Giant Pacific octopus (N = 459) catches from GOA RACE-GAP summer bottom trawl surveys (1993–2019) were most common throughout the central and western GOA (Fig. 299). Five SDMs were considered for inclusion in the ensemble to predict numerical abundance of giant Pacific octopus in the GOA (Table 97); the GAM_{nb} was eliminated by skill testing. The four remaining SDMs had very similar RMSE and were weighted equally in the final ensemble, which attained a fair fit to the observed giant Pacific octopus distribution and abundance data. The ensemble was fair at predicting catches ($\rho = 0.20$), good at discriminating presence-absence (AUC = 0.75), and poor at explaining deviance (PDE = 0.15). Geographic location, sponge presence, and bottom depth accounted for 62.2% of the deviance explained by the ensemble (Table 98). Giant Pacific octopus abundance was predicted to be higher in the central and western GOA, with peak depths between 300-600 m (Fig. 300). The higher CVs from cross-validating these predictions occurred in the eastern GOA (Fig. 300). The probability of encountering giant Pacific octopus was relatively low for most of the GOA continental shelf, with higher values in the central and western GOA near the continental shelf break and upper continental slope (Fig. 301). This reflects that octopus are rarely caught in large numbers in any one place in the GOA. Stock managers have also reported challenges estimating octopus population numbers and biomass (e.g., Ormseth 2019). It is difficult to determine if the actual population density of the species is usually low and spread out, or perhaps just that they are difficult to sample using trawl gear. As this species typically hides in the substrate, trawling may not be an efficient method for

sampling octopodes[59]. Indeed, the highest octopus catch rates have been observed in the central and western GOA as incidental catch in the Pacific cod pot fisheries (Ormseth 2019).

Essential Fish Habitat of giant Pacific octopus life stages in the Gulf of Alaska -- Habitat-related predictions of giant Pacific octopus distribution and abundance from RACE-GAP summer bottom trawl surveys (1993–2019) were mapped as EFH areas and subareas (Fig. 302). Giant Pacific octopus EFH was most extensive in the central and western GOA and along the outer continental shelf and upper continental slope. Core EFH area and EFH hot spots for giant Pacific octopus were concentrated on the GOA continental shelf from east of Kodiak Island and west through the Shumagin Islands, where the presence of EFH hots spots increased. Core EFH areas and EFH hots spots increased with depth on the outer continental shelf and upper continental slope throughout the GOA management area.

Table 97. -- Constituent species distribution models (SDMs) used to construct Essential Fish Habitat (EFH) for giant Pacific octopus: MaxEnt = Maximum entropy; paGAM = presence-absence generalized additive model; hGAM = zero-adjusted Poisson hurdle GAM; GAM_P = standard Poisson GAM; GAM_{nb} = standard negative-binomial GAM; RMSE = root mean square error; ρ (rho) = Spearman's rank correlation coefficient; AUC = area under the receiver operating characteristic curve; and PDE = Poisson deviance explained *. The "--" indicates that this model was not included in the final ensemble.

giant Pacific octopus

Models	**RMSE**	**Relative Weight**	**ρ**	**AUC**	**PDE**	**EFH area (km^2)**
MaxEnt	0.33	0.25	0.14	0.68	0.08	155,700
paGAM	0.33	0.25	0.18	0.73	0.13	129,100
hGAM	0.33	0.25	0.18	0.73	0.12	123,100
GAM_P	0.33	0.25	0.18	0.73	0.12	116,800
GAM_{nb}	0.33	0	--	--	--	--
ensemble	0.33	1	0.20	0.75	0.15	134,900

[59] Incorporating other high quality sources of data if available in future SDM ensemble EFH mapping for this species will be included as a research recommendation from the 2023 EFH 5-year Review.

Table 98. -- Covariates retained in the giant Pacific octopus species distribution model (SDM) final ensembles, the percent contribution to the ensemble deviance explained by each covariate, and the cumulative deviance explained: SD = standard deviation and BPI = bathymetric position index.

giant Pacific octopus

Covariate	% Contribution	Cumulative %
location	35.7	35.7
sponge presence	14.8	50.5
bottom depth	11.7	62.2
current	8.0	70.2
bottom temperature	7.3	77.5
rockiness	6.6	84.1
slope	5.3	89.4
aspect north	3.1	92.5
aspect east	2.6	95.1
current SD	2.4	97.5
tidal maximum	2.2	99.7
BPI	0.2	99.9
curvature	0.1	100.0

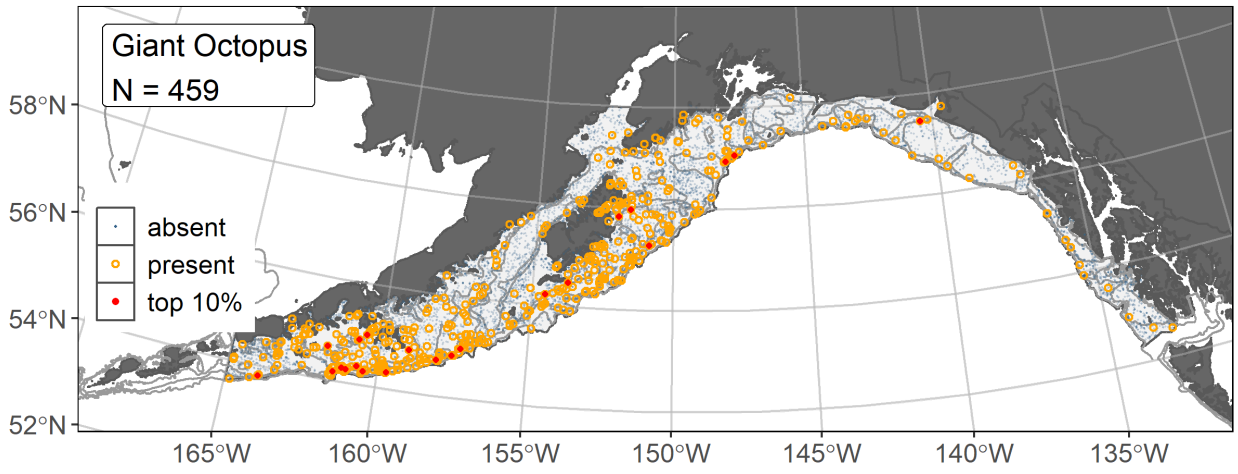

Figure 299. -- Distribution of giant Pacific octopus catches (N = 459) in 1993–2019 AFSC RACE-GAP summer bottom trawl surveys of the Gulf of Alaska with the 100 m, 200 m, and 700 m isobaths indicated; filled red circles indicate locations in top 10% of overall abundance, open orange circles indicate presence in remaining catches, and blue dots indicate stations sampled where the animals were not present.

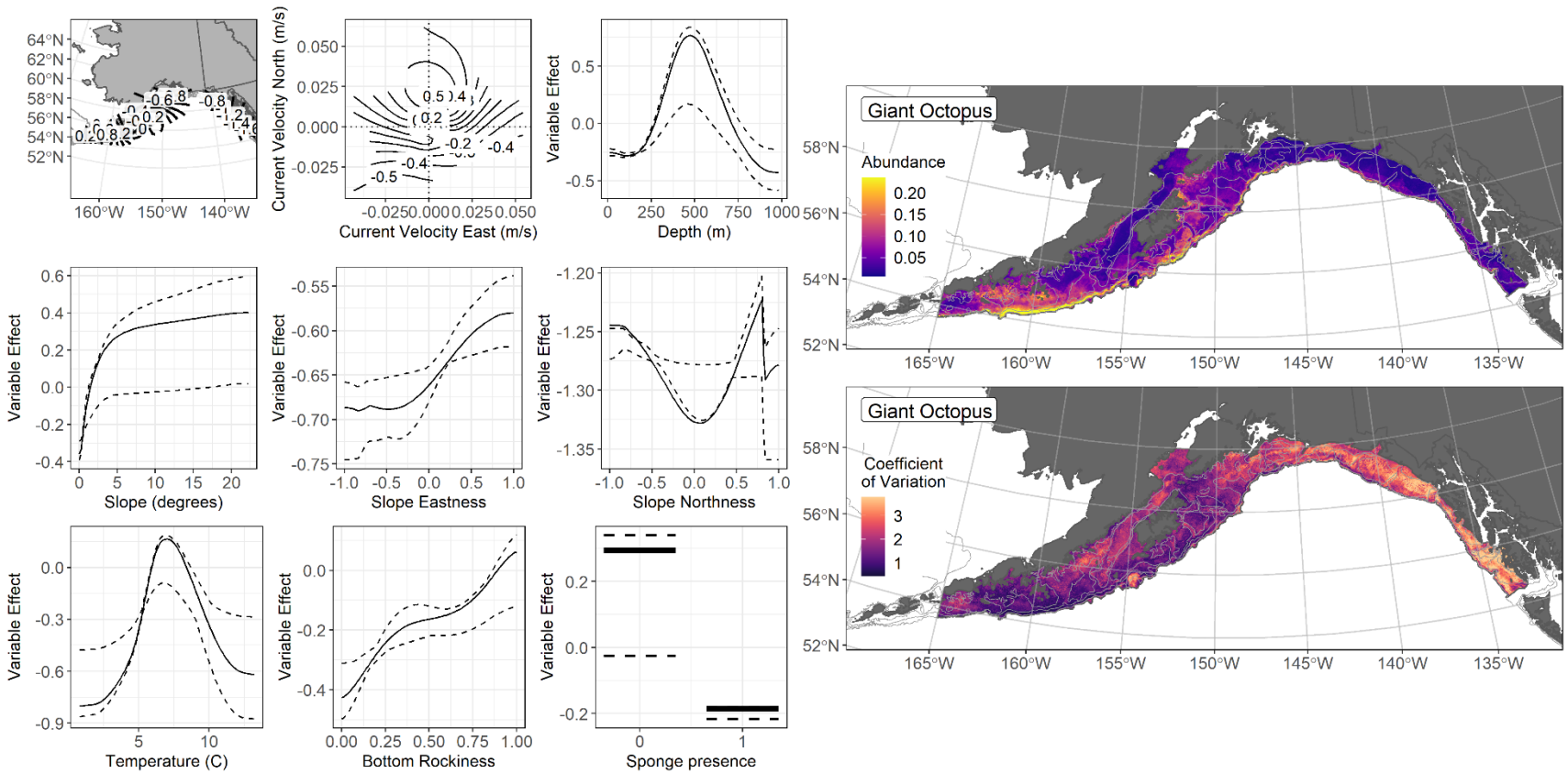

Figure 300. -- The top nine covariate effects (left panel) on ensemble-predicted giant Pacific octopus numerical abundance across the Gulf of Alaska (upper right panel) along with the coefficient of variation (CV) of the ensemble predictions (lower right panel).

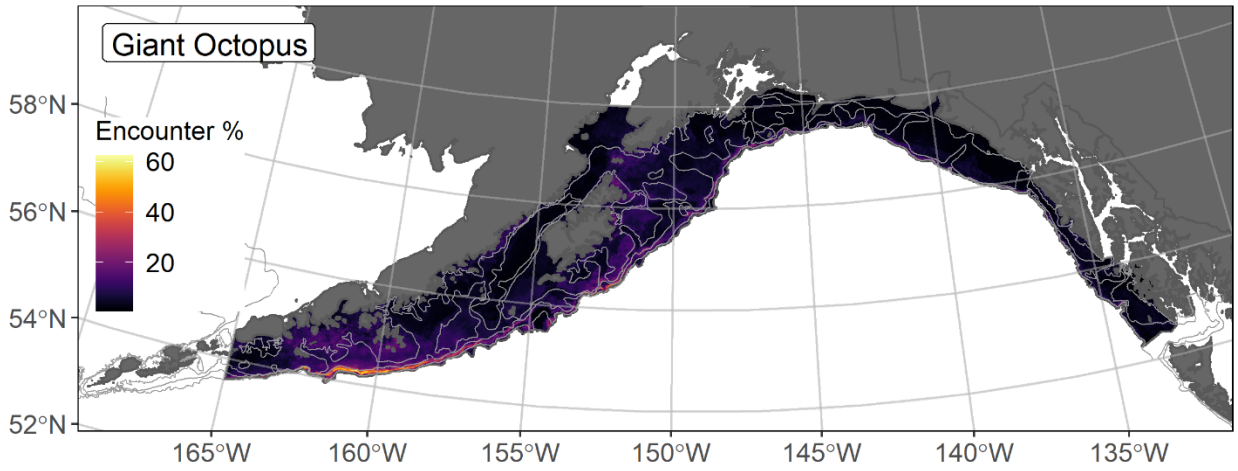

Figure 301. -- Encounter probability of giant Pacific octopus from AFSC RACE-GAP summer bottom trawl surveys (1993–2019) of the Gulf of Alaska with the 100 m, 200 m, and 700 m isobaths indicated.

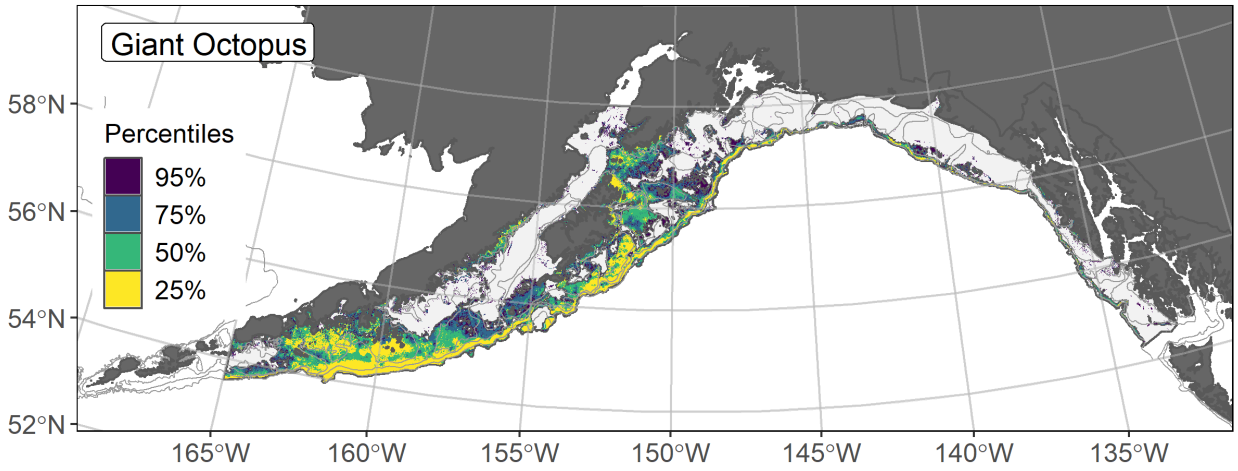

Figure 302. -- Essential fish habitat (EFH) is the area containing the top 95% of occupied habitat (defined as model estimated encounter probabilities greater than 5%) from an SDM ensemble fitted to giant Pacific octopus distribution and abundance from AFSC RACE-GAP Gulf of Alaska (GOA) summer bottom trawl surveys (1993–2019) with 100 m, 200 m, and 700 m isobaths indicated; within the EFH area map are the subareas of the top 25% (EFH hot spots), top 50% (core EFH area), and top 75% (principal EFH area) of habitat-related, ensemble-predicted numerical abundance.

FUTURE RECOMMENDATIONS

The EFH Final Rule requires that Fishery Management Councils and NMFS must periodically review the EFH components of FMPs and revise or amend these components with respect to new information at least every 5 years (50 CFR 600.815(a)(10)) with an overarching consideration that the science related to this effort meets the standards of best available science (NMFS National Standard 2 – Scientific Information 50 CFR 600.315). In the present work, we have adhered to these mandates as we have described and mapped EFH for FMP species in Alaska, using species distribution models (SDMs), incorporating modeling refinements and additional data sources where appropriate. While completing this work, and through conversation and review with stock assessment authors, other species experts, Plan Team members, the Scientific and Statistical Committee (SSC), and additional stakeholders, we have also identified future refinements and recommendations that could be considered for future EFH 5-year Reviews. These recommendations fall into three areas: prioritizing and improving EFH for select species, increasing the scope and applicability of EFH research, and improving process.

Prioritize and improve EFH for select species

The existing methodology for describing EFH works well for most species. However, for others, modified approaches are needed to better capture drivers of density and generate habitat descriptions. These approaches may involve incorporating new datasets (for fish distribution, environmental covariates, or life history parameters), or developing modeling approaches that are amenable to their distributions (e.g., modeling at a broader spatial scale). For some of these species, the need for model improvements has been discussed in the results chapters for the current EFH Review cycle; in the future, it is important to have processes in place (both modeling approaches and communication approaches) for these species. These may include agreed-upon differences in the modeling approach depending on the data needs and model ensemble performance in previous cycles.

Leverage existing species distribution data

Data for species and life stages that are not well-sampled in the RACE GAP summer bottom trawl surveys may need to be augmented with data from other sources. In this study, we combined additional surveys and data sources inshore of the RACE GAP survey area in a single, presence-only SDM (MaxEnt) to more comprehensively describe and map the EFH for the settled early juvenile life stage of 11 groundfish species. Data sets for EFH species, in particular, the settled early juvenile life stage of groundfishes and crabs in nearshore areas, should be further developed to improve EFH descriptions and maps for species in nursery habitats and to improve our understanding of how management decisions affecting nearshore and coastal nursery habitats may affect fishery productivity (e.g., Thorson et al. 2021).

Data other than the RACE-GAP summer bottom trawl survey that could be included in EFH descriptions include data from the North Pacific Observer program[60], the AFSC[61] and IPHC longline surveys[62], and MACE acoustic surveys (e.g., McGowan et al. 2019; Cole C Monnahan et al. 2021). In these and other instances, it is important, at a minimum, to estimate fishing-power corrections between gears, and in some cases might be helpful to identify differences in vertical availability or selectivity ratios (Kotwicki et al. 2017, 2018; Monnahan et al. 2021; see "Develop methodology for combining disparate datasets" section below). The stock assessment author review of the EFH descriptions and identification (maps) (component 1) for the 2023 EFH 5-year Review suggested that the addition of longline survey data may be particularly helpful for arrowtooth flounder, blackspotted and rougheye rockfishes, shortraker rockfish, shortspine thornyhead, sablefish, and Pacific sleeper sharks. In addition, tagging studies and genetic data may be helpful and most useful for fitting process models, which can, in turn, inform SDMs for EFH species (Thorson et al. 2021). These data sources are summarized in

[60] https://www.fisheries.noaa.gov/alaska/fisheries-observers/north-pacific-observer-program
[61] https://www.fisheries.noaa.gov/resource/map/alaska-longline-survey-data-map
[62] https://iphc.int/

Table 99. Data sources to consider incorporating for species distribution.. SDMs that take advantage of multiple data sources may improve the resolution and reliability of existing EFH descriptions.

Incorporating existing datasets into future EFH descriptions and maps may also expand the spatial scope of EFH areas. For example, in the present work, we combined nearshore surveys with offshore surveys in the Gulf of Alaska (GOA) to develop more comprehensive coverage of EFH species and life stages in nearshore areas (see above). There is also a potential for a multiscale approach to EFH that includes paired maps of nearshore and offshore areas, where nearshore maps could be of finer spatial resolution than the offshore maps depending on available data (e.g., Grüss et al. 2021). With enough detailed information from other surveys, identifying biological processes occurring at a subregional scale, such as differences in growth or reproductive output, may also be possible. In the GOA, Dover sole (McGilliard et al. 2019) and rex sole (McGilliard and Palsson 2017) are other species examples where additional survey data may help better distinguish subregional growth differences. Additional information can improve Level 3 EFH information and is useful for stock assessments, especially for species with spatial management (e.g., sablefish; Hanselman et al. 2019). The spatial scope of EFH descriptions and maps will also expand with surveys of untrawlable habitats, including camera surveys.

Combining data between the RACE-GAP bottom trawl surveys and other sources in the SDM ensemble framework presented by this study will require additional research as well as some collaborative guidelines for deciding on criteria for survey and data source inclusion (including non-standard surveys). These criteria may result in the elimination of some datasets from the current RACE GAP summer bottom trawl survey collection. For example, the Eastern Bering Sea slope survey was only conducted in 2002, 2004, 2008, 2010, 2012, and 2016 and may not improve the EFH definitions for Bering Sea species. It will take some modeling effort to determine parameters like gear efficiency ratios that can be used for combining data in SDMs.

Some species have distributions that occupy a narrow subarea within the trawl survey area or have limited data and thus likely require alternative SDM approaches. For these species, it may be

sensible to adopt species-specific modeling approaches where possible to accommodate some of these idiosyncrasies. For example, species like sablefish and shortraker rockfish in the EBS have "long and skinny distributions," which result in poor model fits; species with limited data in a particular region have relatively low ensemble performance compared to other species modeled in the present study, and would benefit from additional survey data to improve ensemble outcomes. In the case of some species at the edge of their distribution, expanding the spatial scope of the modeled area may yield better EFH information (e.g., Atka mackerel EFH in the EBS might be improved by modeling the Bering Sea and Aleutian Islands together); in other cases additional survey data from the same location may be needed (e.g., EBS sablefish from longline surveys).

Table 99. -- Data sources to consider incorporating for species distribution.

Data source	Type of data (presence/absence, density, etc)	Species for which these data are important	Path to SDMs
North Pacific Observer Program	Presence/absence (PA), density, age and length distributions	Commercially targeted species (e.g., pollock, cod, sablefish, yellowfin sole, etc.)	PA and density data can be used directly; age and length distributions can inform individual-based models (IBMs)
IPHC longline surveys	PA, density, age and length distributions	Arrowtooth flounder, blackspotted and rougheye rockfishes, shortraker rockfish, shortspine thornyhead, sablefish, and Pacific sleeper shark, skates	PA and density data can be used directly; age and length distributions can inform IBMs
AFSC longline surveys	PA, density, age and length distributions	Arrowtooth flounder, blackspotted and rougheye rockfishes, shortraker rockfish, shortspine thornyhead, sablefish, and Pacific sleeper shark, skates	PA and density data can be used directly; age and length distributions can inform IBMs
MACE acoustic surveys	PA, density	Prey species, groundfish with more midwater distributions (e.g., pollock)	Include directly in SDMs after estimating gear efficiency ratios
Tagging studies	Movement parameters and nonlocal effects	Sablefish, Pacific cod, arrowtooth flounder, Pacific ocean perch	Parameterize IBMs to inform species distribution models
Genetic data	PA, density	Blackspotted rockfish, Atka mackerel	Include directly in SDMs after estimating gear efficiency ratios and/or spatial sampling precision

Leverage environmental data

The suite of habitat-related covariates used to parameterize SDMs in the present work was extensive, covering static and dynamic metrics ranging from bathymetry and seafloor terrain features to long-term averaged, observed bottom temperatures, and modeled tidal and bottom currents. Ongoing work is exploring the utility of fitting bottom temperature or other covariates over annual time scales, which may provide insight into how well models with long-term averaged covariates explain historical species distributions (e.g., Barnes et al. 2022). Covariates from climatological models (e.g., Bering10K ROMS or GOA 3K ROMS NPZ) can be used for hindcasting and forecasting population responses over a variety of climate scenarios and time scales (Barnes et al. 2022, Rooper et al. 2021, Thorson et al. 2020). In addition, covariates utilized in the present work should be evaluated *post hoc* to determine if some of the present predictors could be eliminated in the next EFH Review.

As of this EFH report, environmental habitat covariates have included geographic position, bottom temperature, depth, bathymetry-derived terrain metrics, tidal and bottom currents, sediment grain size, seafloor rockiness, and the presence of structure-forming invertebrates. Several other covariates may impact groundfish and crab distributions, including 1) irradiance spatially interpolated from net sensors; 2) average (across years and/or seasons) surface chlorophyll from satellites, perhaps broken into size or functional groups; 3) average storm frequency as a proxy for turbulent mixing; 4) average mixed layer depth or other stratification variables; 5) spatially interpolated empirical data or modeled values for secondary producers (copepods and euphausiids) from RPP/MACE/EMA programs and ROMS. Surface chlorophyll covariates were produced for the 2017 EFH report. These data were used for pelagic early life stages in 2017 and could be adapted to future SDMs for pelagic and demersal life stages.

New dynamic covariates can also be explored for inclusion in the SDMs in the future (e.g., prey fields, remote sensing data sets, the Cold Pool or El Niño Southern Oscillation indices, etc.). Many of the covariates in the current report are fixed characteristics of the physical habitat, including substrate and depth. However, for more mobile and/or more pelagic species, important physical habitat may also

include areas with high productivity, prey density, and temperature. We recommend the careful consideration and inclusion of important covariates as they are available in future EFH Reviews. Many of these data are currently available, though some work will be required to properly prepare them for use in SDMs (Table 79). We encourage further evaluation of SDMs with dynamic covariates to leverage high-resolution temporal and spatiotemporal data and improve the accuracy of EFH information. In these cases, we would likely need to average density predictions across some larger number of years.

Existing data should be updated based on ongoing work, including covariate data and species distribution data. For example, bathymetry for the EBS has been updated and should be included in the next EFH report. Some datasets (e.g., trawl data from the Northern Bering Sea prior to 2010) may be used to extend the temporal scope of EFH. Summarizing and communicating data limitations will help prioritize data gaps to fill. Existing data may be used in new ways to inform ecological differences between regions; for example, covariate effects may vary across regions, and this information could be useful for stock assessments and regional management.

Leverage life history information and process studies

The data necessary for using SDMs to describe and map EFH are species-specific response variables (i.e., presence-absence or abundance) and habitat-related predictors (covariates) such as bottom depth or bottom temperature. Because the MSA EFH Regulations specify that EFH descriptions are both species- and life stage-specific, life history updates are integral to incorporating new data and applying best available science to the EFH components of FMPs. Improving life history data and EFH information for ecologically distinct and underrepresented life stages is an ongoing priority.

In this report, species-specific length-based life stage definitions were employed to separate settled early juveniles from subadult stages and subadults from adult stages. We recommend that future EFH work leverages existing data sources and process studies, including novel approaches, to continually improve the available life history information. The next EFH 5-year Review should apply the crab maturity data regularly collected on Bering Sea RACE-GAP bottom trawl surveys to inform life stage-

specific SDMs for these ecologically important species in the BSAI King and Tanner Crabs FMP. This effort should involve collaboration with scientists from the AFSC's Kodiak Laboratory and the Alaska Department of Fish and Game (ADFG), both of which have crab size measurements and maturity data. These data could be used to apportion crab catches to mature and immature life stages in the EBS and to describe and map those life stages for the next EFH 5-year Review.

Existing process studies on species physiology, behavior, and diets can be used to improve the selection of habitat covariates, inform life history and behavioral parameters, generally improve SDMs, and inform mechanistic models that can be used to link environment drivers and ecosystem processes. For example, process studies may inform which life stage of a given species is most likely to be influenced by a given environmental process. Life stage specific parameters can be integrated to obtain growth parameters at the population level. They can also inform biophysical individual-based models (IBMs) that account for life stage-specific habitat needs and behaviors (e.g., foraging, water column position, movement between areas). In 2020, the SSC recommended several pathways by which IBMs could be used to improve habitat information, including mapping of pelagic early life stage habitat (EFH), incorporating ecosystem model outputs in IBMs, and the use of IBMs to estimate the value of different spawning locations. IBMs can also be used to integrate life stage information, and better assess the impacts of human activities (e.g., fishing) at the population scale. Process modeling studies can also incorporate existing IBMs (e.g., Daly et al. 2020, red king crab; Gibson et al. 2019, sablefish; Hinckley et al. 2019, Pacific cod), where life history and behavioral parameters can be updated with new process studies from the laboratory and field and advancements to the modeling environment (e.g., ROMS).

Structural equation models (SEMs) can help better identify environmental drivers and link them mechanistically to population impacts (Thorson et al. 2021). Spatial demographic models accounting for movement rates among areas can help address issues of non-local habitat impacts, impacts of management decisions on non-surveyed age classes, and provide another way to evaluate the combined effects of fishing and habitat impacts at the population scale. Process-based approaches are helpful to

describe and map EFH, inform ecosystem-based fisheries management (EBFM) (e.g., Goldstein et al. 2020), and determine the population-level impacts of management decisions (e.g., Thorson et al. 2021).

Combine disparate datasets

In the present studies, our primary response variable was numerical abundance generated from the fishery-independent RACE-GAP summer bottom trawl surveys. We also modeled settled early juvenile life stage distribution from a variety of inshore and offshore fishery-independent surveys utilizing various sampling modes (e.g., RACE-GAP large mesh bottom trawls, ADFG small mesh bottom trawls, and beach seines) employing MaxEnt modeling of presence as a vehicle to combine these disparate data sources in analyses. A growing body of research could be harnessed in the future to better quantitatively combine data from disparate data sources and fishery-dependent collections, thereby expanding the scope and seasonal availability of species response variables to the SDMs. We recommend combining disparate data sources as a priority area of research development for future EFH Reviews.

One of the refinements we implemented in the present work was to move away from single models for species-specific SDMs to an ensemble modeling approach. Ensemble models have been shown to improve performance (better model fits; Rooper, Zimmermann, and Prescott 2017). Of the five constituent models estimated and considered for the final ensembles in the present work, four were GAMs, and the fifth was a MaxEnt model describing the probability of suitable habitat for each species in a given location. One recommendation for future EFH reviews is to expand the variety and types of models considered in the ensemble approach (e.g., random forest or spatio-temporal models) to expand the range of fitting capabilities across the wide array of distribution patterns encountered in our data sets. As mentioned above, a modeling approach that facilitates combining data from disparate data sources should also be considered since it would expand the number and types of response variables available to the EFH descriptions in space and time.

Several datasets that could be used to either improve existing EFH information within the survey areas or to expand the spatial and temporal extent over which we provide EFH information (e.g., North

Pacific Observer data, AFSC longline survey, ADFG small-mesh bottom trawl survey, etc.). Additional work is needed to combine these disparate datasets in the same SDMs, including the estimation of sampling efficiency ratios for surveys with different gear efficiencies (e.g., O'Leary et al. 2021).

Consider diverse constituent models

SDM approaches are still under development and should be reviewed regularly. As of the present report, MaxEnt models do not directly model absences (Phillips and Dudík 2008) and so may overpredict occupancy based on covariates in the detection areas into areas where a species was not detected. GAM approaches explicitly account for presence/absence and do so in a more ecologically realistic way by modeling presence and absence as a binomial process. In this EFH Review, we presented presence-absence GAMs, hurdle GAMs, standard GAMs using the Poisson distribution, as well as GAMs using the negative binomial distribution to account for overdispersion. In the future, we propose to explore alternatives for modeling distributions. For species with limited data, random forests, boosted regression trees, and other approaches may be more appropriate to include in model ensembles. Our current ensemble framework can be readily expanded to test and incorporate additional constituent SDMs.

Increase scope and applicability of EFH research

Ongoing discussions with the SSC and stock assessment authors have identified conceptual frameworks that should be considered in the future for developing, evaluating, and utilizing EFH descriptions and maps. Considering how EFH is defined in terms of scale and ecological function could improve the utility of this concept for management. The current working definition of EFH equates the area containing 95% of the total estimated occupied habitat with EFH (NMFS 2005[63]), and core habitat as the area containing 50% of occupied habitat. In the present work, occupancy was defined as areas with >5% probability of an encounter based on the RACE GAP bottom trawl survey data. However, this definition may not be as ecologically meaningful for highly mobile species or those with a high degree of

[63] https://repository.library.noaa.gov/view/noaa/17391

uncertainty in the estimate of their population density. For example, the distribution of highly mobile predators might be more strongly impacted by prey availability than by environmental conditions. It may also not be a useful metric if a shrinking proportion of their population is available to the bottom trawl survey, as is the case for species with poleward-shifting distributions. As models describing and predicting species distribution and abundance (density or biomass) become more tightly and realistically linked to habitat and environmental change, there may be opportunity to reconsider how EFH is defined, potentially arriving at a more objective and constrained (less open to interpretation) definition that could be universally applicable across species and regions.

Describe prey species habitat

Many groundfish species are predators of smaller forage species and likely respond to changes in the density of euphausiids and other prey species. They may also be adequate samplers of available forage for predators, and prey biomass (Ng et al. 2021). Approaching groundfish density from the perspective of prey availability aligns with EFH component 7 in the FMPs (Prey Species: "FMPs should list the major prey species for the species in the fishery management unit and discuss the location of prey species' habitat"; 50 CFR 600.815(a)(7)), which includes predator-prey dynamics. Several data sources are available for capturing predator-prey interactions spatially, including data on forage density from midwater acoustic surveys done by the Midwater Assessment and Conservation Engineering (MACE) division and stomach content data from Resource Ecology and Ecosystem Modeling (REEM). For midwater predators especially, data from midwater acoustic surveys may provide useful information on prey fields and therefore distribution. As prey fields shift on short time scales, the appropriate modeling approach will likely be a dynamic approach as opposed to the static EFH maps drawn based on temporal averages.

Stomach contents, behavioral studies, genetics, and other datasets can be used to identify areas of prey abundance, and diet proportions can be analyzed to provide new SDM predictors (Grüss et al. 2020, 2021; Thorson et al. 2021). Predator stomach contents can be fit with environmental

covariates, providing a more mechanistic approach for modeling trophic interactions. We recommend that future studies further explore the potential for predator diets to serve as indices of prey abundance and distribution, including through an SDM framework to develop maps of prey habitat (i.e., EFH component 7 - "location of prey species habitat"). This effort may in turn help identify areas of importance for their EFH species predators.

Expand to EFH Levels 3 and 4 where appropriate

In the present EFH Review, growth, lipid accumulation, and energy loss are the vital rate parameters included to explore Level 3 EFH (habitat-related vital rates). In the future, we recommend adding other vital rates such as lipid consumption or fecundity, as well as Level 4 rates like habitat-related productivity or recruitment. Currently, we have Level 2 EFH information for crab species in the EBS and AI; Level 3 information for crab species could be obtained with growth rate information from surveys carried out by the ADFG and the AFSC's Kodiak Laboratory (see the "Add life stages" section above).

Continue to advance and apply dynamic SDM methods

Ongoing research indicates that dynamic models that capture interannual shifts in density and in habitat covariates describe historical habitat better than static models (Barnes et al. *in review*). Other work shows that many biological processes affecting fish distributions occur on a seasonal timescale or even a weekly basis (e.g., Thorson et al. 2020). In 2020, the SSC asked about the implications of higher or lower sampling frequency for EFH descriptions; considering more dynamic models in the model ensemble would help address this. Continuing to evaluate the impacts of model complexity (including time-varying covariates) on model fit will be necessary to ensure that EFH maps capture relevant processes.

Many of the habitat covariates identified for further exploration are dynamic in nature and require a modeling approach that accounts for this. For example, areas of high productivity or high prey density may be important for higher trophic levels, but their location will shift over time in response to environmental drivers, including currents, light, and the timing of ice retreat. Therefore, dynamic SDMs applied over shorter periods should be considered as an option for presenting dynamic maps alongside

static SDM EFH maps (based on long-term averages) in the next EFH Review. Pairing temporally dynamic and static (long term) approaches to describe and map EFH will improve understanding of how species habitat availability and spatial stock structure shift in space and time, which is needed to improve climate-responsive approaches to EBFM.

Table 100. -- Existing environmental datasets to explore as covariates in future EFH analysis.

Covariate	Source	Current status	Future direction	Data processing needed
Light levels (irradiance)	Bering Sea ROMS model. Vertical profiles of light levels (PAR) available from RPA (EcoFOCI PMEL, EMA) data. Contacts: Jeanette Gann, Phyllis Stabeno.	Water column irradiance could be calculated from ROMS light attenuation and other variables but is not currently a diagnostic output of the ROMS model. In Access database for EMA Bering surveys (2003-present); PMEL mooring survey data also available.	Use light fields to define suitable habitat for visual predators.	If it is to be used as a covariate, irradiance will have to be added as a diagnostic output to future versions of the Bering Sea ROMS model. Then it can be used to calculate other values.
Bottom light levels (optical depth)	Net sensors on bottom trawls (vertical profiles and on bottom in situ irradiance-RACE GAP); vertical profiles of light levels (PAR) available from RPA (EcoFOCI PMEL, EMA) data. Contacts: Jeanette Gann, Phyllis Stabeno.	Available for recent years (EBS: 2004-present, NBS: 2010-present, GOA: 2005-present, AI: 2006-present) (Rohan et al. 2020; Rohan et al. 2021)	Use light fields to define suitable habitat for visual predators. Optical depth (depth × diffuse attenuation coefficient) can be used to identify areas where predators can find prey	Data may require additional kriging; interpolation for years/areas where data are absent
Surface total chlorophyll estimates (satellite)	Satellite data (when cloud cover and sea ice are not interfering). Contact: Jens Nielsen (CICOES).	Includes all phytoplankton together. Data have been organized for including as covariates as of 2017 EFH report.	Test phytoplankton as covariate in SDMs	No further processing needed.
Surface total chlorophyll estimates (discrete/ in situ)	CTD cast data from discrete sampling stations; includes fluorometer for chl a from RPA cruises. Contacts: Jeanette Gann, Colleen Harpold.	Bering Sea data stored in Access; GOA and AI data may not be available yet.	Use as coarser measure of productivity	Unknown
Ice algae	Not available yet	Not yet available	Likely related to sea ice; food resource for crabs and other benthic invertebrates	Unknown

Covariate	Source	Current status	Future direction	Data processing needed
Light levels (irradiance)	Bering Sea ROMS model. Vertical profiles of light levels (PAR) available from RPA (EcoFOCI PMEL, EMA) data. Contacts: Jeanette Gann, Phyllis Stabeno.	Water column irradiance could be calculated from ROMS light attenuation and other variables but is not currently a diagnostic output of the ROMS model. In Access database for EMA Bering surveys (2003-present); PMEL mooring survey data also available.	Use light fields to define suitable habitat for visual predators.	If it is to be used as a covariate, irradiance will have to be added as a diagnostic output to future versions of the Bering Sea ROMS model. Then it can be used to calculate other values.
Size-fractionated surface chlorophyll (discrete / *in situ*)	Taxonomic data collection in progress. Contacts: Lisa Eisner; Jeanette Gann	Bering Sea data stored in Access; GOA and AI data may not be available yet (PI: Lisa Eisner; contact Jeanette Gann with database inquiries)	Larger phytoplankton may be better food (e.g., diatoms) so size fractions might better indicate food availability / quality. There will be a seasonal shift to smaller sizes but persistent hotspots probably have many sizes.	Unknown
Size-fractionated surface chlorophyll (satellite)	Contact: Jens Nielsen	Satellite algorithm still in development. Included in Ecosystem Status Report (ESR) for Eastern Bering Sea.	Larger phytoplankton may be better food (e.g., diatoms) so size fractions might better indicate food availability / quality.	Additional interpolation may be necessary.
Size-fractionated and size-specific or vertically integrated chlorophyll samples (spring and fall)	Contacts: Lisa Eisner, PhD student Jeanette Gann	TBD following collaboration discussion. In Access database for EMA Bering surveys (2003-present); PMEL mooring survey data also available.	Larger phytoplankton may be better food (e.g., diatoms) so size fractions might better indicate food availability / quality. There will be a seasonal shift to smaller sizes but persistent hotspots probably have many sizes.	Additional interpolation may be necessary.
Storm frequency (proxy for turbulent mixing)	May be available from wind speeds (Contact: Pelland) or in ESRs.	Unknown	Turbulent mixing may influence food availability and productivity.	Unknown
Timing and size of spring bloom	Derived from variables described above	Nielsen in ESR for Eastern Bering Sea	For a spatially-varying response, an annual index can still generate interesting differences in distribution among years (Thorson 2019)	Annual indices ready to use for EBS; may be available for other regions.

Covariate	Source	Current status	Future direction	Data processing needed
Light levels (irradiance)	Bering Sea ROMS model. Vertical profiles of light levels (PAR) available from RPA (EcoFOCI PMEL, EMA) data. Contacts: Jeanette Gann, Phyllis Stabeno.	Water column irradiance could be calculated from ROMS light attenuation and other variables but is not currently a diagnostic output of the ROMS model. In Access database for EMA Bering surveys (2003-present); PMEL mooring survey data also available.	Use light fields to define suitable habitat for visual predators.	If it is to be used as a covariate, irradiance will have to be added as a diagnostic output to future versions of the Bering Sea ROMS model. Then it can be used to calculate other values.
Average mixed layer depth	PMEL moorings (seasonal coverage) and oceanographic surveys (PMEL, RPA). Contact: Jeanette Gann, Jens Nielsen, Phyllis Stabeno.	In Access database for EMA Bering surveys (2003-present); PMEL mooring survey data also available.	Mixed layer depth may impact food availability and productivity; may be useful for Component 1 descriptions.	Unknown
Cold Pool Index (CPI)	Net sensors on bottom trawls. CTD data from RPA ecosystem and mooring surveys. Also ROMS model output. Contact: Kelly Kearney.	CPI is fairly standard (O'Leary et al. 2020) but has not been used in EFH so far. Data ready for use.	Use CPI as covariate to improve EFH Component 1 descriptions.	May require additional interpolation.
Secondary producers (other forage including copepods and euphausiids)	RPP/MACE/EMA surveys-zooplankton water column net tows (Contact: Dave Kimmel) and diets in forage fish (Contacts: Dave Kimmel, Alex Andrews). Gut contents from stomach sampling on trawl surveys. ROMS modeled values (e.g., GOA NPZ 3K ROMS small and large copepod fields; Contact Ken Coyle)	Data available	Use prey data to develop prey habitat descriptions for Component 7.	May require additional interpolation and/or diet data to determine important taxa or sizes.
Secondary producers: euphausiids	MACE product from midwater acoustic survey (Contact: Patrick Ressler)	Used annually for ESRs.	Use prey survey data to explore EFH for predators, e.g., euphausiid data can be used as covariate for midwater foragers like walleye pollock	May require additional interpolation. Acoustic data may need additional manipulation.

Covariate	Source	Current status	Future direction	Data processing needed
Light levels (irradiance)	Bering Sea ROMS model. Vertical profiles of light levels (PAR) available from RPA (EcoFOCI PMEL, EMA) data. Contacts: Jeanette Gann, Phyllis Stabeno.	Water column irradiance could be calculated from ROMS light attenuation and other variables but is not currently a diagnostic output of the ROMS model. In Access database for EMA Bering surveys (2003-present); PMEL mooring survey data also available.	Use light fields to define suitable habitat for visual predators.	If it is to be used as a covariate, irradiance will have to be added as a diagnostic output to future versions of the Bering Sea ROMS model. Then it can be used to calculate other values.
Secondary producers: stomach contents as direct measure of foraging success	REEM stomach contents data	Data available	Can be used in a spatial model to interpolate (examples: Grüss et al. 2020; 2021; Ng et al. 2021); methods exist to fit with environmental covariates using GAMs and GLMs	Data may require additional kriging or similar

Improve process and communication

Improving methodological approaches and clearly communicating them is a high priority. Review and input by the Council's SSC, Plan Teams, the stock assessment authors, and other stakeholders is an important part of the iterative EFH 5-year Review process. Expert peer reviews, in particular, can help identify cases where changes are needed to account for species with lower quality data or low availability to the surveys where species data has been used to model and map EFH. Additionally, the EFH process involves communicating model results to a broad stakeholder audience and adapting models when appropriate based on feedback. For example, a species with poor model fits or low stock assessment author confidence in the EFH map might be evaluated using a different SDM, or certain data requirements might be identified early that would lead to that species being modeled differently. Each EFH 5-year Review is an opportunity to improve the process and communication.

We are proud of the process and communication improvements we implemented during this EFH 5-year Review to improve coordination and collaboration between SDM EFH analysts and stock assessment authors. We have implemented SSC suggestions from 2021 about communicating methods and results, including providing descriptions of ensemble modeling methods and probability thresholds, clear descriptions of data, including data transformations and timeframes, and summaries of skill testing results. We (AKRO and AFSC) hosted a stock assessment author summit in January 2021 to discuss and co-develop the review process of the current and new EFH descriptions and maps. We set a timeline that worked for all parties and agreed on the content to be reviewed and the methods, and this was well communicated and executed in an approachable process for the reviewers. In past EFH 5-year Reviews, current EFH descriptions and maps in the FMPs were provided to stock assessment authors with the new EFH maps for review. In this EFH Review, as the SDM ensemble EFH methods represent a significant advancement over the 2017 SDM EFH approach, and expert peer review is an important part of the iterative EFH 5-year Review process; we provided the stock assessment authors with the complete set of regional SDM ensemble EFH methods (3 regions) and species results chapters (118 chapters). Stock

assessment authors are considered subject matter experts whose input was used to ground truth EFH information, including improving the modeling methodology in general and for their species. We recommend that an agreement be reached at the beginning of next 5-year review regarding the process and scope for stock-assessment author review in a way that remains feasible for the EFH analytical team.

Communicate confidence in EFH designations

In 2021, the SSC recommended that analysts define thresholds for excluding or denoting areas where uncertainty is high (e.g., report the ratio of estimated response to uncertainty). This would allow scientists to communicate areas where confidence in the EFH designations was high versus low. Propagating uncertainty through the existing EFH maps in this way is unclear and may lead to "patchy" maps that are more difficult to communicate with stakeholders and regional managers. Additionally, the coefficients of variation (CVs) from cross-validation that we reported in the present results largely track abundance predictions from SDMs, as areas with high abundance tend to have high uncertainty when abundance is Poisson-distributed. Future studies should evaluate uncertainty and find ways to communicate uncertainty in SDM predictions; determine where uncertainty in untrawled/untrawlable areas differs from that in trawled/trawlable areas, and evaluate how these designations might be successfully communicated and addressed in EFH descriptions.

Develop thresholds for EFH mapping and test them

Another aspect where the EFH 5-year Review process and communication can be strengthened is the scientific guidance that informs the various thresholds applied to map EFH from SDMs and evaluate these EFH maps with the fishing effects model (SASI model; Smeltz et al. 2019) and subsequent analysis of stock level impacts by the stock assessment authors (Simpson et al. 2017). Also, conceptual frameworks should be considered in the future for developing, evaluating, and utilizing EFH descriptions and maps within the EFH Regulations (see above section "Increase Scope and Applicability of EFH Research"). We recommend forming a Work Group to develop and communicate scientific guidance on both of these aspects to the SSC prior to the start of the next EFH 5-year Review.

Add more opportunities for communication

Monitoring research, process research, and model development should be coordinated to target knowledge gaps about the relationship between habitat, fishing, and fishery productivity. This coordination should occur across divisions and include conversations with researchers who work outside the existing EFH areas in cases where species ranges are suspected to be shifting. Ongoing conversations with stakeholders about management priorities, risk tolerance, and tradeoffs will help frame process and modeling studies (Thorson et al. 2021). With consistent stakeholder involvement, simulation approaches such as management strategy evaluation (MSE; Punt et al. 2016, Smith 1994) can be used to compare the performance of different management strategies and data collection practices (like survey frequency) under various degrees of uncertainty, including process and model uncertainty.

Streamline workflows and reproducibility

Further improvement of communication about data and code can be achieved with currently available tools. For the next EFH 5-year Review, we recommend augmenting the existing review process with more best practices for open data science, sharing code with reviewers and collaborators, and creating more reproducible workflows to streamline the EFH process (e.g., Lowndes et al. 2017). These changes should include producing reproducible code, making covariate/raster data available through NCEI[64] ERDDAP[65] and AKFIN[66], and automating the generation of EFH reports and presentation slides using Markdown to streamline the creation of EFH products. Reproducible code practices should include the production of an R package for the EFH SDMs so that scientists with species distribution data can easily test model improvements and new data sources instead of waiting for EFH analysts to carry out these comparisons. When data or modeling approaches need to be modified for select species (first section of this chapter), they can be adjusted just for those species, while others are only updated with new data each EFH cycle. Tracking comments and changes to the models, making code available to stock

[64] https://www.ncei.noaa.gov/
[65] https://coastwatch.pfeg.noaa.gov/erddap/index.html
[66] https://akfin.psmfc.org/

assessment authors, and automating some of the map and report generation processes will improve transparency and speed up the generation of EFH products.

Conclusions

We have identified several areas where Essential Fish Habitat research can be advanced in the coming EFH 5-year Review cycles (Table 80). Further work in these areas will identify better SDMs or SDM ensembles for defining EFH, especially for species with less available trawl data. Combining additional species data sources in the SDMs that will add value to the EFH maps will also require additional research to develop the methods to do this well. Advancements in many of the areas we describe here are connected to other topics; for example, the development of approaches for quantifying and describing uncertainty in EFH maps (see the "Modeling" section) will also improve Process and Communication, providing a straightforward way of communicating uncertainty to stock assessment authors and the Council.

The studies recommended here will take longer than one EFH 5-year Review cycle, so some care should be taken to identify priorities for data collection, data setup, and model development. We identify next steps needed for projects involving new covariates in Table 2 and areas where cross-disciplinary collaboration will be especially helpful in Table 80. Cross-divisional collaborations will expand the suite of covariate data that can be incorporated into EFH models and provide a basis for ongoing discussions about ecosystem structure and function as they relate to EFH. Modeling advancements will provide ways to use existing data, account for processes that affect multiple life stages, and account for environmental drivers mechanistically. Finally, discussions with stakeholders and modelers can form a strong foundation for the design of simulation studies that assess the impacts of management decisions on EFH species.

Table 101. -- Summary table of future recommendations for EFH research to advance EFH component 1 descriptions and maps, and how EFH component 1 outputs are evaluated and applied to management.

Area of research	Improvement/advancement	Taxa with potential EFH improvement
Prioritize and improve EFH for select species	Leverage existing species distribution data to expand spatial scope and improve predictions in existing EFH maps	Subset of species where higher-quality EFH information is needed
	Leverage environmental data	All (especially species where higher-quality EFH information is needed)
	Improve life history information with best available science to the extent that the available survey data sets can handle this	All (especially crab species)
	Expand and improve existing SDM EFH mapping to include species and life stages in the nearshore (e.g., at appropriate spatial resolutions)	Many EFH species and their prey that inhabit nearshore habitats
	Develop methodology for combining disparate datasets (e.g., survey/gear intercalibration)	Subset of species where higher-quality EFH information is needed
	Develop process studies to inform EFH descriptions and maps (e.g., vital rates, movement, population dynamics)	All
	Consider diverse constituent models and/or other techniques such as joint species distribution models (jSDM)	Subset of species where higher-quality EFH information is needed; especially those with EFH level 1 information only

Increase scope and applicability of EFH research	Describe prey species habitat (EFH component 7)	Most groundfish, especially those with diets more specialized on forage
	Expand to EFH Levels 3 and 4	All
	Continue to advance and apply dynamic SDM methods in development to map and forecast shifts in EFH and spatial stock structure to improve climate responsive approaches to EFH and EBFM	All
Improve process and communication	Communicate confidence in EFH designations/boundaries	All
	Develop thresholds for mapping EFH with SDMs and SDM EFH applied to the EFH component 2 Fishing Effects Evaluation (e.g., thresholds applied), through research and an expert work group, and communicate this guidance to the SSC prior to the launch of the next EFH 5-year Review. 1-2 SSC members may be interested in joining this team.	All
	Add more opportunities for communication and continually improve communication	All
	Streamline workflows and reproducibility.	All

ACKNOWLEDGEMENTS

We thank Lyle Britt and Stan Kotwicki of the NMFS AFSC Groundfish Assessment Program for their strong support of this work. We wish to thank Gretchen Harrington, Jim Thorson, Cheryl Barnes, Ken Coyle, and Al Hermann for their insightful reviews and important contributions. This work was greatly improved by the time and energy invested by all the stock assessment authors and species experts who contributed to the review of this document. This project was funded by the AKRO/AFSC Essential Fish Habitat Research Plan.

CITATIONS

Abookire, A. A., and B. J. Macewicz. 2003. Latitudinal variation in reproductive biology and growth of female Dover sole (*Microstomus pacificus*) in the North Pacific, with emphasis on the Gulf of Alaska stock. J. Sea Res. 57: 198–208.

Abookire, A. A. 2006. Reproductive biology, spawning season, and growth of female rex sole (*Glyptocephalus zachirus*) in the Gulf of Alaska. Fish. Bull. 104 (3): 350–359.

Abookire, A. A., and K. M. Bailey. 2007. The distribution of life cycle stages of two deep-water pleuronectids, Dover sole (*Microstomus pacificus*) and rex sole (*Glyptocephalus zachirus*), at the northern extent of their range in the Gulf of Alaska. J. Sea Res. 50: 187–197.

Abookire, A. A., J. T. Duffy-Anderson, and C. M. Jump. 2007. Habitat associations and diet of young-of-the-year Pacific cod (*Gadus macrocephalus*) near Kodiak. Alaska. Mar. Biol. 150: 713–726.

Ainsley, S. M., D. A. Ebert, and G. M. Cailliet. 2011. A comparison of reproductive parameters of the Bering skate, *Bathyraja interrupta*, from two Alaskan large marine ecosystems. Mar. Fresh. Res. 62: 557–566.

Allen, M. J., and G. B. Smith. 1988. Atlas and zoogeography of common fishes in the Bering Sea and northeastern Pacific. NOAA Technical Report NMFS-66.

Araujo, M. B., and M. New. 2007. Ensemble forecasting of species distributions. Trends Eco. Evo., 22 (1): 42–47. https://doi.org/10.1016/j.tree.2006.09.010

Bailey, K. M., A. A. Abookire, and J. T. Duffy-Anderson. 2008. Ocean transport paths for the early life history stages of offshore-spawning flatfishes: a case study in the Gulf of Alaska. Fish Fisher. 9: 44–66.

Bailey, K. M., P. J. Stabeno, and D. A. Powers. 1997. The role of larval retention and transport features in mortality and potential gene flow of walleye pollock. J. Fish. Biol. 51 (Suppl. A): 135–154.

Barbeaux, S., B. Ferriss, W. Palsson, S. K. Shotwell, I. Spies, M. Wang, and S. Zador. 2020. Assessment of Pacific cod stock in the Gulf of Alaska. ***In*** Stock Assessment and Fishery Evaluation Report for the Groundfish Resources of the Gulf of Alaska. North Pacific Fishery Management Council, 1007 West Third, Suite 400 Anchorage, AK 99501.

Barnes, C. L., A. H. Beaudreau, M. W. Dorn, K. K. Holsman, and F. J. Mueter. 2020. Development of a predation index to assess trophic stability in the Gulf of Alaska. Ecol. App. 30 (7): e02141. https://doi.org/10.1002/eap.2141.

Barnes, C. L., T. E. Essington, J. L. Pirtle, C. N. Rooper, E. A. Laman, K. K. Holsman, K. Y. Aydin, and J. T. Thorson. 2022. Climate-informed models benefit hindcasting but present challenges when forecasting species–habitat associations. Ecography. 2022: e06189. https://doi.org/10.1111/ecog.06189.

Barry, S. C., and A. H. Welsh 2002. Generalized additive modeling and zero inflated count data. Ecol. Model. 157: 179–188.

Best, D. J., and D. E. Roberts. 1975. Algorithm AS 89: the upper tail probabilities of Spearman's rho. Appl. Stat. 24: 377–379.

Boldt, J. L., T. W. Buckley, C. N. Rooper, and K. Aydin. 2012 Factors influencing cannibalism and abundance of walleye pollock (*Theragra chalcogramma*) on the eastern Bering Sea shelf, 1982-2006. Fish. Bull. 110 (3): 293−306.

Bosley, K. L., J. W. Lavelle, R. D. Brodeur, W. W. Wakefield, R. L. Emmett, E. T. Baker, and K. M. Rehmke. 2004. Biological and physical processes in and around Astoria submarine Canyon, Oregon, USA. Journal of Marine Systems. 50: 21–37.

Brewer, R.S. and B.L. Norcross. 2012. Long-term retention of internal elastomer tags in a wild population of North Pacific giant octopus (*Enteroctopus dofleini*), Fish. Res. 134-136: 17–20. https://doi.org/10.1016/j.fishres.2012.07.020.

Brodeur, R. D. 2001. Habitat-specific distribution of Pacific ocean perch (*Sebastes alutus*) in Pribilof Canyon, Bering Sea. Continent. Shelf Res. 21: 207–224.

Brodeur, R. D. and W. G. Pearcy. 1986. Distribution and relative abundance of pelagic non salmonid nekton off Oregon and Washington, 1979-1984. NOAA Tech. Rep. NMFS-46.

Buckley, T. W., A. Greig, and J. L. Boldt. 2009. Describing summer pelagic habitat over the continental shelf in the eastern Bering Sea, 1982-2006. NOAA Tech. Memo. NMFS-AFSC-196.

Burnham, K. P. and Anderson, D. R., 2002. A practical information-theoretic approach. Model selection and multimodel inference, Second Edition.

Carlson, H. R., and R. R. Straty. 1981. Habitat and nursery grounds of Pacific rockfish, *Sebastes* spp., in rocky coastal areas of Southeastern Alaska. Mar. Fish. Rev. 43: 13–19.

Carlson, P. R., T. R. Bruns, B. F. Molnia, and W. C. Schwab. 1982. Submarine valleys in the northeastern Gulf of Alaska: Characteristics and probable origin. Mar. Geol. 47: 217–242. https://doi:10.1016/0025-3227(82)90070-6.

Chilton, E. 2007. Maturity of female northern rockfish *Sebastes polyspinis* in the central Gulf of Alaska. Ak. Fish. Res. Bull. 12: 264–269. https://www.adfg.alaska.gov/static/home/library/PDFs/afrb/chilv12n2.pdf.

Chilton, E. A. 2010. Maturity and growth of female dusky rockfish (*Sebastes variabilis*) in the central Gulf of Alaska. Fish. Bull. 108 (1): 70–78.

Ciannelli, L., R. D. Brodeur, and J. M. Napp. 2004. Foraging impact on zooplankton by age-0 walleye pollock (*Theragra chalcogramma*) around a front in the southeast Bering Sea. Mar. Biol. 144 (3): 515–526.

Ciannelli, L., P. Fauchald, K. S. Chan, V. N. Agostini, and G. E. Dingsør. 2008. Spatial fisheries ecology: recent progress and future prospects. J. Mar. Sys. 71 (3-4): 223–236.

Clausen, D. M., and J. Heifetz. 2002. The northern rockfish, *Sebastes polyspinis*, in Alaska: Commercial fishery, distribution, and biology. Mar. Fish. Rev. 64: 1–28.

Cochran, W. G. 1977. Sampling Techniques. 3rd ed. Wiley Series in Probability and Mathematical Statistics - Applied. John Wiley & Sons. N.Y., NY 428 p.

Conrath, C. L. 2017. Maturity, spawning omission, and reproductive complexity of deepwater rockfish. Trans. Am. Fish. Soc. 146: 495–507.

Conrath, C. L., and M. E. Conners. 2014. Aspects of the reproductive biology of the North Pacific giant octopus (*Enteroctopus dofleini*) in the Gulf of Alaska. Fish. Bull. 112 (4): 253–260.

Copeman, L. A., B. J. Laurel, M. Spencer, and A. Sremba. 2017. Temperature impacts on lipid allocation among juvenile gadid species at the Pacific Arctic-Boreal interface: an experimental laboratory approach. Mar. Ecol. Prog. Ser. 566: 183–198.

Coyle, K. O., A. J. Hermann, and R. R. Hopcroft. 2019. Modeled spatial-temporal distribution of productivity, chlorophyll, iron and nitrate on the northern Gulf of Alaska shelf relative to field observations. Deep-Sea Res. II. 165: 163–191.

Cragg, J. G. 1971. Some statistical models for limited dependent variables with application to the demand for durable goods. Econometrica. 39: 829–844.

Daly, B, Parada, C, Loher, T, Hinckley, S, Hermann, AJ, Armstrong, D. Red king crab larval advection in Bristol Bay: Implications for recruitment variability. Fish Oceanogr. 2020; 29: 505– 525. https://doi.org/10.1111/fog.12492.

Danielson, S., E. Curchitser, K. Hedstrom, T. Weingartner, and P. Stabeno. 2011. On ocean and sea ice modes of variability in the Bering Sea. J. Geophys. Res. 116: https://doi: 10.1029/2011JC007389.

Diggle, P. J., and P. J. Ribeiro Jr. 2002. Bayesian inference in Gaussian model-based geostatistics. Geo. Environ. Model. 6 (2): 129–146.

Dolan, M. F. J., A. J. Grehan, J. C. Guinan, and C. Brown, C. 2008. Modelling the local distribution of cold-water corals in relation to bathymetric variables: Adding spatial context to deep-sea video data. Deep-Sea Research Part I-Oceanographic Research Papers. 55 (11): 1564–1579. https://doi.org/10.1016/j.dsr.2008.06.010.

Dolan, M. F. J., and V. L. Lucieer. 2014. Variation and Uncertainty in Bathymetric Slope Calculations Using Geographic Information Systems. Marine Geodesy. 37 (2): 187–219. https://doi.org/10.1080/01490419.2014.902888.

Dorn, M. W., A. L. Deary, B. E. Fissel, D. T. Jones, M. Levine, A. L. McCarthy, W. A. Palsson, L. A. Rogers, S. K. Shotwell, K. A. Spalinger, K. Williams, and S. G. Zador. 2020. Assessment of the Walleye Pollock Stock in the Gulf of Alaska. ***In*** Stock Assessment and Fishery Evaluation Report for the Groundfish Resources of the Gulf of Alaska. North Pacific Fishery Management Council, 1007 West Third, Suite 400 Anchorage, AK 99501.

Doyle, M. J., C. Debenham, S. J. Barbeaux, T. W. Buckley, J. L. Pirtle, I. B. Spies, W. T. Stockhausen, S. K. Shotwell, M. T. Wilson, and D. W. Cooper. 2018. A full life history synthesis of Arrowtooth flounder ecology in the Gulf of Alaska: Exposure and sensitivity to potential ecosystem change. J. Sea Res. 142: 28–51.

Doyle, M. J., S. L. Stromb, K. O. Coyle, A. J. Hermann, C. Ladd, A. C. Matarese, S. K. Shotwell, and R. R. Hopcroft. 2019. Early life history phenology among Gulf of Alaska fish species: Strategies, synchronies, and sensitivities. Deep-Sea Res. II 165: 41–73.

Duchon, J. 1977. Splines minimizing rotation-invariant semi-norms in Solobev spaces. ***In*** W. Shemp and K. Zeller (eds) Construction theory of functions of several variables. Springer, Berlin. 85-100.

Ebert, D. A. 2005. Reproductive biology of skates, *Bathyraja* (Ishiyama), along the eastern Bering Sea continental slope. J. Fish Biol. 66 (3): 618–649.

Ebert, D. A., W. D. Smith, D. L. Haas, S. M. Ainsley, and G. M. Cailliet. 2007. Life history and population dynamics of Alaskan skates: providing essential biological information for effective management of bycatch and target species. Final Report to the North Pacific Research Board, Project 510.

Ebert, D. A., W. D. Smith, and G. M. Cailliet. 2008. Reproductive biology of two commercially exploited skates, *Raja binoculata* and *R. rhina*, in the western Gulf of Alaska. Fish. Res. 94 (1): 48–57.

Ebert, D. A., T. W. White, K. J. Goldman, L. J. V. Compagno, T. S. Daly-Engel, and R. D. Ward. 2010. Resurrection and redescriptions of *Squalus suckleyi* (Girard, 1854) from the North Pacific, with comments on the *Squalus acanthias* subgroup (Squaliformes: Squalidae). Zootaxa. 2612: 22–40.

Echave, K. B., D. H. Hanselman, and N. E. Maloney. 2013. Report to industry on the Alaska sablefish tag program, 1972 - 2012. U.S. Dep. Commer., NOAA Tech. Memo. NMFS-AFSC-254, 47 p. Accessed at: https://repository.library.noaa.gov/view/noaa/4434/noaa_4434_DS1.pdf.

Echave, K. B., and P. J. F. Hulson. 2019. Assessment of the Shortraker Rockfish Stock in the Gulf of Alaska. ***In*** Stock assessment and fishery evaluation report for the groundfish resources of the GOA and BS/AI. North Pacific Fishery Management Council, 1007 West Third, Suite 400 Anchorage, AK 99501.

Egbert, G. D., and Erofeeva, S. Y. 2002. Efficient inverse Modeling of barotropic ocean tides. Journal of Atmospheric and Oceanic Technology. 19: 183–204.

Elith, J., S. J. Phillips, T. Hastie, M. Dudík, Y. E. Chee, and C. J. Yates. 2011. A statistical explanation of MaxEnt for ecologists. Divers. Distrib. 17: 43–57.

Fenske, K. H., P. J. F. Hulson, B. Williams, and C. A. O'Leary. 2020. Assessment of the Dusky Rockfish stock in the Gulf of Alaska. ***In*** Stock assessment and fishery evaluation report for the groundfish resources of the GOA and BS/AI. North Pacific Fishery Management Council, 1007 West Third, Suite 400 Anchorage, AK 99501.

Fisheries Leadership and Sustainability Forum. 2016. Regional EFH Profile: North Pacific. National Essential Fish Habitat Summit, 2016. https://www.fisheriesforum.org/our-work/special-projects/efh-summit/efh-profiles/.

Fithian, W., J. Elith, T. Hastie, and D. A. Keith. 2015. Bias correction in species distribution models: pooling survey and collection data for multiple species. Meth. Ecol. Evol. 6: 424–438. https://doi: 10.1111/2041-210X.12242.

Gharrett, A. J., A. P. Matala, E. L. Peterson, A. K. Gray, Z. Li, and J. Heifetz. 2005. Two genetically distinct rougheye rockfish sibling species differ phenotypically? Trans. Am. Fish. Soc. 135: 792–800.

Gibson, G.A., W.T., Stockhausen, K.O. Coyle, S. Hinckley, C. Parada, A.J. Hermann, M. Doyle, and C. Ladd. 2019. An individual-based model for sablefish: Exploring the connectivity between potential spawning and nursery grounds in the Gulf of Alaska. Deep-Sea Res. Pt. II. 165: 89–112.

Goethel, D. R., D. H. Hanselman, C. J., Rodgveller, K. H. Fenske, S. K. Shotwell, K. B. Echave, P. W. Malecha, K. A. Siwicke, and C. R. Lunsford. 2020. Assessment of the sablefish stock in Alaska. ***In*** Stock assessment and fishery evaluation report for the groundfish resources of the GOA and BS/AI. North Pacific Fishery Management Council, 1007 West Third, Suite 400 Anchorage, AK 99501.

Golden, N. E., J. A. Reid, M. Zimmermann, E. N. Lowe, and A. S. Hansen. 2016. Digitized seafloor characterization data from the Gulf of Alaska: U.S. Geological Survey: Santa Cruz, CA, USA, https://dx.doi.org/10.5066/F7CV4FT9.

Goldstein, E. D., J. L. Pirtle, J. T. Duffy-Anderson, W. T. Stockhausen, M. Zimmermann, M. T. Wilson, and C.W. Mordy. 2020. Eddy retention and seafloor terrain facilitate cross-shelf transport and

delivery of fish larvae to suitable nursery habitats. Limnol. Oceanogr. 65: 2800–2818. https://doi: 10.1002/lno.11553.

Grüss, A., Thorson, J. T., Carroll, G., Ng, E. L., Holsman, K. K., Aydin, K., Kotwicki, S., Morzaria-Luna, H. N., Ainsworth, C. H., & Thompson, K. A. (2020). Spatio-temporal analyses of marine predator diets from data-rich and data-limited systems. Fish and Fisheries. 21 (4): 718–739. https://doi.org/10.1111/faf.12457.

Grüss, A., Thorson, J. T., Stawitz, C. C., Reum, J. C. P., Rohan, S. K., & Barnes, C. L. (2021a). Synthesis of interannual variability in spatial demographic processes supports the strong influence of cold-pool extent on eastern Bering Sea walleye pollock (*Gadus chalcogrammus*). Progress in Oceanography. 194: 102569. https://doi.org/10.1016/j.pocean.2021.102569.

Grüss, A., J. L. Pirtle, J. T. Thorson, M. R. Lindeberg, A. D. Neff, S. G. Lewis, and T. E. Essington. 2021. Modeling nearshore fish habitats using Alaska as a regional case study. Fish. Res. 238. https://doi: 10.1016/j.fishres.2021.105905.

Guisan, A., S. Weiss, and A. Weiss. 1999. GLM versus CCA spatial modeling of plant species distribution. Plant Ecol. 143: 107–122.

Guisan, A., N. E. Zimmermann, J. Elith, C. H. Graham, S. Phillips, and A. T. Peterson. 2007. What matters for predicting the occurrences of trees: techniques, data, or species' characteristics?. Ecol. Monogr. 77: 615–630. https://doi.org/10.1890/06-1060.1.

Haas, D. L., D. A. Ebert, and G. M. Cailliet. 2016. Comparative age and growth of the Aleutian skate, *Bathyraja aleutica*, from the eastern Bering Sea and Gulf of Alaska. Env. Biol. Fish. 99: 813–828.

Hannah, R., Parker, S., and Fruth, E. 2002. Length and age at maturity of female petrale sole (*Eopsetta jordani)* determined from samples collected prior to spawning aggregation. U.S. Fish Bulletin 100: 711–719.

Hanselman, D. H., T. J. Quinn II, C. Lunsford, J. Heifetz, and D. M. Clausen. 2001. Spatial implications of adaptive cluster sampling on Gulf of Alaska rockfish. ***In*** Proceedings of the 17th Lowell-Wakefield Symposium: Spatial Processes and Management of Marine Populations, pp. 303-325. Univ. Alaska Sea Grant Program, Fairbanks, AK.

Hanselman, D. H., Rodgveller, C. J., Fenske, K. H., Shotwell, S. K., Echave, K. B., Malecha, P. W., and Lunsford, C. R., 2019. Assessment of the sablefish stock in Alaska. ***In*** Stock Assessment and Fishery Evaluation Report for the Groundfish Resources of the Gulf of Alaska. North Pacific Fishery Management Council, 1007 West Third, Suite 400 Anchorage, AK 99501.

Hart, J. L. 1973. Pacific Fishes of Canada. Canadian Government Publishing Centre, Supply and Services Canada, Ottawa, Canada KIA OS9

Hastie, T. J., and R. J. Tibshirani. 1990. Generalized Additive Models. Monogr. Stat. Appl. Prob. 43. 338 p.

Hastie, T., R. J. Tibshirani, and J. H. Friedman. 2009. The Elements of Statistical Learning: Data Mining, Inference, and Prediction. Second edition. Springer, Berlin, Germany.

Hawley, J. H. 1931. Hydrographic Manual; U.S. Department of Commerce, U.S. Coast and Geodetic Survey, Special Publication No. 143; U.S. Government Printing Office: Washington, DC, USA.

Heifetz, J., and J. T. Fujioka. 1991. Movement dynamics of tagged sablefish in the northeastern Pacific. Fish. Res. 11: 355–374.

Hinckley, S., W. Stockhausen, K. Coyle, B. Laurel, G. Gibson, C. Parada, A. Hermann, M. Doyle, and T. Hurst. 2019. Connectivity between spawning and nursery areas for Pacific cod (*Gadus macrocephalus*) in the Gulf of Alaska. Deep Sea Res. Pt. II. 165-113-126.

Hoff, G. R. 2009. Embryo developmental events and the egg case of the Aleutian skate *Bathyraja aleutica* (Gilbert) and the Alaska skate *Bathyraja parmifera* (Bean). J. Fish. Biol. 74 (3): 438–501.

Hollowed, A. B., E. Brown, P. Livingston, B. Megrey, I. Spies, and C. Wilson. 1995. Walleye pollock. ***In*** Stock Assessment and Fishery Evaluation Report for the 1996 Gulf of Alaska Groundfish Fishery. North Pacific Fishery Management Council, 1007 West Third, Suite 400 Anchorage, AK 99501.

Hollowed, A. B., J. N. Ianelli, and P. A. Livingston. 2000. Including predation mortality in stock assessments: A case study involving Gulf of Alaska walleye pollock. ICES J. Mar. Sci. 57: 279–293.

Horn, B. K. P. 1981. Hill shading and the reflectance map. Proc. IEEE. 69: 14–47.

Hosmer, D. W., and S. Lemeshow. 2005. Assessing the Fit of the Model. *In* Applied Logistic Regression, Second Edition edn, pp. 143-202. John Wiley and Sons, Inc., Hoboken, NJ, USA, 07030.

Howell, K. L., R. Holt, I. P. Endrino, and H. Stewart. 2011. When the species is also a habitat: comparing the predictively modelled distributions of *Lophelia pertusa* and the reef habitat it forms. Biol. Conserv. 144: 2656–2665.

Hulson, P. J. F., C. R. Lunsford, B. Fissel, and D. Jones. 2020. Assessment of the Pacific ocean perch stock in the Gulf of Alaska. ***In*** Stock Assessment and Fishery Evaluation Report for the Groundfish Resources of the Gulf of Alaska. North Pacific Fishery Management Council, 1007 West Third, Suite 400 Anchorage, AK 99501.

Hurst, T. P. *In preparation.* Temperature-dependent growth rates for juvenile flatfishes. Thomas.Hurst@noaa.gov.

Ito, D. H. 1999. Assessing shortraker and rougheye rockfishes in the GOA: addressing a problem of habitat specificity and sampling capability. Ph.D. Dissertation, Univ. Washington, Seattle. 205 pp.

Jackson, D. A. and M. P. Ruccio. 2003. Kodiak, Chignik, and South Peninsula shrimp fisheries and their management: A report to the Alaska Board of Fisheries. https://www.adfg.alaska.gov/FedAidPDFs/rir.4k.2003.07.pdf

Johnson, S. W., A. D. Neff, J. F. Thedinga, M. R. Lindeberg, and J. M. Maselko. 2012. Atlas of nearshore fishes of Alaska: A synthesis of marine surveys from 1998 to 2011. NOAA Tech. Memo. NMFS-AFSC-239. 261 pp.

Jones, D., C. N. Rooper, C. D. Wilson, P. D. Spencer, D. H. Hanselman, and R. E. Wilborn. 2021. Estimates of availability and catchability for select rockfish species based on acoustic-optic surveys in the Gulf of Alaska. Fish. Res. 236.

Jorgensen, E.M. 2009. Field guide to squids and octopods of the eastern North Pacific and Bering Sea. Alaska Sea Grant Pub. No. SG-ED-65, 100 pp.

Kendall, A. W., and A. C. Matarese. 1987. Biology of eggs, larvae, and epipelagic juveniles of sablefish, *Anoplopoma fimbria*, in relation to their potential use in management. Mar. Fish. Rev. 49: 1–13.

Knight, C. A., C. C. Cheng, and A. L. DeVries. 1991. "Adsorption of Alpha-Helical Antifreeze Peptides on Specific Ice Crystal Surface Planes." Biophysical Journal 59 (2): 409–18. https://doi.org/10.1016/S0006-3495(91)82234-2.

Kotwicki, S., Lauth, R.R., Williams, K., Goodman, S.E., 2017. Selectivity ratio: A useful tool for comparing size selectivity of multiple survey gears. Fisheries Research 191, 76–86. https://doi.org/10.1016/j.fishres.2017.02.012.

Kotwicki, S., Ressler, P.H., Ianelli, J.N., Punt, A.E., Horne, J.K., 2018. Combining data from bottom-trawl and acoustic-trawl surveys to estimate an index of abundance for semipelagic species. Can. J. Fish. Aquat. Sci. 75, 60–71. https://doi.org/10.1139/cjfas-2016-0362.

Kramer, D. E., and V. M. O'Connell. 1988. A Guide to Northeast Pacific Rockfishes: Genera *Sebastes* and *Sebastolobus*. ***In*** Alaska Sea Grant Advisory Bulletin 25. National Marine Fisheries Service 2001(a).

Krieger, K. J. and D. H. Ito. 1999. Distribution and abundance of shortraker rockfish, *Sebastes borealis*, and rougheye rockfish, *S. aleutianus*, determined from a manned submersible. Fish. Bull. 97: 264–272.

Krieger, K. J., and B. L. Wing. 2002. Megafauna associations with deepwater corals (*Primnoa* spp.) in the Gulf of Alaska. Hydrobiologia 471: 83–90.

Laman, E. A., C. N. Rooper, K. Turner, S. Rooney, D.W. Cooper, and M. Zimmermann. 2017. Model-based essential fish habitat definitions for Bering Sea groundfish species. U.S. Dep. Commer., NOAA Tech. Memo. NMFS-AFSC-357, 265 p.

Laman, E.A., C.N. Rooper, K. Turner, S. Rooney, D.W. Cooper, and M. Zimmermann. 2018. Using species distribution models to describe essential fish habitat in Alaska. Can. J. Fish. Aquat. Sci. 75 (8): 1230–1255. https://doi.org/10.1139/cjfas-2017-0181.

Lamb, A. and P. Edgell. 2010. Coastal fishes of the Pacific northwest. Second edition. Madeira Park, BC, Canada: Harbor Publishing Co. Ltd., 335 p.

Laurel, B. J., A. W. Stoner, C. H. Ryer, T. P. Hurst, and A. A. Abookire. 2007. Comparative habitat associations in juvenile Pacific cod and other gadids using seines, baited cameras and laboratory techniques. J. Exp. Mar. Biol. Ecol. 351: 42–55.

Laurel, B. J., C. H. Ryer, B. Knoth, and A. W. Stoner. 2009. Temporal and ontogenetic shifts in habitat use of juvenile Pacific cod (*Gadus macrocephalus*). J. Exp. Mar. Biol. Ecol. 377 (1): 28–35.

Laurel, B. J., M. Spencer, P. Iseri, and L. A. Copeman. 2016. Temperature-dependent growth and behavior of juvenile Arctic cod (*Boreogadus saida*) and co-occurring North Pacific gadids. Polar Biology 39: 1127–1135. https://doi/10.1007/s00300-015-1761-5.

Lauth, R. R., S. W. McEntire, and H. H. Zenger. 2007. Geographic Distribution, Depth Range, and Description of Atka Mackerel *Pleurogrammus monopterygius* Nesting Habitat in Alaska. AK Fish. Res. Bull. 12: 165–186.

Legendre, P. and L. Legendre. 2012. Numerical Ecology, Volume 24 - 3rd Edition. Elsevier. https://www.elsevier.com/books/numerical-ecology/legendre/978-0-444-53868-0

Love, M. S., M. Yoklavich, and L. Thorsteinson. 2002. The rockfishes of the Northeast Pacific. University of California Press, Berkeley and Los Angeles. 404 pgs.

Lowe, S. 2019. Assessment of the Atka mackerel stock in the Gulf of Alaska. ***In*** Stock Assessment and Fishery Evaluation Report for the Groundfish Resources of the Gulf of Alaska. North Pacific Fishery Management Council, 1007 West Third, Suite 400 Anchorage, AK 99501.

Lowndes, J.S.S., Best, B.D., Scarborough, C., Afflerbach, J.C., Frazier, M.R., O'Hara, C.C., Jiang, N., Halpern, B.S., 2017. Our path to better science in less time using open data science tools. Nat Ecol Evol 1: 1–7. https://doi.org/10.1038/s41559-017-0160.

Malecha, P.W., D.H. Hanselman, and J. Heifetz. 2007. Growth and mortality of rockfish (Scorpaenidae) from Alaska waters. U.S. Dept. Commer., NOAA Tech. Memo. NMFS F/AFSC-172. 61 p.

Manel, S., Williams, H. C., and Ormerod, S. J. 2001. Evaluating presence-absence models in ecology: the need to account for prevalence. Journal of Applied Ecology, 38: 921–931. Blackwell Science Ltd, Oxford.

McCullagh, P., and J. A. Nelder. 1989. Generalized Linear Models (2nd edition)*,* Chapman and Hall, London, UK. 511 pp. ISBN 0-412-31760-5

McDermott, S. F., and S. A. Lowe. 1997. The reproductive cycle and sexual maturity of Atka mackerel, *Pleurogrammus monopterygius*, in Alaska waters. Fish. Bull., U.S. 95: 321–333.

McGilliard, C. R., and W. Palsson. 2017. Assessment of the rex sole stock in the Gulf of Alaska. ***In*** Stock Assessment and Fishery Evaluation Report for the Groundfish Resources of the Gulf of Alaska. North Pacific Fishery Management Council, 1007 West Third, Suite 400 Anchorage, AK 99501.

McGilliard, C. R., W. Palsson, A. Havron, and S. Zador. 2019. Assessment of the deepwater flatfish stock complex in the Gulf of Alaska. ***In*** Stock Assessment and Fishery Evaluation Report for the Groundfish Resources of the Gulf of Alaska. North Pacific Fishery Management Council, 1007 West Third, Suite 400 Anchorage, AK 99501.

McGowan, D.W., Horne, J.K., Thorson, J.T., Zimmermann, M., 2019. Influence of environmental factors on capelin distributions in the Gulf of Alaska. *Deep Sea Research Part II: Topical Studies in Oceanography, Understanding Ecosystem Processes in the Gulf of Alaska*: Volume 2 165, 238–254. https://doi.org/10.1016/j.dsr2.2017.11.018

Mecklenburg, C. W., T. A. Mecklenburg, and L. K. Thorsteinson. 2002. Fishes of Alaska. American Fisheries Society, Bethesda, MD.

Mienis, F., H. C. de Stigter, M. White, G. Duineveld, H. de Haas, and T. C. E. van Weering. 2007. Hydrodynamic controls on cold-water coral growth and carbonate-mound development at the SW and SE Rockall Trough Margin, NE Atlantic Ocean. Deep Sea Research Part I: Oceanographic Research Papers, 54 (9): 1655–1674. https://doi.org/http://dx.doi.org/10.1016/j.dsr.2007.05.013.

Monnahan, C.C., Thorson, J.T., Kotwicki, S., Lauffenburger, N., Ianelli, J.N., Punt, A.E., 2021. Incorporating vertical distribution in index standardization accounts for spatiotemporal availability to acoustic and bottom trawl gear for semi-pelagic species. *ICES Journal of Marine Science* 78, 1826–1839. https://doi.org/10.1093/icesjms/fsab085

Munk, K. M. 2001. Maximum ages of groundfishes in waters off Alaska and British Columbia and considerations of age determination. Alaska Fish. Res. Bull. 8: 12–21.

National Marine Fisheries Service (NMFS). 2005. Volume I: Final Environmental Impact Statement for Essential Fish Habitat Identification and Conservation in Alaska. https://repository.library.noaa.gov/view/noaa/17391.

Neidetcher, S. K., T. P. Hurst, L. Ciannelli, and E. A. Loggerwell. 2014. Spawning phenology and geography of Aleutian Islands and eastern Bering Sea Pacific cod (*Gadus macrocephalus*). Deep-Sea Res. II: Topical Studies in Oceanography 109: 204–214.

Ng, E. L., Deroba, J. J., Essington, T. E., Grüss, A., Smith, B. E., & Thorson, J. T. (2021). Predator stomach contents can provide accurate indices of prey biomass. *ICES Journal of Marine Science*, *78*(3), 1146–1159. https://doi.org/10.1093/icesjms/fsab026.

O'Connell, V. M., and F. C. Funk. 1987. Age and growth of yelloweye rockfish (*Sebastes ruberrimus*) landed in southeastern Alaska. In Proceedings of the International Rockfish Symposium, 171–185. Alaska Sea Grant Rep. 87–2. Fairbanks.

O'Leary, C. A., Kotwicki, S., Hoff, G. R., Thorson, J. T., Kulik, V. V., Ianelli, J. N., et al. Estimating spatiotemporal availability of transboundary fishes to fishery-independent surveys. Journal of Applied Ecology n/a. https://doi:10.1111/1365-2664.13914.

O'Leary, C. A., Thorson, J. T., Ianelli, J. N., & Kotwicki, S. (2020). Adapting to climate-driven distribution shifts using model-based indices and age composition from multiple surveys in the walleye pollock (*Gadus chalcogrammus*) stock assessment. *Fisheries Oceanography*, *29*(6), 541–557. https://doi.org/10.1111/fog.12494.

Orcutt, H. G. 1950. The life history of the starry flounder *Platichthys stellatus* (Pallas). Calif. Dept. Fish and Game Fish Bull. No. 78, 64 p.

Ormseth, O. A. 2019a. Assessment of the skate stock complex in the Gulf of Alaska. ***In*** Stock Assessment and Fishery Evaluation Report for the Groundfish Resources of the Gulf of Alaska. North Pacific Fishery Management Council, 1007 West Third, Suite 400 Anchorage, AK 99501.

Ormseth, O.A. 2019b. Assessment of the octopus stock complex in the Gulf of Alaska. ***In*** Stock Assessment and Fishery Evaluation Report for the Groundfish Resources of the Gulf of Alaska. North Pacific Fishery Management Council, 1007 West Third, Suite 400 Anchorage, AK 99501.

Ormseth, O. A., and P. D. Spencer. 2011. An assessment of vulnerability in Alaska groundfish. Fish. Res. 112: 127–133.

Orr, J. W. and A. C. Matarese. 2000. Revision of the genus Lepidopsetta Gill, 1862 (Teleostei: Pleuronectidae) based on larval and adult morphology, with a description of a new species from the North Pacific Ocean and Bering Sea. Fish. Bull. 98: 539–582.

Orr, J. W., and J. E. Blackburn. 2004. The dusky rockfishes (Teleostei: Scorpaeniformes) of the North Pacific Ocean: resurrection of *Sebastes variabilis* (Pallas, 1814) and a redescription of *Sebastes ciliatus* (Tilesius, 1813). Fish. Bull., 102 (2): 328–348.

Pearcy, W. G., M. J. Hosie, and S. L. Richardson. 1977. Distribution and duration of pelagic life of larvae of Dover sole, *Microstomus pacificus*; rex sole, *Glyptocephalus zachirus*; and petrale sole, *Eopsetta jordani*, in waters off Oregon. Fish. Bull. 75: 173−183.

Pearson, K. E. and D. R. Gunderson. 2003. Reproductive biology and ecology of shortspine thornyhead rockfish, *Sebastolobus alascanus*, and longspine thornyhead rockfish, *S. altivelis*, from the northeastern Pacific Ocean. Env. Biol. Fish. 67 (2): 117–136.

Phillips S. J., R. P. Anderson, and R. E. Schapire. 2006. Maximum entropy modeling of species geographic distributions. Ecol. Model. 190 (3-4): 231–59.

Phillips, S. J., & Dudík, M. (2008). Modeling of species distributions with Maxent: New extensions and a comprehensive evaluation. Ecography, 31 (2), 161–175. https://doi.org/10.1111/j.0906-7590.2008.5203.x.

Pirtle, J. L. 2005. Habitat-based assessment of structure-forming megafaunal invertebrates and fishes on Cordell Bank, California. 6-10. M.S. thesis, Washington State University. Available at: https://www.benthicecology.org/s/Pirtle-2005-MS_Thesis.pdf.

Pirtle, J. L., T. C. Weber, C. D. Wilson, and C. N. Rooper. 2015. Assessment of trawlable and untrawlable seafloor using multibeam-derived metrics. Methods Oceanogr. 12: 18–35.

Pirtle, J. L., S. K. Shotwell, M. Zimmermann, J. A. Reid, and N. Golden. 2019. Habitat suitability models for groundfish in the Gulf of Alaska. Deep-Sea Res. Pt. II. https://doi:10.1016/j.dsr2.2017.12.005.

Politou, C. Y., G. Tserpes, and J. Dokos. 2008. Identification of deepwater pink shrimp abundance distribution patterns and nursery grounds in the eastern Mediterranean by means of generalized additive modeling. Hydrobiol. 612 (1): 99–107. https://doi:10.1007/s10750-008-9488-8.

Potts, J., and J. Elith. 2006. Comparing species abundance models. Ecol. Model. 199: 153–163.

Porter, S. M. 2005. Temporal and spatial distribution and abundance of flathead sole (*Hippoglossoides elassodon*) eggs and larvae in the western Gulf of Alaska. Fish. Bull. 103: 648–658.

Punt, A.E., Butterworth, D.S., de Moor, C.L., De Oliveira, J.A.A., Haddon, M., 2016. Management strategy evaluation: best practices. Fish and Fisheries 17, 303–334. https://doi.org/10.1111/faf.12104.

R Core Development Team. 2020. R: A Language and Environment for Statistical Computing. R Foundation for Statistical Computing. Vienna, Austria.

Ralston, S. 2005. An assessment of starry flounder off California, Oregon, and Washington. NOAA Fisheries, Southwest Fisheries Science Center.

Rodgveller, C. J., J. W. Stark, K. B. Echave, and P-J. F. Hulson. 2016. Age at maturity, skipped spawning, and fecundity of female sablefish (*Anoplopoma fimbria*) during the spawning season. Fish. Bull. 114 (1): 89–102.

Rodgveller, C. J., K. B. Echave, P-J. F. Hulson, and K. M. Coutré. 2018. Age-at-maturity and fecundity of female sablefish sampled in December of 2011 and 2015 in the Gulf of Alaska. U.S. Dep. Commer., NOAA Tech. Memo. NMFS-AFSC-371, 31 p.

Rohan, S. K., Kotwicki, S., L. L. Britt, E. A. Laman, and K. Aydin. 2020. Deriving apparent optical properties from light measurements obtained using bottom-trawl-mounted archival tags. U.S. Dep. Commer., NOAA Tech. Memo. NMFS-AFSC-403, 91 p.

Rohan, S. K., Kotwicki, S., Kearney, K. A., Schulien, J. A., Laman, E. A., Cokelet, E. D., Beauchamp, D. A., Britt, L. L., Aydin, K. Y., & Zador, S. G. (2021). Using bottom trawls to monitor subsurface water clarity in marine ecosystems. Progress in Oceanography, 194, 102554. https://doi.org/10.1016/j.pocean.2021.102554.

Rooney, S., E. A. Laman, C. N. Rooper, K. Turner, D. W. Cooper, and M. Zimmermann. 2018. Model-based essential fish habitat definitions for Gulf of Alaska groundfish species. U.S. Dep. Commer., NOAA Tech. Memo. NMFS-AFSC-373, 370 p.

Rooper, C. N. 2008. An ecological analysis of rockfish (*Sebastes* spp.) assemblages in the North Pacific Ocean along broad-scale environmental gradients. Fish. Bull. 106: 1–11.

Rooper, C. N., J. L. Boldt, and M. Zimmermann. 2007. An assessment of juvenile Pacific ocean perch (*Sebastes alutus*) habitat use in a deepwater nursery. Estuar. Coastal Shelf Sci. 75: 371–380.

Rooper, C. N., G. R. Hoff, and A. DeRobertis. 2010. Assessing habitat utilization and rockfish (*Sebastes* spp.) biomass on an isolated rocky ridge using acoustics and stereo image analysis. Can. J. Fish. Aquat. Sci. 67 (10): 1658–1670. https://doi.org/10.1139/F10-088.

Rooper, C. N. and M. H. Martin. 2012. Comparison of habitat-based indices of abundance with fishery independent biomass estimates from bottom trawl surveys. Fish. Bull. 110 (1): 21–35.

Rooper, C. N., M. H. Martin, J. L. Butler, D. T. Jones, and M. Zimmerman. 2012a. Estimating species and size composition of rockfishes to verify targets in acoustic surveys of untrawlable areas. Fishery Bulletin 110 (3): 317–331

Rooper, C. N., J. L. Boldt, S. D. Batten, and C. Gburski. 2012b. Growth and production of Pacific ocean perch (*Sebastes alutus*) in nursery habitats of the Gulf of Alaska. Fish. Oceangr. 21 (6): 415–429.

Rooper, C. N., Zimmermann, M., Prescott, M. M., and Hermann, A. J. 2014. Predictive models of coral and sponge distribution, abundance, and diversity in bottom trawl surveys of the Aleutian Islands, Alaska. Mar. Ecol. Prog. Ser. 503: 157–176. https://doi.org/10.3354/meps10710.

Rooper, C. N., M. F., Sigler, P. Goddard, P. Malecha, R. Towler, K. Williams, R. Wilborn, and M. Zimmermann. 2016. Validation and improvement of species distribution models for structure forming invertebrates in the eastern Bering Sea with an independent survey. Mar. Ecol. Prog. Ser. 551: 117–130. https://doi.org/10.3354/meps11703.

Rooper, C. N., R. Wilborn, P. Goddard, K. Williams, R. Towler, and G. R. Hoff. 2017. Validation of deep-sea coral and sponge distribution models in the Aleutian Islands, Alaska. ICES J. Mar. Sci. 75 (1): 199–209.

Rooper C. N., I. Ortiz, A. J. Hermann, E. A. Laman, W. Cheng, K. Kearney, and K. Aydin. 2021. Predicted shifts of groundfish distribution in the eastern Bering Sea under climate change, with implications for fish populations and fisheries management. ICES J. Mar. Sci. 78 (1) 220–234. https://doi.org/10.1093/icesjms/fsaa215.

Rooper, C.N., Zimmermann, M. and Prescott, M.M., 2017. Comparison of modeling methods to predict the spatial distribution of deep-sea coral and sponge in the Gulf of Alaska. Deep Sea Research Part I: Oceanographic Research Papers, 126, pp.148-161.

Rutecki, T. L., and E. R. Varosi. 1997. Distribution, age, and growth of juvenile sablefish, *Anoplopoma fimbria*, in Southeast Alaska. ***In*** Saunders, M., Wilkins, M. (Eds.), Biology and Management of Sablefish (*Anoplopoma fimbria*). U.S. Dep. Commer., NOAA Tech. Rep. NMFS-130.

Sampson, D. B., and S. M. Al-Jufaily. 1999. Geographic variation in the maturity and growth schedules of English sole along the U.S. West Coast. J. Fish Biol. 54: 1–17. https://doi.org/10.1111/j.1095-8649.1999.tb00608.x.

Sasaki, T. 1985. Studies on the sablefish resources in the North Pacific Ocean. Far Seas Fishery Laboratory, Bull. 22. pp. 1-108, Shimizu, 424, Japan. ***In*** Hanselman, D. H., Heifetz, J., Echave, K. B. and Dressel, S. C., 2015. Move it or lose it: movement and mortality of sablefish tagged in Alaska. Can. J. Fish. Aquat. Sci. 72 (2): 238–251.

Schmidt, J., I. S. Evans, and J. Brinkmann, J. 2003. Comparison of polynomial models for land surface curvature calculation. International Journal of Geographical Information Science. 17 (8): 797–814. https://doi.org/10.1080/13658810310001596058.

Shotwell, S. K., and D. H. Hanselman. 2019. Assessment of the rougheye and blackspotted rockfish stock complex in the Gulf of Alaska. ***In*** Stock Assessment and Fishery Evaluation Report for the Groundfish Resources of the Gulf of Alaska. North Pacific Fishery Management Council, 1007 West Third, Suite 400 Anchorage, AK 99501.

Shotwell, S. K., J. L. Pirtle, J. T. Watson, A. L. Deary, M. J. Doyle, S. J. Barbeaux, M. Dorn, G. A. Gibson, E. Goldstein, D. H. Hanselman, A. J. Hermann, P. J. F. Hulson, B. J. Laurel, J. H. Moss, O. Ormseth, D. Robinson, L. A. Rogers, C. N. Rooper, I. Spies, W. Strasburger, R. M. Suryan, and J. J. Vollenweider. 2022. Synthesizing integrated ecosystem research to create informed stock-specific indicators for next generation stock assessments. Deep-Sea Res. II, GOA SI IV. https://doi.org/10.1016/j.dsr2.2022.105070.

Sibson, R. 1981. A Brief Description of Natural Neighbor Interpolation, Chapter 2 *In* V. Barnet (ed.), Interpolating Multivariate Data. John Wiley and Sons, Chichester, West Sussex, UK, PO19 8SQ. pp. 21-36.

Sigler, M. F., C. N. Rooper, G. R. Hoff, R. P. Stone, R. A. McConnaughey, and T. K. Wilderbuer. 2015. Faunal features of submarine canyons on the eastern Bering Sea slope. Mar. Ecol. Prog. Ser. 526: 21–40.

Sigler, M. F., M. P. Eagleton, T. E. Helser, J. V. Olson, J. L. Pirtle, C. N. Rooper, S. C. Simpson, and R. P. Stone. 2017. Alaska Essential Fish Habitat Research Plan: A Research Plan for the National Marine Fisheries Service's Alaska Fisheries Science Center and Alaska Regional Office. AFSC Processed Rep. 2015-05, 22 p. Alaska Fish. Sci. Cent., NOAA, Natl. Mar. Fish. Serv., 7600 Sand Point Way NE, Seattle WA 98115.

Simpson, S. C., M. P. Eagleton, J. V. Olson, G. A. Harrington, and S. R. Kelly. 2017. Final Essential Fish Habitat (EFH) 5-year Review, Summary Report: 2010 through 2015. U.S. Dep. Commer., NOAA Tech. Memo. NMFS-F/AKR-15, 115p

Sinclair, E. H., D. S. Johnson, T. K. Zeppelin, and T. S. Gelatt. 2013. Decadal variation in the diet of western stock Steller sea lions (*Eumetopias jubatus*). U.S. Dep. Commer., NOAA Tech. Memo., NMFS-AFSC-248, 67 p.

Siwicke, K., P. Malecha, C. Rodgveller, and C. Lunsford. 2020. The 2019 longline survey of the Gulf of Alaska and eastern Bering Sea on the FV Ocean Prowler: Cruise Report OP-19-01. AFSC Processed Rep. 2020-02, 30 p. Alaska Fish. Sci. Cent., NOAA, Natl. Mar. Fish. Serv., Auke Bay Laboratories, 17109 Point Lena Loop Road, Juneau, AK 99801.

Siwicke, K., P. Malecha, and C. Rodgveller. 2021. The 2020 longline survey of the Gulf of Alaska and eastern Aleutian Islands on the FV Alaskan Leader: Cruise Report AL-20-01. AFSC Processed Rep. 2021-02, 33 p. Auke Bay Laboratories, Alaska Fish. Sci. Cent., NOAA, Natl. Mar. Fish. Serv., 17109 Point Lena Loop Road Juneau, AK 99801.

Smith, A.D.M., 1994. Management strategy evaluation – the light on the hill, in: In 'Population Dynamics for Fisheries Management.

Spalinger, K. 2020. Special project plan: 2020 small-mesh bottom trawl survey of shrimp and forage fish in the Kodiak District. Alaska Department of Fish and Game, Division of Commercial Fisheries, Regional Information Report 4K20-09, Kodiak. Accessed at: http://www.adfg.alaska.gov/FedAidPDFs/RIR.4K.2020.09.pdf.

Spies, I., K. Aydin, J. N. Ianelli, and W. Palsson. 2019. Assessment of the arrowtooth flounder stock in the Gulf of Alaska. ***In*** Stock Assessment and Fishery Evaluation Report for the Groundfish

Resources of the Gulf of Alaska. North Pacific Fishery Management Council, 1007 West Third, Suite 400 Anchorage, AK 99501.

Spies, I., R., G. G. Thompson, I. Ortiz, E. Siddon, and W. A. Palsson. 2020. Assessment of the Pacific cod stock in the Aleutian Islands. ***In*** Stock Assessment and Fishery Evaluation Report for the Groundfish Resources of the Bering Sea/Aleutian Islands Regions. North Pacific Fishery Management Council, 1007 West Third, Suite 400 Anchorage, AK 99501.

Stabeno, P. J., N. A. Bond, A. J. Hermann, N. B. Kachel, C. W. Mordy, and J. E. Overland. 2004. Meteorology and oceanography of the Northern Gulf of Alaska. Cont. Shelf Res. 24: 859–897. https://doi:10.1016/j.csr.2004.02.007.

Stabeno, P. J., S. Bell, W. Cheng, S. Danielson, N. B. Kachel, and C. W. Mordy. 2016. Long-term observations of Alaska Coastal Current in the northern Gulf of Alaska. Deep-Sea Res. Part II Top. Stud. Oceanogr. 132: 24–40. https://doi:10.1016/j.dsr2.2015.12.016.

Stark. J. W. 2004. A comparison of the maturation and growth of female flathead sole in the central Gulf of Alaska and south-eastern Bering Sea. J. Fish Biol. 64: 876–889. https://doi.org/10.1111/j.1095-8649.2004.00356.x.

Stark, J. W., 2007. Geographic and seasonal variations in maturation and growth of female Pacific cod (*Gadus macrocephalus*) in the Gulf of Alaska and Bering Sea. Fish. Bull. 105 (3): 396–407.

Stark, J. W. 2012a. Female maturity, reproductive potential, relative distribution, and growth compared between arrowtooth flounder (*Atheresthes stomias*) and Kamchatka flounder (*A. evermanni*) indicating concerns for management. J. Appl. Ichthyol. 28: 226–230.

Stark, J. W. 2012b. Contrasting maturation and growth of northern rock sole in the Eastern Bering Sea and Gulf of Alaska for the purpose of stock management. N. Amer. J. Fish. Manage. 32:93-99.

Stark, J. W., and D. A. Somerton. 2002. Maturation, spawning and growth of rock soles off Kodiak Island in the Gulf of Alaska. J. Fish. Bio. 61: 417–431.

Stevenson, D. E., J. W. Orr, G. R. Hoff, and J. D. McEachran. 2007. Sharks, skates and ratfish of Alaska. Fairbanks, AK: Alaska Sea Grant, University of Alaska.

Stewart, I. J., and Hicks, A. C. 2018. Interannual stability from ensemble modelling. Canadian Journal of Fisheries and Aquatic Sciences, 75: 2109–2113.

Stone, R., H. Lehnert, and H. Reiswig. 2011. A guide to the deep-water sponges of the Aleutian Island archipelago. NOAA Professional Paper NMFS 12. Available from https://spo.nmfs.noaa.gov/content/guide-deepwater-sponges-aleutian-island-archipelago.

Sullivan, J., I. Spies, P. Spencer, A. Kingham, T. Tenbrink, and W. Palsson. 2020. Assessment of the Other Rockfish stock complex in the Bering Sea/Aleutian Islands. ***In*** Stock Assessment and Fishery Evaluation Report for the Groundfish Resources of the Bering Sea/Aleutian Islands Regions. North Pacific Fishery Management Council, 1007 West Third, Suite 400 Anchorage, AK 99501.

Tenbrink, T. T., and P. D. Spencer. 2013. Reproductive biology of Pacific ocean perch and northern rockfish in the Aleutian Islands. N. Amer. J. Fish. Manage. 33 (2): 373–383.

Tenbrink, T. T., and T. K. Wilderbuer. 2015. Updated maturity estimates for flatfishes (Pleuronectidae) in the eastern Bering Sea, with implications for fishery management. Mar. Coast. Fish. 7: 474–482. https://doi.org/10.1080/19425120.2015.1091411.

Tenbrink, T. T., and T. E. Helser. 2021. Reproductive biology, size, and age structure of harlequin rockfish: spatial analysis of life history traits. Mar. Coast. Fish. 13 (5): 463–477. https://doi.org/10.1002/mcf2.10172.

Thompson, G. G., J. Conner, S. Kalei Shotwell, B. Fissel, T. Hurst, B. Laurel, L. Rogers, and E. Siddon. 2020. Assessment of the Pacific cod stock in the Eastern Bering Sea. ***In*** Stock Assessment and Fishery Evaluation Report for the Groundfish Resources of the Bering Sea/Aleutian Islands Regions. North Pacific Fishery Management Council, 1007 West Third, Suite 400 Anchorage, AK 99501.

Thorson, J. T. (2019). Measuring the impact of oceanographic indices on species distribution shifts: The spatially varying effect of cold-pool extent in the eastern Bering Sea. Limnology and Oceanography, 64(6), 2632–2645. https://doi.org/10.1002/lno.11238.

Thorson, J.T., Adams, C.F., Brooks, E.N., Eisner, L.B., Kimmel, D.G., Legault, C.M., Rogers, L.A., Yasumiishi, E.M., 2020a. Seasonal and interannual variation in spatio-temporal models for index standardization and phenology studies. ICES Journal of Marine Science 77, 1879–1892. https://doi.org/10.1093/icesjms/fsaa074.

Thorson, J. T., Cheng, W., Hermann, A. J., Ianelli, J. N., Litzow, M. A., O'Leary, C. A., & Thompson, G. G. (2020b). Empirical orthogonal function regression: Linking population biology to spatial varying environmental conditions using climate projections. Global Change Biology, *26*(8), 4638–4649. https://doi.org/10.1111/gcb.15149.

Thorson, J. T., Hermann, A. J., Siwicke, K., & Zimmermann, M. (2021). Grand challenge for habitat science: Stage-structured responses, nonlocal drivers, and mechanistic associations among habitat variables affecting fishery productivity. ICES Journal of Marine Science, 78(6), 1956–1968. https://doi.org/10.1093/icesjms/fsaa236.

Tribuzio, C.A. and G. H. Kruse. 2012. Life history characteristics of a lightly exploited stock of *Squalus suckleyi*. Journal of Fish Biology. 80: 1159–1180.

Tribuzio, C. A., and K. B. Echave. 2019. Assessment of the other rockfish stock complex in the Gulf of Alaska. ***In*** Stock Assessment and Fishery Evaluation Report for the Groundfish Resources of the Gulf of Alaska. North Pacific Fishery Management Council, 1007 West Third, Suite 400 Anchorage, AK 99501.

Tribuzio, C. A., M. E. Matta, K. Echave, and C. Rodgveller. 2020. Assessment of the shark stock stock complex in the Gulf of Alaska. ***In*** Stock Assessment and Fishery Evaluation Report for the Groundfish Resources of the Gulf of Alaska. North Pacific Fishery Management Council, 1007 West Third, Suite 400 Anchorage, AK 99501.

Turner, K., C. N. Rooper, E. A. Laman, S. Rooney, C. W. Cooper, D. W., and M. Zimmermann. 2017. Model-based essential fish habitat definitions for Aleutian Islands groundfish species. U.S. Dep. Commer., NOAA Tech. Memo. NMFS-AFSC-360, 239 p.

Turnock, B. J., C. R. McGilliard, and W. Palsson. 2017a. Assessment of the flathead sole stock in the Gulf of Alaska. ***In*** Stock Assessment and Fishery Evaluation Report for the Groundfish Resources of the Gulf of Alaska. North Pacific Fishery Management Council, 1007 West Third, Suite 400 Anchorage, AK 99501.

Turncock, B. J., M. Bryan, and T. K. Wilderbuer. 2017b. Assessment of the shallow-water Flatfish Stock Complex in the Gulf of Alaska. ***In*** Stock Assessment and Fishery Evaluation Report for the Groundfish Resources of the Gulf of Alaska. North Pacific Fishery Management Council, 1007 West Third, Suite 400 Anchorage, AK 99501.

von Szalay, P. G., and N. W. Raring. 2018. Data Report: 2017 Gulf of Alaska bottom trawl survey. U.S. Dep. Commer., NOAA Tech. Memo. NMFS-AFSC-374, 260 p.

Wakabayashi, K., R. G. Bakkala, and M. S. Alton. 1985. Methods of the Japan demersal trawl surveys, p. 7-29. In R. G. Bakkala and K. Wakabayashi (Editors), Results of cooperative Japan groundfish investigations in the Bering Sea during May-August 1979. Int. N. Pac. Fish. Comm. Bull. 44.

Walbridge, S., N. Slocum, M. Pobuda, and D. J. Wright. 2018. Unified geomorphological analysis workflows with Benthic Terrain Modeler. Geosci. 8:94. Version 3.0 is available at: https://github.com/EsriOceans/btm.

Weinberg, K. L., and S. Kotwicki. 2008. Factors influencing net width and sea floor contact of a survey bottom trawl. Fish. Res. 93: 265–279.

Weiss, A. 2001. Topographic position and landforms analysis. Poster presentation, ESRI User Conference, San Diego, CA.

Wetzel, C.R. 2019. Status of petrale sole (*Eopsetta jordani*) along the U.S. west coast in 2019. Pacific Fishery Management Council, 7700 Ambassador Place NE, Suite 101, Portland, OR 97220.

Williams B. C., G. H. Kruse, and M. W. Dorn. 2016. Interannual and spatial variability in maturity of walleye pollock *Gadus chalcogrammus* and implications for spawning stock biomass estimates in the Gulf of Alaska. PLoS ONE 11 (10): e0164797. https://doi:10.1371/journal.pone.0164797.

Williams, B. C., P. J. F. Hulson, C. R. Lunsford, and C. J. Cunningham. 2020. Assessment of the Northern Rockfish stock in the Gulf of Alaska. ***In*** Stock Assessment and Fishery Evaluation Report for the Groundfish Resources of the Gulf of Alaska. North Pacific Fishery Management Council, 1007 West Third, Suite 400 Anchorage, AK 99501.

Wilson, M. F. J., B. O'Connell, C. Brown, J. C. Guinan, and A. J. Grehan. 2007. Multiscale terrain analysis of multibeam bathymetry data for habitat mapping on the continental slope. Mar. Geodesy 30: 3–35.

Wing, B. L. 1997. Distribution of sablefish, *Anoplopoma fimbria*, larvae in the eastern Gulf of Alaska: Neuston-net tows versus oblique tows, p. 13-25. ***In*** M. E. Wilkins and M. W. Saunders (editors), Biology and management of sablefish, Anoplopoma fimbria. U.S. Dep. Commer., NOAA Tech. Rep. NMFS-130.

Wood, S. N. 2003. Thin plate regression splines. J. R. Statist. Soc. B 65 (1): 95–114.

Wood, S. N. 2017. Generalized Additive Models: An Introduction with R, Second Edition. CRC Press, Taylor & Francis Group. 476 pp.

Wright, D. J., M. Pendleton, J. Boulware, S. Walbridge, B. Gerlt, D. Eslinger, D. Sampson, et al. 2012. ArcGIS Benthic Terrain Modeler (BTM), v. 3.0, Environmental Systems Research Institute, NOAA Coastal Services Center, Massachusetts Office of Coastal Zone Management. Available at: http://esriurl.com/5754.

Yang, M. S. 1993. Food habits of the commercially important groundfishes in the Gulf of Alaska in 1990. U.S. Dept. Commer., NOAA Tech. Memo. NMFS-AFSC-22, 150 p.

Yang, M. S., and P. A. Livingston. 1986. Food habits and diet overlap of two congeneric species, *Atheresthes stomias* and *Atheresthes evermanni*, in the eastern Bering Sea. Fish. Bull. 82: 615–623.

Yeung, C., and D. W. Cooper, 2020. Contrasting the variability in spatial distribution of two juvenile flatfishes in relation to thermal stanzas in the eastern Bering Sea. ICES J. Mar. Sci. 77 (3): 953–963.

Zar, J. H. 1984. Biostatistical Analysis, 2nd Ed., Simon and Schuster Company, New Jersey, USA. 717 pgs.

Zevenbergen, L. W., and Thorne, C. R. 1987. Quantitative analysis of land surface topography. Earth Surface Processes and Landforms, 12: 47–56.

Zimmermann, M., and J. L. Benson. 2013. Smooth sheets: How to work with them in a GIS to derive bathymetry, features and substrates. NOAA Tech. Memo. NMFS-AFSC-249. 52 p.

Zimmermann, M., and M. M. Prescott. 2014. Smooth sheet bathymetry of Cook Inlet, Alaska. NOAA Tech. Memo. NMFS-AFSC-275. 32 p.

Zimmermann, M., and M. M. Prescott. 2015. Smooth sheet bathymetry of the central Gulf of Alaska. NOAA Tech. Memo. NMFS-AFSC-287. 54 p.

Zimmermann, M. 2019. Comparison of the physical attributes of the central and eastern Gulf of Alaska IERP inshore study sites. Deep-Sea Res. II: Understanding Ecosystem Processes in the Gulf of Alaska 2. 165: 280–291. https://doi.org/10.1016/j.dsr2.2018.05.011.

Zimmermann, M., M. M. Prescott, and P. J. Haeussler. 2019. Bathymetry and Geomorphology of Shelikof Strait and the Western Gulf of Alaska. Geosci. 9: 409. https://doi.org/10.3390/geosciences9100409.

Zimmermann, M. 2019. Comparison of the physical attributes of the central and eastern Gulf of Alaska IERP inshore study sites. Deep-Sea Res. II: Understanding Ecosystem Processes in the Gulf of Alaska 2. 165: 280–291. https://doi.org/10.1016/j.dsr2.2018.05.011.

Zuur, A. F., E. N., Ieno, N. J. Walker, A. A. Saveliev, and G. M. Smith. 2009. Mixed Effects Models and Extensions in Ecology with R. Springer Science+Business Media, LLC. New York, N.Y.

U.S. Secretary of Commerce
Gina M. Raimondo

Under Secretary of Commerce for Oceans and Atmosphere
Dr. Richard W. Spinrad

Assistant Administrator, National Marine Fisheries Service
Janet Coit

April 2023

www.nmfs.noaa.gov

OFFICIAL BUSINESS

National Marine Fisheries Service
Alaska Fisheries Science Center
7600 Sand Point Way N.E.
Seattle, WA 98115-6349